

DEVELOPMENT OF NICKEL-CATALYZED ASYMMETRIC REDUCTIVE CROSS-  
COUPLING OF BENZYLIC ELECTROPHILES

Thesis by

Alan Hayden Cherney

In Partial Fulfillment of the Requirements

for the Degree of

Doctor of Philosophy

CALIFORNIA INSTITUTE OF TECHNOLOGY

Pasadena, California

2015

(Defended May 21, 2015)

© 2015

Alan Hayden Cherney

All Rights Reserved

*To my teachers*

## ACKNOWLEDGEMENTS

The five years I have spent at the California Institute of Technology have been a transformational experience because of both the research I have been immersed in and the talented people that surrounded me. Caltech is truly a unique environment that I will remember fondly as I move on in my career.

First and foremost, I would like to thank my research advisor, Prof. Sarah Reisman. I have learned a great deal from her mentorship that will carry me well beyond the walls of Schlinger Laboratory. It has been a privilege to work for such an insightful and diligent advisor who is honestly concerned about the well-being of her students. I have enjoyed watching her evolve from a pre-tenure junior faculty member to a full professor who is known across the globe. Similarly, seeing our research group double in size and witnessing the success of our fellow lab members makes me more aware of all she has accomplished.

I am also grateful to the members of my thesis committee, Profs. Jonas Peters and Gregory Fu, and chairman, Prof. Brian Stoltz. Jonas's organometallic and mechanistic perspective has served an important role in my committee meetings, and Greg's recent move to Caltech has given our lab a new source of guidance and experience in the field of asymmetric catalysis. I am appreciative of our special relationship with the Stoltz group, which has enabled me to receive input from Brian and his lab during joint meetings. The Stoltz group has also been an irreplaceable source of chemicals, equipment, knowledge, and friendship. I believe that this collaborative and open environment is one of the hallmarks of the Caltech experience.

The Caltech staff has played an important role in helping students move their research projects forward. Dr. David Vander Velde has kept the NMR facility running smoothly for the entirety of my tenure. Dr. Scott Virgil and the Caltech Center for Catalysis and Chemical Synthesis have been a tremendous resource for instrumentation, expensive catalysts and ligands, and chemical knowledge. A large component of my research would have proceeded much more slowly if it were not for daily excursions to Scott's facility to use the SFC, rotary stirrers, cooling wells, and much more.

It has been an honor to work with some exceptionally intelligent and dedicated people during my time in the Reisman lab. They inspire me to be a better chemist and have made my time at the bench more enjoyable. The lab as we know it would not be possible without the pioneering efforts of Sarah's first class, Drs. Roger Nani, Lindsay Repka, Julian Codelli, Raul Navarro, and John Yeoman, and her second class of Dr. Jane Ni (as well as Kangway Chuang, who first left Champaign-Urbana, Illinois for Caltech nine years ago). I have been privileged to proceed through all the milestones of graduate school with labmates Madeleine Kieffer and Haoxuan Wang and am excited to be defending my thesis within a week of both of them. I have also enjoyed overlapping with a number of talented post-docs and energetic first-year graduate students who themselves have grown into experienced scientists.

When I first joined the group, Sarah entrusted me with a new project for the lab, and working alone in the trenches has made me appreciate the coworkers who have since joined me on Team Nickel. Nathaniel Kadunce was an invaluable collaborator in our initial development of an asymmetric reductive cross-coupling and is now applying the lessons we have learned toward his own reaction development. His friendship and unique

outlook made the long days in lab go by just a little bit quicker. Dr. Leah Cleary expanded our chemistry in a new direction and gave me fresh ideas and enthusiasm arising from her perspective as a post-doc. I have also benefited from direct and indirect mentoring experiences with several undergraduates and visiting students. Lastly, I am pleased to leave my research efforts in the clever and capable hands of graduate students Julie Hofstra and Kelsey Poremba.

I must also thank my undergraduate research advisor Prof. Martin Burke and mentor Dr. Eric Woerly at the University of Illinois at Urbana-Champaign for initially fostering my passion for synthetic organic chemistry. Without the opportunities they provided me, I would not have been able to find myself in graduate school at Caltech. As I have progressed through my doctoral degree, my appreciation for the time they put into my training has only increased.

Lastly, I would like to thank my friends and family, who have played an important role in my development. My parents' love and continued support throughout my life has driven me to pursue my dreams and ambitions, from dinosaurs in grade school to organic synthesis in graduate school. My brother Michael and sister Elyssa have always been a source of company and friendship, and I remain inspired by their determination to fulfill their own dreams. Jessica Ricci's love, companionship, and patience have sustained me during the long days and weeks of graduate school and have enriched my life in a way I never would have expected when I first moved to California; I look forward to spending more evenings and Sundays with her and Oscar the cat without having to rush back to the lab. As my time at Caltech reaches its end, these are the people that deserve credit for making it all possible.

## ABSTRACT

Over the last forty years, the advent of transition metal-catalyzed cross-coupling has revolutionized the synthetic chemist's ability to generate C–C bonds. Since the 1970s, a parallel effort to control the stereochemical outcome of such transformations has yielded a variety of chiral catalyst complexes that deliver enantioenriched cross-coupled products. Nonetheless, challenges in the use of C(sp<sup>3</sup>)-hybridized coupling partners have limited asymmetric variants to a narrow fraction of the total number of cross-coupling methodologies published each year.

Herein, we report studies on the asymmetric cross-coupling of benzylic groups under either Pd or Ni catalysis. We have developed a Pd-catalyzed Fukuyama cross-coupling of thioesters and secondary benzylzinc halides to deliver racemic ketones under mild conditions. Investigations with chiral catalysts revealed that a promising asymmetric transformation could be achieved to give modestly enantioenriched ketones.

Reductive cross-coupling, involving the union of two different electrophiles, has the added advantage of avoiding harsh or expensive organometallic reagents. We have discovered the first highly enantioselective Ni-catalyzed reductive cross-couplings of two organohalide electrophiles. Treatment of an acid chloride and a secondary benzyl chloride with a chiral nickel/bis(oxazoline) complex and Mn<sup>0</sup> as the stoichiometric reductant furnishes ketone products in good yield and high enantioselectivity. Expanding on this result, we have demonstrated that vinyl bromides and secondary benzyl chlorides can be cross-coupled using a different chiral nickel/bis(oxazoline) complex, illustrating the generality of an asymmetric reductive coupling platform. Preliminary studies directed toward other coupling partners are also disclosed.

**TABLE OF CONTENTS**

<b>CHAPTER 1</b>	<b>1</b>
<i>Enantioselective Transition Metal-Catalyzed Cross-Coupling Reactions of Organometallic Reagents to Prepare C–C Bonds</i>	
<b>1.1 INTRODUCTION.....</b>	<b>1</b>
<b>1.2 REACTIONS OF SECONDARY ALKYL ORGANOMETALLIC REAGENTS .....</b>	<b>4</b>
1.2.1 Organomagnesium Reagents.....	5
1.2.2 Organozinc Reagents.....	14
1.2.3 Organoboron Reagents .....	16
<b>1.3 REACTIONS OF SECONDARY ALKYL ELECTROPHILES .....</b>	<b>17</b>
1.3.1 With Organomagnesium Reagents .....	18
1.3.2 With Organozinc Reagents .....	20
1.3.3 With Organoboron Reagents.....	27
1.3.4 With Organosilicon Reagents.....	33
1.3.5 With Organozirconium Reagents.....	33
1.3.6 With Organoindium Reagents.....	34
<b>1.4 TRANSITION METAL-CATALYZED DESYMMETRIZATION REACTIONS.....</b>	<b>35</b>
1.4.1 With Organozinc Reagents .....	36
1.4.2 With Organoboron Reagents.....	40
<b>1.5 CONCLUDING REMARKS .....</b>	<b>43</b>
<b>1.6 NOTES AND REFERENCES .....</b>	<b>45</b>

**CHAPTER 2** **51**

*Pd-Catalyzed Fukuyama Cross-Coupling of Secondary Organozinc Reagents for the Direct Synthesis of Unsymmetrical Ketones*

<b>2.1 INTRODUCTION.....</b>	<b>51</b>
<b>2.2 DEVELOPMENT OF A RACEMIC FUKUYAMA CROSS-COUPLING OF SECONDARY ORGANOZINC REAGENTS .....</b>	<b>54</b>
<b>2.3 EFFORTS TOWARD AN ENANTIOSELECTIVE FUKUYAMA CROSS-COUPLING .....</b>	<b>61</b>
<b>2.4 CONCLUDING REMARKS .....</b>	<b>70</b>
<b>2.5 EXPERIMENTAL SECTION.....</b>	<b>70</b>
2.5.1 Materials and Methods.....	70
2.5.2 Substrate Synthesis.....	71
2.5.3 General Procedure for Fukuyama Cross-Coupling Reaction .....	76
2.5.4 Procedure for Acid Chloride Cross-Coupling.....	84
<b>2.6 NOTES AND REFERENCES .....</b>	<b>85</b>

**APPENDIX 1** **88**

Spectra Relevant to Chapter 2

**CHAPTER 3** **131**

*Catalytic Asymmetric Reductive Acyl Cross-Coupling: Synthesis of Enantioenriched Acyclic  $\alpha,\alpha$ -Disubstituted Ketones*

<b>3.1 INTRODUCTION.....</b>	<b>131</b>
<b>3.2 DEVELOPMENT OF AN ASYMMETRIC REDUCTIVE ACYL CROSS-COUPLING .....</b>	<b>135</b>

3.2.1 Identification of a Chiral Catalyst System .....	135
3.2.2 Optimization of Reactivity for an Enantioselective Reaction.....	138
3.2.3 Substrate Scope and Further Studies.....	147
<b>3.3 CONCLUDING REMARKS .....</b>	<b>152</b>
<b>3.4 EXPERIMENTAL SECTION.....</b>	<b>152</b>
3.4.1 Materials and Methods.....	152
3.4.2 Substrate Synthesis.....	153
3.4.3 Enantioselective Reductive Cross-Coupling.....	156
3.4.4 SFC Traces of Racemic and Enantioenriched Ketone Products .....	175
<b>3.5 NOTES AND REFERENCES .....</b>	<b>196</b>
<b>APPENDIX 2 .....</b>	<b>200</b>
Spectra Relevant to Chapter 3	
<b>CHAPTER 4 .....</b>	<b>253</b>
<i>Nickel-Catalyzed Asymmetric Reductive Cross-Coupling Between Vinyl and Benzyl Electrophiles</i>	
<b>4.1 INTRODUCTION.....</b>	<b>253</b>
<b>4.2 DEVELOPMENT OF AN ASYMMETRIC REDUCTIVE VINYL CROSS- COUPLING .....</b>	<b>256</b>
4.2.1 Identification of a Chiral Catalyst System .....	256
4.2.2 Optimization of Reactivity for an Enantioselective Reaction.....	258
4.2.3 Substrate Scope and Further Studies.....	264
<b>4.3 CONCLUDING REMARKS .....</b>	<b>270</b>
<b>4.4 EXPERIMENTAL SECTION.....</b>	<b>270</b>
4.4.1 Materials and Methods.....	270

4.4.2 Ligand and Substrate Synthesis.....	272
4.4.3 Enantioselective Reductive Cross-Coupling.....	284
4.4.4 SFC Traces of Racemic and Enantioenriched Products .....	311
<b>4.5 NOTES AND REFERENCES .....</b>	<b>344</b>
 <b>APPENDIX 3</b>	<b>348</b>
Spectra Relevant to Chapter 4	
 <b>CHAPTER 5</b>	<b>433</b>
<i>Toward New Coupling Partners for Asymmetric Ni-Catalyzed Reductive Cross-Coupling</i>	
 <b>5.1 INTRODUCTION.....</b>	<b>433</b>
<b>5.2 DEVELOPMENT OF NEW NI-CATALYZED REDUCTIVE CROSS-COUPPLINGS (RACEMIC OR ACHIRAL) .....</b>	<b>437</b>
<b>5.3 DEVELOPMENT OF NEW NI-CATALYZED REDUCTIVE CROSS-COUPPLINGS (ASYMMETRIC) .....</b>	<b>441</b>
<b>5.4 CONCLUDING REMARKS .....</b>	<b>447</b>
<b>5.5 EXPERIMENTAL SECTION.....</b>	<b>448</b>
5.5.1 Materials and Methods.....	448
5.5.2 Ni-Catalyzed Reductive Cross-Coupling .....	449
<b>5.6 NOTES AND REFERENCES .....</b>	<b>452</b>
 <b>ABOUT THE AUTHOR</b>	<b>454</b>

**LIST OF ABBREVIATIONS**

$[\alpha]_D$	angle of optical rotation of plane-polarized light
Å	angstrom(s)
Ac	acetyl
acac	acetylacetonate
<sup>t</sup> Am	<i>tert</i> -amyl
APCI	atmospheric pressure chemical ionization
app	apparent
aq	aqueous
Ar	aryl group
bathophen	bathophenanthroline
BBN	borabicyclo[3.3.1]nonane
BHT	2,6-di- <i>tert</i> -butyl-4-methylphenol (“ <u>butylated hydroxytoluene</u> ”)
Biox	bi(oxazoline)
BINAP	2,2'-bis(diphenylphosphino)-1,1'-binaphthyl
BINOL	1,1'-bi(2-naphthol)
Bn	benzyl
Boc	<i>tert</i> -butoxycarbonyl
Box	bis(oxazoline)
bp	boiling point
BPPFA	<i>N,N</i> -dimethyl-1-[1',2-bis(diphenylphosphino)ferrocenyl]ethylamine
br	broad

Bu	butyl
<sup>i</sup> Bu	<i>iso</i> -butyl
<sup>n</sup> Bu	butyl or <i>norm</i> -butyl
<sup>s</sup> Bu	<i>sec</i> -butyl
<sup>t</sup> Bu	<i>tert</i> -butyl
Bz	benzoyl
<i>c</i>	concentration of sample for measurement of optical rotation
°C	degrees Celsius
calc'd	calculated
CAM	cerium ammonium molybdate
cm <sup>-1</sup>	wavenumber(s)
cod	1,5-cyclooctadiene
conc.	concentrated
Cp	cyclopentadienyl
Cy	cyclohexyl
Cyp	cyclopentyl
d	doublet
<i>d</i>	dextrorotatory
D	deuterium
dba	dibenzylideneacetone
DFT	density functional theory
DIOP	2,3- <i>O</i> -isopropylidene-2,3-dihydroxy-1,4-bis(diphenylphosphino)butane

DKR	dynamic kinetic resolution
DMA	<i>N,N</i> -dimethylacetamide
DMBA	2,6-dimethylbenzoic acid
DME	1,2-dimethoxyethane
DMF	<i>N,N</i> -dimethylformamide
DMI	1,3-dimethyl-2-imidazolidinone
DMPU	<i>N,N'</i> -dimethylpropylene urea
DMSO	dimethylsulfoxide
dppb	1,4-bis(diphenylphosphino)butane
dppbz	1,2-bis(diphenylphosphino)benzene
dppf	1,1'-bis(diphenylphosphino)ferrocene
dppe	1,2-bis(diphenylphosphino)ethane
dr	diastereomeric ratio
dtbpy	4,4'-di- <i>tert</i> -butyl-2,2'-bipyridine
DYKAT	dynamic kinetic asymmetric transformation
<i>E</i>	trans (entgegen) olefin geometry
ee	enantiomeric excess
EI	electron impact
EPPF	1-diphenylphosphino-2-ethylferrocene
ESI	electrospray ionization
Et	ethyl
FAB	fast atom bombardment
FcPN	1-dimethylaminomethyl-2-diphenyl-phosphinoferrocene

g	gram(s)
GC	gas chromatography
h	hour(s)
$^1\text{H}$	proton
hex	hexyl
HMDS	hexamethyldisilazane
$h\nu$	light
HPLC	high performance liquid chromatography
HRMS	high resolution mass spectrometry
Hz	hertz
IPA	isopropanol
IR	infrared spectroscopy
$J$	coupling constant
$k$	rate constant
L	liter or neutral ligand
$l$	levorotatory
LED	light-emitting diode
m	multiplet or meter(s)
M	molar or molecular ion
$m$	meta
Me	methyl
mg	milligram(s)
MHz	megahertz

min	minute(s)
mL	milliliter(s)
MM	mixed method
mol	mole(s)
MOP	2-(diphenylphosphino)-2'-methoxy-1,1'-binaphthyl
mp	melting point
Ms	methanesulfonyl (mesyl)
MS	molecular sieves or mass spectrometry
<i>m/z</i>	mass-to-charge ratio
naph	naphthyl
Naphos	2,2'-bis(diphenylphosphinomethyl)-1,1'-binaphthyl
nbd	norbornadiene
NBS	<i>N</i> -bromosuccinimide
NMDPP	neomenthyl diphenylphosphine
NMP	<i>N</i> -methyl-2-pyrrolidone
NMR	nuclear magnetic resonance
Norphos	2,3-bis(diphenylphosphino)-bicyclo[2.2.1]hept-5-ene
<i>o</i>	ortho
<i>p</i>	para
Pc	phthalocyanine
Ph	phenyl
pH	hydrogen ion concentration in aqueous solution
phen	1,10-phenanthroline

pin	pinacol
Piv	pivaloyl
$pK_a$	acid dissociation constant
PPFA	<i>N,N</i> -dimethyl-1-[2-(diphenylphosphino)ferrocenyl]ethylamine
Pr	propyl
<sup>i</sup> Pr	isopropyl
<sup>n</sup> Pr	propyl or <i>norm</i> -propyl
Prophos	1,2-bis(diphenylphosphino)propane
py	pyridine
PyBox	pyridine-bis(oxazoline)
PyOx	pyridine-oxazoline
pyphos	(2-diphenylphosphino)ethylpyridine
q	quartet
Quinox	quinoline-oxazoline
R	alkyl group
<i>R</i>	rectus
ref	reference
$R_f$	retention factor
rt	room temperature
s	singlet or seconds
<i>S</i>	sinister
sat.	saturated
SET	single-electron transfer

SFC	supercritical fluid chromatography
t	triplet
TADDOL	$\alpha,\alpha,\alpha,\alpha$ -tetraaryl-1,3-dioxolane-4,5-dimethanol
TBAB	tetra- <i>n</i> -butylammonium bromide
TBAI	tetra- <i>n</i> -butylammonium iodide
TBAT	tetra- <i>n</i> -butylammonium difluorotriphenylsilicate
TBS	<i>tert</i> -butyldimethylsilyl
TDAE	tetrakis(dimethylamino)ethylene
TFA	trifluoroacetic acid
temp	temperature
terpy	2,2':6',2''-terpyridine
THF	tetrahydrofuran
TIPS	triisopropylsilyl
TLC	thin layer chromatography
TMEDA	<i>N,N,N',N'</i> -tetramethylethylenediamine
TMS	trimethylsilyl
TOF	time-of-flight
tol	toluene
UV	ultraviolet
v/v	volume per volume
X	anionic ligand or halide
Z	cis (zusammen) olefin geometry

## **Chapter 1**

### *Enantioselective Transition Metal-Catalyzed Cross-Coupling Reactions of Organometallic Reagents to Prepare C–C Bonds<sup>†</sup>*

#### **1.1 INTRODUCTION**

The stereocontrolled construction of C–C bonds remains one of the foremost challenges in organic synthesis. At the heart of any chemical synthesis of a natural product or designed small molecule is the need to carefully orchestrate a series of chemical reactions to prepare and functionalize a carbon framework. The advent of transition metal catalysis has provided chemists with a broad range of new tools to forge C–C bonds and has resulted in a paradigm shift in synthetic strategy planning. The impact of these methodologies has been recognized with the awarding of the 2010 Nobel Prize in Chemistry to Richard Heck, Ei-ichi Negishi, and Akira Suzuki for their seminal contributions to the development of Pd-catalyzed cross-coupling.

---

<sup>†</sup> Portions of this chapter will be reproduced as a review written in collaboration with Prof. Sarah E. Reisman and Nathaniel T. Kadunce

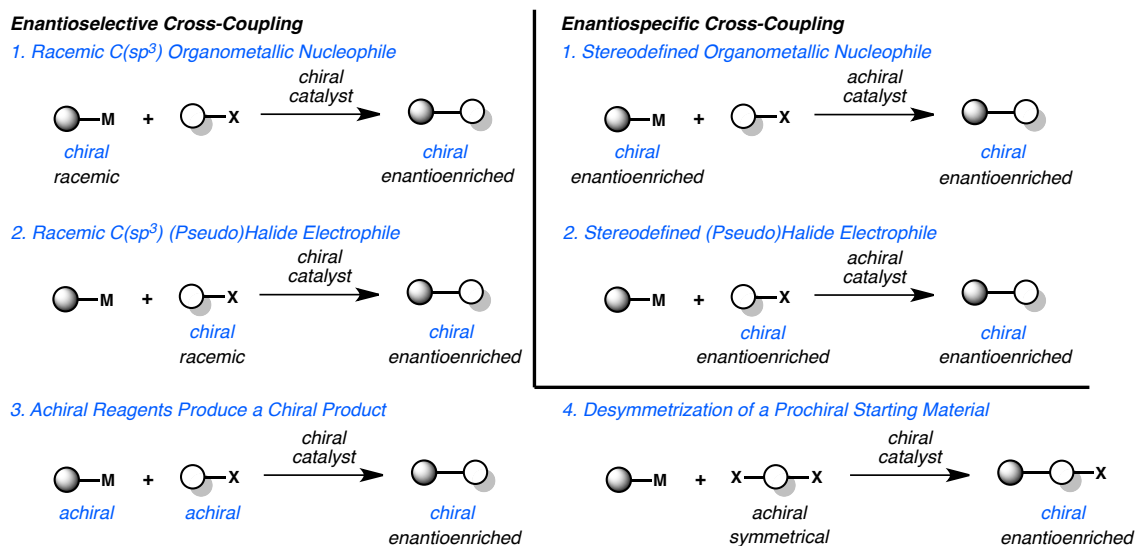
The potential of using transition metal-catalyzed C–C bond formation to prepare enantioenriched molecules was immediately recognized by the synthetic chemistry community. Indeed, the first forays into enantioselective cross-coupling reactions occurred contemporaneously with the development of the transition metal-catalyzed reactions themselves. Here we define *transition metal-catalyzed cross-coupling reactions* as C–C bond forming reactions between an organic electrophile (typically an organic halide or pseudo halide, which in this review includes alcohols, amines, and their derivatives) and an organometallic reagent, mediated by a transition metal catalyst.

Enantio-controlled transition metal-catalyzed cross-coupling reactions to form C–C bonds, in which the stereogenic unit is defined by the C–C bond forming event, can be organized into two general categories. The first group comprises *enantioselective* transition metal-catalyzed cross-coupling reactions, which we define as *reactions in which there is selective formation of one enantiomer over the other as defined by a non-racemic chiral metal catalyst*. There are several different types of enantioselective cross-coupling reactions: those in which (a) racemic, C(sp)<sup>3</sup> organometallic reagents are stereoconvergently coupled to organic electrophiles; (b) racemic, C(sp)<sup>3</sup> organic electrophiles are stereoconvergently coupled to organometallic reagents; (c) achiral organic electrophiles are coupled to achiral organometallic reagents to produce chiral, non-racemic products; and (d) a prochiral starting material (either the organic electrophile or organometallic reagent) is desymmetrized. These reactions are schematically represented in Figure 1.1.

The second group comprises *enantiospecific* transition metal-catalyzed alkyl cross-coupling reactions, which we define as *chirality exchange reactions in which the*

*stereochemistry of a chiral, enantioenriched substrate defines the stereochemistry of the product.* These reactions can be further categorized into those which involve the cross-coupling of (a) a stereodefined organometallic reagent with an electrophile, or (b) a stereodefined electrophile with an organometallic reagent. These types of enantioselective and enantiospecific reactions have been used to prepare molecules exhibiting centro, axial, and planar chirality. This review will encompass enantioselective transition metal-catalyzed cross-coupling reactions of organic electrophiles and organometallic reagents, covering the literature published through the end of the year 2014.

**Figure 1.1.** Strategies for enantiocontrolled cross-coupling.



Despite promising initial reports, highly enantioselective transition metal-catalyzed alkyl cross-coupling reactions were slow to develop, in part because of the general challenges encountered in Pd-catalyzed alkyl cross-coupling reactions. For Pd and other metals that react by polar, two-electron mechanisms, *sec*-alkyl organometallic reagents are typically slower than their *n*-alkyl or C(sp)<sup>2</sup> hybridized counterparts to

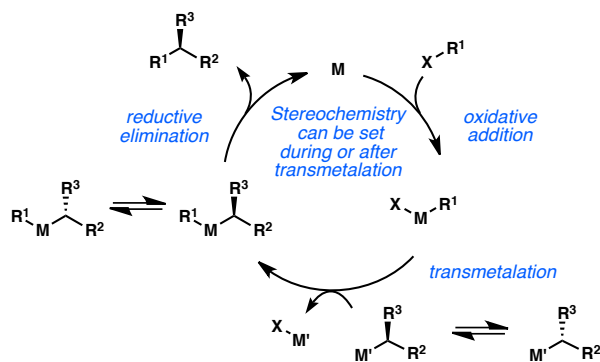
undergo transmetalation.<sup>1</sup> Similarly, *sec*-alkyl electrophiles are frequently slow to undergo oxidative addition to Pd.<sup>2</sup> Moreover, in either case, the resulting *sec*-alkyl transition metal complexes can suffer from rapid, non-productive  $\beta$ -hydride elimination. Thus, the successful realization of enantioselective transition metal-catalyzed alkyl cross-coupling reactions has resulted from fundamental studies of the factors, particularly ligands, which control and influence the efficiency of these transformations. In addition, a renewed interest in Ni catalysts, which can engage with *sec*-alkyl halides through single electron oxidative addition mechanisms, has resulted in a rapidly increasing number of enantioselective alkyl cross-coupling reactions.

## 1.2 REACTIONS OF SECONDARY ALKYL ORGANOMETALLIC REAGENTS

Early efforts to develop enantioselective transition metal-catalyzed alkyl cross-coupling reactions focused primarily on the use of configurationally labile *sec*-alkyl organometallic species such as organomagnesium and organozinc reagents. In general, the configurational stability of an organometallic reagent correlates to the electronegativity of the metal, with less electronegative metals resulting in more configurationally labile *sec*-alkyl reagents.<sup>3</sup> For example, *sec*-alkyl magnesium reagents have been shown to racemize above  $-10\text{ }^{\circ}\text{C}$ , while the corresponding *sec*-alkyl boron reagents are configurationally stable indefinitely at room temperature.<sup>4</sup> In principle, fast equilibration between the two enantiomers of a *sec*-alkyl organometallic reagent or between two diastereomers of a chiral transition metal complex could enable enantioselective cross-coupling through a dynamic kinetic asymmetric transformation

(DYKAT), in which the newly formed stereogenic center is controlled by the chirality of the metal catalyst (Figure 1.2).

**Figure 1.2.** Stereochemical outcome of cross-coupling with secondary nucleophiles.



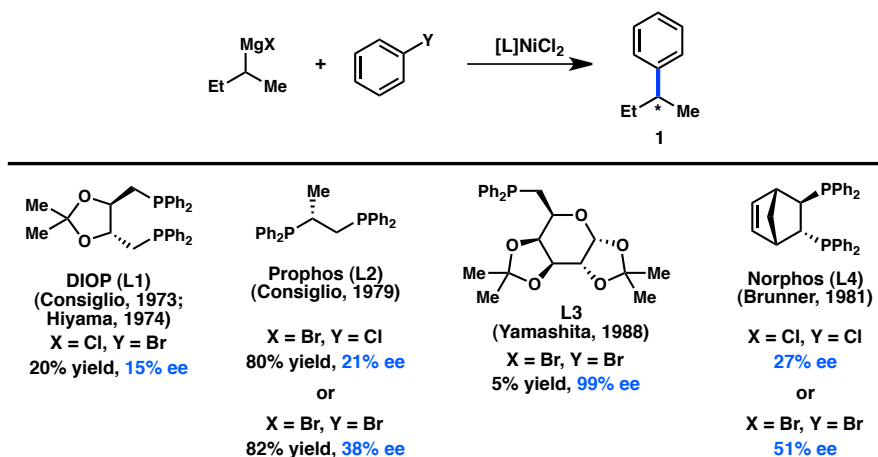
Enantioselective reactions of configurationally stable *sec*-alkyl organometallic reagents can arise from catalyst-controlled kinetic resolution processes, wherein the relative rates of transmetalation for the two enantiomers of the chiral organometallic reagent are substantially different. In this case, an excess of the organometallic reagent must be used to obtain the cross-coupled product in good yield. A third possibility involves a stereoablative mechanism, in which the initial configuration of the starting material is destroyed and then reset by the chiral catalyst during the reaction.

### 1.2.1 Organomagnesium Reagents

In 1972 Corriu and Kumada independently reported the Ni-catalyzed cross-coupling between alkyl organomagnesium halides and aryl or vinyl halides;<sup>5</sup> shortly thereafter the first studies aimed at utilizing chiral transition metal complexes to catalyze these reactions enantioselectively were reported.<sup>6</sup> In 1973 and 1974, respectively, Consiglio and Kumada independently reported that the complex generated from Ni-halide

salts and the chiral bidentate phosphine ligand DIOP (**L1**) catalyzes the reaction between *sec*-butylmagnesium bromide or chloride and bromo- or chlorobenzene to give product **1** with promising enantioinduction (Figure 1.3).<sup>7</sup> These results were an important proof of concept for the area of enantioselective cross-coupling; however, since low yields of product were obtained, it remains ambiguous whether these reactions proceed by kinetic resolution of the *sec*-alkylmagnesium reagent or through a DYKAT. It was subsequently reported that Prophos (**L2**) provides improved enantioinduction and higher yields of **1**.<sup>8</sup> The identity of the halogen on both the organic halide and the organometallic reagent was shown to significantly influence the absolute configuration and the ee of **1**. Further improvements were observed when Norphos (**L4**) was employed as the chiral ligand, providing **1** in 50% ee.<sup>9</sup> A carbohydrate-derived chiral ligand (**L3**) was also reported to deliver **1** in good ee, although with poor yields.<sup>10</sup>

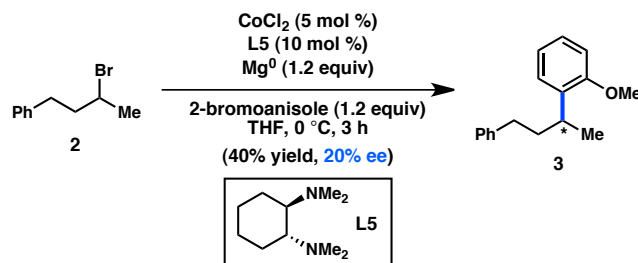
**Figure 1.3.** Stereoconvergent arylation of *s*Bu Grignard reagents.



In 2009, Jacobi von Wangelin and coworkers reported the in situ generation of a secondary Grignard reagent that can subsequently undergo a Co-catalyzed asymmetric cross-coupling with promising enantioinduction (Scheme 1.1).<sup>11</sup> Additional ligand

development and expansion of the substrate scope are imperative, but this initial result represents a solid advance for in situ Grignard formation in stereoconvergent cross-couplings.

**Scheme 1.1.** Stereoselective coupling of a Grignard reagent prepared in situ.



Concurrent to their efforts to develop enantioselective cross-coupling reactions of *sec*-butyl Grignard reagents, Kumada and coworkers investigated the Ni-catalyzed enantioselective coupling between  $\alpha$ -methylbenzyl Grignard reagents and vinyl halides (Figure 1.4). DIOP (**L1**) and the axially chiral Naphos (**L6**) ligand systems provided the product with low enantioinduction.<sup>7b,12</sup> Following up on Kumada's studies, Brunner and coworkers reported that Norphos (**L4**) furnished **4** in 95% yield and 67% ee.<sup>13</sup>

**Figure 1.4.** Stereoconvergent vinylation of benzylic Grignard reagents.

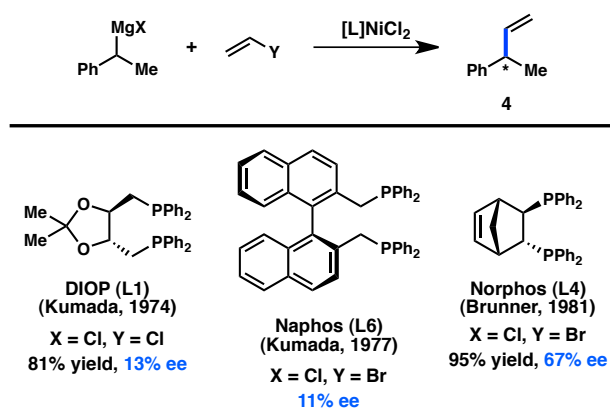
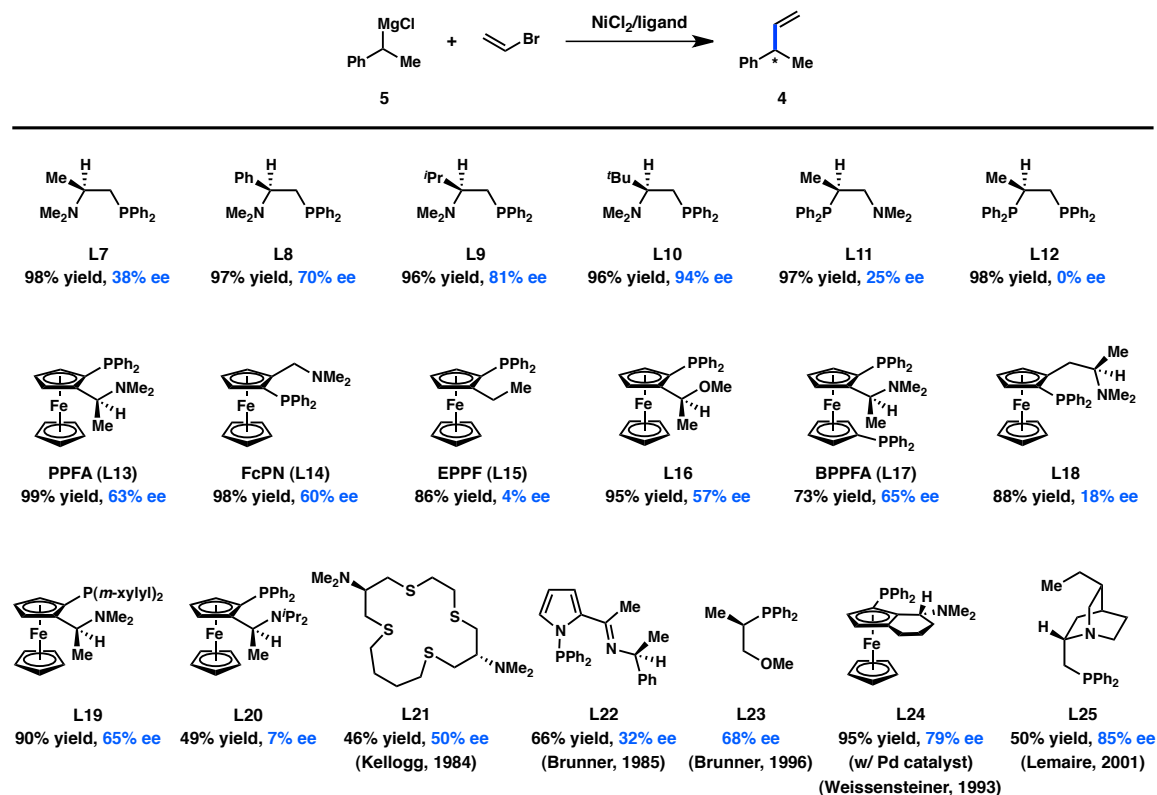


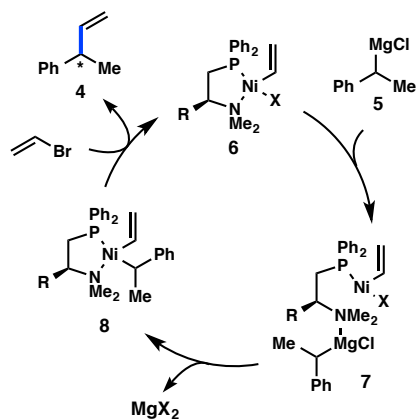
**Figure 1.5.** Chiral ligands developed for the enantioselective cross-coupling of  $\alpha$ -methylbenzyl Grignard reagents.



Since Kumada's initial report, the majority of studies have focused on identifying new ligands to improve the selectivity in the coupling between  $\alpha$ -methylbenzyl Grignard reagents (**5**) and vinyl bromide. Whereas the early studies focused on the use of bidentate bis-phosphine ligands, which delivered modest levels of enantioinduction, later efforts turned to chiral P,N ligands. Kumada, Hayashi, and coworkers reported that chiral ( $\beta$ -aminoalkyl)phosphines—easily prepared from enantiopure amino acids—delivered exceptionally high yields for the cross-coupling between **5** and vinyl bromide (Figure 1.5).<sup>14</sup> Interestingly, whereas the alkyl substitution on the ligand backbone exhibited little influence on the yield of the reaction, it dramatically impacted the enantioselectivity:

increasing the steric profile of the ligand raised the ee from 38% when the chiral tertiary substituent was Me (**L7**) to 94% when this group was <sup>t</sup>Bu (**L10**). In order to probe the origin of asymmetric induction, the isomeric P,N-ligand **L11** was designed. Under the same reaction conditions, **L11** delivered **4** in only 25% ee. Moreover, the analogous bis-phosphine **L12** provided no enantioinduction, suggesting a critical role for the amino group. A proposed catalytic cycle for this reaction is shown in Figure 1.6 and involves precoordination between Grignard reagent **5** and the amino group of the ligand to give complex **7**. The authors hypothesize that this coordination could selectively direct the transmetalation of a single enantiomer of the organometallic reagent, although the importance of this interaction has been debated.<sup>15</sup>

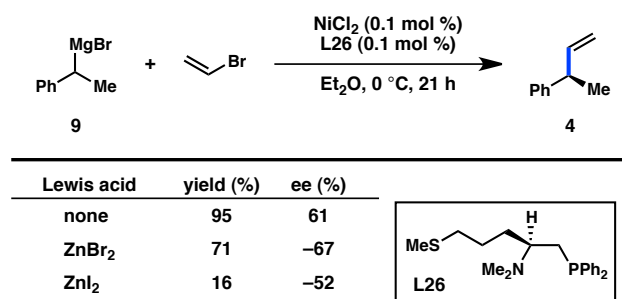
**Figure 1.6.** Proposed catalytic cycle for the enantioselective coupling of  $\alpha$ -methylbenzyl Grignard reagents.



Elaborating on this concept, Kellogg and coworkers investigated the use of ( $\beta$ -aminoalkyl)phosphine ligands bearing pendant heteroatoms, such as those derived from lysine or methionine.<sup>16</sup> The authors reported a reversal of the stereochemical outcome in the presence of exogenous zinc halide salts (Figure 1.7). Control experiments using pre-

generated  $\alpha$ -methylbenzylzinc bromide did not support the intermediacy of an organozinc species; instead it is possible that coordination between the Lewis acidic zinc halide and the sidechain heteroatom could alter or disrupt the ability of the amino group to direct the transmetalation event.

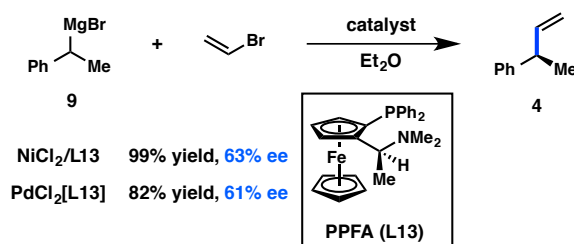
**Figure 1.7.** Addition of exogenous zinc halide salts reverses the sense of enantioinduction when sulfur-containing ligand **L26** is used.



The importance of an amino directing group on the chiral ligand was also reported by Kumada, Hayashi, and coworkers, during their investigations of ferrocenyl phosphines in the Ni-catalyzed coupling between  $\alpha$ -methylbenzyl Grignard reagent **5** and vinyl bromide (Figure 1.5). These bidentate P,N ligands possess both centrochirality at carbon as well as planar chirality. The ligand PPFa (**L13**), furnished **4** in an excellent 99% yield and 63% ee.<sup>17</sup> The ee of the product was determined to remain roughly constant over the course of the reaction.<sup>18</sup> A structure-activity relationship study revealed that FcPN (**L14**), while lacking centrochirality but maintaining planar chirality, gave **4** in 60% ee, demonstrating the dominant role of planar chirality in this system. EPPF (**L15**), which possesses neither centrochirality nor the dimethylamino group, delivered **4** in only 4% ee, validating the importance of the amino group and supporting a role for pre-coordination as proposed in Figure 1.6. Further evidence for the significance of a coordinating group

comes from **L16**, which possesses a methoxy moiety instead of a dimethylamino group and provides **4** in 57% ee. Diphosphine BPPFA (**L17**), which could potentially coordinate through phosphorus in a bidentate fashion, also provides **4** in 65% ee. The similarity of the ee data obtained with **L13** and **L17** suggests that they both coordinate the metal in the same fashion, likely through a P-N mode. Consistent with this observation, changing the steric bulk on the amine of **L13** gives a range of ee values for **4** (see **L20**), while changing the steric environment of the phosphine does not significantly perturb the selectivity (see **L19**). Homologated ligand **L18** delivers **4** in poor ee.<sup>19</sup> Pd catalysts were also investigated and were shown to give comparable results to Ni (Figure 1.8).<sup>17c</sup>

**Figure 1.8.** The use of the P-N ligand PPFA provides similar results in both Ni- and Pd-catalyzed transformations.

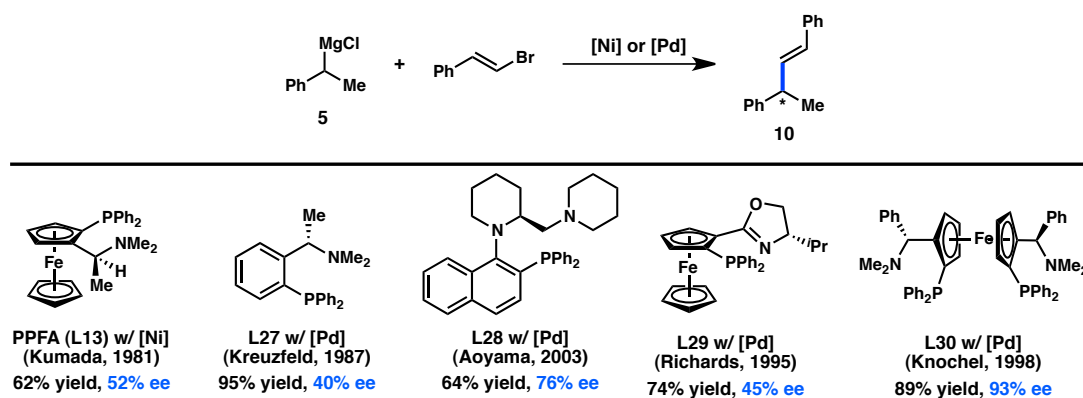


Several other ligand families have been developed for the enantioselective preparation of **4** (Figure 1.5). Catalysts generated from macrocyclic sulfides (**L21**) and nickel salts have been shown to impart moderate enantioselectivity, possibly through a simple kinetic resolution.<sup>20</sup> The use of pyrrole-containing P,N ligand **L22** or phosphine **L23** delivers **4** in 32% ee and 68% ee, respectively, under Ni catalysis.<sup>21,22</sup> Using Pd catalysis, the P,N ligand **L24**, which contains both planar and centrochirality, gives

improved results with respect to PPFA (**L13**).<sup>23</sup> High ee can also be achieved with phosphine-quincoridine **L25**.<sup>24</sup>

Despite the advances made through ligand tuning when vinyl bromide is used as an electrophile, the scope of the asymmetric alkyl cross-coupling is poor. Disubstituted alkenes were typically found to be less enantioselective; for example, the reaction of *E*-bromostyrene using PPFA (**L13**) as the ligand delivered **10** in only 52% ee and moderate yield (Figure 1.9).<sup>17c,25</sup> While the yield could be improved using the simpler aminophosphine **L27**, the ee of **10** decreased.<sup>26</sup> **L28**, designed to induce axial chirality upon coordination to a transition metal, was able to induce 76% ee for **10**.<sup>27</sup> Moderate ee could also be attained with phosphine-oxazoline ligand **L29**.<sup>28</sup> Knochel and coworkers reported *C*<sub>2</sub>-symmetric ferrocenyl phosphine **L30** as being capable of delivering excellent ee for the coupling of bromostyrene, although the reaction scope is still limited.<sup>29</sup>

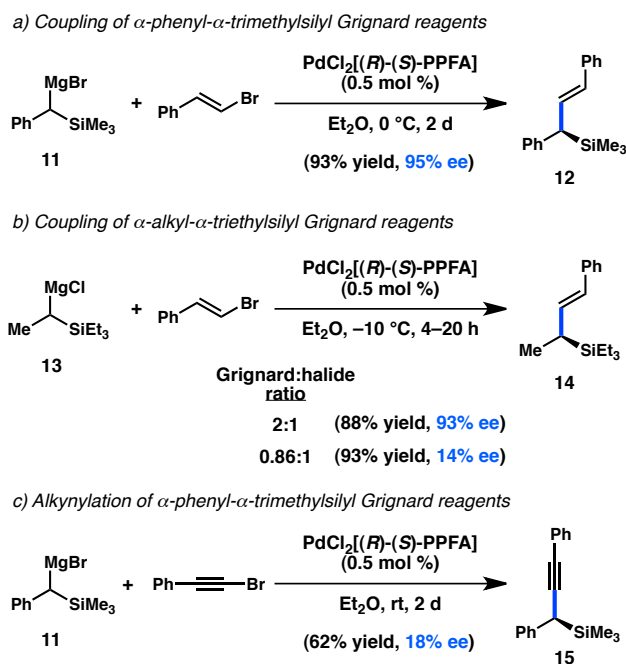
**Figure 1.9.** Asymmetric Kumada–Corriu cross-coupling of bromostyrene.

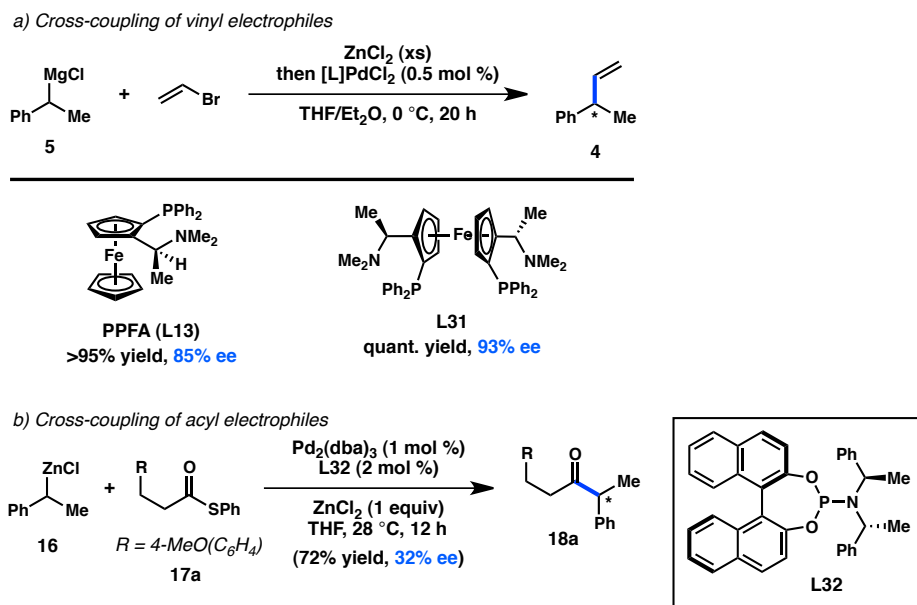


The asymmetric cross-coupling of organomagnesium reagents has been extended to  $\alpha$ -trialkylsilyl Grignard reagents (**11** and **13**). When vinyl halides are used as the coupling partners, the products are allylsilanes, which are versatile reagents for the construction of C–C bonds. In initial studies, Kumada, Hayashi, and coworkers reported

that Ni catalysts delivered poor yields of the desired allylsilane. However, the chiral  $\text{PdCl}_2[\text{PPFA}]$  complex furnished **12** in 93% yield and 95% ee (Scheme 1.2, a).<sup>30</sup> *E*-Vinyl bromides were found to provide higher selectivities than the corresponding *Z*-substrates, and the enantioselectivity was independent of the ratio of Grignard reagent to vinyl bromide. In contrast, the coupling of alkyl-substituted Grignard **13** proceeded in 93% ee when excess organomagnesium reagent was employed, but the ee fell precipitously when Grignard **13** was used as the limiting reagent (Scheme 1.2, b). These findings might suggest that for Grignard **13**, the rate of racemization is slow relative to the rate of C–C bond formation, resulting in a simple kinetic resolution instead of a DKR. A similar kinetic resolution had been observed previously in the diastereoselective coupling of non-benzylic Grignard reagents.<sup>31</sup> Lastly, an ee of 18% could be achieved in the alkylation of **11** in the presence of  $\text{PdCl}_2[\text{PPFA}]$  (Scheme 1.2, c).<sup>30,32</sup>

**Scheme 1.2.** Diphosphine ligands in the coupling of  $\alpha$ -silyl Grignard reagents.



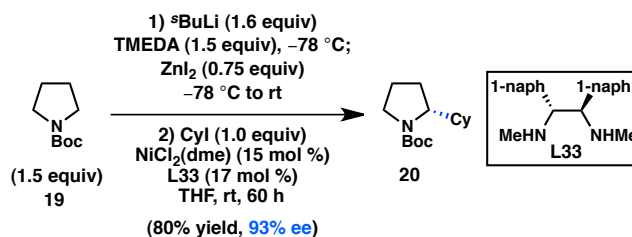
**Figure 1.10.** Enantioselective alkyl Negishi-type cross-couplings.

## 1.2.2 Organozinc Reagents

The pioneering studies of enantioselective transition metal-catalyzed alkyl cross-coupling reactions were initially performed using Ni catalysts and organomagnesium reagents—a species expected to exhibit configurational lability. Advances in the development of the Negishi cross-coupling subsequently enabled the use of organozinc reagents in asymmetric alkyl cross-coupling reactions, with Hayashi, Kumada, and coworkers reporting the first examples in 1983.<sup>33</sup> Preliminary studies investigated the coupling of the organozinc chloride prepared from transmetalation of **5** with  $\text{ZnCl}_2$ ; however, Ni catalysts were determined to be poorly reactive. On the other hand, the combination of Pd and PPFA (**L13**) delivered **4** in 85% ee (Figure 1.10, a). Significantly, when the organometallic was prepared by direct insertion of  $\text{Zn}^0$  into the organic chloride, the same enantioselectivity is achieved, albeit with a lower yield. Such an

outcome implicates  $\text{RZnCl}$  as the transmetalating agent, rather than  $\text{ZnCl}_2$  behaving as a Lewis acid to otherwise effect the transformation.<sup>16a</sup> Lower selectivities are obtained with the corresponding Grignard reagent under similar conditions. Additional improvements in ligand design revealed that **4** is formed in 93% ee when **L31** is used.<sup>34</sup> Despite a growing interest in the enantioselective cross-coupling reactions of organozinc reagents over the past three decades, successful efforts to further expand upon the enantioselective alkyl Negishi cross-coupling have been limited. Recently, Reisman and coworkers reported the Pd-catalyzed coupling between thioester **17a** and organozinc **16** to form ketone **18a** using chiral phosphoramidite **L32** (Figure 1.10, b).<sup>35</sup> While the enantioselectivity of the transformation is still low, the study represents a proof of concept for the possibility of employing organozinc reagents in enantioselective acyl cross-coupling reactions.

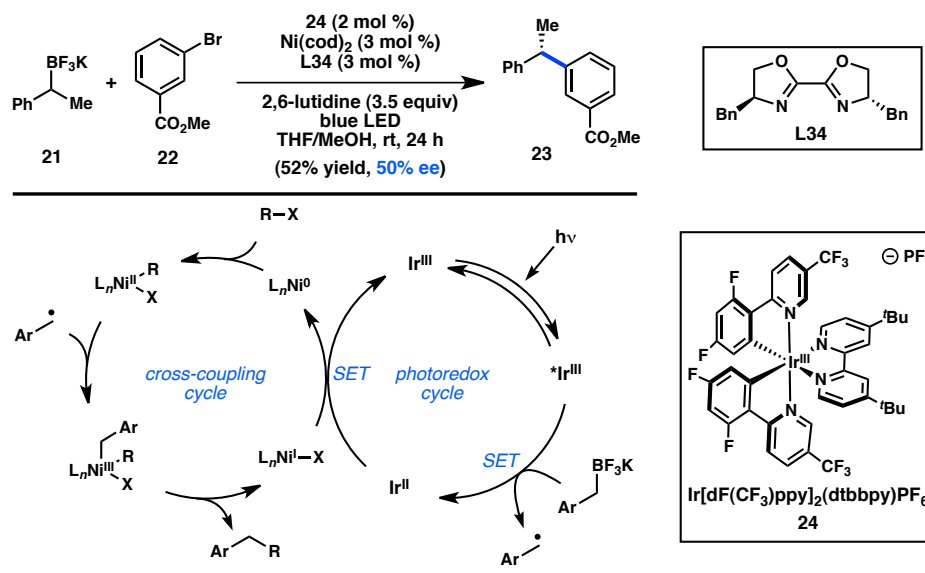
**Scheme 1.3.** Enantioselective functionalization of pyrrolidine.



In a seminal 2013 report, Fu reinvestigated the Negishi cross-coupling of  $\alpha$ -zincated *N*-Boc-pyrrolidine, which Campos and coworkers had previously shown can undergo stereospecific Pd-catalyzed cross-coupling to deliver enantioenriched  $\alpha$ -arylpiperidine products.<sup>36</sup> Under Ni catalysis, in the absence of a chiral ligand, coupling of the stereodefined organozinc reagent with cyclohexyl iodide produced the coupled product in almost racemic form. Alternatively, when the chiral Ni/**L33** complex was used as the catalyst, coupling of racemic **19** with cyclohexyl iodide furnished **20** with high ee

in a stereoconvergent fashion, representing the first enantioconvergent alkyl-alkyl coupling of a racemic organometallic reagent (Scheme 1.3).<sup>37</sup> Mechanistic studies have determined that this stereoconvergence does not arise from a series of  $\beta$ -hydride elimination/alkene insertion processes of the organometallic reagent.

**Figure 1.11.** Dual catalysis approach to asymmetric cross-coupling.

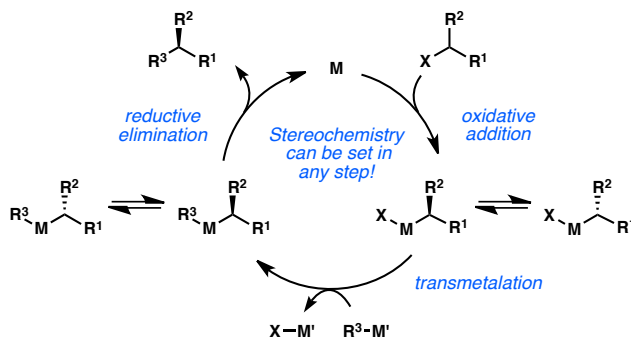


### 1.2.3 Organoboron Reagents

Trifluoroborate salts are often used in the Suzuki–Miyaura cross-coupling due to their improved stability with respect to boronic acids and esters. The two-electron mechanism of transmetalation typically believed to be operative in Suzuki–Miyaura reactions innately favors transmetalation in a stereospecific manner. However, Molander and coworkers hypothesized that transmetalation through a single electron pathway could favor transfer of a C(sp<sup>3</sup>)-hybridized alkyl fragment via a stereoconvergent, radical process. In order to generate a radical from an organoboron reagent, the authors

envisaged a dual catalysis mechanism in which Ni-catalyzed cross-coupling and Ir-catalyzed photoredox events occur synergistically (Figure 1.11).<sup>38</sup> In an important proof of concept, chiral bioxazoline (BiOX) **L34** was used to furnish **23** in 50% ee. Electron transfer to an excited state  $^*Ir^{III}$  complex from an organoboron species would generate an alkyl radical. The alkyl radical can then combine with a chiral  $Ni^{II}$  complex to form a  $Ni^{III}$  species that can reductively eliminate the desired product. The resulting  $Ni^I$  can be reduced by  $Ir^{II}$  to complete both catalytic cycles. Additional investigations toward asymmetric catalysis would be valuable.

**Figure 1.12.** Stereochemical outcome of cross-coupling with secondary electrophiles.

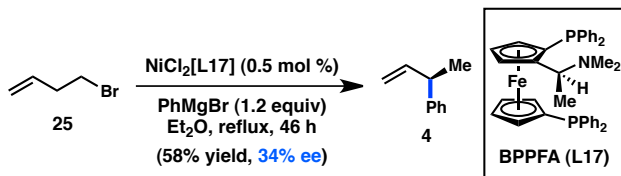


### 1.3 REACTIONS OF SECONDARY ALKYL ELECTROPHILES

The challenges associated with oxidative addition of *sec*-alkyl electrophiles, as well as the propensity for alkyl transition metal complexes to undergo rapid  $\beta$ -hydride elimination, conspired to make the cross-coupling of these electrophiles difficult to realize using Pd, which had emerged as the metal of choice for cross-coupling in the 1980s. In the early 2000's, researchers began re-investigating first-row transition metals

for the cross-coupling of *sec*-alkyl halides and organometallic reagents.<sup>2</sup> Following the first reports of alkyl cross-coupling to form stereogenic C(sp<sup>3</sup>) centers, the systematic examination of asymmetric induction in these processes became a chief objective. In these systems, catalysts that favor a single-electron oxidative addition mechanism may undergo a stereoconvergent oxidative addition to set the ultimate stereochemistry of the product. Alternatively, rapidly equilibrating mixtures of diastereomeric transition metal complexes can result in preferential transmetalation or reductive elimination of one diastereomer over the other (Figure 1.12).

**Scheme 1.4.** Primary-to-secondary isomerization in asymmetric cross-coupling.

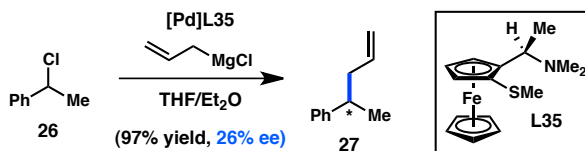


### 1.3.1 With Organomagnesium Reagents

The earliest example of an enantioselective transition metal-catalyzed cross-coupling reaction between an alkyl electrophile and an organomagnesium reagent was disclosed by Kumada and coworkers in 1977, the result of a surprising alkyl group isomerization observed during the coupling between homoallylic halide **25** and  $\text{PhMgBr}$  (Scheme 1.4).<sup>39</sup> In the presence of the chiral catalyst  $\text{NiCl}_2[\text{BPPFA}]$ , **4** was formed in 34% ee. While the isomerization of secondary organometallic reagents to primary species is a well-known side reaction in cross-coupling chemistry, the inverse isomerization is much more rarely observed.<sup>40</sup> Although this preliminary result was not further developed

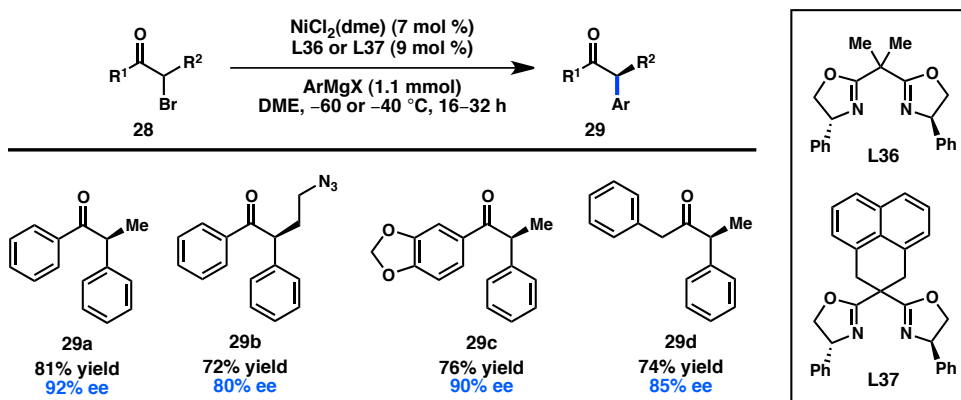
by Kumada and coworkers, it presaged the explosion of asymmetric cross-couplings of *sec*-alkyl electrophiles that would emerge in the literature nearly two decades later.

**Scheme 1.5.** Asymmetric  $C(sp^3)$ – $C(sp^3)$  Kumada–Corriu cross-coupling.



In 1988, the Pd-catalyzed enantioselective cross-coupling between allylmagnesium chloride and racemic (1-chloroethyl)benzene (**26**) was reported by Brubaker and coworkers. A variety of bidentate S,N and Se,N ligands bearing planar and centrochirality were prepared and used to generate chiral Pd complexes.<sup>41</sup> The complex derived from **L35** catalyzed the formation of **27** in a high yield and modest, yet promising, ee (Scheme 1.5). Mechanistic studies to elucidate whether the enantioenriched product arises from a stereoconvergent process were not disclosed. The same group later studied Ni complexes of these ligands in the same transformation, obtaining similar levels of enantioinduction.

**Figure 1.13.** Stereoconvergent Kumada–Corriu coupling of  $\alpha$ -haloketones.



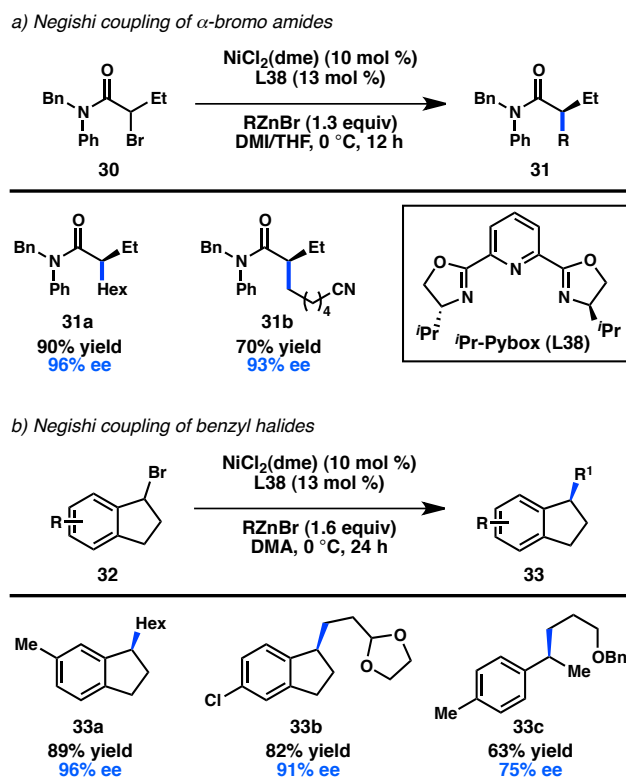
The first synthetically useful enantioselective, stereoconvergent cross-coupling between a *sec*-alkyl electrophile and a Grignard reagent was reported two decades later by Fu and coworkers. In this seminal report, the combination of NiCl<sub>2</sub>(dme) and bidentate bis(oxazoline) ligand **L36** or **L37** was found to promote the coupling of  $\alpha$ -haloketones **28** and arylmagnesium halides to give  $\alpha$ -aryl ketones (Figure 1.13).<sup>42</sup> Notably, the reaction can be run at some of the lowest temperatures reported for the cross-coupling of alkyl electrophiles (–60 °C); the low temperature prevents the racemization of ketone product **29** through enolization by the Brønsted basic Grignard reagent. Both alkyl and aryl ketones can be prepared by this method, and these products can be diastereoselectively derivatized to access chiral alcohols and amines.<sup>43</sup>

### 1.3.2 With Organozinc Reagents

In 2005, two reports from the Fu laboratory demonstrated the first utilization of secondary alkyl electrophiles in highly enantioselective cross-coupling reactions. In one example, treatment of  $\alpha$ -bromo amide **30** with an alkylzinc reagent and a Ni/**L38** catalyst delivered **31** in good yield and high ee (Figure 1.14, a).<sup>44</sup> The identity of the amide substituents played a key role in achieving high enantioselectivity. When the organozinc reagent is used as a limiting reagent, the  $\alpha$ -bromo amide is recovered as a racemate, suggesting that the reaction does not proceed by a kinetic resolution. In a second example by Fu and coworkers, the Ni/**L38**-catalyzed coupling of 1-bromoindanes and alkyl halides produced chiral indane **33** in good yield and high ee (Figure 1.14, b).<sup>45</sup> The use of acyclic 1-(1-bromoethyl)-4-methylbenzene furnished **33c** with more modest

enantioselectivity. In both cases, only primary organozinc reagents were compatible with the reaction conditions. A computational investigation by Lin and coworkers proposed that a  $\text{Ni}^{\text{I}}/\text{Ni}^{\text{III}}$  mechanism consisting of transmetalation/oxidative addition/reductive elimination is more energetically favorable than a  $\text{Ni}^0/\text{Ni}^{\text{II}}$  mechanism.<sup>46</sup> The enantioselectivity of the reaction was also correlated to the difference in free energy between the two transition states for reductive elimination.

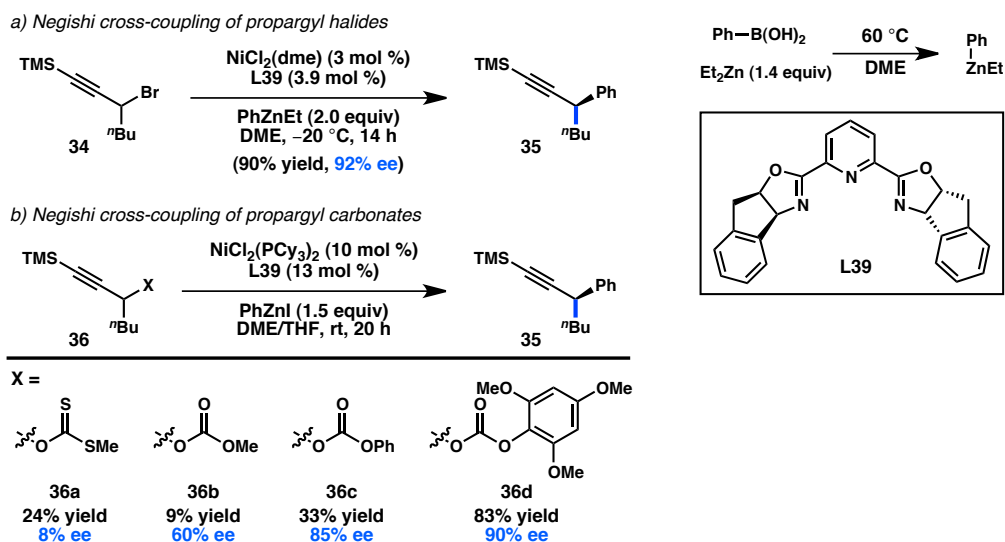
**Figure 1.14.** Seminal stereoconvergent cross-couplings of secondary alkyl halides.



In spite of Fu's promising results for the asymmetric, stereoconvergent Negishi cross-coupling of *alkylzinc* reagents, the extension to *arylzinc* species proved challenging. After a lengthy investigation, it was discovered that  $\text{Ni}/\text{L39}$  complexes catalyze the cross-coupling between propargyl halide **34** and  $\text{Ph}_2\text{Zn}$  to furnish **35** in a high yield and ee (Figure 1.15, a).<sup>47</sup> Since relatively few diarylzinc reagents are

commercially available, the group sought to identify other arylzinc reagents that were effective for this transformation. Unfortunately, the use of arylzinc halides or in situ-prepared diarylzincs, generated from transmetalation of the corresponding organolithium or –magnesium reagent, was unsuccessful. However, the group determined that  $\text{ArZnEt}$ , prepared from  $\text{ArB(OH)}_2$  and  $\text{Et}_2\text{Zn}$ , could react to provide comparable results. In contrast to the stereospecific Pd-catalyzed coupling of propargyl halides, no allene formation arising from  $\text{S}_{\text{N}}2'$  oxidative addition was observed.<sup>48</sup>

**Figure 1.15.** Stereoconvergent Negishi cross-coupling of propargylic electrophiles.

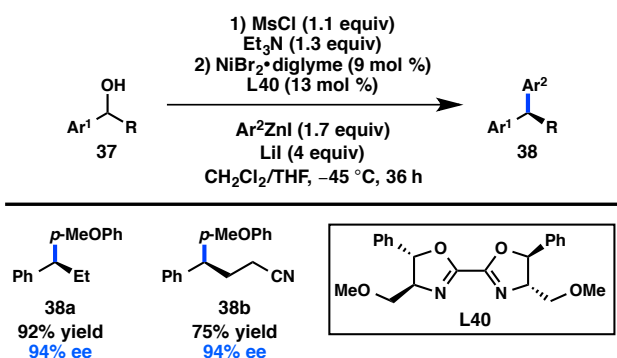


Organic halides are frequently prepared from the corresponding alcohols, and for certain substrates this functional group interconversion can be low yielding. Recognizing the synthetic advantage of using oxygen-based electrophiles directly in cross-coupling reactions, Fu and colleagues turned their attention to the asymmetric cross-coupling of propargylic alcohol derivatives. Hypothesizing that the reaction would proceed through a radical-based oxidative addition to Ni, a xanthate was chosen as a potential leaving group, due to its propensity toward radical cleavage in Barton-McCombie-type

transformations. However, these substrates performed poorly, producing **35** in low yield and ee. (Figure 1.15, b).<sup>49</sup> On the other hand, simple carbonate **36b** underwent cross-coupling with improved enantioselectivity. Further investigation revealed that both the yield and ee could be improved by use of aryl-substituted carbonates, with **36d** delivering **35** in 83% yield and 90% ee. The optimized reaction conditions proved to be general not just for propargyl carbonates, but also for the coupling of propargyl chlorides and bromides.

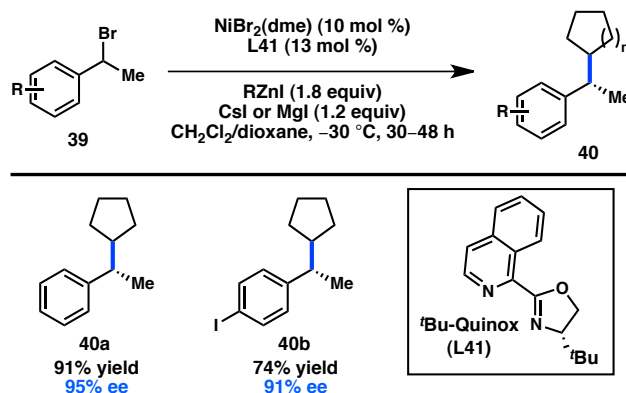
In 2013, Fu and coworkers published a stereoconvergent Negishi coupling of benzylic mesylates that could be prepared from the corresponding alcohols immediately prior to the coupling and used without purification (Figure 1.16).<sup>50</sup> Bi-oxazoline **L40** was identified as the optimal ligand, with more traditional Pybox and Box ligands delivering poor enantioselectivity. LiI was employed to allow in situ displacement of the mesylate to form a reactive benzylic iodide. A wide substrate scope was demonstrated for the cross-coupling; a slight erosion of ee is observed when R = Me. Although several stereospecific routes to diarylalkanes have been developed to date,<sup>51</sup> this reaction provides a complementary approach.

**Figure 1.16.** Stereoconvergent Negishi cross-coupling of benzylic alcohol derivatives.



A long-term objective in the area of enantioselective alkyl cross-coupling is to couple *sec*-alkyl electrophiles with *sec*-alkyl organometallic reagents. The Fu laboratory made a significant advance toward this objective in 2012 when they reported the asymmetric Negishi cross-coupling between benzylic bromide **39** and cyclic organozinc halides (Figure 1.17).<sup>40</sup> Isoquinoline-oxazoline ligand **L41** delivered the products in high yields and ee's, in contrast to the more commonly employed PyBox and Box ligands. Acyclic secondary organozinc halides resulted in a mixture of branched and linear products; surprisingly, primary organozinc halides also resulted in a mixture of branched and linear products.

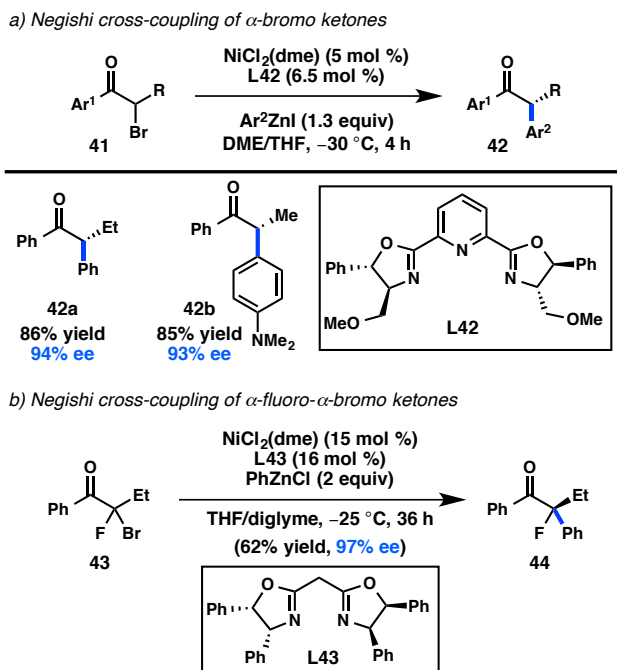
**Figure 1.17.** Enantioconvergent Negishi cross-coupling of secondary organozinc reagents.



Prior to their disclosure of the enantioselective cross-coupling between  $\alpha$ -bromoketones and aryl Grignard reagents (see Figure 1.13), the Fu laboratory developed a Ni/**L42**-catalyzed asymmetric cross-coupling of  $\alpha$ -bromoketones and arylzinc reagents (Figure 1.18, a).<sup>43</sup> The low basicity of the organozinc reagent, as well as a reduced reaction temperature, accounts for the configurational stability of the potentially sensitive tertiary stereocenter in **42**. The synthesis of dialkyl ketones proceeded with lower

enantioinduction; however, this substrate limitation is addressed by their subsequently developed Kumada–Corriu conditions.<sup>42</sup> A recent modification of the reaction conditions has permitted the use of  $\alpha$ -halo- $\alpha$ -fluoroketones, enabling the asymmetric formation of tertiary fluorides (Figure 1.18, b).<sup>52</sup>

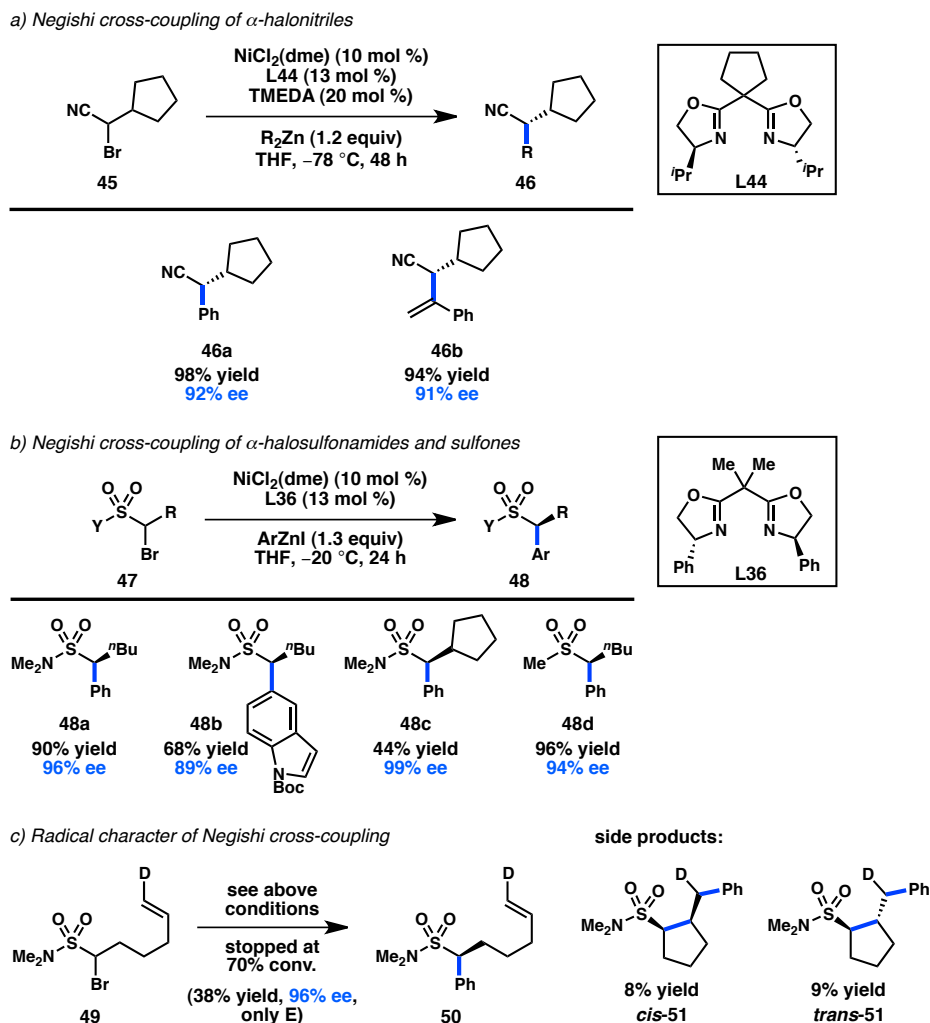
**Figure 1.18.** Asymmetric Negishi cross-coupling of  $\alpha$ -halo ketones.



The Fu group has further expanded the scope of alkyl electrophiles amenable to Ni-catalyzed stereoconvergent Negishi cross-coupling to include  $\alpha$ -bromonitriles.<sup>53</sup> Coupling of  $\alpha$ -bromonitrile **45** and  $\text{R}_2\text{Zn}$  in the presence of  $\text{NiCl}_2(\text{dme})$  and **L44** at  $-78\text{ }^\circ\text{C}$  furnishes **46** in high yield and ee (Figure 1.19, a).<sup>54</sup> For the first time, alkenylzinc reagents were suitable coupling partners, delivering **46b** in 94% yield and 91% ee. Somewhat unexpectedly, a variant of **46** containing a pendant alkene failed to cyclize under the reaction conditions, in contrast to what was observed in the related coupling of simple unactivated halide electrophiles.<sup>55</sup> A more comprehensive mechanistic analysis is

thus required to elucidate the mechanism of oxidative addition for the given transformation.

**Figure 1.19.** Other directing groups in asymmetric Ni-catalyzed Negishi cross-coupling.



The previous examples of Ni-catalyzed stereoconvergent Negishi cross-coupling reactions from the Fu laboratory have focused on the use of activated secondary electrophiles; in 2014, they reported the coupling between  $\alpha$ -halosulfonamides (**47**) and arylzinc reagents (Figures 1.19, b).<sup>56</sup> Since sulfonyl groups do not significantly stabilize

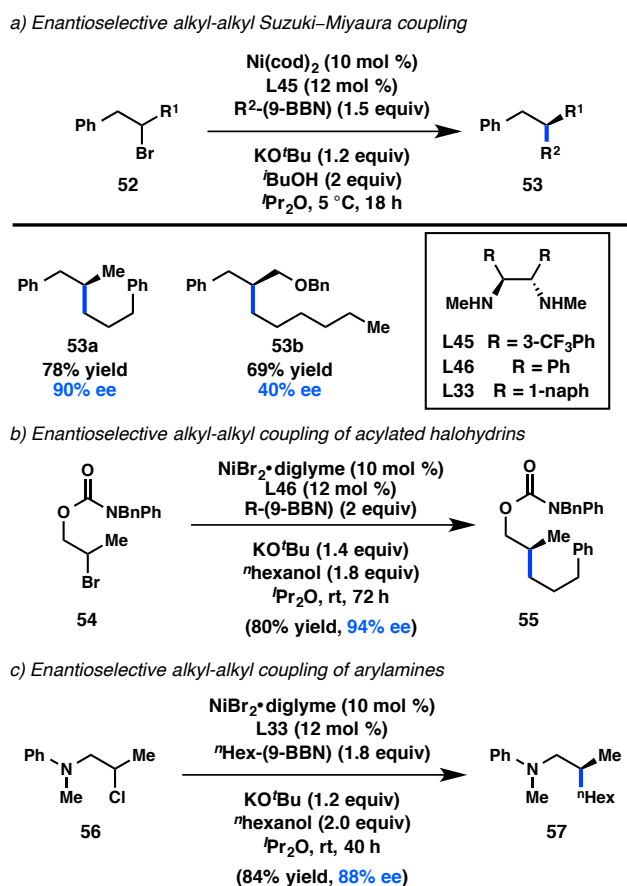
$\alpha$ -radicals, **47** can be considered as an unactivated electrophile. Investigations of the substrate scope revealed that sulfones are also suitable substrates without any change in the reaction conditions, furnishing **48d** in high yield and ee. Subjection of radical clock substrate **49** to the reaction conditions provided a mixture of **50**, *cis*-**51** and *trans*-**51**; the ratio of uncyclized product to cyclized product was found to increase linearly with increased Ni loading. These data could suggest that the reaction proceeds through a noncaged radical species, and also illustrates the dichotomy between the coupling of electrophiles **45** and **47**.

### 1.3.3 With Organoboron Reagents

Seminal contributions to the transition metal-catalyzed enantioselective cross-coupling of *sec*-alkyl electrophiles with organoboron reagents have been made by the Fu laboratory. Shortly after disclosing the Ni-catalyzed cross-coupling of *sec*-alkyl electrophiles with alkylboranes to prepare racemic products,<sup>57</sup> Fu and coworkers reported that use of catalytic Ni(cod)<sub>2</sub> in conjunction with chiral 1,2-diamine ligand **L45** enabled the enantioselective coupling of homobenzylic bromides (**52**) with organoboranes (Figure 1.20, a).<sup>58</sup> The Ni catalyst was proposed to engage in a secondary interaction with the benzylic substituent on **52**, allowing for differentiation between the two alkyl groups of the starting material. While a variety of homobenzylic bromides were tolerated, poor enantioselectivity was attained in the formation of **53b**. Fu hypothesized that the ether might also interact with the Ni catalyst, leading to poor asymmetric induction. Based on this hypothesis, the group subsequently reported that carbamate-protected halohydrins

(**54**) can also be coupled with alkylboranes in high enantioselectivity using a chiral 1,2-diamine **L46** (Figure 1.20, b).<sup>59</sup> Modified conditions permitted the enantioselective coupling of a homologated halohydrin. Further expansion of the substrate scope determined that halides (**56**) bearing proximal arylamines as directing groups can be coupled with alkylboranes in high enantioselectivity as well (Figure 1.20, c).<sup>60</sup> The reaction was found to be directed by the nitrogen atom of the arylamine group.

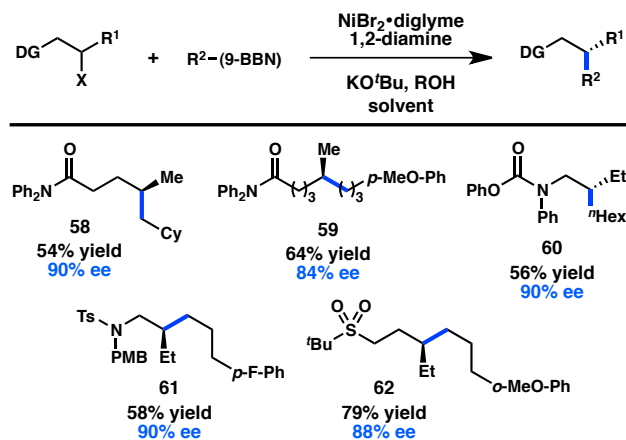
**Figure 1.20.** Enantioconvergent Ni-catalyzed alkyl-alkyl Suzuki–Miyaura coupling.



The early examples of enantioconvergent alkyl-alkyl Suzuki–Miyaura couplings all involved alkyl halide substrates with a directing group capable of coordinating the Ni center. Subsequent efforts turned to identifying new directing groups and to exploring

how far removed the directing group could be from the reacting C–halide bond. Illustrating that distal functional groups are still capable of directing highly enantioselective reactions, both  $\gamma$ - and  $\delta$ -chloroamides were shown to undergo Suzuki–Miyaura cross-coupling with good asymmetric induction to form **58** and **59**, respectively (Figure 1.21).<sup>61</sup> Various halides proximal to protected amines, such as carbamates or sulfonamides, were also optimized toward enantioconvergent cross-coupling.<sup>62</sup> After confirming that the oxygen of the sulfonamide was the key directing atom, Fu and coworkers examined sulfone-containing electrophiles and reported that good enantioselectivity can still be maintained for these substrates.<sup>62a</sup>

**Figure 1.21.** Examples of directing groups for the enantioconvergent Suzuki–Miyaura coupling.

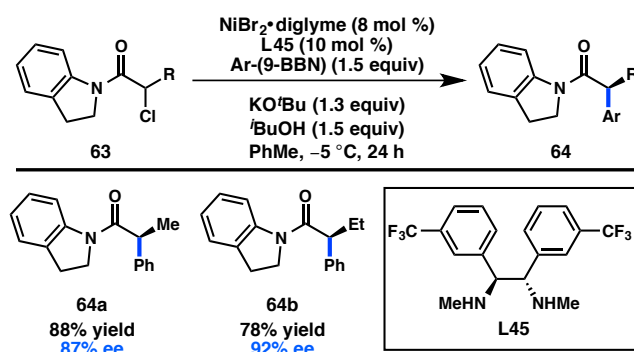


In addition to the Ni-catalyzed cross-coupling of organomagnesium and organozinc reagents to  $\alpha$ -halocarbonyl compounds, the Fu laboratory has identified conditions for the enantioselective coupling between  $\alpha$ -haloamides and arylboron reagents. After first investigating several different amides, it was found that the combination of  $\text{NiBr}_2 \cdot \text{diglyme}$  and **L45** catalyzed the coupling between  $\alpha$ -chloroamides

(**63**) and Ar-(9-BBN) reagents to furnish **64** in good yields and high ee's (Figure 1.22).<sup>63</sup>

The identity of the amide substituents was important for good enantioinduction: diphenyl amides and Weinreb amides delivered nearly racemic products. In contrast to previous stereoconvergent couplings of secondary electrophiles, a modest kinetic resolution of **63** was observed. Further studies confirmed an irreversible oxidative addition step.  $\gamma$ -Haloamides can also be arylated with Ph-(9-BBN) in good ee but only moderate yield.<sup>61</sup>

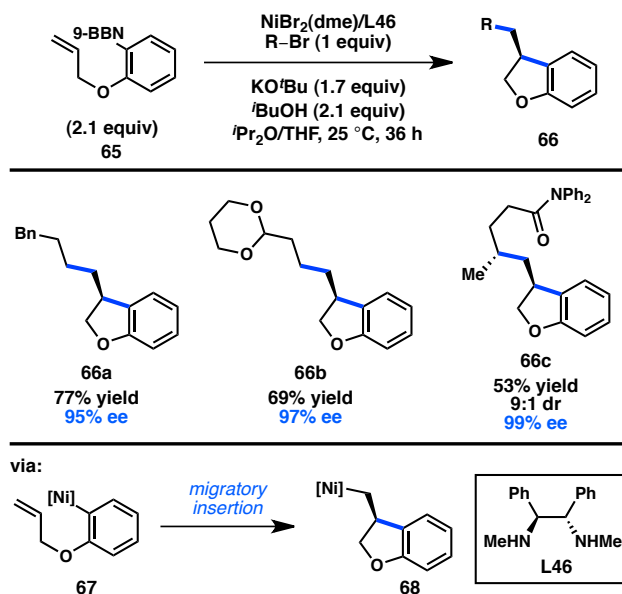
**Figure 1.22.** Asymmetric Suzuki–Miyaura coupling of  $\alpha$ -haloamides.



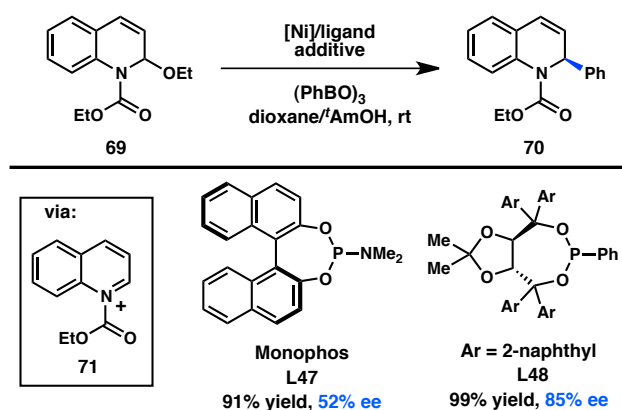
Building off their growing mechanistic understanding of Ni-catalyzed stereoconvergent alkyl cross-coupling reactions, Fu and coworkers have developed a cascade cyclization/cross-coupling to forge two C–C bonds in one step with both excellent ee and high dr (Figure 1.23).<sup>64</sup> Key to this transformation was the insight that a “transmetalation first” mechanism could be operative, and that organonickel complex **67** might undergo migratory insertion faster than oxidative addition of the alkyl halide. This theory was validated in the Ni-catalyzed asymmetric cascade cyclization/cross-coupling reaction between arylborane **65** and several simple alkyl bromides, in which heterocyclic products **66** were obtained in excellent ee. Realizing the compatibility of their reaction conditions with those previously optimized for coupling of

$\gamma$ -haloamides (see Figure 1.21), a  $\gamma$ -haloamide was also used as an electrophile.<sup>61</sup> Remarkably, a single Ni complex controls the stereochemical outcome of two distinct C–C bond forming processes, giving product **66c** in good yield, good dr, and excellent ee.

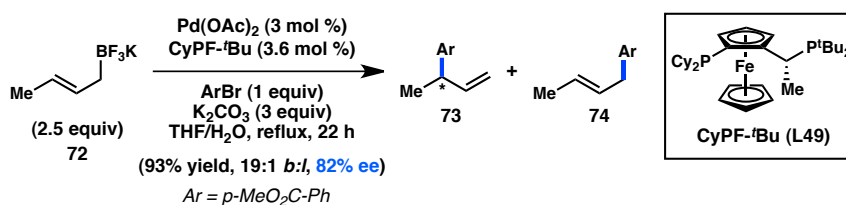
**Figure 1.23.** Asymmetric cascade cyclization/cross-coupling.



The Doyle laboratory has focused on expanding the scope of electrophiles suitable for transition metal catalysis, investigating the cross-coupling reactions of acetals and *N,O*-acetals. These efforts led to the discovery that Ni(cod)<sub>2</sub> catalyzes the addition of various aryl boroxines to *N,O*-acetal **69**, presumably via the intermediacy of quinolinium ion **71**.<sup>65</sup> When chiral phosphoramidite **L47** is used as a supporting ligand, **70** is formed in 52% ee (Figure 1.24). A unique oxidative addition mechanism, in which the Lewis acidic boroxine promotes ionization of the leaving group and results in an S<sub>N</sub>1-type addition of Ni<sup>0</sup>, was discovered for this coupling.<sup>66</sup> A wider survey of ligands showed that improved ee could be realized with TADDOL-based phosphonite **L48**.<sup>67</sup> In an extension, the addition of arylzinc reagents into pyridinium ions was subsequently reported.<sup>68</sup>

**Figure 1.24.** Asymmetric addition into quinolinium ions.

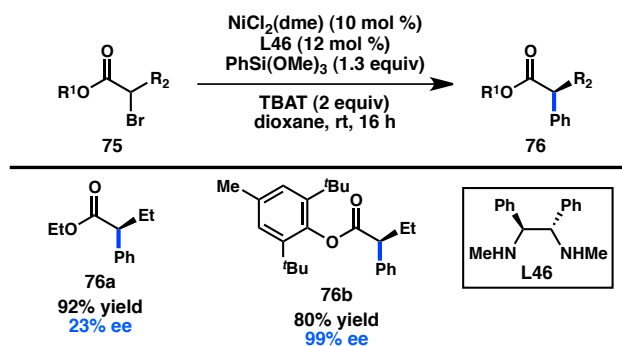
In 2006, Yamamoto, Miyaura, and coworkers reported a novel strategy for the preparation of enantioenriched products from achiral starting material. Bidentate phosphine ligands allowed for high  $\gamma$ -selectivity in the Pd-catalyzed coupling between allylic trifluoroborate salts and aryl bromides.<sup>69</sup> Bulky, Josiphos-type ligand **L49** promoted formation of **73** in 82% ee while still maintaining high selectivity for  $\gamma$ -addition (Scheme 1.6).<sup>70</sup> DFT studies support a  $S_E2'$  (open) transition state for transmetalation, whereas the corresponding closed transition state was of slightly higher energy;<sup>71</sup> transmetalation was also proposed to be the stereochemistry-determining step, followed by a fast reductive elimination to forge the desired product. Similar  $\gamma$ -selectivity was observed in the stereospecific couplings of allylic boronates<sup>72</sup> and silanes.<sup>73</sup>

**Scheme 1.6.** Enantioselective cross-coupling of allylic trifluoroborate salts.

### 1.3.4 With Organosilicon Reagents

Only a single example of an asymmetric cross-coupling between *sec*-alkyl organic halides and organosilicon reagents has been reported to date. Fu and colleagues developed a Ni/L46-catalyzed stereoconvergent coupling of  $\alpha$ -bromoesters (**75**) and aryl siloxanes to furnish  $\alpha$ -aryl esters in good yields and with high enantioinduction (Figure 1.25).<sup>74</sup> While simple ethyl esters gave good yield but poor ee, the use of the BHT ester resulted in formation of **76b** in a remarkable 99% ee. The nature of the fluoride source and the steric profile of R<sup>2</sup> also affected the level of enantioinduction. In the same report, the optimized reaction conditions were extended to the coupling of alkenyl silanes as well.

**Figure 1.25.** Stereoconvergent coupling of aryl silanes.

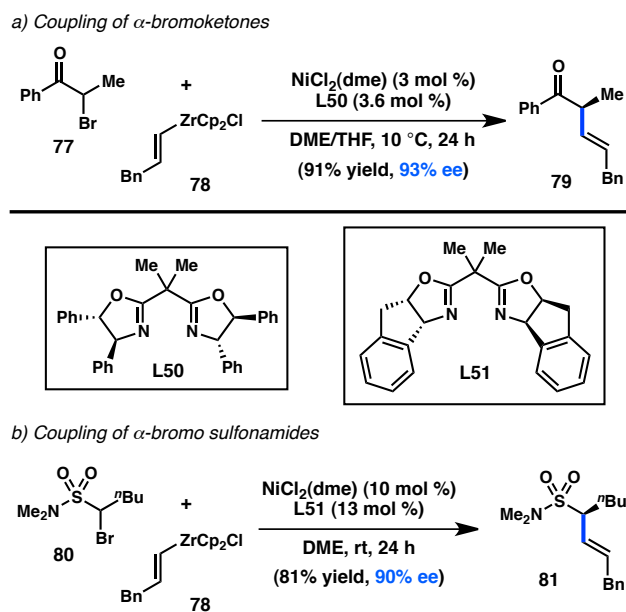


### 1.3.5 With Organozirconium Reagents

Alkenylzirconium complexes are attractive vinyl organometallic species for use in organic synthesis because they can be easily prepared from Schwartz's reagent and an alkyne. While Fu has disclosed a remarkable variety of stereoconvergent arylation reactions, most of the reaction conditions could not easily be extended to the cross-

coupling of alkenyl metal species, with alkenyl silicon<sup>74</sup> and zinc<sup>54</sup> reagents being the most promising. In 2010, Fu and coworkers published the Ni/**L50**-catalyzed asymmetric cross-coupling of alkenylzirconium reagents and  $\alpha$ -bromoketones, allowing access to **79** in 93% ee (Figure 1.26, a).<sup>75</sup> The versatility of this approach has been exemplified by the efficient coupling of both aryl-alkyl ketones and dialkyl ketones under the same conditions. Alkenylzirconium complexes have also been shown to react with  $\alpha$ -bromosulfonamides in high yield and ee (Figure 1.26, b).<sup>56</sup>

**Figure 1.26.** Stereoconvergent coupling of alkenylzirconium reagents.

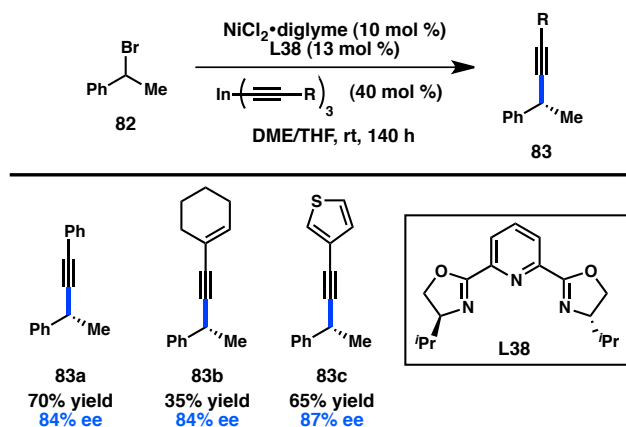


### 1.3.6 With Organoindium Reagents

Shortly after the publication of Fu's seminal examples of Ni-catalyzed stereoconvergent cross-coupling reactions between *sec*-alkyl electrophiles and either C(sp<sup>3</sup>)- or C(sp<sup>2</sup>)-hybridized organometallic reagents,<sup>44-45</sup> Sestelo, Sarandeses, and

coworkers investigated the asymmetric coupling between C(sp)-hybridized organometallic reagents and benzylic bromides. Alkynylindium reagents exhibited clean cross-coupling under Ni-catalysis, and were selected for further study. Pybox ligand **L38** was optimal, delivering cross-coupled product **83** in up to 87% ee for several different alkynes (Figure 1.27).<sup>76</sup> Further work on the asymmetric coupling of C(sp) organometallic reagents has not been disclosed.

**Figure 1.27.** Alkynyl organometallic reagents in stereoconvergent cross-coupling.

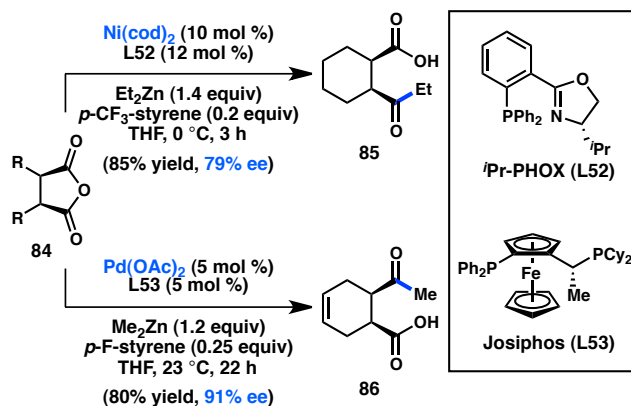


## 1.4 TRANSITION METAL-CATALYZED DESYMMETRIZATION REACTIONS

One approach to generating enantioenriched products through transition metal-catalyzed alkyl cross-coupling reactions is to perform desymmetrization reactions of *meso* compounds. In this case, the C(sp<sup>3</sup>)-hybridized carbon at the site of C–C bond formation is not necessarily stereogenic; instead, the C–C bond formation is used to break symmetry through a catalyst-controlled process, giving rise to a molecule with centrochirality. Most of the work in this area has focused on the desymmetrization of

*meso* electrophiles; however, some researchers have investigated the desymmetrization of *meso* bis-organometallic reagents or processes that involve desymmetrization by C-H functionalization.

**Scheme 1.7.** Alkylative desymmetrization of *meso*-anhydrides.

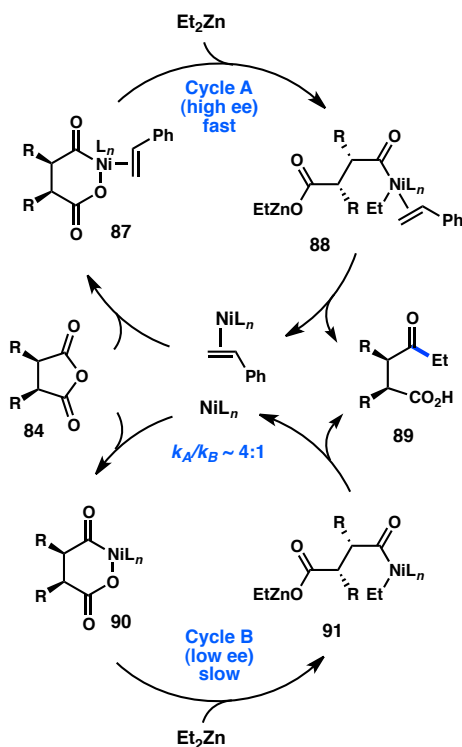


### 1.4.1 Organozinc Reagents

The desymmetrization of *meso*-anhydrides has emerged as a robust method for the synthesis of enantiopure products.<sup>77</sup> Rovis and coworkers<sup>78</sup> have developed a monofunctionalization of cyclic anhydrides through a Ni-catalyzed Negishi coupling with  $\text{Et}_2\text{Zn}$ .<sup>79</sup> The transformation was sensitive to the bite angle of the ligand and required an electron-deficient styrene additive, which has been demonstrated by Knochel to accelerate reductive elimination over  $\beta$ -hydride elimination.<sup>80</sup> Based on these initial findings, the authors sought to develop a desymmetrizing Negishi reaction of *meso*-cyclic anhydride **84**, and determined that the catalyst prepared from  $\text{Ni}(\text{cod})_2$  and <sup>t</sup>Pr-PHOX (**L52**) furnished **85** in 79% ee (Scheme 1.7).<sup>81</sup> Surprisingly, omission of the *p*-CF<sub>3</sub>-styrene

additive reduced the ee to 4%, prompting Rovis and coworkers to more closely examine the mechanism of the reaction.

**Figure 1.28.** Competing mechanisms in the Ni-catalyzed desymmetrization of meso-anhydrides.

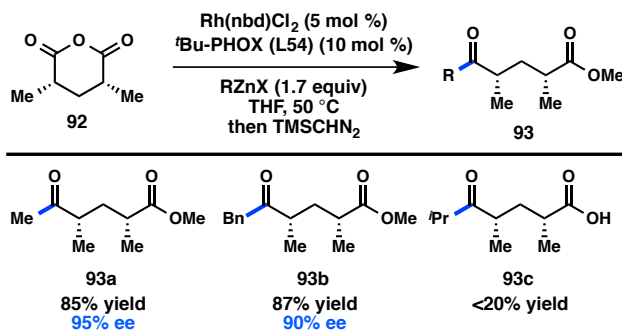


Kinetic analysis of the reaction revealed two competing mechanisms for the formation of **85** (Figure 1.28).<sup>82</sup> One occurred in the absence of styrene and proceeded with low enantioselectivity (cycle B). The other involved coordination of styrene and provided **89** in high ee (cycle A). For both reactions, the rate-determining step was realized to be oxidative addition. However, in contrast to the initial proposal that *p*-CF<sub>3</sub>-styrene would accelerate reductive elimination, it was instead shown to increase the rate of oxidative addition. While the origin of this rate enhancement is unclear, it was hypothesized that *p*-CF<sub>3</sub>-styrene might coordinate to Ni and facilitate deligation of cod,

providing a three-coordinate Ni complex capable of undergoing oxidative addition. The kinetic analysis determined that cycle A proceeds approximately four times faster than cycle B and is roughly consistent with the somewhat modest enantioselectivities obtained under these conditions.

The Pd-catalyzed desymmetrization of succinic anhydrides was also developed by Rovis and coworkers (Scheme 1.7). Treatment of **84** with  $\text{Me}_2\text{Zn}$  in the presence of  $\text{Pd}(\text{OAc})_2$  and the bidentate phosphine Josiphos (**L53**) furnished **86** in 91% ee; the use of *p*-F-styrene as an additive was crucial to achieving the high level of enantioselectivity.<sup>83</sup>

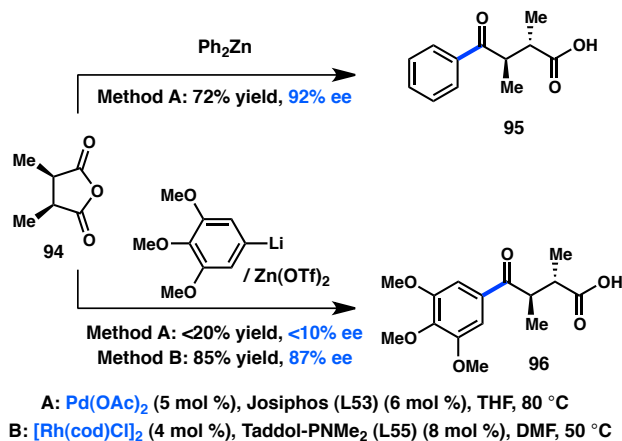
**Figure 1.29.** Rh-catalyzed desymmetrization of glutaric anhydrides.



One hurdle in the Pd-catalyzed desymmetrization was the catalyst's sensitivity to halide salts, meaning that the organozinc reagent could not be prepared in situ from the more readily available organomagnesium or -lithium reagents. Investigation of Rh catalysts in the desymmetrization of glutaric anhydride, a substrate that reacts poorly in the presence of Pd, revealed that high yields and good ee's could be attained, allowing access to *syn*-deoxypolypropionate synthons (Figure 1.29).<sup>84</sup> This reaction is proposed to proceed through a  $\text{Rh}^{\text{I}}/\text{Rh}^{\text{III}}$  catalytic cycle, with transmetalation occurring prior to oxidative addition of the anhydride. Furthermore, the organozinc reagent could now be prepared in situ. The desymmetrization of glutaric anhydrides is an enantioselective

alternative to Breit's enantiospecific Kumada–Corriu coupling for the synthesis of deoxypolypropionates.<sup>85</sup>

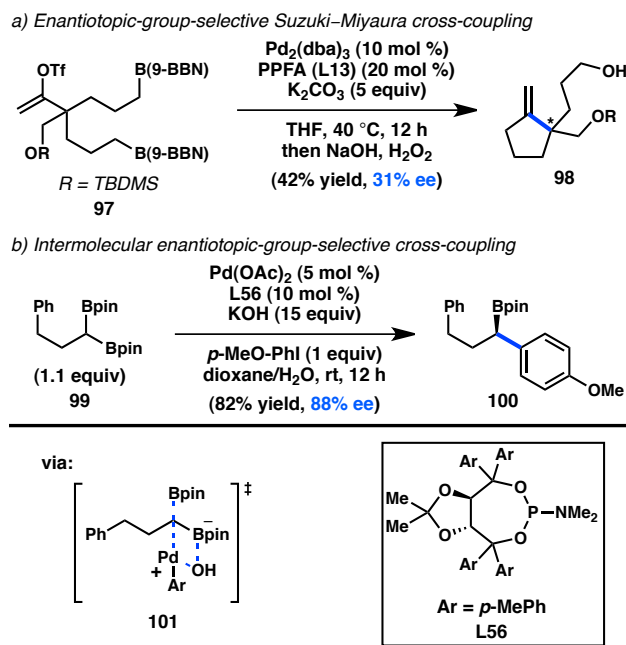
**Figure 1.30.** Pd- and Rh-catalyzed desymmetrization with arylzinc reagents.



Efforts by Rovis and coworkers to affect an alkylative desymmetrization of *meso*-anhydrides have been complemented by attempts to use arylzinc reagents in similar transformations. In the presence of a Pd/Josiphos catalyst system, 1,4-ketoacid **95** could be prepared from commercially available Ph<sub>2</sub>Zn in good yield and high ee (Figure 1.30).<sup>83</sup> In contrast to Rovis' alkylation methodology, excess fluorostyrene is not necessary to achieve a high enantioinduction. While Ph<sub>2</sub>Zn was reactive in the Pd-catalyzed transformation, lower yields and ee's were observed when the organozinc reagent was prepared in situ from the corresponding organolithium. In fact, simple exposure of **94** and Ph<sub>2</sub>Zn to LiX under the standard reaction conditions led to a sharp drop in enantioselectivity. As a result, Rovis next turned to Rh complexes, which are well known to be less prone to interaction with Lewis bases like halides. After optimizing toward a chiral phosphoramidite ligand, **96** could be furnished in 85% yield and 87% ee.<sup>84b,86</sup> A variety of in situ-prepared arylzinc reagents can be coupled under the Rh-catalyzed

conditions with uniformly good enantioselectivity, leading the authors to propose that the stereochemistry-determining step occurs independent of the organometallic reagent. These reaction conditions could not be extended to the coupling of alkylzinc reagents.

**Figure 1.31.** Enantiotopic-group-selective cross-coupling.



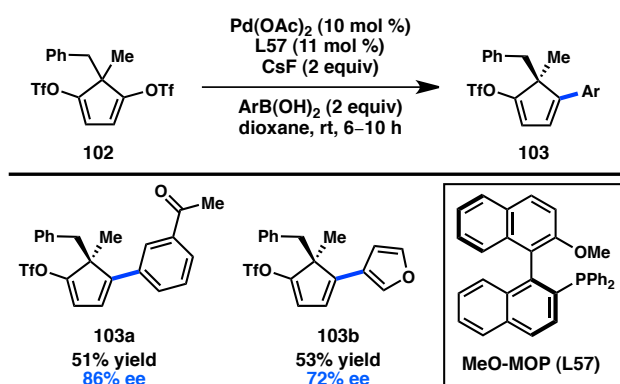
### 1.4.2 Organoboron Reagents

In 1998, Shibasaki and coworkers reported a Pd-catalyzed intramolecular enantiotopic group-selective Suzuki–Miyaura coupling of alkylboranes (**97**) to prepare exo-methylene cyclopentanes, but the highest ee value obtained was 31% (Figure 1.31, a).<sup>87</sup> More recently, Morken demonstrated that prochiral diboronate **99** can be cross-coupled with an aryl halide in the presence of  $\text{Pd}(\text{OAc})_2$  and phosphoramidite **L56** to forge benzylic boronate **100** with good enantioinduction (Figure 1.31, b).<sup>88</sup> Enantioenriched boronate **100** can undergo a subsequent stereospecific cross-coupling to

generate an enantioenriched diarylalkane.<sup>51a</sup> Prior studies by Shibata and coworkers had demonstrated that geminal bis(boronate) **99** is activated toward transmetalation and proposed that the “ate” complex of one boronate can coordinate to Pd and assist in an S<sub>E</sub>2 transmetalation of the second boronate.<sup>89</sup> The resulting monoboronate **100** lacks this mode of activation, avoiding the formation of diarylated products.

In a distinct desymmetrization approach, Willis and coworkers reported the asymmetric Suzuki–Miyaura cross-coupling of *meso*-ditriflate **102**.<sup>90</sup> The catalyst generated from Pd(OAc)<sub>2</sub> and chiral biaryl phosphine **L57** furnished mono-arylated **103** bearing a stereodefined quaternary center (Figure 1.32). Even though the yield of the transformation was moderate, good enantioselectivity was still accomplished. The remaining triflate on **103** was shown to serve as a versatile handle for further diversification of the reaction products.

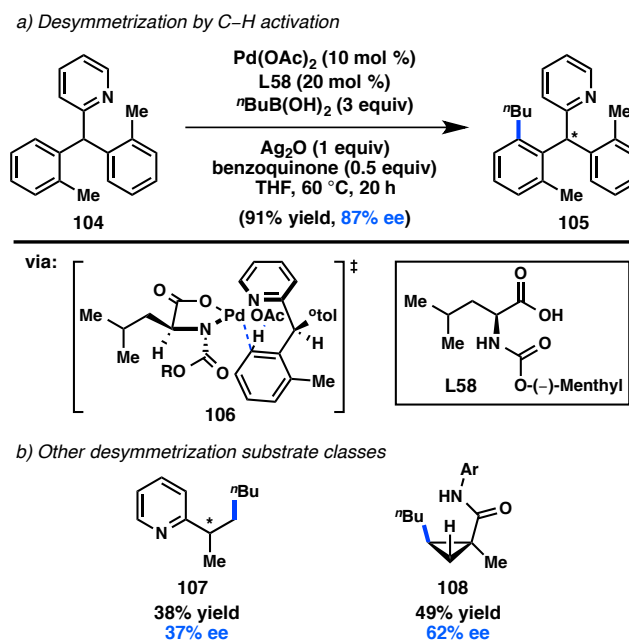
**Figure 1.32.** Enantioselective desymmetrization of a *meso*-ditriflate.



Yu and coworkers reported the first enantioselective C–H activation/cross-coupling via a desymmetrization process in 2008. Prochiral pyridyl-diarylmethane **104** was selected for these studies because of the relatively low temperatures required for C–H activation.<sup>91</sup> Following a thorough ligand study, the use of monoprotected amino

acid **L58** in conjunction with Pd(OAc)<sub>2</sub> was found to impart a high degree of asymmetric induction for the C–H activation/cross-coupling between **104** and butylboronic acid to give **105** (Figure 1.33, a). The *N*-protecting group on **L58** was a critical element for generating high ee. The reaction is hypothesized to proceed through concerted metalation/deprotonation transition state **106**, in which the unreactive aryl group is positioned *anti* to the carbamate protecting group of the ligand.<sup>92</sup>

**Figure 1.33.** Desymmetrizing enantioselective C–H activation/cross-coupling.



Yu and coworkers were subsequently able to expand this chemistry to the desymmetrization of cyclopropanes and cyclobutanes. After extensive re-engineering of the ligand, the combination of Pd(OAc)<sub>2</sub> and monoprotected amino acid **L59** was found to catalyze C–H arylation of cyclopropyl amide **109** with phenyl boronate ester to produce **110** in good yield and high ee (Scheme 1.8, a).<sup>92</sup> Unfortunately, these conditions could not be extended toward the less acidic C–H bonds of a cyclobutane. The authors



coupling, allowing chemists to leverage the flexibility of cross-coupling to streamline the synthesis of complex molecules. However, there remain challenges at the forefront of this field. Whereas enantiocontrolled cross-couplings of *sec*-alkyl partners with *n*-alkyl or C(sp<sup>2</sup>) partners have been well-explored, the analogous asymmetric cross-coupling reactions of *tert*-alkyl partners represent a largely-undeveloped area of great synthetic promise. Similarly, the completely stereocontrolled cross-coupling of two *sec*-alkyl partners is yet to be realized. These reactions would provide entry to molecules with all carbon-quaternary centers or vicinal tertiary centers, respectively—motifs that are present in many bioactive small molecules and natural product targets. The promise of enantiocontrolled cross-coupling methodologies has been made clear in the years since their inception. We anticipate that their development and application will continue to address long-standing challenges in the field of organic synthesis.

## 1.6 NOTES AND REFERENCES

- (1) Jana, R.; Pathak, T. P.; Sigman, M. S. *Chem. Rev.* **2011**, *111*, 1417.
- (2) Rudolph, A.; Lautens, M. *Angew. Chem., Int. Ed.* **2009**, *48*, 2656.
- (3) (a) Whitesides, G. M.; Roberts, J. D. *J. Am. Chem. Soc.* **1965**, *87*, 4878. (b) Whitesides, G. M.; Witanowski, M.; Roberts, J. D. *J. Am. Chem. Soc.* **1965**, *87*, 2854. (c) Witanowski, M.; Roberts, J. D. *J. Am. Chem. Soc.* **1966**, *88*, 737.
- (4) Hoffmann, R. W.; Hölzer, B.; Knopff, O.; Harms, K. *Angew. Chem., Int. Ed.* **2000**, *39*, 3072.
- (5) (a) Corriu, R. J. P.; Masse, J. P. *J. Chem. Soc., Chem. Commun.* **1972**, 144. (b) Tamao, K.; Sumitani, K.; Kumada, M. *J. Am. Chem. Soc.* **1972**, *94*, 4374. (c) Tamao, K. *J. Organomet. Chem.* **2002**, *653*, 23.
- (6) Hayashi, T. *J. Organomet. Chem.* **2002**, *653*, 41.
- (7) (a) Consiglio, G.; Botteghi, C. *Helv. Chim. Acta* **1973**, *56*, 460. (b) Kiso, Y.; Tamao, K.; Miyake, N.; Yamamoto, K.; Kumada, M. *Tetrahedron Lett.* **1974**, 3.
- (8) Consiglio, G.; Piccolo, O. *J. Organomet. Chem.* **1979**, *177*, C13.
- (9) (a) Consiglio, G.; Morandini, F.; Piccolo, O. *Tetrahedron* **1983**, *39*, 2699. (b) Consiglio, G.; Indolese, A. *J. Organomet. Chem.* **1991**, *417*, C36.
- (10) Iida, A.; Yamashita, M. *Bull. Chem. Soc. Jpn.* **1988**, *61*, 2365.
- (11) Czaplik, W. M.; Mayer, M.; Jacobi von Wangelin, A. *Synlett* **2009**, 2931.
- (12) Tamao, K.; Yamamoto, H.; Matsumoto, H.; Miyake, N.; Hayashi, T.; Kumada, M. *Tetrahedron Lett.* **1977**, *18*, 1389.
- (13) Brunner, H.; Pröbster, M. *J. Organomet. Chem.* **1981**, *209*, C1.
- (14) (a) Hayashi, T.; Fukushima, M.; Konishi, M.; Kumada, M. *Tetrahedron Lett.* **1980**, *21*, 79. (b) Hayashi, T.; Nagashima, N.; Kumada, M. *Tetrahedron Lett.* **1980**, *21*, 4623. (c) Hayashi, T.; Konishi, M.; Fukushima, M.; Kanehira, K.; Hioki, T.; Kumada, M. *J. Org. Chem.* **1983**, *48*, 2195.
- (15) Baker, K. V.; Brown, J. M.; Cooley, N. A.; Hughes, G. D.; Taylor, R. J. *J. Organomet. Chem.* **1989**, *370*, 397.

- (16) (a) Cross, G. A.; Kellogg, R. M. *J. Chem. Soc., Chem. Commun.* **1987**, 1746. (b) Cross, G.; Vriesema, B. K.; Boven, G.; Kellogg, R. M.; van Bolhuis, F. *J. Organomet. Chem.* **1989**, 370, 357.
- (17) (a) Hayashi, T.; Tajika, M.; Tamao, K.; Kumada, M. *J. Am. Chem. Soc.* **1976**, 98, 3718. (b) Tamao, K.; Hayashi, T.; Matsumoto, H.; Yamamoto, H.; Kumada, M. *Tetrahedron Lett.* **1979**, 2155. (c) Hayashi, T.; Konishi, M.; Fukushima, M.; Mise, T.; Kagotani, M.; Tajika, M.; Kumada, M. *J. Am. Chem. Soc.* **1982**, 104, 180. (d) Hayashi, T.; Kumada, M. *Acc. Chem. Res.* **1982**, 15, 395.
- (18) Indolese, A.; Consiglio, G. *J. Organomet. Chem.* **1993**, 463, 23.
- (19) Hayashi, T.; Konishi, M.; Hioki, T.; Kumada, M.; Ratajczak, A.; Niedbala, H. *Bull. Chem. Soc. Jpn.* **1981**, 54, 3615.
- (20) (a) Lemaire, M.; Buter, J.; Vriesema, B. K.; Kellogg, R. M. *J. Chem. Soc., Chem. Commun.* **1984**, 309. (b) Vriesema, B. K.; Lemaire, M.; Buter, J.; Kellogg, R. M. *J. Org. Chem.* **1986**, 51, 5169.
- (21) Brunner, H.; Li, W.; Weber, H. *J. Organomet. Chem.* **1985**, 288, 359.
- (22) Terfort, A.; Brunner, H. *J. Chem. Soc., Perkin Trans. 1* **1996**, 1467.
- (23) Jedlicka, B.; Kratky, C.; Weissensteiner, W.; Widhalm, M. *J. Chem. Soc., Chem. Commun.* **1993**, 1329.
- (24) Pellet-Rostaing, S.; Saluzzo, C.; Halle, R. T.; Breuzard, J.; Vial, L.; Le Guyader, F.; Lemaire, M. *Tetrahedron: Asymmetry* **2001**, 12, 1983.
- (25) (a) Hayashi, M.; Takaoki, K.; Hashimoto, Y.; Saigo, K. *Enantiomer* **1997**, 2, 293. (b) Yamago, S.; Yanagawa, M.; Nakamura, E. *J. Chem. Soc., Chem. Commun.* **1994**, 2093. (c) Yamago, S.; Yanagawa, M.; Mukai, H.; Nakamura, E. *Tetrahedron* **1996**, 52, 5091.
- (26) (a) Kreuzfeld, H. J.; Döbler, C.; Abicht, H. P. *J. Organomet. Chem.* **1987**, 336, 287. (b) Döbler, C.; Kreuzfeld, H. J. *J. Organomet. Chem.* **1988**, 344, 249.
- (27) (a) Horibe, H.; Kazuta, K.; Kotoku, M.; Kondo, K.; Okuno, H.; Murakami, Y.; Aoyama, T. *Synlett* **2003**, 2047. (b) Hideo, H.; Fukuda, Y.; Kondo, K.; Okuno, H.; Murakami, Y.; Aoyama, T. *Tetrahedron* **2004**, 60, 10701.
- (28) (a) Richards, C. J.; Hibbs, D. E.; Hursthouse, M. B. *Tetrahedron Lett.* **1995**, 36, 3745. (b) Lloyd-Jones, G. C.; Butts, C. P. *Tetrahedron* **1998**, 54, 901.
- (29) Schwink, L.; Knochel, P. *Chem. Eur. J.* **1998**, 4, 950.

- (30) (a) Hayashi, T.; Konishi, M.; Ito, H.; Kumada, M. *J. Am. Chem. Soc.* **1982**, *104*, 4962. (b) Hayashi, T.; Konishi, M.; Okamoto, Y.; Kabeta, K.; Kumada, M. *J. Org. Chem.* **1986**, *51*, 3772.
- (31) Hayashi, T.; Kanehira, K.; Hioki, T.; Kumada, M. *Tetrahedron Lett.* **1981**, *22*, 137.
- (32) Hayashi, T.; Okamoto, Y.; Kumada, M. *Tetrahedron Lett.* **1983**, *24*, 807.
- (33) Hayashi, T.; Hagihara, T.; Katsuro, Y.; Kumada, M. *Bull. Chem. Soc. Jpn.* **1983**, *56*, 363.
- (34) Hayashi, T.; Yamamoto, A.; Hojo, M.; Ito, Y. *J. Chem. Soc., Chem. Commun.* **1989**, 495.
- (35) Cherney, A. H.; Reisman, S. E. *Tetrahedron* **2014**, *70*, 3259.
- (36) Campos, K. R.; Klapars, A.; Waldman, J. H.; Dormer, P. G.; Chen, C.-y. *J. Am. Chem. Soc.* **2006**, *128*, 3538.
- (37) Cordier, C. J.; Lundgren, R. J.; Fu, G. C. *J. Am. Chem. Soc.* **2013**, *135*, 10946.
- (38) Tellis, J. C.; Primer, D. N.; Molander, G. A. *Science* **2014**, *345*, 433.
- (39) Zembayashi, M.; Tamao, K.; Hayashi, T.; Mise, T.; Kumada, M. *Tetrahedron Lett.* **1977**, *18*, 1799.
- (40) Binder, J. T.; Cordier, C. J.; Fu, G. C. *J. Am. Chem. Soc.* **2012**, *134*, 17003.
- (41) (a) Okoroafor, M. O.; Ward, D. L.; Brubaker, C. H. *Organometallics* **1988**, *7*, 1504. (b) Naiini, A. A.; Lai, C.-K.; Ward, D. L.; Brubaker, C. H. *J. Organomet. Chem.* **1990**, *390*, 73. (c) Ali, H. M.; Brubaker, C. H. *J. Mol. Cat.* **1990**, *60*, 331.
- (42) Lou, S.; Fu, G. C. *J. Am. Chem. Soc.* **2010**, *132*, 1264.
- (43) Lundin, P. M.; Esquivias, J.; Fu, G. C. *Angew. Chem., Int. Ed.* **2009**, *48*, 154.
- (44) Fischer, C.; Fu, G. C. *J. Am. Chem. Soc.* **2005**, *127*, 4594.
- (45) Arp, F. O.; Fu, G. C. *J. Am. Chem. Soc.* **2005**, *127*, 10482.
- (46) Lin, X.; Sun, J.; Xi, Y.; Lin, D. *Organometallics* **2011**, *30*, 3284.
- (47) Smith, S. W.; Fu, G. C. *J. Am. Chem. Soc.* **2008**, *130*, 12645.
- (48) Partridge, B. M.; Chausset-Boissarie, L.; Burns, M.; Pulis, A. P.; Aggarwal, V. K. *Angew. Chem., Int. Ed.* **2012**, *51*, 11795.

- (49) Oelke, A. J.; Sun, J.; Fu, G. C. *J. Am. Chem. Soc.* **2012**, *134*, 2966.
- (50) Do, H.-Q.; Chandrashekar, E. R. R.; Fu, G. C. *J. Am. Chem. Soc.* **2013**, *135*, 16288.
- (51) (a) Imao, D.; Glasspoole, B. W.; Laberge, V. S.; Crudden, C. M. *J. Am. Chem. Soc.* **2009**, *131*, 5024. (b) Taylor, B. L. H.; Swift, E. C.; Waetzig, J. D.; Jarvo, E. R. *J. Am. Chem. Soc.* **2011**, *133*, 389. (c) Greene, M. A.; Yonova, I. M.; Williams, F. J.; Jarvo, E. R. *Org. Lett.* **2012**, *14*, 4293. (d) Yonova, I. M.; Johnson, A. G.; Osborne, C. A.; Moore, C. E.; Morrissette, N. S.; Jarvo, E. R. *Angew. Chem., Int. Ed.* **2014**, *53*, 2422. (e) Zhou, Q.; Srinivas, H. D.; Dasgupta, S.; Watson, M. P. *J. Am. Chem. Soc.* **2013**, *135*, 3307. (f) Maity, P.; Shacklady-McAtee, D. M.; Yap, G. P. A.; Sirianni, E. R.; Watson, M. P. *J. Am. Chem. Soc.* **2013**, *135*, 280. (g) Shacklady-McAtee, D. M.; Roberts, K. M.; Basch, C. H.; Song, Y.-G.; Watson, M. P. *Tetrahedron* **2014**, *70*, 4257.
- (52) Liang, Y.; Fu, G. C. *J. Am. Chem. Soc.* **2014**, *136*, 5520.
- (53) He, A.; Falck, J. R. *J. Am. Chem. Soc.* **2010**, *132*, 2524.
- (54) Choi, J.; Fu, G. C. *J. Am. Chem. Soc.* **2012**, *134*, 9102.
- (55) (a) Powell, D. A.; Maki, T.; Fu, G. C. *J. Am. Chem. Soc.* **2005**, *127*, 510. (b) Gonzalez-Bobes, F.; Fu, G. C. *J. Am. Chem. Soc.* **2006**, *128*, 5360.
- (56) Choi, J.; Martín-Gago, P.; Fu, G. C. *J. Am. Chem. Soc.* **2014**, *136*, 12161.
- (57) Saito, B.; Fu, G. C. *J. Am. Chem. Soc.* **2007**, *129*, 9602.
- (58) Saito, B.; Fu, G. C. *J. Am. Chem. Soc.* **2008**, *130*, 6694.
- (59) Owston, N. A.; Fu, G. C. *J. Am. Chem. Soc.* **2010**, *132*, 11908.
- (60) Lu, Z.; Wilsily, A.; Fu, G. C. *J. Am. Chem. Soc.* **2011**, *133*, 8154.
- (61) Zultanski, S. L.; Fu, G. C. *J. Am. Chem. Soc.* **2011**, *133*, 15362.
- (62) (a) Wilsily, A.; Tramutola, F.; Owston, N. A.; Fu, G. C. *J. Am. Chem. Soc.* **2012**, *134*, 5794. (b) Jiang, X.; Sakthivel, S.; Kulbitski, K.; Nisnevich, G.; Gandelman, M. *J. Am. Chem. Soc.* **2014**, *136*, 9548.
- (63) Lundin, P. M.; Fu, G. C. *J. Am. Chem. Soc.* **2010**, *132*, 11027.
- (64) Cong, H.; Fu, G. C. *J. Am. Chem. Soc.* **2014**, *136*, 3788.
- (65) Graham, T. J. A.; Shields, J. D.; Doyle, A. G. *Chem. Sci.* **2011**, *2*, 980.

- (66) Sylvester, K. T.; Wu, K.; Doyle, A. G. *J. Am. Chem. Soc.* **2012**, *134*, 16967.
- (67) Shields, J. D.; Ahneman, D. T.; Graham, T. J. A.; Doyle, A. G. *Org. Lett.* **2014**, *16*, 142.
- (68) Chau, S. T.; Lutz, J. P.; Wu, K.; Doyle, A. G. *Angew. Chem., Int. Ed.* **2013**, *52*, 9153.
- (69) Yamamoto, Y.; Takada, S.; Miyaura, N. *Chem. Lett.* **2006**, *35*, 704.
- (70) Yamamoto, Y.; Takada, S.; Miyaura, N. *Chem. Lett.* **2006**, *35*, 1368.
- (71) Yamamoto, Y.; Takada, S.; Miyaura, N.; Iyama, T.; Tachikawa, H. *Organometallics* **2009**, *28*, 152.
- (72) Chausset-Boissarie, L.; Ghozati, K.; LaBine, E.; Chen, J. L.-Y.; Aggarwal, V. K.; Crudden, C. M. *Chem. Eur. J.* **2013**, *19*, 17698.
- (73) (a) Hatanaka, Y.; Goda, K.-I.; Hiyama, T. *Tetrahedron Lett.* **1994**, *35*, 1279. (b) Denmark, S. E.; Werner, N. S. *J. Am. Chem. Soc.* **2010**, *132*, 3612.
- (74) Dai, X.; Strotman, N. A.; Fu, G. C. *J. Am. Chem. Soc.* **2008**, *130*, 3302.
- (75) Lou, S.; Fu, G. C. *J. Am. Chem. Soc.* **2010**, *132*, 5010.
- (76) Caeiro, J.; Pérez Sestelo, J.; Sarandeses, L. A. *Chem. Eur. J.* **2008**, *14*, 741.
- (77) (a) Willis, M. C. *J. Chem. Soc., Perkin Trans. 1* **1999**, 1765. (b) Chen, Y.; McDaid, P.; Deng, L. *Chem. Rev.* **2003**, *103*, 2965. (c) Díaz de Villegas, M. D.; Gálvez, J. A.; Etayo, P.; Badorrey, R.; López-Ram-de-Víu, P. *Chem. Soc. Rev.* **2011**, *40*, 5564.
- (78) Johnson, J. B.; Rovis, T. *Acc. Chem. Res.* **2008**, *41*, 327.
- (79) Bercot, E. A.; Rovis, T. *J. Am. Chem. Soc.* **2005**, *127*, 247.
- (80) (a) Giovannini, R.; Stüdemann, T.; Dussin, G.; Knochel, P. *Angew. Chem., Int. Ed.* **1998**, *37*, 2387. (b) Giovannini, R.; Stüdemann, T.; Devasagayaraj, A.; Dussin, G.; Knochel, P. *J. Org. Chem.* **1999**, *64*, 3544.
- (81) Bercot, E. A.; Rovis, T. *J. Am. Chem. Soc.* **2002**, *124*, 174.
- (82) Johnson, J. B.; Bercot, E. A.; Rowley, J. M.; Coates, G. W.; Rovis, T. *J. Am. Chem. Soc.* **2007**, *129*, 2718.
- (83) Bercot, E. A.; Rovis, T. *J. Am. Chem. Soc.* **2004**, *126*, 10248.

- (84) (a) Cook, M. J.; Rovis, T. *J. Am. Chem. Soc.* **2007**, *129*, 9302. (b) Johnson, J. B.; Cook, M. J.; Rovis, T. *Tetrahedron* **2009**, *65*, 3202. (c) Cook, M. J.; Rovis, T. *Synthesis* **2009**, 335.
- (85) Brand, G. J.; Studte, C.; Breit, B. *Org. Lett.* **2009**, *11*, 4668.
- (86) Johnson, J. B.; Bercot, E. A.; Williams, C. M.; Rovis, T. *Angew. Chem., Int. Ed.* **2007**, *46*, 4514.
- (87) Cho, S. Y.; Shibasaki, M. *Tetrahedron: Asymmetry* **1998**, *9*, 3751.
- (88) Sun, C.; Potter, B.; Morken, J. P. *J. Am. Chem. Soc.* **2014**, *136*, 6534.
- (89) Endo, K.; Ohkubo, T.; Hirokami, M.; Shibata, T. *J. Am. Chem. Soc.* **2010**, *132*, 11033.
- (90) Willis, M. C.; Powell, L. H. W.; Claverie, C. K.; Watson, S. J. *Angew. Chem., Int. Ed.* **2004**, *43*, 1249.
- (91) Shi, B.-F.; Mangel, N.; Zhang, Y.-H.; Yu, J.-Q. *Angew. Chem., Int. Ed.* **2008**, *47*, 4882.
- (92) Wasa, M.; Engle, K. M.; Lin, D. W.; Yoo, E. J.; Yu, J.-Q. *J. Am. Chem. Soc.* **2011**, *133*, 19598.
- (93) Xiao, K.-J.; Lin, D. W.; Miura, M.; Zhu, R.-Y.; Gong, W.; Wasa, M.; Yu, J.-Q. *J. Am. Chem. Soc.* **2014**, *136*, 8138.

## Chapter 2

### *Pd-Catalyzed Fukuyama Cross-Coupling of Secondary Organozinc Reagents for the Direct Synthesis of Unsymmetrical Ketones<sup>†</sup>*

#### 2.1 INTRODUCTION

Transition metal-catalyzed cross-coupling reactions have emerged as a transformative methodology in the field of organic synthesis, enabling the rapid generation of complex molecules under mild, selective, and catalytic conditions. While initial reports focused on C(sp<sup>2</sup>)-C(sp<sup>2</sup>) couplings, the burgeoning field of C(sp<sup>3</sup>) bond-forming processes has rapidly expanded in the past decade.<sup>1</sup> In a seminal report, Hayashi and coworkers found that Pd complexes supported by bulky, bidentate phosphines with large bite angles (e.g., 1,1'-bis(diphenylphosphino)ferrocene) (dppf) can catalyze the cross-coupling between aryl or vinyl halides and primary or secondary organomagnesium and organozinc reagents.<sup>2</sup> In 2003, Fu and coworkers demonstrated that similar bulky,

---

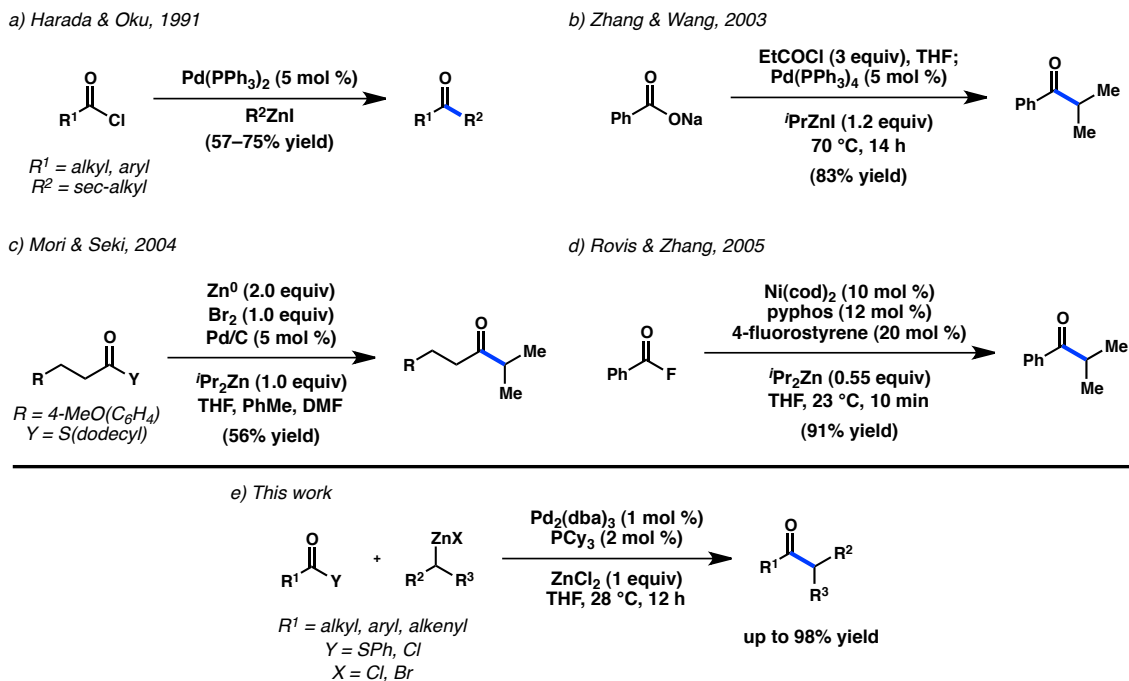
<sup>†</sup> Portions of this chapter have been reproduced from published studies (see reference 19) and the supporting information found therein.

electron-rich phosphines enable a general Pd-catalyzed Negishi coupling of C(sp<sup>3</sup>)-hybridized electrophiles with alkyl, alkenyl, and aryl nucleophiles.<sup>3</sup> In the decade that has followed, steady advances have been made in Pd- and Ni-catalyzed cross-coupling reactions of both *secondary* C(sp<sup>3</sup>) organometallic reagents and *secondary* C(sp<sup>3</sup>) electrophiles, giving rise to a wide variety of products now accessible via simple alkyl building blocks.<sup>4,5,6</sup>

One transformation that remains underdeveloped is the transition metal-catalyzed cross-coupling reaction between carboxylic acid derivatives and C(sp<sup>3</sup>) organometallic reagents to prepare ketones, despite the fact that the Pd-catalyzed reaction between acid chlorides and alkyl tin reagents was first reported over thirty years ago.<sup>7</sup> In 1998, Fukuyama and coworkers disclosed the Pd-catalyzed coupling of thioesters and primary alkyl organozinc or hydride reagents, generating ketone or aldehyde products, respectively.<sup>8</sup> A number of functional groups are tolerated due to the relative stability of both coupling components. Seki and coworkers have since developed both heterogeneous and phosphine-free Pd-catalyzed Fukuyama couplings, as well as a Ni-catalyzed Fukuyama coupling.<sup>9</sup> Despite these advances, the use of *secondary* C(sp<sup>3</sup>) organometallic reagents still proves challenging. While  $\alpha,\alpha$ -disubstituted ketones can be prepared by direct attack of a variety of strongly nucleophilic organometal species onto acyl electrophiles, such protocols are frequently accompanied by over-addition products due to the electrophilicity of the newly formed ketone.<sup>10</sup> Specialized acyl derivatives such as Weinreb amides can minimize over-addition, but require the use of organolithium or Grignard reagents, which suffer from poor functional group tolerance.<sup>11</sup> Recent strategies

to eliminate the need for alkyl organometallic reagents in ketone synthesis include reverse-polarity cross-couplings<sup>12</sup> and reductive cross-couplings (see Chapter 3).<sup>13</sup>

**Figure 2.1.** Acyl cross-coupling reactions of secondary organozinc reagents.

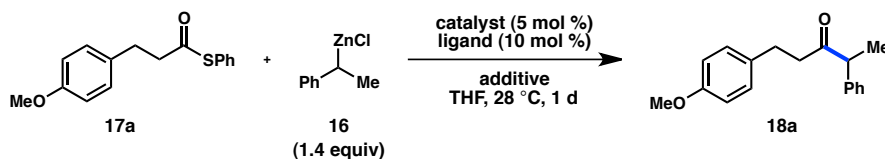


Although substantial progress has been made on the transition metal-catalyzed cross-coupling between acyl electrophiles and primary alkyl organometallic reagents, there are far fewer reports describing the coupling of secondary alkyl organometallics. In an early study, Harada and Oku disclosed the coupling of secondary organozinc reagents with acid chlorides and obtained moderate to good yields of the ketone product, although the functional group tolerance of the reaction was not further explored (Figure 2.1).<sup>14</sup> Zhang and Wang reported a high-yielding reaction between *i*PrZnI and the mixed anhydride generated from sodium benzoate; however, additional substrate scope was not disclosed.<sup>15</sup> Subsequently, Mori and Seki reported a Pd-catalyzed coupling between a thioester and *i*Pr<sub>2</sub>Zn that proceeds in moderate yield.<sup>16</sup> Rovis and Zhang have also

reported a single case of a high-yielding coupling reaction between an acid fluoride and  $i\text{Pr}_2\text{Zn}$ .<sup>17</sup> Organoboron reagents are another class of nucleophiles utilized in the related Liebskind–Srogl cross-coupling of thioesters. However, these reactions only proceed with primary organoboron reagents despite efforts to extend the reaction to secondary reagents.<sup>18</sup> With the objective of expanding the synthetic utility of metal-catalyzed acyl cross-coupling reactions, herein we report a general method for the cross-coupling of *secondary* organozinc reagents and thioesters.<sup>19</sup>

## 2.2 DEVELOPMENT OF A RACEMIC FUKUYAMA CROSS-COUPLING OF SECONDARY ORGANOZINC REAGENTS

The scarcity of *sec*-alkylmetal couplings with acyl derivatives is indicative of the inherent difficulties of transition metal-catalyzed reactions involving  $\text{C}(\text{sp}^3)$ -hybridized coupling partners.<sup>1d</sup> In general, alkyl organometallic reagents are prone to  $\beta$ -hydride elimination as well as proto-demetalation under typical cross-coupling reaction conditions. Additionally, many alkyl organometallics suffer from slow transmetalation to the transition metal catalyst. Furthermore, reductive elimination from a transition metal is also slow due to  $\sigma$ -donation of the alkyl group to the metal. The sluggishness of reductive elimination enhances side reactions such as  $\beta$ -hydride elimination and isomerization. Acceleration of the reductive elimination pathway, either through catalyst and ligand tuning or through the use of additives, can prevent this undesired isomerization. Significantly, alkylzinc reagents display relatively broad use in  $\text{C}(\text{sp}^3)$  cross-couplings because of their ability to undergo a facile transmetalation with Pd as compared to other organometallic partners used in cross-coupling chemistry.

**Table 2.1.** Optimization of reaction conditions.

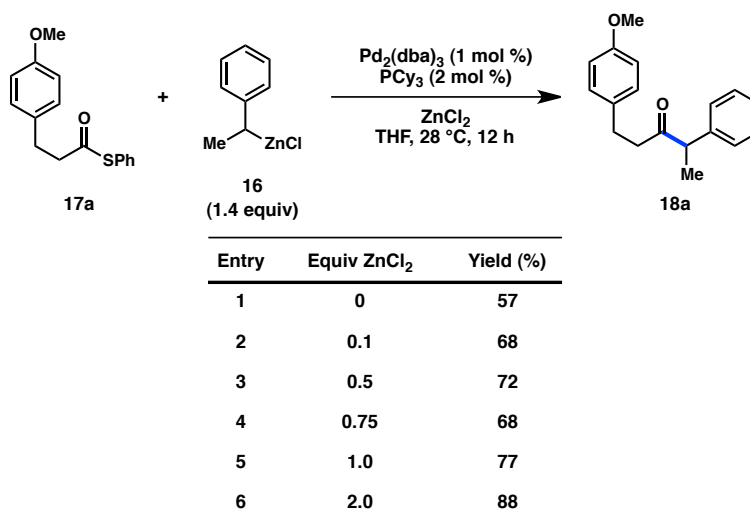
Entry	Catalyst	Ligand <sup>a</sup>	Additive	Conversion (%) <sup>b</sup>	Yield (%) <sup>b</sup>
1	Ni(acac) <sub>2</sub> <sup>c</sup>	-	-	75	10
2	NiCl <sub>2</sub> (dme) <sup>c</sup>	-	-	83	14
3	Pd <sub>2</sub> (dba) <sub>3</sub>	-	-	94	13
4	Pd(OAc) <sub>2</sub> <sup>c</sup>	-	-	75	15
5	PdCl <sub>2</sub> (dppf) <sup>c</sup>	-	-	88	20
6	Pd <sub>2</sub> (dba) <sub>3</sub>	PPh <sub>3</sub>	-	92	16
7	Pd <sub>2</sub> (dba) <sub>3</sub>	PCy <sub>3</sub>	-	89	34
8	Pd <sub>2</sub> (dba) <sub>3</sub>	SPhos	-	93	16
9	Pd <sub>2</sub> (dba) <sub>3</sub>	XPhos	-	82	14
10	Pd <sub>2</sub> (dba) <sub>3</sub>	PCy <sub>3</sub>	DMF <sup>e</sup>	78	52
11	Pd <sub>2</sub> (dba) <sub>3</sub>	PMe <sub>3</sub>	DMF <sup>e</sup>	100	23
12	Pd <sub>2</sub> (dba) <sub>3</sub>	PEt <sub>3</sub>	DMF <sup>e</sup>	80	35
13	Pd <sub>2</sub> (dba) <sub>3</sub>	P <sup>n</sup> Bu <sub>3</sub>	DMF <sup>e</sup>	90	32
14	Pd <sub>2</sub> (dba) <sub>3</sub>	P <sup>t</sup> Bu <sub>3</sub>	DMF <sup>e</sup>	88	22
15	Pd <sub>2</sub> (dba) <sub>3</sub> <sup>d</sup>	PCy <sub>3</sub>	DMF <sup>e</sup> /ZnCl <sub>2</sub> <sup>f</sup>	100	83
16	Pd <sub>2</sub> (dba) <sub>3</sub> <sup>d</sup>	PCy <sub>3</sub>	ZnCl <sub>2</sub> <sup>f</sup>	93	89
17	Pd <sub>2</sub> (dba) <sub>3</sub> <sup>d</sup>	dCyb	ZnCl <sub>2</sub> <sup>f</sup>	49	44

<sup>a</sup> 1:1 Pd:phosphine was used. <sup>b</sup> Conversion of **17a** and yield of **18a** were calculated by <sup>1</sup>H NMR analysis with internal standard. <sup>c</sup> 10 mol % was used. <sup>d</sup> 1 mol % was used. <sup>e</sup> 10 vol % was added. <sup>f</sup> 1 equiv was added.

We therefore began our studies by evaluating the cross-coupling between thioester **17a** and organozinc **16**. An analysis of metal catalysts revealed that Ni sources performed poorly (Table 2.1, entries 1–2), whereas PdCl<sub>2</sub>(dppf) was more promising (Table 2.1, entry 5). A screen of several phosphine ligands revealed that the bulky, monodentate, electron-rich ligand PCy<sub>3</sub> furnished ketone **18a** in 34% yield (entries 6–9). Despite their success in a number of Negishi couplings, the Buchwald ligands SPhos and XPhos showed low reactivity.<sup>20</sup> On the other hand, use of 10 vol % DMF as a polar cosolvent further increased the yield to 52% (entry 10), although additional DMF had no

effect on the reaction. Other trialkylphosphines resulted in lower yields of **18a** (entries 11–14). Interestingly, these conditions of Pd<sub>2</sub>(dba)<sub>3</sub>/PCy<sub>3</sub>/DMF closely resemble Fu's general conditions (Pd<sub>2</sub>(dba)<sub>3</sub>/PCyp<sub>3</sub>/NMI) for Negishi cross-couplings of alkyl electrophiles.<sup>3</sup> Notably, *no isomerized linear product was observed*.

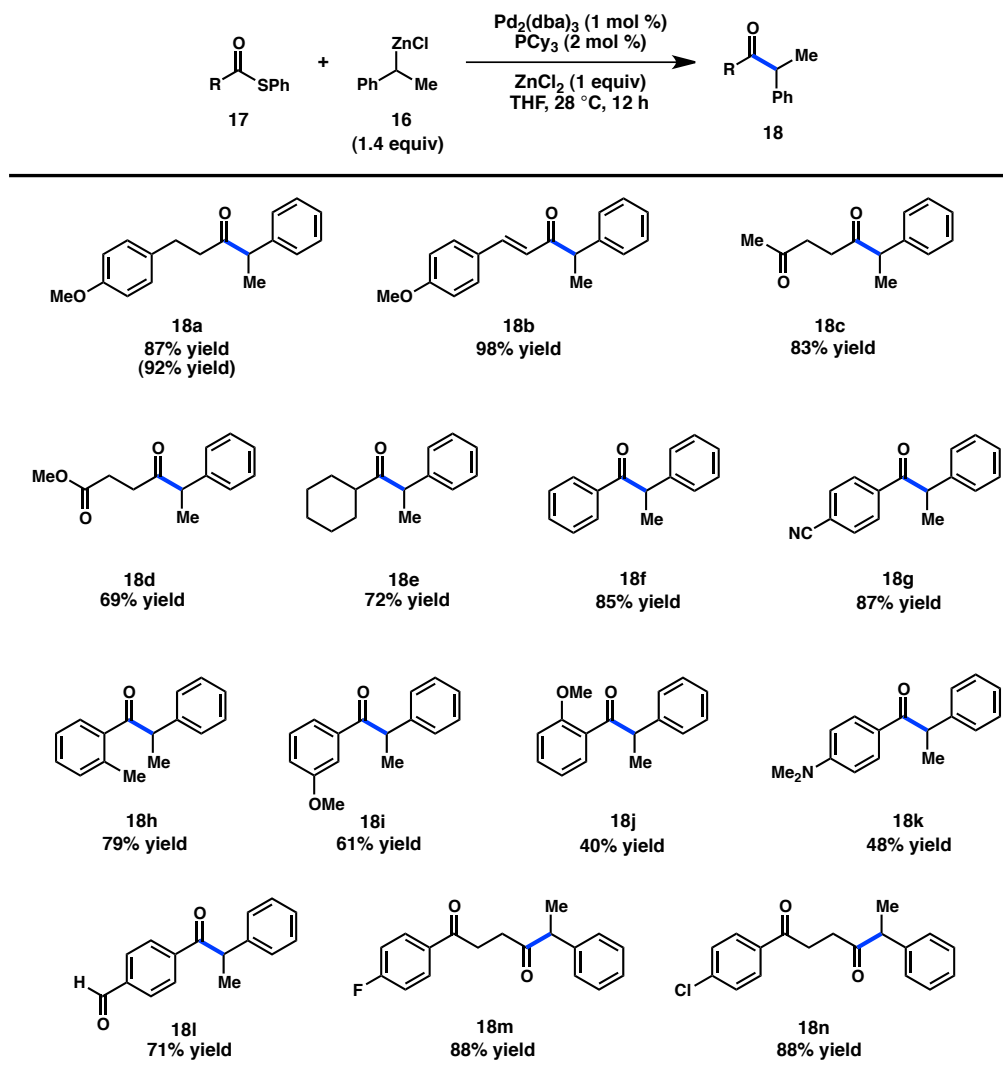
**Table 2.2.** Effect of zinc chloride on the Fukuyama cross-coupling.



Previous studies of the Fukuyama coupling have noted that addition of inorganic zinc salts may shift the Schlenk equilibrium of the organozinc reagent toward a more reactive organozinc halide and may also activate Pd toward oxidative addition.<sup>9</sup> Gratifyingly, addition of ZnCl<sub>2</sub> increased both the conversion and yield of the reaction, while allowing the catalyst loading to be reduced to 1 mol % Pd<sub>2</sub>(dba)<sub>3</sub> without an appreciable decrease in yield (entry 15). Use of ZnCl<sub>2</sub> as the sole additive also obviated the need for DMF, delivering **18a** in 89% yield (entry 16). Replacement of PCy<sub>3</sub> for a bidentate phosphine analog, 1,4-bis(dicyclohexylphosphino)butane (dCyb), resulted in a lower conversion of **17a** and a lower yield of **18a**. To understand the effect of ZnCl<sub>2</sub>, an analysis of additive loading revealed that as increasing amounts of ZnCl<sub>2</sub> are used, the

yield of ketone **18a** rises (Table 2.2). This behavior is consistent with  $\text{ZnCl}_2$  modulating a Schlenk equilibrium, although further studies to establish its exact role are desirable.

**Figure 2.2.** Thioester substrate scope.

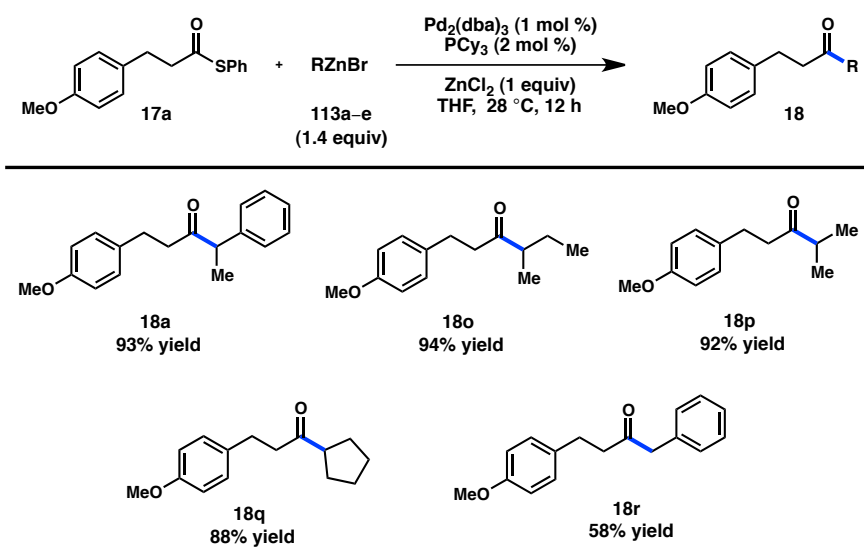


Isolated yields; reactions conducted on a 0.2 mmol scale under an  $\text{N}_2$  atmosphere in a glovebox. Number in parentheses indicates reaction conducted on a 1.0 mmol scale under an  $\text{N}_2$  atmosphere on the benchtop using standard Schlenk techniques.

Having developed optimized coupling conditions for secondary organozinc halides, we applied our  $\text{Pd}_2(\text{dba})_3/\text{PCy}_3/\text{ZnCl}_2$  system to a series of thioesters to determine the scope of the reaction (Figure 2.2). The cross-coupling reaction proceeds in excellent

yields for alkyl (**17a**), aryl (**17f–l**), and  $\alpha,\beta$ -unsaturated thioesters (**17b**). A variety of thioesters with electrophilic functional groups such as a ketone (**17c**, **17m**, **17n**), aldehyde (**17l**), ester (**17d**), or nitrile (**17g**), all of which would be incompatible with standard Weinreb ketone synthesis conditions, generate the desired coupling products in high yields. Aryl fluorides (**17m**) and chlorides (**17n**) both react with the thioester chemoselectively. The reaction can also tolerate a more sterically encumbered thioester to form **18h** in 79% yield. In contrast, a decreased yield was observed when **17j**, containing an *o*-methoxy group, was employed.  $\alpha,\alpha$ -Disubstituted thioester **17e** furnishes the desired product in 72% yield despite the increased steric hindrance. To illustrate the robustness of the methodology, the cross-coupling reaction was performed on a 1.0 mmol scale on the benchtop using standard Schlenk techniques, under which conditions **18a** was obtained in 92% yield.

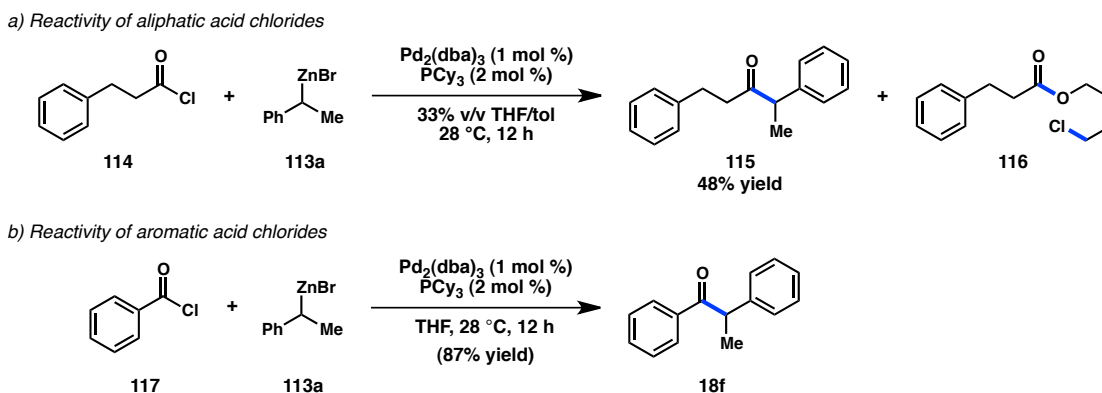
**Figure 2.3.** Organozinc substrate scope.



Isolated yields; reactions conducted on a 0.2 mmol scale under an  $\text{N}_2$  atmosphere in a glovebox.

Given that organozinc **16** was prepared via direct insertion of  $\text{Zn}^0$  into (1-chloroethyl)benzene (see Experimental Section), we sought to test whether commercial Rieke organozinc reagents,<sup>21</sup> possessing a different mixture of solubilized salts, would be equally active under our cross-coupling conditions. We were pleased to observe that ketone **18a** could be prepared in 93% yield when using Rieke organozinc reagent **113a** (Figure 2.3). Non-activated cyclic and acyclic Rieke organozinc bromides furnished the desired products in excellent yields. In the case of **18o** and **18p**, no isomerized linear product was observed.

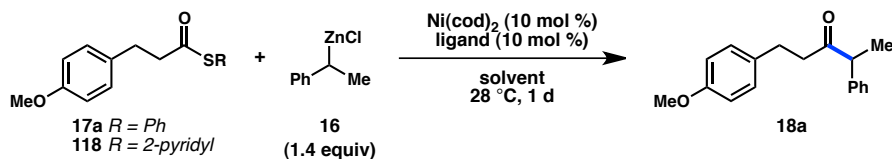
**Scheme 2.1.** Extension to acid chlorides.



While thioesters are air- and moisture-stable building blocks, acid chlorides represent one of the most commonly used types of acyl electrophile. As such, our optimized conditions were tested against several acid chloride coupling partners. Under conditions developed for the coupling of thioesters, aliphatic acid chlorides reacted slowly and primarily underwent a competitive Lewis acid-mediated reaction with THF to form ester **116** (Scheme 2.1, a).<sup>22</sup> However, treatment of acid chloride **114** with organozinc **113a** in a mixed solvent system, and in the absence of excess  $\text{ZnCl}_2$ , delivered ketone **115** in 48% yield. Aromatic acid chlorides proved to be more reactive toward

cross-coupling than their aliphatic counterparts: in the absence of excess  $\text{ZnCl}_2$ , benzoyl chloride (**117**) could be coupled to generate **18f** in 87% yield (Scheme 2.1, b).

**Table 2.3.** Optimization of a Ni-catalyzed Fukuyama cross-coupling.



Entry	Thioester	Ligand	Solvent	Conversion (%) <sup>a</sup>	Yield (%) <sup>a</sup>
1 <sup>b</sup>	17a	$\text{PCy}_3$	THF		0
2 <sup>b</sup>	17a	phen	THF	32	0
3	17a	phen	THF	54	11
4	17a	phen	4:1 THF/DMF	56	23
5	17a	bipy	4:1 THF/DMF	37	12
6	17a	terpy	4:1 THF/DMF	49	7
7	17a	bathophen	4:1 THF/DMF	54	21
8	118	phen	4:1 THF/DMF	100	71
9	118	phen	THF	100	70

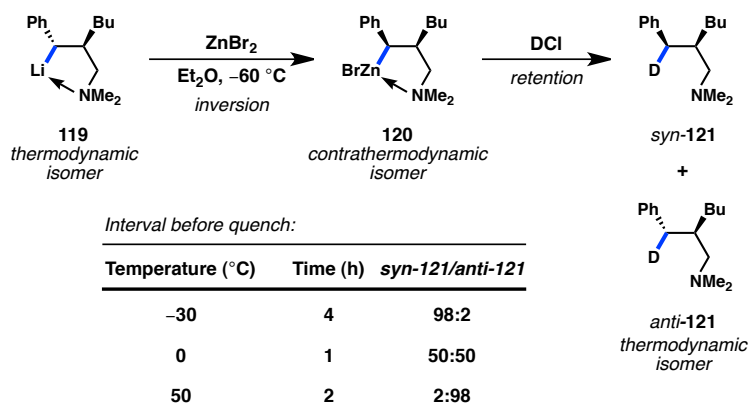
<sup>a</sup> Conversion of **17a** and **118** and yield of **18a** were calculated by  $^1\text{H}$  NMR analysis with internal standard. <sup>b</sup> 1 equiv  $\text{ZnCl}_2$  was added.

Having successfully identified conditions for a Pd-catalyzed Fukuyama cross-coupling between thioesters and secondary organozinc reagents, the potential for Ni catalysis was reinvestigated. The presence of excess  $\text{ZnCl}_2$  prevented product formation when either phosphorus or nitrogen ligands were employed (Table 2.3, entries 1–3). A screen of cosolvents revealed that the addition of DMF, with phenanthroline serving as a bidentate ligand, produced ketone **18a** in 23% yield (entry 4). A further evaluation of nitrogen-based ligands failed to increase the conversion of thioester **17a** or the yield of ketone **18a** (entries 5–7). In contrast, utilization of 2-pyridyl thioester **118** provided full conversion of the starting material and furnished **18a** in 70% yield when THF was employed as the sole solvent (entries 8 and 9).<sup>23</sup>

## 2.3 EFFORTS TOWARD AN ENANTIOSELECTIVE FUKUYAMA CROSS-COUPLING

Having identified conditions for the coupling of thioesters and secondary organozinc reagents, we initiated an investigation of whether the coupling between organozinc **16** and thioester **17a** would be amenable to asymmetric catalysis. We realized that benzylzinc halides might possess a suitable configurational lability about the C–Zn bond, permitting a fast equilibration between the two enantiomers of organometallic **16**. If this equilibration is rapid in relation to transmetalation, then an appropriate chiral catalyst could selectively react with a single enantiomer of the nucleophile and cause a dynamic kinetic resolution (DKR). Indeed, Marek and coworkers have demonstrated that benzylzinc halides epimerize rapidly at elevated temperatures and at a moderate rate at 0 °C (Figure 2.4).<sup>24</sup> Only when cooled to –30° C is epimerization of **120** minimized, providing *syn*-**121** after quenching with DCl.

**Figure 2.4.** Configurational lability of benzylzinc halides.



A series of chiral ligand scaffolds were evaluated under our previously optimized conditions in order to assess the validity of the proposed DKR. Several common chiral

bidentate phosphine ligands failed to deliver ketone **18a** in appreciable yields (Figure 2.5). Notably, ferrocenylphosphine **L17**, which has previously been demonstrated to promote asymmetric Kumada–Corriu cross-couplings through a DKR mechanism, was ineffective in this system.<sup>25</sup> On the other hand, we were pleased to realize that monodentate phosphines, including NMDPP (**L64**) and Monophos (**L65**), delivered moderate yields of the desired product, albeit with little enantioinduction. Nitrogen-based ligands from the PHOX, Box, and PyBox families provided poor yields and ee's of the desired ketone.

**Figure 2.5.** Preliminary study of chiral ligand scaffolds.

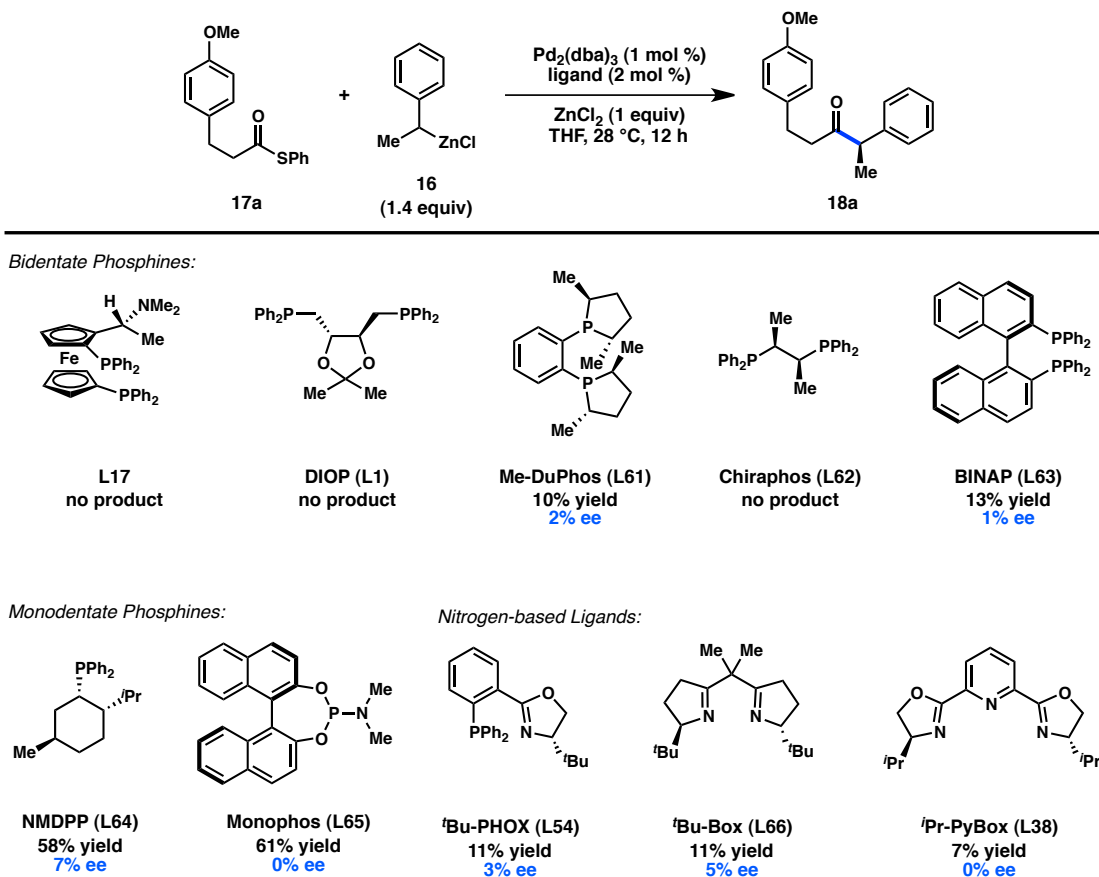
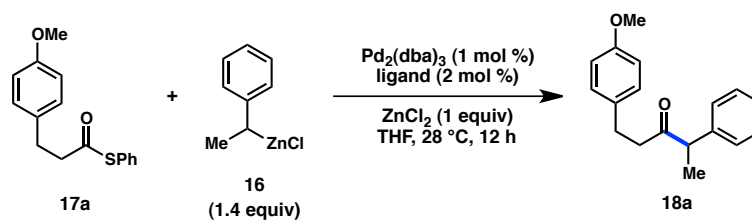
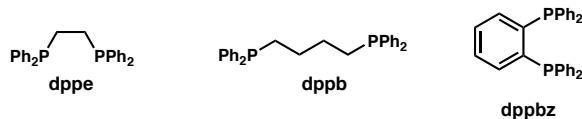


**Table 2.4.** Activity of monodentate and bidentate phosphine ligands.



Entry	Ligand	Pd:Ligand	Conversion (%)	Yield (%)
1	$\text{PPh}_3$	2:1	95	55
2	$\text{PPh}_3$	1:1	100	90
3	$\text{PPh}_3$	1:2	100	82
4	$\text{PPh}_3$	1:4	81	74
5	dppe	1:1	12	9
6	dppb	1:1	31	13
7	dppbz	1:1	11	10



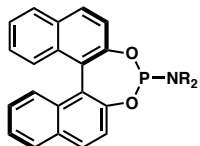
In order to better understand the divergent activity of monodentate and bidentate phosphines, additional mechanistic studies were conducted prior to further ligand development. Variation of the metal/ligand ratio revealed that complete conversion and excellent yields are realized when a 1:1 ratio is employed (Table 2.4, entries 1–4). When an excess of ligand is utilized, a systematic decrease in product yield is observed. These results corroborate the superiority of a 1:1 stoichiometry between metal and ligand, but they also suggest that excess phosphine may exhibit an inhibitory effect on Pd, as evidenced by the incomplete conversion witnessed when four equivalents of phosphine are used relative to Pd (entry 4). In contrast to  $\text{PPh}_3$ , bidentate ligands strongly disfavor formation of monoligated Pd species; indeed, switching to such ligands delivers poor yields of ketone **18a** and additionally inhibits conversion of thioester **17a**. These results

indicate that additional investigation of chiral ligand scaffolds should focus on chiral monodentate ligands as opposed to their bidentate counterparts.

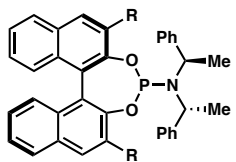
While good yields were expected with NMDPP (**L64**) because of its steric and electronic similarity to PCy<sub>3</sub>, we were pleased that Monophos (**L65**) also displayed similar reactivity (see Figure 2.5). In contrast to NMDPP, phosphoramidites have seen widespread use in asymmetric catalysis, including in monophosphine-metal-catalyzed reactions.<sup>26</sup> Despite finding diverse applications in conjugate addition and allylic substitution chemistry, few examples exist of phosphoramidites being used in Pd-catalyzed non-Heck cross-couplings.<sup>27</sup> Inspired by these other successes using phosphoramidites, we sought to evaluate more members of the ligand family under our previously optimized reaction conditions. In a first generation approach, incorporation of simple amine groups into the phosphoramidite framework provided measurable asymmetric induction (Figure 2.6, **L67–L69**). In a second generation of ligand synthesis, we reasoned that phosphoramidites bearing chiral amines might better impart high levels of enantioinduction. Gratifyingly, phosphoramidite **L70** delivered ketone **18a** in 72% yield and 32% ee, while the ligand diastereomer **L71** only provided the product in 25% ee. A structure-activity study revealed the important nature of both the phenyl rings and the chiral centers on the amine (**L72–L76**). Replacement of the phenyl groups with other aromatic moieties did not succeed in increasing the enantioselectivity of the Fukuyama coupling (**L77–L79**). Lastly, chiral diaryl pyrrolidines, acting as tethered analogues of **L70**, resulted in reduced ee's of ketone **18a** (**L80** and **L81**). Having identified an optimal amine substituent, third generation ligands were prepared with substitution at the 3,3' position on the BINOL backbone. In all cases, substitution delivered ketone **18a** in lower

**Figure 2.6.** Phosphoramidite ligands in the Fukuyama cross-coupling.

Backbone for First and Second Generation Ligands



Backbone for Third Generation Ligands



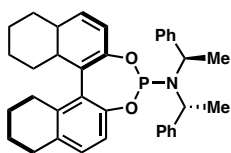
First Generation Ligands - Simple Amines

Entry	NR <sub>2</sub>	Ligand	Yield (%)	ee (%)
1		L65	61	0
2		L67	35	12
3		L68	35	8
4		L69	53	2

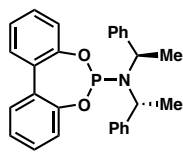
Third Generation Ligands - BINOL Substitution

Entry	R	Ligand	Yield (%)	ee (%)
1	Me	L82	19	1
2	Ph	L83	15	9
3	F	L84	20	10

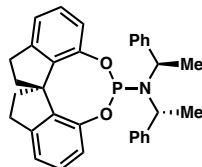
Fourth Generation Ligands - Other Backbones



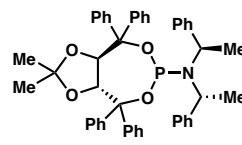
L85  
82% yield  
27% ee



L86  
76% yield  
12% ee



L87  
21% yield  
23% ee



L88  
16% yield  
7% ee

Second Generation Ligands - Chiral Amines

Entry	NR <sub>2</sub>	Ligand	Yield (%)	ee (%)
1		L70	72	32
2		L71	58	25
3		L72	61	28
4		L73	66	32
5		L74	55	20
6		L75	39	19
7		L76	51	12
8		L77	41	17
9		L78	56	27
10		L79	68	23
11		L80	63	20
12		L81	52	19

yield and ee than when **L70** was utilized (**L82–L84**). Fourth generation ligands focused on novel backbone structures: the octahydro-BINOL backbone provided similar results to **L70**, while a biphenyl backbone provided ketone **18a** in lower ee, illustrating the importance of an interplay between both the central and axial chirality of **L70**. Spirocyclic and TADDOL backbones also did not form product in greater ee than **L70**.

**Table 2.5.** TADDOL-Based phosphoramidites in the Fukuyama cross-coupling.

Entry	NR <sub>2</sub>	Ligand	Yield (%)	ee (%)	Entry	NR <sub>2</sub>	Ligand	Yield (%)	ee (%)
1		L55	83	24	5		L92	39	21
2		L89	72	28	6		L93	66	19
3		L90	16	6	7		L94	55	19
4		L91	16	-11	8		L95	83	24

Entry	NR <sub>2</sub>	Ligand	Yield (%)	ee (%)
9		L96	43	9
10		L97	51	7

For entries 1–8:

For entries 9 and 10:

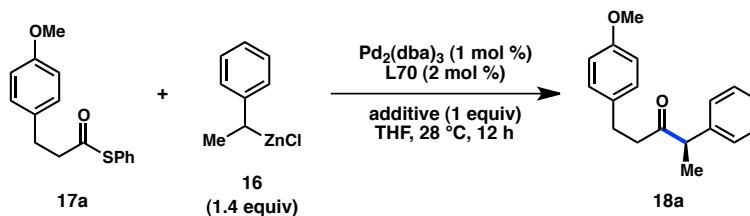
Ar = 2-naphthyl

While only low enantioinduction could be achieved with BINOL-based phosphoramidites, commercially-available TADDOL-based ligand **L55** delivered a promising 83% yield and 24% ee of ketone **18a** (Table 2.5, entry 1). Unfortunately, evaluation of a series of TADDOL-based phosphoramidites bearing simple amines did not significantly raise the level of asymmetric induction (**L89–L95**). Utilization of a bulkier TADDOL backbone, as in the case of **L96** and **L97**, led to a reduction in

enantioselectivity. In contrast to the BINOL-based ligands, use of chiral amine groups did not lead to an increase in the ee of ketone **18a** (see Figure 2.6, **L88**).

As phosphoramidite **L70** furnished ketone **18a** in the greatest ee, we began to explore **L70** with other parameters to enhance the asymmetric induction. Altering the catalyst loading, Pd:L ratio, Pd source, and solvent gave little improvement in ee. Use of either an analogous *S*-ethyl thioester or an acid chloride generated ketone products in similar ee's, suggesting that these leaving groups have little effect on the stereochemistry-determining step.

**Table 2.6.** Effect of zinc halides on enantioinduction.

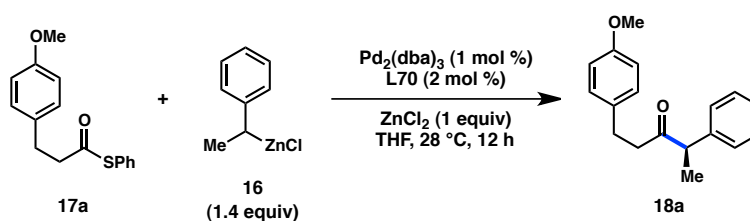


Entry	Additive	Yield (%)	ee (%)
1	none	51	22
2	$\text{ZnF}_2$	59	28
3	$\text{ZnCl}_2$	68	31
4	$\text{ZnBr}_2$	77	27
5	$\text{ZnI}_2$	79	12

A series of salts were assessed to evaluate the role of inorganic additives on enantioinduction.  $\text{ZnCl}_2$  was observed to have a positive effect on the ee of ketone **18a** when compared with no additive (Table 2.6, entries 1 and 3). While  $\text{ZnBr}_2$  and  $\text{ZnI}_2$  gave slightly improved yields of the ketone product, the ee decreased to 27% and 12%, respectively (entries 4 and 5). This observed counterion effect may result from an exchange of the halide moiety of organozinc **16**: less electronegative counterions on **16** would increase the covalency of the C–Zn bond, hindering its propensity to invert and

establish a DKR. Polar additives have also been shown to increase enantioselectivity in organozinc additions to aldehydes by sequestering diorganozinc species that contribute to background reactivity. Unfortunately, NMP nearly shut down the reaction, DMF decreased the ee, and TMEDA had little effect on the reaction outcome. To date  $\text{ZnCl}_2$  remains the most potent additive for increasing the enantioselectivity of the reaction.

**Table 2.7.** Understanding the origin of enantioinduction.



Effect of conversion on ee:

Entry	Time (h)	Conversion (%)	ee (%)
1	0.25	20	30
2	3	73	30
3	23	100	28

Effect of equivalents of organozinc reagent on ee:

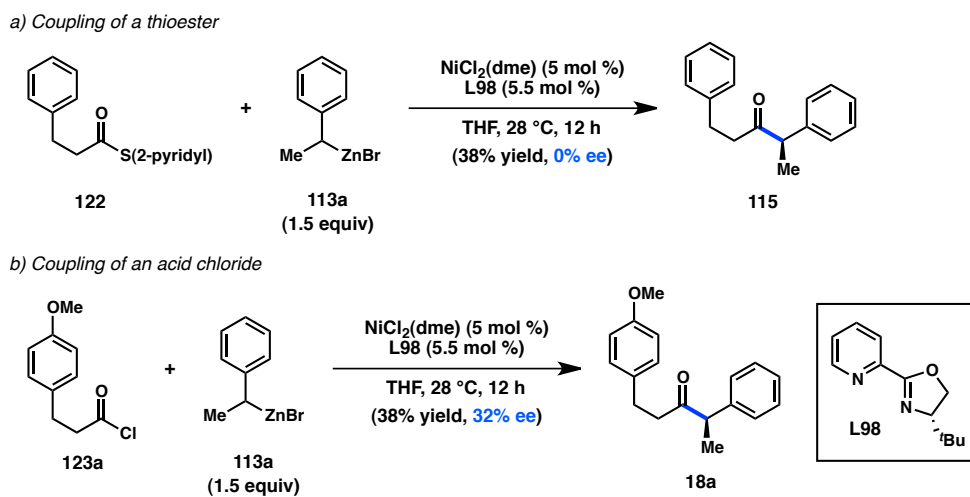
Entry	Equivalents	Yield (%)	ee (%)
1	1.2	68	26
2	2.4	87	28
3	3.6	90	29

Several experiments have been conducted to better understand the origin of enantioinduction in this system. Measuring the enantioselectivity as a function of conversion reveals that asymmetric induction is independent of reaction progress (Table 2.7). This result supports enantioinduction arising from a DYKAT instead of a simple kinetic resolution, as simple kinetic resolutions often lead to erosion of ee as all the starting material is consumed. It has also been determined that the ee of ketone **18a** is independent of the organozinc loading. If interconversion of the enantiomers of **16** was slow and a simple kinetic resolution was taking place, then addition of excess reagent would be expected to increase the enantioselectivity of the transformation significantly. Taken together, these results suggest that the asymmetric transformation proceeds

according to a DYKAT instead of a simple kinetic resolution. To date, there is not enough data to determine whether a fast racemization of organozinc **16** relative to transmetalation (as in a DKR) or a subsequent epimerization of diastereomeric Pd complexes is the cause of the enantioinduction. Likewise, further studies are necessary to determine whether the stereochemistry-determining step is transmetalation or reductive elimination.

A preliminary study of an asymmetric Ni-catalyzed acyl cross-coupling was conducted with an array of chiral bidentate nitrogen ligands. In the presence of 2-pyridyl thioester **122**, moderate yields but no enantioinduction was observed for all ligands that were tested (Scheme 2.2). Surprisingly, treatment of acid chloride **123a** with <sup>t</sup>Bu-PyOx (**L98**) delivered ketone **18a** in 38% yield and 32% ee. Other chiral ligands, including additional members of the PyOx ligand family, failed to impart any asymmetric induction. These results illustrate the non-innocent nature of the 2-pyridyl leaving group in this asymmetric cross-coupling.

**Scheme 2.2.** Asymmetric Ni-catalyzed acyl cross-coupling.



## 2.4 CONCLUDING REMARKS

In conclusion, a practical method for the Pd-catalyzed Fukuyama cross-coupling of thioesters and *secondary* organozinc reagents has been developed. The Pd<sub>2</sub>(dba)<sub>3</sub>/PCy<sub>3</sub>/ZnCl<sub>2</sub> system furnishes high yields of complex ketone products in a convergent fashion. These conditions also allow for the Negishi coupling of aryl acid chlorides to proceed in high yield. An analysis of chiral ligands revealed that modestly enantioenriched ketone products could be achieved in the presence of a chiral phosphoramidite ligand. Mechanistic studies currently favor a DYKAT instead of a simple kinetic resolution to explain the origin of enantioinduction. Efforts to increase the synthetic utility of the Fukuyama coupling and further extension to asymmetric catalysis are ongoing in our laboratory.

## 2.5 EXPERIMENTAL SECTION

### 2.5.1 *Materials and Methods*

Unless otherwise stated, reactions were performed under a nitrogen atmosphere using freshly dried solvents. Tetrahydrofuran (THF) and methylene chloride (CH<sub>2</sub>Cl<sub>2</sub>) were dried by passing through activated alumina columns. Triethylamine (Et<sub>3</sub>N) was distilled over calcium hydride prior to use. Unless otherwise stated, chemicals and reagents were used as received. Pd<sub>2</sub>(dba)<sub>3</sub> and PCy<sub>3</sub> were purchased from Aldrich and used as received. Phosphoramidite ligands were either purchased from Aldrich or synthesized according to literature procedures. All reactions were monitored by thin-layer chromatography using EMD/Merck silica gel 60 F254 pre-coated plates (0.25 mm) and were visualized by UV,

*p*-anisaldehyde, or KMnO<sub>4</sub> staining. Flash column chromatography was performed as described by Still et al.<sup>28</sup> using silica gel (particle size 0.032-0.063) purchased from Silicycle. <sup>1</sup>H and <sup>13</sup>C NMR spectra were recorded on a Varian 400 MR (at 400 MHz and 101 MHz, respectively) or a Varian Inova 500 (at 500 MHz and 126 MHz, respectively), and are reported relative to internal chloroform (<sup>1</sup>H, δ = 7.26, <sup>13</sup>C, δ = 77.0). Data for <sup>1</sup>H NMR spectra are reported as follows: chemical shift (δ ppm) (multiplicity, coupling constant (Hz), integration). Multiplicity and qualifier abbreviations are as follows: s = singlet, d = doublet, t = triplet, q = quartet, m = multiplet, br = broad. IR spectra were recorded on a Perkin Elmer Paragon 1000 spectrometer and are reported in frequency of absorption (cm<sup>-1</sup>). Analytical SFC was performed with a Mettler SFC supercritical CO<sub>2</sub> analytical chromatography system with Chiralcel AD-H, OD-H, AS-H, OB-H, and OJ-H columns (4.6 mm x 25 cm). HRMS were acquired using an Agilent 6200 Series TOF with an Agilent G1978A Multimode source in electrospray ionization (ESI), atmospheric pressure chemical ionization (APCI), or mixed (MM) ionization mode.

### 2.5.2 Substrate Synthesis

#### General Procedure 1 for Synthesis of Thioesters

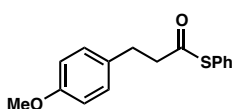
According to the protocol of Tanabe and coworkers,<sup>29</sup> a flask was charged with 3-(4-methoxyphenyl)propionic acid (58.2 mmol, 1 equiv) followed by MeCN (60 mL) and *N*-methyl imidazole (174.6 mmol, 3 equiv). The solution was cooled to 0 °C and tosyl chloride (1.5 M solution in MeCN, 87.3 mmol, 1.5 equiv) was added. The reaction was stirred at 0 °C under N<sub>2</sub> for 0.5 h, after which time thiophenol (1.0 M solution in MeCN,

58.2 mmol, 1 equiv) was added. The reaction was stirred at 0 °C under N<sub>2</sub> for 2 h and then allowed to warm to room temperature. The resulting solution was diluted with ether and water. The aqueous layer was extracted with ether and the combined organic layers were washed with water, dried (MgSO<sub>4</sub>), filtered, and concentrated. The crude residue was purified by silica gel chromatography.

### General Procedure 2 for Synthesis of Thioesters

A flame-dried flask was charged with 4-cyanobenzoic acid (5.8 mmol, 1 equiv) and CH<sub>2</sub>Cl<sub>2</sub> (12 mL). The reaction was cooled to 0 °C and isobutyl chloroformate (6.38 mmol, 1.1 equiv) and Et<sub>3</sub>N (5.8 mmol, 1 equiv) were added dropwise. The resulting mixture was stirred vigorously for 10 min under N<sub>2</sub>, after which time Et<sub>3</sub>N (5.8 mmol, 1 equiv) and thiophenol (12.76 mmol, 2.2 equiv) were added dropwise. The reaction was stirred at 0 °C under N<sub>2</sub> for 1 h. The reaction was warmed to room temperature and washed with 1 M HCl, water, 1 M NaOH, water, and brine. The combined aqueous layers were extracted with CH<sub>2</sub>Cl<sub>2</sub>. The combined organic layers were dried (MgSO<sub>4</sub>), filtered, and concentrated. The crude residue was purified by column chromatography.

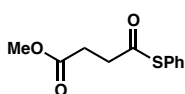
### S-Phenyl 3-(4-methoxyphenyl)propanethioate (17a)



Prepared from 3-(4-methoxyphenyl)propionic acid (10.5 g, 58.2 mmol) following General Procedure 1. The crude residue was purified by silica gel chromatography (2:98 to 10:90 EtOAc:hexanes) to yield 13.19 g (83% yield) of **17a** as a white solid, mp 31 – 32 °C. <sup>1</sup>H NMR (500 MHz, CDCl<sub>3</sub>) δ 7.47 – 7.36 (m, 5H), 7.18 – 7.09 (m, 2H), 6.89 – 6.81 (m, 2H), 3.80 (s, 3H), 3.03 – 2.89 (m, 4H);

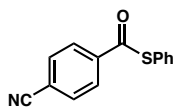
$^{13}\text{C}$  NMR (125 MHz,  $\text{CDCl}_3$ )  $\delta$  196.7, 158.1, 134.5, 131.9, 129.3, 129.2, 129.1, 127.6, 113.9, 55.2, 45.4, 30.5; IR (NaCl/thin film): 2932, 2834, 1706, 1611, 1512, 1477, 1440, 1247  $\text{cm}^{-1}$ ; HRMS (MM) calc'd for  $[\text{M}-\text{H}]^-$  271.0798, found 271.0799.

#### Methyl 4-oxo-4-(phenylthio)butanoate (**17d**)



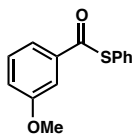
Prepared from monomethyl succinate (2.56 g, 19.4 mmol) following General Procedure 1. The crude residue was purified by silica gel chromatography (2:98 to 20:80 EtOAc:hexanes) to yield 2.21 g (51% yield) of **17d** as a slightly yellow oil.  $^1\text{H}$  NMR (500 MHz,  $\text{CDCl}_3$ )  $\delta$  7.46 – 7.36 (m, 5H), 3.69 (s, 3H), 3.00 (t,  $J = 6.9$  Hz, 2H), 2.69 (t,  $J = 6.9$  Hz, 2H);  $^{13}\text{C}$  NMR (125 MHz,  $\text{CDCl}_3$ )  $\delta$  196.14, 172.2, 134.5, 129.5, 129.2, 127.2, 51.9, 38.0, 28.9; IR (NaCl/thin film): 3061, 2997, 2952, 1739, 1707, 1478, 1440  $\text{cm}^{-1}$ ; HRMS (MM) calc'd for  $[\text{M}-\text{H}]^-$  223.0434, found 223.0285.

#### S-Phenyl 4-cyanobenzothioate (**17g**)



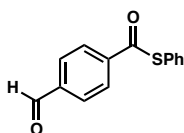
Prepared from 4-cyanobenzoic acid (859 mg, 5.8 mmol) following General Procedure 2. The crude residue was recrystallized from ether to yield 991 mg (71% yield) of **17g** as a slightly yellow solid, mp 127 – 129  $^\circ\text{C}$ .  $^1\text{H}$  NMR (500 MHz,  $\text{CDCl}_3$ ) 8.17 – 8.06 (m, 2H), 7.84 – 7.76 (m, 2H), 7.57 – 7.44 (m, 5H);  $^{13}\text{C}$  NMR (125 MHz,  $\text{CDCl}_3$ )  $\delta$  189.1, 139.8, 134.9, 132.6, 130.0, 129.5, 127.9, 126.2, 117.8, 116.9; IR (NaCl/thin film): 3089, 2231, 1683, 1668, 1479, 1404, 1207, 1172  $\text{cm}^{-1}$ ; HRMS (MM) calc'd for  $[\text{M}-\text{H}]^-$  238.0332, found 238.0327.

### S-Phenyl 3-methoxybenzothioate (17i)



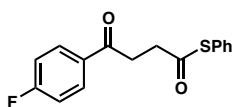
Prepared from 3-methoxybenzoic acid (2.95 g, 19.4 mmol) following General Procedure 1. The crude residue was purified by silica gel chromatography (2:98 to 20:80 EtOAc:hexanes) to yield 2.41 g (51% yield) of **17i** as a slightly yellow oil.  $^1\text{H}$  NMR (500 MHz,  $\text{CDCl}_3$ )  $\delta$  7.70 – 7.63 (m, 1H), 7.57 – 7.35 (m, 7H), 7.16 (ddd,  $J = 8.2, 2.6, 0.9$  Hz, 1H), 3.87 (s, 3H);  $^{13}\text{C}$  NMR (125 MHz,  $\text{CDCl}_3$ )  $\delta$  190.1, 159.8, 137.9, 135.0, 129.7, 129.5, 129.3, 129.2, 127.3, 120.0, 111.7, 55.5; IR (NaCl/thin film): 3060, 3004, 2938, 2835, 1679, 1597, 1583, 1484, 1440, 1288, 1260  $\text{cm}^{-1}$ ; HRMS (MM) calc'd for  $[\text{M}-\text{H}]^-$  242.0485, found 242.0462.

### S-Phenyl 4-formylbenzothioate (17l)



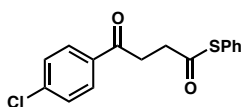
Prepared from 4-formylbenzoic acid (870 mg, 5.8 mmol) following General Procedure 1. The crude residue was purified by silica gel chromatography (2:98 EtOAc:hexanes) to yield 88 mg (6% yield) of **17l** as a white solid.  $^1\text{H}$  NMR (500 MHz,  $\text{CDCl}_3$ )  $\delta$  10.12 (s, 1H), 8.22 – 8.12 (m, 2H), 8.06 – 7.95 (m, 2H), 7.58 – 7.43 (m, 5H);  $^{13}\text{C}$  NMR (125 MHz,  $\text{CDCl}_3$ )  $\delta$  191.4, 189.6, 141.0, 139.4, 134.9, 129.9 (2C), 129.4, 128.0, 126.6; IR (NaCl/thin film): 3064, 2844, 2744, 1700, 1676, 1575, 1438, 1383, 1198  $\text{cm}^{-1}$ ; HRMS (MM) calc'd for  $[\text{M}-\text{CHO}]^-$  213.0374, found 213.0373.

**S-Phenyl 4-(4-fluorophenyl)-4-oxobutanethioate (17m)**



Prepared from 3-(4-fluorobenzoyl)propionic acid (1.14 g, 5.8 mmol) following General Procedure 2. The crude residue was purified by silica gel chromatography (2:98 to 20:80 EtOAc:hexanes) to yield 1.44 g (86% yield) of **17m** as a slightly yellow oil.  $^1\text{H}$  NMR (500 MHz,  $\text{CDCl}_3$ )  $\delta$  8.05 – 7.94 (m, 2H), 7.49 – 7.35 (m, 5H), 7.19 – 7.07 (m, 2H), 3.34 (t,  $J = 6.6$  Hz, 2H), 3.14 (t,  $J = 6.6$  Hz, 2H);  $^{13}\text{C}$  NMR (125 MHz,  $\text{CDCl}_3$ )  $\delta$  196.8, 195.9, 165.8 (d,  $J_{\text{C-F}} = 254.8$  Hz), 134.5, 132.8, 130.7 (d,  $J_{\text{C-F}} = 9.0$  Hz), 129.4, 129.2, 127.5, 115.7 (d,  $J_{\text{C-F}} = 21.8$  Hz), 37.3, 33.3; IR (NaCl/thin film): 3075, 2915, 1705, 1687, 1597, 1506, 1478, 1441, 1409, 1234  $\text{cm}^{-1}$ ; HRMS (MM) calc'd for  $[\text{M-H}]^-$  287.0548, found 287.0542.

**S-Phenyl 4-(4-chlorophenyl)-4-oxobutanethioate (17n)**



Prepared from 3-(4-chlorobenzoyl)propionic acid (1.23 g, 5.8 mmol) following General Procedure 2. The crude residue was purified by silica gel chromatography (2:98 to 20:80 EtOAc:hexanes) to yield 1.08 g (61% yield) of **17n** as a slightly yellow oil.  $^1\text{H}$  NMR (500 MHz,  $\text{CDCl}_3$ )  $\delta$  7.97 – 7.85 (m, 2H), 7.48 – 7.35 (m, 7H), 3.33 (t,  $J = 6.6$  Hz, 2H), 3.14 (t,  $J = 6.5$  Hz, 2H);  $^{13}\text{C}$  NMR (125 MHz,  $\text{CDCl}_3$ )  $\delta$  196.7, 196.3, 139.7, 134.6, 134.5, 129.4, 129.3, 129.2, 128.9, 127.4, 37.2, 33.4; IR (NaCl/thin film): 3060, 2914, 1706, 1685, 1590, 1478, 1441, 1400  $\text{cm}^{-1}$ ; HRMS (MM) calc'd for  $[\text{M+H}]^+$  305.0398, found 305.0406.

### **Preparation of Organozinc 16**

According to the protocol of Orito and coworkers,<sup>30</sup> a flame-dried Schlenk flask was charged with zinc dust (2.80 g, 42.6 mmol, 1.5 equiv), TMSCl (0.14 mL, 1.12 mmol, 0.04 equiv), and THF (14 mL). The reaction was stirred at room temperature under N<sub>2</sub> for 15 min. To the reaction was added (1-chloroethyl)benzene (4.00 g, 28.4 mmol, 1 equiv) dropwise. The reaction was stirred at 40 °C under N<sub>2</sub> for 4 h. The mixture was cooled to room temperature and the excess zinc dust was allowed to settle. The solution was titrated with I<sub>2</sub> according to Knochel and coworkers.<sup>31</sup> The yellow organozinc solution was transferred to a flame-dried flask and stored under N<sub>2</sub> at –20 °C. Concentrations of 1.0 M were obtained.

### **General Procedure for Synthesis of Phosphoramidite Ligands**

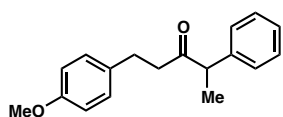
A flame-dried flask was charged with PCl<sub>3</sub> (1 mmol, 1 equiv) and CH<sub>2</sub>Cl<sub>2</sub> (5 mL). The reaction was cooled to 0 °C and Et<sub>3</sub>N (5 mmol, 5 equiv) was added dropwise, followed by addition of amine (1 mmol, 1 equiv). The reaction was stirred at 23 °C under N<sub>2</sub> for 5 h. Diol (1 mmol, 1 equiv) was added and the reaction was stirred at 23 °C under N<sub>2</sub> for 11 h. The reaction was filtered and concentrated. The crude residue was purified by column chromatography (100% CH<sub>2</sub>Cl<sub>2</sub>) to obtain a white foamy solid.

### **2.5.3 General Procedure for Fukuyama Cross-Coupling Reaction**

In a glovebox, a vial was charged with Pd<sub>2</sub>(dba)<sub>3</sub> (0.002 mmol, 0.01 equiv), PCy<sub>3</sub> (0.004 mmol, 0.02 equiv), and THF (1 mL). The deep purple solution was stirred at 28 °C for 10

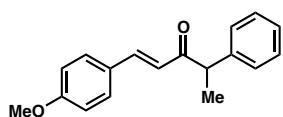
min. The thioester substrate **17** (0.2 mmol, 1 equiv), the (1-phenylethyl)zinc(II) chloride (**16**, 1.0 M THF, 0.28 mmol, 1.4 equiv), and ZnCl<sub>2</sub> (1.0 M THF, 0.2 mmol, 1 equiv) were added to the reaction. The reaction was stirred at 28 °C for 12 h, after which time it was removed from the glovebox, quenched with 0.1 mL sat. aq. NH<sub>4</sub>Cl, dried (MgSO<sub>4</sub>), filtered, and concentrated. The crude residue was purified by silica gel chromatography.

### 1-(4-methoxyphenyl)-4-Phenylpentan-3-one (**18a**)



Prepared from *S*-phenyl 3-(4-methoxyphenyl)propanethioate (**17a**, 54.1 mg, 0.2 mmol). The crude residue was purified by silica gel chromatography (2:98 to 20:80 EtOAc:hexanes) to yield 46.8 mg (87% yield) of **18a** as a slightly yellow oil. <sup>1</sup>H NMR (500 MHz, CDCl<sub>3</sub>) δ 7.37 – 7.21 (m, 3H), 7.22 – 7.14 (m, 2H), 7.05 – 6.96 (m, 2H), 6.84 – 6.75 (m, 2H), 3.79 (s, 3H), 3.72 (q, *J* = 7.0 Hz, 1H), 2.88 – 2.57 (m, 4H), 1.39 (d, *J* = 7.0 Hz, 3H); <sup>13</sup>C NMR (125 MHz, CDCl<sub>3</sub>) δ 210.0, 157.8, 140.4, 133.0, 129.2, 128.9, 127.8, 127.1, 113.7, 55.2, 53.2, 42.8, 29.1, 17.3; IR (NaCl/thin film): 3060, 3027, 2973, 2931, 2834, 1713, 1611, 1513, 1493, 1452, 1300, 1247 cm<sup>-1</sup>; HRMS (MM) calc'd for [M-H]<sup>-</sup> 267.1391, found 267.1391.

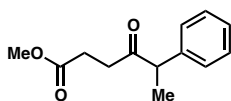
### (*E*)-1-(4-methoxyphenyl)-4-Phenylpent-1-en-3-one (**18b**)



Prepared from (*E*)-*S*-phenyl 3-(4-methoxyphenyl)prop-2-enethioate (**17b**, 54.1 mg, 0.2 mmol). The crude residue was purified by silica gel chromatography (2:98 to 20:80 EtOAc:hexanes) to yield 52.0 mg (98% yield) of **18b** as a slightly yellow oil. <sup>1</sup>H NMR (500 MHz, CDCl<sub>3</sub>) δ 7.59 (d, *J* = 15.9 Hz, 1H), 7.47 – 7.39 (m, 2H), 7.37 – 7.19 (m, 5H), 6.91 – 6.80 (m, 2H), 6.60 (d, *J* =

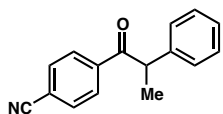
15.9 Hz, 1H), 4.01 (q,  $J = 6.9$  Hz, 1H), 3.81 (s, 3H), 1.49 (d,  $J = 6.9$  Hz, 3H);  $^{13}\text{C}$  NMR (125 MHz,  $\text{CDCl}_3$ )  $\delta$  199.4, 161.4, 142.4, 140.9, 130.0, 128.9, 128.0, 127.2, 127.0, 122.4, 114.2, 55.3, 51.7, 17.9; IR (NaCl/thin film): 2971, 2930, 2837, 1684, 1654, 1598, 1572, 1511, 1254  $\text{cm}^{-1}$ ; HRMS (MM) calc'd for  $[\text{M}-\text{H}]^-$  265.1234, found 265.1239.

#### Methyl 4-oxo-5-phenylhexanoate (18d)



Prepared from methyl 4-oxo-4-(phenylthio)butanoate (**17d**, 44.9 mg, 0.2 mmol). The crude residue was purified by silica gel chromatography (2:98 to 20:80 EtOAc:hexanes) to yield 30.3 mg (69% yield) of **18d** as a slightly yellow oil.  $^1\text{H}$  NMR (500 MHz,  $\text{CDCl}_3$ )  $\delta$  7.39 – 7.16 (m, 5H), 3.79 (q,  $J = 7.0$  Hz, 1H), 3.63 (s, 3H), 2.77 – 2.38 (m, 4H), 1.41 (d,  $J = 7.0$  Hz, 3H);  $^{13}\text{C}$  NMR (125 MHz,  $\text{CDCl}_3$ )  $\delta$  209.0, 173.2, 140.4, 128.9, 127.9, 127.2, 52.9, 51.7, 35.6, 27.9, 17.3; IR (NaCl/thin film): 3062, 3027, 2977, 2952, 2932, 1739, 1716, 1494, 1453, 1437, 1372, 1356, 1211  $\text{cm}^{-1}$ ; HRMS (MM) calc'd for  $[\text{M}+\text{H}]^+$  221.1172, found 221.1173.

#### 4-(2-phenylpropanoyl)Benzonitrile (18g)

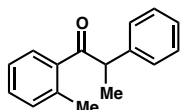


Prepared from *S*-phenyl 4-cyanobenzothioate (**17g**, 47.9 mg, 0.2 mmol). The crude residue was purified by silica gel chromatography (2:98 to 20:80 EtOAc:hexanes) to yield 40.8 mg (87% yield) of **18g** as a slightly yellow oil.  $^1\text{H}$  NMR (500 MHz,  $\text{CDCl}_3$ )  $\delta$  8.04 – 7.94 (m, 2H), 7.71 – 7.61 (m, 2H), 7.39 – 7.17 (m, 5H), 4.61 (q,  $J = 6.8$  Hz, 1H), 1.54 (d,  $J = 6.8$  Hz, 3H);  $^{13}\text{C}$  NMR (125 MHz,  $\text{CDCl}_3$ )  $\delta$  198.8, 140.4, 139.5, 132.3, 129.3, 129.1, 127.6, 127.3, 117.9, 115.9, 48.6, 19.3; IR

(NaCl/thin film): 3061, 2976, 2930, 2230, 1685, 1600, 1452, 1404, 1218, 1199  $\text{cm}^{-1}$ ;

HRMS (MM) calc'd for  $[\text{M}-\text{H}]^-$  234.0924, found 234.0932.

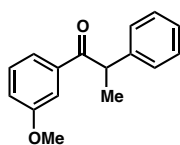
### 2-Phenyl-1-(*o*-tolyl)propan-1-one (**18h**)



Prepared from *S*-phenyl 2-methylbenzothioate (**17h**, 45.7 mg, 0.2 mmol).

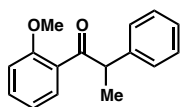
The crude residue was purified by silica gel chromatography (2:98 EtOAc:hexanes) to yield 35.6 mg (79% yield) of **18h** as a slightly yellow oil.  $^1\text{H}$  NMR (500 MHz,  $\text{CDCl}_3$ )  $\delta$  7.53 (d,  $J = 7.7$  Hz, 1H), 7.36 – 7.06 (m, 8H), 4.53 (q,  $J = 6.9$  Hz, 1H), 2.34 (s, 3H), 1.55 (d,  $J = 6.9$  Hz, 3H);  $^{13}\text{C}$  NMR (125 MHz,  $\text{CDCl}_3$ ) 204.6, 140.4, 138.5, 137.8, 131.5, 130.7, 128.8, 127.9, 127.8, 126.9, 125.3, 50.7, 20.8, 18.5; IR (NaCl/thin film): 3061, 3026, 2971, 2929, 2870, 1685, 1600, 1492, 1452, 1220  $\text{cm}^{-1}$ ; HRMS (MM) calc'd for  $[\text{M}-\text{H}]^-$  238.1128, found 238.1128.

### 1-(3-methoxyphenyl)-2-Phenylpropan-1-one (**18i**)



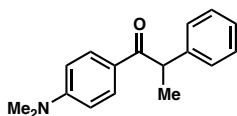
Prepared from *S*-phenyl 3-methoxybenzothioate (**17i**, 48.9 mg, 0.2 mmol). The crude residue was purified by silica gel chromatography (2:98 EtOAc:hexanes) to yield 29.2 mg (61% yield) of **18i** as a slightly yellow oil.  $^1\text{H}$  NMR (500 MHz,  $\text{CDCl}_3$ )  $\delta$  7.56 – 7.44 (m, 2H), 7.34 – 7.25 (m, 5H), 7.24 – 7.15 (m, 1H), 7.02 (ddd,  $J = 8.2, 2.7, 0.9$  Hz, 1H), 4.67 (q,  $J = 6.9$  Hz, 1H), 3.80 (s, 3H), 1.53 (d,  $J = 6.8$  Hz, 3H);  $^{13}\text{C}$  NMR (125 MHz,  $\text{CDCl}_3$ )  $\delta$  200.1, 159.7, 141.5, 137.8, 129.4, 129.0, 127.7, 126.9, 121.4, 119.3, 113.1, 55.3, 48.0, 19.5; IR (NaCl/thin film): 3062, 3025, 2973, 2930, 2835, 1681, 1596, 1581, 1488, 1451, 1426, 1263  $\text{cm}^{-1}$ ; HRMS (MM) calc'd for  $[\text{M}-\text{H}]^-$  239.1078, found 239.1088.

### 1-(2-methoxyphenyl)-2-Phenylpropan-1-one (18j)



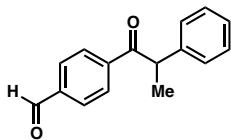
Prepared from *S*-phenyl 2-methoxybenzothioate (**17j**, 48.9 mg, 0.2 mmol). The crude residue was purified by silica gel chromatography (2:98 EtOAc:hexanes) to yield 19.2 mg (40% yield) of **18j** as a slightly yellow oil. <sup>1</sup>H NMR (500 MHz, CDCl<sub>3</sub>) δ 7.48 (dd, *J* = 7.6, 1.8 Hz, 1H), 7.39 (ddd, *J* = 8.3, 7.3, 1.8 Hz, 1H), 7.34 – 7.13 (m, 5H), 6.95 – 6.89 (m, 2H), 4.75 (q, *J* = 7.0 Hz, 1H), 3.88 (s, 3H), 1.54 (d, *J* = 6.9 Hz, 3H); <sup>13</sup>C NMR (125 MHz, CDCl<sub>3</sub>) δ 204.1, 157.5, 141.3, 135.1, 132.7, 130.4, 128.4, 128.1, 126.6, 120.5, 111.3, 55.3, 51.8, 18.7; IR (NaCl/thin film): 2929, 1736, 1666, 1597, 1485, 1466, 1284, 1245, 1198 cm<sup>-1</sup>; HRMS (MM) calc'd for [M+H]<sup>+</sup> 241.1223, found 241.1223.

### 1-(4-(dimethylamino)phenyl)-2-Phenylpropan-1-one (18k)



Prepared from *S*-phenyl 4-(dimethylamino)benzothioate (**17k**, 51.5 mg, 0.2 mmol). The crude residue was purified by silica gel chromatography (2:98 to 20:80 EtOAc:hexanes) to yield 24.4 mg (48% yield) of **18k** as a slightly yellow oil. <sup>1</sup>H NMR (500 MHz, CDCl<sub>3</sub>) δ 7.95 – 7.85 (m, 2H), 7.36 – 7.23 (m, 4H), 7.23 – 7.13 (m, 1H), 6.62 – 6.55 (m, 2H), 4.64 (q, *J* = 6.9 Hz, 1H), 3.00 (s, 6H), 1.51 (d, *J* = 6.9 Hz, 3H); <sup>13</sup>C NMR (125 MHz, CDCl<sub>3</sub>) δ 198.3, 153.1, 142.6, 131.0, 130.9, 128.7, 126.5, 124.3, 110.6, 46.9, 39.9, 19.6; IR (NaCl/thin film): 3027, 2974, 2928, 2820, 1651, 1615, 1492, 1448, 1234, 1198 cm<sup>-1</sup>; HRMS (MM) calc'd for [M+H]<sup>+</sup> 254.1539, found 254.1543.

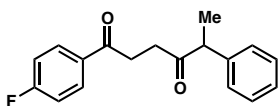
#### 4-(2-phenylpropanoyl)Benzaldehyde (**18l**)



Prepared from *S*-phenyl 4-formylbenzothioate (**17l**, 48.5 mg, 0.2 mmol). The crude residue was purified by silica gel chromatography (2:98 to 20:80 EtOAc:hexanes) to yield 33.7 mg (71% yield) of **18l**

as a slightly yellow oil.  $^1\text{H}$  NMR (500 MHz,  $\text{CDCl}_3$ )  $\delta$  10.03 (s, 1H), 8.11 – 7.98 (m, 2H), 7.95 – 7.75 (m, 2H), 7.45 – 7.12 (m, 5H), 4.67 (q,  $J = 6.8$  Hz, 1H), 1.55 (d,  $J = 6.9$  Hz, 3H);  $^{13}\text{C}$  NMR (125 MHz,  $\text{CDCl}_3$ )  $\delta$  199.7, 191.5, 140.7, 138.6, 129.7, 129.2, 128.9, 127.7, 127.2, 126.8, 48.6, 19.3; IR (NaCl/thin film): 3060, 3026, 2975, 2929, 1700, 1684, 1606, 1452, 1219  $\text{cm}^{-1}$ ; HRMS (MM) calc'd for  $[\text{M}-\text{H}]^-$  237.0921, found 237.0909.

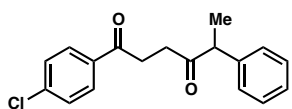
#### 1-(4-fluorophenyl)-5-Phenylhexane-1,4-dione (**18m**)



Prepared from *S*-phenyl 4-(4-fluorophenyl)-4-oxobutanethioate (**17m**, 57.7 mg, 0.2 mmol). The crude residue was purified by

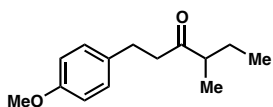
silica gel chromatography (2:98 to 10:90 EtOAc:hexanes) to yield 50.3 mg (88% yield) of **18m** as a slightly yellow oil.  $^1\text{H}$  NMR (500 MHz,  $\text{CDCl}_3$ )  $\delta$  8.03 – 7.92 (m, 2H), 7.41 – 7.33 (m, 2H), 7.30 – 7.21 (m, 3H), 7.16 – 7.05 (m, 2H), 3.90 (q,  $J = 7.0$  Hz, 1H), 3.28 (ddd,  $J = 18.1, 7.6, 5.8$  Hz, 1H), 3.06 (dt,  $J = 18.1, 6.0$  Hz, 1H), 2.88 (ddd,  $J = 18.2, 7.6, 5.7$  Hz, 1H), 2.72 (dt,  $J = 18.2, 6.0$  Hz, 1H), 1.44 (d,  $J = 7.0$  Hz, 3H);  $^{13}\text{C}$  NMR (125 MHz,  $\text{CDCl}_3$ )  $\delta$  209.5, 197.0, 165.7 (d,  $J_{\text{C-F}} = 254.4$  Hz), 140.6, 133.1, 130.7 (d,  $J_{\text{C-F}} = 9.1$  Hz), 128.9, 127.9, 127.2, 115.6 (d,  $J_{\text{C-F}} = 21.8$  Hz), 53.1, 34.8, 32.5, 17.4; IR (NaCl/thin film): 2975, 2913, 1714, 1685, 1597, 1506, 1410, 1231  $\text{cm}^{-1}$ ; HRMS (MM) calc'd for  $[\text{M}-\text{H}]^-$  283.1140, found 283.1141.

### 1-(4-chlorophenyl)-5-Phenylhexane-1,4-dione (**18n**)



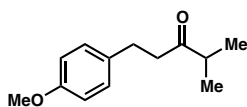
Prepared from *S*-phenyl 4-(4-chlorophenyl)-4-oxobutanethioate (**17n**, 61.0 mg, 0.2 mmol). The crude residue was purified by silica gel chromatography (2:98 to 10:90 EtOAc:hexanes) to yield 52.8 mg (88% yield) of **18n** as a slightly yellow oil. <sup>1</sup>H NMR (500 MHz, CDCl<sub>3</sub>) δ 7.91 – 7.83 (m, 2H), 7.48 – 7.22 (m, 7H), 3.89 (q, *J* = 7.0 Hz, 1H), 3.26 (ddd, *J* = 18.1, 7.5, 5.8 Hz, 1H), 3.04 (dt, *J* = 18.2, 5.9 Hz, 1H), 2.87 (ddd, *J* = 18.2, 7.6, 5.6 Hz, 1H), 2.72 (dt, *J* = 18.2, 6.0 Hz, 1H), 1.44 (d, *J* = 7.0 Hz, 3H); <sup>13</sup>C NMR (125 MHz, CDCl<sub>3</sub>) δ 209.5, 197.4, 140.6, 139.5, 134.9, 129.4, 128.9, 128.8, 127.9, 127.2, 53.1, 34.8, 32.5, 17.4; IR (NaCl/thin film): 3062, 3026, 2974, 2913, 1713, 1685, 1590, 1493, 1452, 1400, 1199 cm<sup>-1</sup>; HRMS (MM) calc'd for [M-H]<sup>-</sup> 299.0844, found 299.0870.

### 1-(4-methoxyphenyl)-4-Methylhexan-3-one (**18o**)



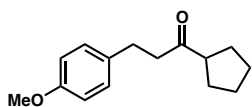
Prepared from *S*-phenyl 3-(4-methoxyphenyl)propanethioate (**17a**, 54.5 mg, 0.2 mmol) and Rieke organozinc **113b** (0.5 M THF, 0.56 mL, 0.28 mmol). The crude residue was purified by silica gel chromatography (5:95 EtOAc:hexanes) to yield 41.4 mg (94% yield) of **18o** as a slightly yellow oil. <sup>1</sup>H NMR (500 MHz, CDCl<sub>3</sub>) δ 7.15 – 7.05 (m, 2H), 6.87 – 6.76 (m, 2H), 3.78 (s, 3H), 2.83 (t, *J* = 7.2 Hz, 2H), 2.81 – 2.66 (m, 2H), 2.41 (h, *J* = 6.9 Hz, 1H), 1.71 – 1.58 (m, 1H), 1.44 – 1.29 (m, 1H), 1.03 (d, *J* = 6.9 Hz, 3H), 0.83 (t, *J* = 7.4 Hz, 3H); <sup>13</sup>C NMR (125 MHz, CDCl<sub>3</sub>) δ 213.9, 157.3, 133.4, 129.2, 113.8, 55.2, 48.0, 43.0, 28.8, 25.82, 15.7, 11.6; IR (NaCl/thin film): 2964, 2933, 2875, 2835, 1710, 1612, 1513, 1462, 1300, 1247 cm<sup>-1</sup>; HRMS (MM) calc'd for [M]<sup>+</sup> 220.1458, found 220.1414.

### 1-(4-methoxyphenyl)-4-Methylpentan-3-one (18p)



Prepared from *S*-phenyl 3-(4-methoxyphenyl)propanethioate (**17a**, 54.5 mg, 0.2 mmol) and Rieke organozinc **113c** (0.5 M THF, 0.56 mL, 0.28 mmol). The crude residue was purified by silica gel chromatography (5:95 EtOAc:hexanes) to yield 38.2 mg (92% yield) of **18p** as a slightly yellow oil.  $^1\text{H}$  NMR (500 MHz,  $\text{CDCl}_3$ )  $\delta$  7.13 – 7.06 (m, 2H), 6.87 – 6.78 (m, 2H), 3.78 (s, 3H), 2.87 – 2.78 (m, 2H), 2.78 – 2.68 (m, 2H), 2.56 (hept,  $J = 7.0$  Hz, 1H), 1.06 (d,  $J = 6.9$  Hz, 6H);  $^{13}\text{C}$  NMR (125 MHz,  $\text{CDCl}_3$ )  $\delta$  214.0, 157.8, 133.4, 129.2, 113.8, 55.2, 42.2, 41.0, 28.9, 18.1; IR (NaCl/thin film): 2968, 2933, 2873, 2835, 1710, 1612, 1513, 1465, 1300, 1246  $\text{cm}^{-1}$ ; HRMS (MM) calc'd for  $[\text{M}-\text{H}]^-$  205.1234, found 205.1575.

### 1-Cyclopentyl-3-(4-methoxyphenyl)propan-1-one (18q)



Prepared from *S*-phenyl 3-(4-methoxyphenyl)propanethioate (**17a**, 54.5 mg, 0.2 mmol) and Rieke organozinc **113d** (0.5 M THF, 0.56 mL, 0.28 mmol). The crude residue was purified by silica gel chromatography (5:95 EtOAc:hexanes) to yield 41.0 mg (88% yield) of **18q** as a slightly yellow oil.  $^1\text{H}$  NMR (500 MHz,  $\text{CDCl}_3$ )  $\delta$  7.15 – 7.05 (m, 2H), 6.87 – 6.78 (m, 2H), 3.78 (s, 3H), 2.88 – 2.76 (m, 3H), 2.78 – 2.69 (m, 2H), 1.84 – 1.49 (m, 8H);  $^{13}\text{C}$  NMR (125 MHz,  $\text{CDCl}_3$ )  $\delta$  212.4, 157.8, 133.4, 129.2, 113.8, 55.2, 51.5, 43.6, 29.0, 28.7, 25.9; IR (NaCl/thin film): 2953, 2868, 1707, 1612, 1513, 1300, 1247  $\text{cm}^{-1}$ ; HRMS (MM) calc'd for  $[\text{M}-\text{H}]^-$  233.1536, found 233.1530.

### **2.5.4 Procedure for Acid Chloride Cross-Coupling**

In a glovebox, a vial was charged with Pd<sub>2</sub>(dba)<sub>3</sub> (0.002 mmol, 0.01 equiv), PCy<sub>3</sub> (0.004 mmol, 0.02 equiv), and THF (1 mL). The deep purple solution was stirred at 28 °C for 10 min. Acid chloride **117** (0.2 mmol, 1 equiv) and Rieke organozinc bromide **113a** (0.5 M THF, 0.56 mmol, 1.4 equiv) were added to the reaction. The reaction was stirred at 28 °C for 12 h, after which time it was removed from the glovebox, quenched with 0.1 mL sat. NH<sub>4</sub>Cl, dried (MgSO<sub>4</sub>), filtered, and concentrated. The crude residue was purified by silica gel chromatography.

## 2.6 NOTES AND REFERENCES

- (1) For reviews on alkyl halides in cross-couplings: (a) Netherton, M. R.; Fu, G. C. *Adv. Synth. & Catal.* **2004**, *346*, 1525. (b) Frisch, A. C.; Beller, M. *Angew. Chem., Int. Ed.* **2005**, *44*, 674. (c) Rudolph, A.; Lautens, M. *Angew. Chem., Int. Ed.* **2009**, *48*, 2656. For a review on alkyl organometallics in cross-couplings: (d) Jana, R.; Pathak, T. P.; Sigman, M. S. *Chem. Rev.* **2011**, *111*, 1417.
- (2) Hayashi, T.; Konishi, M.; Kobori, Y.; Kumada, M.; Higuchi, T.; Hirotsu, K. *J. Am. Chem. Soc.* **1984**, *106*, 158.
- (3) Zhou, J.; Fu, G. C. *J. Am. Chem. Soc.* **2003**, *125*, 12527.
- (4) For selected examples of Ni-catalyzed C(sp<sup>3</sup>)-C(sp<sup>3</sup>) couplings: (a) Giovannini, R.; Stüdemann, T.; Dussin, G.; Knochel, P. *Angew. Chem., Int. Ed.* **1998**, *37*, 2387. (b) Giovannini, R.; Stüdemann, T.; Devasagayaraj, A.; Dussin, G.; Knochel, P. *J. Org. Chem.* **1999**, *64*, 3544. (c) Jensen, A. E.; Knochel, P. *J. Org. Chem.* **2001**, *67*, 79.
- (5) For selected Ni-catalyzed stereoconvergent cross-couplings of secondary alkyl electrophiles: (a) Fischer, C.; Fu, G. C. *J. Am. Chem. Soc.* **2005**, *127*, 4594. (b) Arp, F. O.; Fu, G. C. *J. Am. Chem. Soc.* **2005**, *127*, 10482. (c) Dai, X.; Strotman, N. A.; Fu, G. C. *J. Am. Chem. Soc.* **2008**, *130*, 3302. (d) Lundin, P. M.; Esquivias, J.; Fu, G. C. *Angew. Chem., Int. Ed.* **2009**, *48*, 154. (e) Lou, S.; Fu, G. C. *J. Am. Chem. Soc.* **2010**, *132*, 1264. (f) Lou, S.; Fu, G. C. *J. Am. Chem. Soc.* **2010**, *132*, 5010.
- (6) For selected examples of Pd-catalyzed cross-couplings of secondary alkyl organometallics: (a) Dreher, S. D.; Dormer, P. G.; Sandrock, D. L.; Molander, G. A. *J. Am. Chem. Soc.* **2008**, *130*, 9257. (b) Han, C.; Buchwald, S. L. *J. Am. Chem. Soc.* **2009**, *131*, 7532. (c) Joshi-Pangu, A.; Ganesh, M.; Biscoe, M. R. *Org. Lett.* **2011**, *13*, 1218. (d) Li, L.; Wang, C.-Y.; Huang, R.; Biscoe, M. R. *Nature Chem.* **2013**, *5*, 607. (e) Li, L.; Zhao, S.; Joshi-Pangu, A.; Diane, M.; Biscoe, M. R. *J. Am. Chem. Soc.* **2014**, *136*, 14027.
- (7) Seminal examples of acyl cross-coupling: (a) Milstein, D.; Stille, J. K. *J. Am. Chem. Soc.* **1978**, *100*, 3636. (b) Negishi, E.; Bagheri, V.; Chatterjee, S.; Luo, F.-T.; Miller, J. A.; Stoll, A. T. *Tetrahedron Lett.* **1983**, *24*, 5181. (c) Haddach, M.; McCarthy, J. R. *Tetrahedron Lett.* **1999**, *40*, 3109.
- (8) (a) Tokuyama, H.; Yokoshima, S.; Yamashita, T.; Fukuyama, T. *Tetrahedron Lett.* **1998**, *39*, 3189. (b) Tokuyama, H.; Yokoshima, S.; Yamashita, T.; Lin, S. C.; Li, L. P.; Fukuyama, T. *J. Braz. Chem. Soc.* **1998**, *9*, 381. (c) Miyazaki, T.; Hanaya, Y.; Tokuyama, H.; Fukuyama, T. *Synlett* **2004**, 477. (d) For a review, see: Fukuyama, T.; Tokuyama, H. *Aldrichimica Acta* **2004**, *37*, 87.

- (9) Mori, Y.; Seki, M. *Adv. Synth. Catal.* **2007**, *349*, 2027.
- (10) Dieter, R. K. *Tetrahedron* **1999**, *55*, 4177.
- (11) Nahm, S.; Weinreb, S. M. *Tetrahedron Lett.* **1981**, *22*, 3815.
- (12) Schmink, J. R.; Krska, S. W. *J. Am. Chem. Soc.* **2011**, *133*, 19574.
- (13) (a) Wotal, A. C.; Weix, D. J. *Org. Lett.* **2012**, *14*, 1476. (b) Wu, F.; Lu, W.; Qian, Q.; Ren, Q.; Gong, H. *Org. Lett.* **2012**, *14*, 3044. (c) Cherney, A. H.; Kadunce, N. T.; Reisman, S. E. *J. Am. Chem. Soc.* **2013**, *135*, 7442.
- (14) Harada, T.; Kotani, Y.; Katsuhira, T.; Oku, A. *Tetrahedron Lett.* **1991**, *32*, 1573.
- (15) Wang, D.; Zhang, Z. *Org. Lett.* **2003**, *5*, 4645.
- (16) Mori, Y.; Seki, M. *Tetrahedron Lett.* **2004**, *45*, 7343.
- (17) Zhang, Y.; Rovis, T. *J. Am. Chem. Soc.* **2004**, *126*, 15964.
- (18) Yu, Y.; Liebeskind, L. S. *J. Org. Chem.* **2004**, *69*, 3554.
- (19) Cherney, A. H.; Reisman, S. E. *Tetrahedron* **2014**, *70*, 3259.
- (20) Milne, J. E.; Buchwald, S. L. *J. Am. Chem. Soc.* **2004**, *126*, 13028.
- (21) Zhu, L.; Wehmeyer, R. M.; Rieke, R. D. *J. Org. Chem.* **1991**, *56*, 1445.
- (22) (a) Cloke, J. B.; Pilgrim, F. J. *J. Am. Chem. Soc.* **1939**, *61*, 2667. (b) Bhar, S.; Ranu, B. C. *J. Org. Chem.* **1995**, *60*, 745
- (23) (a) Zhang, Y.; Rovis, T. *J. Am. Chem. Soc.* **2004**, *126*, 15964. (b) Onaka, M.; Matsuoka, Y.; Mukaiyama, T. *Chem. Lett.* **1981**, *10*, 531.
- (24) (a) Marek, I.; Normant, J. F. *J. Org. Chem.* **1994**, *59*, 2925. (b) Marek, I.; Normant, J. F. *Chem. Eur. J.* **1999**, *5*, 2055.
- (25) (a) Hayashi, T.; Tajika, M.; Tamao, K.; Kumada, M. *J. Am. Chem. Soc.* **1976**, *98*, 3718. (b) Tamao, K.; Hayashi, T.; Matsumoto, H.; Yamamoto, H.; Kumada, M. *Tetrahedron Lett.* **1979**, 2155. (c) Hayashi, T.; Konishi, M.; Fukushima, M.; Mise, T.; Kagotani, M.; Tajika, M.; Kumada, M. *J. Am. Chem. Soc.* **1982**, *104*, 180. (d) Hayashi, T.; Kumada, M. *Acc. Chem. Res.* **1982**, *15*, 395.
- (26) For a review, see: Teichert, J. F.; Feringa, B. L. *Angew. Chem., Int. Ed.* **2010**, *49*, 2486.

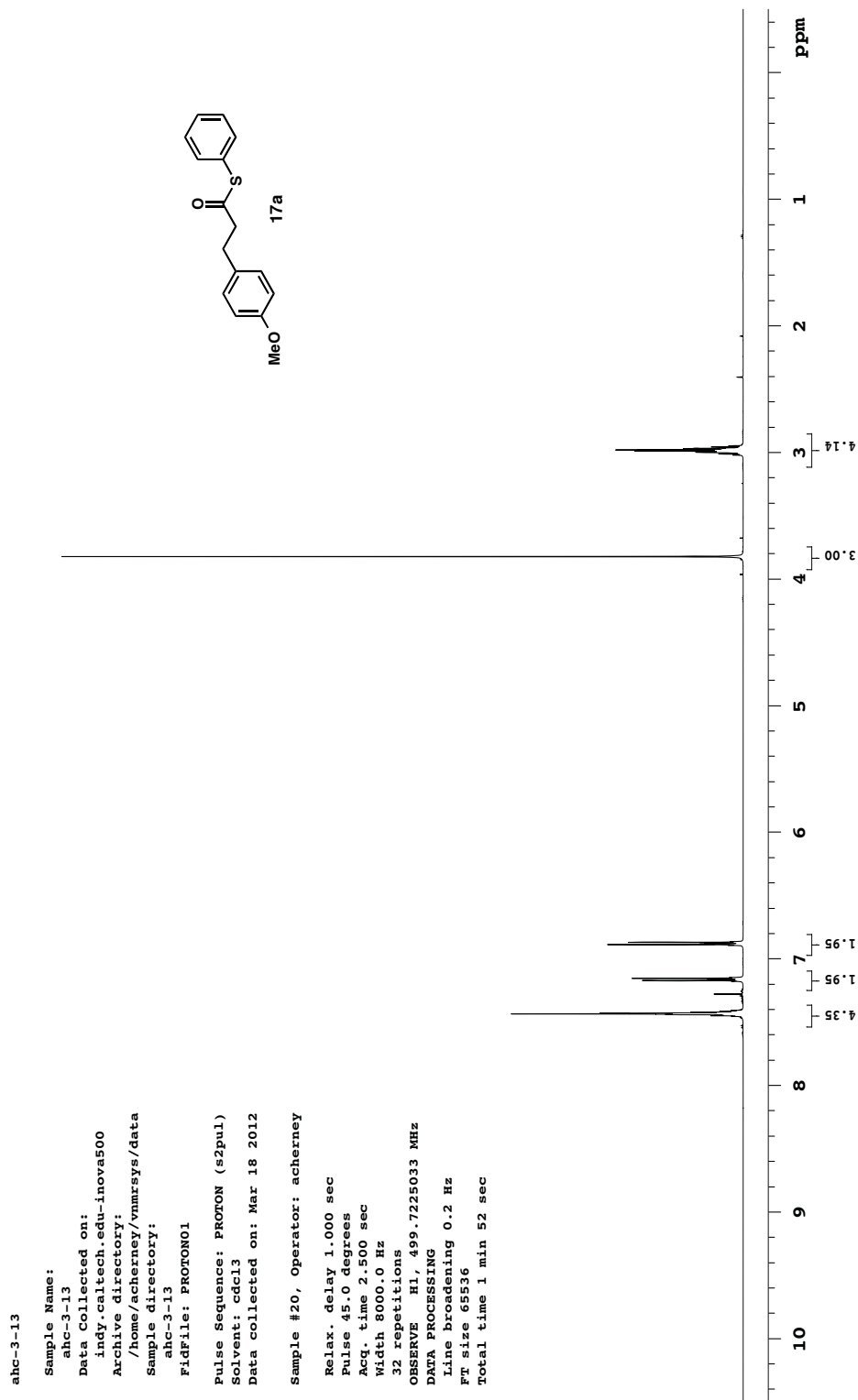
- (27) Zhang, Z. J.; Mao, J. C.; Wang, R. L.; Wu, F.; Chen, H. L.; Wan, B. S. *J. Mol. Catal. A* **2006**, 243, 239.
- (28) Still, W. C.; Kahn, M.; Mitra, A. *J. Org. Chem.* **1978**, 43, 2923.
- (29) Wakasugi, K.; Iida, A.; Misaki, T.; Nishii, Y.; Tanabe, Y. *Adv. Synth. Catal.* **2003**, 345, 1209.
- (30) Yuguchi, M.; Tokuda, M.; Orito, K. *J. Org. Chem.* **2004**, 69, 908.
- (31) Krasovskiy, A.; Knochel, P. *Synthesis* **2006**, 890.

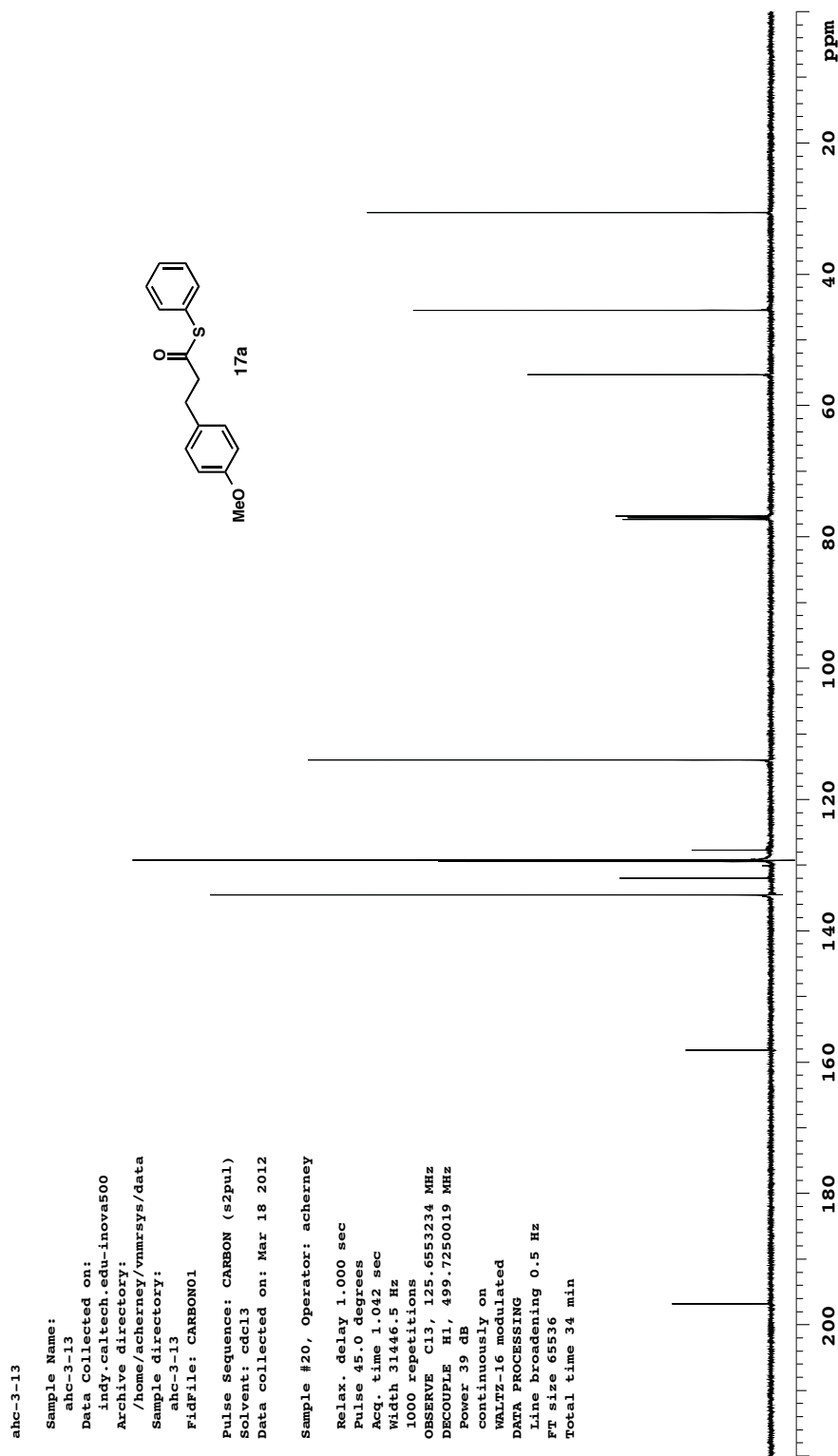
## **APPENDIX 1**

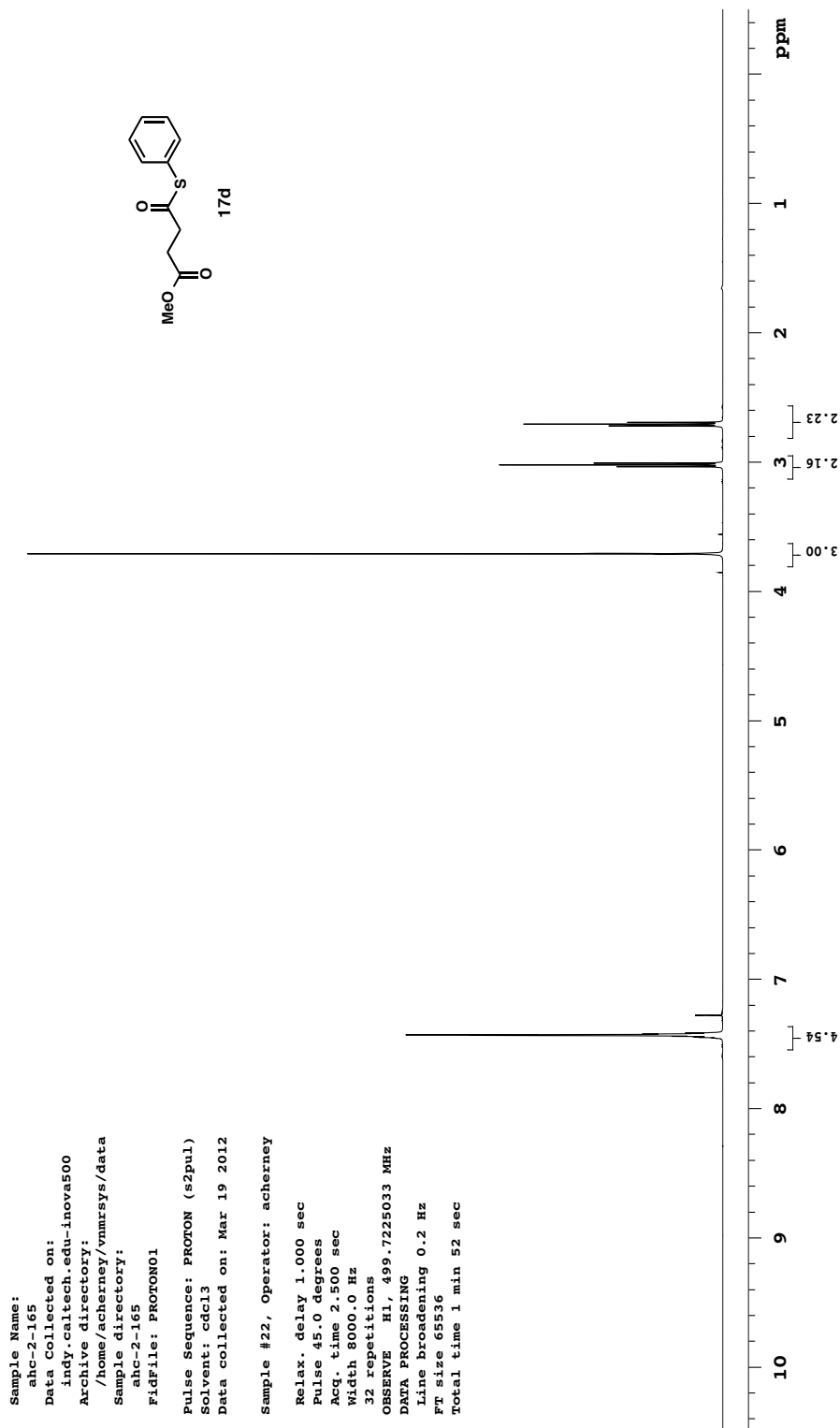
*Spectra Relevant to Chapter 2:*

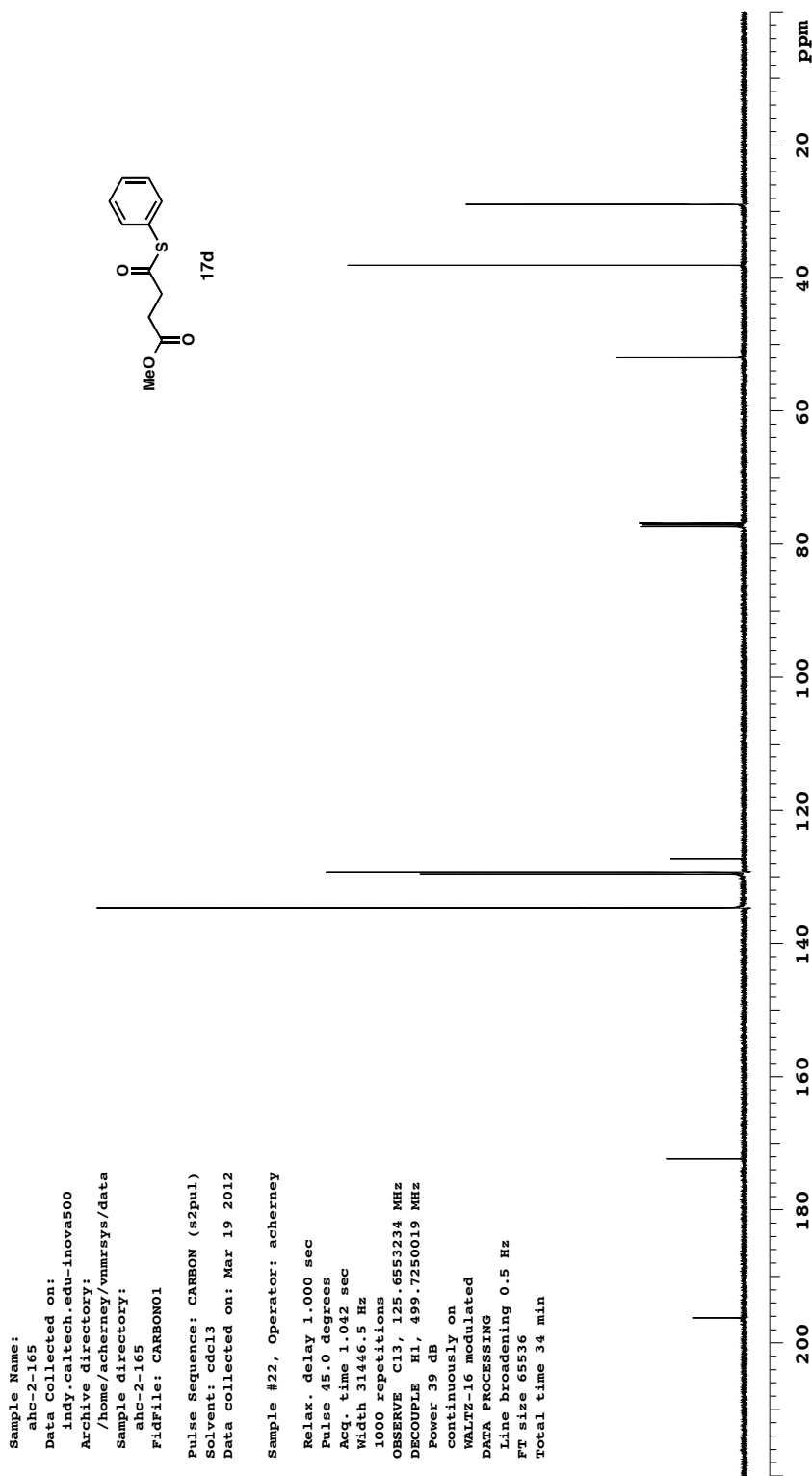
*Pd-Catalyzed Fukuyama Cross-Coupling of Secondary Organozinc*

*Reagents for the Direct Synthesis of Unsymmetrical Ketones*

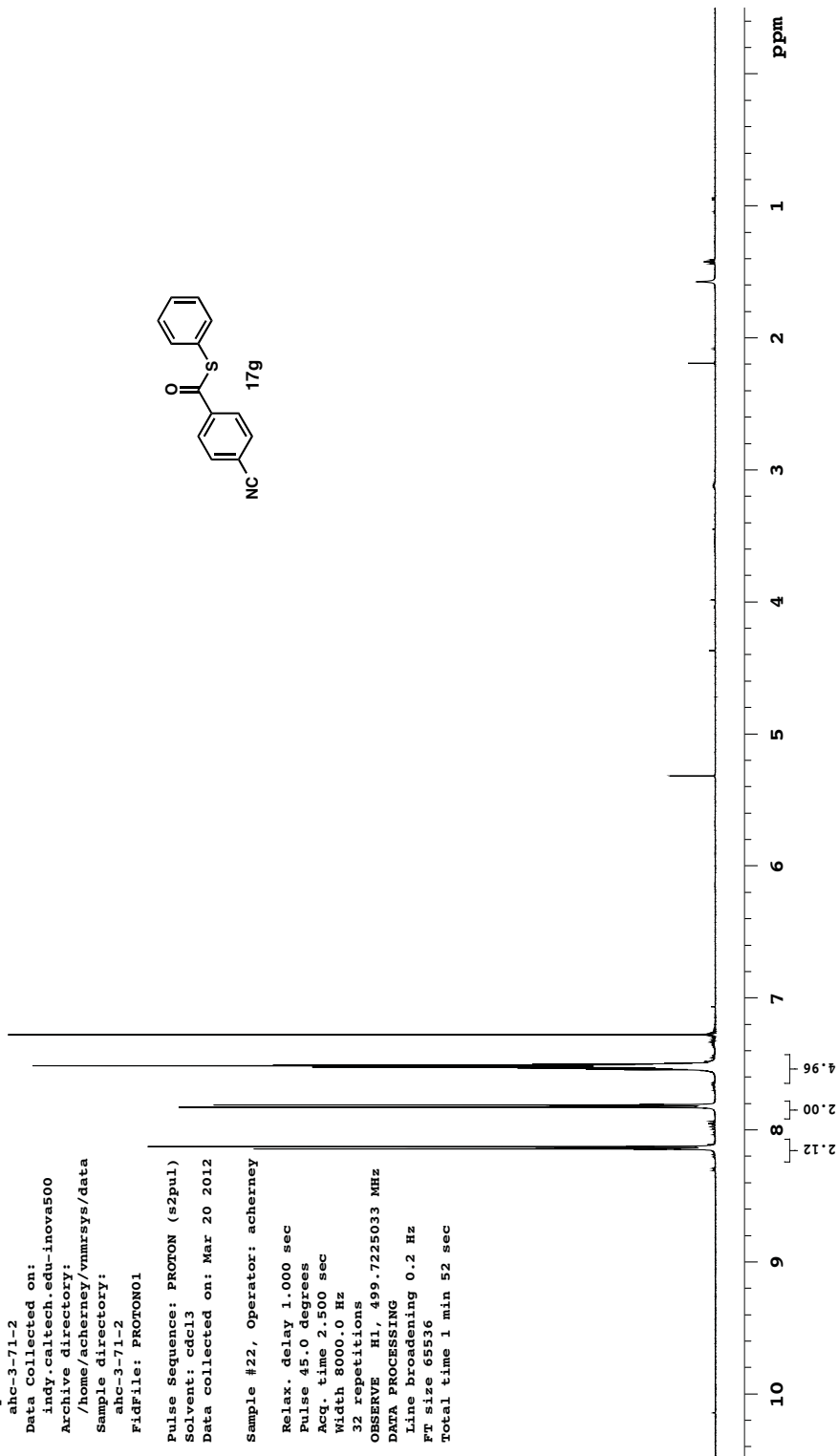
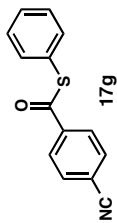


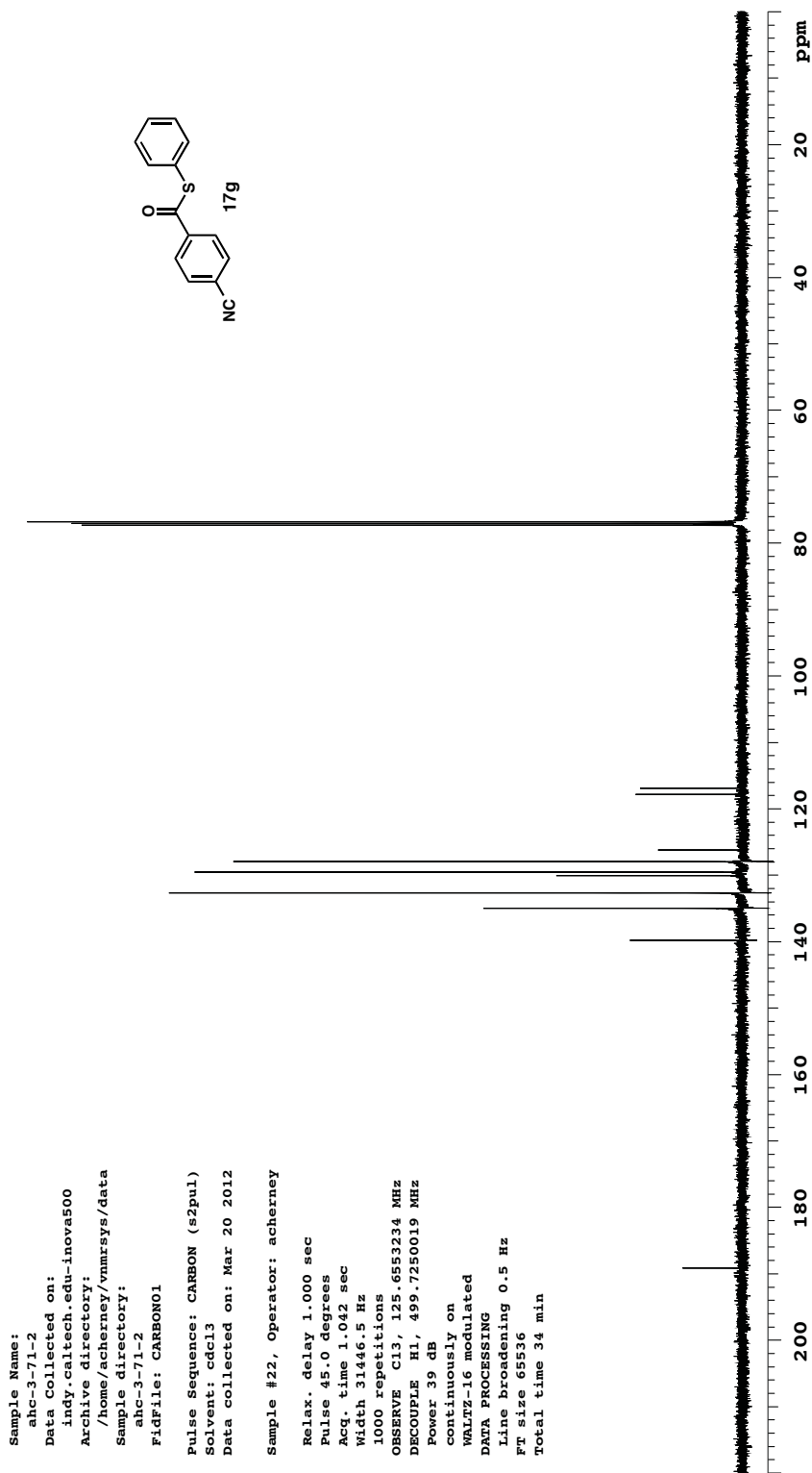




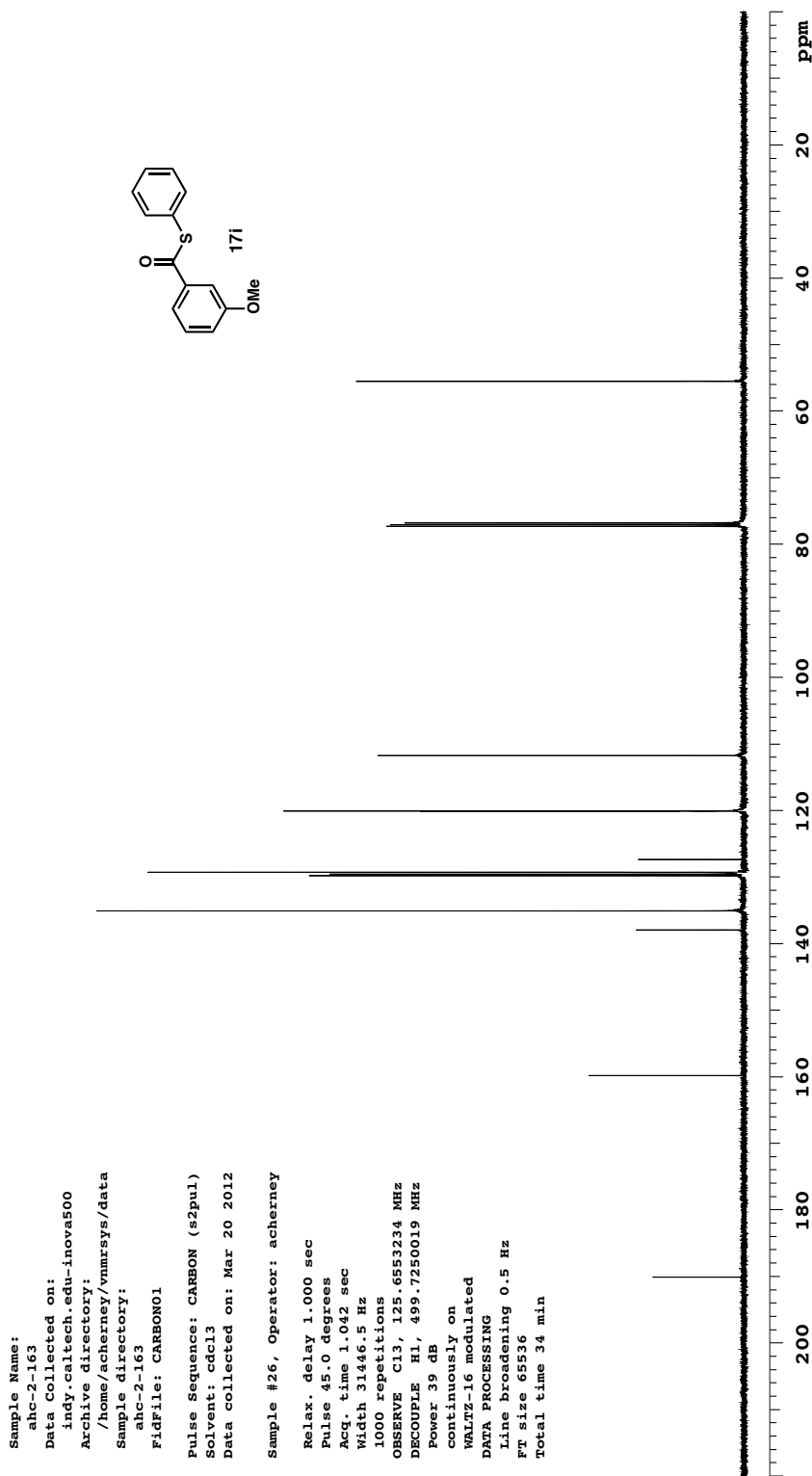


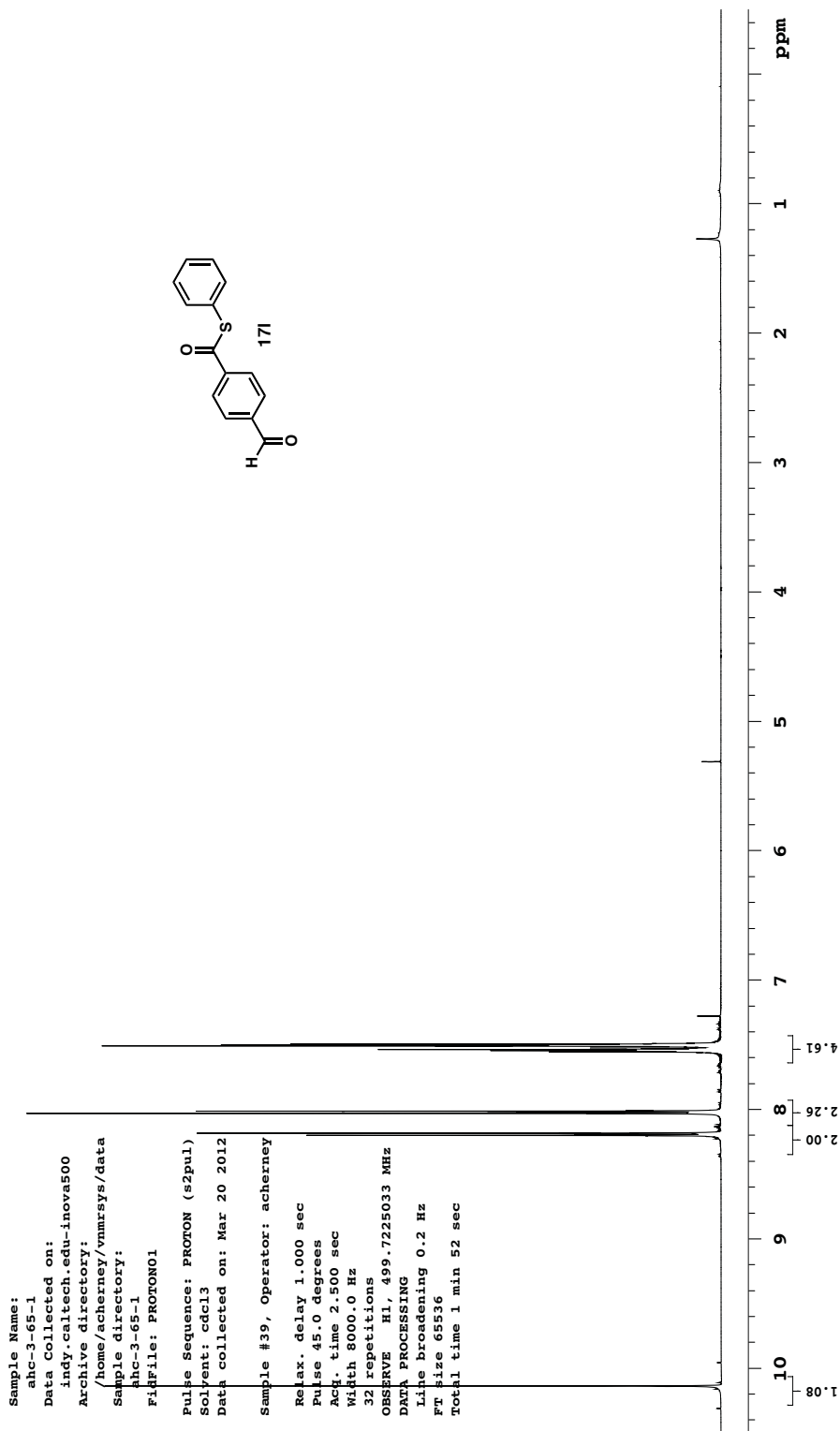
Sample Name:  
 ahc-3-71-2  
 Data Collected on:  
 indy.caltech.edu-inova500  
 Archive directory:  
 /home/acherney/vnmrSYS/data  
 Sample directory:  
 ahc-3-71-2  
 FidFile: PROTON01  
 Pulse Sequence: PROTON (s2pul)  
 Solvent: cdcl3  
 Data collected on: Mar 20 2012  
 Sample #22, Operator: acherney  
 Relax. delay 1.000 sec  
 Pulse 45.0 degrees  
 Acq. time 2.500 sec  
 Width 8000.0 Hz  
 32 repetitions  
 OBSERVE H1, 499.725033 MHz  
 DATA PROCESSING  
 Line broadening 0.2 Hz  
 FT size 65536  
 Total time 1 min 52 sec

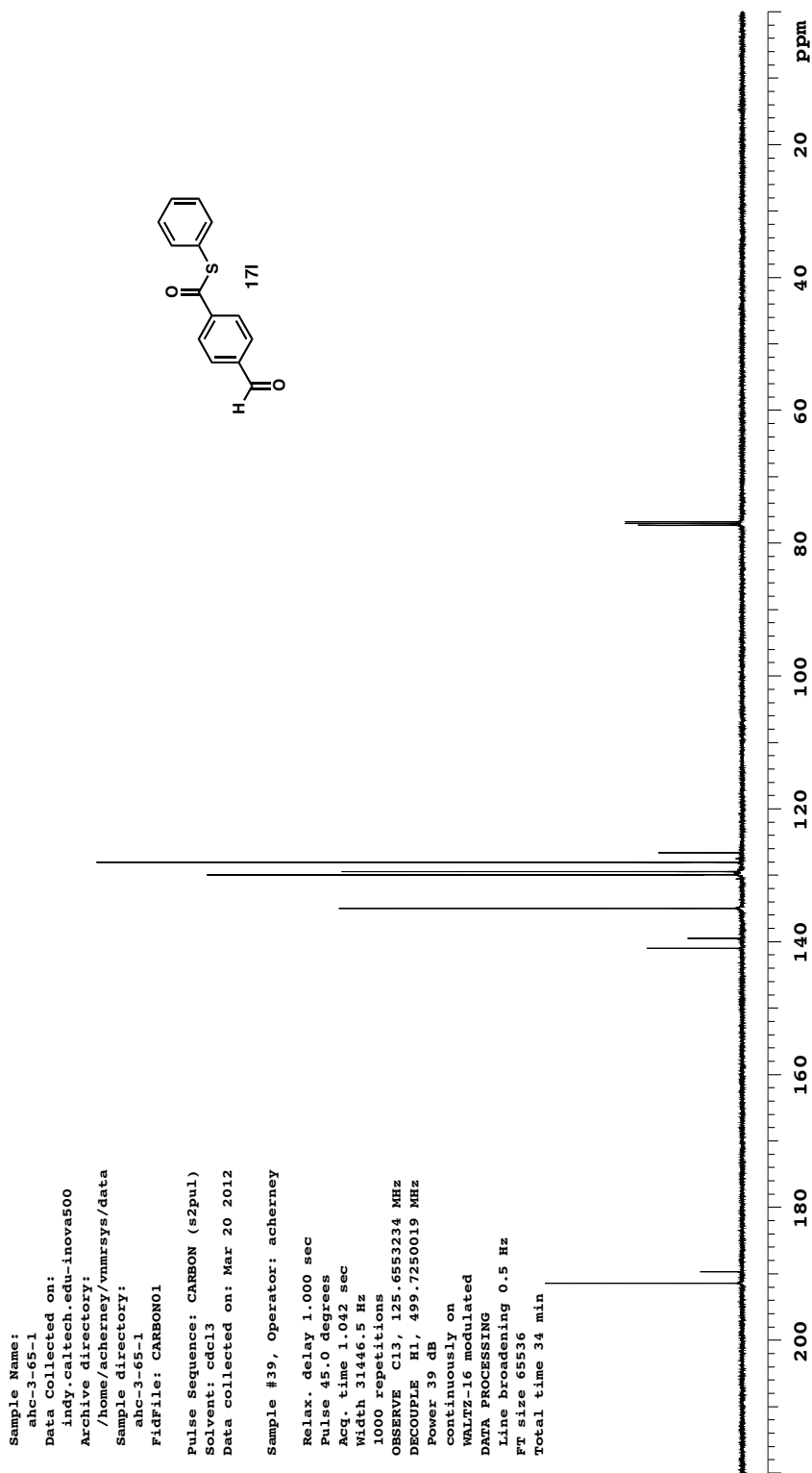


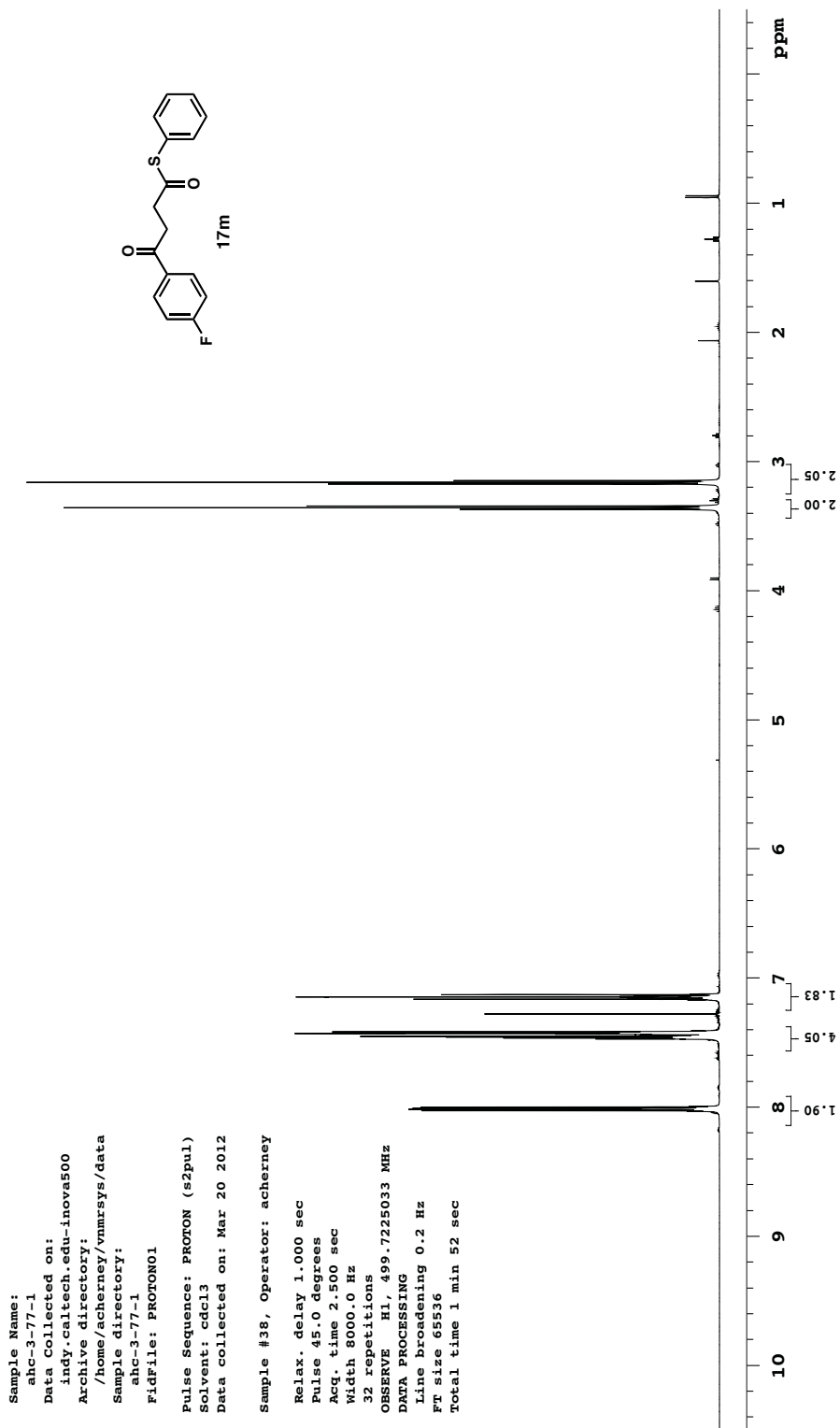


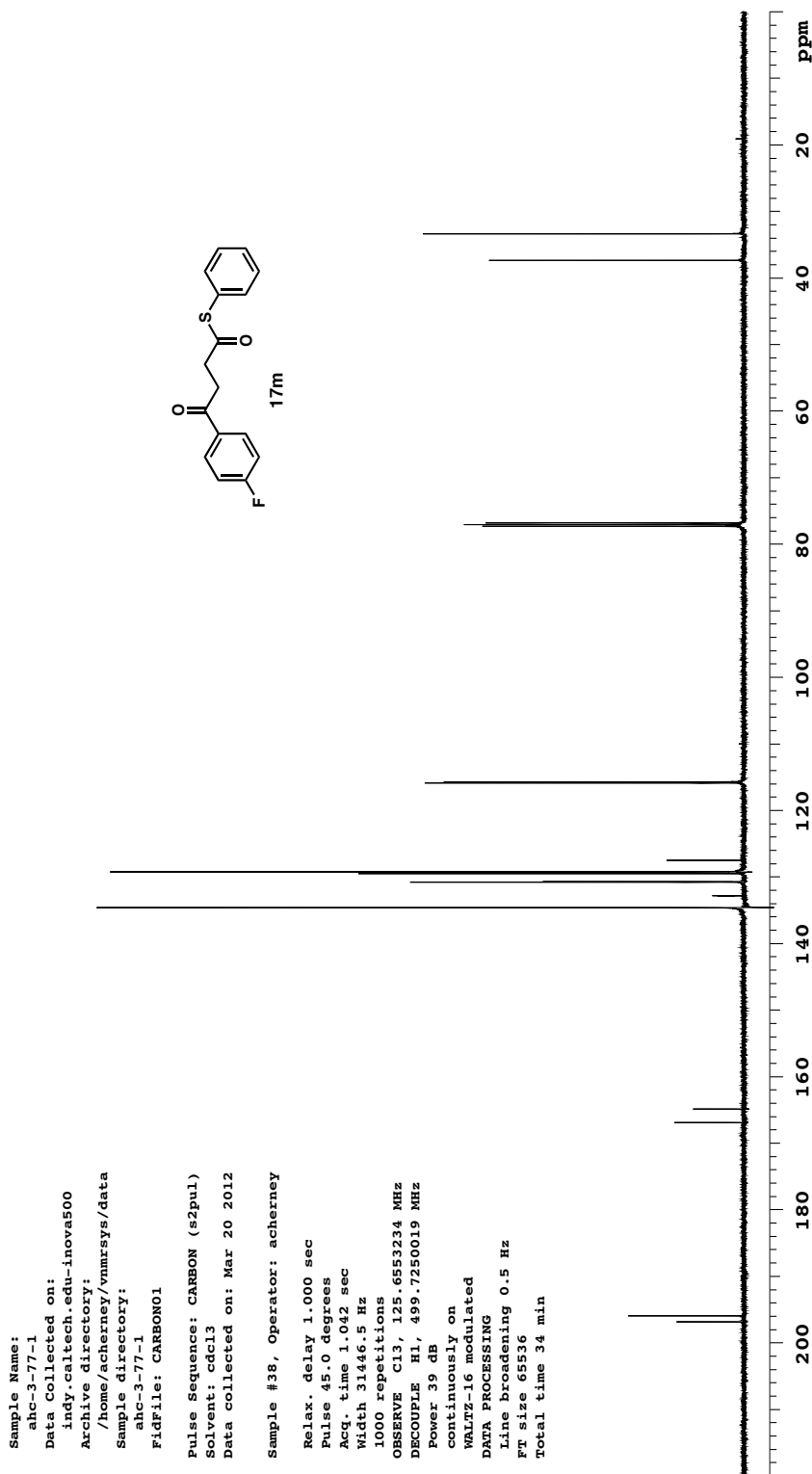


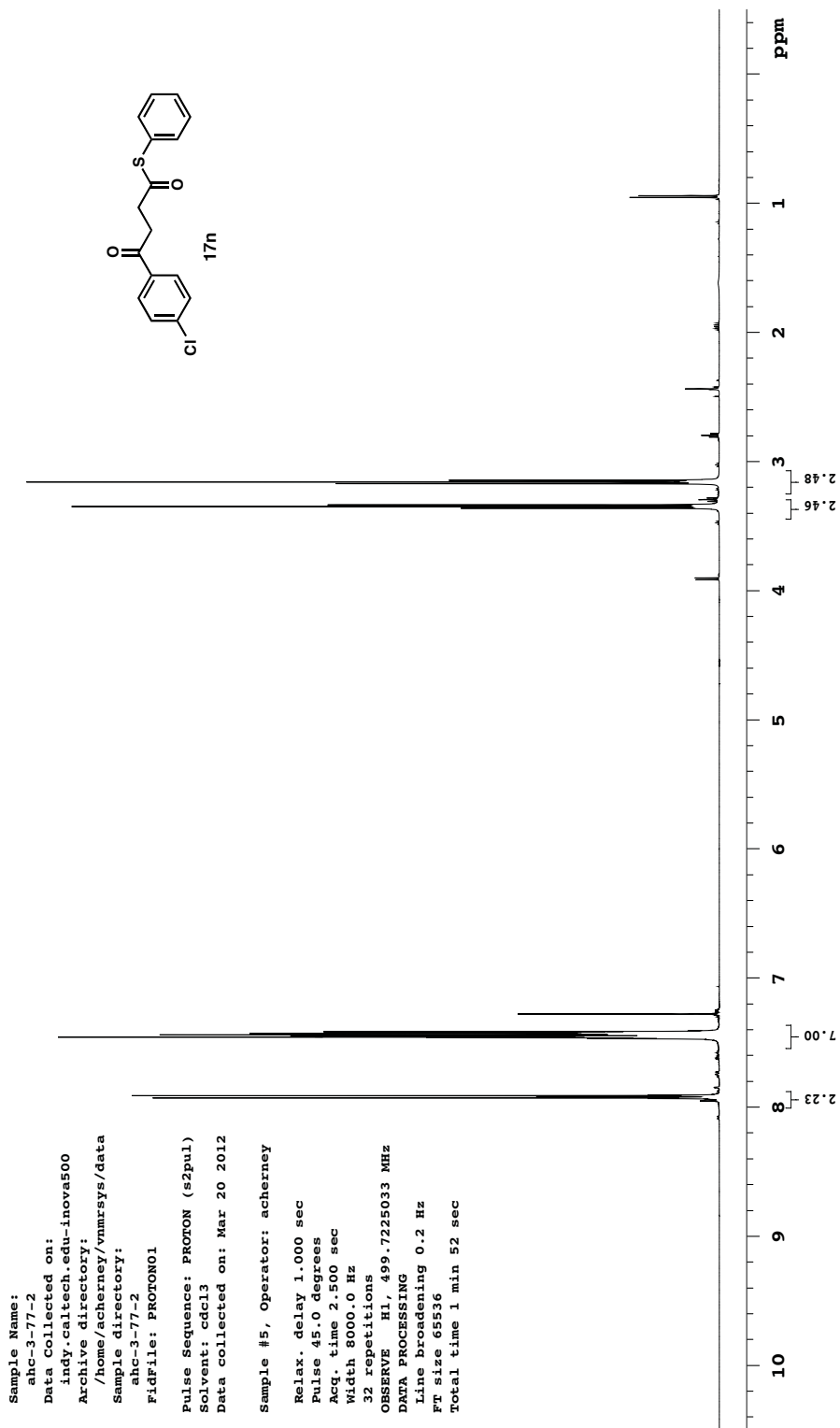


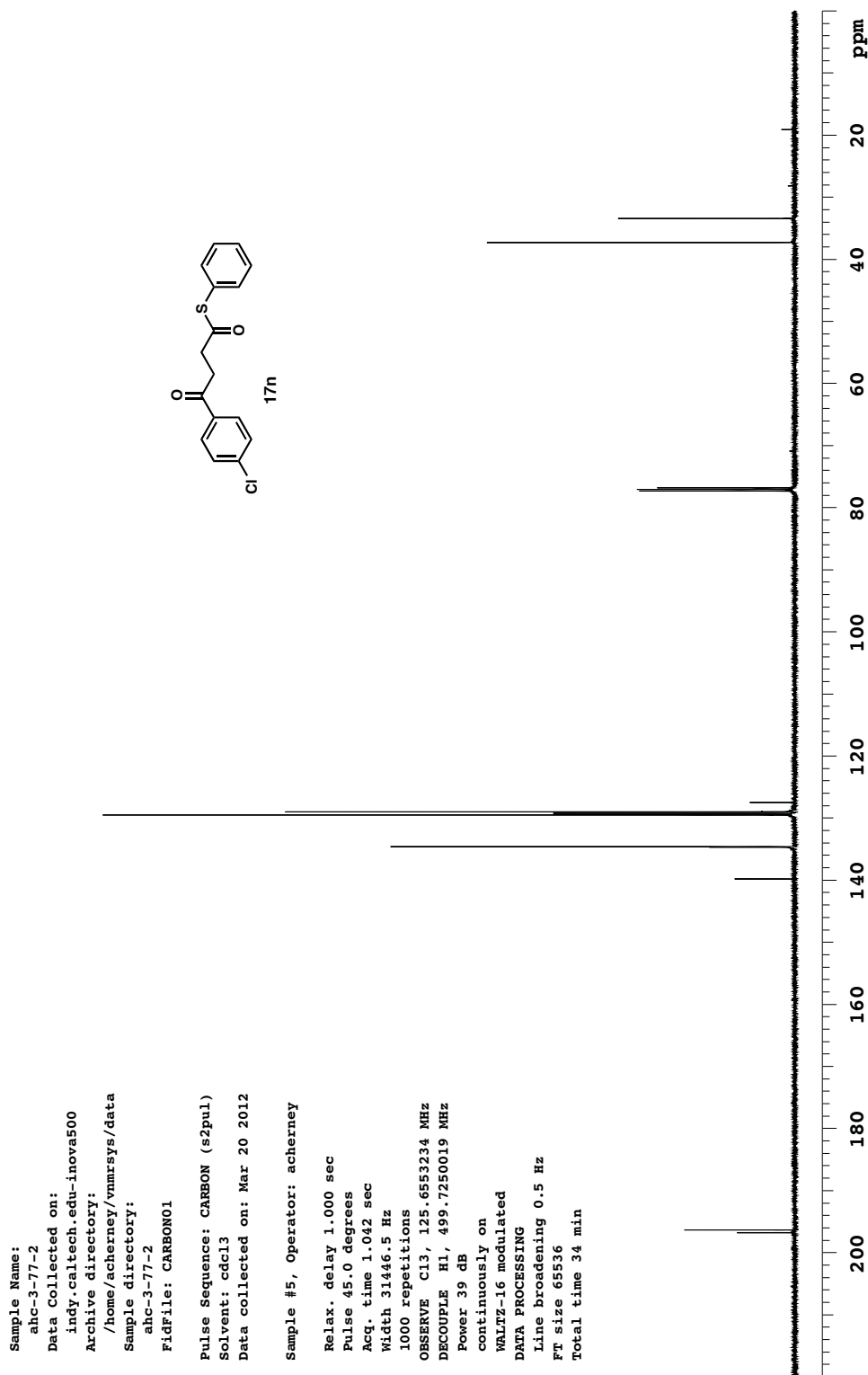


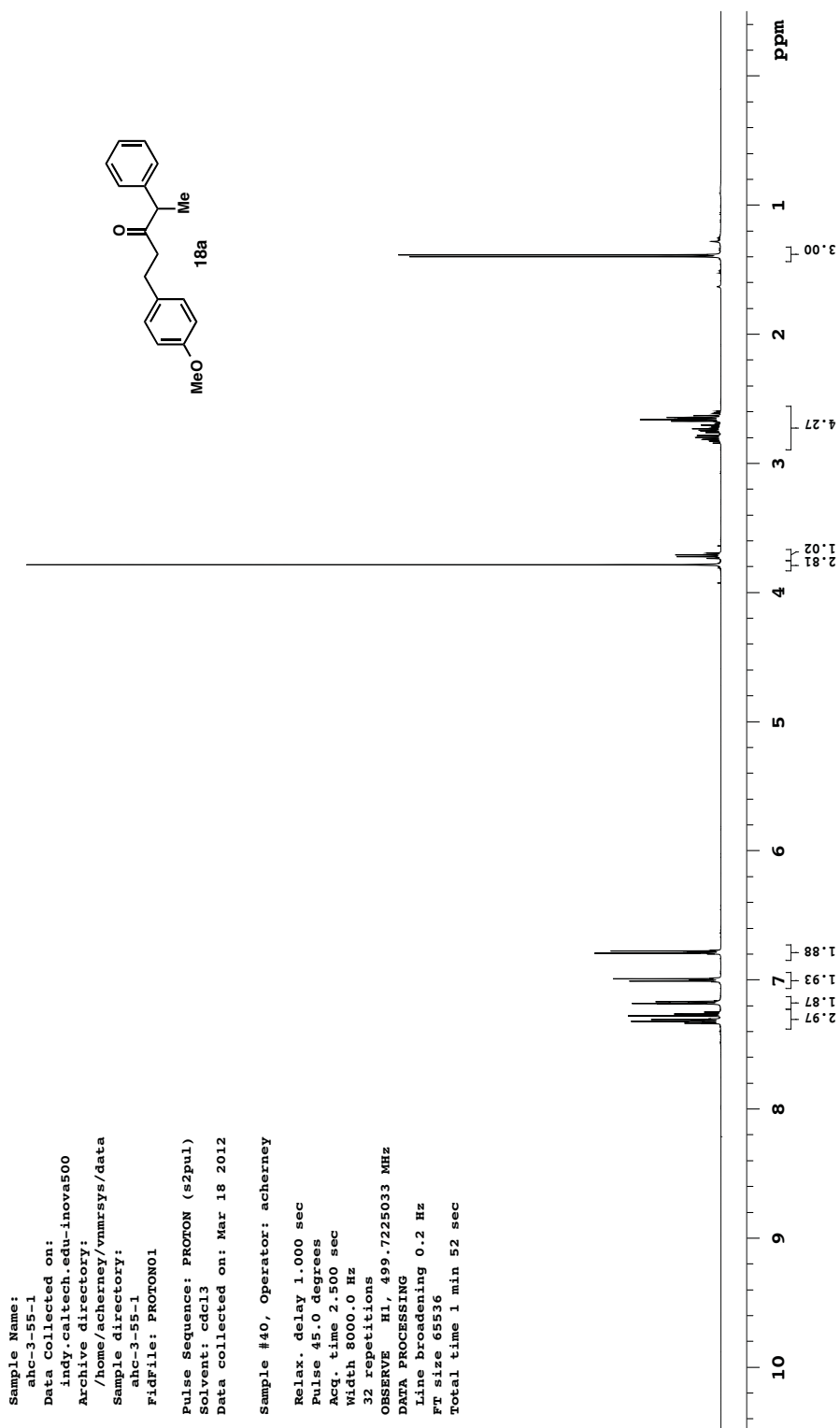


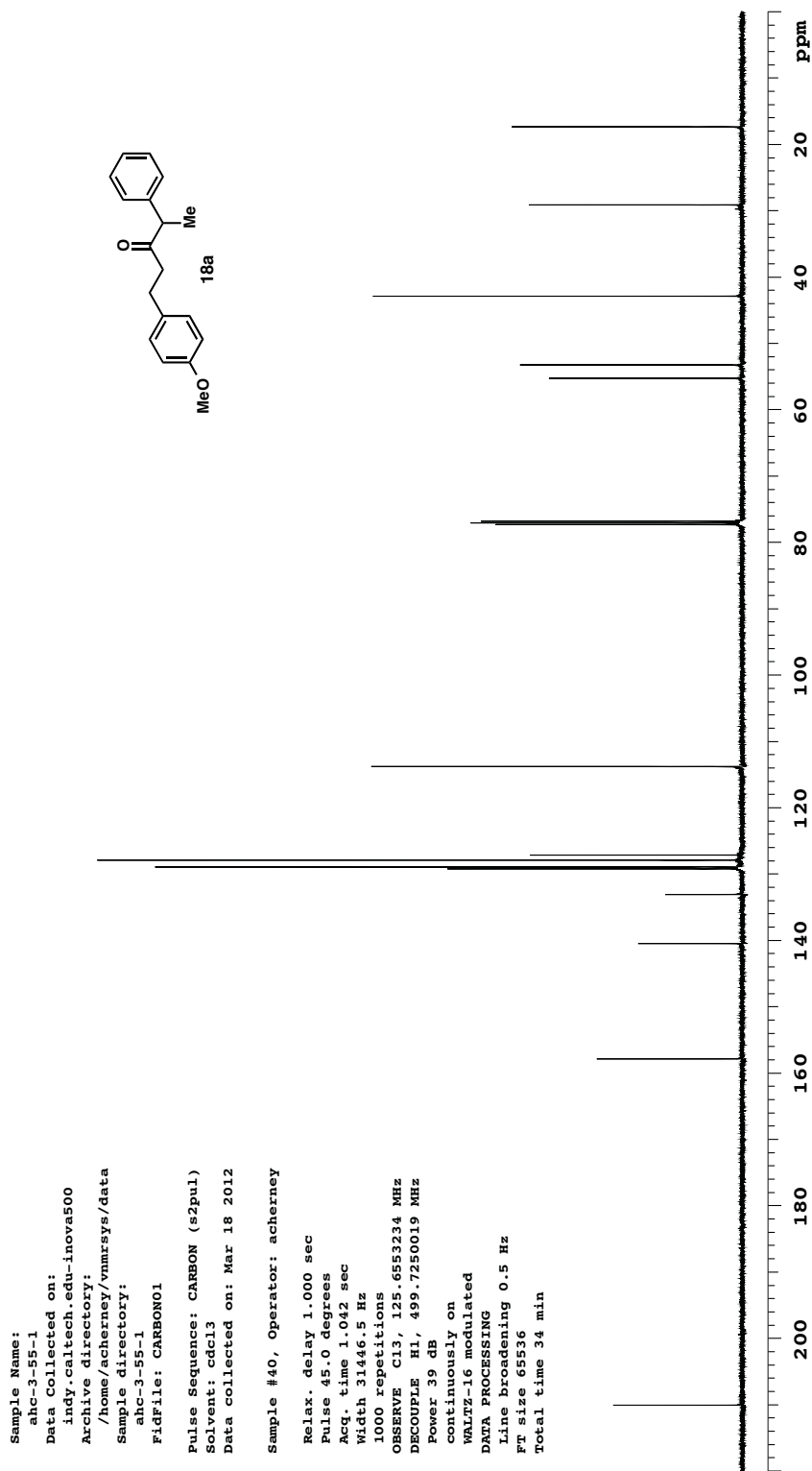


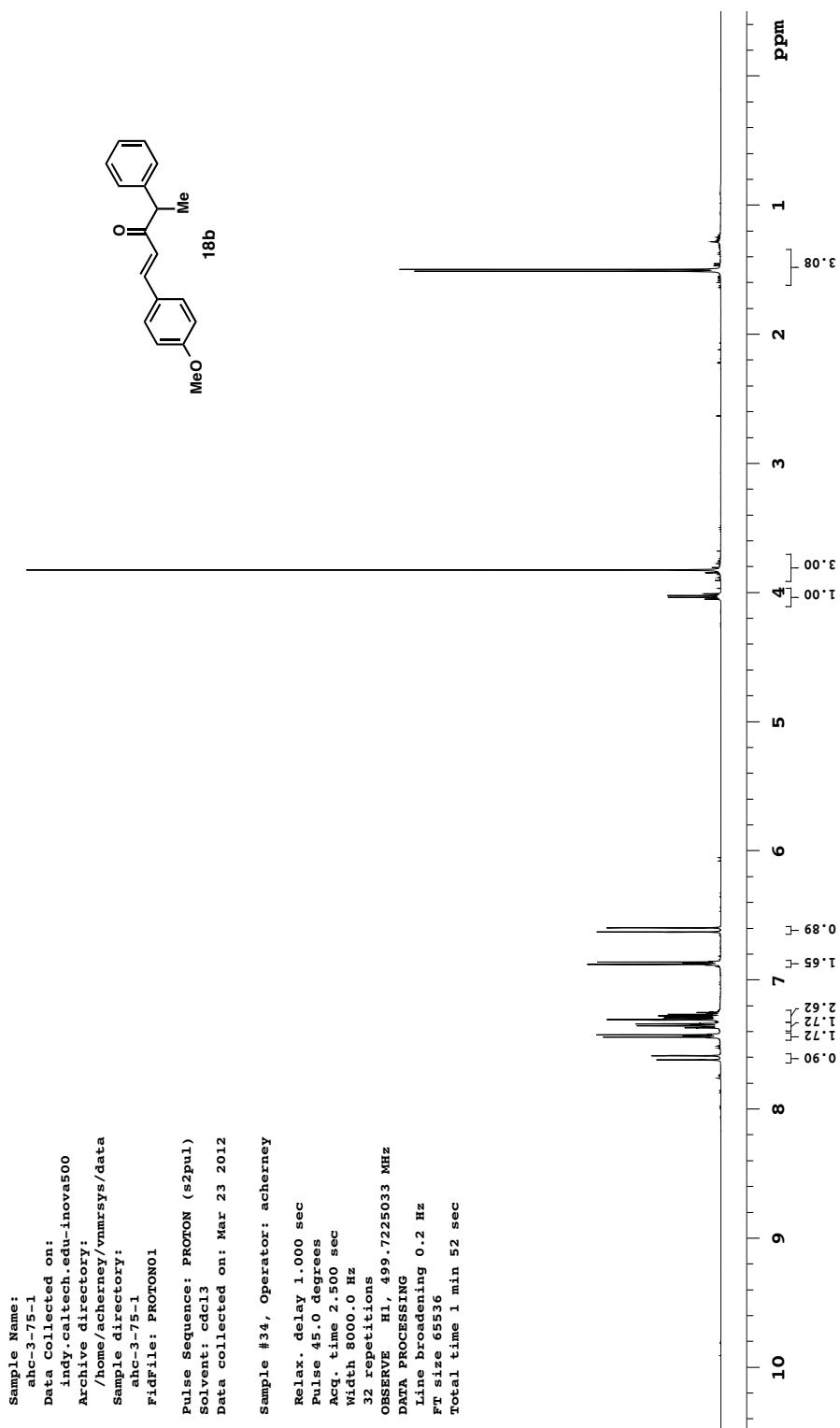


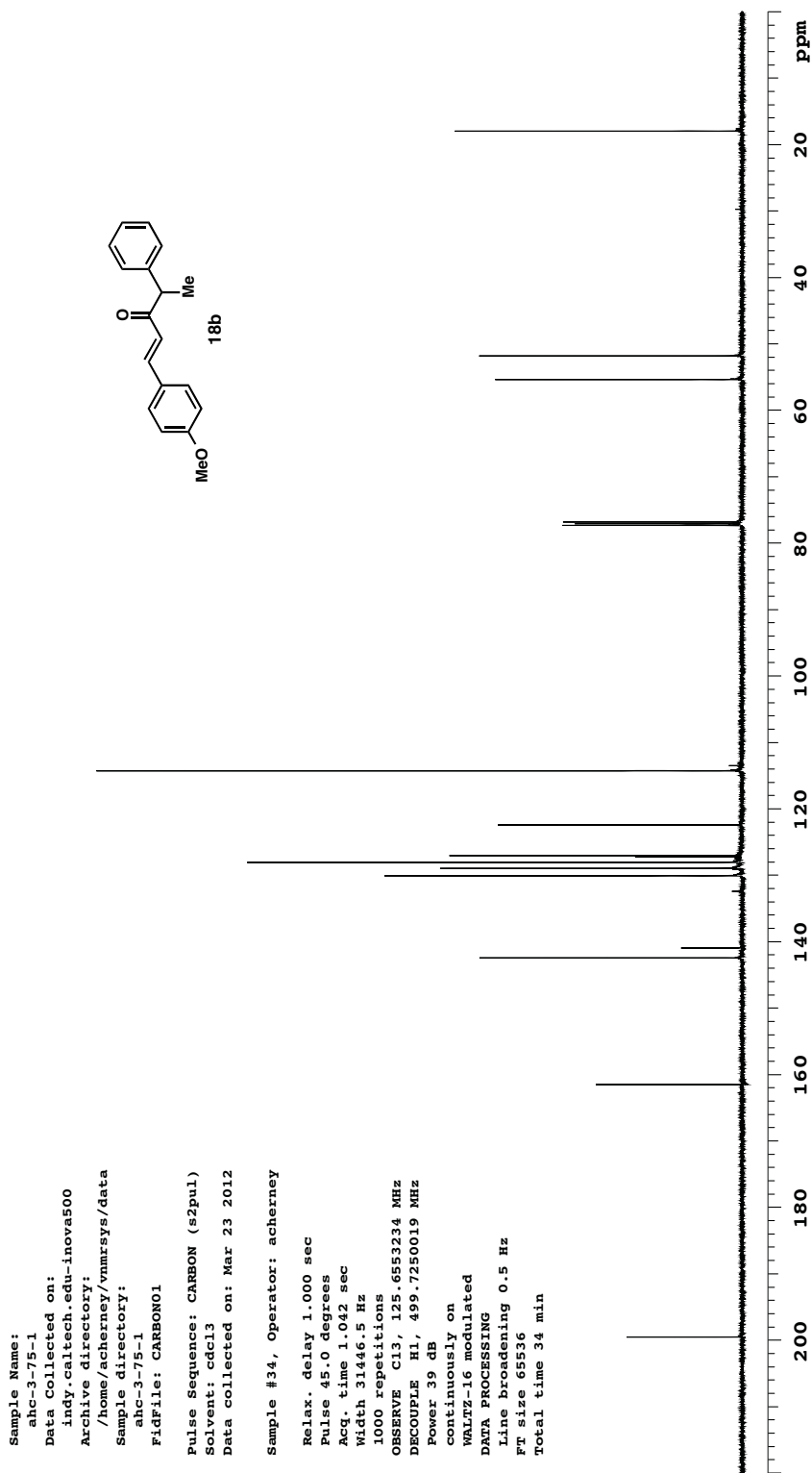


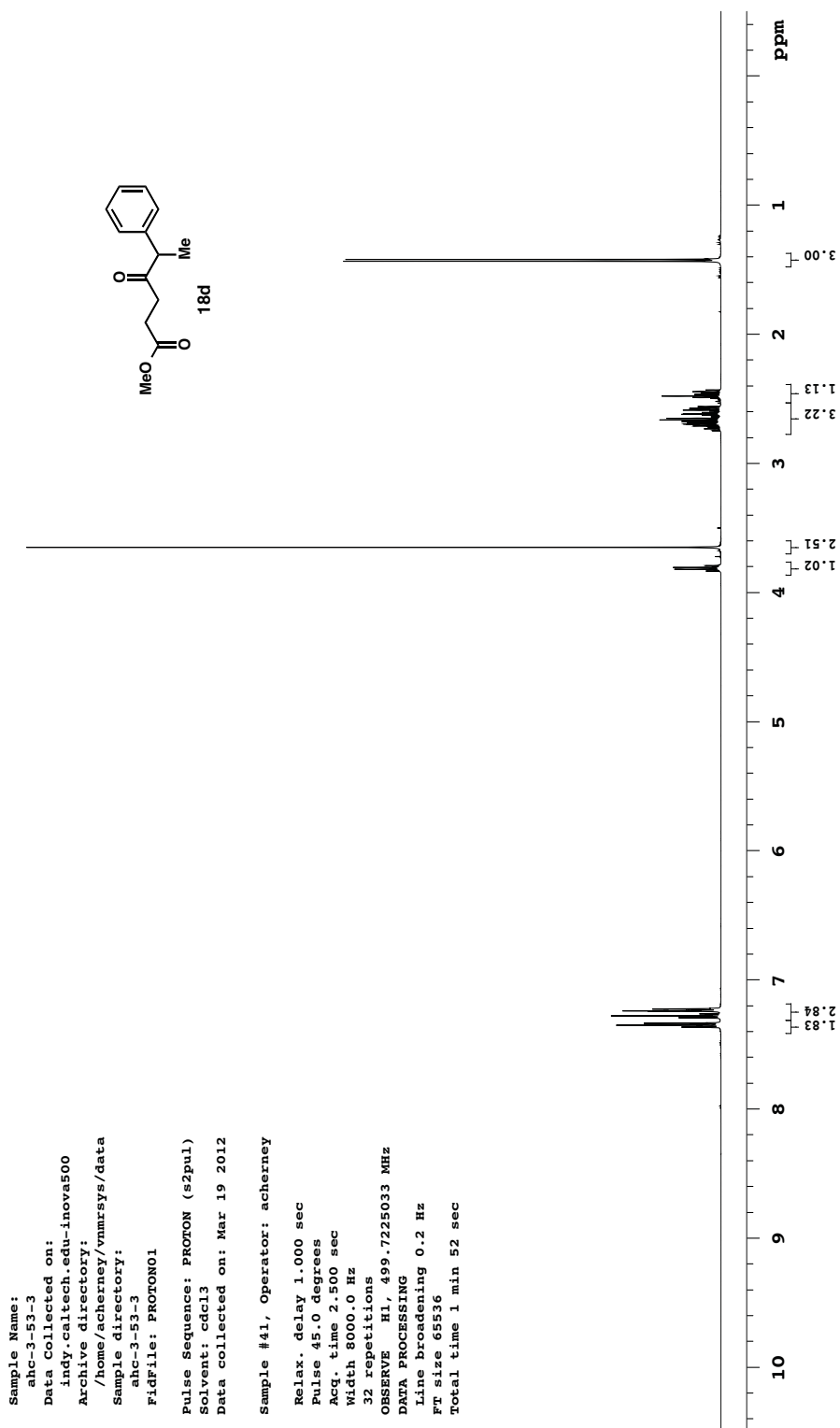


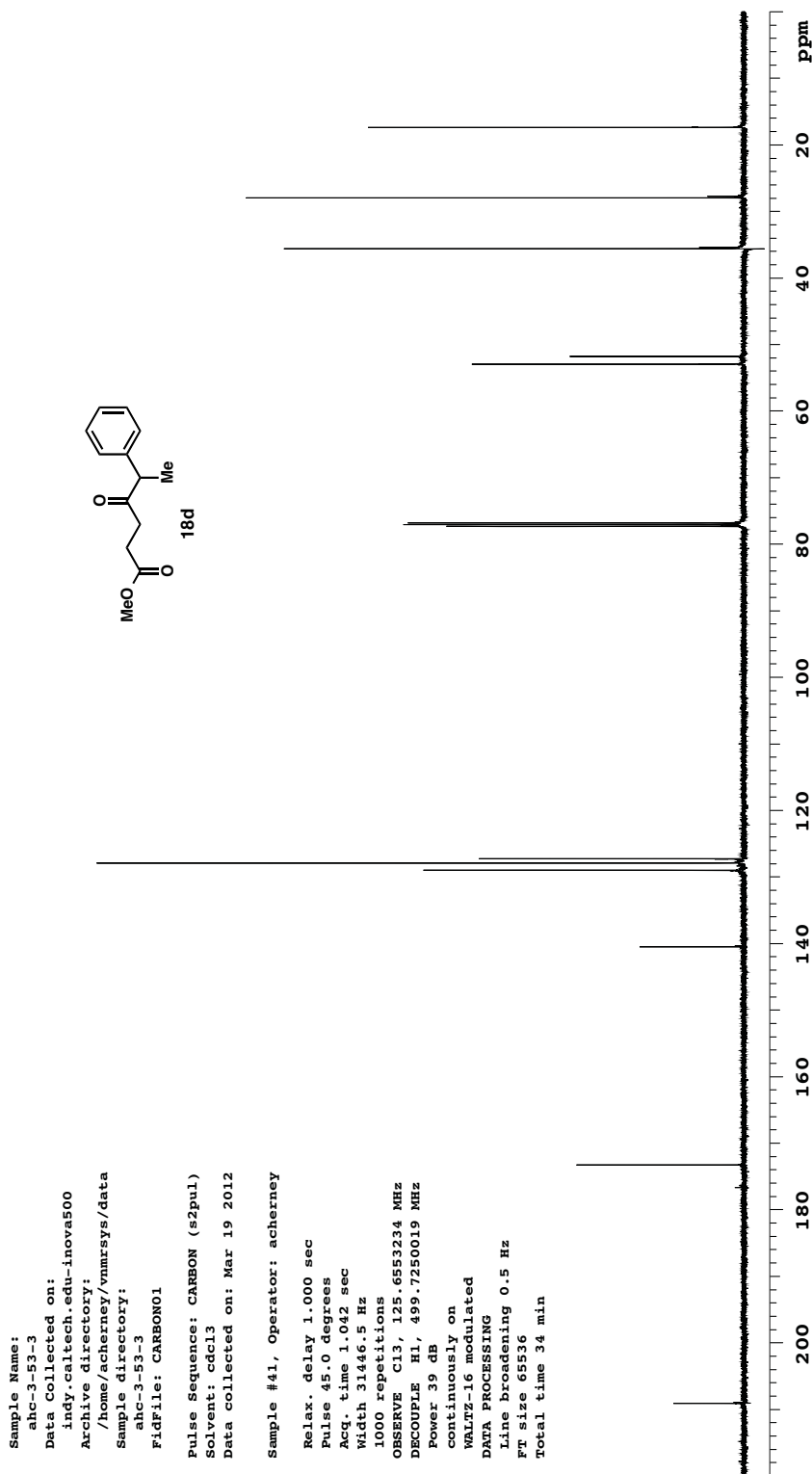


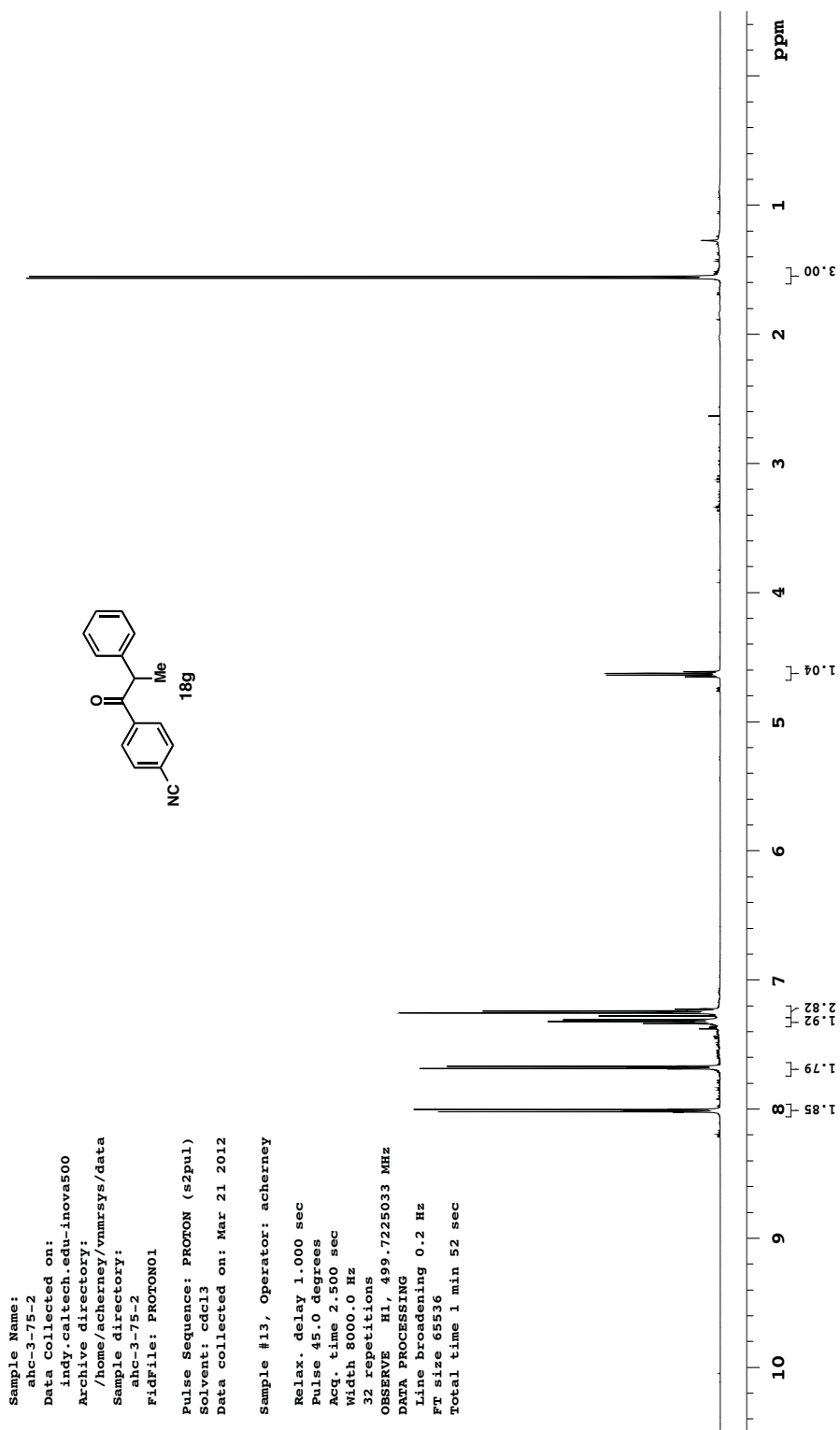


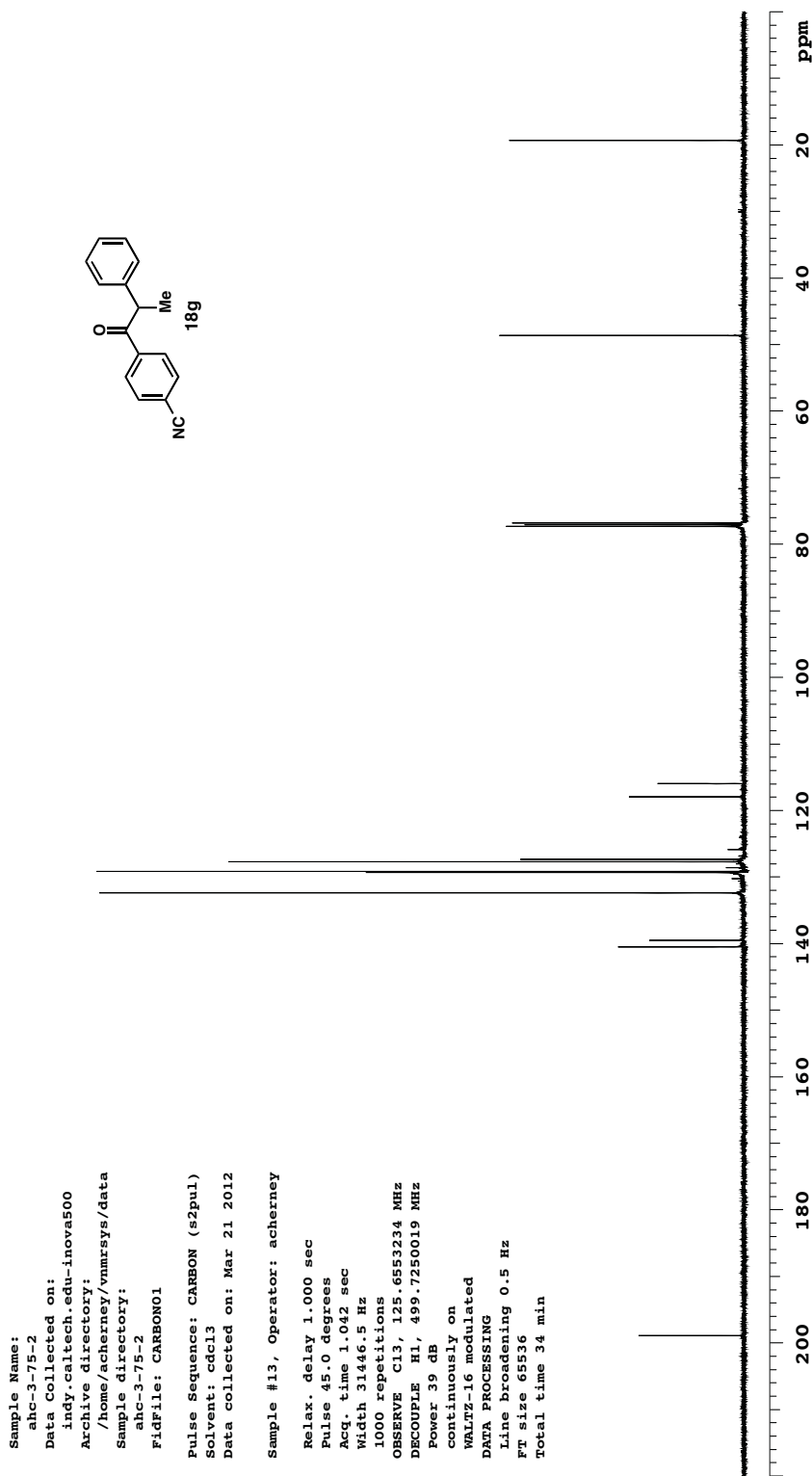


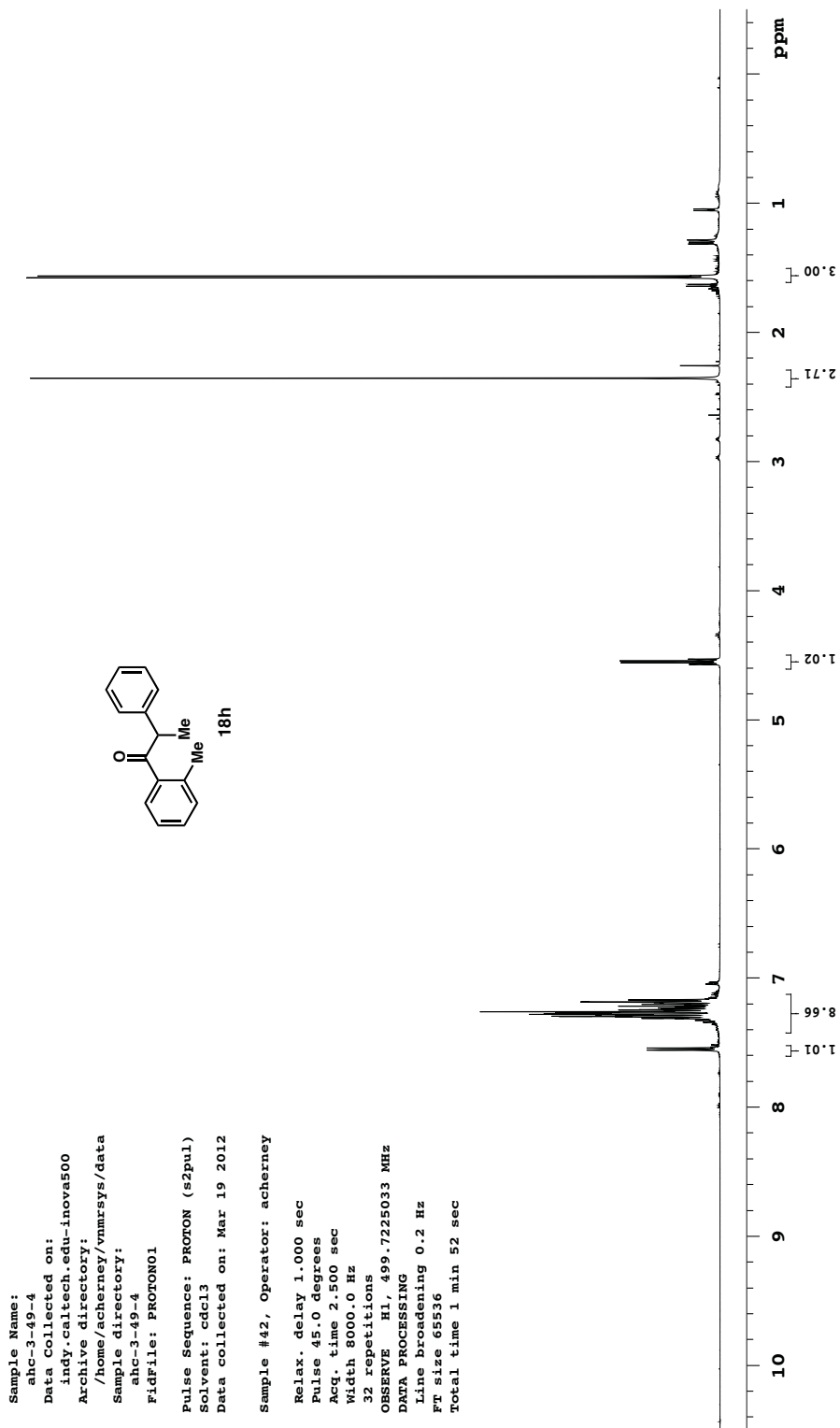




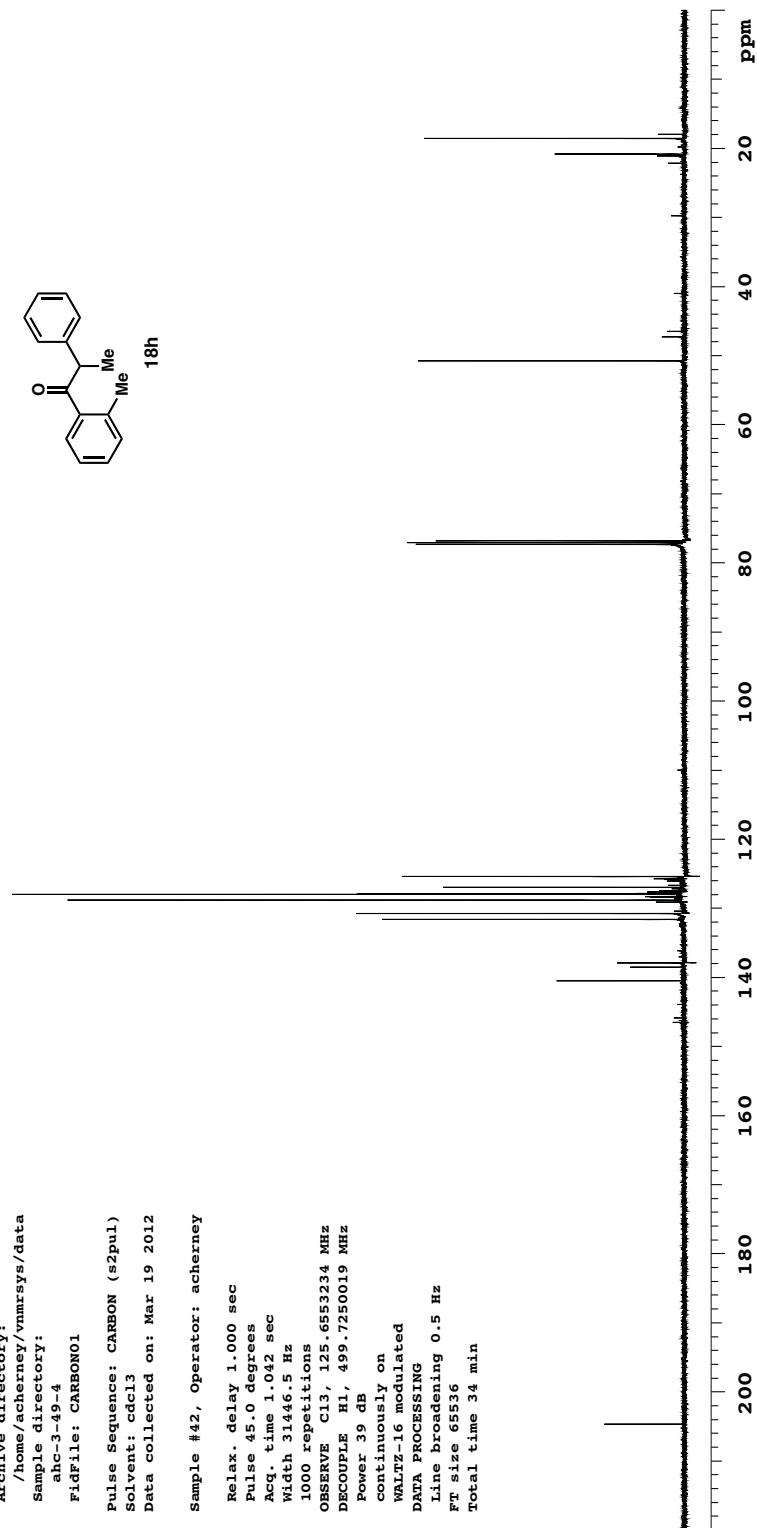
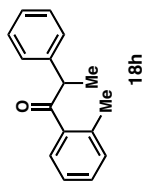




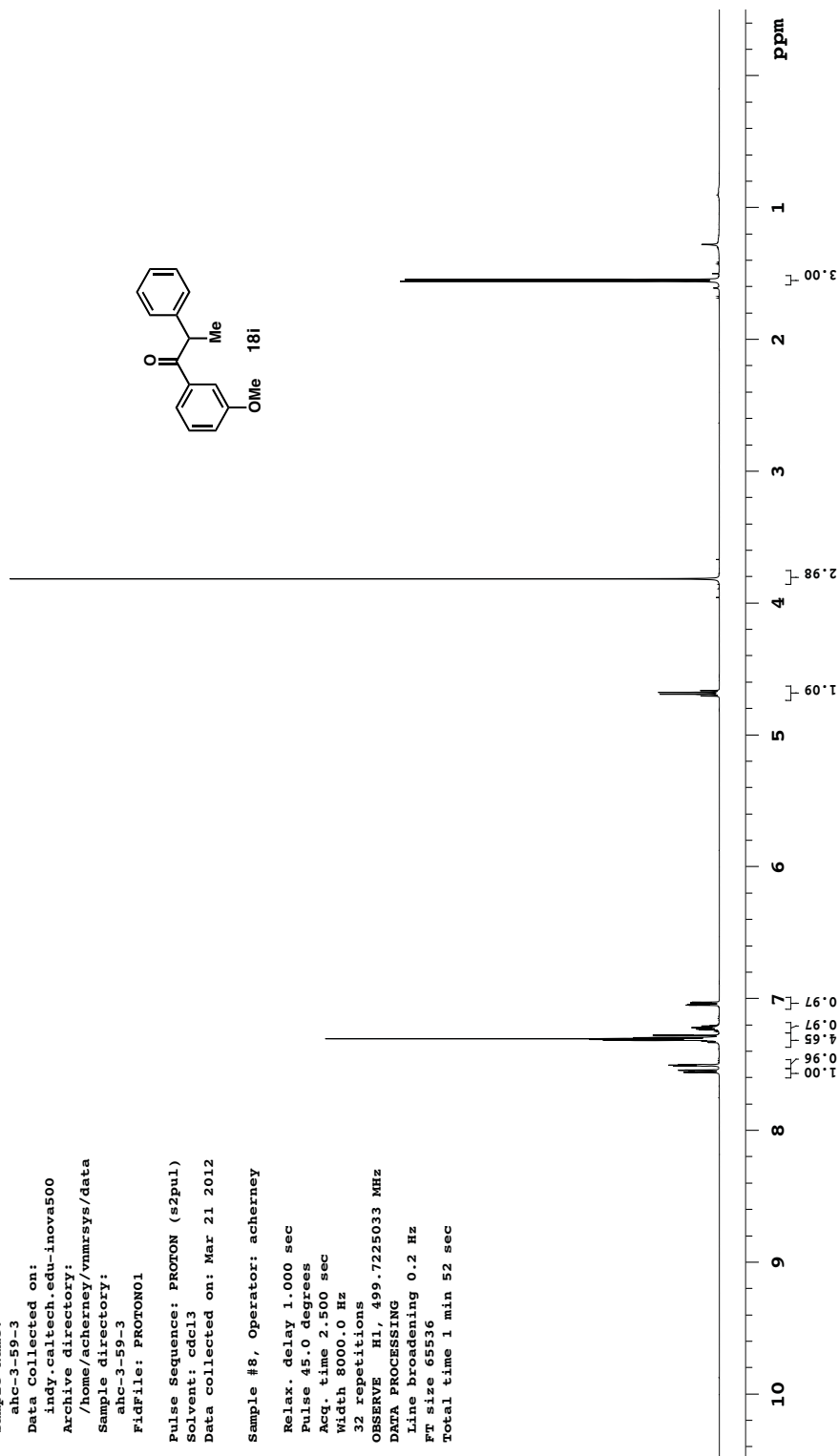
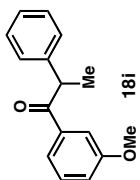


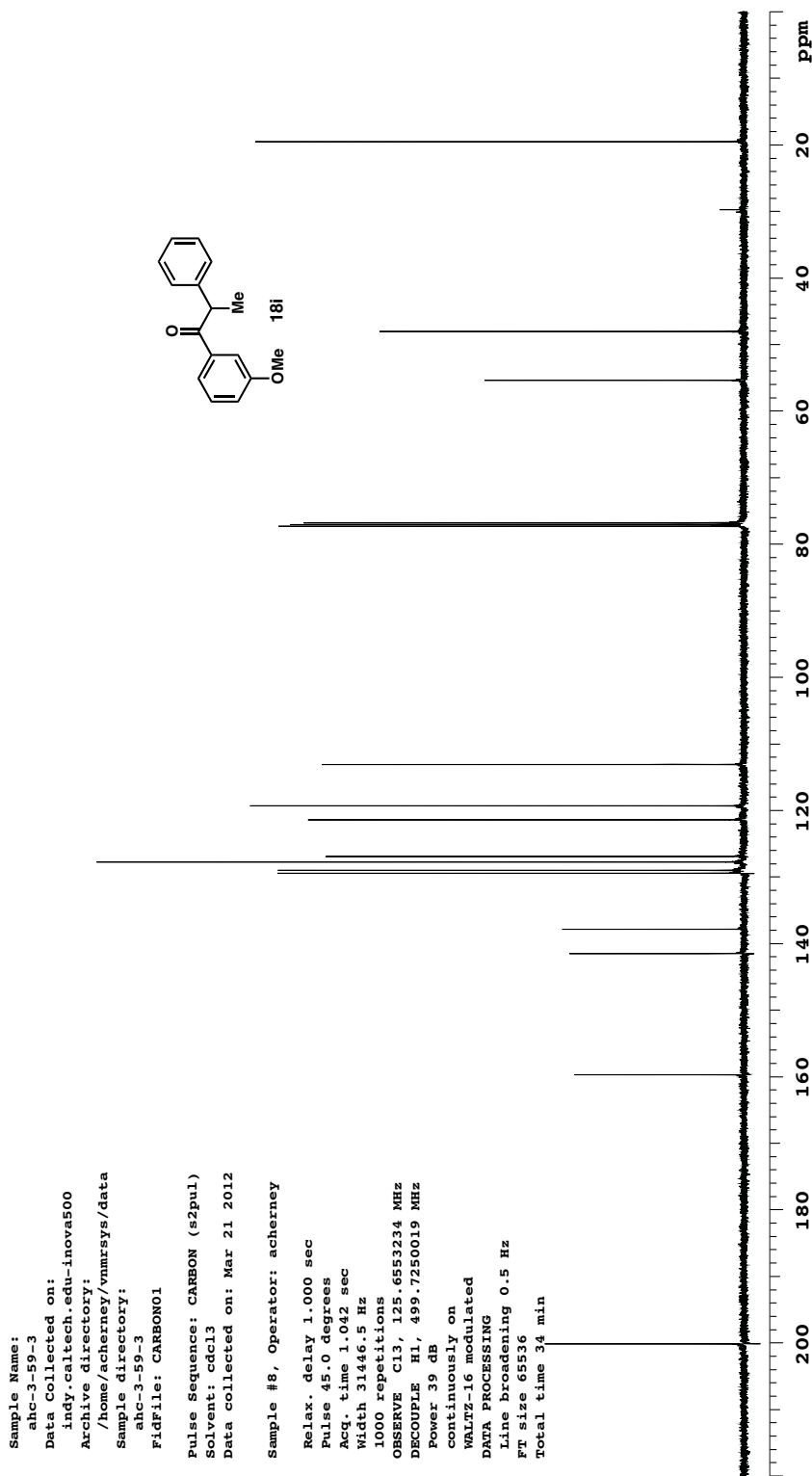


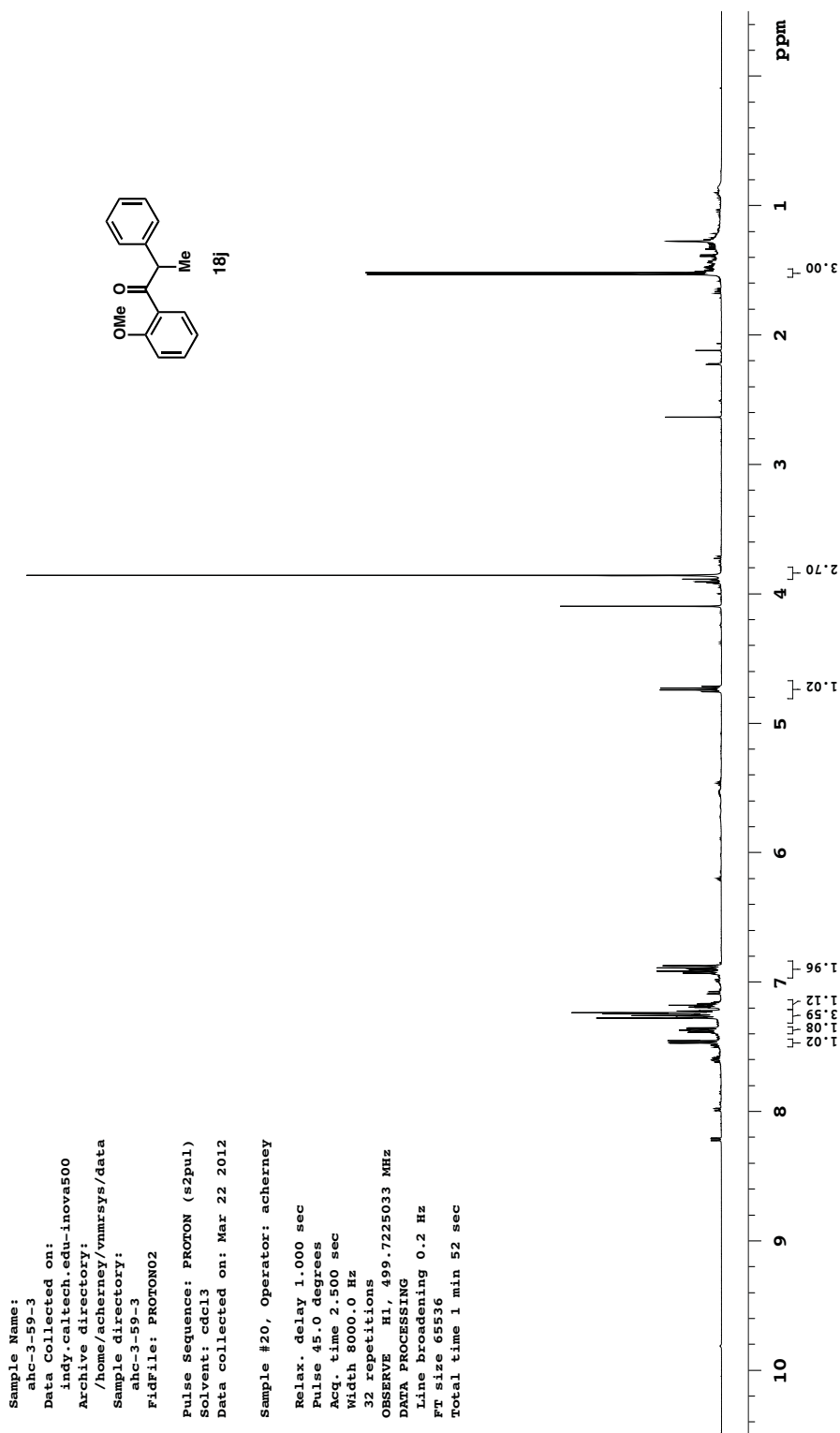
Sample Name:  
 ahc-3-49-4  
 Data Collected on:  
 indy.caltech.edu-inova500  
 Archive directory:  
 /home/acherney/vnmrsys/data  
 Sample directory:  
 ahc-3-49-4  
 Fidfile: CARBONO1  
 Pulse Sequence: CARBON (s2pul)  
 Solvent: cdcl3  
 Data collected on: Mar 19 2012  
 Sample #42, Operator: acherney  
 Relax. delay 1.000 sec  
 Pulse 45.0 degrees  
 Acq. time 1.042 sec  
 Width 31446.5 Hz  
 1000 repetitions  
 OBSERVE C13, 125.6553234 MHz  
 DECOUPLE H1, 499.7250019 MHz  
 Power 39 dB  
 continuously on  
 WALTZ-16 modulated  
 DATA PROCESSING  
 Line broadening 0.5 Hz  
 F1 size 65536  
 Total time 34 min

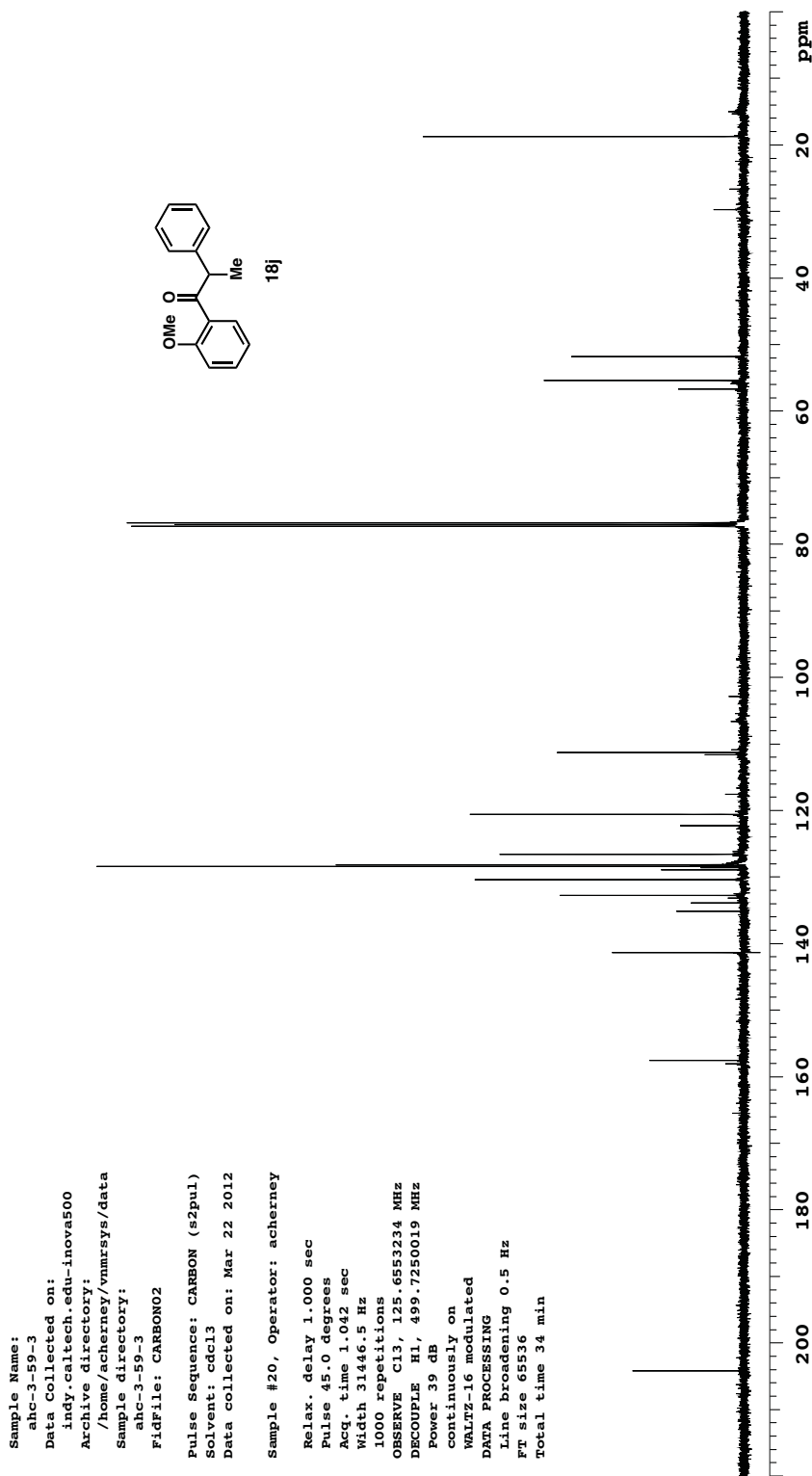


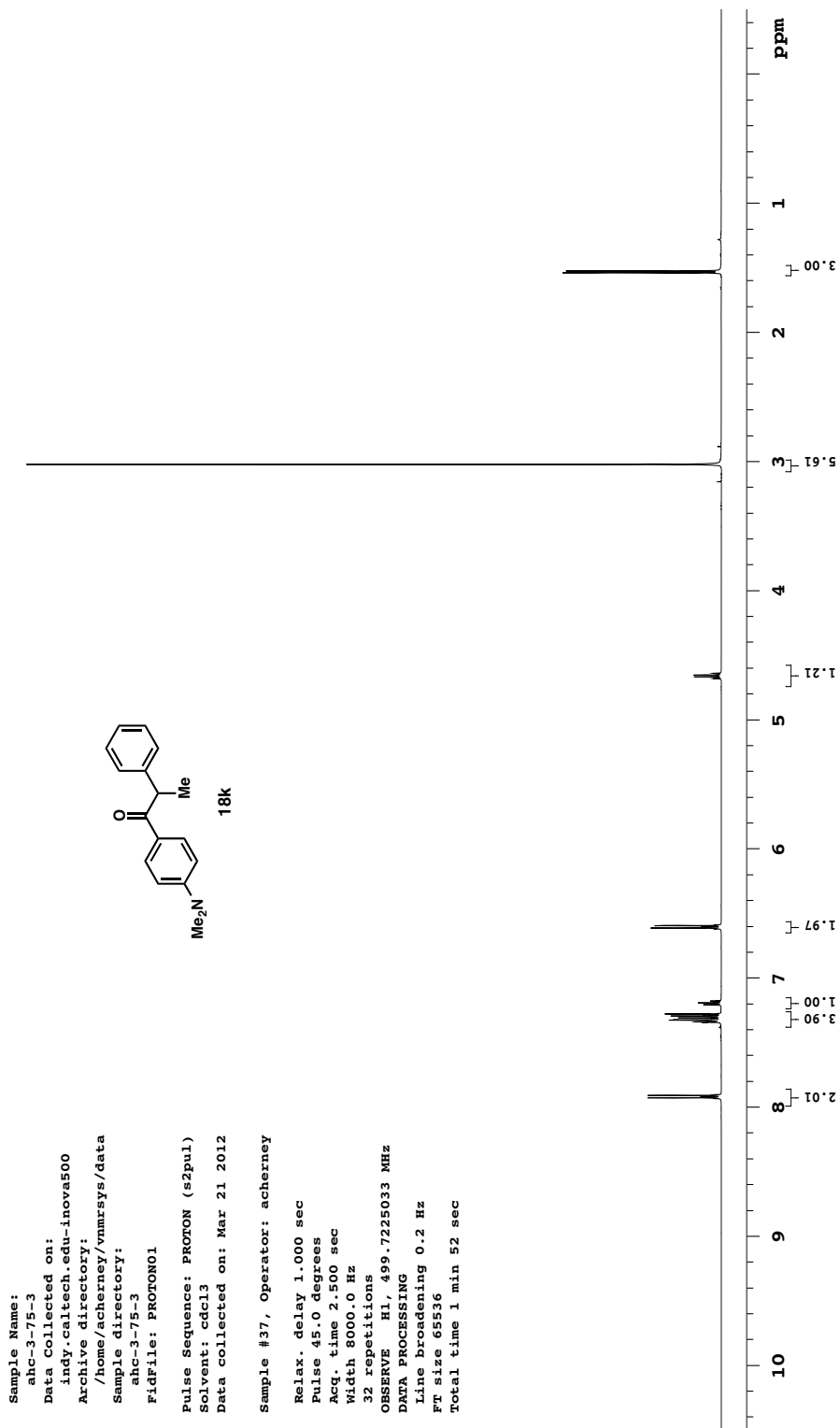
Sample Name:  
 ahc-3-59-3  
 Data Collected on:  
 indy.caltech.edu-inova500  
 Archive directory:  
 /home/acherney/vnmrSYS/data  
 Sample directory:  
 ahc-3-59-3  
 FidFile: PROTON01  
 Pulse Sequence: PROTON (s2pul)  
 Solvent: cdcl3  
 Data collected on: Mar 21 2012  
 Sample #8, Operator: acherney  
 Relax. delay 1.000 sec  
 Pulse 45.0 degrees  
 Acq. time 2.500 sec  
 Width 8000.0 Hz  
 32 repetitions  
 OBSERVE H1, 499.725033 MHz  
 DATA PROCESSING  
 Line broadening 0.2 Hz  
 FT size 65536  
 Total time 1 min 52 sec

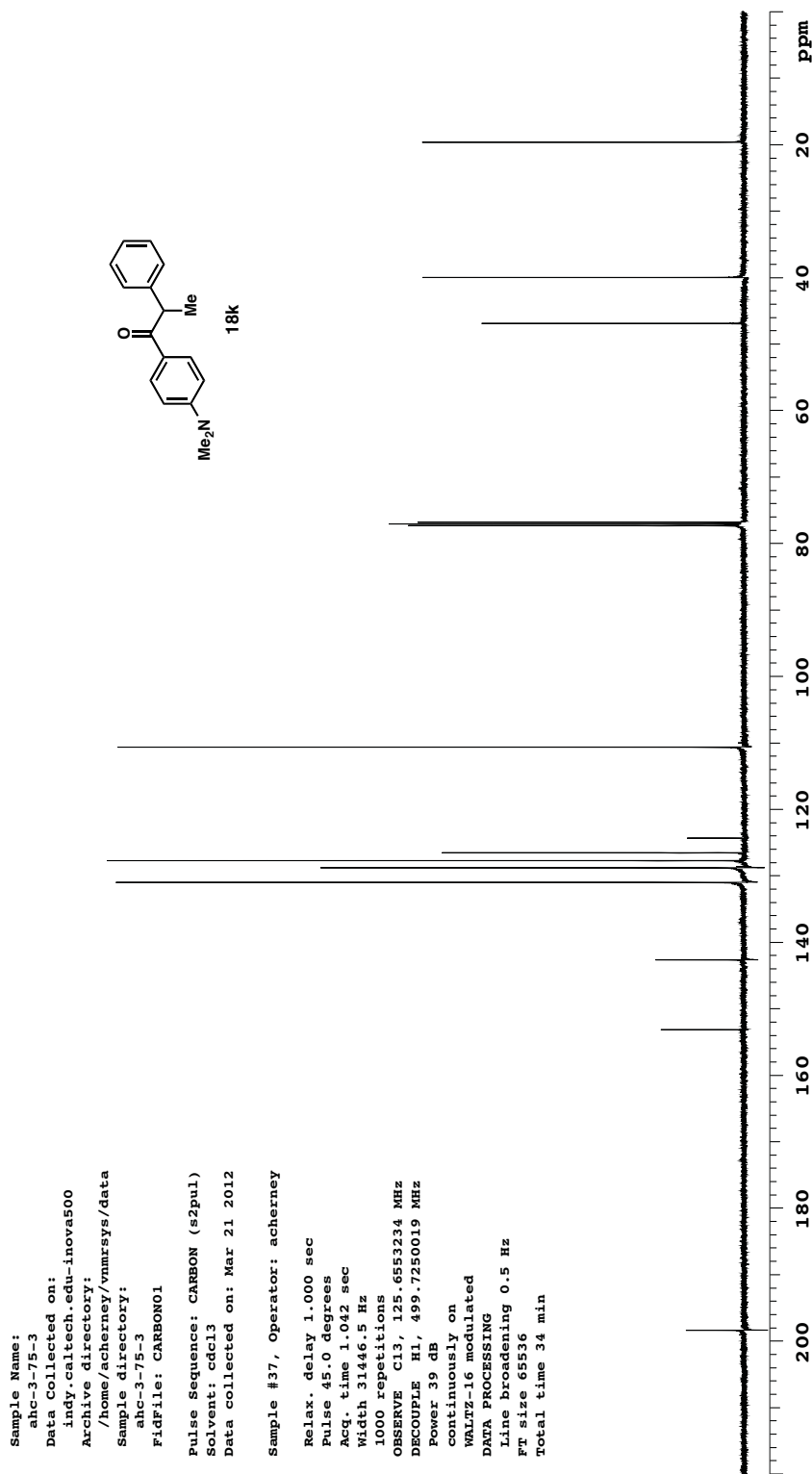












## STANDARD PROTON PARAMETERS

Sample Name:  
ahc-3-69-2-column  
Data Collected on:  
hg2.caltech.edu-mercury300  
Archive directory:

Sample directory:

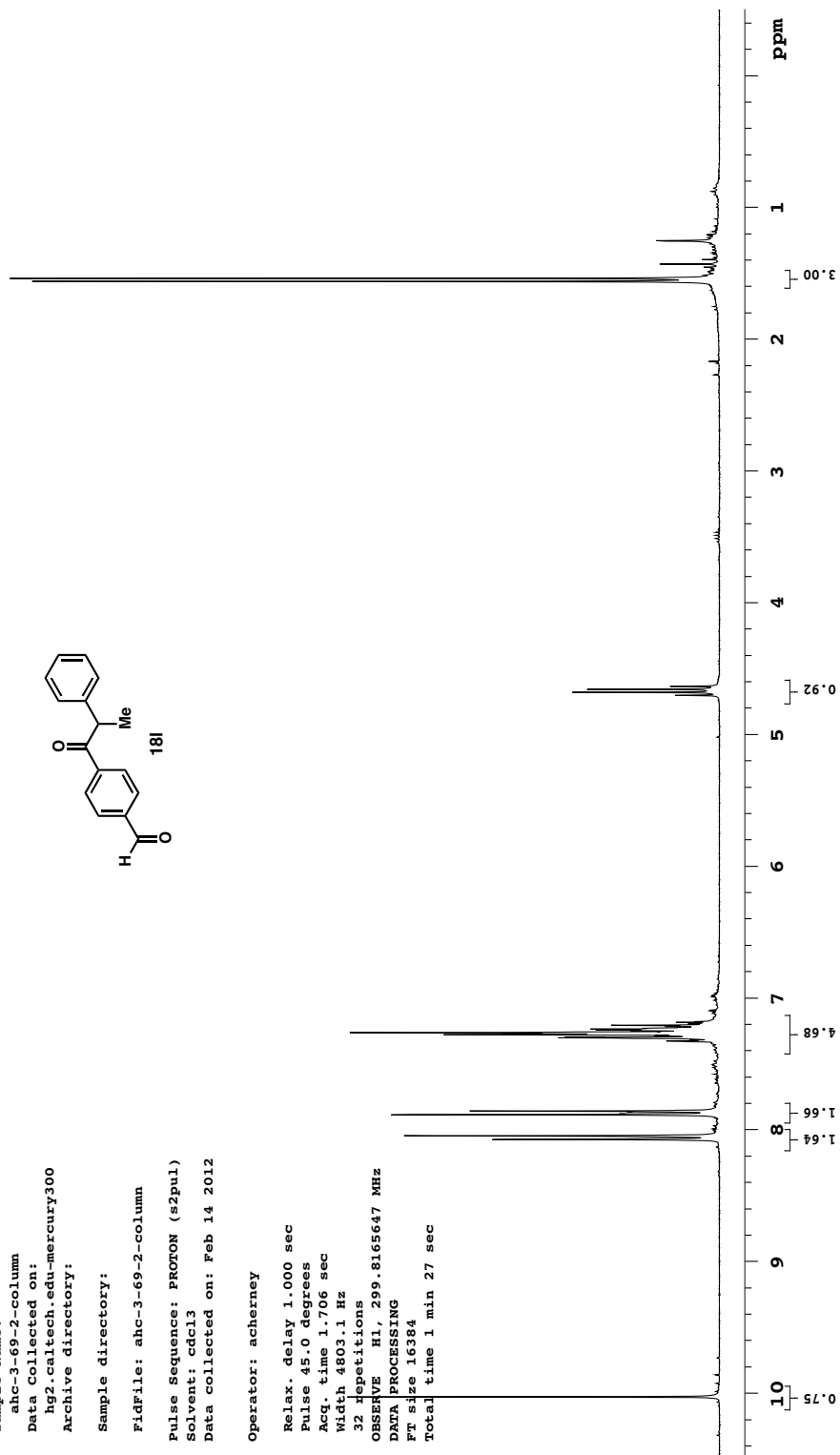
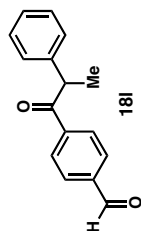
FidFile: ahc-3-69-2-column

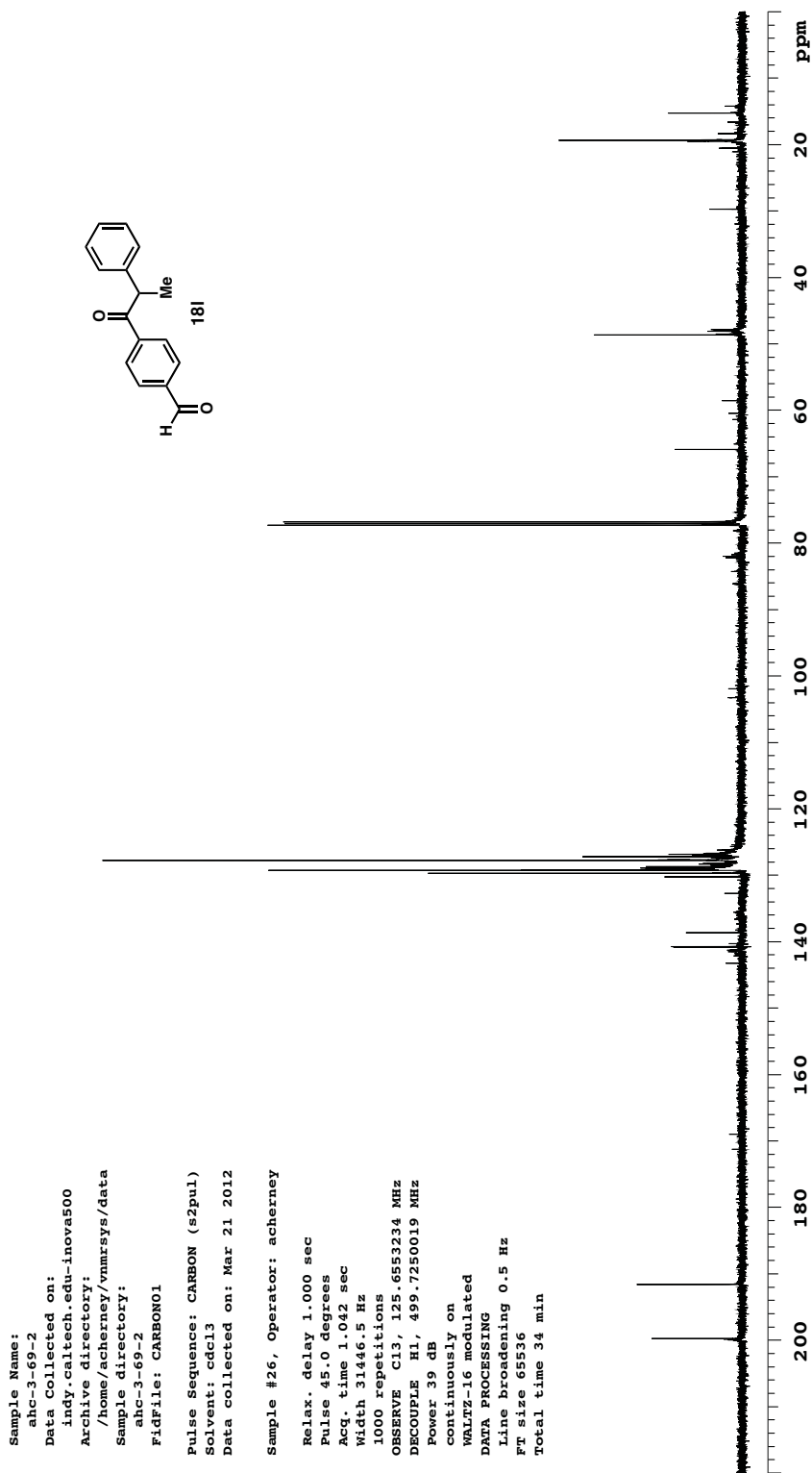
Pulse Sequence: PROTON (s2pul)

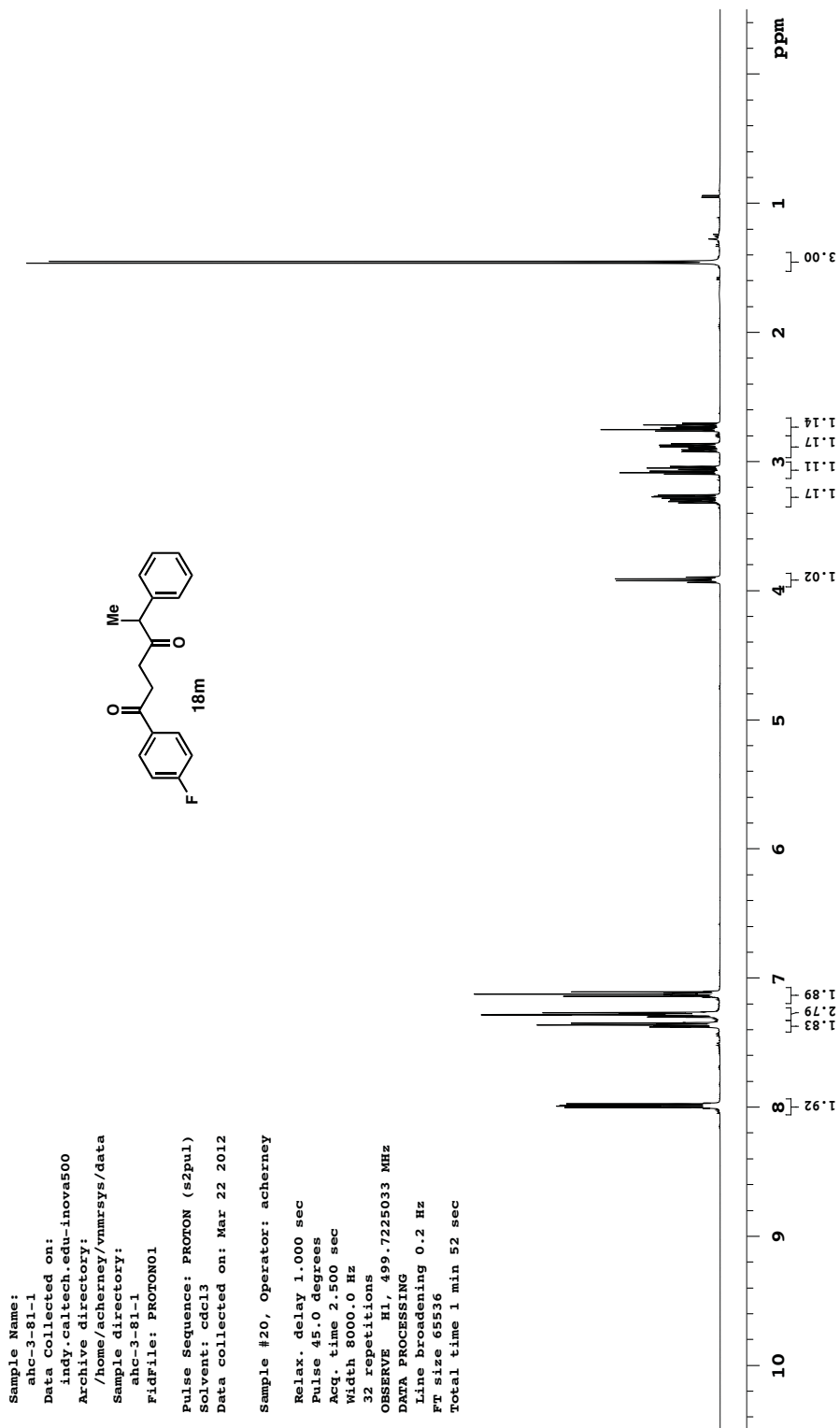
Solvent: cdcl3  
Data collected on: Feb 14 2012

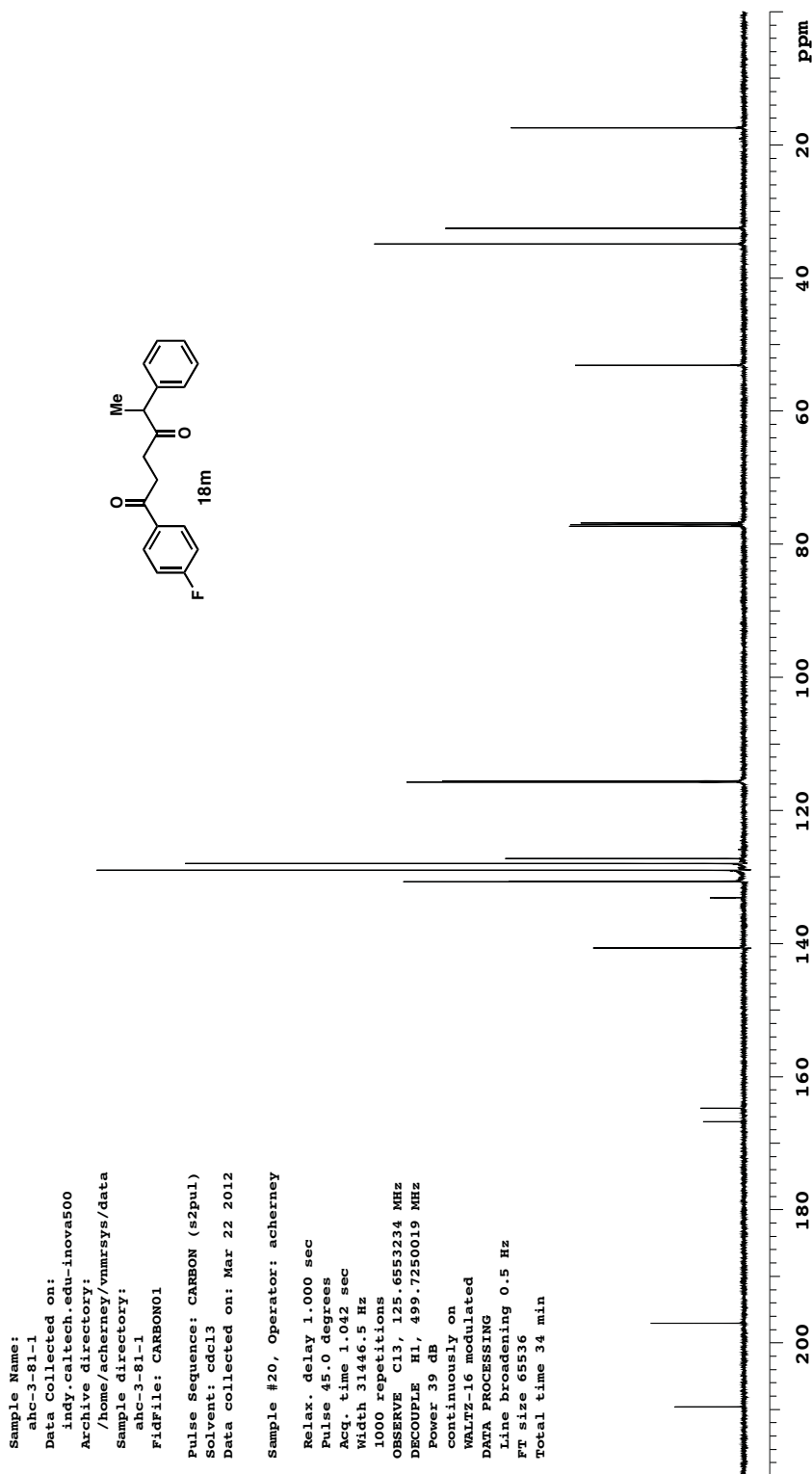
Operator: acherney

Relax. delay 1.000 sec  
Pulse 45.0 degrees  
Acq. time 1.706 sec  
Width 4803.1 Hz  
32 repetitions  
OBSERVE H1, 299.8165647 MHz  
DATA PROCESSING  
Ft size 16384  
Total time 1 min 27 sec



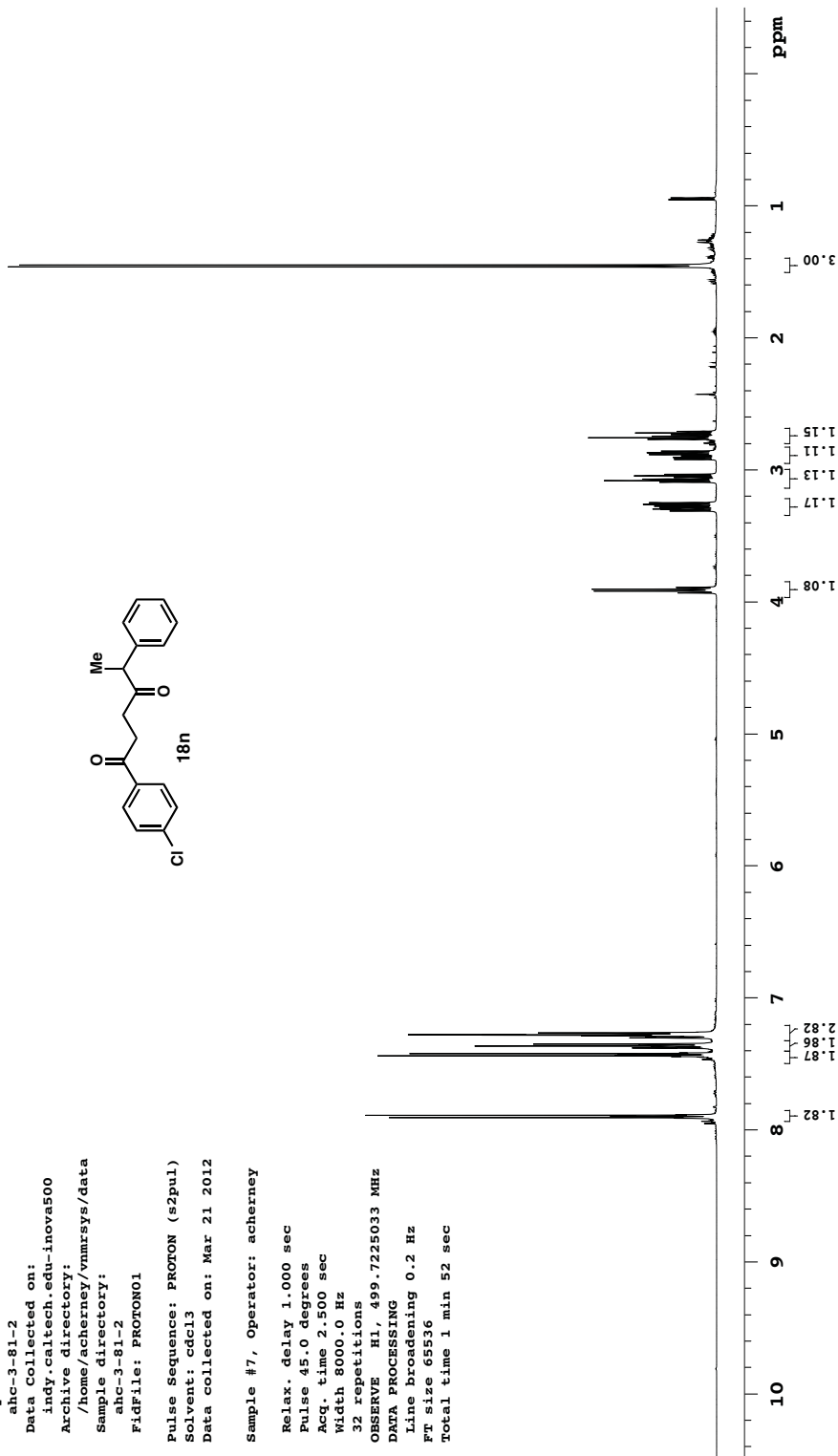
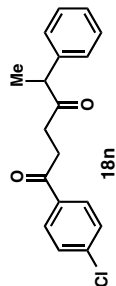


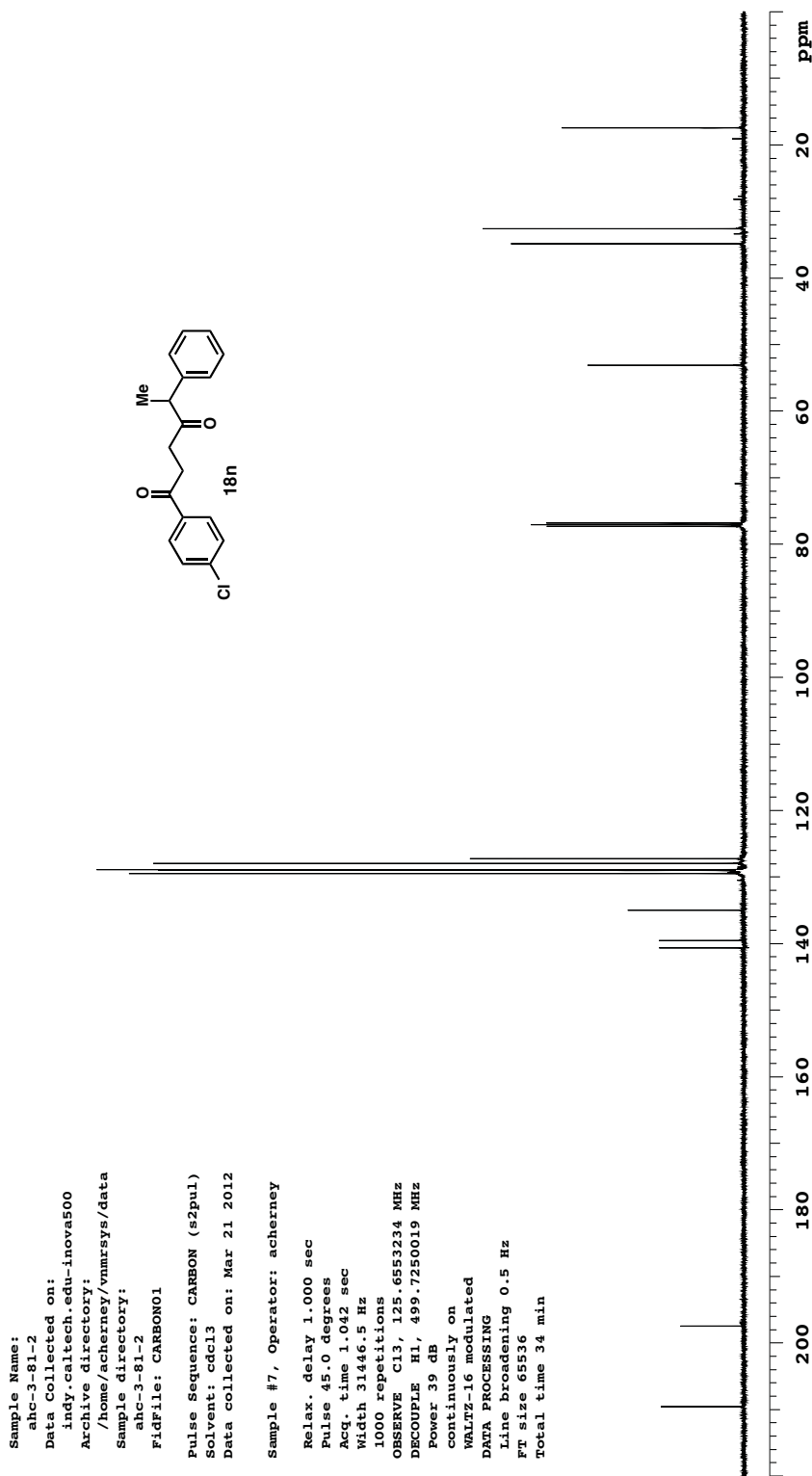


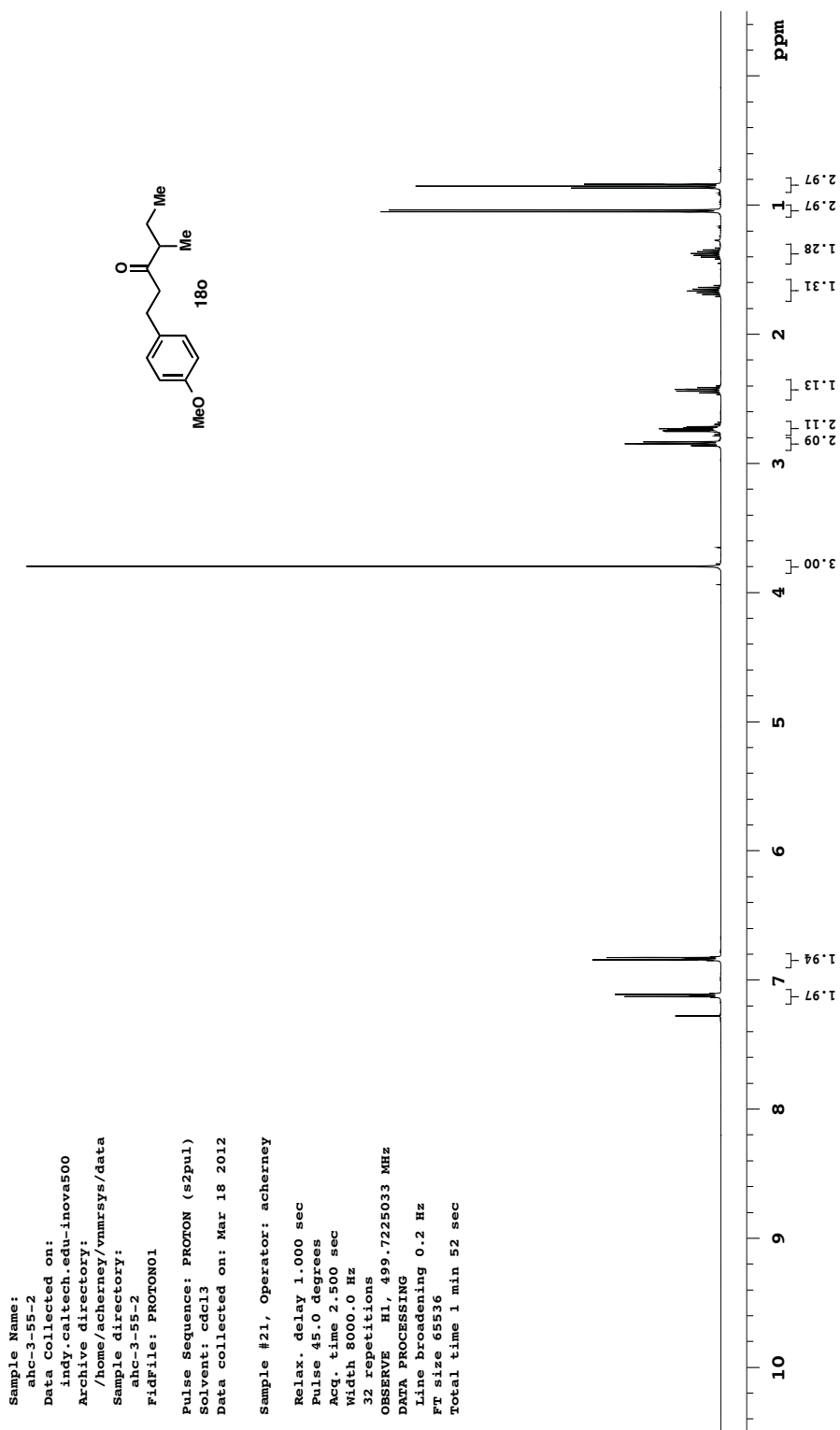


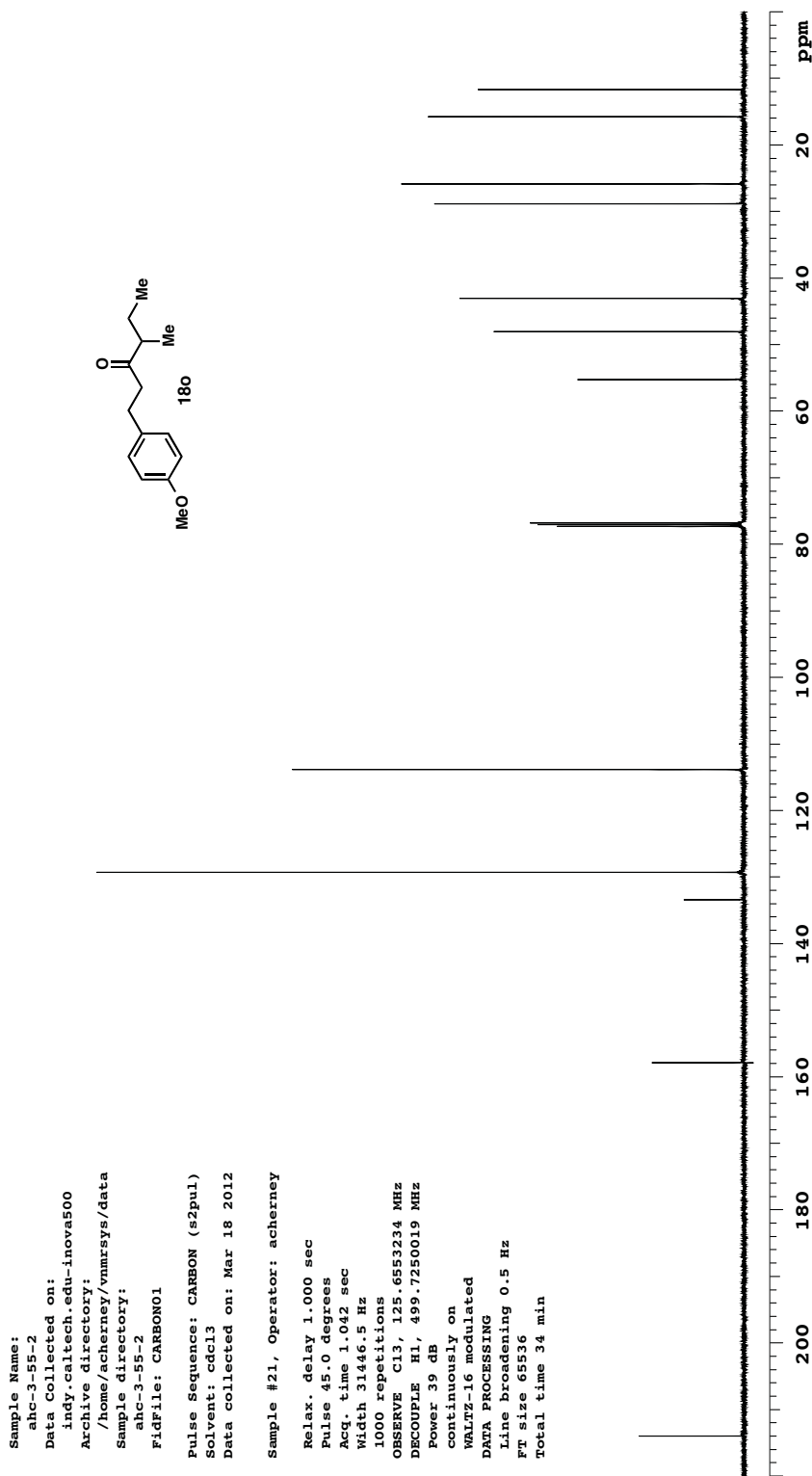
Sample Name:  
 ahc-3-81-2  
 Data Collected on:  
 indy.caltech.edu-inova500  
 Archive directory:  
 /home/acherney/vnmrSYS/data  
 Sample directory:  
 ahc-3-81-2  
 FidFile: PROTON01  
 Pulse Sequence: PROTON (s2pul)  
 Solvent: cdcl3  
 Data collected on: Mar 21 2012

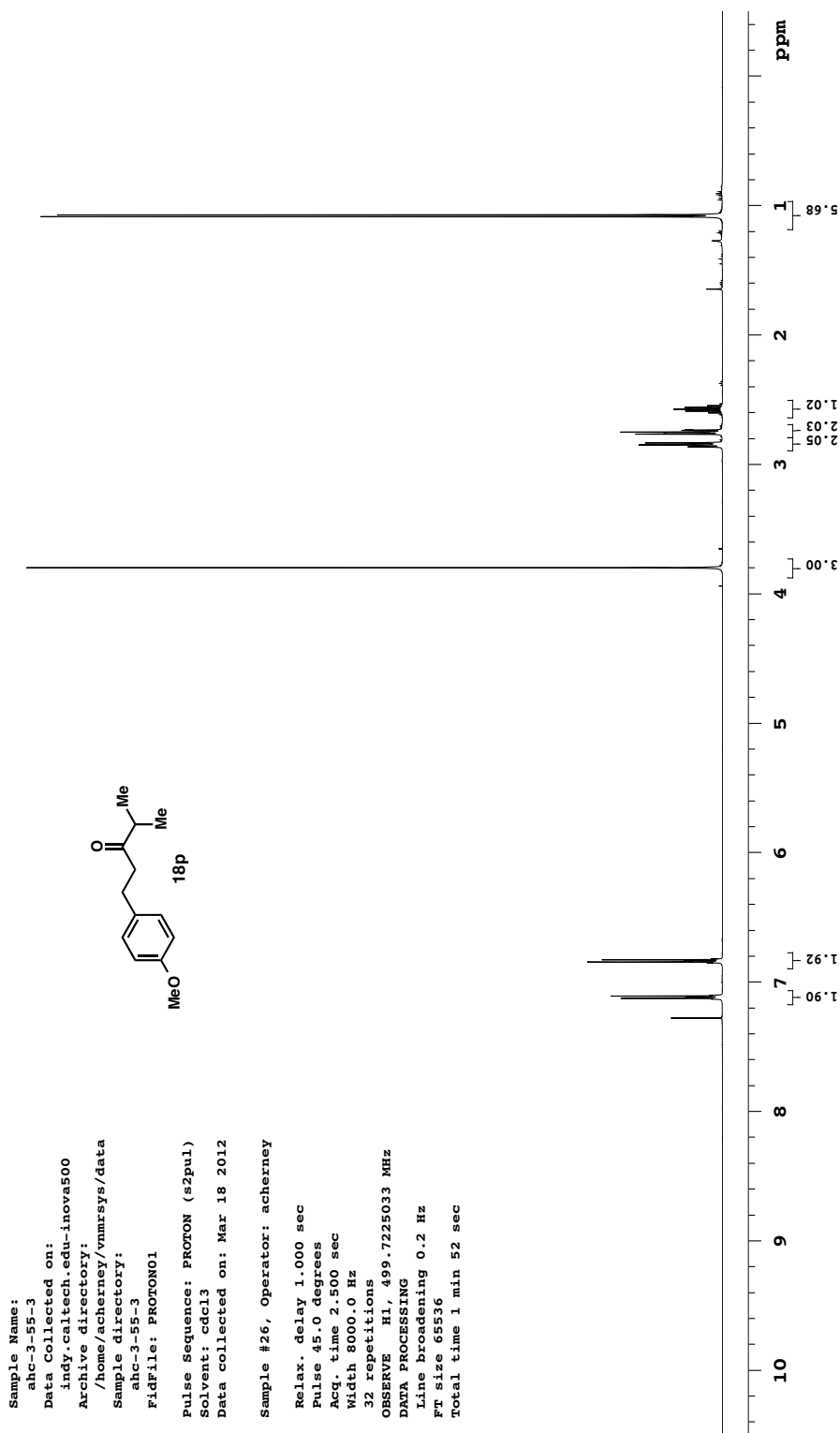
Sample #7, Operator: acherney  
 Relax. delay 1.000 sec  
 Pulse 45.0 degrees  
 Acq. time 2.500 sec  
 Width 8000.0 Hz  
 32 repetitions  
 OBSERVE H1, 499.7225033 MHz  
 DATA PROCESSING  
 Line broadening 0.2 Hz  
 FT size 65536  
 Total time 1 min 52 sec

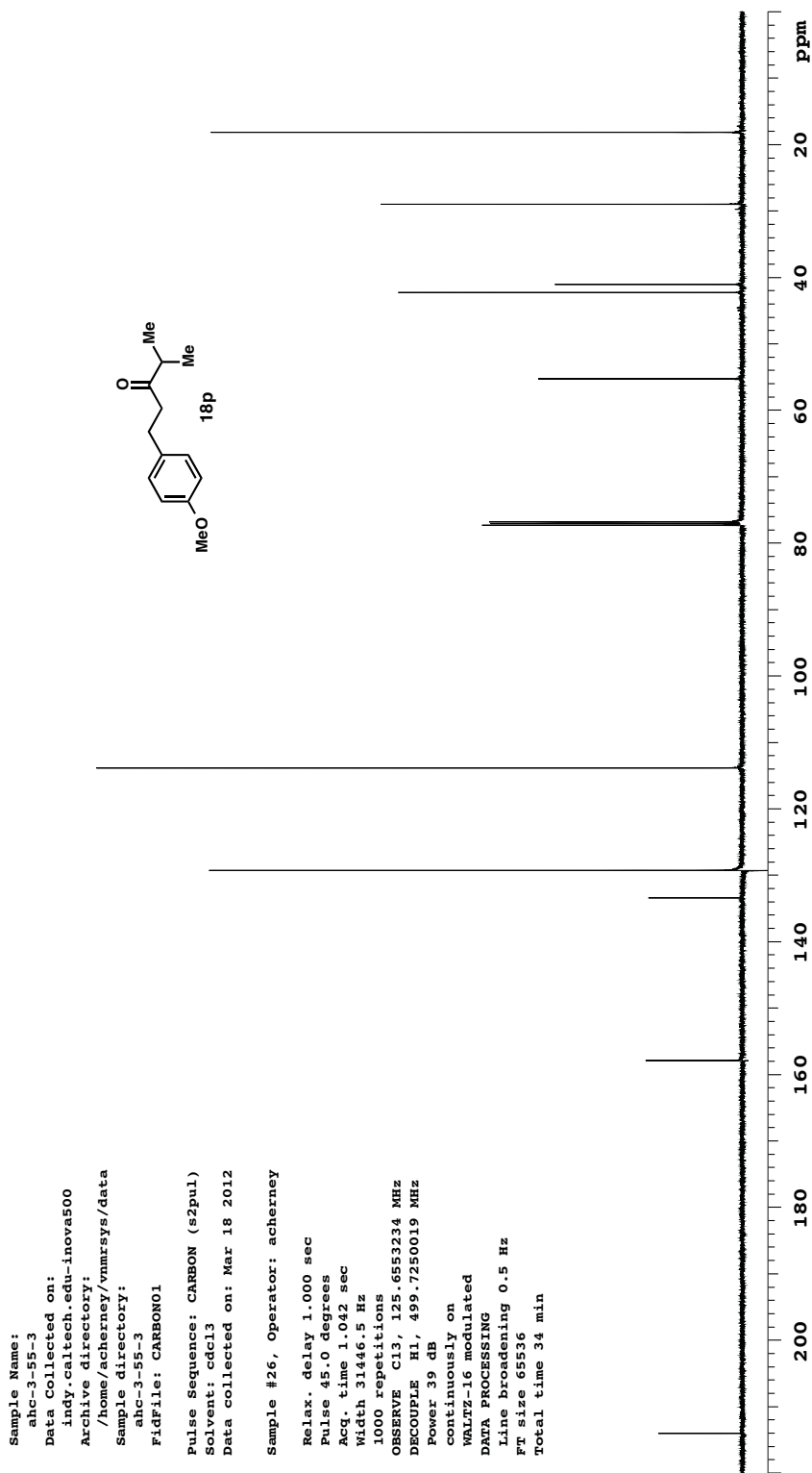


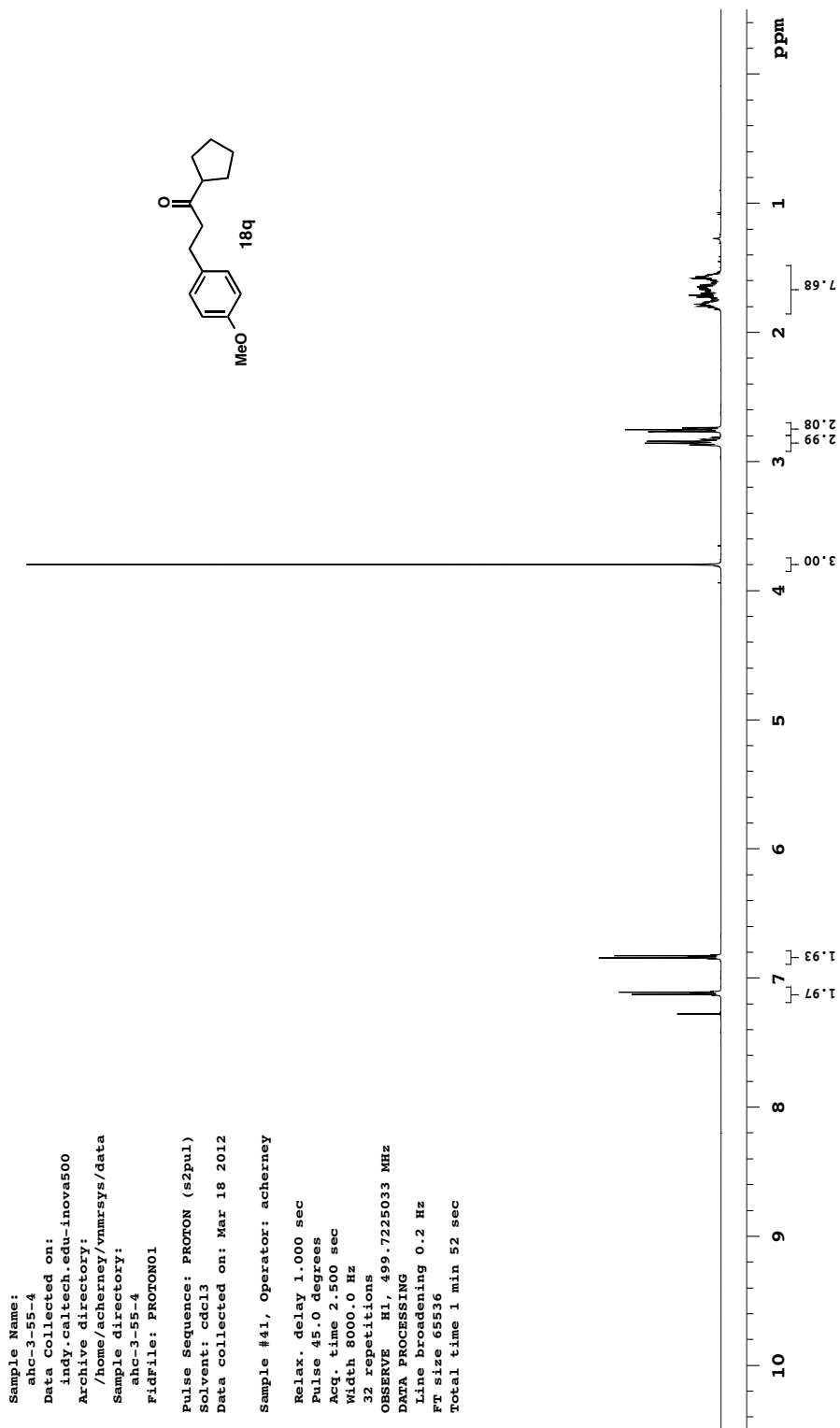


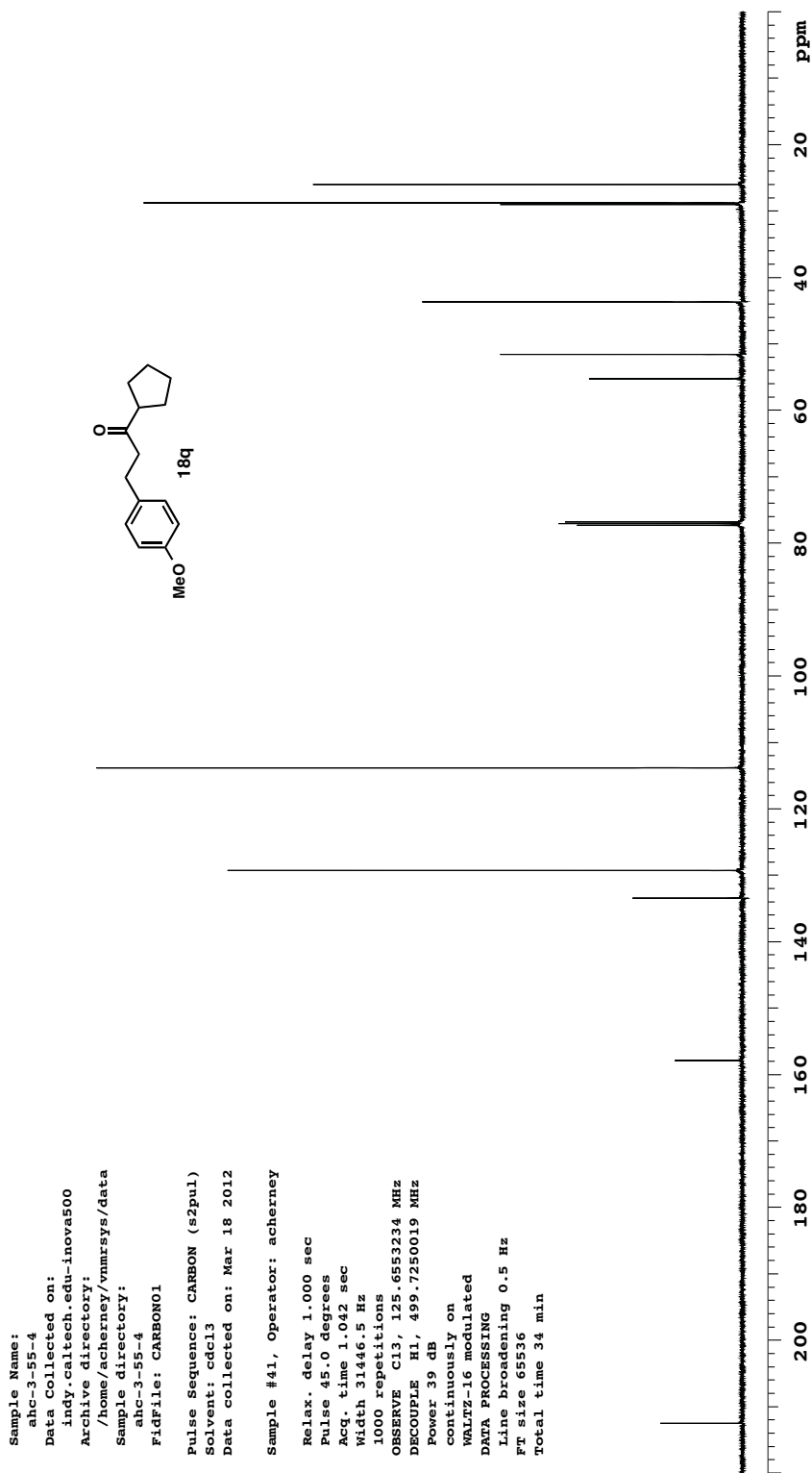












## Chapter 3

### *Catalytic Asymmetric Reductive Acyl Cross-Coupling: Synthesis of Enantioenriched Acyclic $\alpha,\alpha$ -Disubstituted Ketones<sup>†</sup>*

#### 3.1 INTRODUCTION

Enantioenriched acyclic  $\alpha,\alpha$ -disubstituted carbonyl compounds are versatile synthetic intermediates for the synthesis of natural products and pharmaceutical agents. Due to their ubiquity and utility, the development of new synthetic methods to prepare such compounds has been the subject of intense research. In addition to numerous chiral auxiliary-based strategies,<sup>1</sup> there are an increasing number of catalytic asymmetric  $\alpha$ -alkylation,<sup>2</sup> -alkenylation,<sup>3</sup> and -arylation<sup>4</sup> reactions that provide products with  $\alpha$ -tertiary

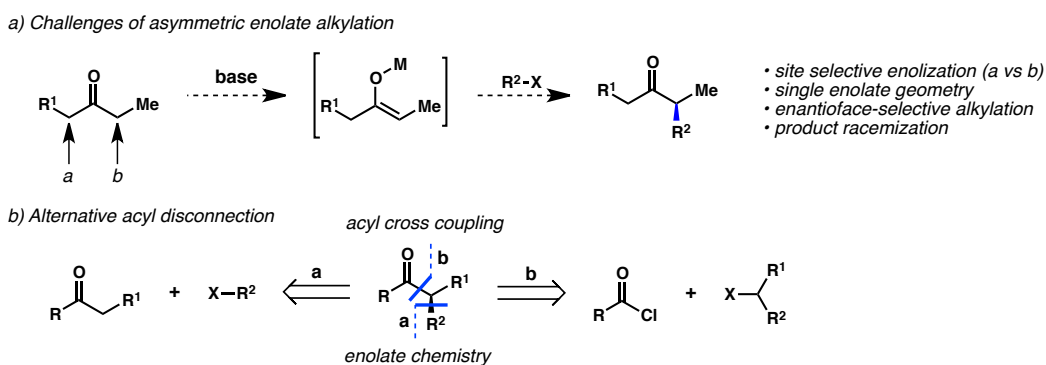
---

<sup>†</sup> Portions of this chapter have been reproduced from published studies (see reference 21) and the supporting information found therein. The research presented in this chapter was completed in collaboration with Nathaniel T. Kadunce, a graduate student in the Reisman group.

stereogenic centers. Collectively, these methods represent a versatile array of tools that are indispensable to synthetic chemists.

The vast majority of  $\alpha$ -functionalization reactions described above proceed via the intermediacy of enolates or enolate equivalents. As a result, the stereochemistry of C–C bond formation is typically influenced by both the enolate geometry and the  $\pi$ -facial selectivity. The synthesis of acyclic  $\alpha,\alpha$ -disubstituted ketones presents the added requirements of 1) site-selective enolization and 2) mild conditions that prevent racemization of the newly formed tertiary stereogenic center (Figure 3.1, a).<sup>5,6</sup> Strategically, we envisioned that transition metal-catalyzed acyl cross-coupling reactions — which typically occur at low temperatures and circumvent enolate intermediates altogether — could represent an alternative approach to prepare enantioenriched acyclic  $\alpha,\alpha$ -disubstituted ketones in a convergent and regioselective fashion (Figure 3.1, b).<sup>7</sup>

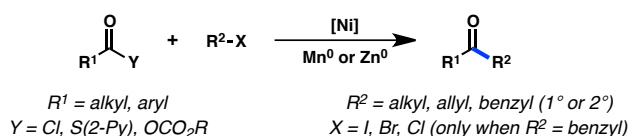
**Figure 3.1.** Approach to asymmetric acyl cross-coupling.



Specifically, we hypothesized that Ni-catalyzed *reductive* coupling reactions<sup>8,9</sup> between carboxylic acid derivatives and secondary alkyl halides<sup>10</sup> could be amenable to asymmetric catalysis. While Ni-mediated reductive homocoupling of organohalide electrophiles was first reported by Semmelhack and coworkers in 1971,<sup>11</sup> a renewed

interest in reductive, or cross-electrophile, methodologies in recent years has been spearheaded by the laboratories of Weix<sup>12</sup> and Gong.<sup>13</sup> Building off of electrochemical studies,<sup>14</sup> Weix and coworkers reported in 2012 the reductive cross-coupling of aliphatic acid chlorides or thioesters with alkyl halides, including benzylic chlorides (Scheme 3.1).<sup>15</sup> Concurrently, Gong and coworkers disclosed a related coupling of aromatic acid chlorides with alkyl halides.<sup>16</sup> Significantly, both transformations demonstrate the ability of Ni catalysts to cross-couple hindered C(sp<sup>3</sup>)-hybridized secondary alkyl halides.

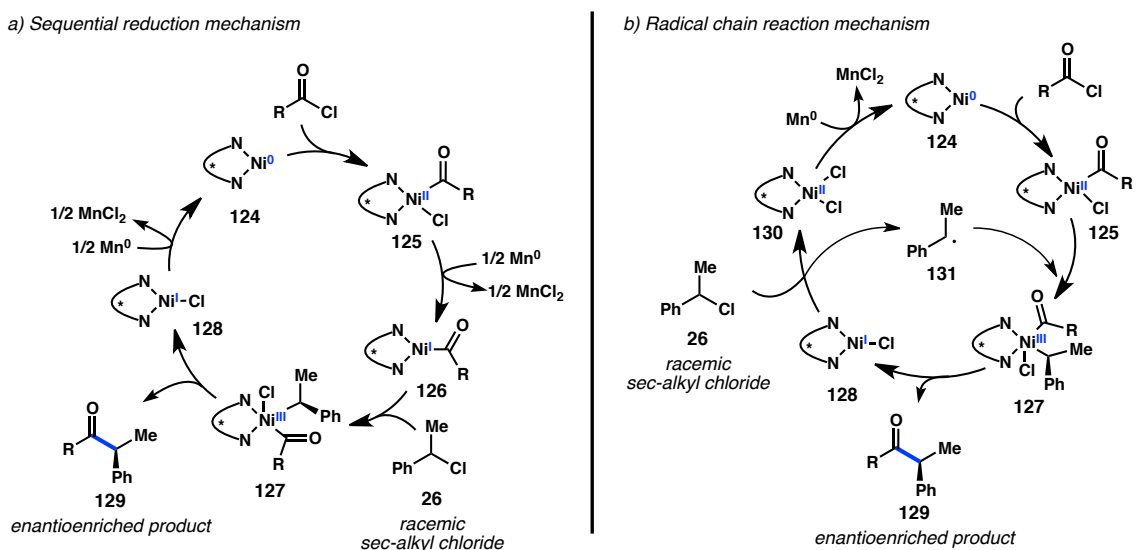
**Scheme 3.1.** Racemic Reductive Cross-Coupling of Acyl Electrophiles.



Although several different mechanisms have been proposed for these reactions, two limiting cases can be considered.<sup>12b</sup> In a sequential reduction mechanism, oxidative addition of the acid chloride could generate Ni<sup>II</sup>-acyl complex **125**, which could be reduced by Mn<sup>0</sup> to give Ni<sup>I</sup>-acyl species **126** (Figure 3.2).<sup>17</sup> Subsequent oxidative addition of benzyl chloride **26** by a radical process would then generate Ni<sup>III</sup> complex **127**, converging both enantiomers of **26** to a single diastereomer.<sup>18</sup> Reductive elimination of ketone **129** from **127** followed by reduction of the Ni<sup>I</sup>-chloride complex would close the catalytic cycle. An alternative proposal is the radical chain reaction mechanism, wherein Ni<sup>II</sup>-acyl complex **125**, formed by reaction of Ni<sup>0</sup> with an acid chloride, combines with free benzylic radical **131** to produce Ni<sup>III</sup> complex **127**. Reductive elimination delivers ketone **129** and Ni<sup>I</sup>-chloride **128**, which can abstract a halide from starting material **26**. The resultant benzylic radical (**131**) is free to escape the solvent cage, while Ni<sup>II</sup>-

dichloride **130** is reduced by  $\text{Mn}^0$  to reform  $\text{Ni}^0$  complex **124**. The key conceptual difference between these two proposed mechanisms is simply the lifetime of benzylic radical **131**. Recent mechanistic studies by Weix and coworkers support a radical chain mechanism for the reductive coupling of aryl and alkyl halides.<sup>12c</sup>

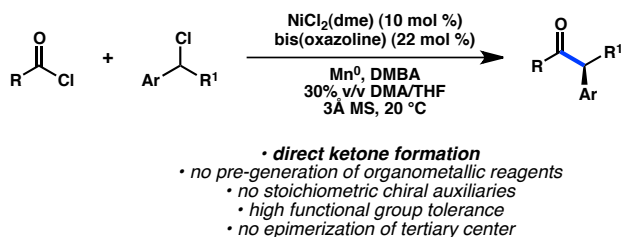
**Figure 3.2.** Two potential mechanisms for Ni-catalyzed reductive cross-coupling.



Regardless of which mechanism is operative under our reaction conditions, we hypothesized that an appropriate chiral catalyst could promote a stereoconvergent transformation of benzyl chloride **26** because of the stereoablative nature with which **26** interacts with Ni. Indeed, Fu and coworkers have shown that Ni catalysts promote stereoconvergent cross-couplings of racemic secondary electrophiles and organometallic reagents under similar reaction conditions.<sup>19</sup> While a stereoconvergent oxidative addition is plausible, Molander and Kozlowski have also recently demonstrated the feasibility of a stereochemistry-determining reductive elimination.<sup>20</sup> Based on this mechanistic understanding, we questioned whether the use of a chiral Ni catalyst could enable the stereoconvergent synthesis of enantioenriched  $\alpha,\alpha$ -disubstituted ketones from racemic

alkyl halides. Herein we report the successful execution of this plan, which has resulted in the development of the first enantioselective Ni-catalyzed reductive cross-coupling reaction between acid chlorides and secondary alkyl halides (Figure 3.3).<sup>21</sup>

**Figure 3.3.** This work: Asymmetric reductive acyl cross-coupling.



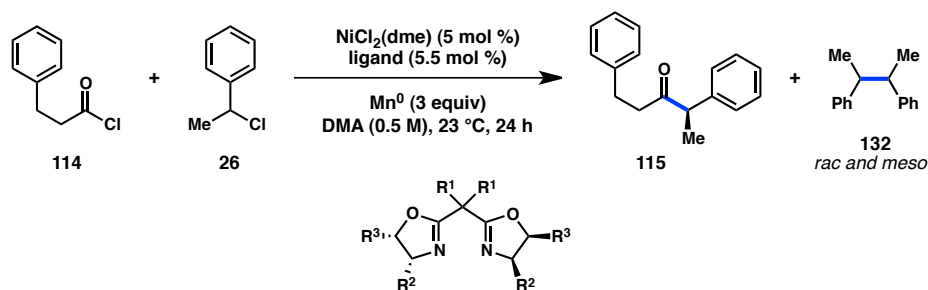
## 3.2 DEVELOPMENT OF AN ASYMMETRIC REDUCTIVE ACYL CROSS-COUPLING

### 3.2.1 Identification of a Chiral Catalyst System

Our investigations began with the reductive coupling of hydrocinnamoyl chloride (**114**) and (1-chloroethyl)benzene (**26**). Using catalytic  $\text{NiCl}_2(\text{dme})$  in *N,N*-dimethylacetamide (DMA) with  $\text{Mn}^0$  as the stoichiometric reductant — conditions previously reported to promote the coupling of acid chlorides and alkyl halides<sup>15a</sup> — a screen of chiral ligands was conducted. Evaluation of a set of bis(oxazoline) ligands revealed that both phenyl substitution and an isopropylidene linker were critical for imparting moderate enantioinduction (entries 1–5). Elaboration to tetrasubstituted ligands (entries 6 and 7) or indanyl-substituted ligands (entries 8–10) produced ketone **115** with reduced enantioselectivity. Other bidentate and tridentate ligand scaffolds (**L38**, **L105**–**L108**) delivered the product with little asymmetric induction. While we were encouraged

by the unique activity of bis(oxazoline) **L36**, use of this ligand delivered ketone **115** in only 7% yield, with homocoupled product **132** being the major side product. Nonetheless, we proceeded to investigate other reaction conditions to further increase the enantioselectivity of the transformation.

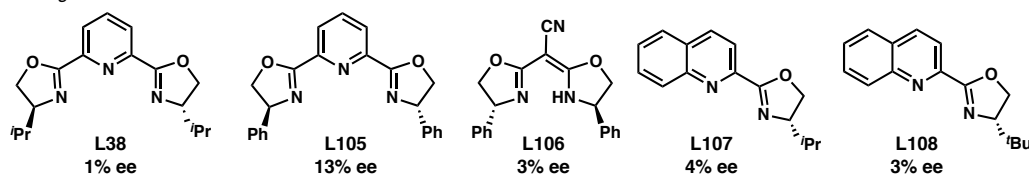
**Figure 3.4.** Evaluation of chiral ligand frameworks.



Bis(oxazoline) Ligand Scaffold

Entry	R <sup>1</sup>	R <sup>2</sup>	R <sup>3</sup>	Ligand	ee (%)
1	Me	<sup>i</sup> Pr	H	L99	27
2	Me	<sup>t</sup> Bu	H	L66	5
3	Me	Bn	H	L100	37
4	Me	Ph	H	L36	66
5	H	Ph	H	L101	12
6	H	Ph	Ph	L43	9
7	-CH <sub>2</sub> CH <sub>2</sub> -	Ph	Ph	L102	55
8	H	indanyl		L103	8
9	Me	indanyl		L51	7
10	-CH <sub>2</sub> CH <sub>2</sub> -	indanyl		L104	10

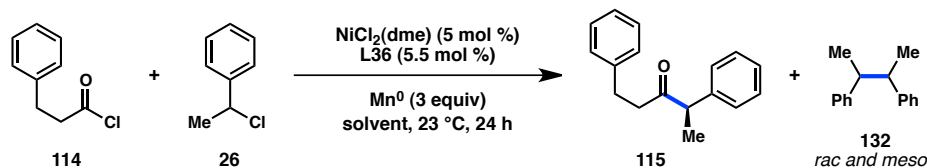
Other Ligand Scaffolds



After conducting a screen of various solvents, we were pleased to observe that less strongly coordinating solvents provided a higher degree of asymmetric induction (Table 3.1). Accordingly, in the presence of THF, ketone **115** was obtained in 92% ee but

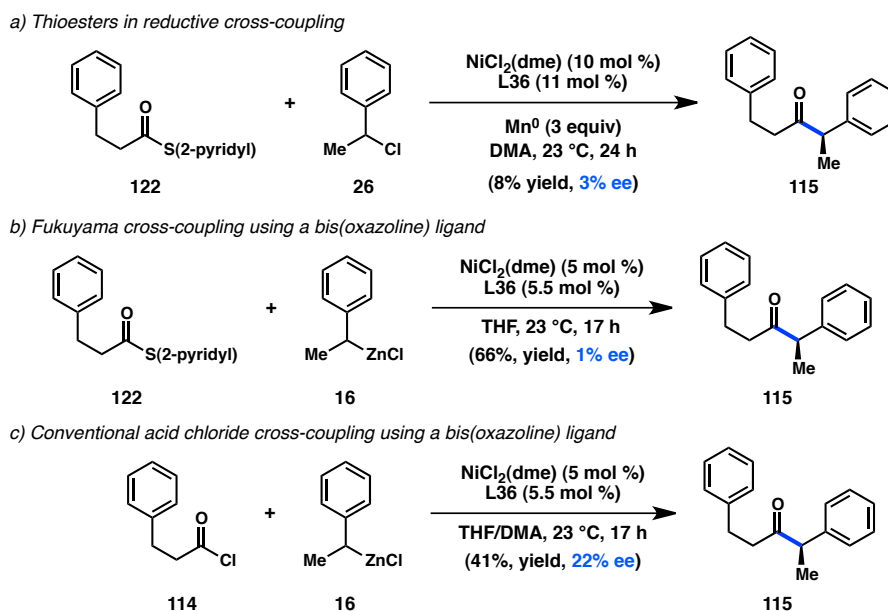
only 19% yield (entry 6). Unfortunately, the reaction did not provide full conversion of benzyl chloride **26**, and homocoupling of **26** was competitive.

**Table 3.1.** Evaluation of solvents.



Entry	Solvent	ee (%)	Entry	Solvent	ee (%)
1	DMPU	37	4	DME	72
2	DMF	50	5	EtOAc	82
3	DMA	66	6	THF	92

At this stage, the role of the leaving group on enantioselectivity was examined. Reductive coupling of benzyl chloride **26** with 2-pyridyl thioester **122** in the presence of **L36** failed to impart any enantioselectivity (Figure 3.5, a). In this case, following oxidative addition, the bidentate thiolate leaving group may inhibit the chiral catalyst, and the poor selectivity may arise from racemic background reactivity. Similarly, as was observed in previous studies on an asymmetric Fukuyama cross-coupling (see Chapter 2), exposure of 2-pyridyl thioester **122** and organozinc halide **16** to  $\text{NiCl}_2(\text{dme})$  and **L36** delivered the desired ketone in 66% yield but only 1% ee (Figure 3.5, b), confirming the non-innocent nature of the thiolate leaving group. We next studied a conventional cross-coupling of acid chloride **114** and organozinc halide **16**, but the reaction did not proceed in THF. Alternatively, a mixed solvent system of THF and DMA allowed ketone **115** to be formed in 22% ee (Figure 3.5, c). This disparity in enantioinduction for the conventional Negishi-type and reductive cross-couplings suggests a difference in the chiral catalyst structure during the enantiodetermining step of the transformation.

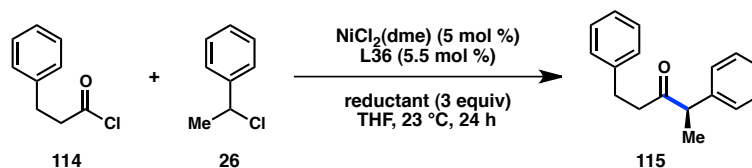
**Figure 3.5.** Study of enantioselectivity with thioesters and organozinc halides.

### 3.2.2 Optimization of Reactivity for an Enantioselective Reaction

Having identified conditions for a highly enantioselective reductive cross-coupling, we proceeded to optimize the yield of the reaction. When THF was utilized as a solvent, the Ni catalyst was poorly reactive, delivering low conversions of benzyl chloride **26** and no selectivity for ketone formation over benzylic homocoupling. Furthermore, the sluggishness of the reactivity induced acid chloride **114** to react with THF, affording ester **133**.<sup>22</sup> We hypothesized that as we transitioned from solvents with high dielectric constants (e.g., DMA, DMPU, and DMF) to THF, the electron-transfer step might become rate-limiting. Unfortunately, a screen of other reductants failed to provide better yields than  $\text{Mn}^0$  (Table 3.2, entry 1).  $\text{Zn}^0$  provided complete conversion of the starting materials but favored homocoupling over heterocoupling (entry 2). The

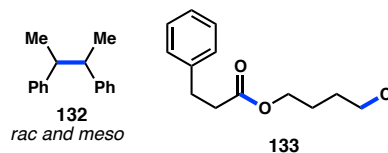
soluble reductant cobaltocene ( $\text{CoCp}_2$ ) was also ineffective at promoting cross-coupling (entry 6).

**Table 3.2.** Evaluation of stoichiometric reductants.



Entry	Reductant	Conversion (%)	Yield (%)	ee (%)
1	$\text{Mn}^0$	43	19	92
2	$\text{Zn}^0$	100	13	46
3	$\text{Mg}^0$	100	trace	20
4	$\text{Co}^0$	0	0	--
5	$\text{Fe}^0$	0	0	--
6	$\text{CoCp}_2$	0	0	--

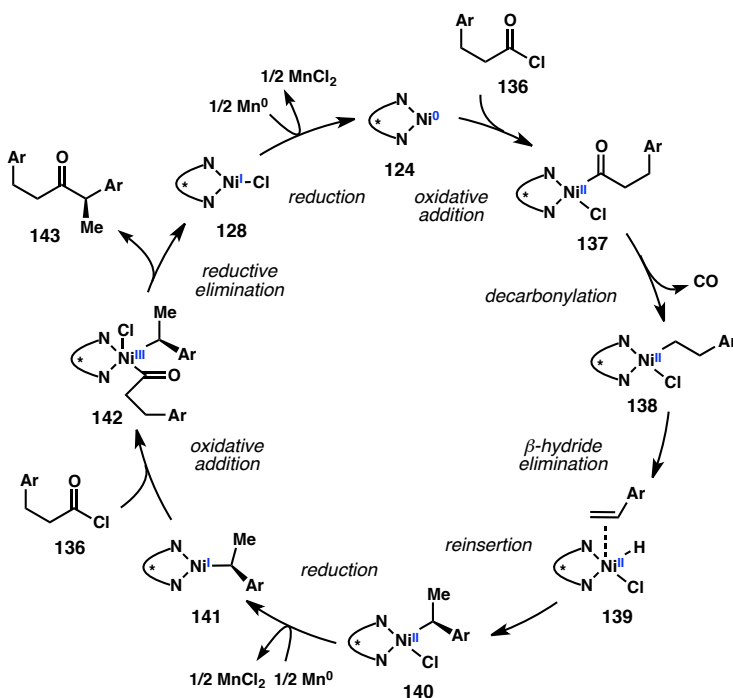
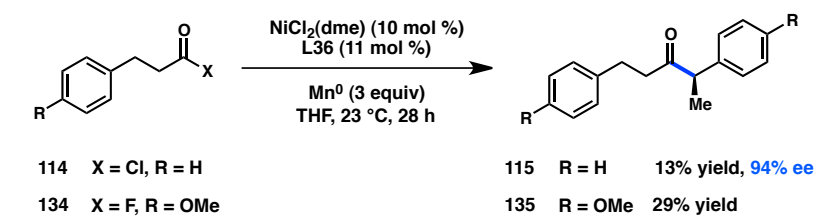
Side Products:



The sluggish reactivity toward benzyl chloride **26** in THF also resulted in unexpected rearrangement products. During the course of our studies, we observed that in the absence of benzyl coupling partner **26**, treatment of acid chloride **114** with  $\text{NiCl}_2(\text{dme})$ , **L36**, and  $\text{Mn}^0$  in THF still produced **115** in 13% yield and 94% ee (Figure 3.6). Further optimization demonstrated that acid fluoride **134** delivers ketone **135** in 29% yield. Surprisingly, no product is detected when the reaction is performed using DMA as a cosolvent. A possible catalytic cycle is displayed in Figure 3.6. Oxidative addition of  $\text{Ni}^0$  to acid chloride **136** forms  $\text{Ni}^{\text{II}}$ -acyl complex **137**. If reduction by  $\text{Mn}^0$  in THF is slow, then decarbonylation can give  $\text{Ni}^{\text{II}}$ -alkyl **138** and release CO. A  $\beta$ -hydride elimination/reinsertion sequence can provide isomerized  $\text{Ni}^{\text{II}}$ -alkyl **140**, which can then

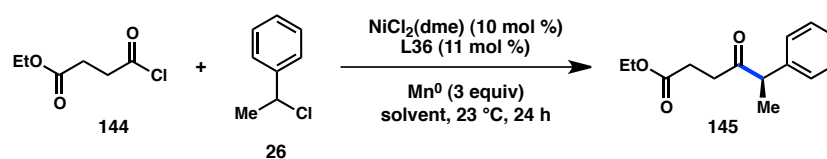
be reduced to a  $\text{Ni}^{\text{I}}$  complex. A second oxidative addition to acid chloride **136** furnishes  $\text{Ni}^{\text{III}}$  complex **142**, intercepting an intermediate from our typical cross-coupling mechanism. Reductive elimination and a subsequent single-electron reduction delivers ketone **143** and reforms  $\text{Ni}^{\text{I}}$ . Interestingly, the acid chloride dimerization proceeds with identical enantioselectivity as the typical cross-coupling reaction. Based on the above results, it is possible that coupling of acid chloride **114** and benzyl chloride **26** can produce ketone **115** by competing heterocoupling and acid chloride dimerizations.

**Figure 3.6.** Unexpected dimerization of acid chlorides.



While the lower dielectric constant of THF compared to DMA may slow down electron transfer events, it is also possible that low conversion of benzyl chloride **26** is the result of dimerization or aggregation of Ni species in less strongly polar solvents, resulting in catalyst inhibition or death.<sup>17</sup> In either case, we reasoned that a mixed solvent system between THF and DMA would maintain high levels of enantioselectivity while also accelerating the rate of product formation. Indeed, using 10 mol % catalyst, THF provides a 24% yield and 86% ee of ketone **145** and DMA delivers a 59% yield and 73% ee of the product (Table 3.3, entries 1 and 8). The cross-coupling proved to be highly sensitive to the amount of DMA that was used as a cosolvent. Lower levels of DMA provided reduced conversion of benzyl chloride **26** (entries 2 and 3), while a higher proportion of DMA resulted in lower asymmetric induction (entries 6 and 7). Gratifyingly, 30% v/v DMA in THF furnishes ketone **145** in 62% yield and 86% ee, preserving the yield seen in DMA and the selectivity seen in THF (entry 4).

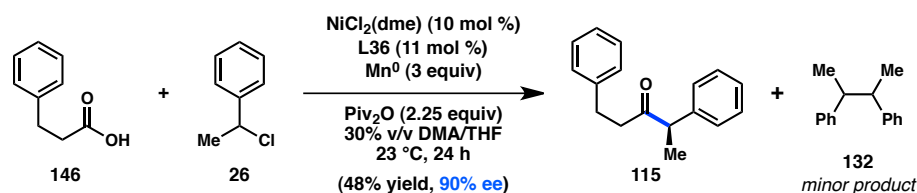
**Table 3.3.** Evaluation of mixed solvent systems.



Entry	Solvent	Conversion (%)	Yield (%)	ee (%)
1	THF	72	24	86
2	10% DMA in THF	45	46	87
3	20% DMA in THF	57	47	87
4	30% DMA in THF	90	62	86
5	40% DMA in THF	87	36	82
6	50% DMA in THF	100	43	74
7	75% DMA in THF	100	52	64
8	DMA	100	59	73

Having increased the reactivity of our system without diminishing the enantioselectivity, we next sought to increase the product yield further by improving the preference for heterocoupling over homocoupling.<sup>23</sup> Previous studies on reductive cross-couplings have minimized homodimer formation through structural modification of the Ni/ligand complex or through statistical manipulation by adding an excess of one reagent.<sup>8a</sup> The sensitivity of our enantioinduction to changes in ligand and a desire to develop an efficient transformation dissuaded us from these approaches. After an extensive analysis of reaction parameters and additives, we became aware of two important considerations: 1) reproducibility of reaction outcomes was hampered because not all trials would exhibit a consistent ratio of product to homocoupling, and 2) the cross-coupling of an in situ-generated mixed anhydride, formed by treatment with pivalic anhydride, proceeded with a low level of homodimer formation (Scheme 3.2).<sup>24</sup>

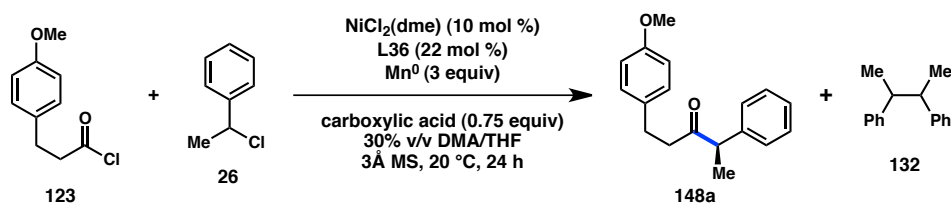
**Scheme 3.2.** Reductive cross-coupling of in situ-generated mixed anhydrides.



To explain these effects, we rationalized that adventitious water might result in irreproducible reaction outcomes because of hydrolysis of the acid chloride to a carboxylic acid. Similarly, we realized that the mixed anhydride cross-coupling resulted in a full equivalent of a free carboxylic acid being present in the reaction medium. Based on these observations, we hypothesized that a free carboxylic acid might be able to modulate the selectivity for ketone formation over homocoupling. A wide screen of

carboxylic acids revealed that 2,6-dimethylbenzoic acid (DMBA, **147**) delivered the greatest selectivity for product formation over homocoupling (Table 3.4). Further optimization of the reaction concentration, the ligand-to-metal ratio, and addition of 3Å molecular sieves permitted ketone **148a** to be obtained in 85% yield and 93% ee, with only a 4% yield of homodimer.

**Table 3.4.** Effect of carboxylic acids on the ratio of ketone to homodimer formation.

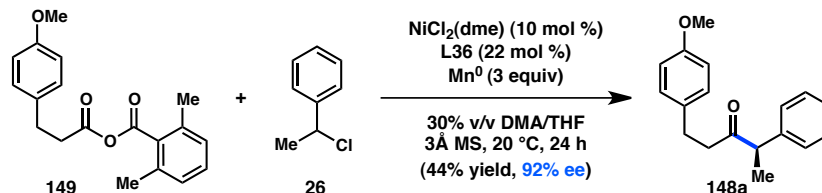


Entry	Acid	Yield <b>132</b> (%)	Yield <b>148a</b> (%)	ee (%)
1	--	22	52	94
2	AcOH	17	65	92
3	BzOH	14	40	92
4	DMBA ( <b>147</b> )	4	85	93

The mechanistic role of the carboxylic acid additive is still unclear. We currently speculate that the carboxylic acid can coordinate to the Ni catalyst at some point during the catalytic cycle as opposed to interacting with either substrate. We do not observe formation of the mixed anhydride during the reaction, and the mixed anhydride is not isolated by treatment of the acid chloride with DMBA and mol sieves in DMA/THF. Nonetheless, pregenerated mixed anhydride **149** produces the desired product in 44% yield and 92% ee (Scheme 3.3), suggesting that **149** is a competent starting material but not confirming its role as a reaction intermediate. Interestingly, DMBA displays the greatest inhibitory effect on homocoupling when THF is the sole solvent and has the least activity when DMA is the sole solvent. This may be explained by the reduced

coordinating ability of DMBA in highly polar solvents like DMA, when it has to compete with DMA for open coordination sites on Ni.

**Scheme 3.3.** Employing a pregenerated mixed anhydride.

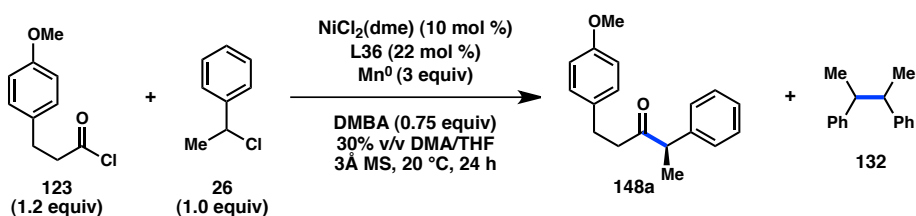


Two possible actions of the carboxylic acid additive are promotion of ketone formation or inhibition of homodimer formation. Given that the enantioselectivity of the cross-coupling is not affected by the choice of acid, it appears that the additive is not coordinated to the catalyst during the stereochemistry-determining step. Instead, the carboxylic acid may assist with initial oxidative addition of  $\text{Ni}^0$  to the acid chloride over the benzyl chloride, with addition of  $\text{Ni}^0$  to benzyl chloride ultimately resulting in homocoupling. Reactions run in the presence of DMBA generally proceed in lower conversion than in the absence of DMBA, suggesting that the carboxylic acid reduces the rate of the reaction or facilitates catalyst inhibition. While additional mechanistic studies are necessary, we speculate that DMBA might coordinate to  $\text{Ni}^0$  and decelerate oxidative addition to benzyl chloride **26** relative to acid chloride **123**, providing greater selectivity for heterocoupling over homocoupling.

At this point, we reevaluated several important reaction parameters. These results are summarized in Table 3.5. Control experiments determined that ketone **148a** is not produced in the absence of  $\text{Mn}^0$  or Ni catalyst, although low yields of **148a** can be observed in the absence of ligand (Table 3.5, entries 2–4). Removal of DMBA was found

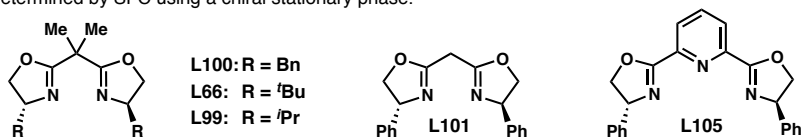
to increase the formation of homocoupled product **132** and decrease the yield of **148a** (entry 5). Molecular sieves were discovered to further increase the yield of **148a**, although freshly-dried molecular sieves did not provide a yield enhancement (entry 6). Given that  $Mn^0$  mediates homocoupling of benzyl chloride **26** in the absence of Ni (entry 3), several alternative stoichiometric inorganic and organic reductants were investigated with the objective of shutting down this undesired pathway. Unfortunately,  $Zn^0$  was the only reductant that furnished detectable quantities of **148a**, and it did not provide improvements with respect to  $Mn^0$  (entry 7). Use of  $Ni(cod)_2$  as a pre-catalyst delivered **148a** with comparable ee (entry 8); however, the yield was reduced relative to  $NiCl_2(dme)$ . The use of other metal salts such as  $CoCl_2$  were ineffective (entry 9).

A reinvestigation of ligands under the optimized conditions confirmed that **L36** provides higher ee's than other substituted bis(oxazolines) (entries 10–14). Furthermore, the isopropylidene bridge of **L36** proved to be critical, as **L101** afforded **148a** with no stereoinduction. Use of tridentate ligands such as **L105** led to almost exclusive homocoupling.<sup>25</sup> The mixed solvent system was found to provide the appropriate balance of reactivity and selectivity (entries 16–18). Whereas the best ee's were obtained in THF, the reactivity was poor and the yields were low. On the other hand, DMA provided higher conversions, but also resulted in increased production of homodimer **132**. Reducing the **L36**:Ni ratio to 1.1:1 led to a slight reduction in yield of **148a** (entry 15). Excess ligand might be beneficial to prevent the formation of dimeric  $Ni^I$  complexes that can act as a catalyst sink.<sup>17</sup> Coupling of (1-bromoethyl)benzene under otherwise identical reaction conditions provided **148a** in the same ee, but in lower yield due to increased formation of homodimer **132** (entry 19).<sup>26</sup>

**Table 3.5.** Impact of reaction parameters on Ni-catalyzed asymmetric reductive coupling.

Entry	Deviation from standard conditions <sup>a</sup>	Conversion 26 (%) <sup>b</sup>	Yield 132 (%) <sup>b</sup>	Yield 148a (%) <sup>b</sup>	ee 148a (%) <sup>c</sup>
1	none	90	4	85	92
2	no Mn <sup>0</sup>	0	0	0	--
3	no NiCl <sub>2</sub> (dme)	35	35	0	--
4	no L36	73	5	8	--
5	no DMBA (147)	100	22	52	94
6	no 3Å MS	100	7	76	90
7	Zn <sup>0</sup> instead of Mn <sup>0</sup>	85	26	31	88
8	Ni(cod) <sub>2</sub> instead of NiCl <sub>2</sub> (dme)	98	18	68	92
9	CoCl <sub>2</sub> instead of NiCl <sub>2</sub> (dme)	73	24	0	--
10	L100 instead of L36	61	24	22	45
11	L66 instead of L36	98	62	14	2
12	L99 instead of L36	89	52	40	69
13	L101 instead of L36	15	1	10	0
14	L105 instead of L36	99	53	4	9
15	11 mol % L36	82	3	72	92
16	DMA as solvent	99	43	30	88
17	THF as solvent	25	<1	26	94
18	MeCN as solvent	28	4	16	45
19	(1-bromoethyl)benzene instead of 26	100	42	58	92

<sup>a</sup> Reactions conducted on 0.2 mmol scale under an N<sub>2</sub> atmosphere in a glovebox. <sup>b</sup> Determined by GC versus an internal standard. <sup>c</sup> Determined by SFC using a chiral stationary phase.



Several additional experiments were performed to gain additional insight into the observed reactivity. When the reaction between **123** and **26** is conducted in the presence of 0.5 equiv of the radical inhibitor 2,6-bis(1,1-dimethylethyl)-4-methylphenol (BHT),

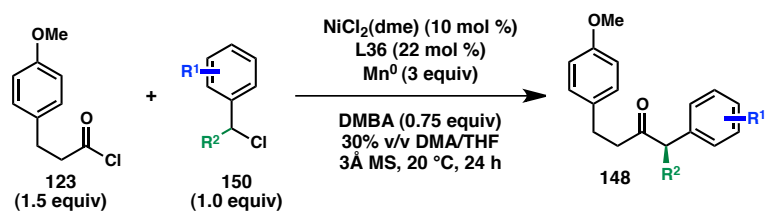
ketone **148a** is isolated in 80% yield and 92% ee. Alternatively, use of the electron transfer inhibitor 1-chloro-2,4-dinitrobenzene completely shuts down the reaction. These findings are consistent with the sequential reduction mechanism proposed in Figure 3.2. Additionally, the ee of ketone **148a** is constant over the course of reaction, whereas the ee of recovered benzyl chloride **26** gradually increases to 17% at 94% conversion. These results suggest that the two enantiomers of **26** react at comparable rates, as only a very modest kinetic resolution occurs. When enantioenriched **26** is employed, ketone **148a** is obtained in 92% ee and **26** is recovered without erosion of ee. Lastly, to assess the intermediacy of organomanganese intermediates, **26** was converted to the corresponding benzylmanganese halide via Grignard formation/transmetalation. Ketone **148a** was not observed after exposure of the organomanganese to our optimized reaction conditions.<sup>27</sup>

### 3.2.3 Substrate Scope and Further Studies

With optimized conditions in hand, we investigated the scope of the benzyl chloride (Table 3.6). Coupling of **123** with benzyl chlorides bearing electron-releasing substituents furnished the corresponding ketones in high ee; however, these substrates reacted slowly relative to **150a** and required higher **L36**:Ni ratios (3.3:1) to obtain good conversions (entries 2–5). In contrast, benzyl chlorides bearing electron-withdrawing substituents reacted rapidly and proceeded to full conversion. In the case of the trifluoromethyl-substituted substrate (entry 8), the higher reactivity was accompanied by increased side product formation and somewhat reduced enantioselectivity. Both 4-chloro and 4-bromobenzyl chlorides can be coupled with complete chemoselectivity, providing

products suitable for further elaboration. Under our standard conditions, the coupling of **150g** resulted in higher-than-usual levels of homocoupling; this was mitigated via addition of excess DMBA (entry 7). Unfortunately, *o*-substituted benzyl chlorides (e.g. **150d**, entry 4) were poor substrates, providing the ketone products in low yields and ee's.

**Table 3.6.** Substrate scope of benzyl chlorides.



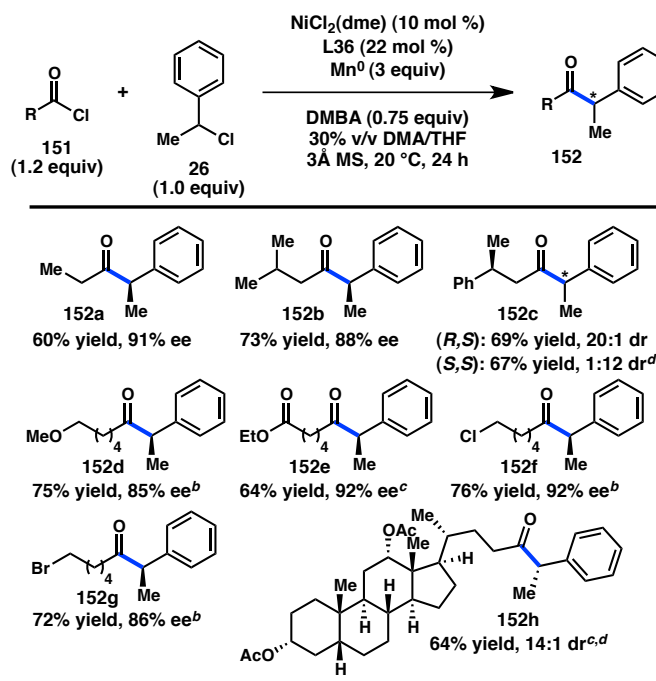
Entry	R <sup>1</sup>	R <sup>2</sup>	Pdt	Yield (%) <sup>a</sup>	ee (%) <sup>b</sup>
1	H	Me	148a	79	93
2 <sup>c</sup>	4-Me	Me	148b	74	93
3 <sup>c</sup>	3-Me	Me	148c	75	93
4 <sup>c</sup>	2-Me	Me	148d	35	72
5 <sup>c</sup>	4-OMe	Me	148e	56	86
6	4-Cl	Me	148f	76	91
7 <sup>d</sup>	4-Br	Me	148g	73	86
8 <sup>e</sup>	4-CF <sub>3</sub>	Me	148h	64	82
9 <sup>c</sup>	2-naphthyl	Me	148i	65	91
10	H	Et	148j	50	94
11	Cl	Et	148k	65	90
12	H	Bn	148l	79	92
13 <sup>f</sup>	H	CH <sub>2</sub> OTBS	148m	51	89
14	H	4-pentenyl	148n	38	92
15	2,3-dihydro-1 <i>H</i> -inden-1-yl		148o	68	78

<sup>a</sup> Isolated yield, reactions conducted on 0.2 mmol scale under an N<sub>2</sub> atmosphere in a glovebox. <sup>b</sup> Determined by SFC using a chiral stationary phase. <sup>c</sup> Run with 33 mol % **L36**. <sup>d</sup> Run with 1.25 equiv DMBA <sup>e</sup> Run in 20% v/v DMA/THF. <sup>f</sup> Run in 50% v/v DMA/THF.

We were pleased to discover that  $\beta$ -substituted benzyl chlorides provide access to  $\alpha$ -aryl- $\alpha$ -alkyl ketones with high enantioselectivity (entries 10–14). In general, these substrates react more slowly and do not achieve complete conversion; however, they also exhibit low propensity toward homocoupling. Notably, the mild conditions of the

reductive coupling enable formation of **148m** in moderate yield without any observed elimination (entry 13). Interestingly, **148n** was formed without any detectable quantities of the 5-*exo* cyclization product (entry 14). This result suggests that if oxidative addition takes place via a radical pathway, then radical recombination occurs faster than cyclization or that the radical cyclization is reversible.<sup>28</sup> The cyclic substrate 1-chloro-2,3-dihydro-1*H*-indene reacted to provide ketone **148o** in good yield, albeit modest ee (entry 15). The reaction can be run on preparative scale: coupling of acid chloride **123** and benzyl chloride **150a** on a 1.0 mmol scale at the bench top delivered ketone **148a** in 70% yield and 93% ee.

The scope of the acid chloride coupling partner was also investigated (Figure 3.7). Alkyl halide and ester functionalities are well tolerated; these findings are noteworthy because such groups would not be compatible in their native form with the more conventional synthesis involving auxiliary-controlled alkylation followed by Weinreb ketone synthesis.<sup>29</sup> For several of the acid chlorides shown in Figure 3.7, the efficiency of the coupling proved to be sensitive to the DMA:THF ratio, with improved yields often being observed with lower levels of the amide solvent. Depending on the enantiomer of **L36** that is employed, the coupling of benzyl chloride **26** with enantiopure acid chloride **151c** provides access to either diastereomer with high diastereoselectivity. A standard enolate alkylation approach to **152c** would not be anticipated to provide such high levels of 1,4-stereoselection. The power of this methodology is further demonstrated by the diastereoselective preparation of ketone **152h**. While  $\beta$ -substituted acid chlorides are well-tolerated,  $\alpha,\alpha$ -disubstituted acid chlorides result in lower levels of enantioselectivity and increases in benzylic homocoupling.

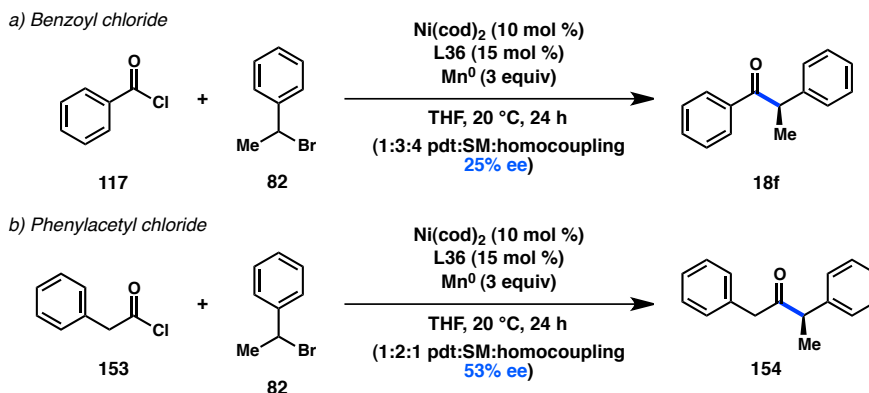
**Figure 3.7.** Substrate scope of acid chlorides.<sup>a</sup>

<sup>a</sup> Isolated yield, reactions conducted on 0.2 mmol scale under an  $\text{N}_2$  atmosphere in a glovebox. % ee determined by SFC using a chiral stationary phase. <sup>b</sup> Run in 20% v/v DMA/THF. <sup>c</sup> Run in 10% v/v DMA/THF. <sup>d</sup> Run with *ent*-L36.

We next attempted to expand our substrate scope from aliphatic acid chlorides to aromatic ones. Unfortunately, under the optimized conditions, no product was observed when benzoyl chloride (**117**) was employed as a starting material. Transitioning to the more reactive benzyl bromide **82**, we realized that only a trace yield of product was detected when DMA was used as a solvent. The yield increased when the reaction was run with  $\text{Ni}(\text{cod})_2$  in THF, albeit with no enantioinduction. Surprisingly, lowering the concentration from 0.375 M to 0.15 M delivered ketone **18f** in 25% ee (Scheme 3.4). The origin of this concentration-dependent enantioselectivity remains unclear, although a similar concentration effect was also observed for the coupling of phenylacetyl chloride

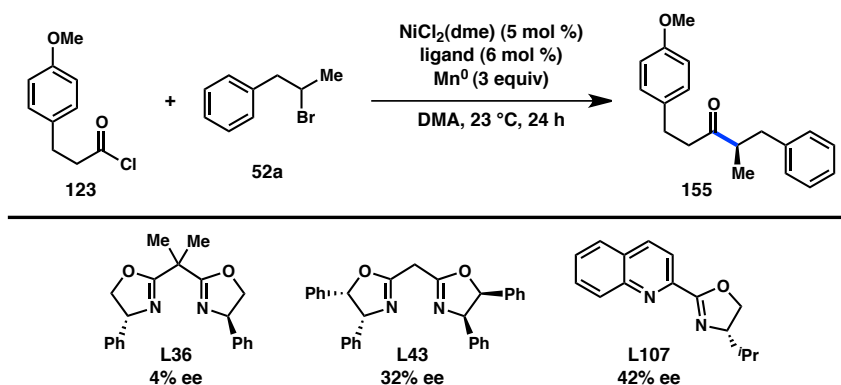
(153). Evaluation of other chiral ligands for the couplings of acid chlorides **117** or **153** failed to provide higher levels of enantioinduction

**Scheme 3.4.** Expansion of acid chloride substrate scope.



We questioned whether homobenzylic halides might also undergo an enantioselective reductive cross-coupling. Treatment of acid chloride **123** and bromide **52a** with  $\text{NiCl}_2(\text{dme})$  and **L36** furnished product **155** in 4% ee, demonstrating the critical role that the aryl group plays in our standard cross-coupling (Figure 3.8). A screen of different chiral ligand scaffolds revealed that ketone **155** could be generated in up to 42% ee, highlighting the  $\beta$ -aryl substituent's decreased ability to behave as a directing group in the cross-coupling when compared to an  $\alpha$ -aryl substituent.

**Figure 3.8.** Reductive cross-coupling of a homobenzylic halide.



### 3.3 CONCLUDING REMARKS

In conclusion, the first Ni-catalyzed asymmetric reductive acyl cross-coupling reaction has been developed. This mild, chemoselective reaction provides access to a variety of  $\alpha$ -aryl- $\alpha$ -alkyl ketones in good yields and high enantioselectivity. The reaction is highly convergent and functional group-tolerant, which enables the rapid construction of complex ketones from bench stable and easy-to-handle starting materials. The further development and application of this reaction, as well as study of the mechanism, is the focus of ongoing research in our laboratory.

### 3.4 EXPERIMENTAL SECTION

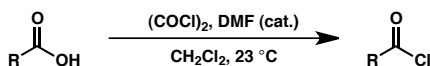
#### 3.4.1 Materials and Methods

Unless otherwise stated, reactions were performed under a nitrogen atmosphere using freshly dried solvents. Tetrahydrofuran (THF), methylene chloride ( $\text{CH}_2\text{Cl}_2$ ), and acetonitrile (MeCN) were dried by passing through activated alumina columns. Anhydrous dimethylacetamide (DMA) was purchased from Aldrich and stored under inert atmosphere. Manganese powder (-325 mesh, 99.3%) was purchased from Alfa Aesar. Unless otherwise stated, chemicals and reagents were used as received. All reactions were monitored by thin-layer chromatography using EMD/Merck silica gel 60 F254 pre-coated plates (0.25 mm) and were visualized by UV, *p*-anisaldehyde, or  $\text{KMnO}_4$  staining. Flash column chromatography was performed as described by Still et al.<sup>30</sup> using silica gel (partical size 0.032-0.063) purchased from Silicycle. Optical rotations were measured on a Jasco P-2000 polarimeter using a 100 mm path-length cell at 589 nm.  $^1\text{H}$

and  $^{13}\text{C}$  NMR spectra were recorded on a Varian 400 MR (at 400 MHz and 101 MHz, respectively) or a Varian Inova 500 (at 500 MHz and 126 MHz, respectively), and are reported relative to internal  $\text{CHCl}_3$  ( $^1\text{H}$ ,  $\delta = 7.26$ ) or acetone ( $^1\text{H}$ ,  $\delta = 2.05$ ), and  $\text{CDCl}_3$  ( $^{13}\text{C}$ ,  $\delta = 77.0$ ) or acetone ( $^{13}\text{C}$ ,  $\delta = 29.8$ ). Data for  $^1\text{H}$  NMR spectra are reported as follows: chemical shift ( $\delta$  ppm) (multiplicity, coupling constant (Hz), integration). Multiplicity and qualifier abbreviations are as follows: s = singlet, d = doublet, t = triplet, q = quartet, m = multiplet, br = broad, app = apparent. IR spectra were recorded on a Perkin Elmer Paragon 1000 spectrometer and are reported in frequency of absorption ( $\text{cm}^{-1}$ ). HRMS were acquired using an Agilent 6200 Series TOF with an Agilent G1978A Multimode source in electrospray ionization (ESI) or mixed (MM) ionization mode, or obtained from the Caltech Mass Spectral Facility in fast-atom bombardment mode (FAB). Analytical SFC was performed with a Mettler SFC supercritical  $\text{CO}_2$  analytical chromatography system with Chiralcel AD-H, OD-H, AS-H, OB-H, and OJ-H columns (4.6 mm x 25 cm) with visualization at 210 nm. Analytical achiral GC was performed with an Agilent 6850 GC utilizing an Agilent DB-WAX (30.0 m x 0.25 mm) column (1.0 mL/min He carrier gas flow).

### 3.4.2 Substrate Synthesis

#### General Procedure 1: Acid Chloride Synthesis



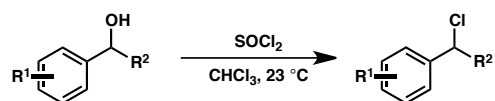
A flask was charged with the appropriate carboxylic acid (1.0 equiv) and  $\text{CH}_2\text{Cl}_2$  (0.5 M). Two drops of DMF and oxalyl chloride (1.2 equiv) were added dropwise. The solution

was stirred at 23 °C for 3 h and then concentrated. The crude acid chloride was used without any further purification.

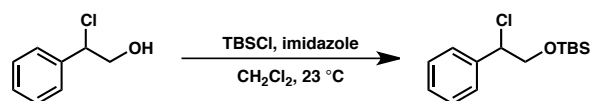
### 3-(4-methoxyphenyl)propanoic 2,6-dimethylbenzoic anhydride (**149**)



A flame-dried flask was charged with 2,6-dimethylbenzoic acid (1.0 mmol, 1 equiv) and CH<sub>2</sub>Cl<sub>2</sub> (0.33 M). To the solution was added NaH (60% dispersion in oil, 1.05 mmol, 1.05 equiv) and the reaction was allowed to stir for 3 h. 3-(4-methoxyphenyl)propanoyl chloride (**123**, 1.0 mmol, 1 equiv) was added dropwise to the reaction mixture and the reaction was stirred overnight. The crude mixture was filtered through a small plug of celite and concentrated to afford a light yellow oil (291.1 mg, 93% yield). <sup>1</sup>H NMR (500 MHz, CDCl<sub>3</sub>)  $\delta$  7.24 (t,  $J$  = 7.7 Hz, 1H), 7.13 (d,  $J$  = 8.7 Hz, 2H), 7.06 (d,  $J$  = 7.5 Hz, 2H), 6.84 (d,  $J$  = 8.7 Hz, 4H), 3.79 (s, 3H), 2.97 (t,  $J$  = 7.6 Hz, 2H), 2.82 (dd,  $J$  = 4879.7, 7.5 Hz, 4H), 2.37 (d,  $J$  = 0.7 Hz, 6H); <sup>13</sup>C NMR (126 MHz, CDCl<sub>3</sub>)  $\delta$  168.5, 165.1, 158.2, 135.8, 131.7, 131.6, 130.4, 129.3, 127.9, 114.0, 55.3, 37.5, 29.4, 20.0; FTIR (NaCl, thin film): 2955, 2931, 2836, 1811, 1740, 1612, 1595, 1584, 1513, 1466, 1301, 1248, 1179, 1124, 1079, 1036, 990, 827, 775 cm<sup>-1</sup>; LRMS (ESI) calc'd for [M+Na]<sup>+</sup> 335.1, found 335.1.

**General Procedure 2: Benzyl Chloride Synthesis**

A flask was charged with the appropriate benzyl alcohol (1.0 equiv) and  $\text{CHCl}_3$  (1.5 M). Thionyl chloride (1.05 equiv) was added dropwise. Evolved gas was quenched via cannula by aqueous  $\text{NaHCO}_3$ . The solution was stirred at 23 °C for 12 h and then concentrated to afford a yellow oil. The crude residue was purified by Kugelrohr distillation to isolate a clear oil. Spectral data for all compounds matched those reported in the literature.

**[1-chloro-2-(*t*-butyldimethylsiloxy)ethyl]benzene (150m).**

To a flask was added 2-chloro-2-phenylethanol (8.5 mmol, 1.0 equiv) and  $\text{CH}_2\text{Cl}_2$  (18 mL, 0.5 M) followed by imidazole (10.2 mmol, 1.2 equiv) and *tert*-butyldimethylsilyl chloride (10.2 mmol, 1.2 equiv). The reaction was stirred at 23 °C for 24 h and then quenched by pouring into water (40 mL). The aqueous and organic layers were separated and the aqueous layer was extracted with  $\text{CH}_2\text{Cl}_2$  (2 X 20 mL). The combined organic layers were washed with brine (1 X 20 mL) and dried ( $\text{Na}_2\text{SO}_4$ ), filtered, and concentrated. The crude residue was filtered through a thick pad of silica with hexanes and concentrated to afford a clear oil (2.21 g, 96% yield).  $^1\text{H}$  NMR (500 MHz,  $\text{CDCl}_3$ )  $\delta$  7.43 – 7.27 (m, 5H), 4.87 (t,  $J = 6.6$  Hz, 1H), 4.00 (dd,  $J = 10.7, 6.8$  Hz, 1H), 3.92 (dd,  $J = 10.7, 6.5$  Hz, 1H), 0.85 (s, 9H), 0.01 (s, 3H),  $-0.04$  (s, 3H);  $^{13}\text{C}$  NMR (126 MHz,  $\text{CDCl}_3$ )

$\delta$  139.0, 128.39, 128.37, 127.6, 68.5, 63.3, 25.7, -5.4, -5.5; FTIR (NaCl, thin film):  
2955, 2928, 2884, 2856, 1494, 1472, 1361, 1257, 1123, 1080, 837, 778  $\text{cm}^{-1}$ ; HRMS  
(FAB) calc'd for  $[\text{M}+\text{H}]^+$  271.1279, found 271.1290.

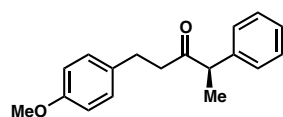
### 3.4.3 Enantioselective Reductive Cross-Coupling

#### General Procedure 3 (Table 3.5)

On a bench-top, to a 1/2 dram vial was added the appropriate ligand (0.044 mmol, 22 mol %), carboxylic acid (0.15 mmol, 0.75 equiv), 3 Å mol sieves (30 mg/0.2 mmol benzyl chloride), reductant (0.6 mmol, 3 equiv), and nickel source (0.02 mmol, 10 mol %). Under an inert atmosphere in a glovebox, the vial was charged with the appropriate solvent (0.53 mL, 0.375 M) followed by benzyl chloride (**26**, 0.2 mmol, 1 equiv), acid chloride (**123**, 0.24 mmol, 1.2 equiv), and dodecane (internal standard). The mixture was stirred at 240 rpm, ensuring that the reductant was uniformly suspended. Stirring continued at 20 °C under inert atmosphere for 24 h. The black slurry was transferred to a separatory funnel using 1 M HCl (5 mL) and diethyl ether (10 mL). The mixture was diluted with H<sub>2</sub>O (10 mL) and the aqueous and organic layers were separated. The aqueous layer was extracted with diethyl ether (2 X 10 mL) and the combined organic layers were washed with brine (1 X 15 mL) and dried (MgSO<sub>4</sub>), filtered, and concentrated. The crude residue was analyzed by GC.

**General Procedure 4: Enantioselective Reductive Coupling of Benzyl Chlorides and  
Acid Chlorides**

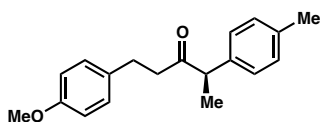
On a bench-top, to a 1/2 dram vial was added (*R,R*)-**L36** (0.044 mmol, 22 mol %), 2,6-DMBA (0.15 mmol, 0.75 equiv), 3 Å mol sieves (30 mg/0.2 mmol benzyl chloride), manganese powder (0.6 mmol, 3 equiv), and NiCl<sub>2</sub>(dme) (0.02 mmol, 10 mol %). Under an inert atmosphere in a glovebox, the vial was charged with 30% v/v DMA/THF (0.53 mL, 0.375 M) followed by benzyl chloride (**150**, 0.2 mmol, 1 equiv) and acid chloride (**123**, Table 3.6: 0.3 mmol, 1.5 equiv; **151**, Figure 3.7: 0.24 mmol, 1.2 equiv). The mixture was stirred at 240 rpm, ensuring that the manganese powder was uniformly suspended. Stirring continued at 20 °C under inert atmosphere for 24 h. The black slurry was transferred to a separatory funnel using 1 M HCl (5 mL) and diethyl ether (10 mL). The mixture was diluted with H<sub>2</sub>O (10 mL) and the aqueous and organic layers were separated. The aqueous layer was extracted with diethyl ether (2 X 10 mL) and the combined organic layers were washed with brine (1 X 15 mL) and dried (MgSO<sub>4</sub>), filtered, and concentrated. The crude residue was purified by flash chromatography.

**(*R*)-1-(4-methoxyphenyl)-4-Phenylpentan-3-one (148a)**

Prepared from (1-chloroethyl)benzene (**150a**, 0.20 mmol) and 3-(4-methoxyphenyl)propanoyl chloride (**123**, 0.30 mmol) according to General Procedure 4. The crude residue was purified by silica gel chromatography (5% ethyl acetate/hexanes) to yield **148a** (42.3 mg, 79% yield) in 93% ee as a clear oil. The enantiomeric excess was determined by chiral SFC analysis (OD-H, 2.5 mL/min, 5% IPA in CO<sub>2</sub>,  $\lambda = 210$  nm):  $t_R$  (minor) = 9.2 min,  $t_R$  (major) = 9.8 min.

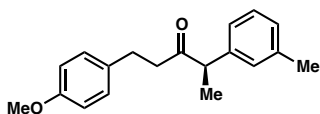
$[\alpha]_D^{25} = -102.3^\circ$  ( $c = 1.10$ ,  $\text{CHCl}_3$ );  $^1\text{H NMR}$  (500 MHz,  $\text{CDCl}_3$ )  $\delta$  7.37 – 7.21 (m, 3H), 7.22 – 7.14 (m, 2H), 7.05 – 6.96 (m, 2H), 6.84 – 6.75 (m, 2H), 3.79 (s, 3H), 3.72 (q,  $J = 7.0$  Hz, 1H), 2.88 – 2.57 (m, 4H), 1.39 (d,  $J = 7.0$  Hz, 3H);  $^{13}\text{C NMR}$  (126 MHz,  $\text{CDCl}_3$ )  $\delta$  210.0, 157.8, 140.4, 133.0, 129.2, 128.9, 127.8, 127.1, 113.7, 55.2, 53.2, 42.8, 29.1, 17.3; FTIR (NaCl, thin film): 3060, 3027, 2973, 2931, 2834, 1713, 1611, 1513, 1493, 1452, 1300, 1247  $\text{cm}^{-1}$ ; HRMS (MM) calc'd for  $[\text{M}-\text{H}]^-$  267.1391, found 267.1391.

**(*R*)-1-(4-methoxyphenyl)-4-(*p*-tolyl)Pentan-3-one (148b)**



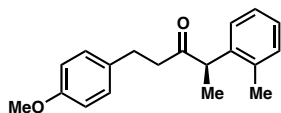
Prepared from 1-(1-chloroethyl)-4-methylbenzene (**150b**, 0.20 mmol) and 3-(4-methoxyphenyl)propanoyl chloride (**123**, 0.30 mmol) according to General Procedure 4 except using 33 mol % (*R,R*)-**L36** (0.066 mmol). The crude residue was purified by silica gel chromatography (5% ethyl acetate/hexanes) to yield **148b** (41.8 mg, 74% yield) in 93% ee as a clear oil. The enantiomeric excess was determined by chiral SFC analysis (OD-H, 2.5 mL/min, 5% IPA in  $\text{CO}_2$ ,  $\lambda = 210$  nm):  $t_R$  (minor) = 9.0 min,  $t_R$  (major) = 9.8 min.  $[\alpha]_D^{25} = -84.9^\circ$  ( $c = 1.37$ ,  $\text{CHCl}_3$ );  $^1\text{H NMR}$  (500 MHz,  $\text{CDCl}_3$ )  $\delta$  7.11 (d,  $J = 7.9$  Hz, 2H), 7.05 (d,  $J = 7.9$  Hz, 2H), 6.99 (d,  $J = 9.0$  Hz, 2H), 6.77 (d,  $J = 8.6$  Hz, 2H), 3.77 (s, 3H), 3.66 (q,  $J = 6.9$  Hz, 1H), 2.84 – 2.55 (m, 4H), 2.33 (s, 3H), 1.35 (d,  $J = 7.0$  Hz, 3H);  $^{13}\text{C NMR}$  (126 MHz,  $\text{CDCl}_3$ )  $\delta$  210.2, 157.8, 137.4, 136.7, 133.1, 129.6, 129.2, 127.7, 113.8, 55.2, 52.8, 42.8, 29.1, 21.0, 17.3; FTIR (NaCl, thin film): 2930, 2834, 1713, 1612, 1584, 1513, 1454, 1300, 1246, 1178, 1036, 824  $\text{cm}^{-1}$ ; HRMS (MM) calc'd for  $[\text{M}+\text{H}]^+$  283.1647, found 283.1693.

**(R)-1-(4-methoxyphenyl)-4-(*m*-tolyl)Pentan-3-one (148c)**



Prepared from 1-(1-chloroethyl)-3-methylbenzene (**150c**, 0.20 mmol) and 3-(4-methoxyphenyl)propanoyl chloride (**123**, 0.30 mmol) according to General Procedure 4 except using 33 mol % (*R,R*)-**L36** (0.066 mmol). The crude residue was purified by silica gel chromatography (5% ethyl acetate/hexanes) to yield **148c** (42.5 mg, 75% yield) in 93% ee as a clear oil. The enantiomeric excess was determined by chiral SFC analysis (OD-H, 2.5 mL/min, 5% IPA in CO<sub>2</sub>,  $\lambda = 210$  nm):  $t_R$  (minor) = 9.1 min,  $t_R$  (major) = 9.9 min.  $[\alpha]_D^{25} = -90.4^\circ$  (c = 1.46, CHCl<sub>3</sub>); <sup>1</sup>H NMR (500 MHz, CDCl<sub>3</sub>)  $\delta$  7.19 (t, J = 7.5 Hz, 1H), 7.09 – 7.01 (m, 1H), 7.02 – 6.92 (m, 4H), 6.77 (d, J = 8.5 Hz, 2H), 3.77 (s, 3H), 3.66 (q, J = 6.9 Hz, 1H), 2.84 – 2.56 (m, 4H), 2.31 (s, 3H), 1.36 (d, J = 6.9 Hz, 3H); <sup>13</sup>C NMR (126 MHz, CDCl<sub>3</sub>)  $\delta$  210.1, 157.8, 140.4, 138.6, 133.1, 129.2, 128.8, 128.6, 127.9, 125.0, 113.8, 55.2, 53.1, 42.8, 29.1, 21.4, 17.3; FTIR (NaCl, thin film): 2931, 2834, 1714, 1611, 1584, 1513, 1453, 1300, 1246, 1178, 1036, 825 cm<sup>-1</sup>; HRMS (MM) calc'd for [M+H]<sup>+</sup> 283.1693, found 283.1557.

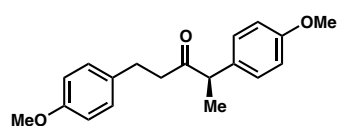
**(R)-1-(4-methoxyphenyl)-4-(*o*-tolyl)Pentan-3-one (148d)**



Prepared from 1-(1-chloroethyl)-2-methylbenzene (**150d**, 0.20 mmol) and 3-(4-methoxyphenyl)propanoyl chloride (**123**, 0.30 mmol) according to General Procedure 4 except using 33 mol % (*R,R*)-**L36** (0.066 mmol). The crude residue was purified by silica gel chromatography (5% ethyl acetate/hexanes) to yield **148d** (19.8 mg, 35% yield) in 72% ee as a clear oil. The enantiomeric excess was determined by chiral SFC analysis (OD-H, 2.5 mL/min, 10%

IPA in CO<sub>2</sub>,  $\lambda = 210$  nm):  $t_R$  (minor) = 5.3 min,  $t_R$  (major) = 5.7 min.  $[\alpha]_D^{25} = -72.3^\circ$  (c = 0.56, CHCl<sub>3</sub>); <sup>1</sup>H NMR (500 MHz, CDCl<sub>3</sub>)  $\delta$  7.21 – 7.09 (m, 3H), 7.02 – 6.92 (m, 3H), 6.77 (d, J = 8.6 Hz, 2H), 3.87 (q, J = 6.9 Hz, 1H), 3.76 (s, 3H), 2.85 – 2.68 (m, 2H), 2.64 – 2.47 (m, 2H), 2.33 (s, 3H), 1.32 (d, J = 6.9 Hz, 3H); <sup>13</sup>C NMR (126 MHz, CDCl<sub>3</sub>)  $\delta$  210.4, 157.9, 140.0, 135.7, 133.1, 130.8, 129.2, 127.0, 126.6, 113.8, 55.2, 49.2, 42.8, 29.2, 19.7, 16.7; FTIR (NaCl, thin film): 2931, 2834, 1712, 1611, 1513, 1491, 1463, 1300, 1246, 1171, 1036, 828 cm<sup>-1</sup>; HRMS (MM) calc'd for M<sup>+</sup> 282.1614, found 282.1543.

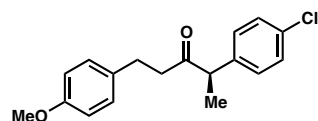
**(R)-1,4-bis(4-methoxyphenyl)Pentan-3-one (148e)**



Prepared from 1-(1-chloroethyl)-4-methoxybenzene (**150e**, 0.20 mmol) and 3-(4-methoxyphenyl)propanoyl chloride (**123**, 0.30 mmol) according to General Procedure 4 except using 33 mol % (*R,R*)-**L36** (0.066 mmol). The crude residue was purified by silica gel chromatography (5% ethyl acetate/hexanes) to yield **148e** (33.4 mg, 56% yield) in 86% ee as a clear oil. The enantiomeric excess was determined by chiral SFC analysis (OB-H, 2.5 mL/min, 10% IPA in CO<sub>2</sub>,  $\lambda = 210$  nm):  $t_R$  (minor) = 6.8 min,  $t_R$  (major) = 7.4 min.  $[\alpha]_D^{25} = -77.2^\circ$  (c = 1.22, CHCl<sub>3</sub>); <sup>1</sup>H NMR (500 MHz, CDCl<sub>3</sub>)  $\delta$  7.10 (d, J = 8.3 Hz, 2H), 6.98 (d, J = 8.0 Hz, 2H), 6.83 (d, J = 9.0 Hz, 2H), 6.76 (d, J = 9.0 Hz, 2H), 3.79 (s, 3H), 3.77 (s, 3H), 3.64 (q, J = 6.9 Hz, 1H), 2.83 – 2.54 (m, 4H), 1.34 (d, J = 7.0 Hz, 3H); <sup>13</sup>C NMR (126 MHz, CDCl<sub>3</sub>)  $\delta$  210.3, 158.7, 157.9, 133.1, 132.4, 129.2, 128.9, 114.3, 113.8, 55.24, 55.23, 52.3, 42.7, 29.1, 17.3 ; FTIR (NaCl, thin film): 2930, 2834, 1710, 1611, 1582, 1512,

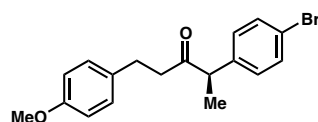
1463, 1301, 1246, 1177, 1034, 827  $\text{cm}^{-1}$ ; HRMS (MM) calc'd for  $\text{M}^+$  298.1563, found 298.1622.

**(R)-4-(4-chlorophenyl)-1-(4-methoxyphenyl)Pentan-3-one (148f)**



Prepared from 1-chloro-4-(1-chloroethyl)benzene (**150f**, 0.20 mmol) and 3-(4-methoxyphenyl)propanoyl chloride (**123**, 0.30 mmol) according to General Procedure 4. The crude residue was purified by silica gel chromatography (5% ethyl acetate/hexanes) to yield **148f** (45.9 mg, 76% yield) in 91% ee as a clear oil. The enantiomeric excess was determined by chiral SFC analysis (OD-H, 2.5 mL/min, 3% IPA in  $\text{CO}_2$ ,  $\lambda = 210$  nm):  $t_R$  (minor) = 19.6 min,  $t_R$  (major) = 20.6 min.  $[\alpha]_D^{25} = -64.1^\circ$  ( $c = 0.79$ ,  $\text{CHCl}_3$ );  $^1\text{H}$  NMR (500 MHz,  $\text{CDCl}_3$ )  $\delta$  7.25 (d,  $J = 8.8$  Hz, 2H), 7.06 (d,  $J = 8.8$  Hz, 2H), 6.97 (d,  $J = 8.8$  Hz, 2H), 6.76 (d,  $J = 8.4$  Hz, 2H), 3.77 (s, 3H), 3.67 (q,  $J = 7.0$  Hz, 1H), 2.83 – 2.55 (m, 4H), 1.34 (d,  $J = 7.0$  Hz, 3H);  $^{13}\text{C}$  NMR (126 MHz,  $\text{CDCl}_3$ )  $\delta$  209.4, 157.9, 138.8, 133.0, 132.8, 129.2, 129.0, 113.8, 55.2, 52.5, 42.9, 29.0, 17.3; FTIR (NaCl, thin film): 2932, 1713, 1611, 1513, 1491, 1300, 1247, 1178, 1093, 1036, 1014, 825  $\text{cm}^{-1}$ ; HRMS (MM) calc'd for  $\text{M}^+$  302.1068, found 302.1001.

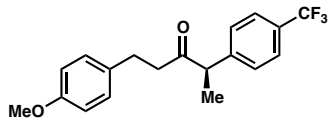
**(R)-4-(4-bromophenyl)-1-(4-methoxyphenyl)Pentan-3-one (148g)**



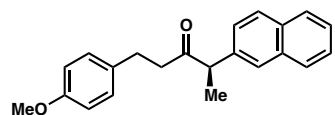
Prepared from 1-bromo-4-(1-chloroethyl)benzene (**150g**, 0.20 mmol) and 3-(4-methoxyphenyl)propanoyl chloride (**123**, 0.30 mmol) according to General Procedure 4 except using 1.25 equiv 2,6-DMBA (0.25 mmol). The crude residue was purified by silica gel chromatography (5% ethyl acetate/hexanes) to yield **148g** (51.0 mg, 73% yield) in 86% ee as a clear oil. The

enantiomeric excess was determined by chiral SFC analysis (OD-H, 2.5 mL/min, 5% IPA in CO<sub>2</sub>,  $\lambda = 210$  nm):  $t_R$  (minor) = 25.4 min,  $t_R$  (major) = 27.0 min.  $[\alpha]_D^{25} = -53.5^\circ$  (c = 1.44, CHCl<sub>3</sub>); <sup>1</sup>H NMR (500 MHz, CDCl<sub>3</sub>)  $\delta$  7.41 (d, J = 8.6 Hz, 2H), 7.01 (d, J = 8.4 Hz, 2H), 6.97 (d, J = 8.6 Hz, 2H), 6.76 (d, J = 9.2 Hz, 2H), 3.77 (s, 3H), 3.65 (q, J = 7.0 Hz, 1H), 2.83 – 2.55 (m, 4H), 1.34 (d, J = 7.0 Hz, 3H); <sup>13</sup>C NMR (126 MHz, CDCl<sub>3</sub>)  $\delta$  209.3, 157.9, 139.3, 132.8, 132.0, 129.6, 129.2, 121.1, 113.8, 55.2, 52.6, 42.9, 29.0, 17.3; FTIR (NaCl, thin film): 2932, 2834, 1714, 1611, 1513, 1487, 1453, 1300, 1247, 1178, 1036, 1010, 825 cm<sup>-1</sup>; HRMS (MM) calc'd for M<sup>+</sup> 346.0563, found 346.0463.

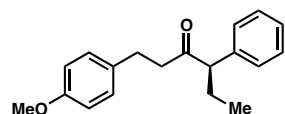
**(R)-1-(4-methoxyphenyl)-4-(4-(trifluoromethyl)phenyl)Pentan-3-one (148h)**



Prepared from 1-(1-chloroethyl)-4-(trifluoromethyl)benzene (**148h**, 0.20 mmol) and 3-(4-methoxyphenyl)propanoyl chloride (**123**, 0.30 mmol) according to General Procedure 4 except using 20% v/v DMA/THF. The crude residue was purified by silica gel chromatography (5% ethyl acetate/hexanes) to yield **148h** (42.8 mg, 64% yield) in 82% ee as a clear oil. The enantiomeric excess was determined by chiral SFC analysis (OJ-H, 2.5 mL/min, 5% IPA in CO<sub>2</sub>,  $\lambda = 210$  nm):  $t_R$  (major) = 6.0 min,  $t_R$  (minor) = 7.3 min.  $[\alpha]_D^{25} = -50.8^\circ$  (c = 1.01, CHCl<sub>3</sub>); <sup>1</sup>H NMR (500 MHz, CDCl<sub>3</sub>)  $\delta$  7.53 (d, J = 7.8 Hz, 2H), 7.25 (d, J = 7.7 Hz, 2H), 6.97 (d, J = 8.8 Hz, 2H), 6.80 (d, J = 9.0 Hz, 2H), 3.80 – 3.74 (m, 4H), 2.85 – 2.60 (m, 4H), 1.38 (d, J = 7.0 Hz, 3H); <sup>13</sup>C NMR (126 MHz, CDCl<sub>3</sub>)  $\delta$  209.0, 158.0, 144.2, 132.7, 129.3, 129.2, 128.2, 125.8, 113.9, 113.8, 55.2, 53.0, 43.1, 28.9, 17.3; FTIR (NaCl, thin film): 2934, 2837, 1717, 1616, 1584, 1513, 1419, 1326, 1247, 1165, 1124, 1070, 1036, 825 cm<sup>-1</sup>; HRMS (MM) calc'd for M<sup>+</sup> 336.1332, found 336.1342.

**(R)-1-(4-methoxyphenyl)-4-(naphthalen-2-yl)Pentan-3-one (148i)**

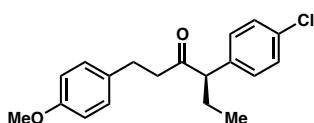
Prepared from 2-(1-chloroethyl)naphthalene (**150i**, 0.20 mmol) and 3-(4-methoxyphenyl)propanoyl chloride (**123**, 0.30 mmol) according to General Procedure 4 except using 33 mol % (*R,R*)-**L36** (0.066 mmol). The crude residue was purified by silica gel chromatography (5% ethyl acetate/hexanes) to yield **148i** (41.7 mg, 65% yield) in 91% ee as a clear oil. The enantiomeric excess was determined by chiral SFC analysis (AS-H, 2.5 mL/min, 5% IPA in CO<sub>2</sub>,  $\lambda = 210$  nm):  $t_R$  (minor) = 10.7 min,  $t_R$  (major) = 11.3 min.  $[\alpha]_D^{25} = -100.4^\circ$  ( $c = 1.00$ , CHCl<sub>3</sub>); <sup>1</sup>H NMR (500 MHz, CDCl<sub>3</sub>)  $\delta$  7.85 – 7.73 (m, 3H), 7.59 (s, 1H), 7.52 – 7.42 (m, 2H), 7.29 – 7.23 (m, 1H), 6.95 (d,  $J = 8.8$  Hz, 2H), 6.71 (d,  $J = 8.8$  Hz, 2H), 3.86 (q,  $J = 6.9$  Hz, 1H), 3.73 (s, 3H), 2.85 – 2.60 (m, 4H), 1.46 (d,  $J = 6.9$  Hz, 3H); <sup>13</sup>C NMR (126 MHz, CDCl<sub>3</sub>)  $\delta$  210.0, 157.8, 137.9, 133.6, 132.9, 132.5, 129.2, 128.7, 127.7, 127.6, 126.6, 126.2, 125.9, 113.7, 55.2, 53.3, 42.9, 29.0, 17.3; FTIR (NaCl, thin film): 3055, 2972, 2931, 2834, 1713, 1611, 1583, 1511, 1455, 1374, 1300, 1245, 1178, 1035, 822, 750 cm<sup>-1</sup>; LRMS (ESI) calc'd for [M+H]<sup>+</sup> 319.2, found 319.2.

**(R)-1-(4-methoxyphenyl)-4-Phenylhexan-3-one (148j)**

Prepared from (1-chloropropyl)benzene (**150j**, 0.20 mmol) and 3-(4-methoxyphenyl)propanoyl chloride (**123**, 0.30 mmol) according to General Procedure 4. The crude residue was purified by silica gel chromatography (5% ethyl acetate/hexanes) to yield **148j** (28.1 mg, 50% yield) in 94% ee as a clear oil. The enantiomeric excess was determined by chiral SFC analysis (OB-H, 2.5 mL/min, 5% IPA in CO<sub>2</sub>,  $\lambda = 210$  nm):  $t_R$  (minor) = 6.2 min,  $t_R$  (major) = 6.9 min.

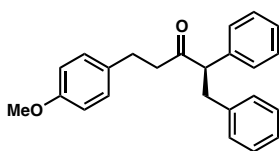
$[\alpha]_D^{25} = -97.9^\circ$  ( $c = 0.96$ ,  $\text{CHCl}_3$ );  $^1\text{H NMR}$  (500 MHz,  $\text{CDCl}_3$ )  $\delta$  7.33 – 7.20 (m, 3H), 7.19 – 7.12 (m, 2H), 6.98 (d,  $J = 8.8$  Hz, 2H), 6.76 (d,  $J = 8.5$  Hz, 2H), 3.76 (s, 3H), 3.48 (t,  $J = 7.4$  Hz, 1H), 2.84 – 2.56 (m, 4H), 2.11 – 1.99 (m, 1H), 1.77 – 1.64 (m, 1H), 0.80 (t,  $J = 7.4$  Hz, 3H);  $^{13}\text{C NMR}$  (126 MHz,  $\text{CDCl}_3$ )  $\delta$  209.7, 157.8, 138.8, 133.1, 129.2, 128.8, 128.3, 127.1, 113.8, 61.0, 55.2, 43.6, 29.0, 25.1, 12.1; FTIR (NaCl, thin film): 2961, 2932, 1711, 1611, 1513, 1492, 1453, 1300, 1247, 1178, 1036, 821  $\text{cm}^{-1}$ ; HRMS (MM) calc'd for  $\text{M}^+$  282.1614, found 282.1631.

**(R)-4-(4-chlorophenyl)-1-(4-methoxyphenyl)Hexan-3-one (148k)**



Prepared from 1-chloro-4-(1-chloropropyl)benzene (**150k**, 0.20 mmol) and 3-(4-methoxyphenyl)propanoyl chloride (**123**, 0.30 mmol) according to General Procedure 4. The crude residue was purified by silica gel chromatography (5% ethyl acetate/hexanes) to yield **148k** (41.2 mg, 65% yield) in 91% ee as a clear oil. The enantiomeric excess was determined by chiral SFC analysis (OD-H, 2.5 mL/min, 3% IPA in  $\text{CO}_2$ ,  $\lambda = 210$  nm):  $t_R$  (minor) = 18.1 min,  $t_R$  (major) = 19.4 min.  $[\alpha]_D^{25} = -79.7^\circ$  ( $c = 1.85$ ,  $\text{CHCl}_3$ );  $^1\text{H NMR}$  (500 MHz,  $\text{CDCl}_3$ )  $\delta$  7.24 (d,  $J = 8.6$  Hz, 2H), 7.06 (d,  $J = 8.9$  Hz, 2H), 6.97 (d,  $J = 9.1$  Hz, 2H), 6.76 (d,  $J = 8.6$  Hz, 2H), 3.77 (s, 3H), 3.48 – 3.41 (m, 1H), 2.83 – 2.55 (m, 4H), 2.01 (dp,  $J = 14.4, 7.3$  Hz, 1H), 1.72 – 1.62 (m, 1H), 0.78 (t,  $J = 7.4$  Hz, 3H);  $^{13}\text{C NMR}$  (126 MHz,  $\text{CDCl}_3$ )  $\delta$  209.2, 157.9, 137.1, 133.0, 132.8, 129.6, 129.2, 128.9, 113.7, 60.3, 55.2, 43.7, 28.9, 25.1, 12.0; FTIR (NaCl, thin film): 2962, 2932, 2834, 1711, 1611, 1583, 1512, 1490, 1463, 1300, 1246, 1178, 1092, 1036, 1014, 819  $\text{cm}^{-1}$ ; LRMS (ESI) calc'd for  $[\text{M}+\text{H}]^+$  317.1, found 317.1.

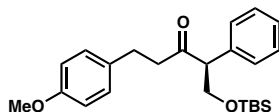
**(R)-5-(4-methoxyphenyl)-1,2-Diphenylpentan-3-one (148l)**



Prepared from (1-chloroethane-1,2-diyl)dibenzene (**150l**, 0.20 mmol) and 3-(4-methoxyphenyl)propanoyl chloride (**123**, 0.30 mmol) according to General Procedure 4. The crude residue was purified by silica gel chromatography (5% ethyl acetate/hexanes) to yield **148l** (54.6 mg, 79% yield) in 92% ee as a clear oil. The enantiomeric excess was determined by chiral SFC analysis (AS-H, 2.5 mL/min, 10% IPA in CO<sub>2</sub>,  $\lambda = 210$  nm):  $t_R$  (major) = 4.5 min,  $t_R$  (minor) = 5.3 min.  $[\alpha]_D^{25} = -166.8^\circ$  ( $c = 0.85$ , CHCl<sub>3</sub>); <sup>1</sup>H NMR (500 MHz, CDCl<sub>3</sub>)  $\delta$  7.32 – 7.08 (m, 8H), 7.06 – 6.96 (m, 2H), 6.92 (d,  $J = 8.3$  Hz, 2H), 6.74 (d,  $J = 8.3$  Hz, 2H), 3.87 (t,  $J = 7.4$  Hz, 1H), 3.77 (s, 3H), 3.42 (dd,  $J = 13.7, 7.7$  Hz, 1H), 2.90 (dd,  $J = 13.7, 7.0$  Hz, 1H), 2.80 – 2.59 (m, 3H), 2.58 – 2.45 (m, 1H); <sup>13</sup>C NMR (126 MHz, CDCl<sub>3</sub>)  $\delta$  209.0, 157.8, 139.7, 138.3, 132.9, 129.1, 129.0, 128.9, 128.4, 128.2, 127.3, 126.1, 113.8, 61.1, 55.2, 44.1, 38.6, 28.9; FTIR (NaCl, thin film): 3027, 2930, 2834, 1712, 1611, 1583, 1513, 1495, 1453, 1300, 1247, 1178, 1035, 824 cm<sup>-1</sup>; HRMS (MM) calc'd for [M+H]<sup>+</sup> 345.1849, found 345.1831.

**(S)-1-((tert-butyldimethylsilyloxy)-5-(4-methoxyphenyl)-2-Phenylpentan-3-one**

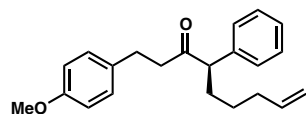
**(148m)**



Prepared from [1-chloro-2-(*t*-butyldimethylsilyloxy)ethyl]benzene (**150m**, 0.20 mmol) and 3-(4-methoxyphenyl)propanoyl chloride (**123**, 0.30 mmol) according to General Procedure 4 except using 50% v/v DMA/THF. The crude residue was purified by silica gel chromatography (5% ethyl acetate/hexanes) to yield **148m** (40.4 mg, 51% yield) in 89% ee as a clear oil. The enantiomeric excess

was determined by chiral SFC analysis (AS-H, 2.5 mL/min, 5% IPA in CO<sub>2</sub>,  $\lambda$  = 210 nm):  $t_R$  (major) = 3.3 min,  $t_R$  (minor) = 3.8 min.  $[\alpha]_D^{25} = -50.0^\circ$  (c = 0.90, CHCl<sub>3</sub>); <sup>1</sup>H NMR (500 MHz, CDCl<sub>3</sub>)  $\delta$  7.33 – 7.23 (m, 3H), 7.20 (dd, J = 8.1, 1.6 Hz, 2H), 7.01 (d, J = 8.8 Hz, 2H), 6.77 (d, J = 8.8 Hz, 2H), 4.23 (dd, J = 9.7, 8.5 Hz, 1H), 3.92 (dd, J = 8.5, 5.7 Hz, 1H), 3.77 (s, 3H), 3.73 (dd, J = 9.7, 5.7 Hz, 1H), 2.88 – 2.68 (m, 4H), 0.84 (s, 9H), –0.01 (s, 3H), –0.03 (s, 3H); <sup>13</sup>C NMR (126 MHz, CDCl<sub>3</sub>)  $\delta$  208.8, 157.8, 135.9, 133.1, 129.2, 128.7, 128.5, 127.5, 113.8, 65.0, 61.0, 55.2, 45.1, 28.6, 25.8, 18.2, –5.57, –5.60; FTIR (NaCl, thin film): 2953, 2928, 2855, 1718, 1612, 1583, 1513, 1463, 1361, 1248, 1099, 835 cm<sup>-1</sup>; HRMS (MM) calc'd for [M+H]<sup>+</sup> 399.2350, found 399.2198.

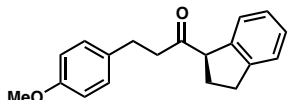
**(R)-1-(4-methoxyphenyl)-4-Phenylnon-8-en-3-one (148n)**



Prepared from (1-chlorohex-5-en-1-yl)benzene (**150n**, 0.20 mmol) and 3-(4-methoxyphenyl)propanoyl chloride (**123**, 0.30 mmol) according to General Procedure 4. The crude residue was purified by silica gel chromatography (5% ethyl acetate/hexanes) to yield **148n** (24.6 mg, 38% yield) in 92% ee as a clear oil. The enantiomeric excess was determined by chiral SFC analysis (AD-H, 2.5 mL/min, 5% IPA in CO<sub>2</sub>,  $\lambda$  = 210 nm):  $t_R$  (major) = 10.9 min,  $t_R$  (minor) = 11.9 min.  $[\alpha]_D^{25} = -90.9^\circ$  (c = 0.47, CHCl<sub>3</sub>); <sup>1</sup>H NMR (500 MHz, CDCl<sub>3</sub>)  $\delta$  7.35 – 7.20 (m, 3H), 7.18 – 7.11 (m, 2H), 6.98 (d, J = 8.4 Hz, 2H), 6.76 (d, J = 8.9 Hz, 2H), 5.73 (ddt, J = 16.9, 10.2, 6.7 Hz, 1H), 5.02 – 4.88 (m, 2H), 3.76 (s, 3H), 3.55 (t, J = 7.4 Hz, 1H), 2.84 – 2.54 (m, 4H), 2.09 – 1.93 (m, 3H), 1.74 – 1.63 (m, 1H), 1.37 – 1.15 (m, 2H); <sup>13</sup>C NMR (126 MHz, CDCl<sub>3</sub>)  $\delta$  209.6, 157.9, 138.8, 138.4, 133.0, 129.2, 128.9, 128.3, 127.2, 114.7, 113.8, 59.1, 55.2, 43.6, 33.6, 31.4, 29.0, 26.7; FTIR (NaCl, thin film): 2930, 1712, 1640,

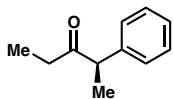
1611, 1583, 1513, 1453, 1300, 1247, 1177, 1036, 824  $\text{cm}^{-1}$ ; HRMS (MM) calc'd for  $[\text{M}+\text{H}]^+$  323.2006, found 323.1945.

**(R)-1-(2,3-dihydro-1H-inden-1-yl)-3-(4-methoxyphenyl)Propan-1-one (148o)**



Prepared from 1-chloro-2,3-dihydro-1H-indene (**150o**, 0.20 mmol) and 3-(4-methoxyphenyl)propanoyl chloride (**123**, 0.30 mmol) according to General Procedure 4. The crude residue was purified by silica gel chromatography (5% ethyl acetate/hexanes) to yield **148o** (38.3 mg, 68% yield) in 78% ee as a clear oil. The enantiomeric excess was determined by chiral SFC analysis (AD-H, 2.5 mL/min, 10% IPA in  $\text{CO}_2$ ,  $\lambda = 210$  nm):  $t_R$  (minor) = 7.9 min,  $t_R$  (major) = 8.9 min.  $[\alpha]_D^{25} = 11.3^\circ$  ( $c = 0.179$ ,  $\text{CHCl}_3$ );  $^1\text{H}$  NMR (500 MHz,  $\text{CDCl}_3$ )  $\delta$  7.30 – 7.10 (m, 4H), 7.07 (d,  $J = 8.9$  Hz, 2H), 6.83 (d,  $J = 8.7$  Hz, 3H), 4.08 (t,  $J = 7.1$  Hz, 1H), 3.78 (s, 3H), 3.05 (d,  $J = 7.9$  Hz, 1H), 2.98 – 2.67 (m, 5H), 2.37 – 2.18 (m, 2H);  $^{13}\text{C}$  NMR (126 MHz,  $\text{CDCl}_3$ )  $\delta$  210.0, 157.9, 144.6, 140.8, 133.2, 129.3, 127.5, 124.9, 124.8, 113.9, 113.8, 58.4, 55.3, 42.4, 31.9, 28.9, 28.5; FTIR (NaCl, thin film): 2932, 2849, 1709, 1611, 1583, 1513, 1458, 1300, 1247, 1178, 1036, 826, 755  $\text{cm}^{-1}$ ; LRMS (ESI) calc'd for  $[\text{M}+\text{H}]^+$  281.2, found 281.1.

**(R)-2-Phenylpentan-3-one (152a)**

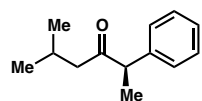


Prepared from (1-chloroethyl)benzene (**26**, 0.20 mmol) and propionyl chloride (**151a**, 0.24 mmol) according to General Procedure 4 except using 20% v/v DMA/THF. The crude residue was purified by silica gel chromatography (2% ethyl acetate/hexanes) to yield **152a** (19.5 mg, 60% yield) in 91% ee as a clear oil.

The enantiomeric excess was determined by chiral SFC analysis (AS-H, 2.5 mL/min, 1% IPA in CO<sub>2</sub>,  $\lambda = 210$  nm):  $t_R$  (minor) = 1.8 min,  $t_R$  (major) = 2.0 min.  $[\alpha]_D^{25} = -225.9^\circ$  (c = 0.57, CHCl<sub>3</sub>); <sup>1</sup>H NMR (500 MHz, CDCl<sub>3</sub>)  $\delta$  7.36 – 7.29 (m, 2H), 7.28 – 7.23 (m, 1H), 7.23 – 7.19 (m, 2H), 3.76 (q, J = 7.0 Hz, 1H), 2.42 – 2.33 (m, 2H), 1.39 (d, J = 7.0 Hz, 3H), 0.97 (t, J = 7.3 Hz, 3H); <sup>13</sup>C NMR (126 MHz, CDCl<sub>3</sub>)  $\delta$  211.5, 140.9, 128.8, 127.8, 127.0, 52.7, 34.2, 17.5, 8.0; FTIR (NaCl, thin film): 3027, 2976, 2935, 1716, 1600, 1494, 1453, 1374, 1130, 1070, 1029, 957, 758 cm<sup>-1</sup>; LRMS (ESI) calc'd for [M+H]<sup>+</sup> 163.1, found 163.1.

The optical rotation of the product generated in the presence of (*R,R*)-**L36** was measured as  $[\alpha]_D^{25} = -225.9^\circ$  (c = 0.57, CHCl<sub>3</sub>). Lit:  $[\alpha]_D^{25} = -76^\circ$  (c = 1.2, CHCl<sub>3</sub>, *R* enantiomer, 95% ee)<sup>26</sup> and  $[\alpha]_D^{21} = -47.2$  (c = 1.00, CHCl<sub>3</sub>; 73% ee).<sup>5e</sup> Based on the literature precedent, we assign our product as the *R* enantiomer.

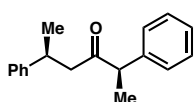
### (*R*)-5-Methyl-2-phenylhexan-3-one (**152b**)



Prepared from (1-chloroethyl)benzene (**26**, 0.20 mmol) and isovaleroyl chloride (**151b**, 0.24 mmol) according to General Procedure 4. The crude residue was purified by silica gel chromatography (2% ethyl acetate/hexanes) to yield **152b** (27.5 mg, 73% yield) in 88% ee as a clear oil. The enantiomeric excess was determined by chiral SFC analysis (OD-H, 2.5 mL/min, 1% IPA in CO<sub>2</sub>,  $\lambda = 210$  nm):  $t_R$  (minor) = 2.2 min,  $t_R$  (major) = 2.7 min.  $[\alpha]_D^{25} = -205.8^\circ$  (c = 0.92, CHCl<sub>3</sub>); <sup>1</sup>H NMR (500 MHz, CDCl<sub>3</sub>)  $\delta$  7.35 – 7.29 (m, 2H), 7.28 – 7.23 (m, 1H), 7.23 – 7.18 (m, 2H), 3.72 (q, J

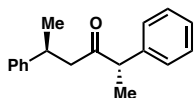
= 6.9 Hz, 1H), 2.29 – 2.16 (m, 2H), 2.10 (hept, J = 6.7 Hz, 1H), 1.38 (d, J = 7.0 Hz, 3H), 0.84 (d, J = 6.6 Hz, 3H), 0.75 (d, J = 6.6 Hz, 3H);  $^{13}\text{C}$  NMR (126 MHz,  $\text{CDCl}_3$ )  $\delta$  210.5, 140.5, 128.8, 127.9, 127.0, 53.3, 50.0, 24.3, 22.6, 22.2, 17.4; FTIR (NaCl, thin film): 3027, 2957, 2871, 1712, 1600, 1493, 1453, 1366, 1143, 1071, 1024, 761  $\text{cm}^{-1}$ ; LRMS (ESI) calc'd for  $[\text{M}+\text{H}]^+$  191.1, found 191.2.

**(2*R*,5*S*)-2,5-Diphenylhexan-3-one ((*R,S*)-**152c**)**



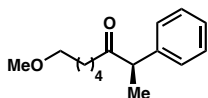
Prepared from (1-chloroethyl)benzene (**26**, 0.20 mmol) and (*S*)-3-phenylbutyryl chloride ((*S*)-**151c**, 0.24 mmol) according to General Procedure 4. The crude residue was purified by silica gel chromatography (2% ethyl acetate/hexanes) to yield (*R,S*)-**152c** (34.8 mg, 69% yield) as a clear oil and as a 20:1 mixture of diastereomers (determined by NMR analysis of the purified product).  $[\alpha]_D^{25} = -122.2^\circ$  ( $c = 1.71$ ,  $\text{CHCl}_3$ );  $^1\text{H}$  NMR (500 MHz,  $\text{CDCl}_3$ )  $\delta$  7.30 – 7.17 (m, 5H), 7.17 – 7.12 (m, 1H), 7.10 – 7.02 (m, 4H), 3.69 (q, J = 7.0 Hz, 1H), 3.30 (h, J = 7.0 Hz, 1H), 2.70 (dd, J = 16.8, 6.8 Hz, 1H), 2.58 (dd, J = 16.8, 7.5 Hz, 1H), 1.34 (d, J = 6.9 Hz, 3H), 1.20 (d, J = 7.0 Hz, 3H);  $^{13}\text{C}$  NMR (126 MHz,  $\text{CDCl}_3$ )  $\delta$  209.3, 146.1, 140.2, 128.8, 128.3, 127.0, 126.74, 126.73, 126.1, 53.5, 49.2, 35.2, 21.9, 17.2; FTIR (NaCl, thin film): 3061, 3027, 2967, 2930, 1714, 1601, 1493, 1452, 1373, 1125, 1069, 1029, 759  $\text{cm}^{-1}$ ; LRMS (ESI) calc'd for  $[\text{M}+\text{H}]^+$  253.2, found 253.2.

**(2*S*,5*S*)-2,5-Diphenylhexan-3-one ((*S,S*)-**152c**)**



Prepared from (1-chloroethyl)benzene (**26**, 0.20 mmol) and (*S*)-3-phenylbutyryl chloride ((*S*)-**151c**, 0.24 mmol) according to General Procedure 4 except using (*S,S*)-**L36**. The crude residue was purified by silica gel chromatography (2% ethyl acetate/hexanes) to yield (*S,S*)-**152c** (33.7 mg, 67% yield) as a clear oil and as a 12:1 mixture of diastereomers (determined by NMR analysis of the purified product).  $[\alpha]_D^{25} = 121.3^\circ$  ( $c = 1.59$ ,  $\text{CHCl}_3$ );  $^1\text{H NMR}$  (500 MHz,  $\text{CDCl}_3$ )  $\delta$  7.37 – 7.31 (m, 2H), 7.31 – 7.24 (m, 3H), 7.22 – 7.13 (m, 5H), 3.54 (q,  $J = 6.9$  Hz, 1H), 3.29 (h,  $J = 7.3$  Hz, 1H), 2.67 (dd,  $J = 16.3, 6.4$  Hz, 1H), 2.56 (dd,  $J = 16.3, 7.9$  Hz, 1H), 1.32 (d,  $J = 6.9$  Hz, 3H), 1.11 (d,  $J = 7.0$  Hz, 3H);  $^{13}\text{C NMR}$  (126 MHz,  $\text{CDCl}_3$ )  $\delta$  209.5, 146.3, 140.3, 128.9, 128.5, 128.0, 127.1, 126.8, 126.2, 53.4, 49.6, 35.4, 21.5, 17.2; FTIR (NaCl, thin film): 3061, 3027, 2968, 2930, 1714, 1601, 1494, 1452, 1374, 1125, 1068, 1029, 1004, 763  $\text{cm}^{-1}$ ; LRMS (ESI) calc'd for  $[\text{M}+\text{H}]^+$  253.2, found 253.1.

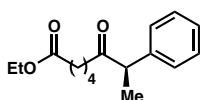
**(*R*)-8-Methoxy-2-phenyloctan-3-one (**152d**)**



Prepared from (1-chloroethyl)benzene (**26**, 0.20 mmol) and 6-methoxyhexanoyl chloride (**151d**, 0.24 mmol) according to General Procedure 4 except using 20% v/v DMA/THF. The crude residue was purified by silica gel chromatography (5-10% ethyl acetate/hexanes) to yield **152d** (35.0 mg, 75% yield) in 85% ee as a clear oil. The enantiomeric excess was determined by chiral SFC analysis (OD-H, 2.5 mL/min, 3% IPA in  $\text{CO}_2$ ,  $\lambda = 210$  nm):  $t_R$  (minor) = 5.4 min,  $t_R$  (major) = 5.8 min.  $[\alpha]_D^{25} = -146.0^\circ$  ( $c = 1.14$ ,  $\text{CHCl}_3$ );  $^1\text{H NMR}$  (500 MHz,  $\text{CDCl}_3$ )  $\delta$  7.35 – 7.29 (m, 2H), 7.28 – 7.23 (m, 1H), 7.22 – 7.18 (m, 2H), 3.74 (q,  $J = 7.0$  Hz, 1H), 3.31 – 3.25 (m,

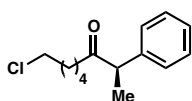
5H), 2.38 – 2.32 (m, 2H), 1.57 – 1.42 (m, 2H), 1.38 (d,  $J = 7.0$  Hz, 3H), 1.26 – 1.17 (m, 2H);  $^{13}\text{C}$  NMR (126 MHz,  $\text{CDCl}_3$ )  $\delta$  210.9, 140.7, 128.9, 127.9, 127.1, 72.5, 58.5, 53.0, 40.9, 29.3, 25.6, 23.6, 17.4; FTIR (NaCl, thin film): 2931, 2866, 2360, 1714, 1600, 1494, 1453, 1373, 1119, 1072, 1029, 761  $\text{cm}^{-1}$ ; LRMS (ESI) calc'd for  $[\text{M}+\text{H}]^+$  235.2, found 235.2.

**(R)-Ethyl 6-oxo-7-phenyloctanoate (152e)**



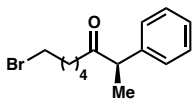
Prepared from (1-chloroethyl)benzene (**26**, 0.20 mmol) and ethyl 6-chloro-6-oxohexanoate (**151e**, 0.24 mmol) according to General Procedure 4 except using 10% v/v DMA/THF. The crude residue was purified by silica gel chromatography (5% ethyl acetate/hexanes) to yield **152e** (33.8 mg, 64% yield) in 92% ee as a clear oil. The enantiomeric excess was determined by chiral SFC analysis (AD-H, 2.5 mL/min, 4% IPA in  $\text{CO}_2$ ,  $\lambda = 210$  nm):  $t_{\text{R}}$  (minor) = 4.9 min,  $t_{\text{R}}$  (major) = 5.3 min.  $[\alpha]_{\text{D}}^{25} = -146.8^\circ$  ( $c = 0.85$ ,  $\text{CHCl}_3$ );  $^1\text{H}$  NMR (500 MHz,  $\text{CDCl}_3$ )  $\delta$  7.35 – 7.29 (m, 2H), 7.28 – 7.23 (m, 1H), 7.22 – 7.18 (m, 2H), 4.09 (q,  $J = 7.1$  Hz, 2H), 3.73 (q,  $J = 7.0$  Hz, 1H), 2.44 – 2.28 (m, 2H), 2.25 – 2.15 (m, 2H), 1.58 – 1.44 (m, 4H), 1.38 (d,  $J = 7.0$  Hz, 3H), 1.22 (t,  $J = 7.1$  Hz, 3H);  $^{13}\text{C}$  NMR (126 MHz,  $\text{CDCl}_3$ )  $\delta$  210.4, 173.4, 140.6, 128.9, 127.8, 127.1, 60.2, 53.0, 40.5, 34.0, 24.3, 23.2, 17.4, 14.2; FTIR (NaCl, thin film): 2977, 2932, 1733, 1714, 1600, 1494, 1453, 1375, 1248, 1181, 1029, 761  $\text{cm}^{-1}$ ; LRMS (ESI) calc'd for  $[\text{M}+\text{H}]^+$  263.2, found 263.2.

**(R)-8-Chloro-2-phenyloctan-3-one (152f)**



Prepared from (1-chloroethyl)benzene (**26**, 0.20 mmol) and 6-chlorohexanoyl chloride (**151f**, 0.24 mmol) according to General Procedure 4 except using 20% v/v DMA/THF. The crude residue was purified by silica gel chromatography (2% ethyl acetate/hexanes) to yield **152f** (36.3 mg, 76% yield) in 92% ee as a clear oil. The enantiomeric excess was determined by chiral SFC analysis (OD-H, 2.5 mL/min, 3% IPA in CO<sub>2</sub>,  $\lambda = 210$  nm):  $t_R$  (minor) = 5.8 min,  $t_R$  (major) = 6.5 min.  $[\alpha]_D^{25} = -163.3^\circ$  (c = 0.78, CHCl<sub>3</sub>); <sup>1</sup>H NMR (500 MHz, CDCl<sub>3</sub>)  $\delta$  7.36 – 7.30 (m, 2H), 7.29 – 7.23 (m, 1H), 7.23 – 7.18 (m, 2H), 3.74 (q, J = 7.0 Hz, 1H), 3.45 (t, J = 6.7 Hz, 2H), 2.46 – 2.28 (m, 2H), 1.73 – 1.61 (m, 2H), 1.57 – 1.44 (m, 2H), 1.39 (d, J = 7.0 Hz, 3H), 1.34 – 1.24 (m, 2H); <sup>13</sup>C NMR (126 MHz, CDCl<sub>3</sub>)  $\delta$  210.6, 140.6, 128.9, 127.8, 127.2, 53.1, 44.8, 40.6, 32.3, 26.2, 23.0, 17.4; FTIR (NaCl, thin film): 2932, 2867, 2360, 1711, 1599, 1493, 1452, 1374, 1122, 1069, 1029, 760 cm<sup>-1</sup>; LRMS (ESI) calc'd for [M+H]<sup>+</sup> 239.1, found 239.1.

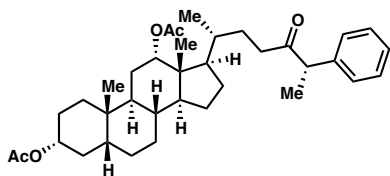
**(R)-8-Bromo-2-phenyloctan-3-one (152g)**



Prepared from (1-chloroethyl)benzene (**26**, 0.20 mmol) and 6-bromohexanoyl chloride (**151g**, 0.24 mmol) according to General Procedure 4 except using 10% v/v DMA/THF. The crude residue was purified by silica gel chromatography (2% ethyl acetate/hexanes) to yield **152g** (40.8 mg, 72% yield) in 86% ee as a clear oil. The enantiomeric excess was determined by chiral SFC analysis (OD-H, 2.5 mL/min, 3% IPA in CO<sub>2</sub>,  $\lambda = 210$  nm):  $t_R$  (minor) = 7.3 min,  $t_R$  (major) = 8.1 min.  $[\alpha]_D^{25} = -146.8^\circ$  (c = 1.57, CHCl<sub>3</sub>); <sup>1</sup>H NMR (500 MHz, CDCl<sub>3</sub>)  $\delta$  7.37 – 7.30 (m,

2H), 7.29 – 7.24 (m, 1H), 7.23 – 7.18 (m, 2H), 3.74 (q,  $J = 7.0$  Hz, 1H), 3.32 (t,  $J = 6.8$  Hz, 2H), 2.46 – 2.28 (m, 2H), 1.80 – 1.70 (m, 2H), 1.56 – 1.44 (m, 2H), 1.39 (d,  $J = 7.0$  Hz, 3H), 1.37 – 1.24 (m, 2H);  $^{13}\text{C}$  NMR (126 MHz,  $\text{CDCl}_3$ )  $\delta$  210.5, 140.6, 128.9, 127.9, 127.2, 53.1, 40.6, 33.6, 32.4, 27.5, 22.9, 17.4; FTIR (NaCl, thin film): 2932, 2867, 1713, 1600, 1494, 1453, 1373, 1252, 1069, 1029, 761  $\text{cm}^{-1}$ ; LRMS (ESI) calc'd for  $[\text{M}+\text{H}]^+$  283.1, found 283.1.

**(3*R*,5*R*,8*R*,9*S*,10*S*,12*S*,13*R*,14*S*,17*R*)-10,13-Dimethyl-17-((2*R*,6*S*)-5-oxo-6-phenylheptan-2-yl)hexadecahydro-1*H*-cyclopenta[*a*]phenanthrene-3,12-diyl diacetate (**152h**)**



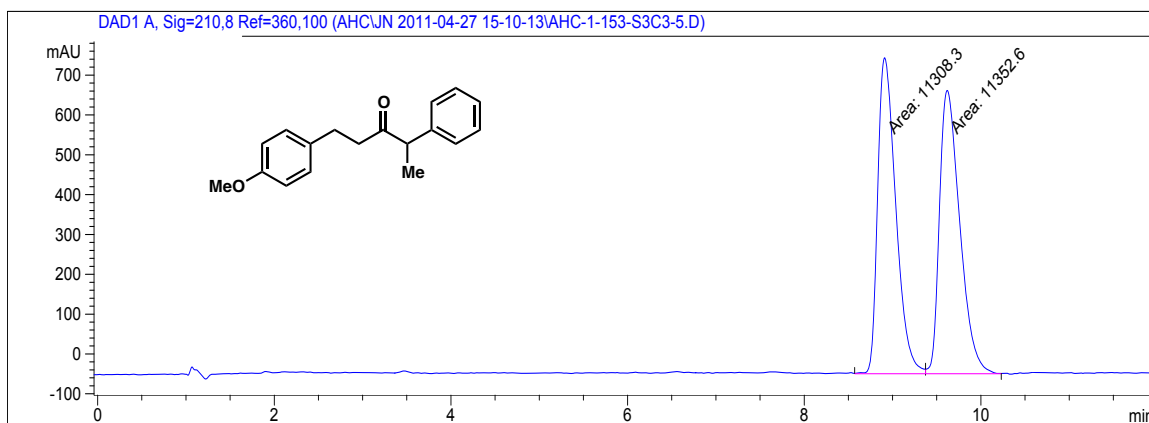
Prepared from (1-chloroethyl)benzene (**26**, 0.20 mmol) and acid chloride **151h** (0.24 mmol) according to General Procedure 4 except using 10% v/v DMA/THF

and (*S,S*)-**L36**. Following extraction, the combined organic layers were washed with sat. aq.  $\text{NaHCO}_3$  (1 X 10 mL) and brine (1 X 15 mL). The crude residue was purified by silica gel chromatography (15% ethyl acetate/hexanes) to yield **152h** (72.5 mg, 64% yield) as a fluffy white solid and as a 14:1 mixture of diastereomers (determined by NMR analysis of the purified product).  $[\alpha]_D^{25} = 146.0^\circ$  ( $c = 2.05$ ,  $\text{CHCl}_3$ );  $^1\text{H}$  NMR (500 MHz, Acetone- $d_6$ )  $\delta$  7.39 – 7.31 (m, 2H), 7.30 – 7.22 (m, 3H), 4.99 (t,  $J = 3.0$  Hz, 1H), 4.63 (tt,  $J = 11.4, 4.6$  Hz, 1H), 3.90 (q,  $J = 6.9$  Hz, 1H), 2.45 – 2.29 (m, 2H), 2.01 (s, 3H), 1.98 – 1.40 (m, 17H), 1.37 – 0.99 (m, 13H), 0.95 (s, 3H), 0.72 (s, 3H), 0.69 (d,  $J = 6.9$  Hz, 3H);  $^{13}\text{C}$  NMR (126 MHz,  $\text{CDCl}_3$ )  $\delta$  209.8, 169.5, 169.3, 141.3, 128.7, 127.8, 126.9, 75.2, 73.5, 52.4, 49.4, 47.4, 44.9, 41.7, 37.3, 35.6, 34.6, 34.5, 34.3, 33.9, 32.1, 29.6, 27.0, 26.7,

26.4, 25.8, 25.3, 23.2, 22.5, 20.4, 20.3, 17.1, 16.9, 11.8; FTIR (NaCl, thin film): 2937, 2869, 1735, 1493, 1452, 1377, 1363, 1245, 1194, 1029, 971  $\text{cm}^{-1}$ ; LRMS (ESI) calc'd for  $[\text{M}+\text{H}_2\text{O}]^+$  582.4, found 582.4.

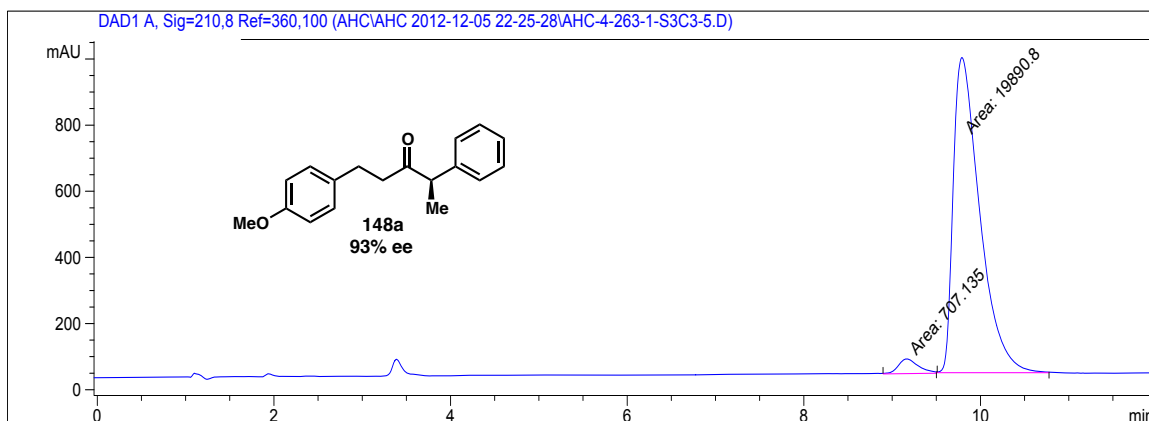
### 3.4.4 SFC Traces of Racemic and Enantioenriched Ketone Products

**148a (Table 3.6, entry 1): racemic**

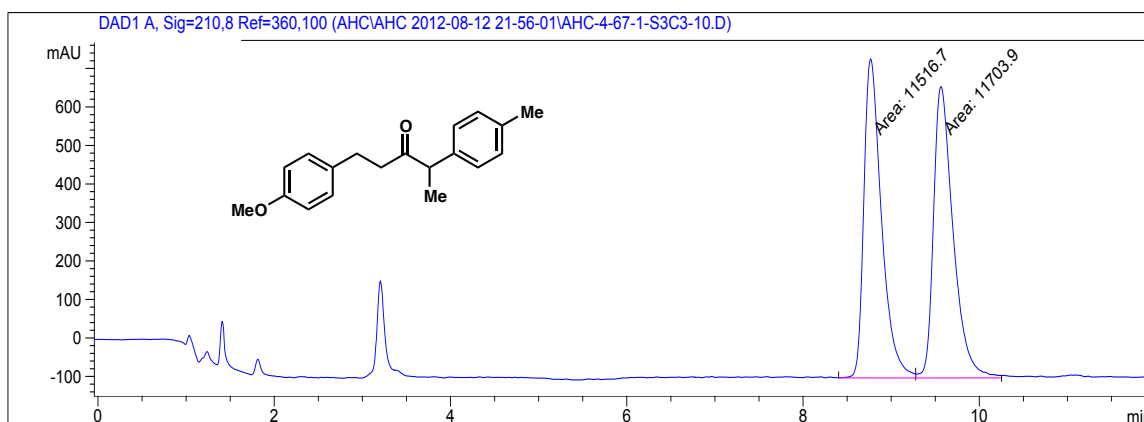


Peak #	RetTime [min]	Type	Width [min]	Area [mAU*s]	Height [mAU]	Area %
1	8.911	MM	0.2376	1.13083e4	793.28162	49.9021
2	9.619	MM	0.2660	1.13526e4	711.29791	50.0979

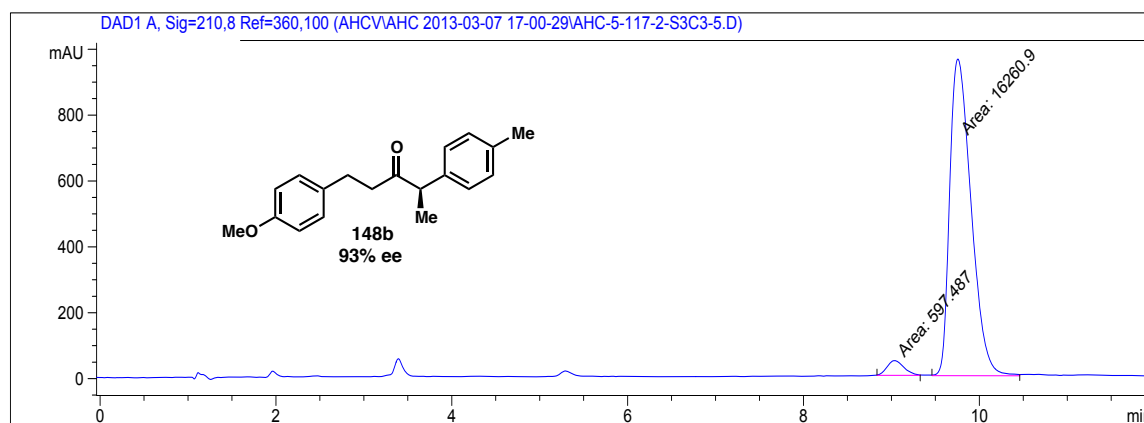
**148a (Table 3.6, entry 1): enantioenriched, 93% ee**



Peak #	RetTime [min]	Type	Width [min]	Area [mAU*s]	Height [mAU]	Area %
1	9.164	MM	0.2646	707.13519	44.53406	3.4330
2	9.790	MM	0.3479	1.98908e4	952.85913	96.5670

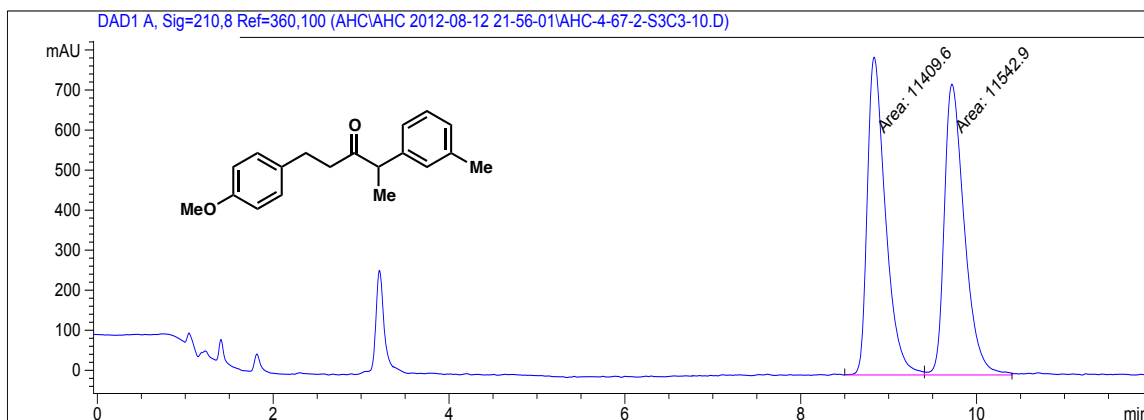
**148b (Table 3.6, entry 2): racemic**

Peak #	RetTime [min]	Type	Width [min]	Area [mAU*s]	Height [mAU]	Area %
1	8.766	MM	0.2315	1.15167e4	829.08398	49.5970
2	9.564	MM	0.2576	1.17039e4	757.13312	50.4030

**148b (Table 3.6, entry 2): enantioenriched, 93% ee**

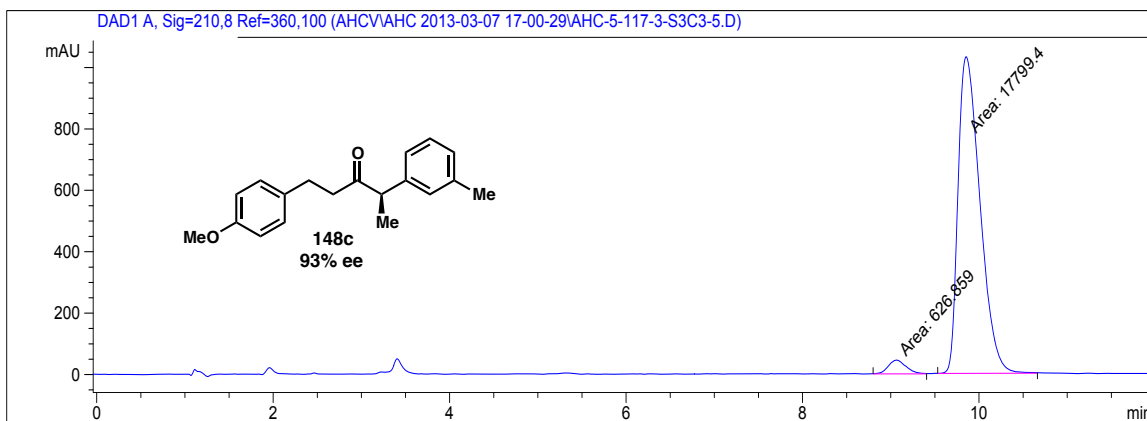
Peak #	RetTime [min]	Type	Width [min]	Area [mAU*s]	Height [mAU]	Area %
1	9.036	MM	0.2206	597.48749	45.14814	3.5442
2	9.756	MM	0.2819	1.62609e4	961.42609	96.4558

**148c (Table 3.6, entry 3): racemic**

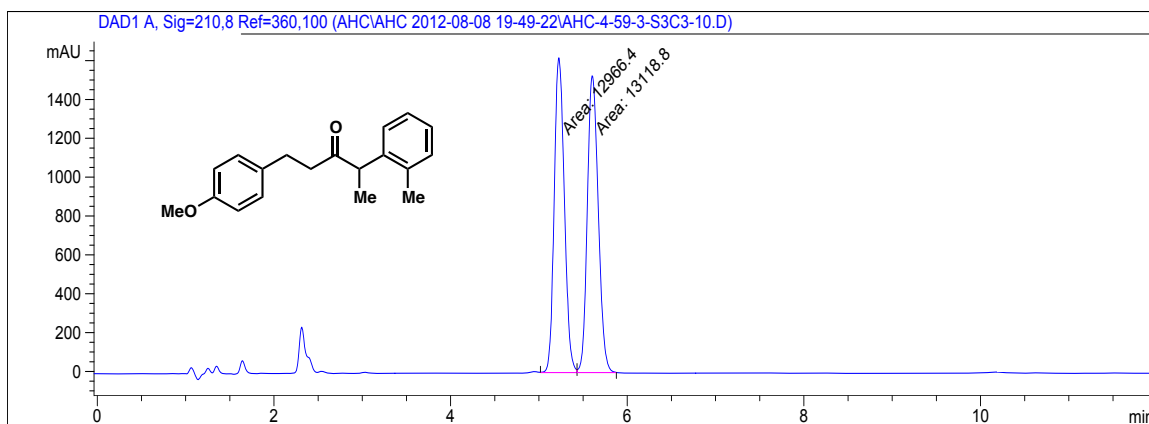


Peak #	RetTime [min]	Type	Width [min]	Area [mAU*s]	Height [mAU]	Area %
1	8.835	MM	0.2395	1.14096e4	794.09918	49.7095
2	9.720	MM	0.2647	1.15429e4	726.79602	50.2905

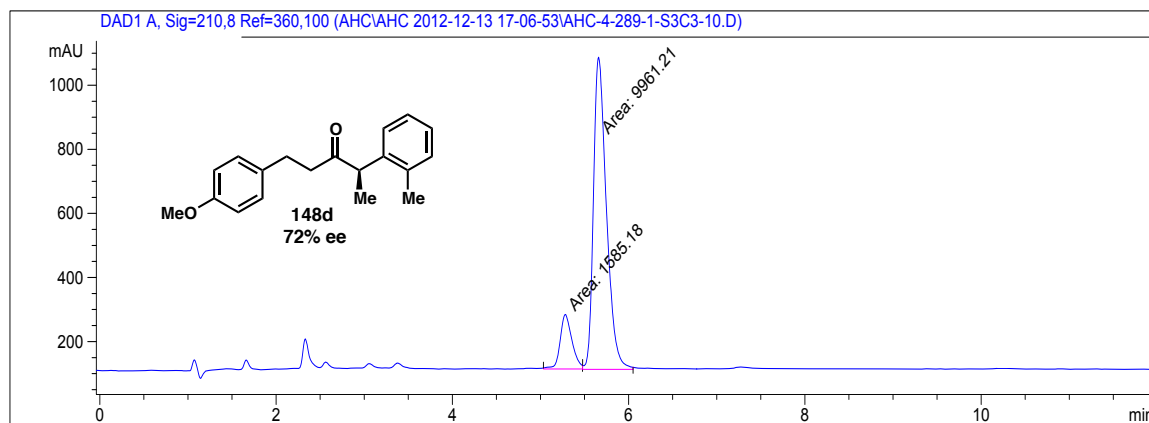
**148c (Table 3.6, entry 3): enantioenriched, 93% ee**



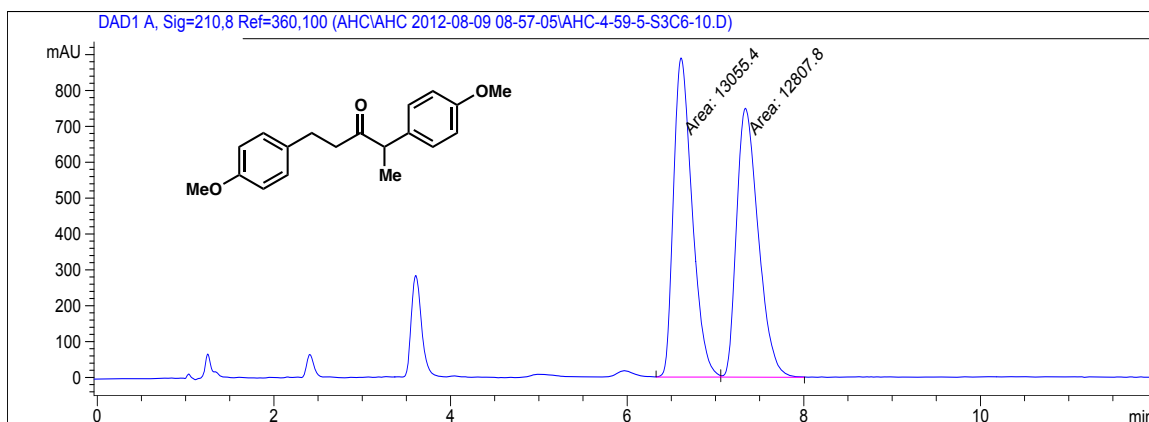
Peak #	RetTime [min]	Type	Width [min]	Area [mAU*s]	Height [mAU]	Area %
1	9.064	MM	0.2335	626.85852	44.73974	3.4020
2	9.854	MM	0.2876	1.77994e4	1031.51978	96.5980

**148d (Table 3.6, entry 4): racemic**

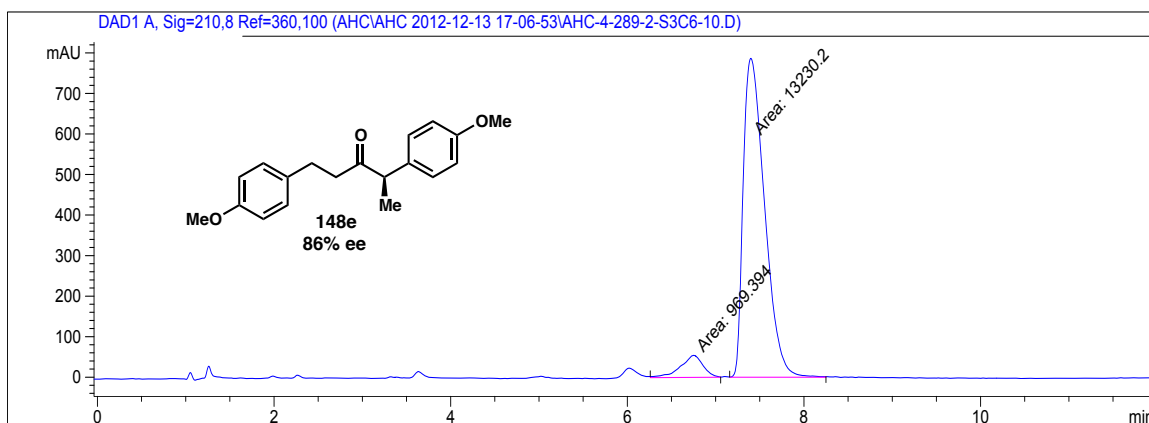
Peak #	RetTime [min]	Type	Width [min]	Area [mAU*s]	Height [mAU]	Area %
1	5.225	MM	0.1332	1.29664e4	1622.72693	49.7079
2	5.604	MM	0.1430	1.31188e4	1529.25037	50.2921

**148d (Table 3.6, entry 4): enantioenriched, 72% ee**

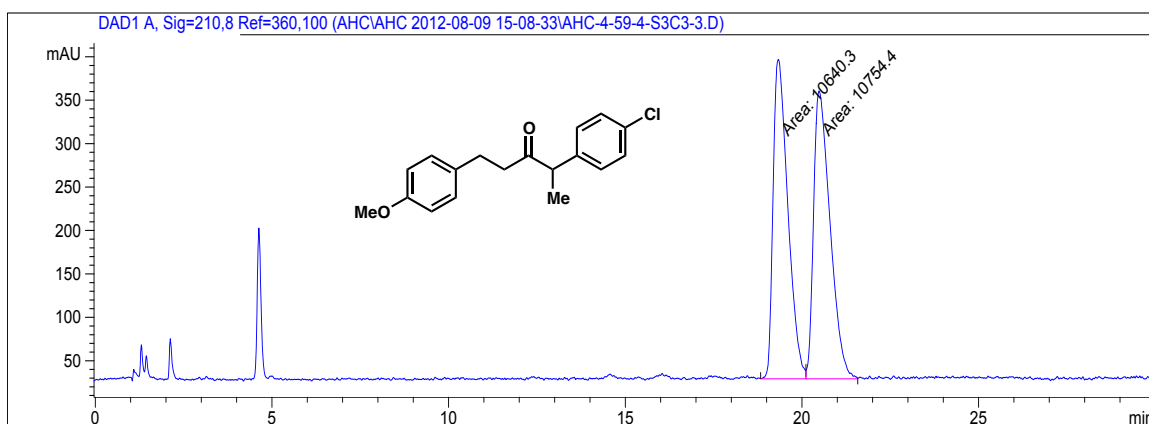
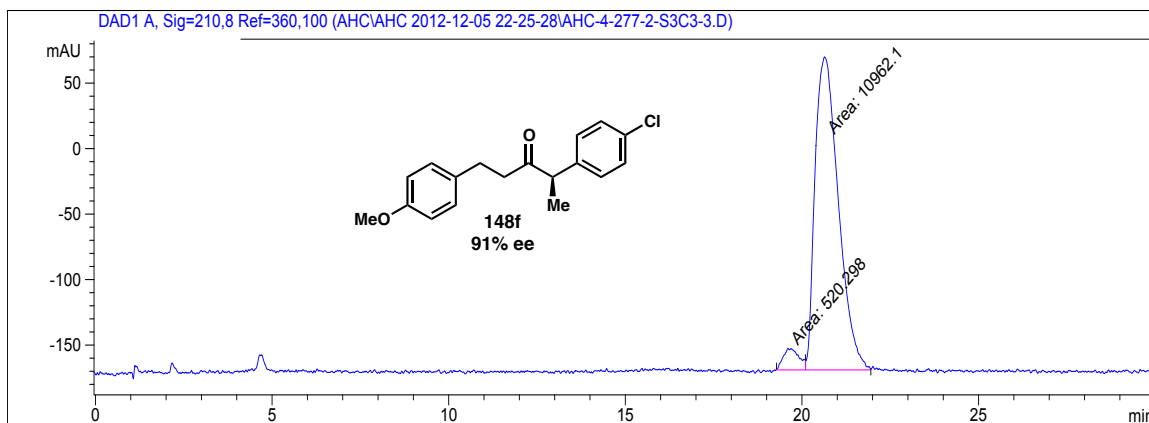
Peak #	RetTime [min]	Type	Width [min]	Area [mAU*s]	Height [mAU]	Area %
1	5.282	MM	0.1551	1585.18311	170.37230	13.7288
2	5.659	MM	0.1703	9961.21484	974.66937	86.2712

**148e (Table 3.6, entry 5): racemic**

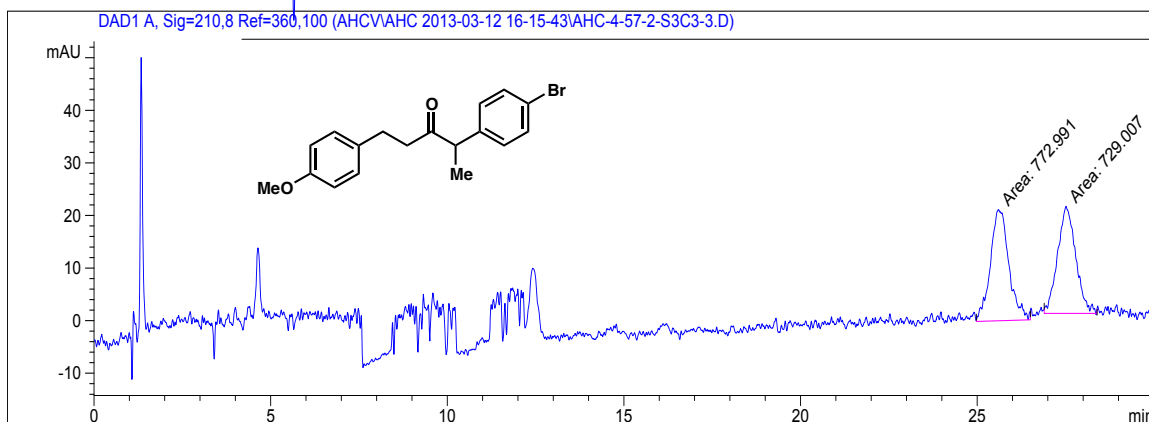
Peak #	RetTime [min]	Type	Width [min]	Area [mAU*s]	Height [mAU]	Area %
1	6.610	MM	0.2445	1.30554e4	889.75983	50.4785
2	7.339	MM	0.2848	1.28078e4	749.64392	49.5215

**148e (Table 3.6, entry 5): enantioenriched, 86% ee**

Peak #	RetTime [min]	Type	Width [min]	Area [mAU*s]	Height [mAU]	Area %
1	6.750	MM	0.2970	969.39368	54.40509	6.8269
2	7.399	MM	0.2801	1.32302e4	787.11755	93.1731

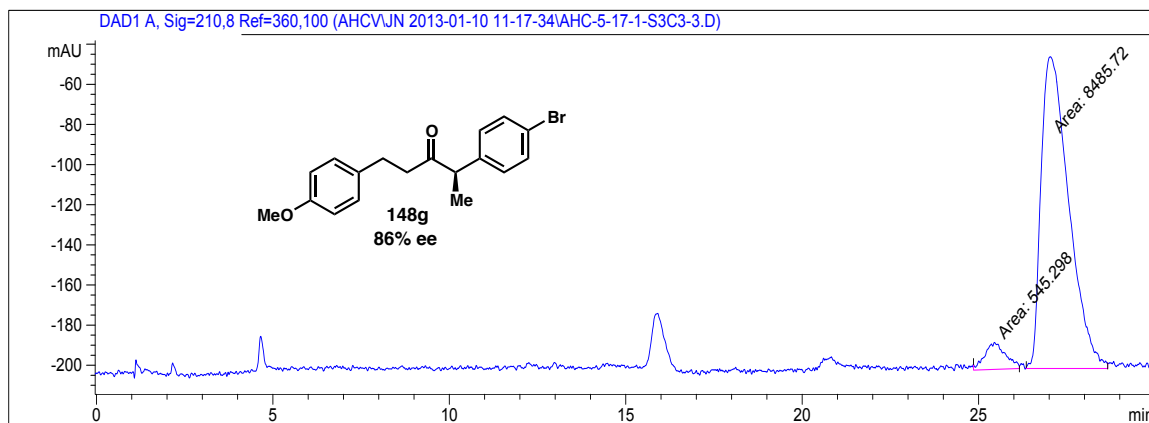
**148f (Table 3.6, entry 6): racemic****148f (Table 3.6, entry 6): enantioenriched, 91% ee**

**148g (Table 3.6, entry 7): racemic**

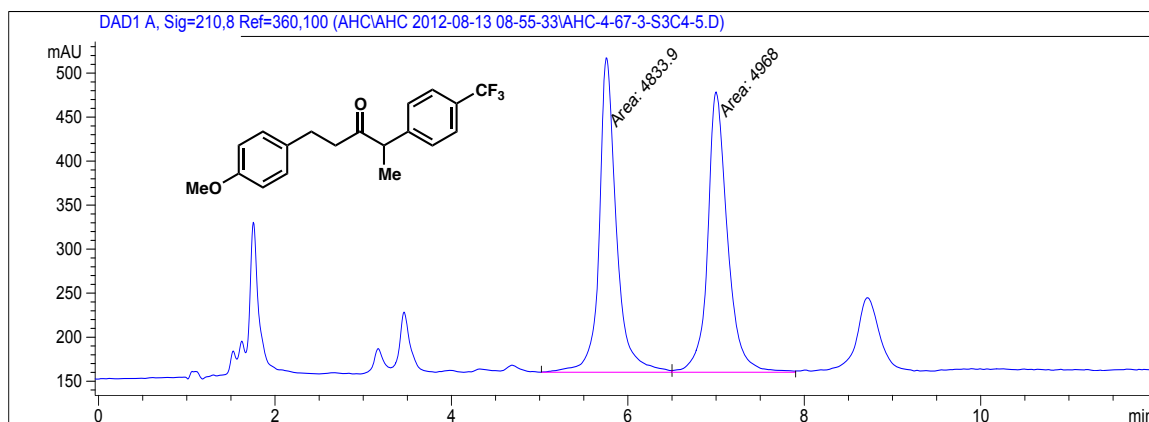


Peak #	RetTime [min]	Type	Width [min]	Area [mAU*s]	Height [mAU]	Area %
1	25.604	MM	0.6090	772.99146	21.15472	51.4642
2	27.518	MM	0.5962	729.00677	20.37799	48.5358

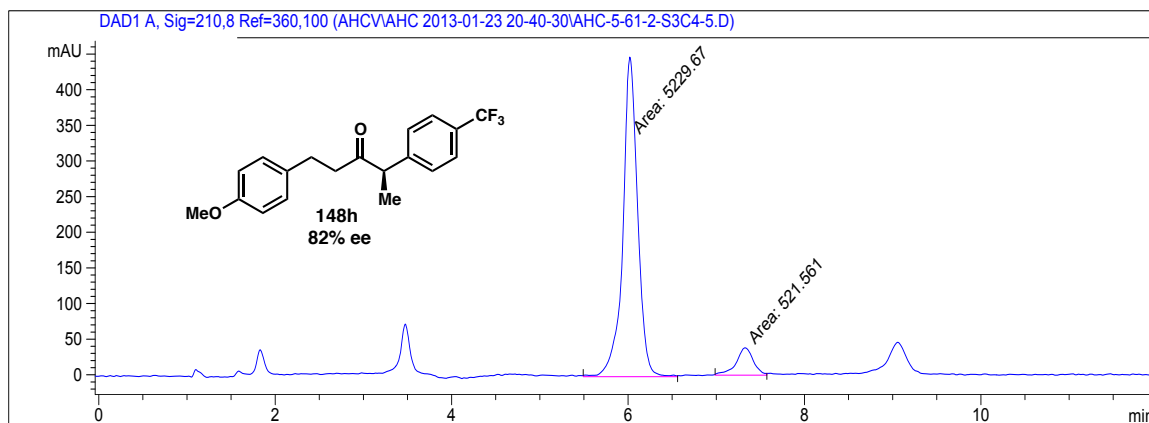
**148g (Table 3.6, entry 7): enantioenriched, 86% ee**



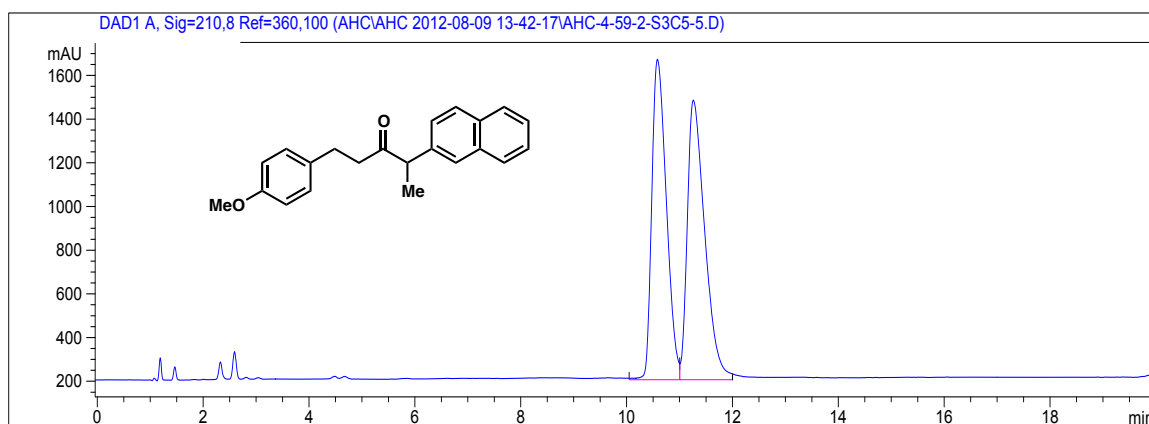
Peak #	RetTime [min]	Type	Width [min]	Area [mAU*s]	Height [mAU]	Area %
1	25.449	MM	0.6766	545.29791	13.43136	6.0381
2	27.030	MM	0.9105	8485.72363	155.33823	93.9619

**148h (Table 3.6, entry 8): racemic**

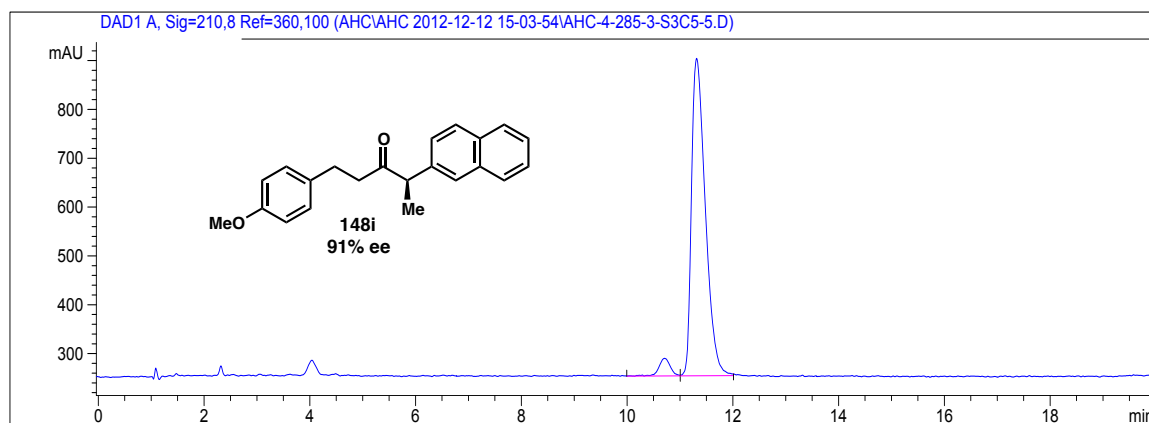
Peak #	RetTime [min]	Type	Width [min]	Area [mAU*s]	Height [mAU]	Area %
1	5.757	MM	0.2253	4833.89893	357.65167	49.3159
2	6.999	MM	0.2598	4967.99951	318.66217	50.6841

**148h (Table 3.6, entry 8): enantioenriched, 82% ee**

Peak #	RetTime [min]	Type	Width [min]	Area [mAU*s]	Height [mAU]	Area %
1	6.020	MM	0.1943	5229.66602	448.69507	90.9313
2	7.327	MM	0.2264	521.56061	38.39449	9.0687

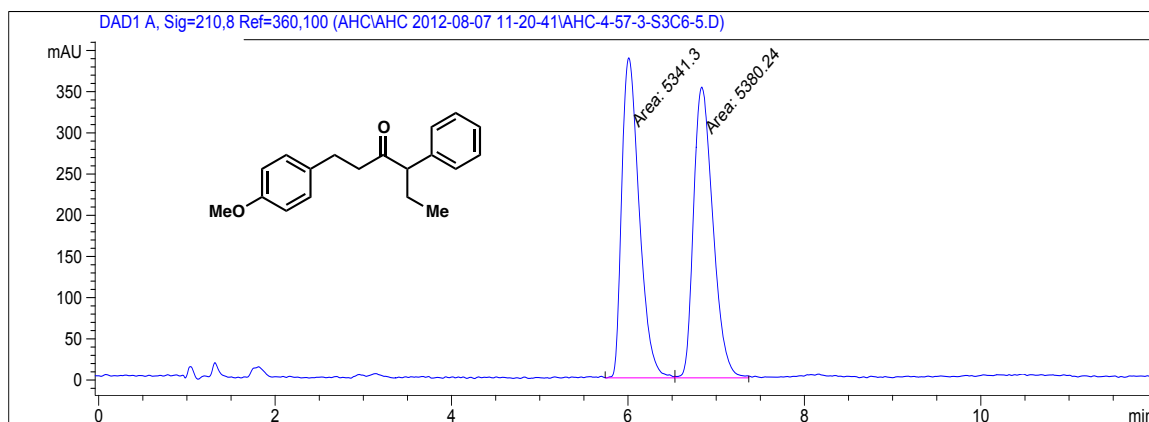
**148i (Table 3.6, entry 9): racemic**

Peak #	RetTime [min]	Type	Width [min]	Area [mAU*s]	Height [mAU]	Area %
1	10.584	VV	0.3032	2.80499e4	1465.87903	48.9009
2	11.263	VBA	0.3473	2.93108e4	1279.38000	51.0991

**148i (Table 3.6, entry 9): enantioenriched, 91% ee**

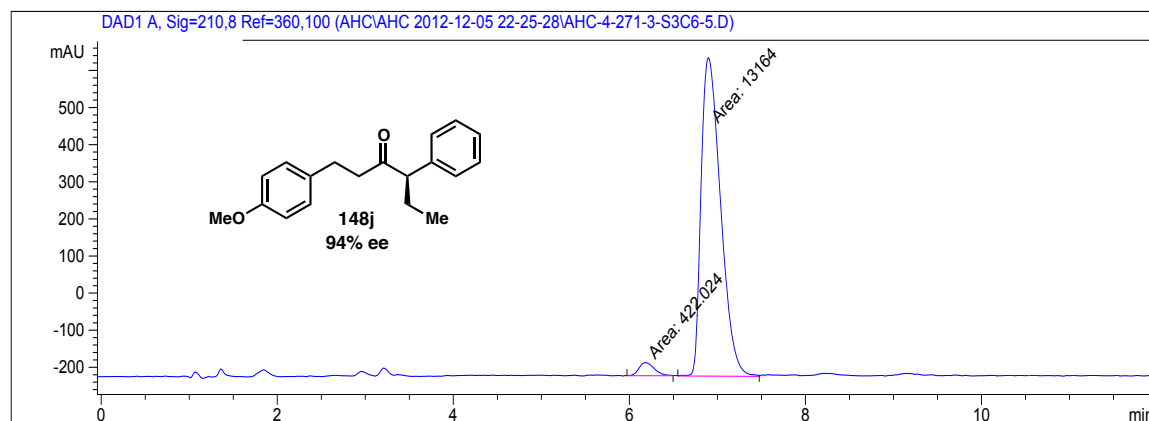
Peak #	RetTime [min]	Type	Width [min]	Area [mAU*s]	Height [mAU]	Area %
1	10.708	VV	0.2364	545.21796	36.05198	4.4227
2	11.316	VBA	0.2797	1.17825e4	649.47711	95.5773

**148j (Table 3.6, entry 10): racemic**

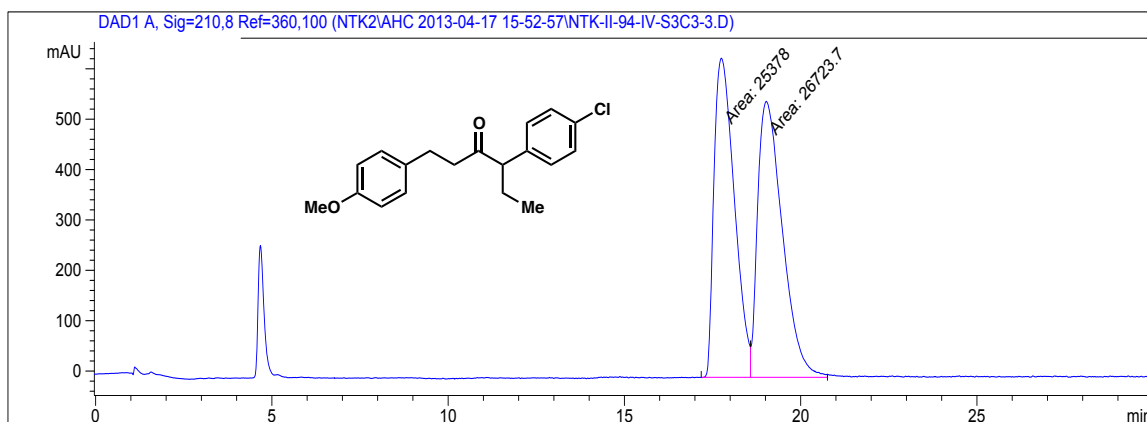


Peak #	RetTime [min]	Type	Width [min]	Area [mAU*s]	Height [mAU]	Area %
1	6.009	MM	0.2291	5341.29736	388.53415	49.8184
2	6.837	MM	0.2540	5380.24316	353.03430	50.1816

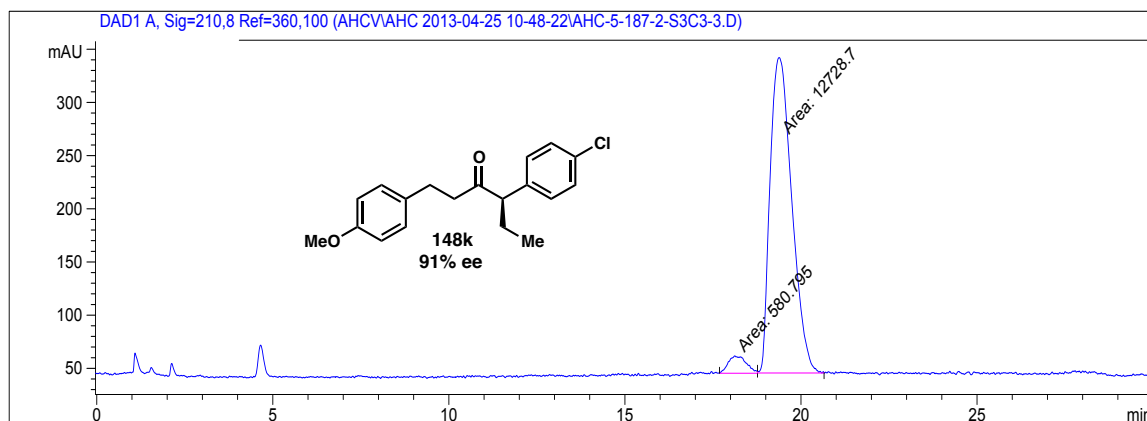
**148j (Table 3.6, entry 10): enantioenriched, 94% ee**



Peak #	RetTime [min]	Type	Width [min]	Area [mAU*s]	Height [mAU]	Area %
1	6.179	MM	0.1983	422.02435	35.47295	3.1063
2	6.898	MM	0.2556	1.31640e4	858.35632	96.8937

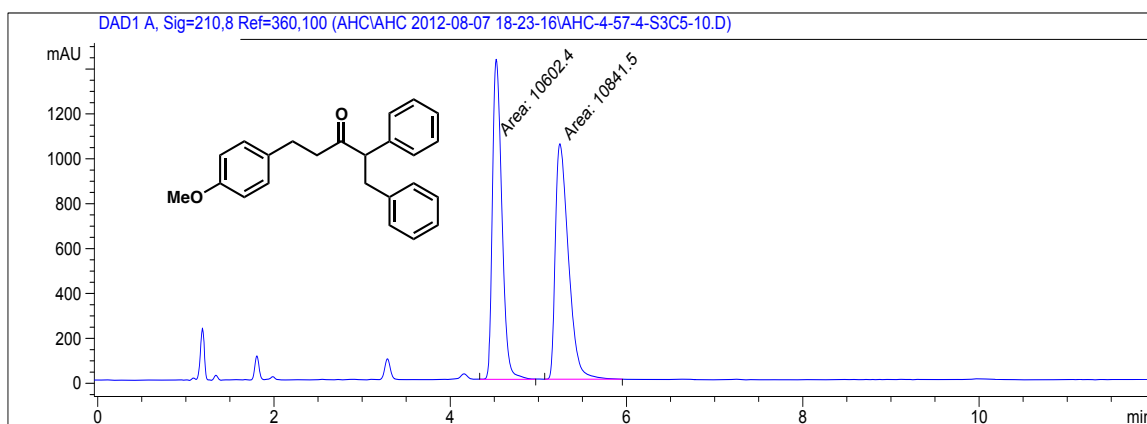
**148k (Table 3.6, entry 11): racemic**

Peak #	RetTime [min]	Type	Width [min]	Area [mAU*s]	Height [mAU]	Area %
1	17.749	MM	0.6673	2.53780e4	633.81763	48.7086
2	19.022	MM	0.8126	2.67237e4	548.09839	51.2914

**148k (Table 3.6, entry 11): enantioenriched, 91% ee**

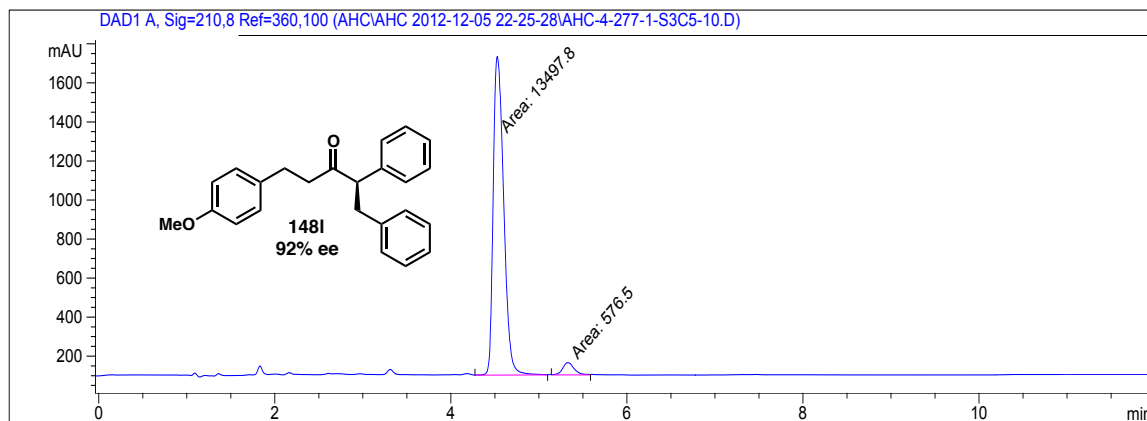
Peak #	RetTime [min]	Type	Width [min]	Area [mAU*s]	Height [mAU]	Area %
1	18.118	MM	0.5944	580.79498	16.28630	4.3637
2	19.381	MM	0.7154	1.27287e4	296.55020	95.6363

**148l (Table 3.6, entry 12): racemic**

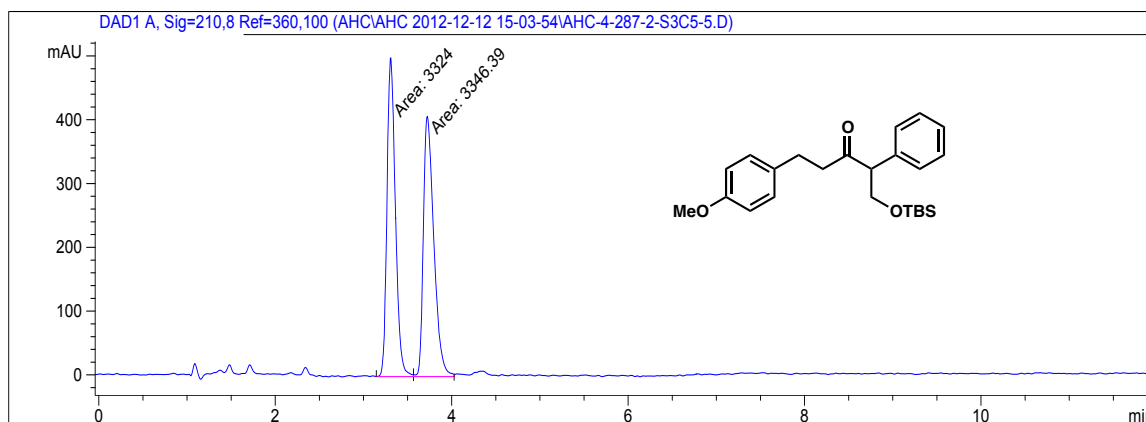


Peak #	RetTime [min]	Type	Width [min]	Area [mAU*s]	Height [mAU]	Area %
1	4.522	MM	0.1239	1.06024e4	1426.70251	49.4425
2	5.244	MM	0.1721	1.08415e4	1050.01685	50.5575

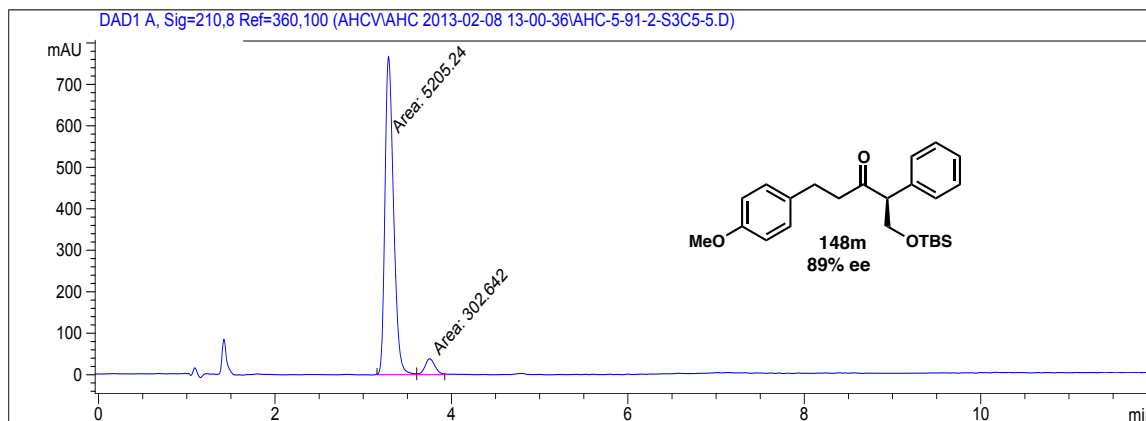
**148l (Table 3.6, entry 12): enantioenriched, 92% ee**



Peak #	RetTime [min]	Type	Width [min]	Area [mAU*s]	Height [mAU]	Area %
1	4.528	MM	0.1377	1.34978e4	1634.09204	95.9039
2	5.330	MM	0.1513	576.49988	63.49461	4.0961

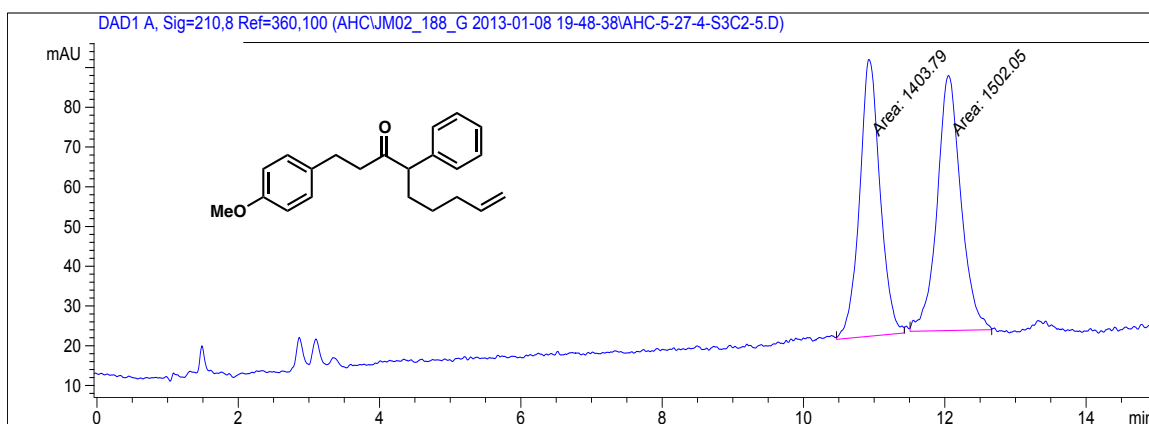
**148m (Table 3.6, entry 13): racemic**

Peak #	RetTime [min]	Type	Width [min]	Area [mAU*s]	Height [mAU]	Area %
1	3.308	MM	0.1105	3324.00073	501.56870	49.8322
2	3.723	MM	0.1365	3346.39185	408.55920	50.1678

**148m (Table 3.6, entry 13): enantioenriched, 89% ee**

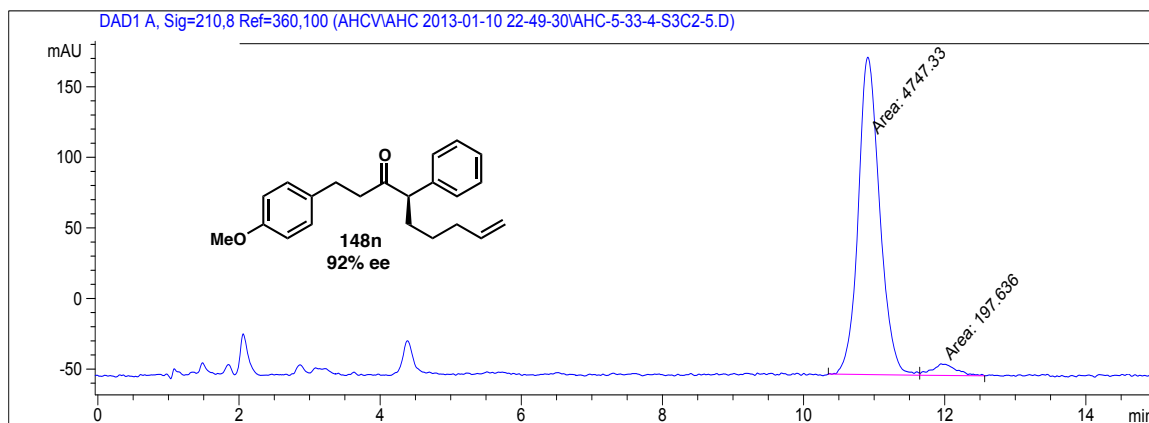
Peak #	RetTime [min]	Type	Width [min]	Area [mAU*s]	Height [mAU]	Area %
1	3.287	MM	0.1129	5205.23877	768.54687	94.5053
2	3.754	MM	0.1313	302.64224	38.40394	5.4947

**148n (Table 3.6, entry 14): racemic**



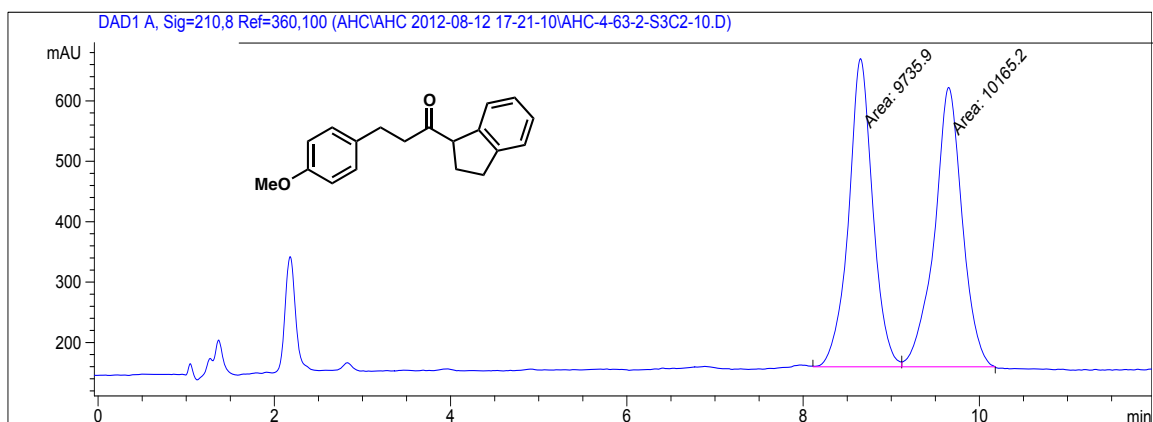
Peak #	RetTime [min]	Type	Width [min]	Area [mAU*s]	Height [mAU]	Area %
1	10.925	MM	0.3357	1403.79077	69.69751	48.3093
2	12.051	MM	0.3898	1502.04858	64.21613	51.6907

**148n (Table 3.6, entry 14): enantioenriched, 92% ee**



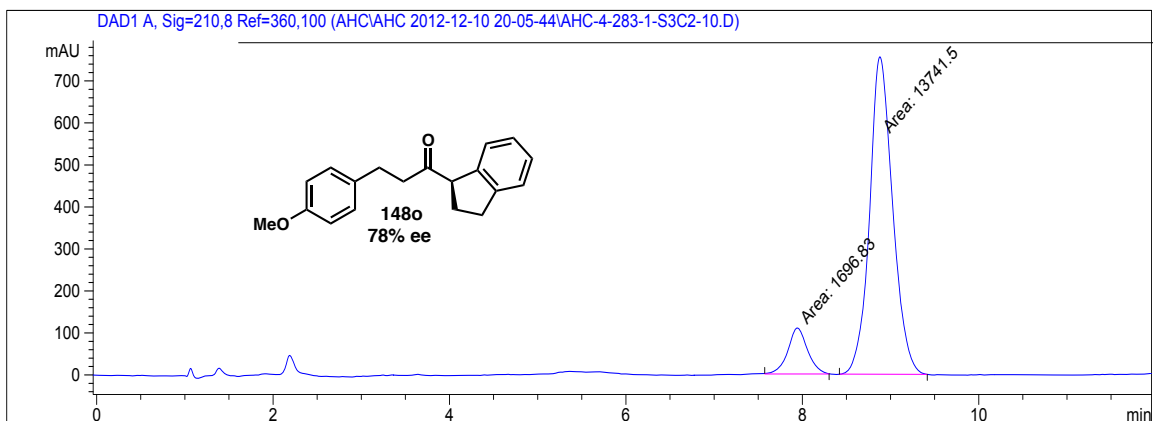
Peak #	RetTime [min]	Type	Width [min]	Area [mAU*s]	Height [mAU]	Area %
1	10.911	MM	0.3519	4747.33496	224.86562	96.0033
2	11.946	MM	0.4028	197.63620	8.17804	3.9967

**148o (Table 3.6, entry 15): racemic**

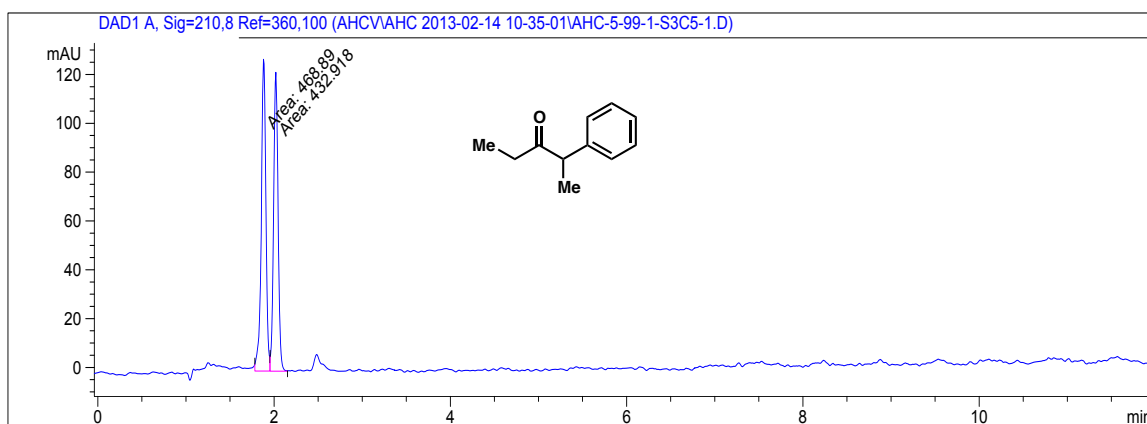


Peak #	RetTime [min]	Type	Width [min]	Area [mAU*s]	Height [mAU]	Area %
1	8.651	MM	0.3179	9735.89941	510.35568	48.9213
2	9.651	MM	0.3663	1.01652e4	462.52780	51.0787

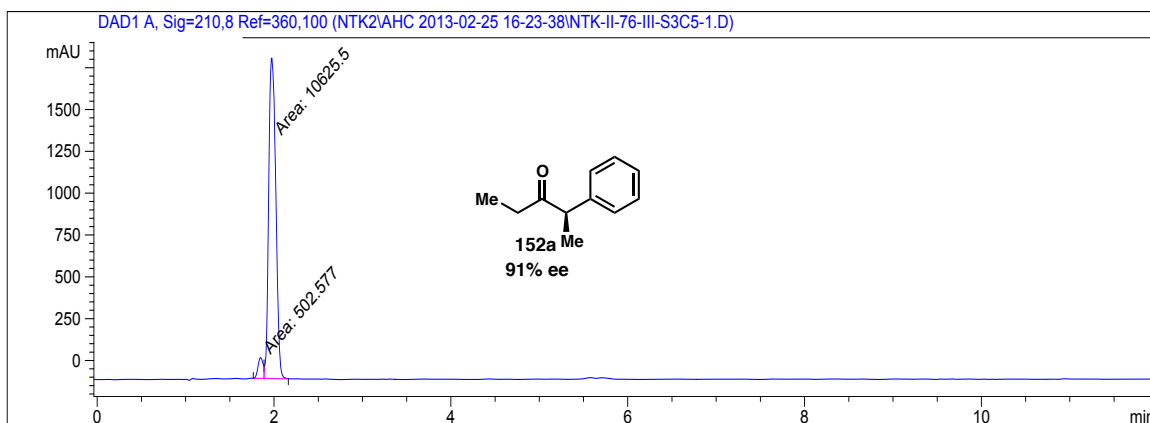
**148o (Table 3.6, entry 15): enantioenriched, 78% ee**



Peak #	RetTime [min]	Type	Width [min]	Area [mAU*s]	Height [mAU]	Area %
1	7.943	MM	0.2586	1696.82703	109.37256	10.9910
2	8.880	MM	0.3030	1.37415e4	755.81702	89.0090

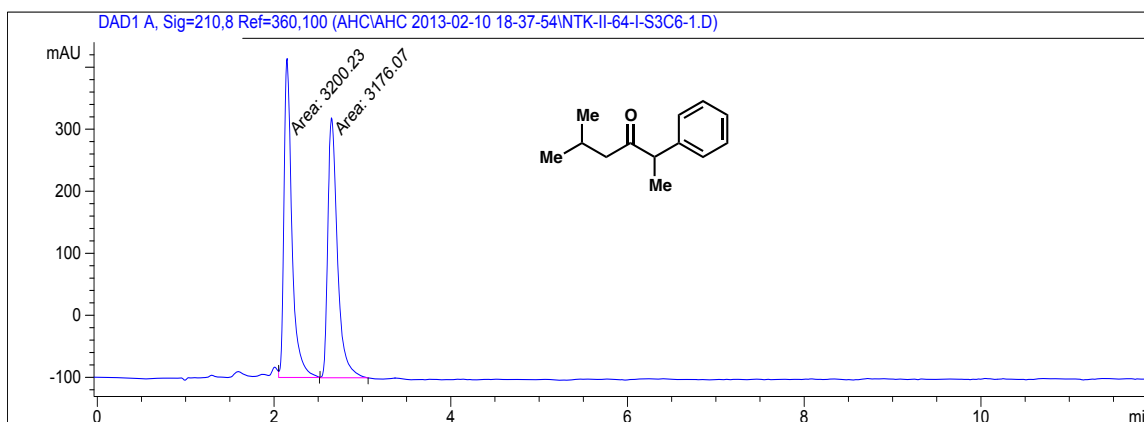
**152a (Table 3.7): racemic**

Peak #	RetTime [min]	Type	Width [min]	Area [mAU*s]	Height [mAU]	Area %
1	1.882	MM	0.0607	468.89008	128.69202	51.9944
2	2.020	MM	0.0587	432.91794	122.82136	48.0056

**152a (Table 3.7): enantioenriched, 89% ee**

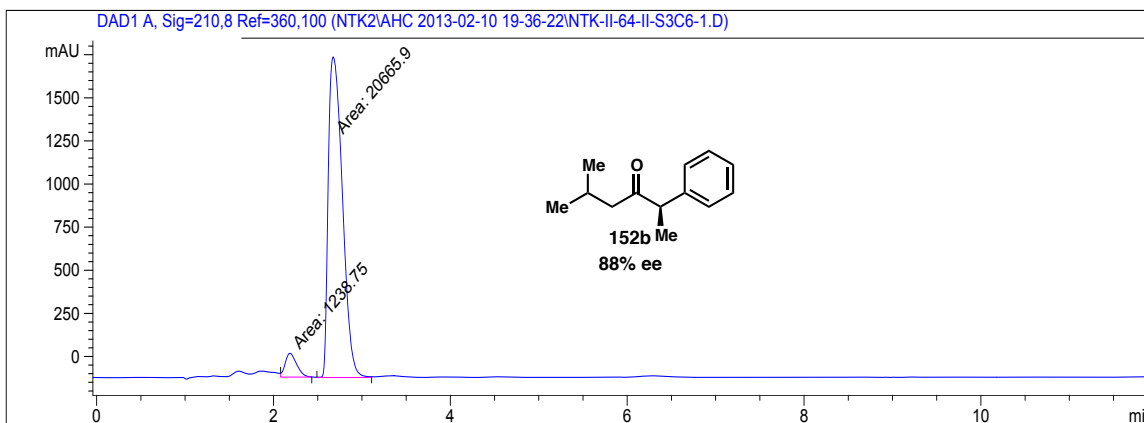
Peak #	RetTime [min]	Type	Width [min]	Area [mAU*s]	Height [mAU]	Area %
1	1.848	MM	0.0672	502.57666	124.59120	4.5163
2	1.973	MM	0.0923	1.06255e4	1918.92407	95.4837

**152b (Table 3.7): racemic**



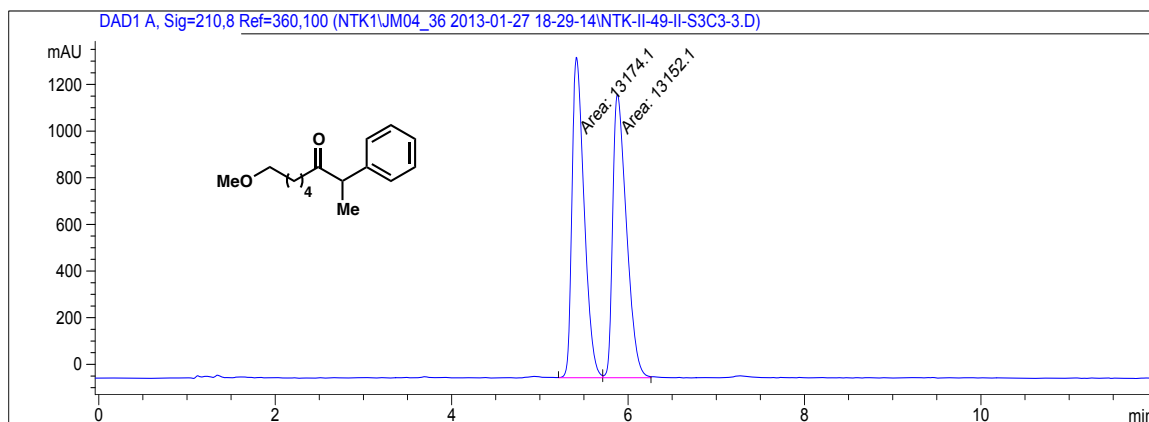
Peak #	RetTime [min]	Type	Width [min]	Area [mAU*s]	Height [mAU]	Area %
1	2.147	MM	0.1035	3200.22705	515.47467	50.1894
2	2.651	MM	0.1261	3176.07007	419.70117	49.8106

**152b (Table 3.7): enantioenriched, 88% ee**



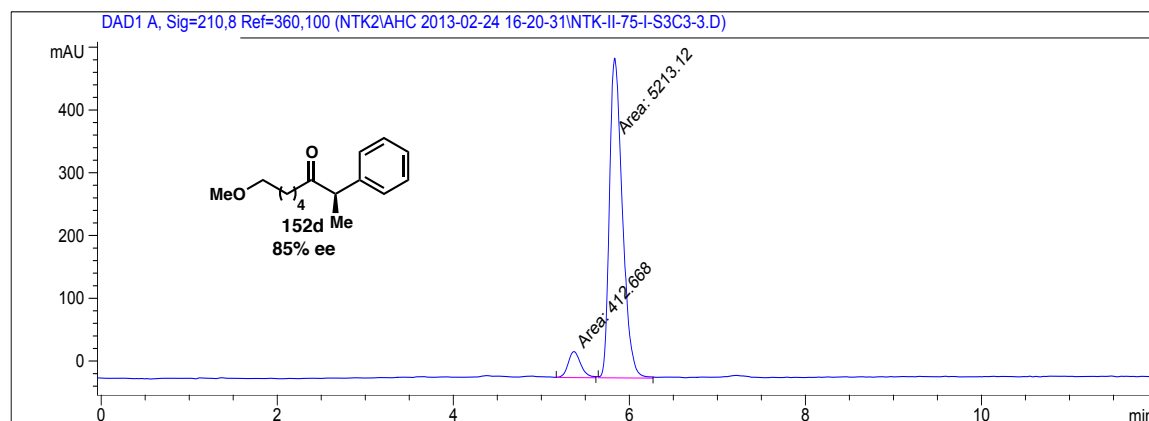
Peak #	RetTime [min]	Type	Width [min]	Area [mAU*s]	Height [mAU]	Area %
1	2.186	MM	0.1493	1238.74841	138.30533	5.6552
2	2.675	MM	0.1852	2.06659e4	1859.45630	94.3448

**152d (Table 3.7): racemic**

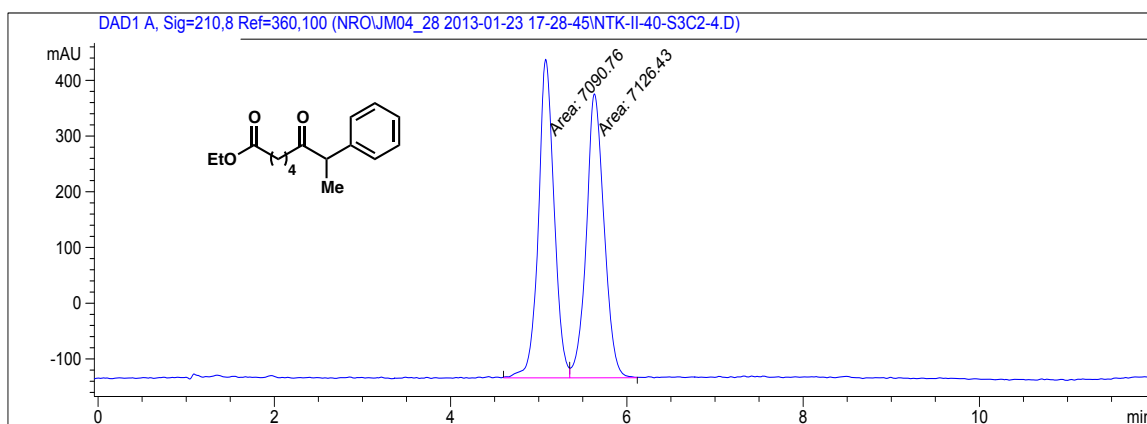


Peak #	RetTime [min]	Type	Width [min]	Area [mAU*s]	Height [mAU]	Area %
1	5.415	MM	0.1596	1.31741e4	1375.35034	50.0417
2	5.880	MM	0.1802	1.31521e4	1216.19214	49.9583

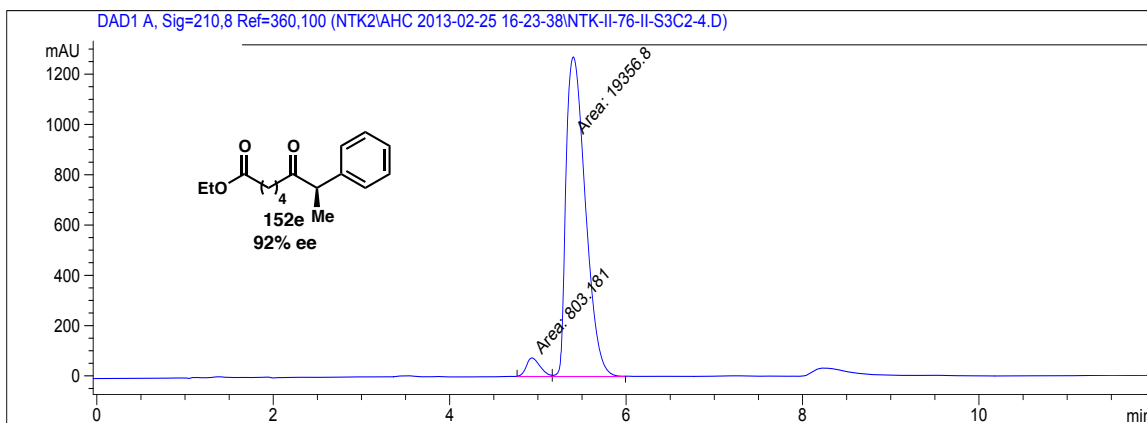
**152d (Table 3.7): enantioenriched, 85% ee**



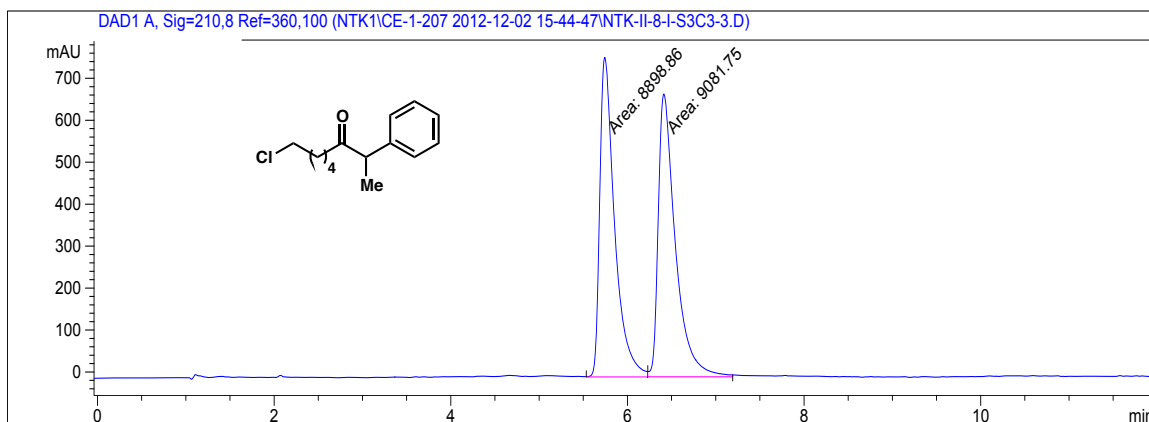
Peak #	RetTime [min]	Type	Width [min]	Area [mAU*s]	Height [mAU]	Area %
1	5.371	MM	0.1661	412.66797	41.40784	7.3353
2	5.833	MM	0.1703	5213.12402	510.12839	92.6647

**152e (Table 3.7): racemic**

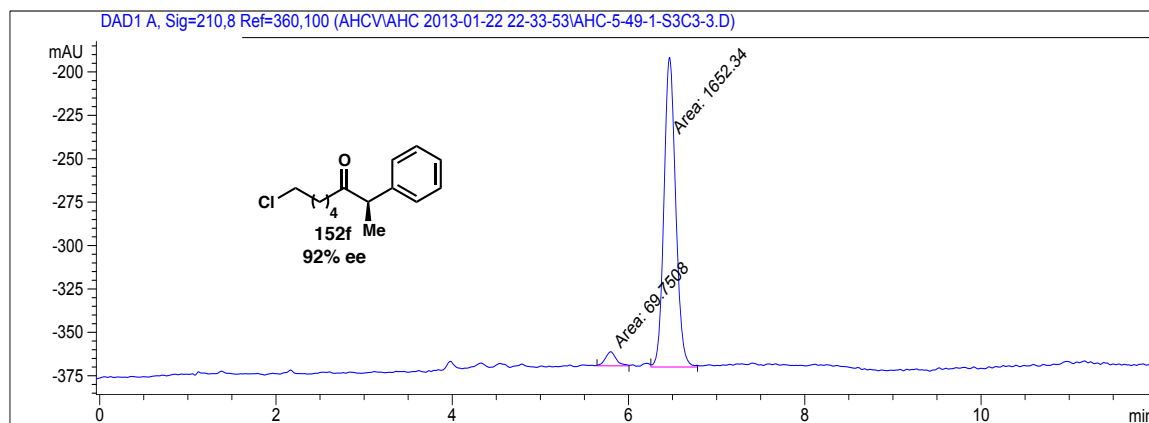
Peak #	RetTime [min]	Type	Width [min]	Area [mAU*s]	Height [mAU]	Area %
1	5.079	MM	0.2066	7090.76221	572.01874	49.8746
2	5.631	MM	0.2330	7126.43066	509.79788	50.1254

**152e (Table 3.7): enantioenriched, 92% ee**

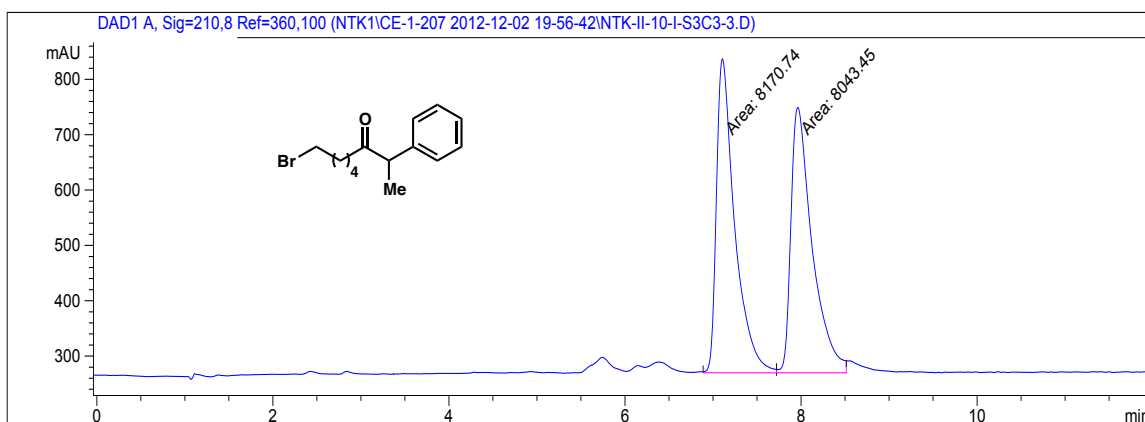
Peak #	RetTime [min]	Type	Width [min]	Area [mAU*s]	Height [mAU]	Area %
1	4.932	MM	0.1805	803.18146	74.16300	3.9840
2	5.401	MM	0.2538	1.93568e4	1271.19958	96.0160

**152f (Table 3.7): racemic**

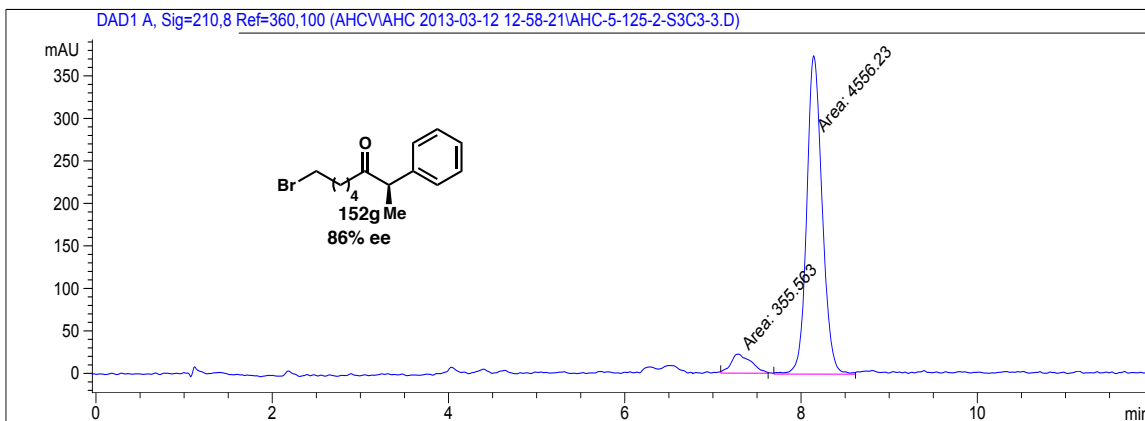
Peak #	RetTime [min]	Type	Width [min]	Area [mAU*s]	Height [mAU]	Area %
1	5.744	MM	0.1945	8898.86133	762.63263	49.4914
2	6.413	MM	0.2244	9081.74902	674.62744	50.5086

**152f (Table 3.7): enantioenriched, 92% ee**

Peak #	RetTime [min]	Type	Width [min]	Area [mAU*s]	Height [mAU]	Area %
1	5.798	MM	0.1418	69.75076	8.19656	4.0504
2	6.465	MM	0.1542	1652.33777	178.58195	95.9496

**152g (Table 3.7): racemic**

Peak #	RetTime [min]	Type	Width [min]	Area [mAU*s]	Height [mAU]	Area %
1	7.107	MM	0.2399	8170.74316	567.72528	50.3925
2	7.963	MM	0.2795	8043.45215	479.56842	49.6075

**152g (Table 3.7): enantioenriched, 86% ee**

Peak #	RetTime [min]	Type	Width [min]	Area [mAU*s]	Height [mAU]	Area %
1	7.295	MM	0.2652	355.56323	22.34372	7.2390
2	8.144	MM	0.2027	4556.22852	374.71005	92.7610

### 3.5 NOTES AND REFERENCES

- (1) Seminal reports: (a) Meyers, A. I.; Knaus, G.; Kamata, K. *J. Am. Chem. Soc.* **1974**, *95*, 268. (b) Evans, D. A.; Ennis, M. D.; Mathre, D. J. *J. Am. Chem. Soc.* **1982**, *104*, 1737. (c) Sonnet, P.; Heath, R. R. *J. Org. Chem.* **1980**, *45*, 3137 (d) Oppolzer, W.; Moretti, R.; Thomi, S. *Tetrahedron Lett.* **1989**, *30*, 5603. (e) Myers, A. G.; Yang, B. H.; Chen, H.; McKinsty, L.; Kopecky, D. J.; Gleason, J. L. *J. Am. Chem. Soc.* **1997**, *119*, 6496. (f) A recent example of a “traceless” auxiliary: Stivala, C. E.; Zakarian, A. *J. Am. Chem. Soc.* **2011**, *133*, 11936.
- (2) (a) Beeson, T. D.; Mastracchio, A.; Hong, J.-B.; Ashton, K.; MacMillan, D. W. C. *Science* **2007**, *316*, 582. (b) Nicewicz, D. A.; MacMillan, D. W. C. *Science* **2008**, *322*, 77. (c) Shih, H.-W.; Vander Wal, M. N.; Grange, R. L.; MacMillan, D. W. C. *J. Am. Chem. Soc.* **2010**, *132*, 13600. (d) Chen, J.; Ding, C.; Liu, W.; Hou, X.; Dai, L. *J. Am. Chem. Soc.* **2010**, *132*, 15493.
- (3) (a) Kim, H.; MacMillan, D. W. C. *J. Am. Chem. Soc.* **2008**, *130*, 398. (b) Dai, X.; Strotman, N. A.; Fu, G. C. *J. Am. Chem. Soc.* **2008**, *130*, 3302. (c) Skucas, E.; MacMillan, D. W. *J. Am. Chem. Soc.* **2012**, *134*, 9090.
- (4) (a) Alemán, J.; Cabrera, S.; Maerten, E.; Overgaard, J.; Jørgensen, K. A. *Angew. Chem., Int. Ed.* **2007**, *46*, 5520. (b) Allen, A. E.; MacMillan, D. W. *J. Am. Chem. Soc.* **2011**, *133*, 4260. (c) Bigot, A.; Williamson, A. E.; Gaunt, M. J. *J. Am. Chem. Soc.* **2011**, *133*, 13778. (d) Harvey, J. S.; Simonovich, S. P.; Jamison, C. R.; MacMillan, D. W. C. *J. Am. Chem. Soc.* **2011**, *133*, 13782.
- (5) Catalytic asymmetric synthesis of acyclic  $\alpha,\alpha$ -disubstituted ketones: (a) Trost, B. M.; Xu, J. *J. Am. Chem. Soc.* **2005**, *127*, 17180–17181. (b) Yan, X.-X.; Liang, C.-G.; Zhang, Y.; Hong, W.; Cao, B.-X.; Dai, L.-X.; Hou, X.-L. *Angew. Chem., Int. Ed.* **2005**, *44*, 6544–6546. (c) Zheng, W.-H.; Zheng, B.-H.; Zhang, Y.; Hou, X.-L. *J. Am. Chem. Soc.* **2007**, *129*, 7718. (d) Lundin, P. M.; Esquivias, J.; Fu, G. C. *Angew. Chem., Int. Ed.* **2009**, *48*, 154. (e) Lou, S.; Fu, G. C. *J. Am. Chem. Soc.* **2010**, *132*, 1264. (f) Lou, S.; Fu, G. C. *J. Am. Chem. Soc.* **2010**, *132*, 5010. (g) Liang, Y.; Fu, G. C. *J. Am. Chem. Soc.* **2014**, *136*, 5520.
- (6) The catalytic asymmetric synthesis of  $\alpha$ -quaternary ketones has been more extensively developed. Selected examples: (a) Åhman, J.; Wolfe, J. P.; Troutman, M. V.; Palucki, M.; Buchwald, S. L. *J. Am. Chem. Soc.* **1998**, *120*, 1918. (b) Hamada, T.; Chieffi, A.; Åhman, J.; Buchwald, S. L. *J. Am. Chem. Soc.* **2002**, *124*, 1261. (c) Behenna, D. C.; Stoltz, B. M. *J. Am. Chem. Soc.* **2004**, *126*, 15044. (d) Trost, B. M.; Xu, J. *J. Am. Chem. Soc.* **2005**, *127*, 2846. (e) Chen, G.; Kwong, F. Y.; Chan, H. O.; Yu, W.-Y.; Chan, A. S. C. *Chem. Commun.* **2006**, 1413. (f) Doyle, A. G.; Jacobsen, E. N. *Angew. Chem., Int. Ed.* **2007**, *46*, 3701–3705. (e) Liao, X.; Weng, Z.; Hartwig, J. F. *J. Am. Chem. Soc.* **2008**, *130*, 195. (g) Ge, S.;

- Hartwig, J. F. *J. Am. Chem. Soc.* **2011**, *133*, 16330. (h) Evans, P. A.; Oliver, S.; Chae, J. *J. Am. Chem. Soc.* **2012**, *134*, 19314.
- (7) Seminal examples of acyl cross coupling: (a) Milstein, D.; Stille, J. K. *J. Am. Chem. Soc.* **1978**, *100*, 3636. (b) Negishi, E.-i.; Bagheri, V.; Chatterjee, S.; Luo, F.-T.; Miller, J. A.; Stoll, A. T. *Tetrahedron Lett.* **1983**, *24*, 5181. (c) Haddach, M.; McCarthy, J. R. *Tetrahedron Lett.* **1999**, *40*, 3109. For a review, see: (d) Dieter, R. K. *Tetrahedron* **1999**, *55*, 4177.
- (8) For reviews on reductive cross-coupling: Everson, D. A.; Weix, D. J. *J. Org. Chem.* **2014**, *79*, 4793; Knappke, C. E. I.; Grupe, S.; Gärtner, D.; Corpet, M.; Gosmini, C.; Jacobi von Wangelin, A. *Chem. Eur. J.* **2014**, *20*, 6828; Moragas, T.; Correa, A.; Martin, R. *Chem. Eur. J.* **2014**, *79*, 8242.
- (9) Co-catalyzed reductive coupling reactions have also been reported: (a) Amatore, M.; Gosmini, C. *Angew. Chem., Int. Ed.* **2008**, *47*, 2089. (b) Amatore, M.; Gosmini, C. *Chem. Eur. J.* **2010**, *16*, 5848. For a related Co-catalyzed reaction proposed to proceed by *in situ* formation of a Grignard reagent, see: (c) Czaplik, W.; Mayer, M.; Jacobi von Wangelin, A. *Synlett* **2009**, 2931.
- (10) Reviews on alkyl halides in cross-couplings: (a) Netherton, M. R.; Fu, G. C. *Adv. Synth. & Catal.* **2004**, *346*, 1525. (b) Frisch, A. C.; Beller, M. *Angew. Chem., Int. Ed.* **2005**, *44*, 674. (c) Rudolph, A.; Lautens, M. *Angew. Chem., Int. Ed.* **2009**, *48*, 2656.
- (11) Semmelhack, M. F.; Helquist, P. M.; Jones, L. D. *J. Am. Chem. Soc.* **1971**, *93*, 5908.
- (12) (a) Everson, D. A.; Shrestha, R.; Weix, D. J. *J. Am. Chem. Soc.* **2010**, *132*, 920. (b) Everson, D. A.; Jones, B. A.; Weix, D. J. *J. Am. Chem. Soc.* **2012**, *134*, 6146. (c) Biswas, S.; Weix, D. J. *J. Am. Chem. Soc.* **2013**, *135*, 16192.
- (13) (a) Yu, X.; Yang, T.; Wang, S.; Xu, H.; Gong, H. *Org. Lett.* **2011**, *13*, 2138. (b) Wang, S.; Qian, Q.; Gong, H. *Org. Lett.* **2012**, *14*, 3352. (c) Xu, H.; Zhao, C.; Qian, Q.; Deng, W.; Gong, H. *Chem. Sci.* **2013**, *4*, 4022.
- (14) Metal-catalyzed electrochemical synthesis of ketones: (a) Habeeb, J. J.; Tuck, D. G. *J. Chem. Soc., Chem. Commun.* **1976**, 696. (b) Shono, T.; Nishiguchi, I.; Ohmizu, H. *Chem. Lett.* **1977**, *6*, 1021. (c) Dincan, E.; Sibille, S.; Périchon, J.; Moingeon, M.-O.; Chaussard, J. *Tetrahedron Lett.* **1986**, *27*, 4175. (d) Marzouk, H.; Rollin, Y.; Folest, J. C.; Nédélec, J. Y.; Périchon, J. *J. Organomet. Chem.* **1989**, *369*, 47. (e) Amatore, C.; Jutand, A.; Périchon, J.; Rollin, Y. *Monatsh. Chem.* **2000**, *131*, 1293.

- (15) (a) Wotal, A. C.; Weix, D. J. *Org. Lett.* **2012**, *14*, 1476. (b) Wotal, A. C.; Ribson, R. D.; Weix, D. J. *Organometallics* **2014**, *33*, 5874.
- (16) (a) Wu, F.; Lu, W.; Qian, Q.; Ren, Q.; Gong, H. *Org. Lett.* **2012**, *14*, 3044. (b) Yin, H.; Zhao, C.; You, H.; Lin, K.; Gong, H. *Chem. Commun.* **2012**, *48*, 7034. (c) Zhao, C.; Jia, X.; Wang, X.; Gong, H. *J. Am. Chem. Soc.* **2014**, *136*, 17645.
- (17) Amatore, C.; Jutand, A. *Organometallics* **1988**, *7*, 2203.
- (18) (a) Anderson, T. J.; Jones, G. D.; Vivic, D. A. *J. Am. Chem. Soc.* **2004**, *126*, 8100. (b) Fischer, C.; Fu, G. C. *J. Am. Chem. Soc.* **2005**, *127*, 4594. (c) Arp, F. O.; Fu, G. C. *J. Am. Chem. Soc.* **2005**, *127*, 10482. (d) Jones, G. D.; Martin, J. L.; McFarland, C.; Allen, O. R.; Hall, R. E.; Haley, A. D.; Brandon, R. J.; Konovalova, T.; Desrochers, P. J.; Pulay, P.; Vivic, D. A. *J. Am. Chem. Soc.* **2006**, *128*, 13175. (e) Lin, X.; Sun, J.; Xi, Y.; Lin, D. *Organometallics* **2011**, *30*, 3284.
- (19) For selected examples see refs 5d–g.
- (20) Gutierrez, O.; Tellis, J. C.; Primer, D. N.; Molander, G. A.; Kozlowski, M. C. *J. Am. Chem. Soc.* **2015**, *137*, 4896.
- (21) Cherney, A. H.; Kadunce, N. T.; Reisman, S. E. *J. Am. Chem. Soc.* **2013**, *135*, 7442.
- (22) (a) Cloke, J. B.; Pilgrim, F. J. *J. Am. Chem. Soc.* **1939**, *61*, 2667. (b) Bhar, S.; Ranu, B. C. *J. Org. Chem.* **1995**, *60*, 745
- (23) For mechanistic studies on homodimer formation see: (a) Yamamoto, T.; Kohara, T.; Yamamoto, A. *Bull. Chem. Soc. Jpn.* **1981**, *54*, 2010. (b) Yamamoto, T.; Kohara, T.; Osakada, K.; Yamamoto, A. *Bull. Chem. Soc. Jpn.* **1983**, *56*, 2147.
- (24) Gong and coworkers concurrently published the reductive cross-coupling of in situ-generated mixed anhydrides and alkyl halides: Yin, H.; Zhao, C.; You, H.; Lin, K.; Gong, H. *Chem. Commun.* **2012**, *48*, 7034.
- (25) Prinsell, M. R.; Everson, D. A.; Weix, D. J. *Chem. Commun.* **2010**, *46*, 5743.
- (26) The absolute stereochemistry was assigned by comparison of the optical rotation to literature reported data. (a) Rodríguez, C.; de Gonzalo, G.; Fraaije, M. W.; Gotor, V. *Tetrahedron: Asymmetry* **2007**, *18*, 1338. The assignment of all other compounds was made by analogy.

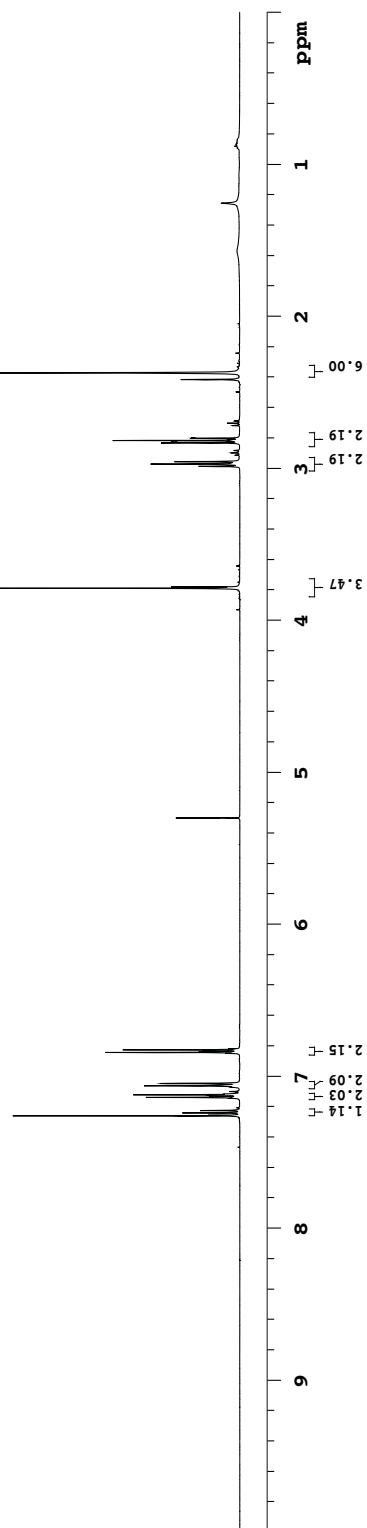
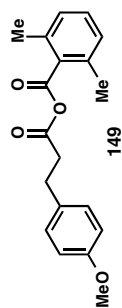
- (27) Formation of organomanganese reagents: (a) Boucley, C.; Cahiez, G.; Carini, S.; Cerè, V.; Comes-Franchini, M.; Knochel, P.; Pollicino, S.; Ricci, A. *J. Organomet. Chem.* **2001**, 624, 223. (b) Cahiez, G.; Duplais, C.; Buendia, J. *Chem. Rev.* **2009**, 109, 1434. (c) Peng, Z.; Knochel, P. *Org. Lett.* **2011**, 13, 3198.
- (28) Choi, J.; Fu, G. C. *J. Am. Chem. Soc.* **2012**, 134, 9102.
- (29) Nahm, S.; Weinreb, S. M. *Tetrahedron Lett.* **1981**, 22, 3815.
- (30) Still, W. C.; Kahn, M.; Mitra, A. *J. Org. Chem.* **1978**, 43, 2923.

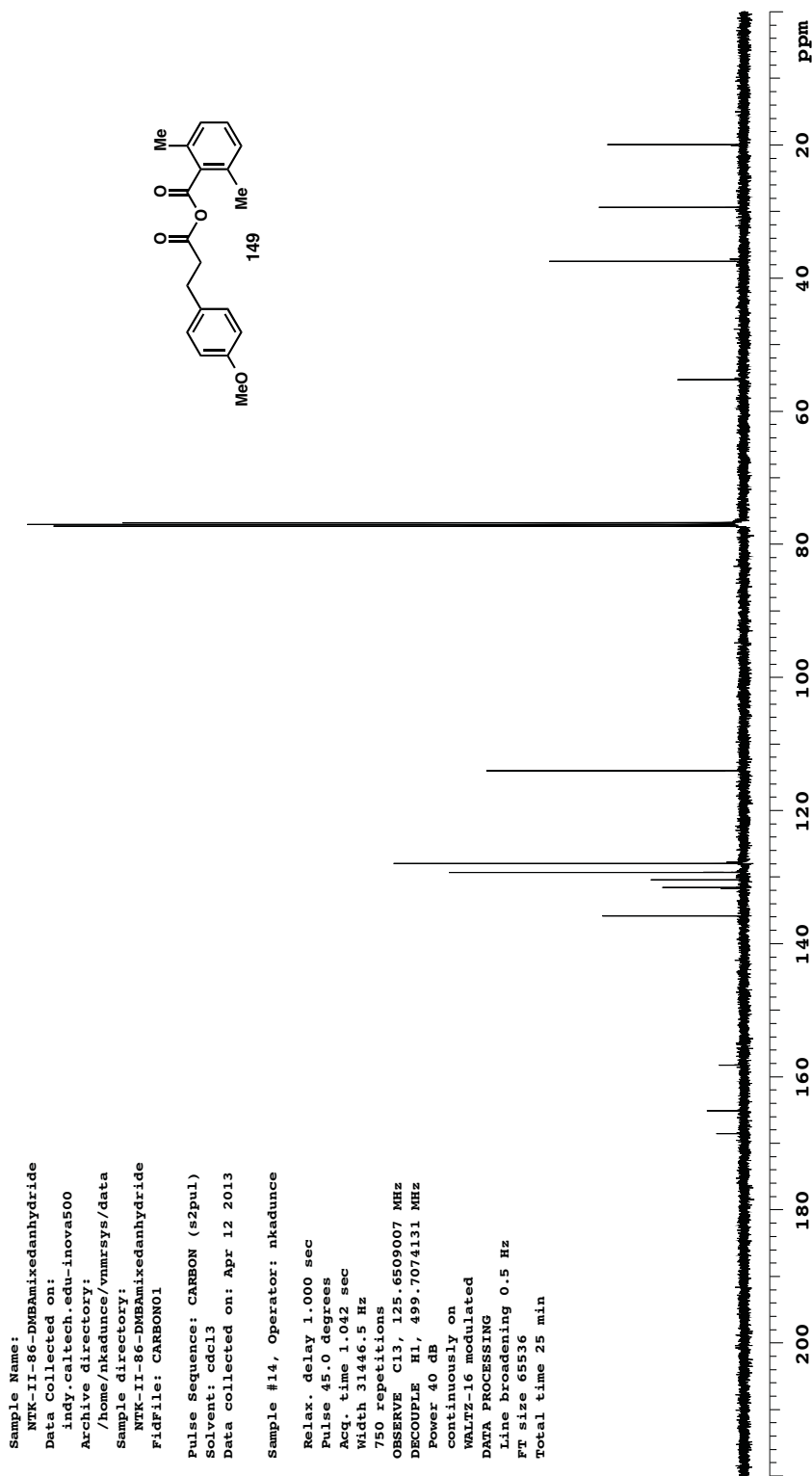
## **APPENDIX 2**

*Spectra Relevant to Chapter 3:*

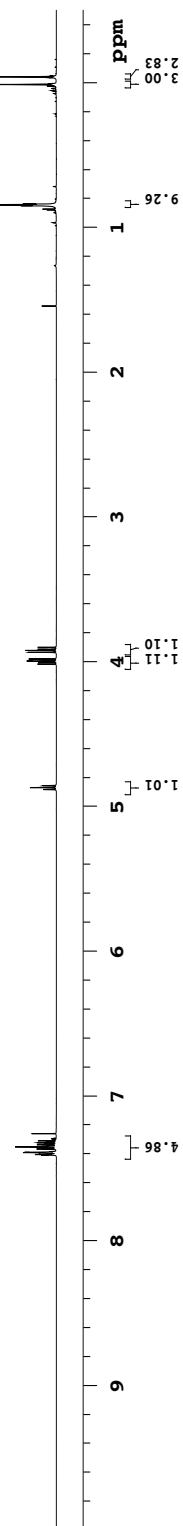
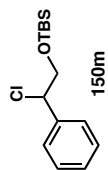
*Catalytic Asymmetric Reductive Acyl Cross-Coupling: Synthesis of  
Enantioenriched Acyclic  $\alpha,\alpha$ -Disubstituted Ketones*

Sample Name:  
 NTK-II-86-DMBAmixedanhydride  
 Data Collected on:  
 indy.caltech.edu-inova500  
 Archive directory:  
 /home/nkadunce/vnmrSYS/data  
 Sample directory:  
 NTK-II-86-DMBAmixedanhydride  
 FidFile: PROTON01  
 Pulse Sequence: PROTON (s2pul)  
 Solvent: cdcl3  
 Data collected on: Apr 12 2013  
 Sample #14, Operator: nkadunce  
 Relax. delay 1.000 sec  
 Pulse 45.0 degrees  
 Acq. time 3.000 sec  
 Width 8000.0 Hz  
 32 repetitions  
 OBSERVE H1, 499.7049145 MHz  
 DATA PROCESSING  
 Line broadening 0.2 Hz  
 FT size 65536  
 Total time 2 min 8 sec

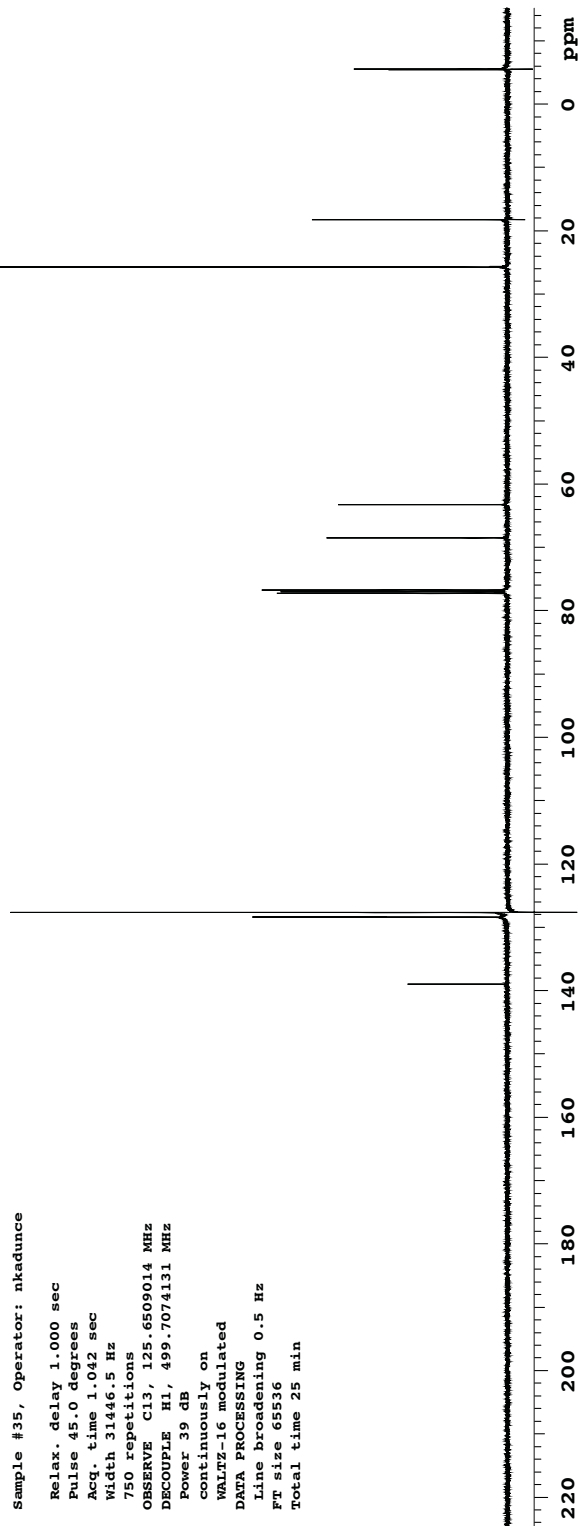
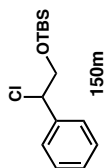




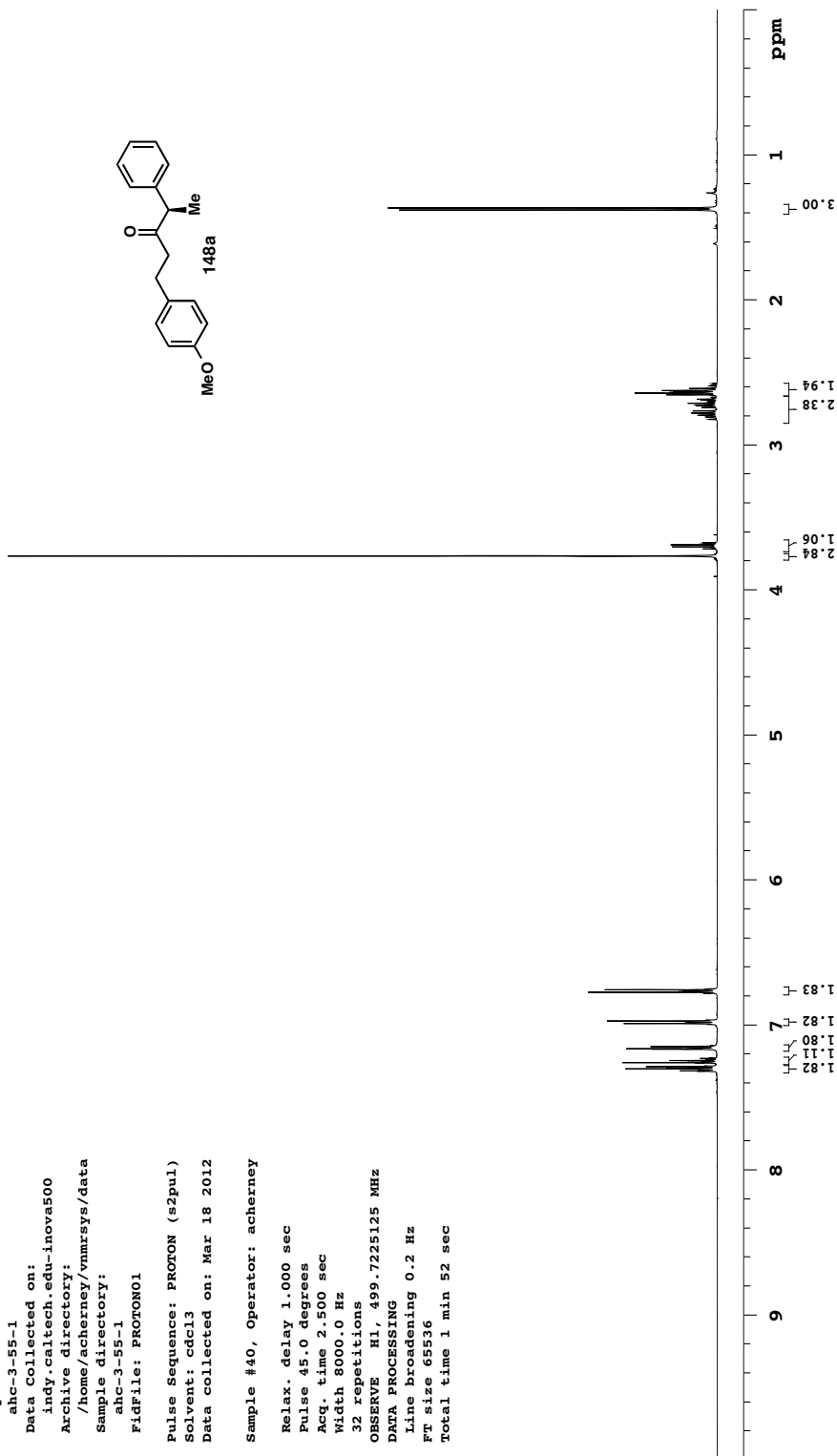
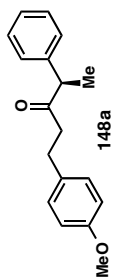
Sample Name:  
 NTK-I-289-II  
 Data Collected on:  
 indy.caltech.edu-inova500  
 Archive directory:  
 /home/nkadunce/vnmrSYS/data  
 Sample directory:  
 NTK-I-289-II  
 FidFile: PROTON01  
 Pulse Sequence: PROTON (s2pul)  
 Solvent: cdcl3  
 Data collected on: Feb 26 2013  
 Sample #35, Operator: nkadunce  
 Relax. delay 1.000 sec  
 Pulse 45.0 degrees  
 Acq. time 3.000 sec  
 Width 8000.0 Hz  
 32 repetitions  
 OBSERVE H1, 499.7049145 MHz  
 DATA PROCESSING  
 Line broadening 0.2 Hz  
 FT size 65536  
 Total time 2 min 8 sec

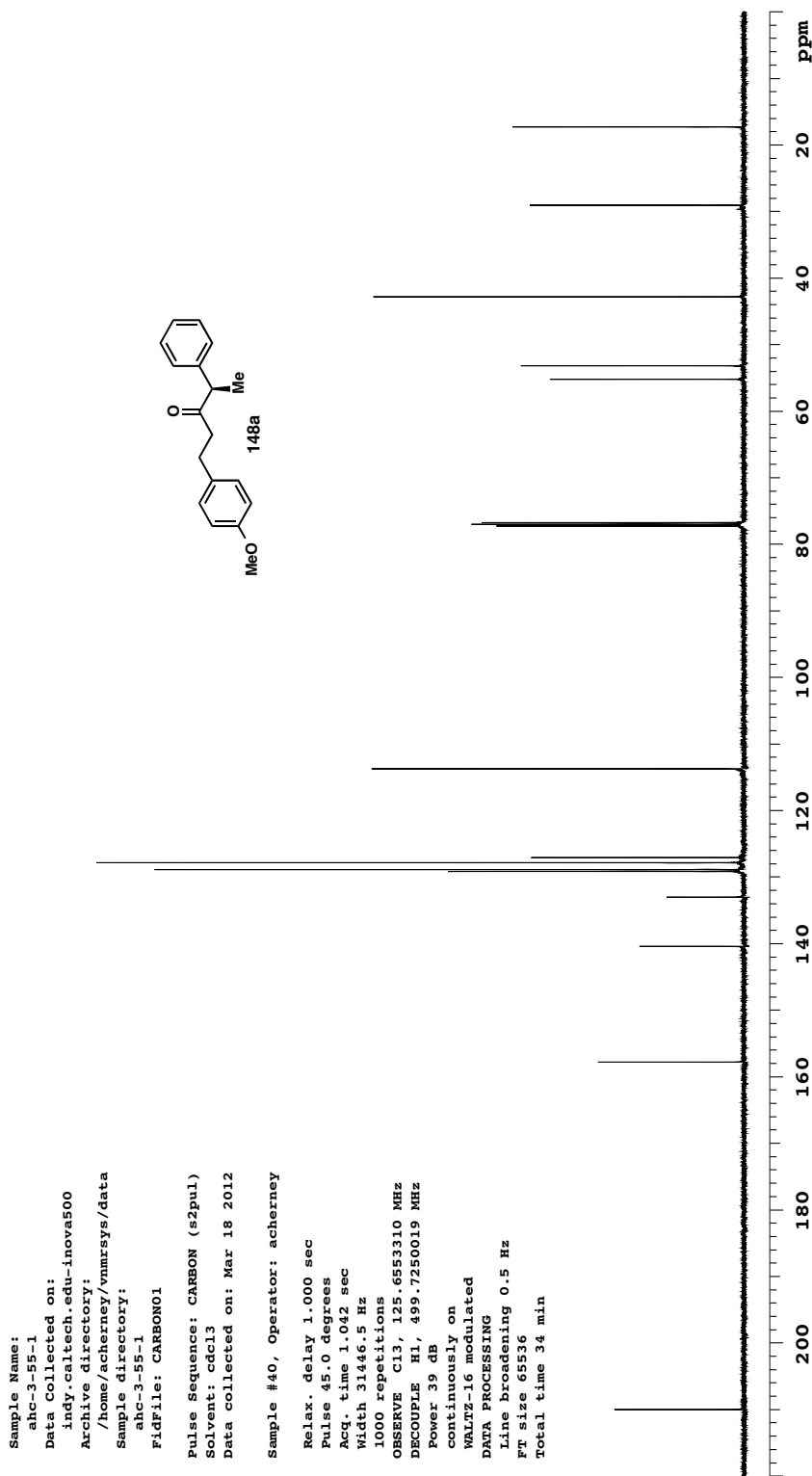


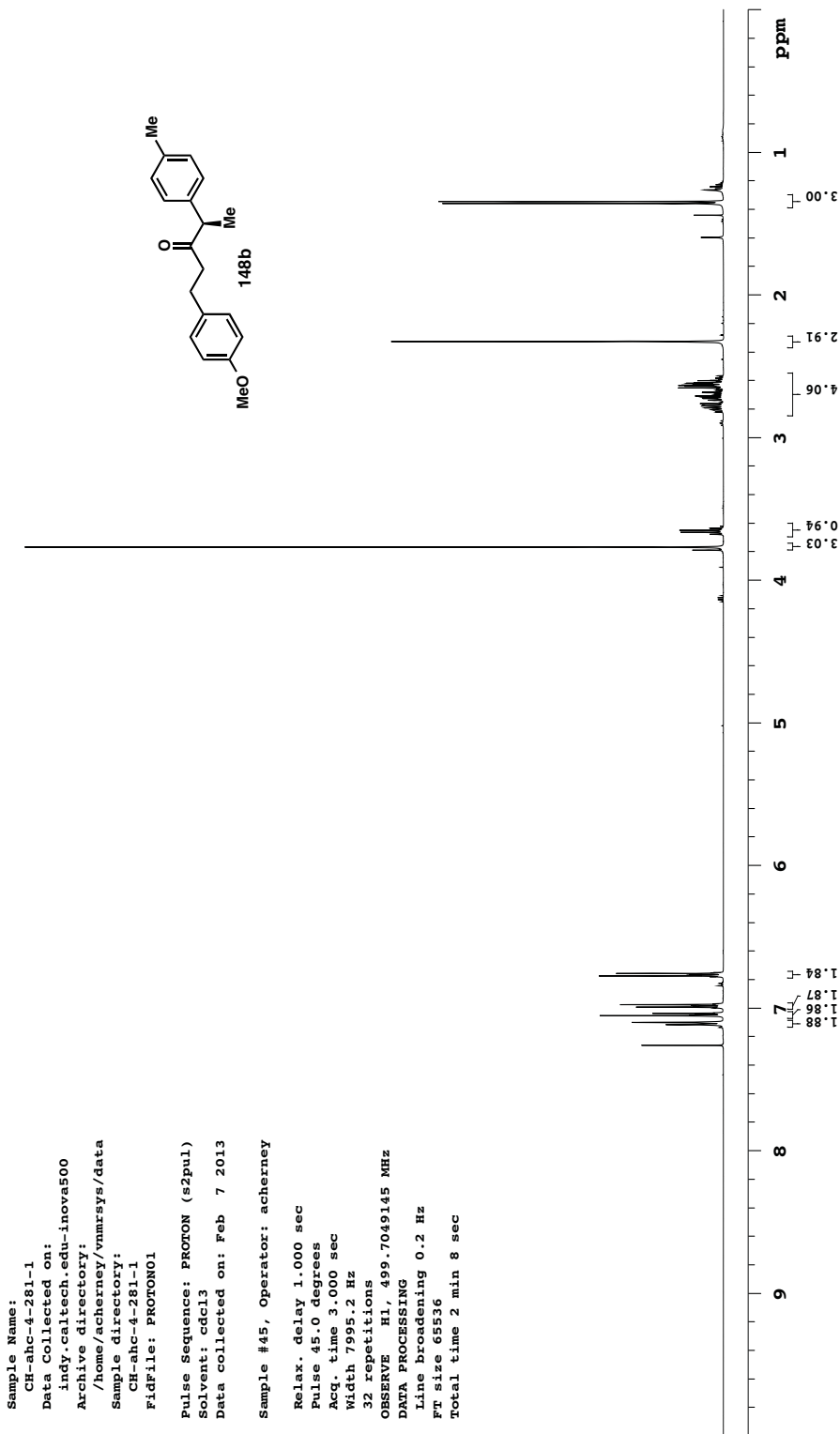
Sample Name:  
 NTK-I-289-II  
 Data Collected on:  
 indy.caltech.edu-inova500  
 Archive directory:  
 /home/nkadance/vnmrSYS/data  
 Sample directory:  
 NTK-I-289-II  
 FidFile: CARBONO1  
 Pulse Sequence: CARBON (s2pul)  
 Solvent: cdcl3  
 Data collected on: Feb 26 2013  
 Sample #35, Operator: nkadance  
 Relax. delay 1.000 sec  
 Pulse 45.0 degrees  
 Acq. time 1.042 sec  
 Width 31446.5 Hz  
 750 repetitions  
 OBSERVE C13, 125.6509014 MHz  
 DECOUPLE H1, 499.7074131 MHz  
 Power 39 dB  
 continuously on  
 WALTZ-16 modulated  
 DATA PROCESSING  
 Line broadening 0.5 Hz  
 F1 size 65536  
 Total time 25 min

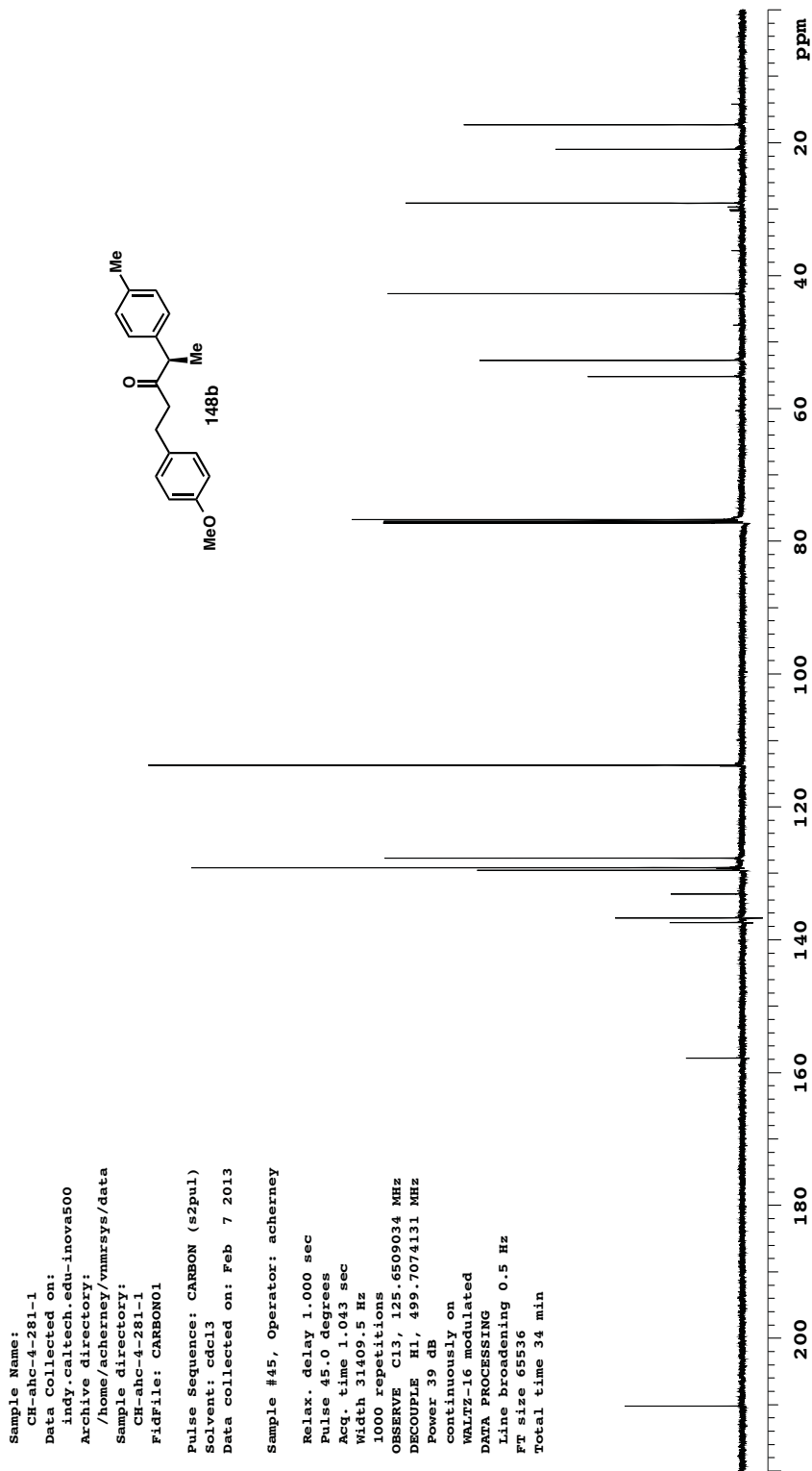


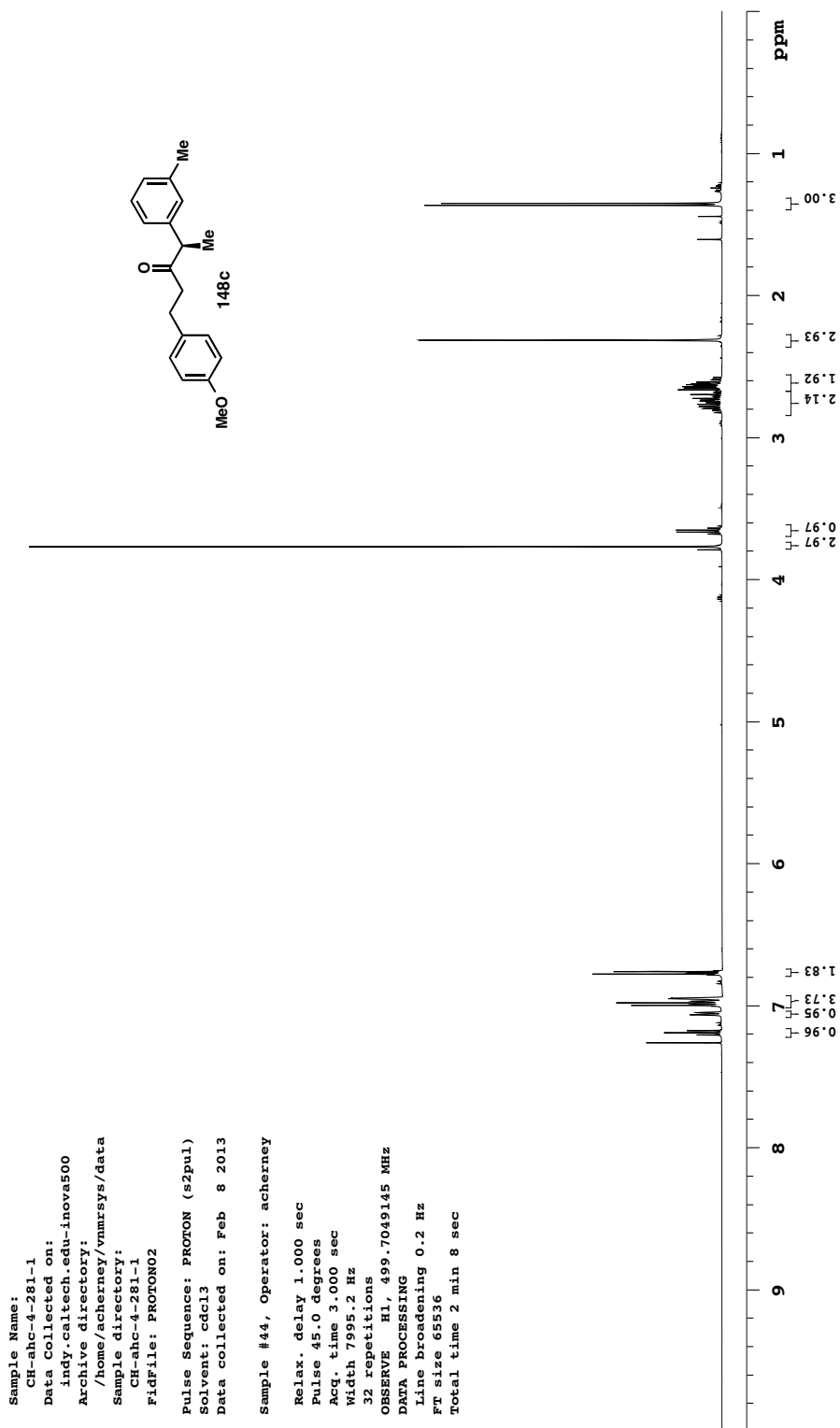
Sample Name:  
 ahc-3-55-1  
 Data Collected on:  
 indy.caltech.edu-inova500  
 Archive directory:  
 /home/acherney/vnmrSYS/data  
 Sample directory:  
 ahc-3-55-1  
 FidFile: PROTON01  
 Pulse Sequence: PROTON (s2pul)  
 Solvent: cdcl3  
 Data collected on: Mar 18 2012  
 Sample #40, Operator: acherney  
 Relax. delay 1.000 sec  
 Pulse 45.0 degrees  
 Acq. time 2.500 sec  
 Width 8000.0 Hz  
 32 repetitions  
 OBSERVE H1, 499.725125 MHz  
 DATA PROCESSING  
 Line broadening 0.2 Hz  
 FT size 65536  
 Total time 1 min 52 sec





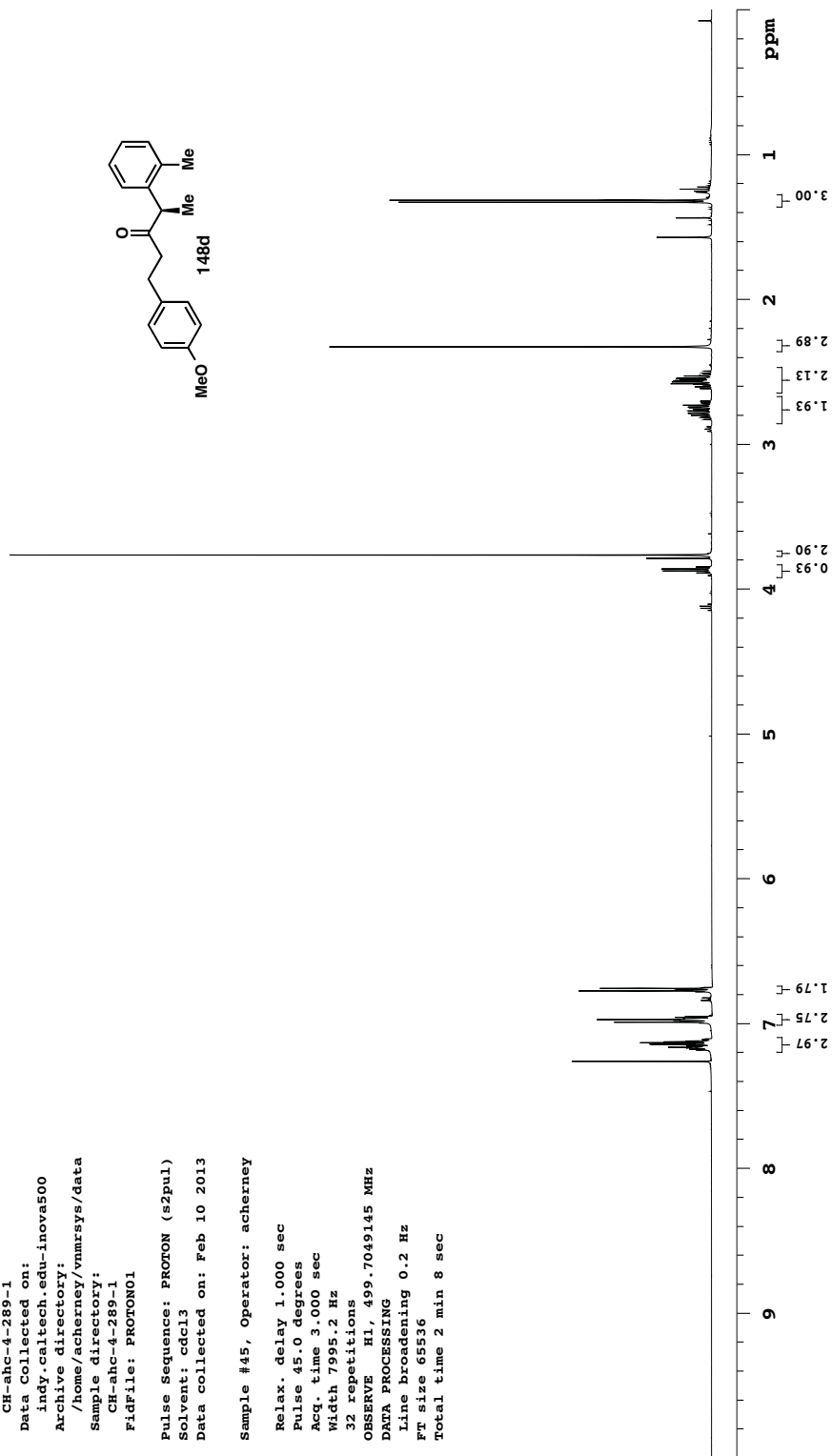
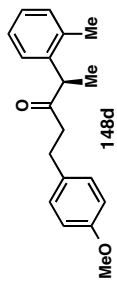


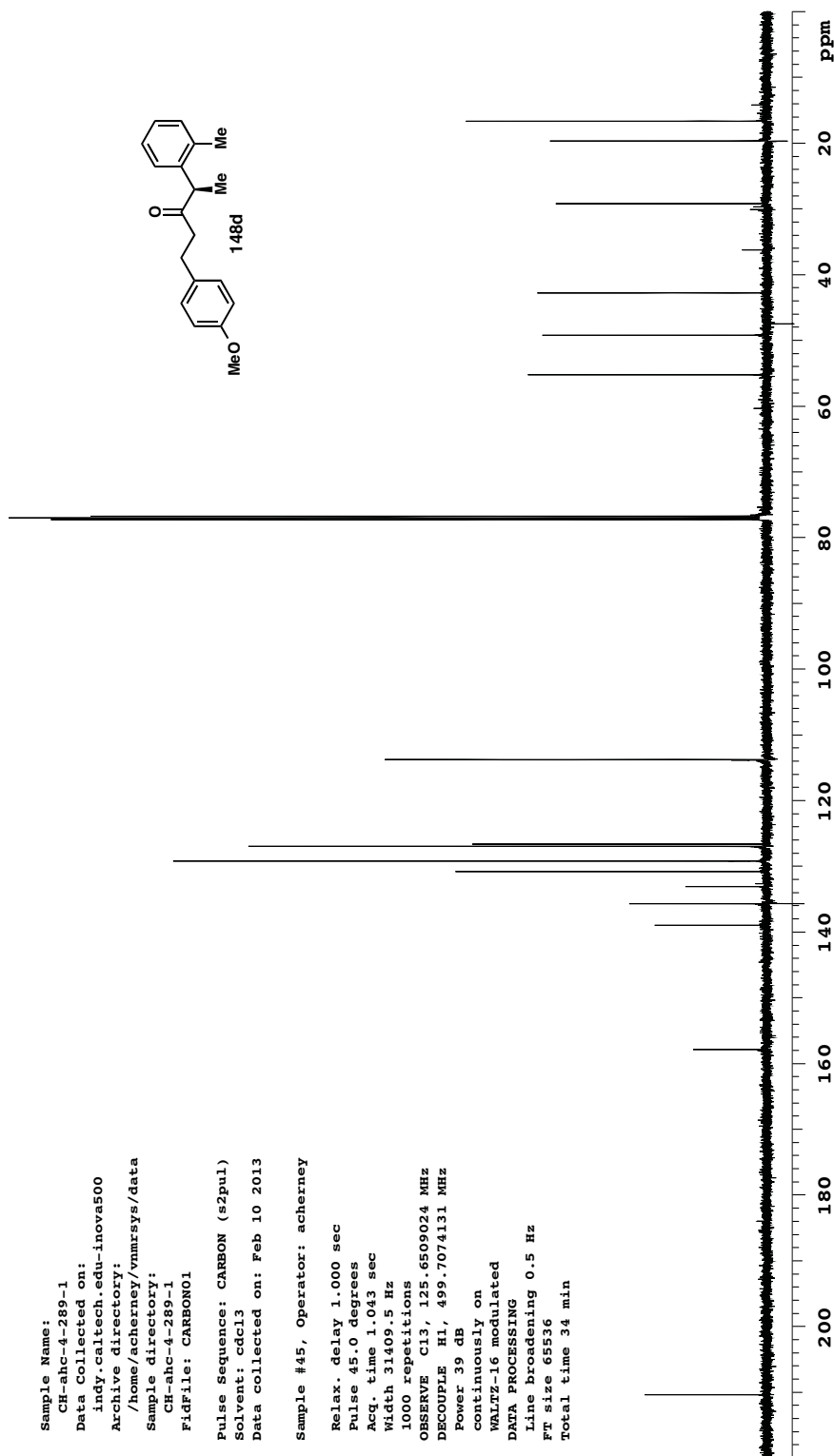


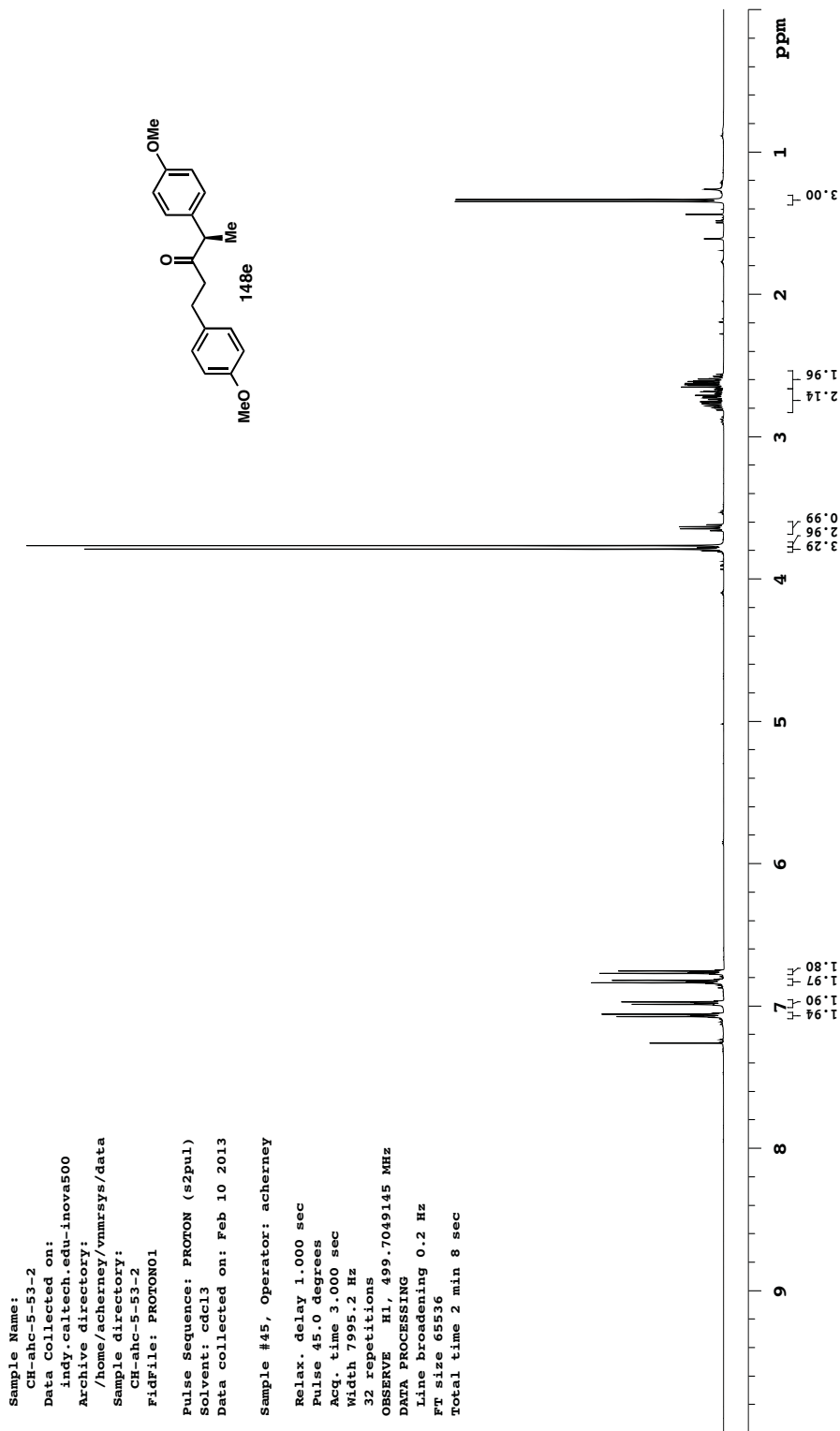


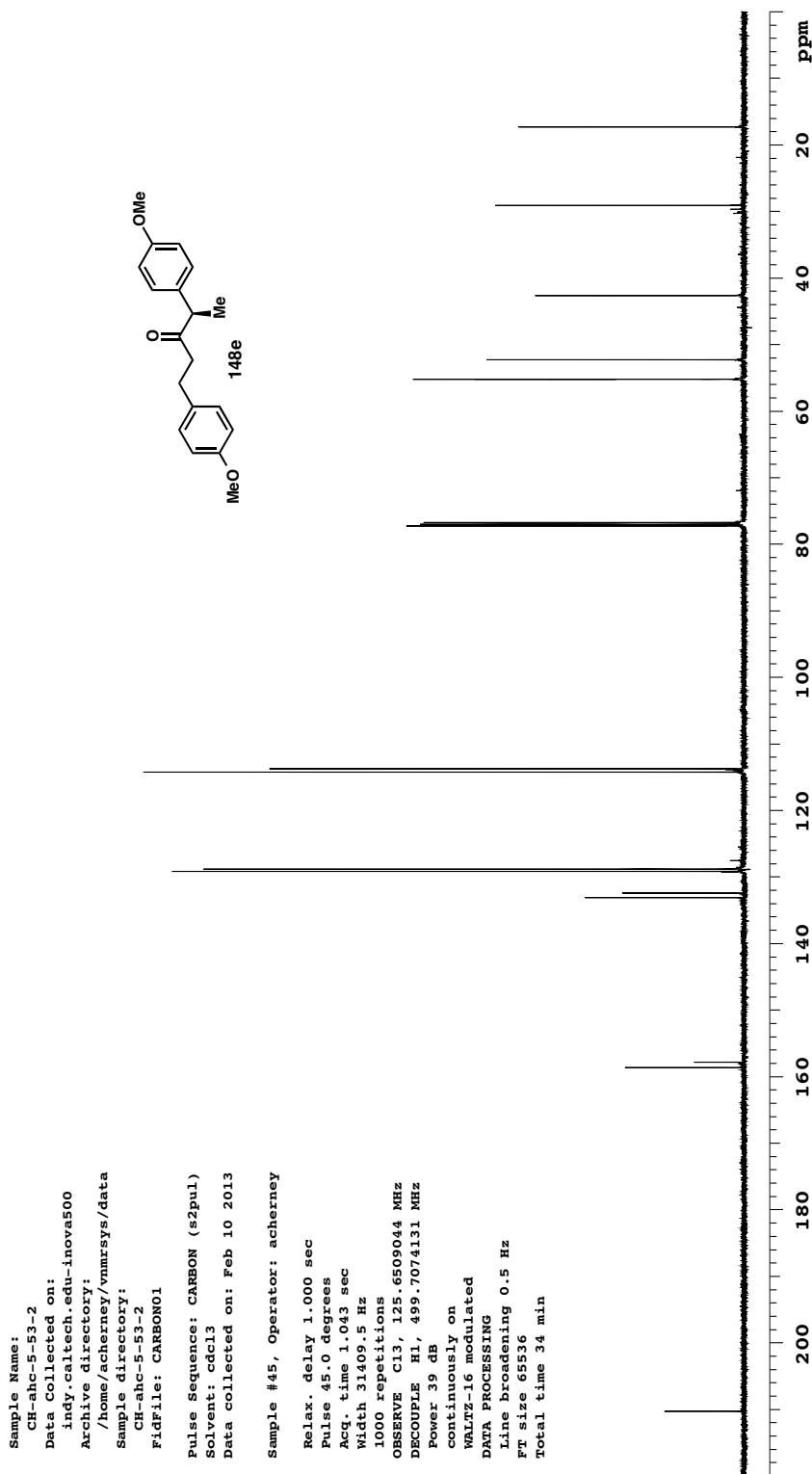


Sample Name: CH-ahc-4-289-1  
 Data Collected on: indy.caltech.edu-inova500  
 Archive directory: /home/acherney/vnmrsys/data  
 Sample directory: CH-ahc-4-289-1  
 FidFile: PROTON01  
 Pulse Sequence: PROTON (s2pul)  
 Solvent: cdcl3  
 Data collected on: Feb 10 2013  
 Sample #45, Operator: acherney  
 Relax. delay 1.000 sec  
 Pulse 45.0 degrees  
 Acq. time 3.000 sec  
 Width 7995.2 Hz  
 32 repetitions  
 OBSERVE H1, 499.7049145 MHz  
 DATA PROCESSING  
 Line broadening 0.2 Hz  
 FT size 65536  
 Total time 2 min 8 sec

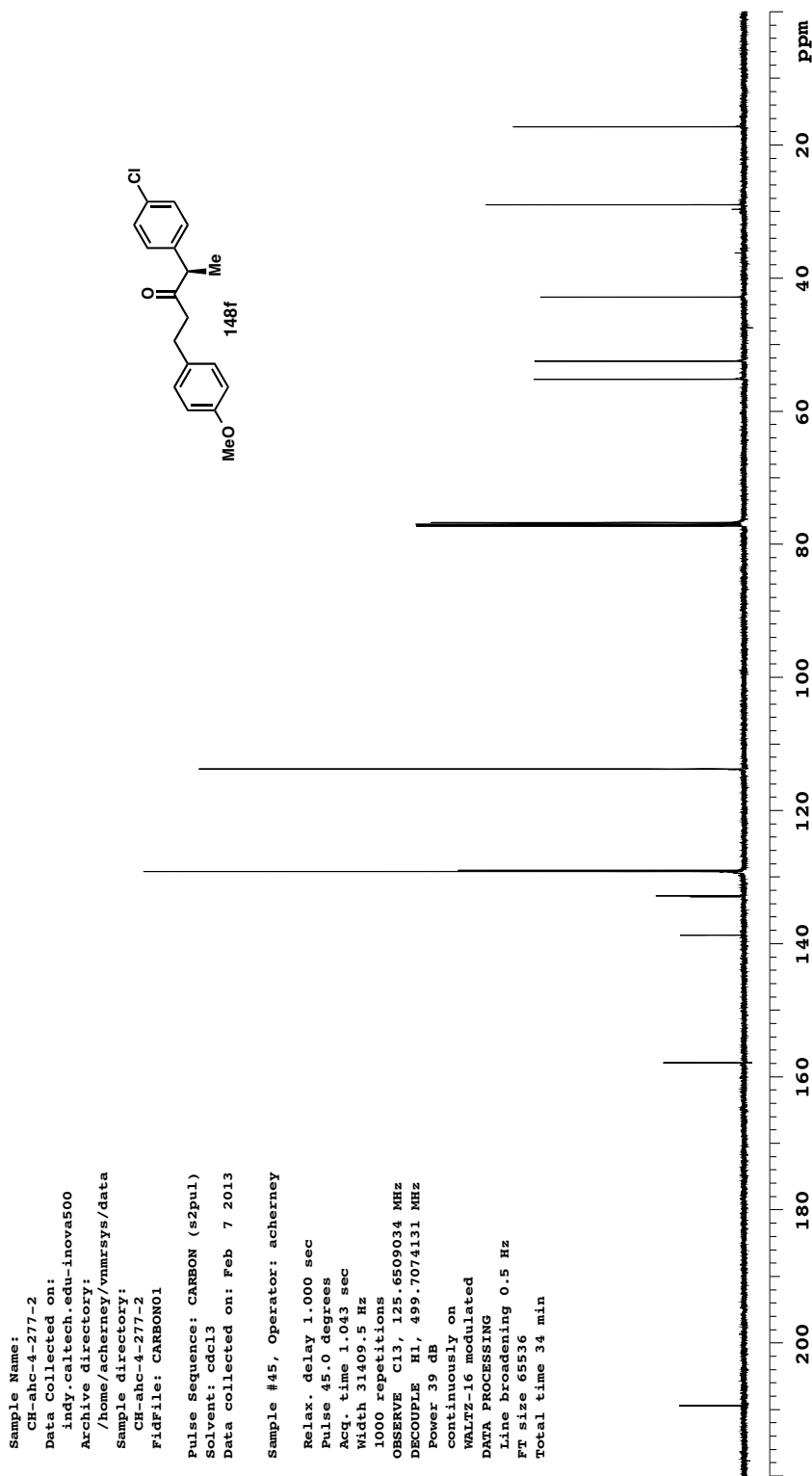


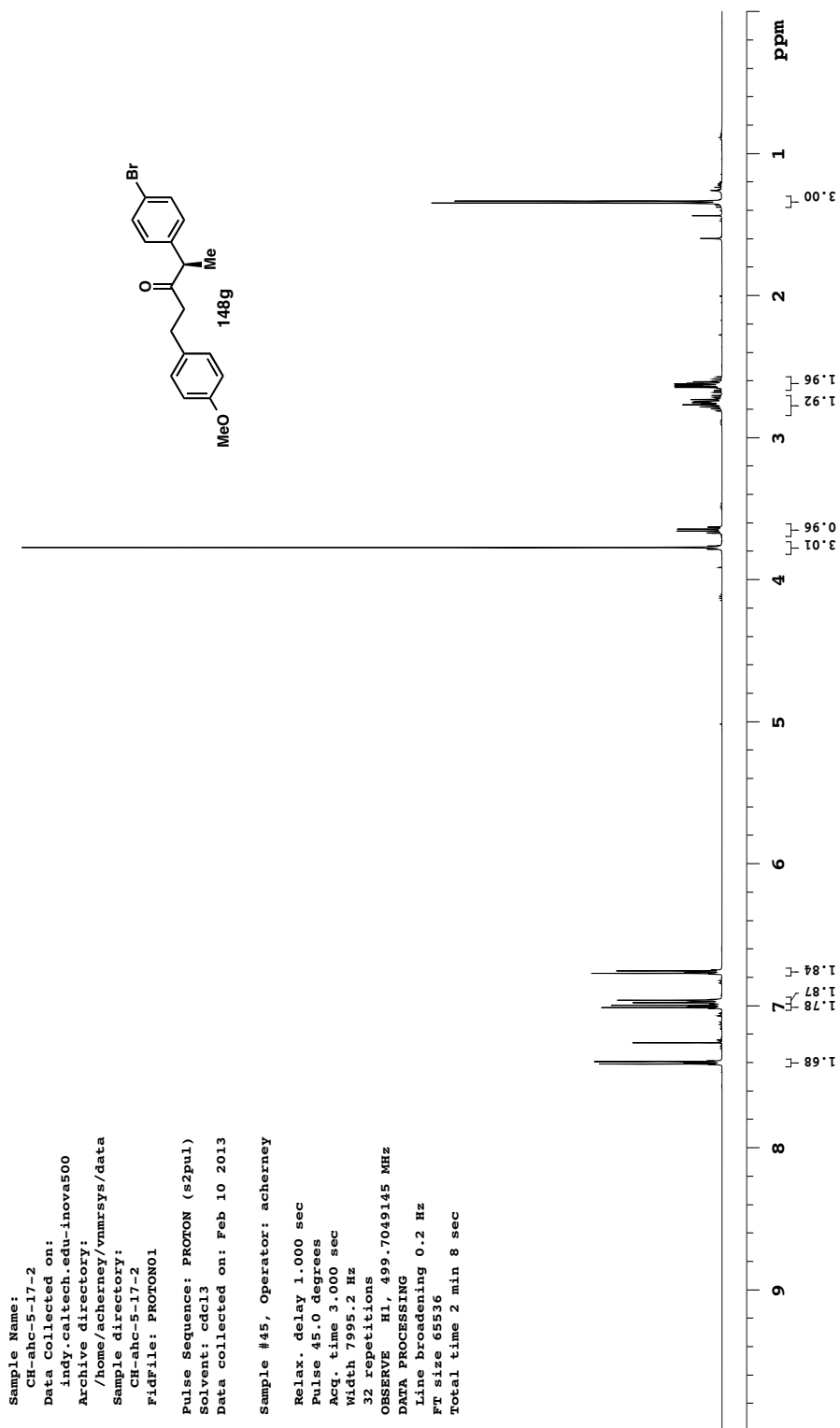


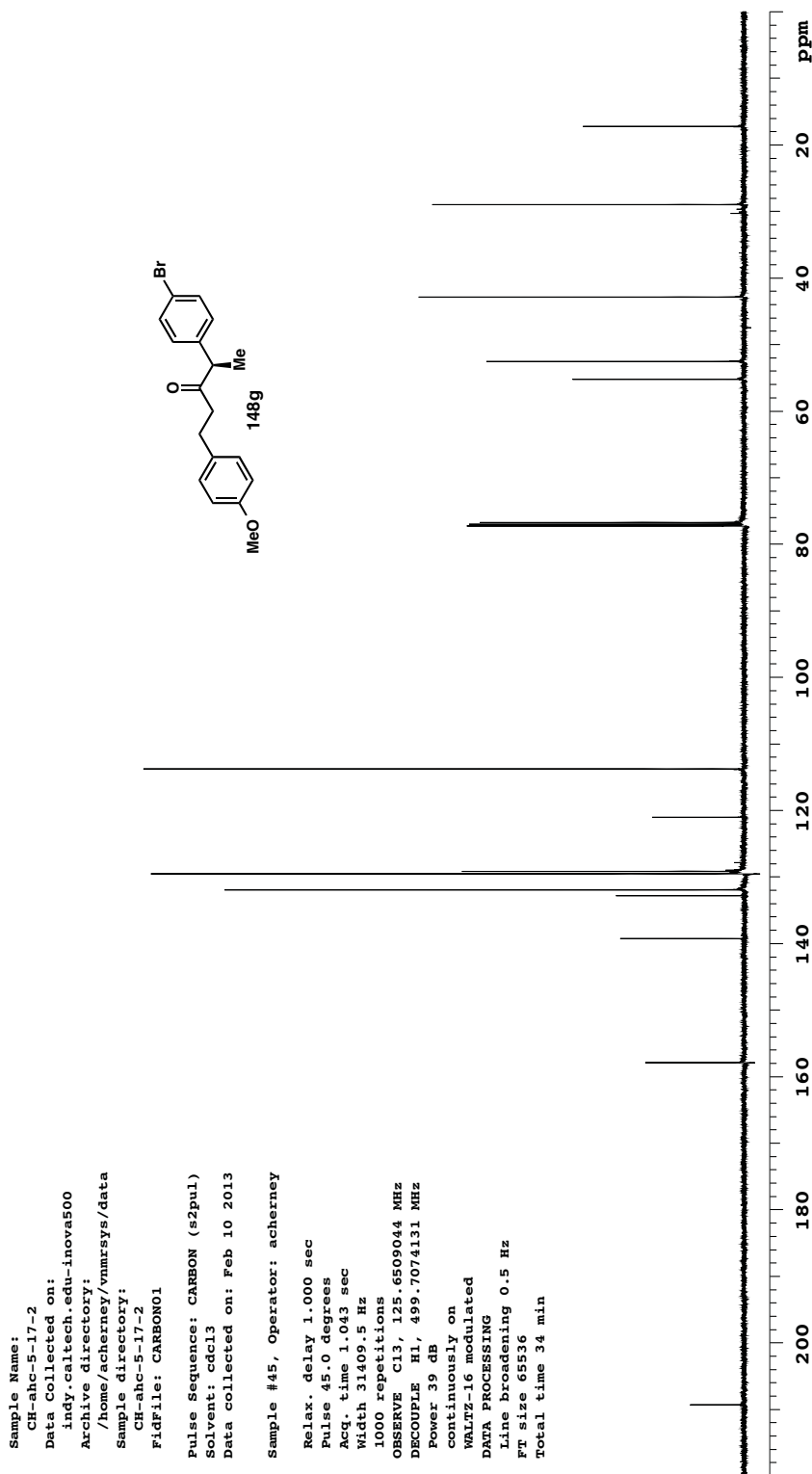


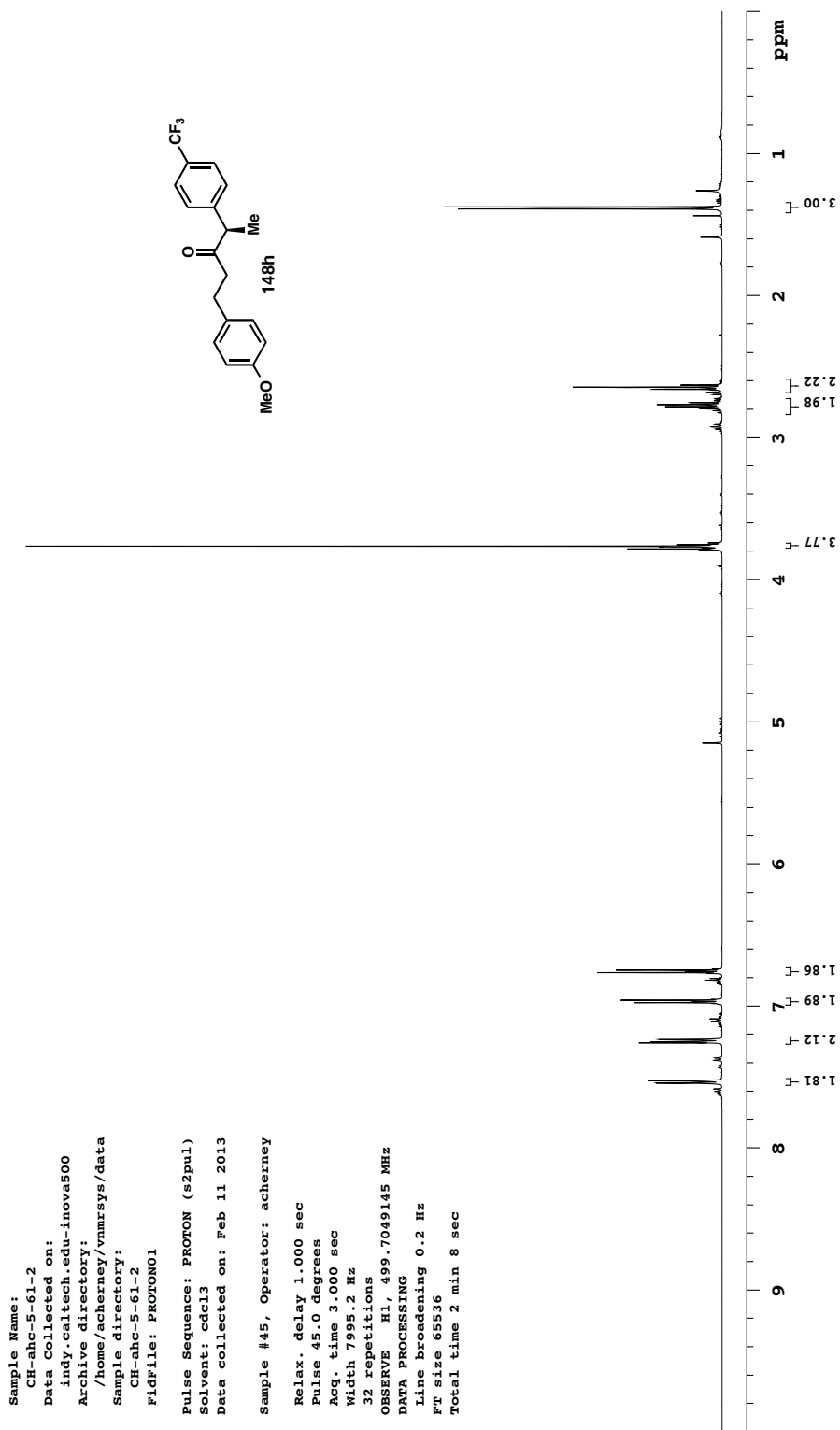


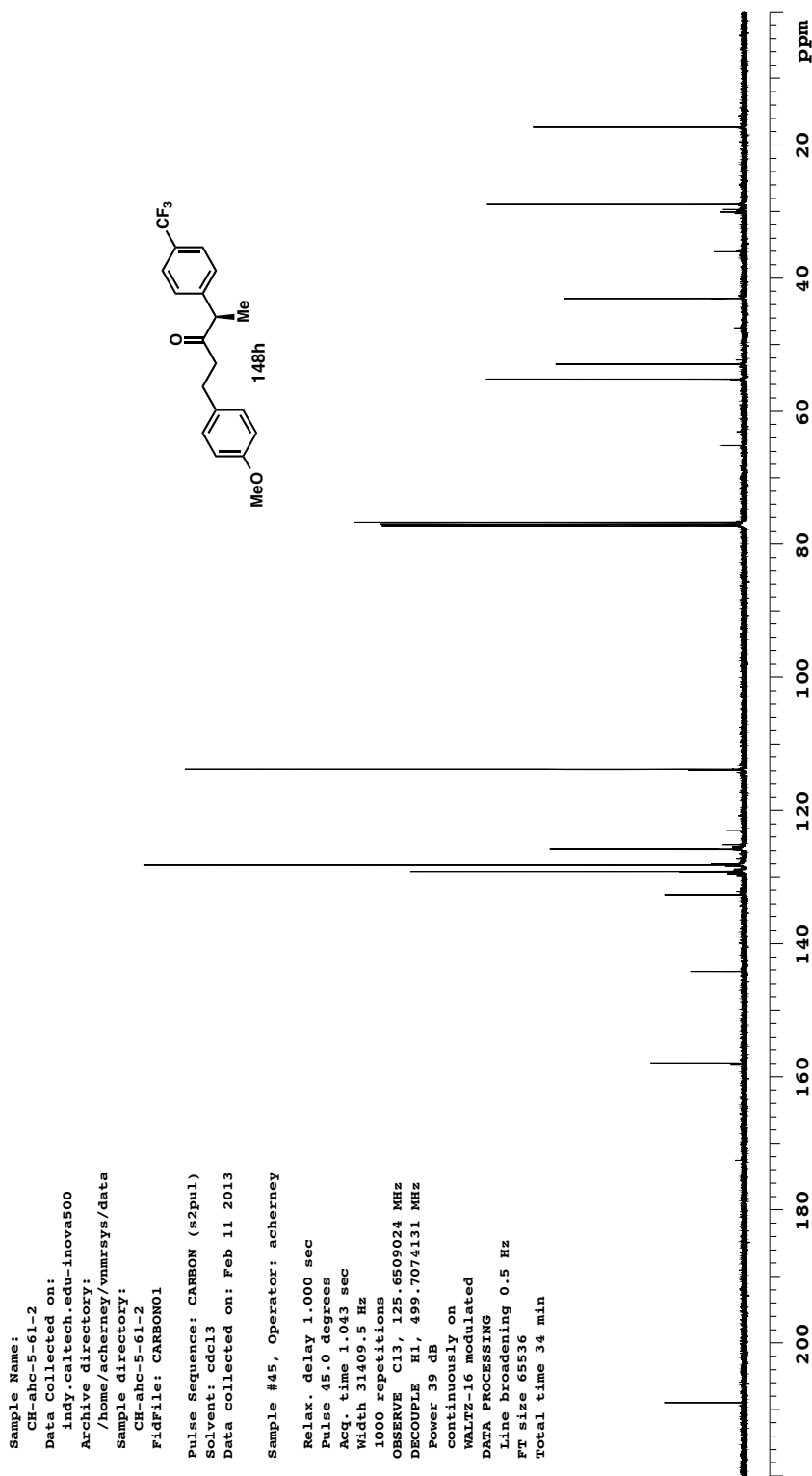




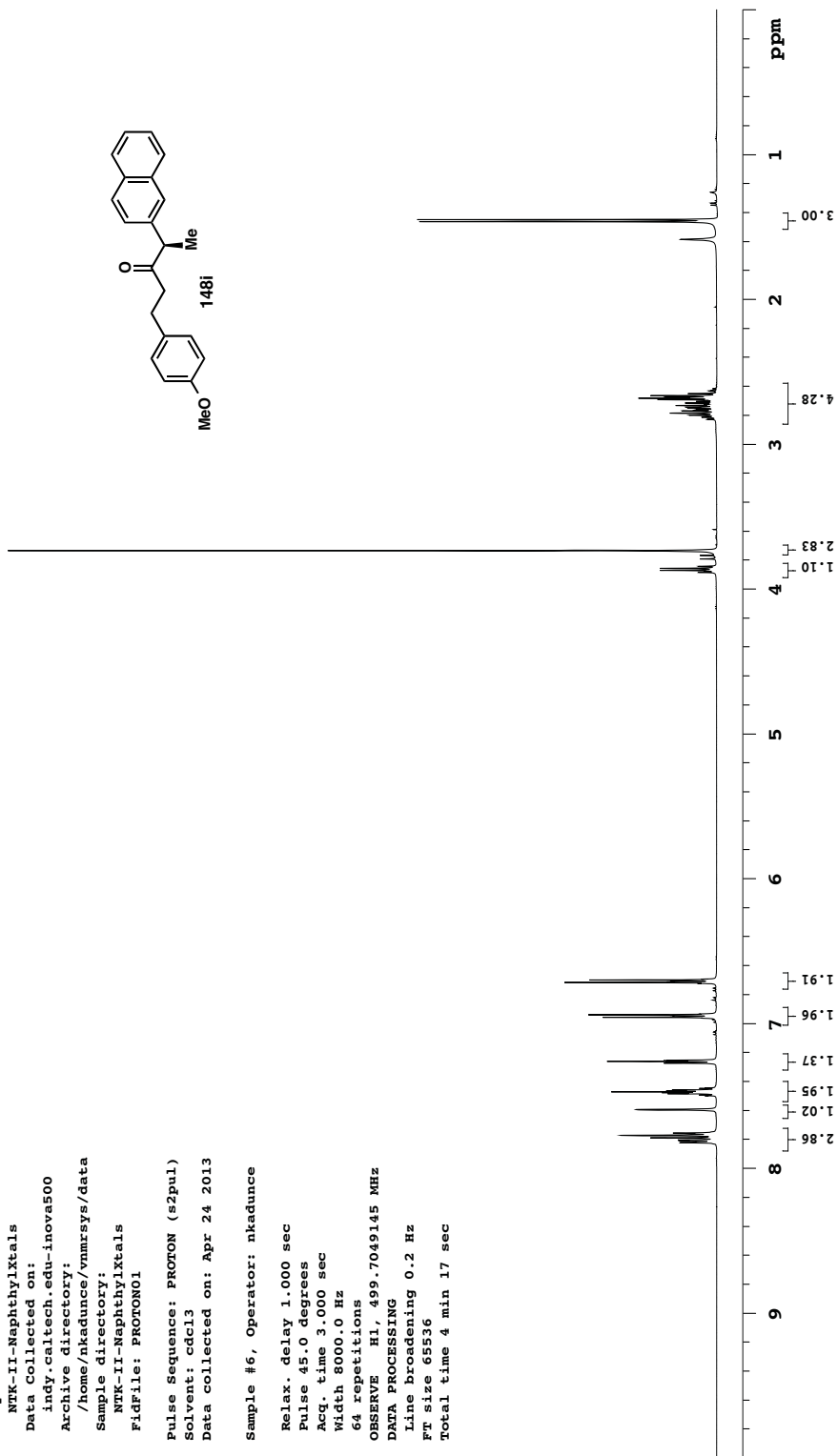
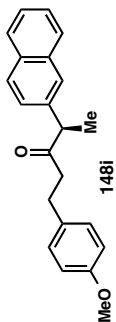


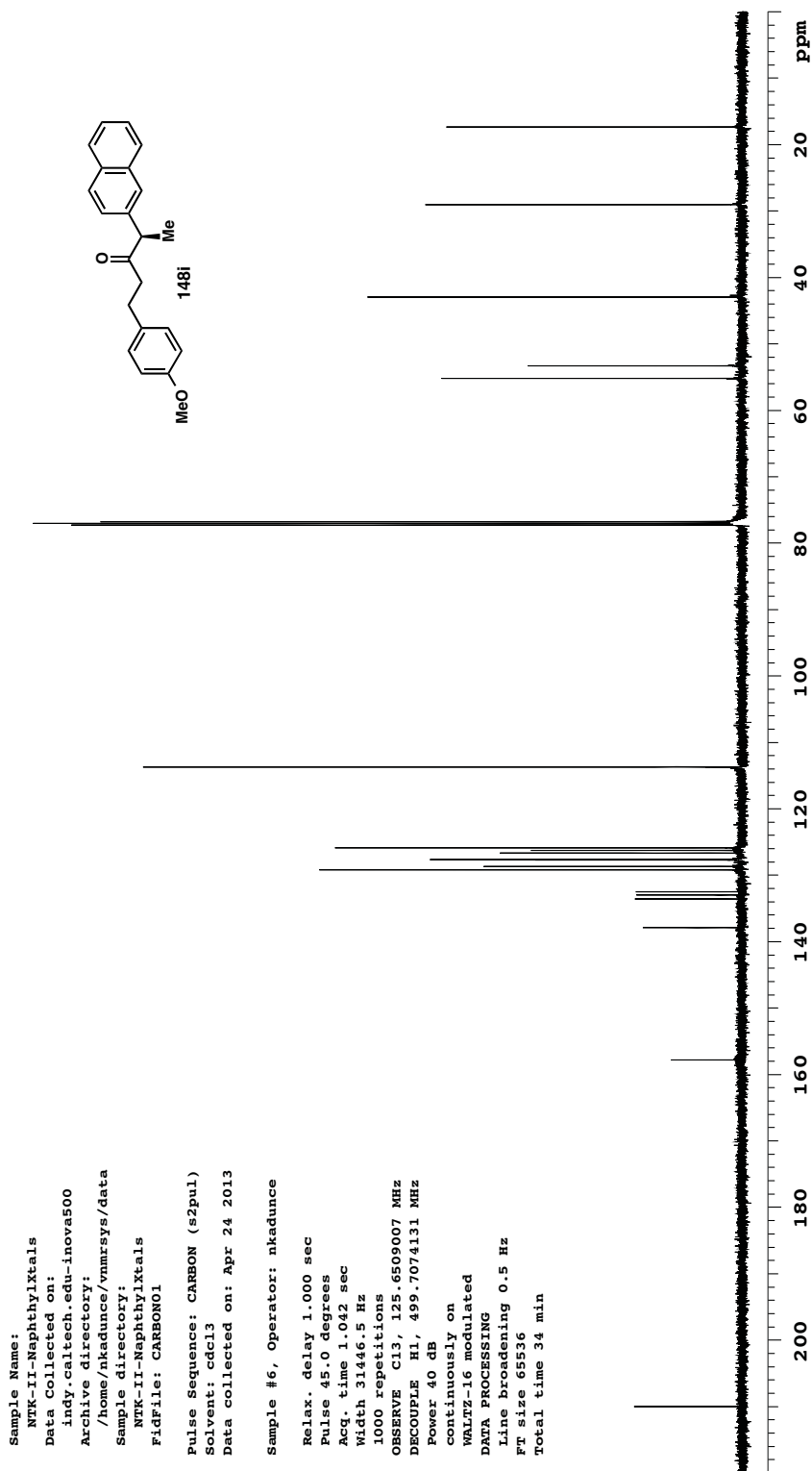


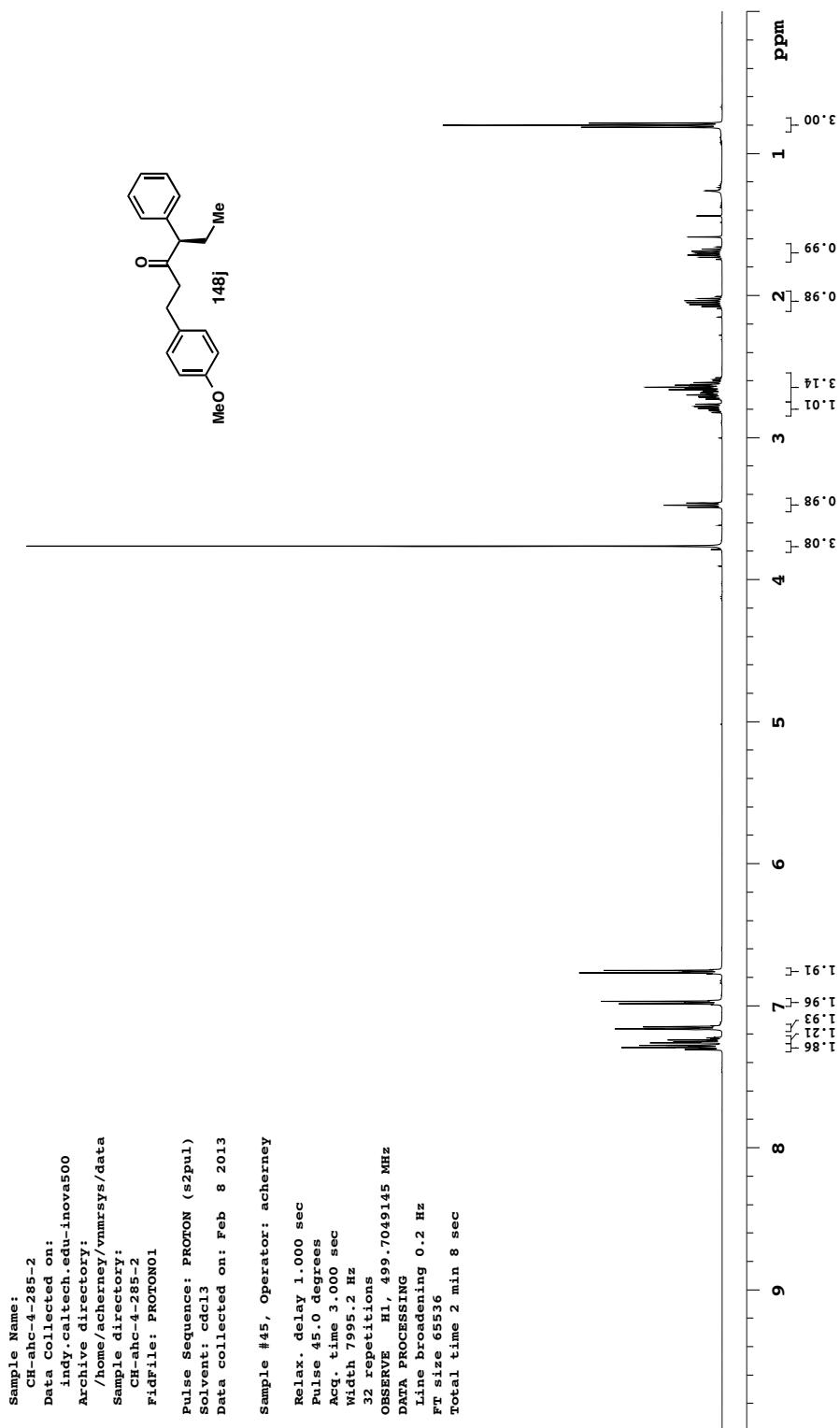


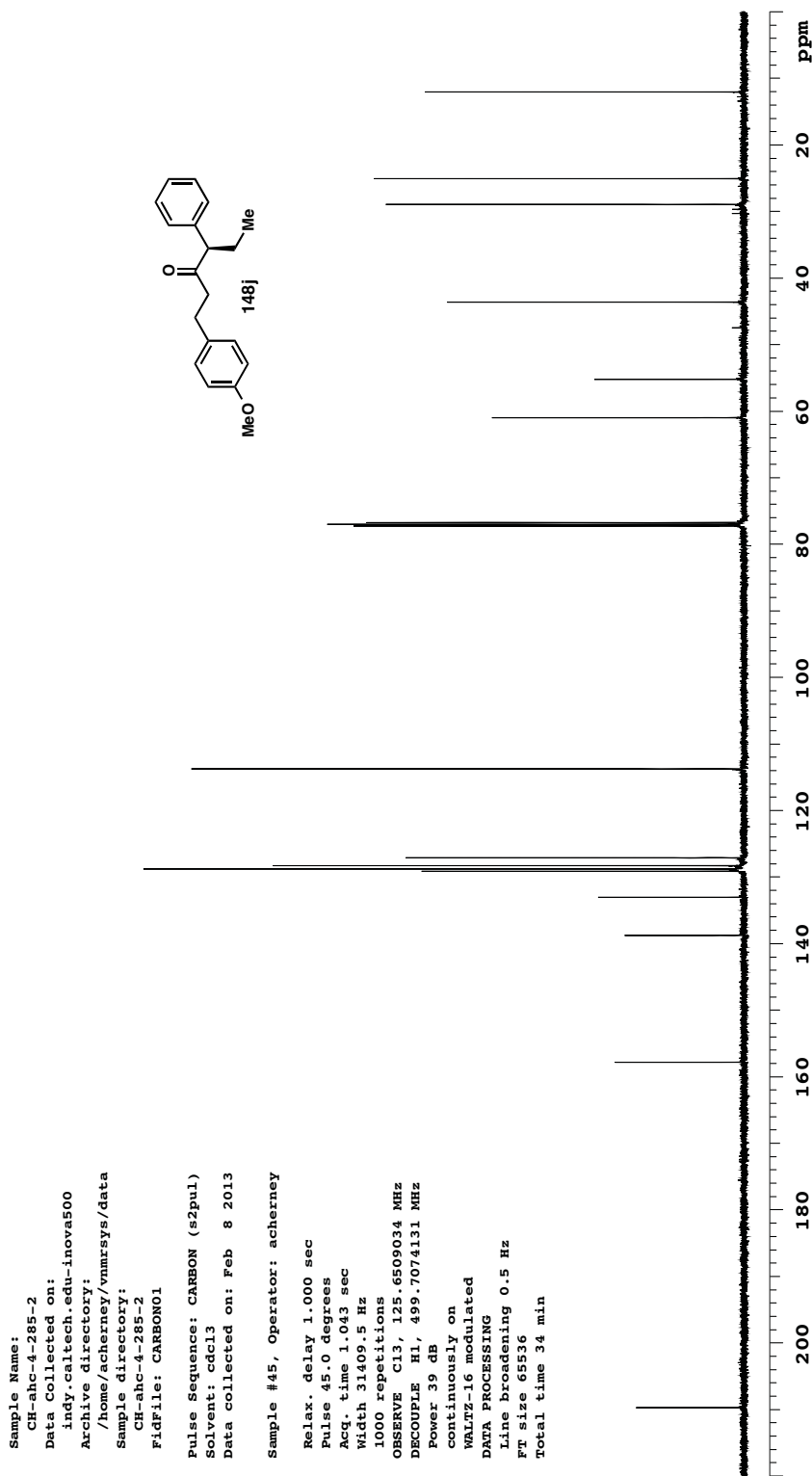


Sample Name: NTK-II-NaphthylXtals  
 Data Collected on: indy.caltech.edu-inova500  
 Archive directory: /home/nkadance/vnmrSYS/data  
 Sample directory: NTK-II-NaphthylXtals  
 FidFile: PROTON01  
 Pulse Sequence: PROTON (s2pul)  
 Solvent: cdcl3  
 Data collected on: Apr 24 2013  
 Sample #6, Operator: nkadance  
 Relax. delay 1.000 sec  
 Pulse 45.0 degrees  
 Acq. time 3.000 sec  
 Width 8000.0 Hz  
 64 repetitions  
 OBSERVE H1, 499.7049145 MHz  
 DATA PROCESSING  
 Line broadening 0.2 Hz  
 FT size 65536  
 Total time 4 min 17 sec

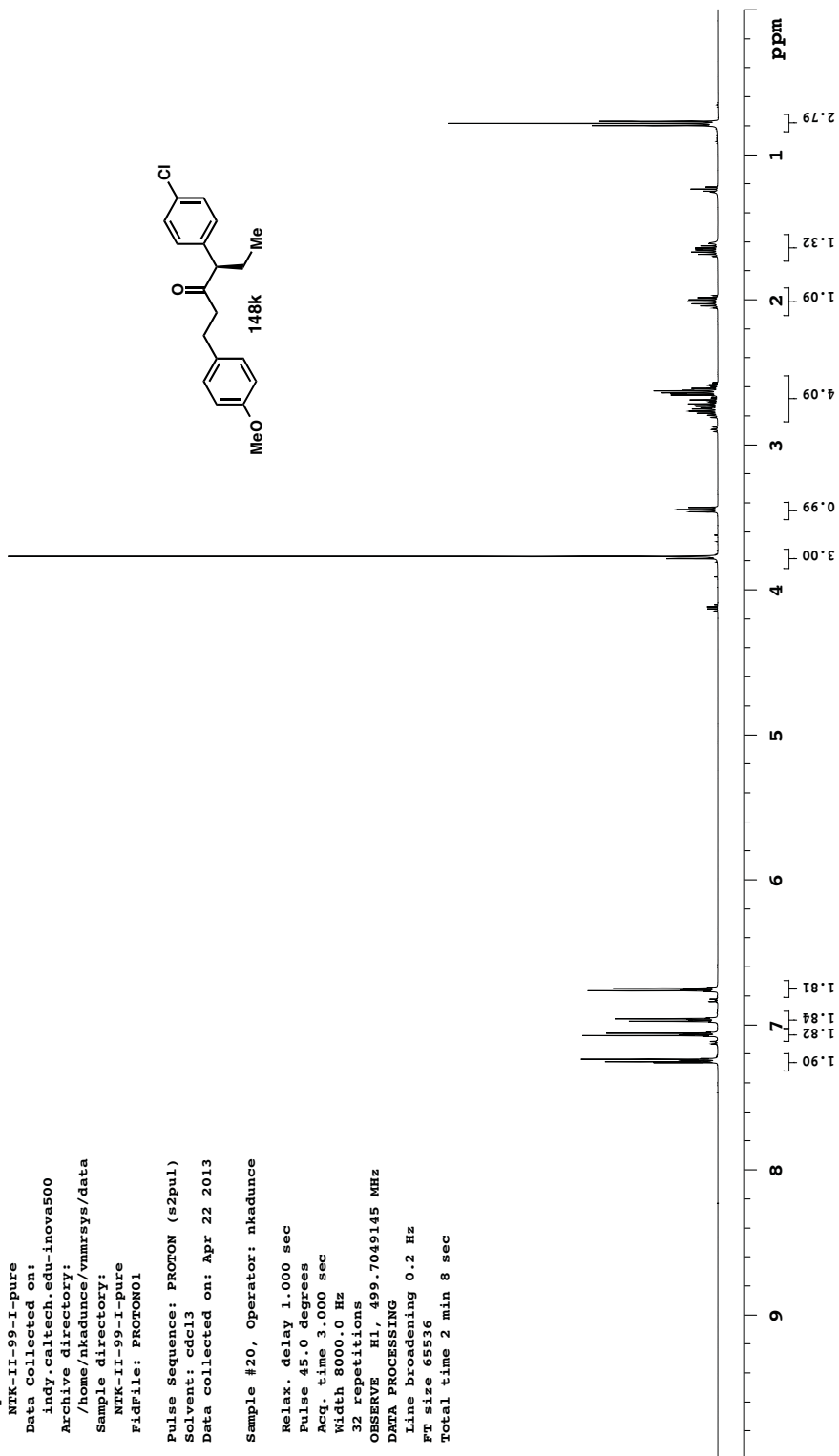


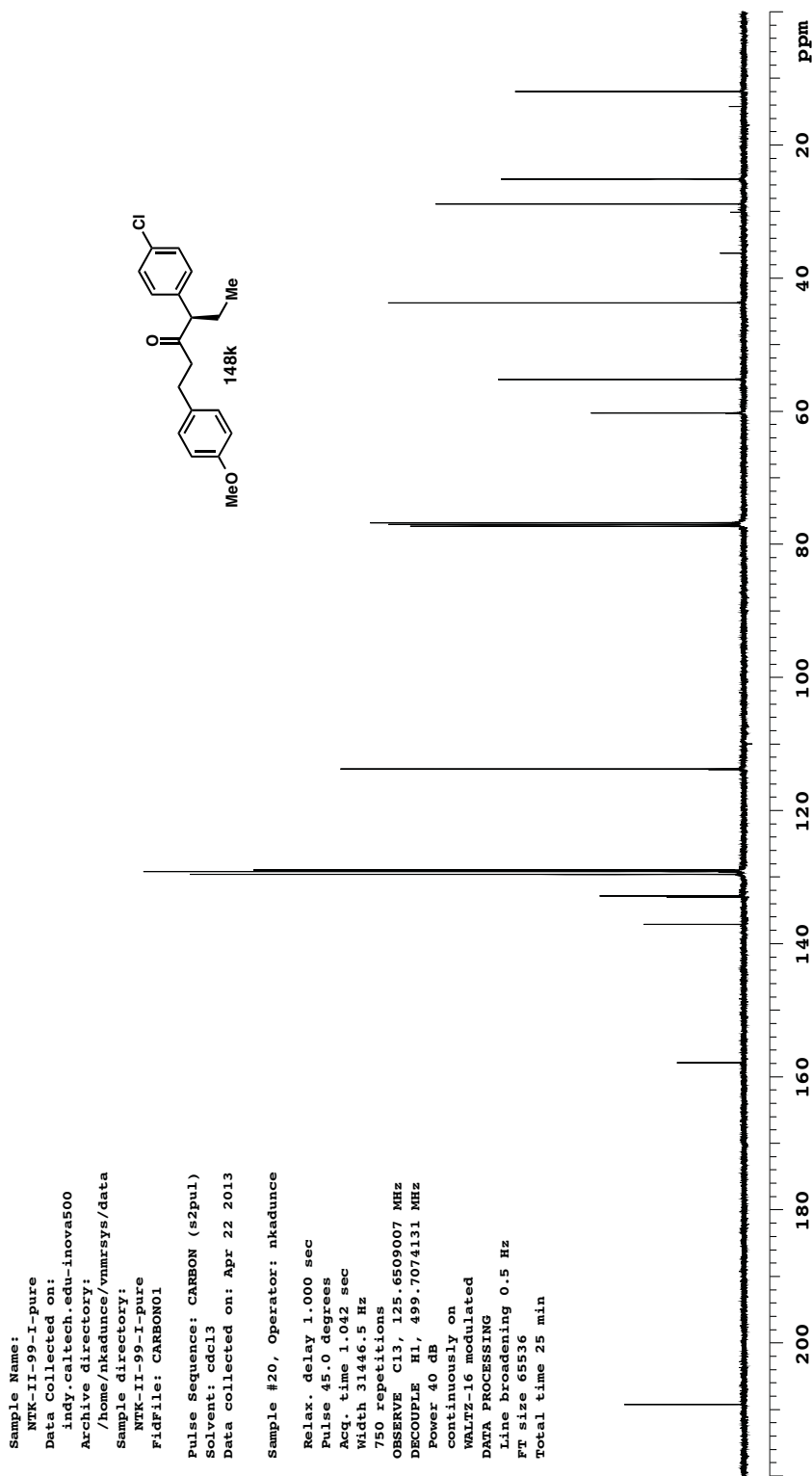






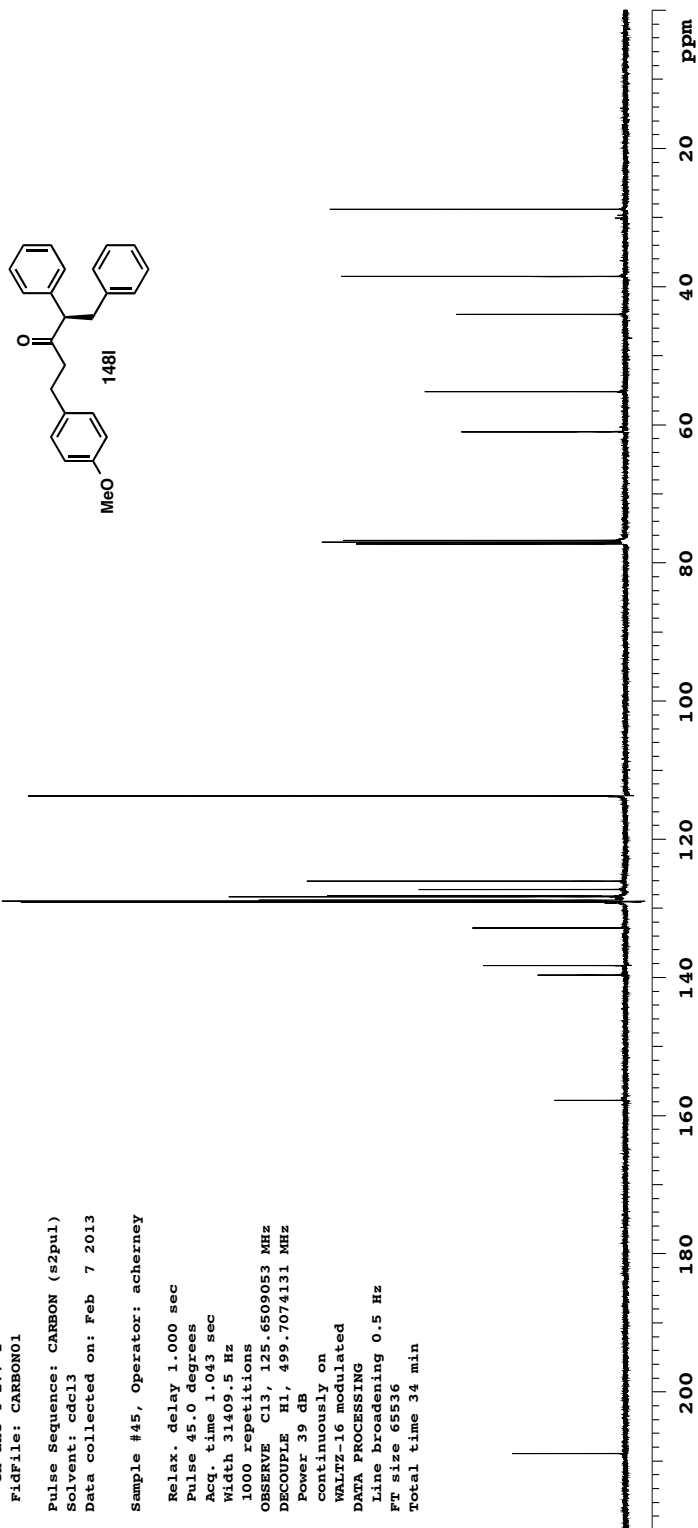
Sample Name:  
 NTK-II-99-I-pure  
 Data Collected on:  
 indy.caltech.edu-inova500  
 Archive directory:  
 /home/nkadunce/vnmrSYS/data  
 Sample directory:  
 NTK-II-99-I-pure  
 FidFile: PROTON01  
 Pulse Sequence: PROTON (s2pul)  
 Solvent: cdcl3  
 Data collected on: Apr 22 2013  
 Sample #20, Operator: nkadunce  
 Relax. delay 1.000 sec  
 Pulse 45.0 degrees  
 Acq. time 3.000 sec  
 Width 8000.0 Hz  
 32 repetitions  
 OBSERVE H1, 499.7049145 MHz  
 DATA PROCESSING  
 Line broadening 0.2 Hz  
 FT size 65536  
 Total time 2 min 8 sec



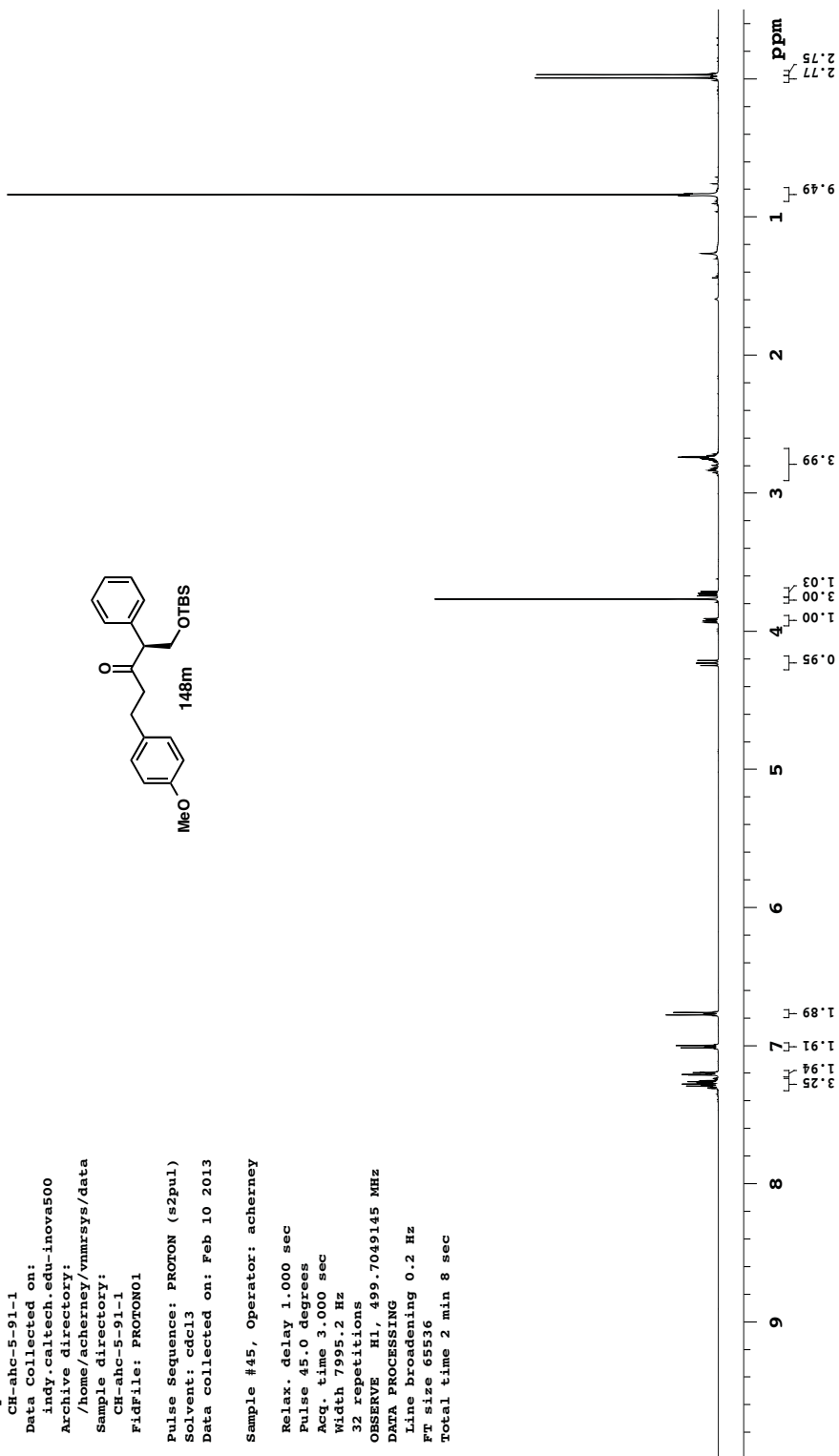
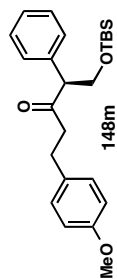


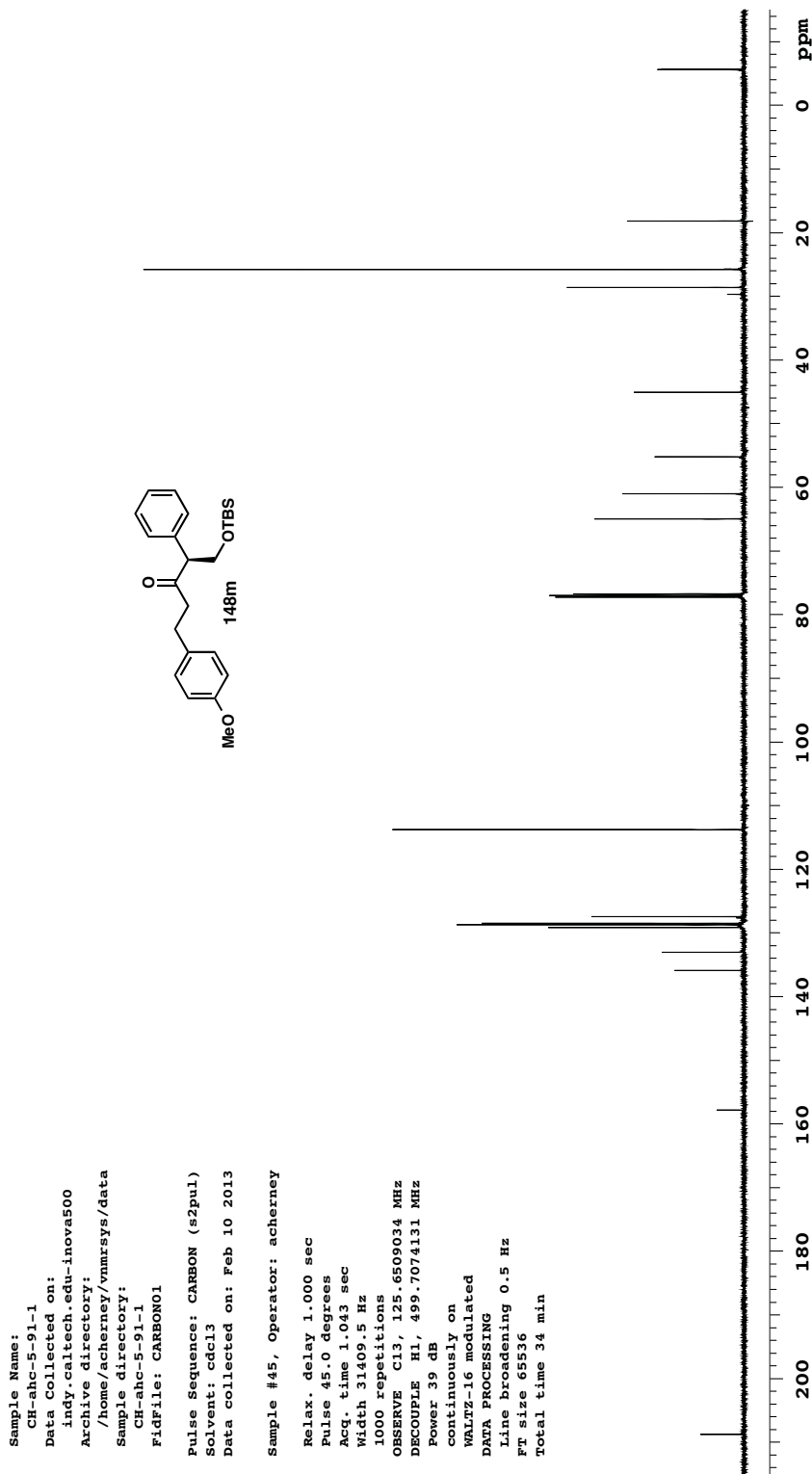


Sample Name:  
 CH-ahc-4-277-1  
 Data Collected on:  
 indy.caltech.edu-inova500  
 Archive directory:  
 /home/acherney/vnmrsys/data  
 Sample directory:  
 CH-ahc-4-277-1  
 FidFile: CARBONO1  
 Pulse Sequence: CARBON (s2pul)  
 Solvent: cdcl3  
 Data collected on: Feb 7 2013  
 Sample #45, Operator: acherney  
 Relax. delay 1.000 sec  
 Pulse 45.0 degrees  
 Acq. time 1.043 sec  
 Width 31409.5 Hz  
 1000 repetitions  
 OBSERVE C13, 125.6509053 MHz  
 DECOUPLE H1, 499.7074131 MHz  
 Power 39 dB  
 continuously on  
 WALTZ-16 modulated  
 DATA PROCESSING  
 Line broadening 0.5 Hz  
 F1 size 65536  
 Total time 34 min

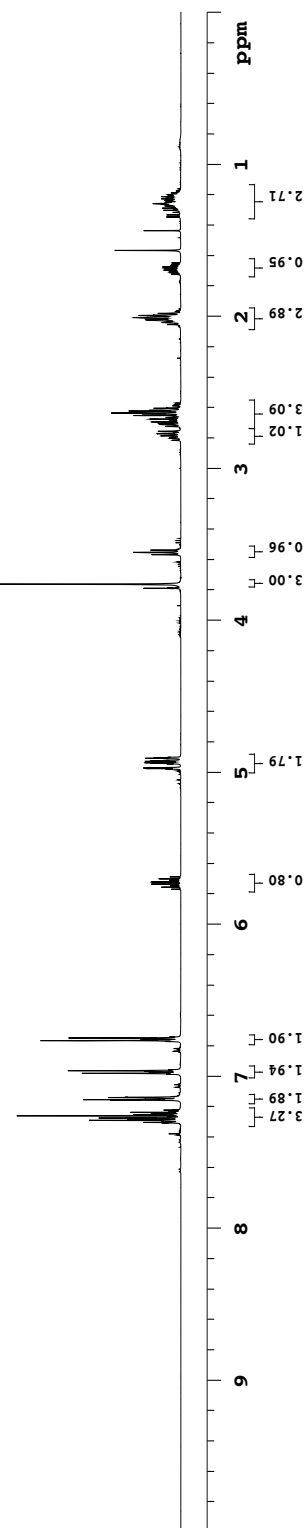
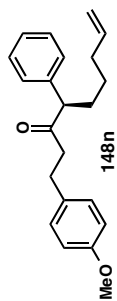


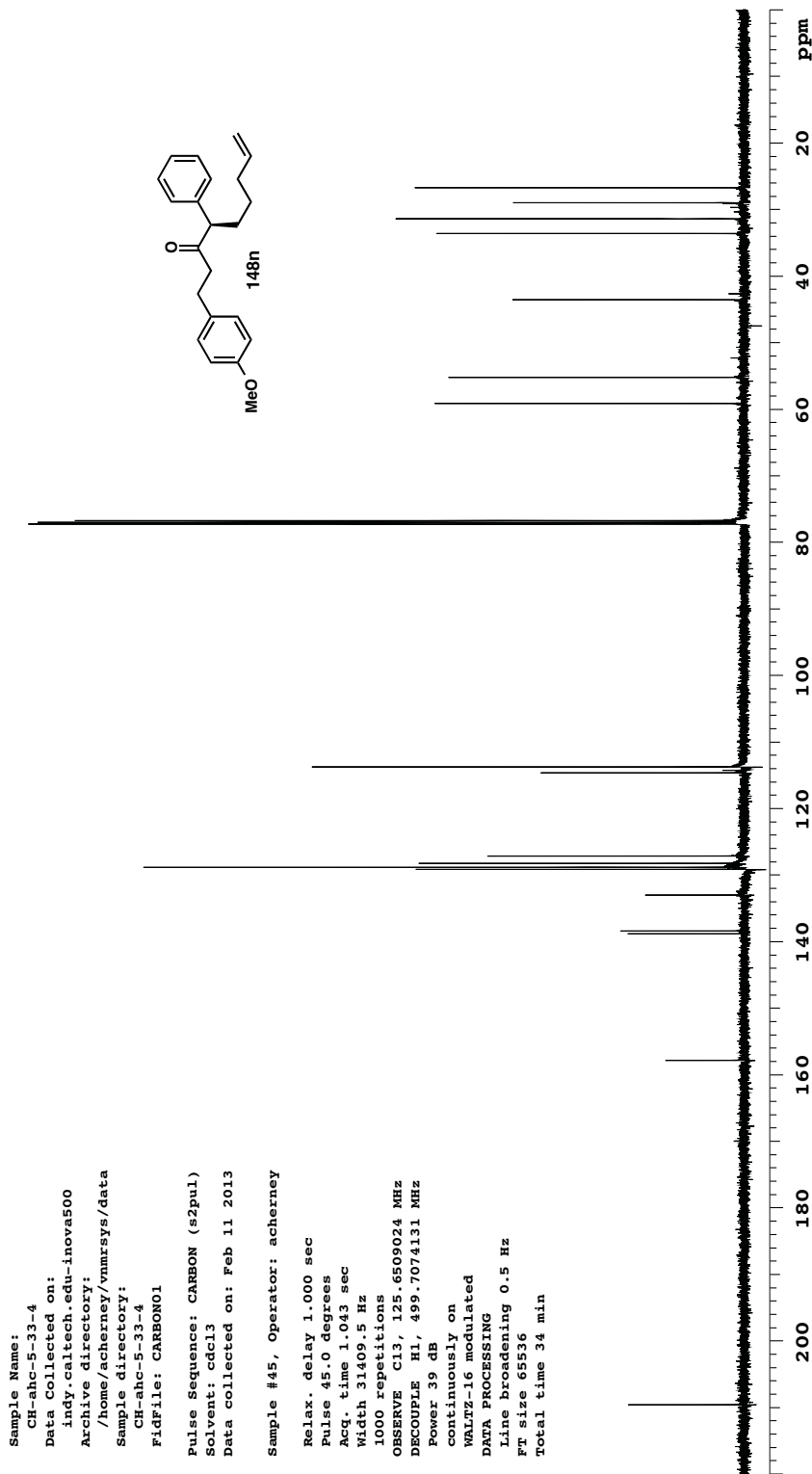
Sample Name: CH-ahc-5-91-1  
 Data Collected on: indy.caltech.edu-inova500  
 Archive directory: /home/acherney/vnmrsys/data  
 Sample directory: CH-ahc-5-91-1  
 FidFile: PROTON01  
 Pulse Sequence: PROTON (s2pul)  
 Solvent: cdcl3  
 Data collected on: Feb 10 2013  
 Sample #45, Operator: acherney  
 Relax. delay 1.000 sec  
 Pulse 45.0 degrees  
 Acq. time 3.000 sec  
 Width 7995.2 Hz  
 32 repetitions  
 OBSERVE H1, 499.7049145 MHz  
 DATA PROCESSING  
 Line broadening 0.2 Hz  
 FT size 65536  
 Total time 2 min 8 sec

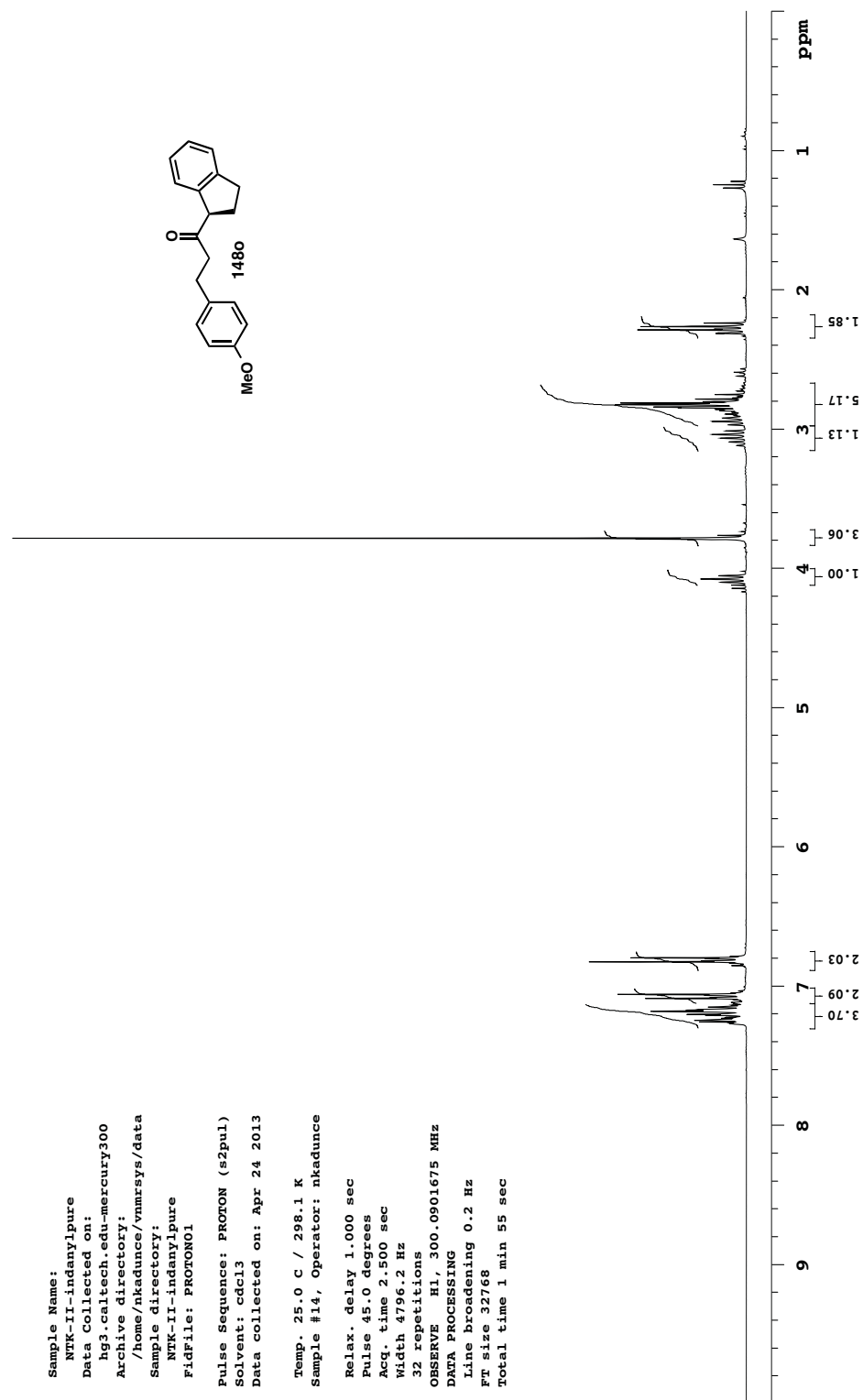


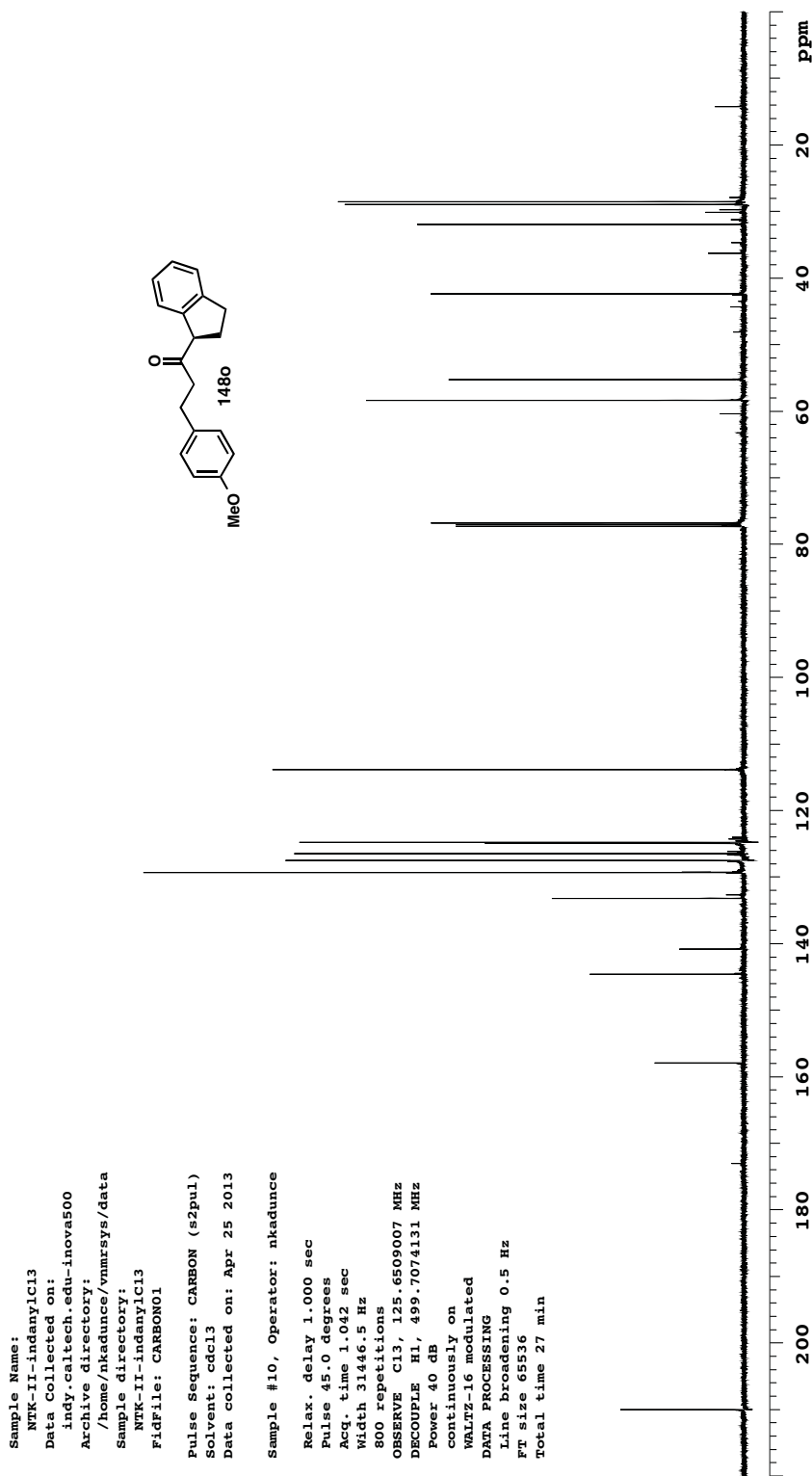


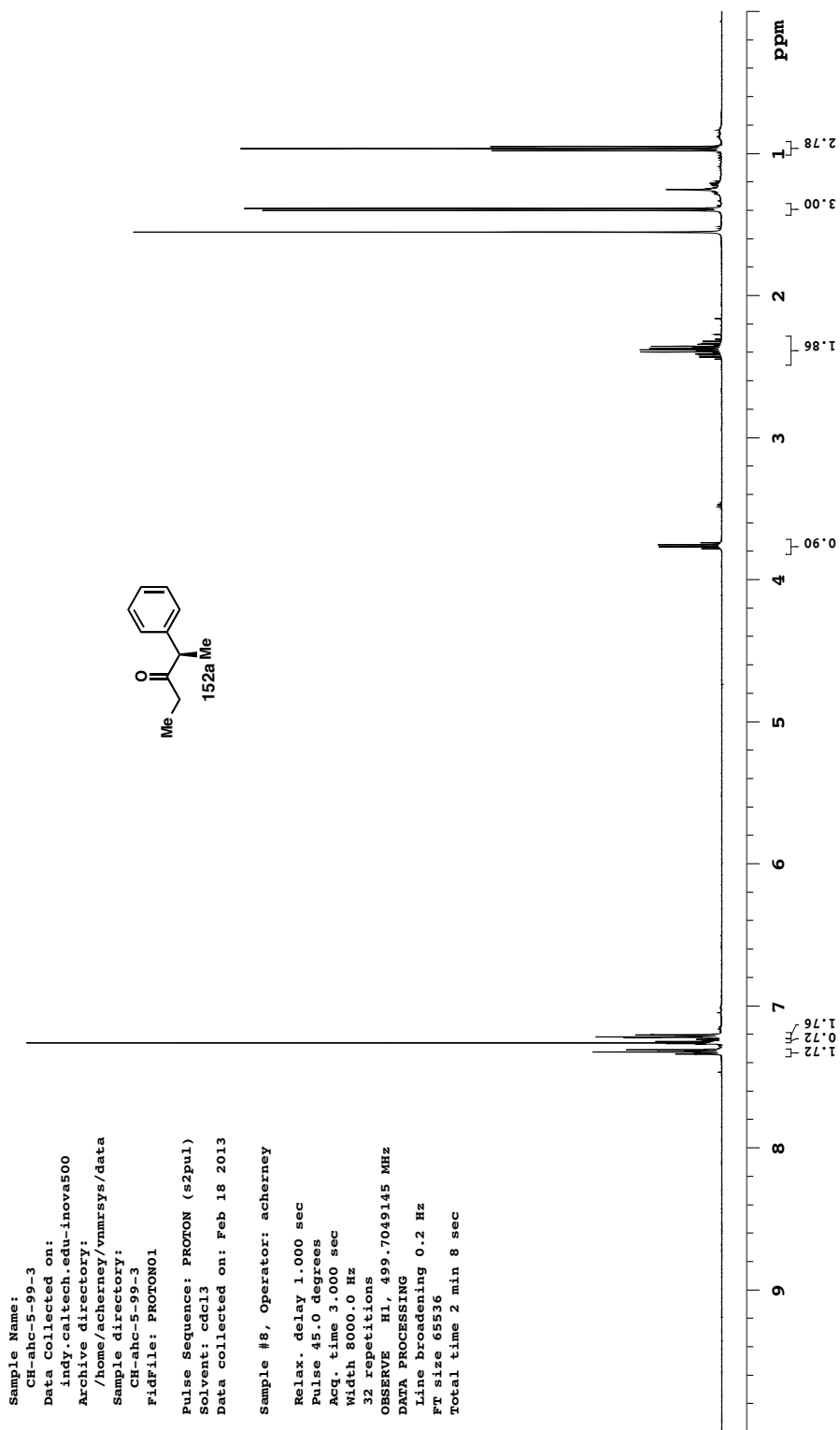
Sample Name:  
 CH-ahc-5-33-4  
 Data Collected on:  
 indy.caltech.edu-inova500  
 Archive directory:  
 /home/acherney/vnmrsys/data  
 Sample directory:  
 CH-ahc-5-33-4  
 FidFile: PROTON01  
 Pulse Sequence: PROTON (s2pul)  
 Solvent: cdcl3  
 Data collected on: Feb 11 2013  
 Sample #45, Operator: acherney  
 Relax. delay 1.000 sec  
 Pulse 45.0 degrees  
 Acq. time 3.000 sec  
 Width 7995.2 Hz  
 32 repetitions  
 OBSERVE H1, 499.7049145 MHz  
 DATA PROCESSING  
 Line broadening 0.2 Hz  
 FT size 65536  
 Total time 2 min 8 sec

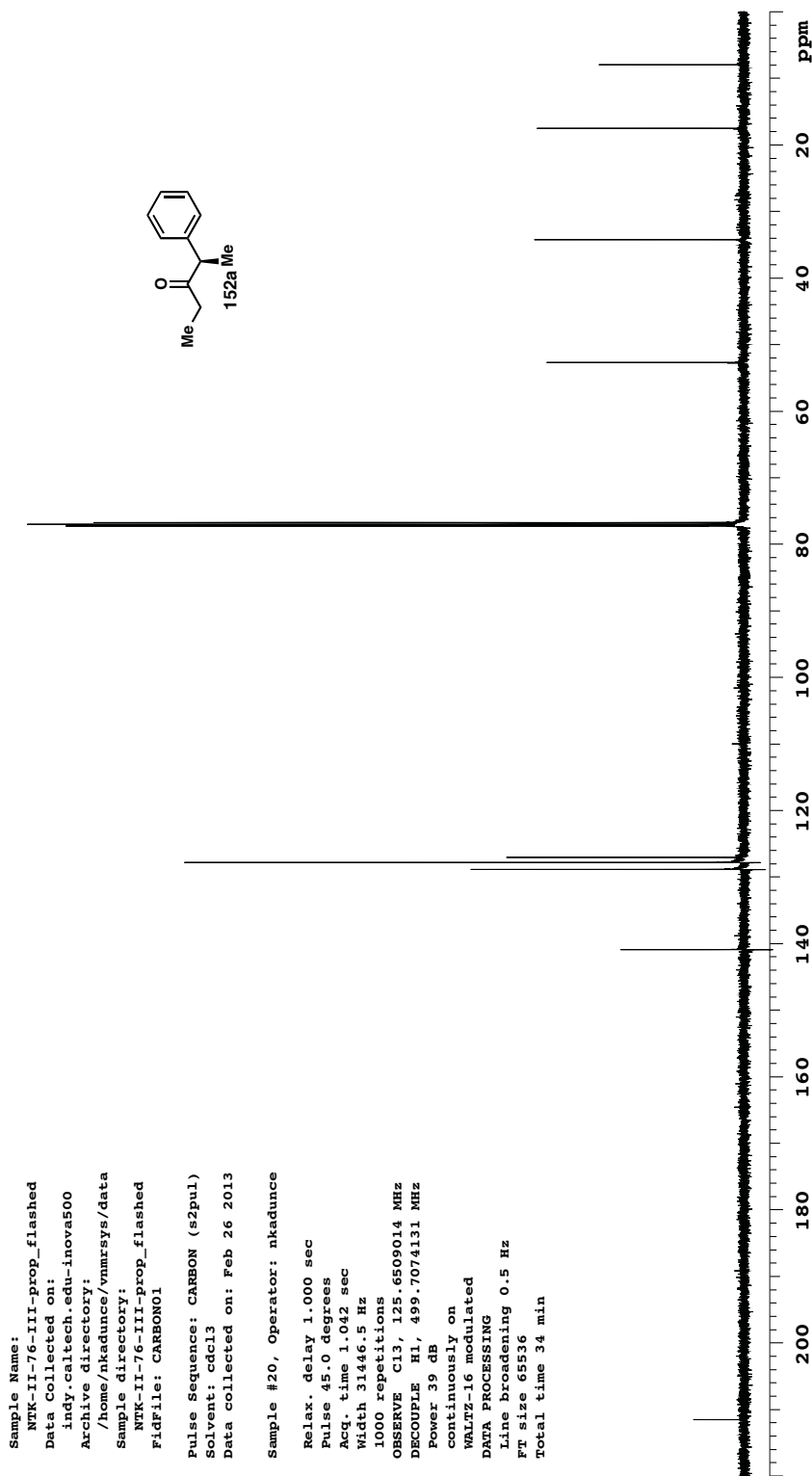




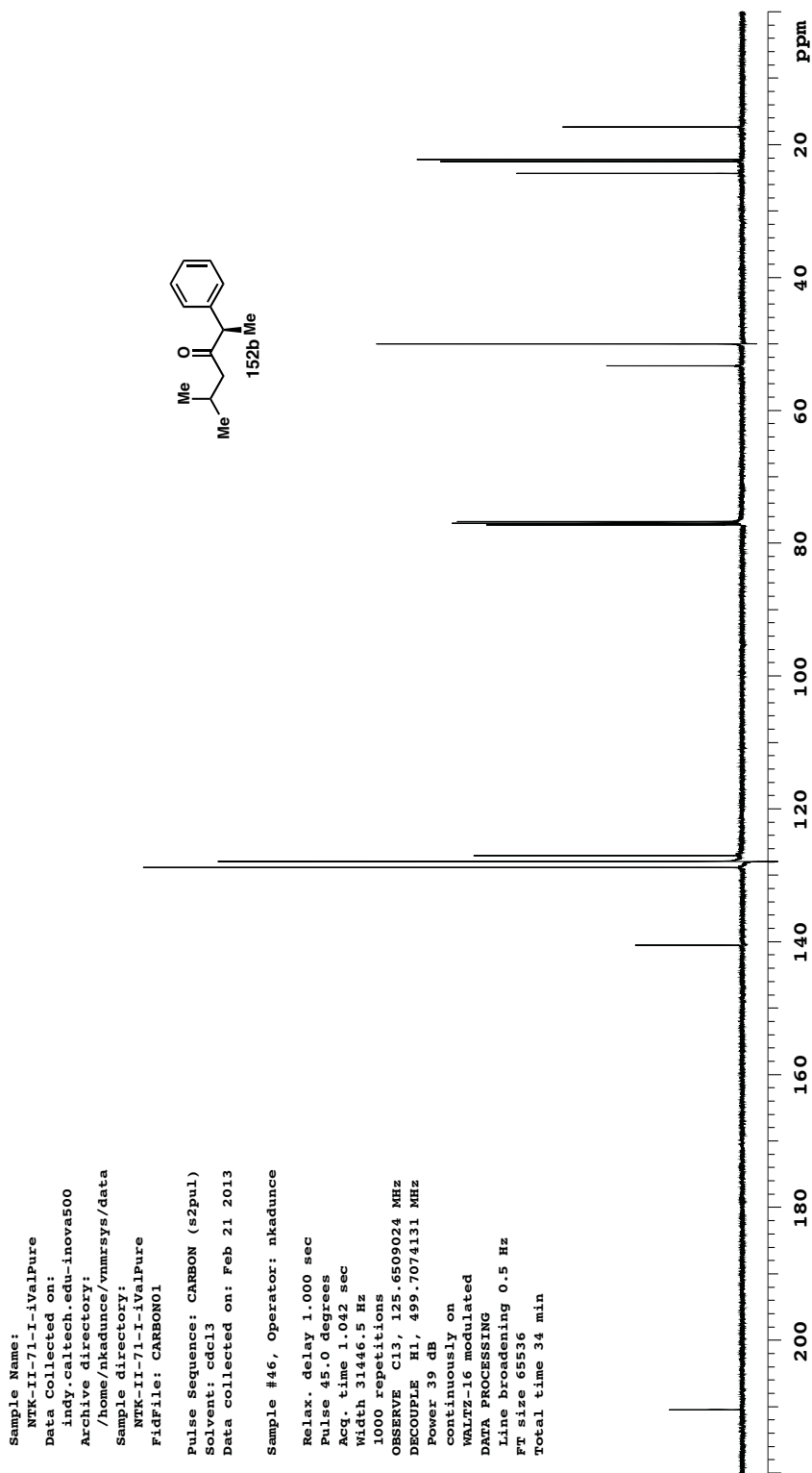




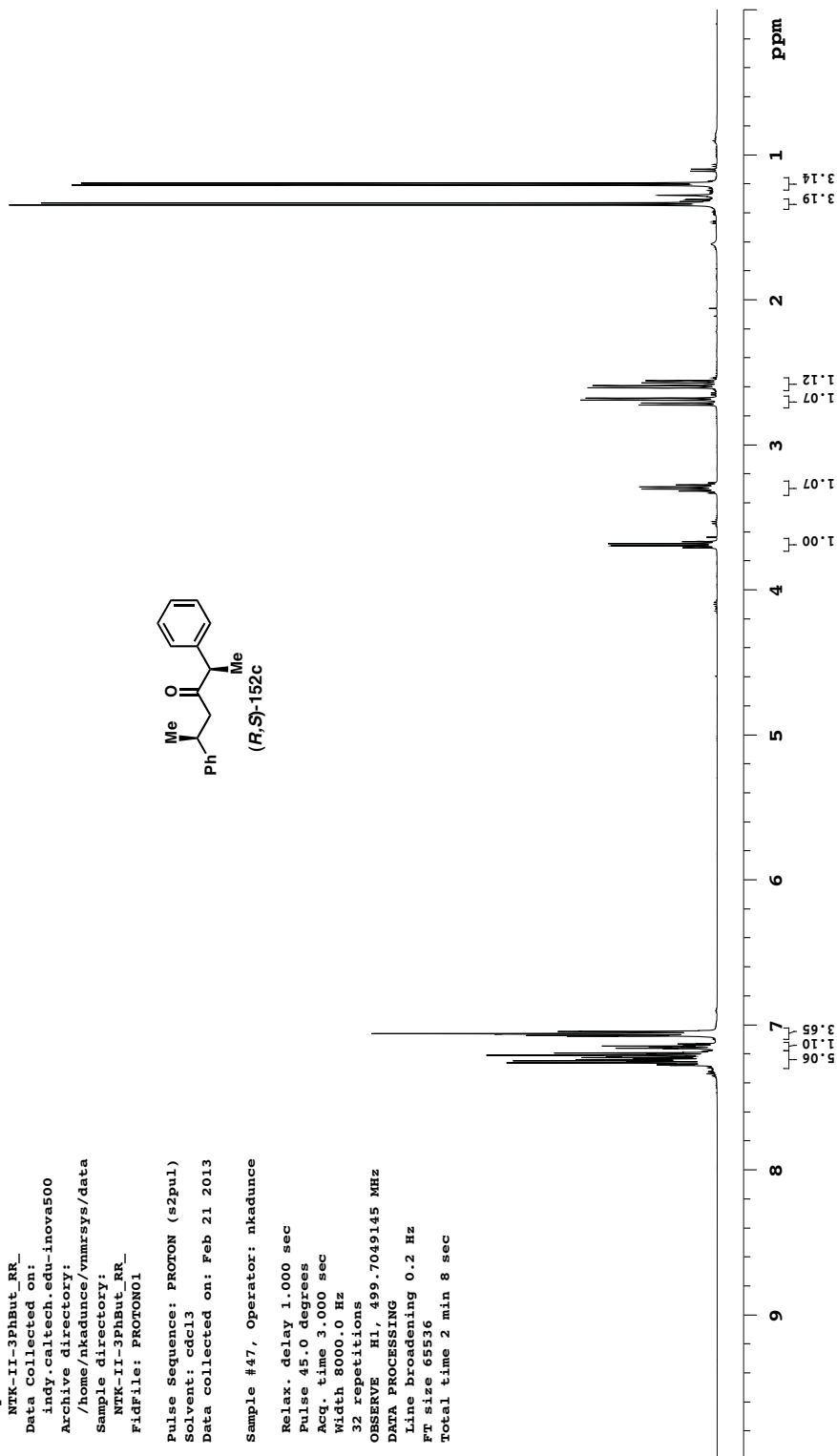
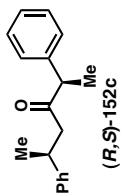


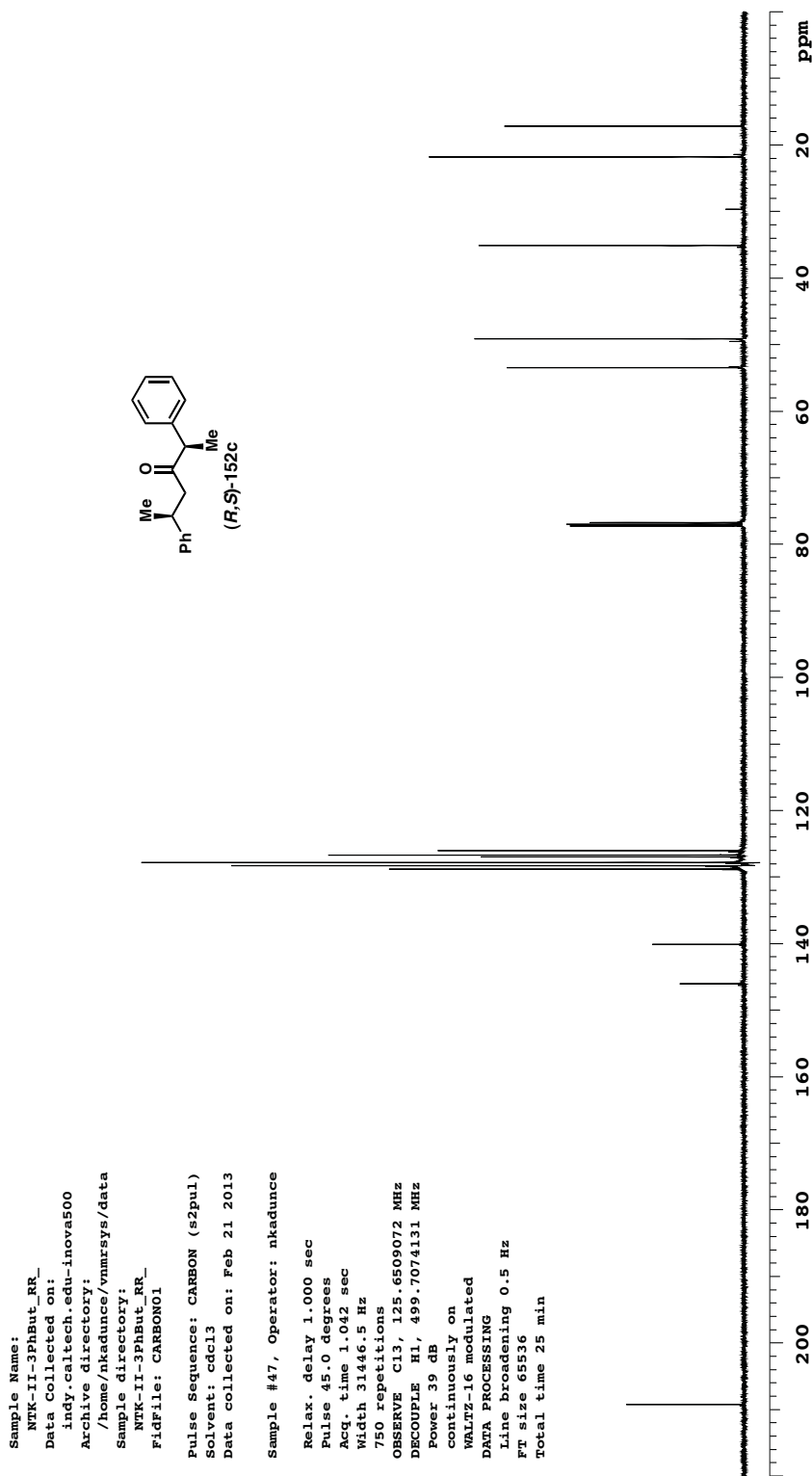


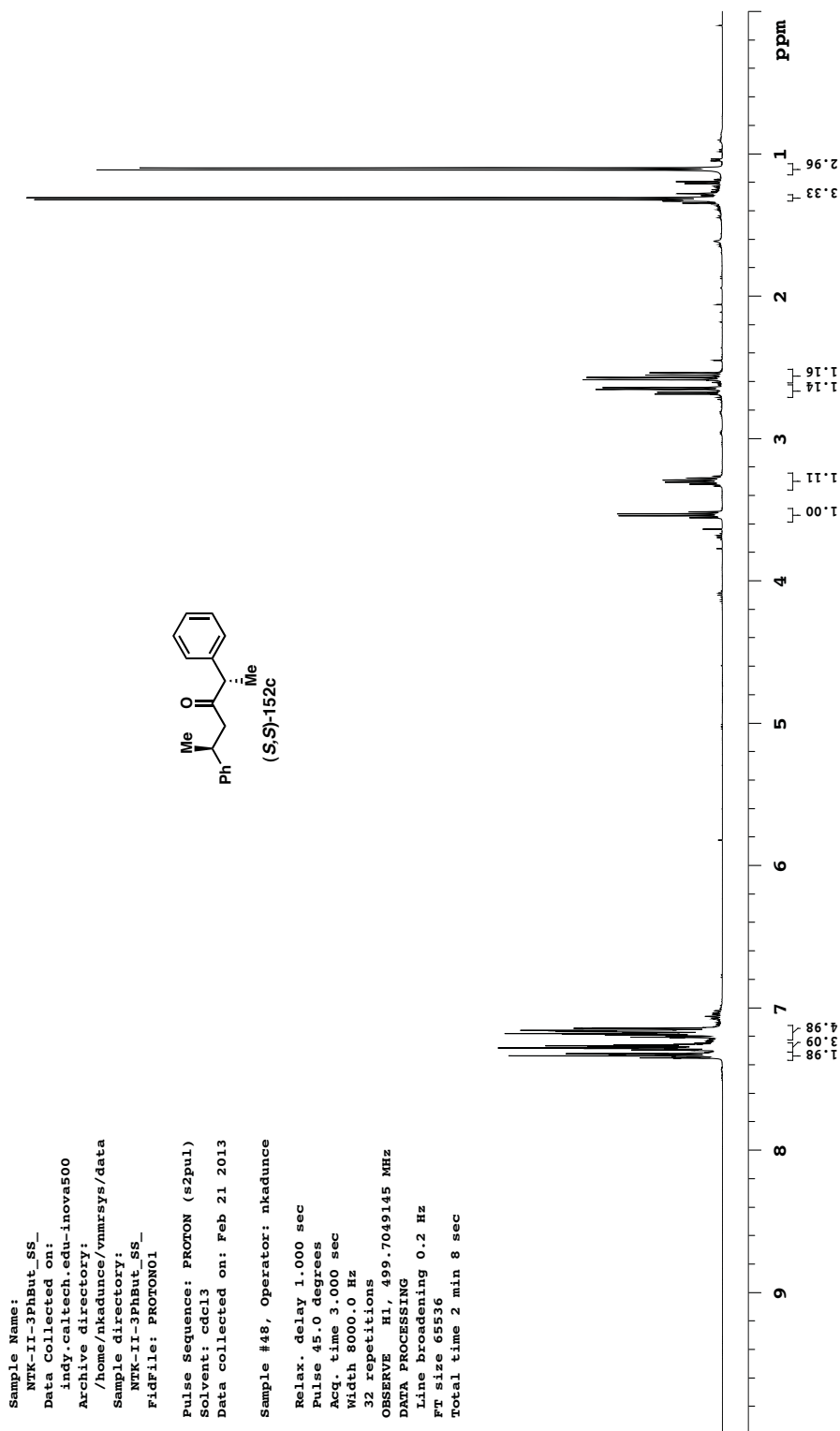


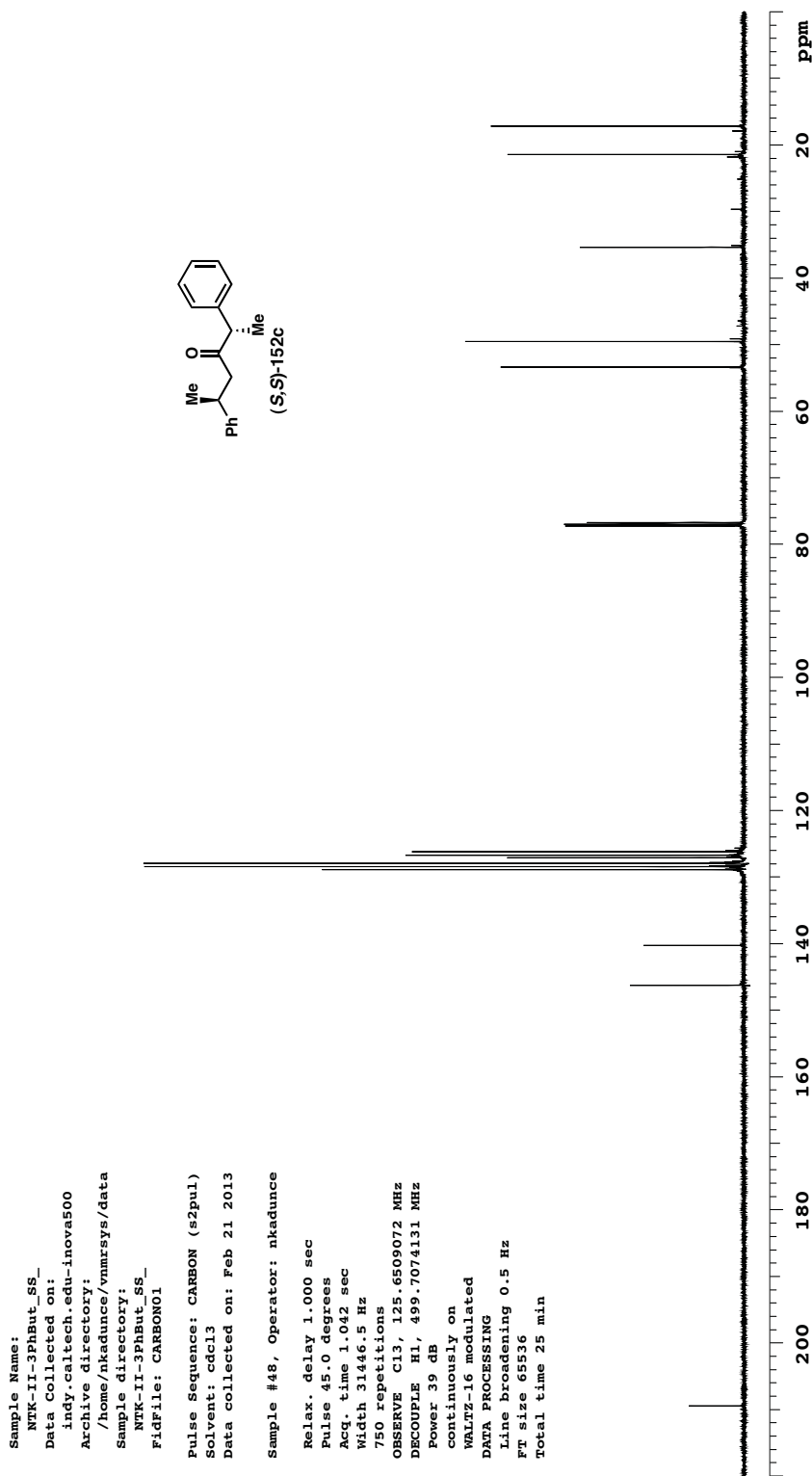


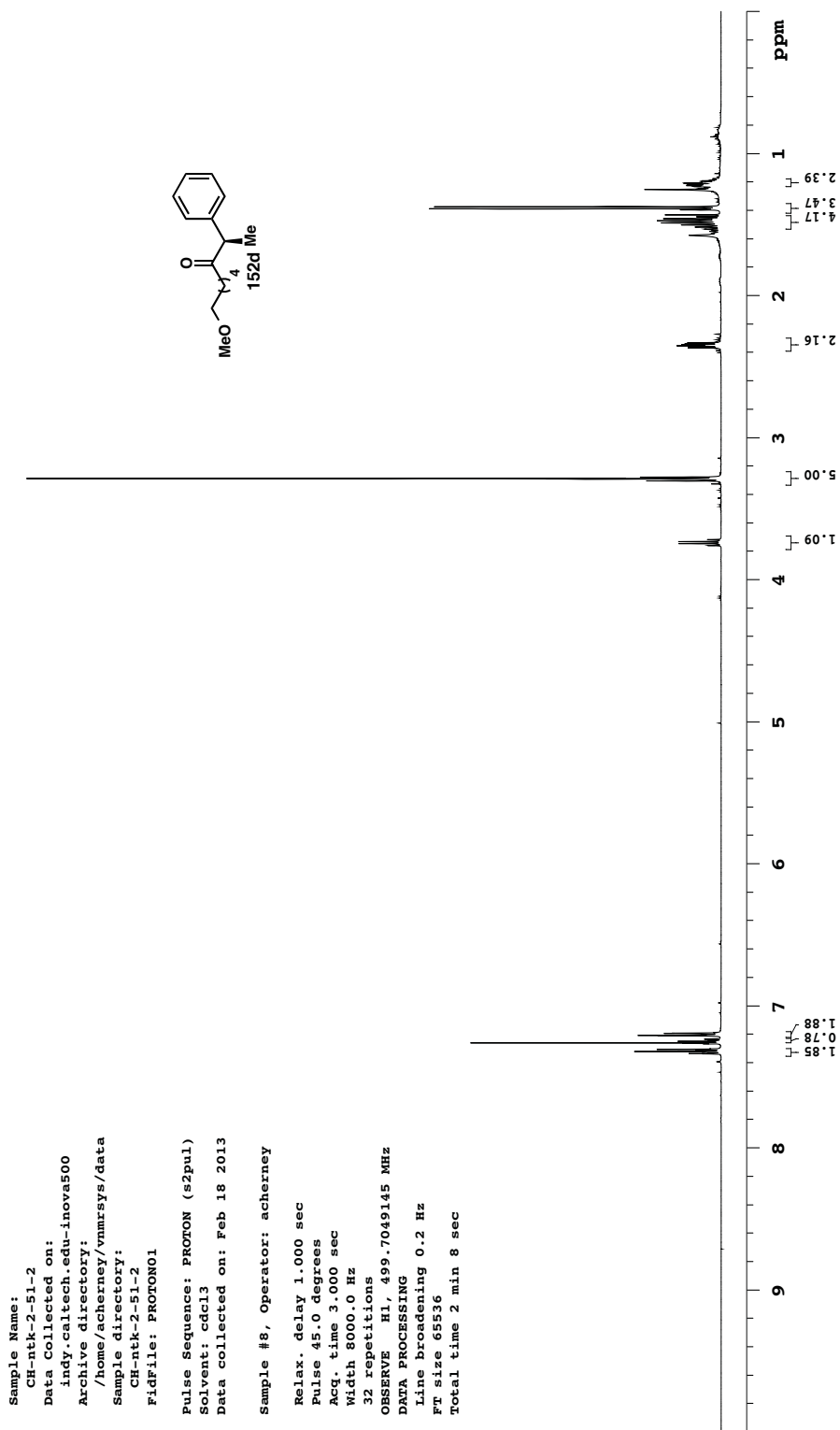
Sample Name: NTK-II-3PhBut\_RR\_  
 Data Collected on: indy.caltech.edu-inova500  
 Archive directory: /home/nkadance/vnmrsys/data  
 Sample directory: NTK-II-3PhBut\_RR\_  
 FidFile: PROTON01  
 Pulse Sequence: PROTON (s2pul)  
 Solvent: cdcl3  
 Data collected on: Feb 21 2013  
 Sample #47, Operator: nkadance  
 Relax. delay 1.000 sec  
 Pulse 45.0 degrees  
 Acq. time 3.000 sec  
 Width 8000.0 Hz  
 32 repetitions  
 OBSERVE H1, 499.7049145 MHz  
 DATA PROCESSING  
 Line broadening 0.2 Hz  
 FT size 65536  
 Total time 2 min 8 sec

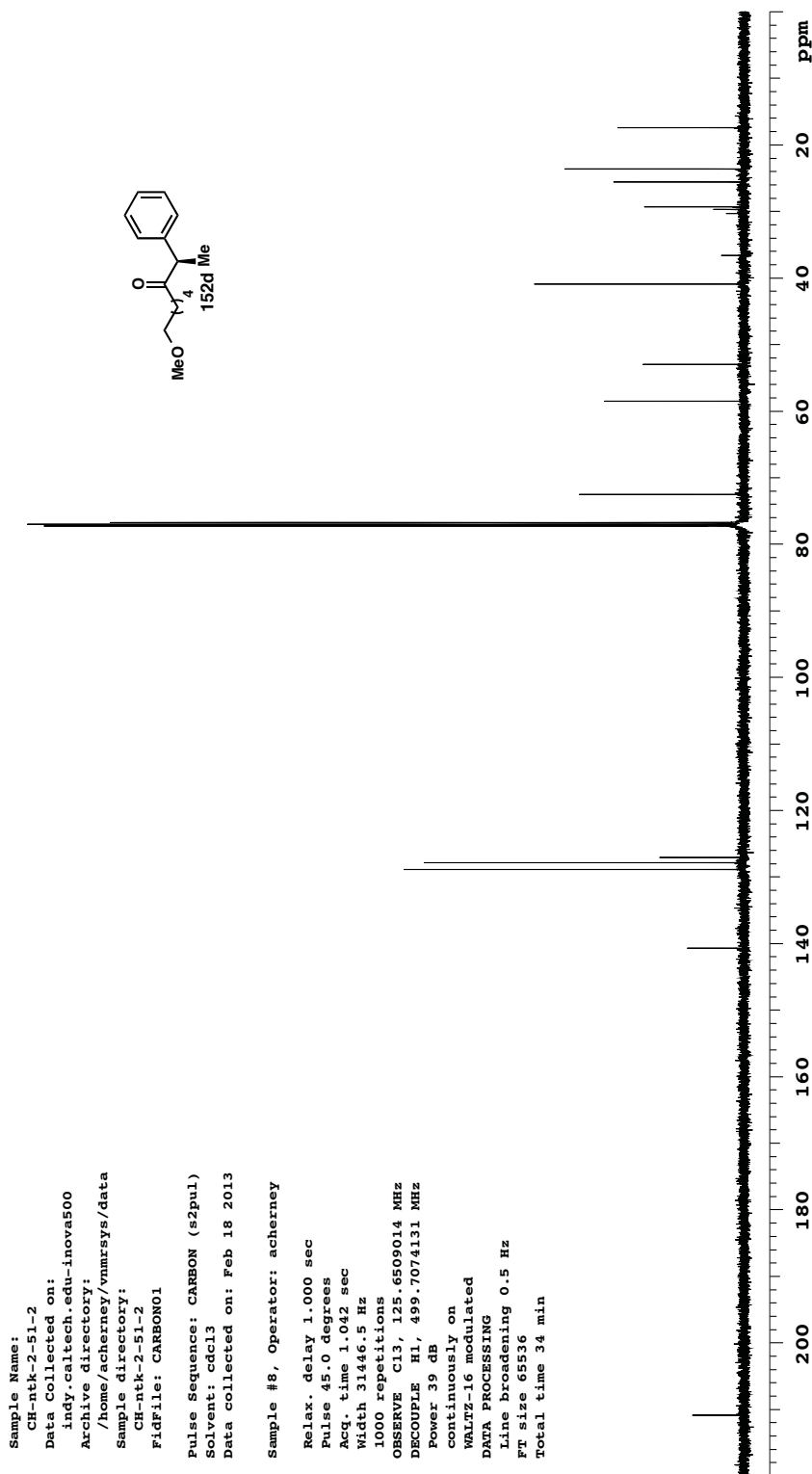




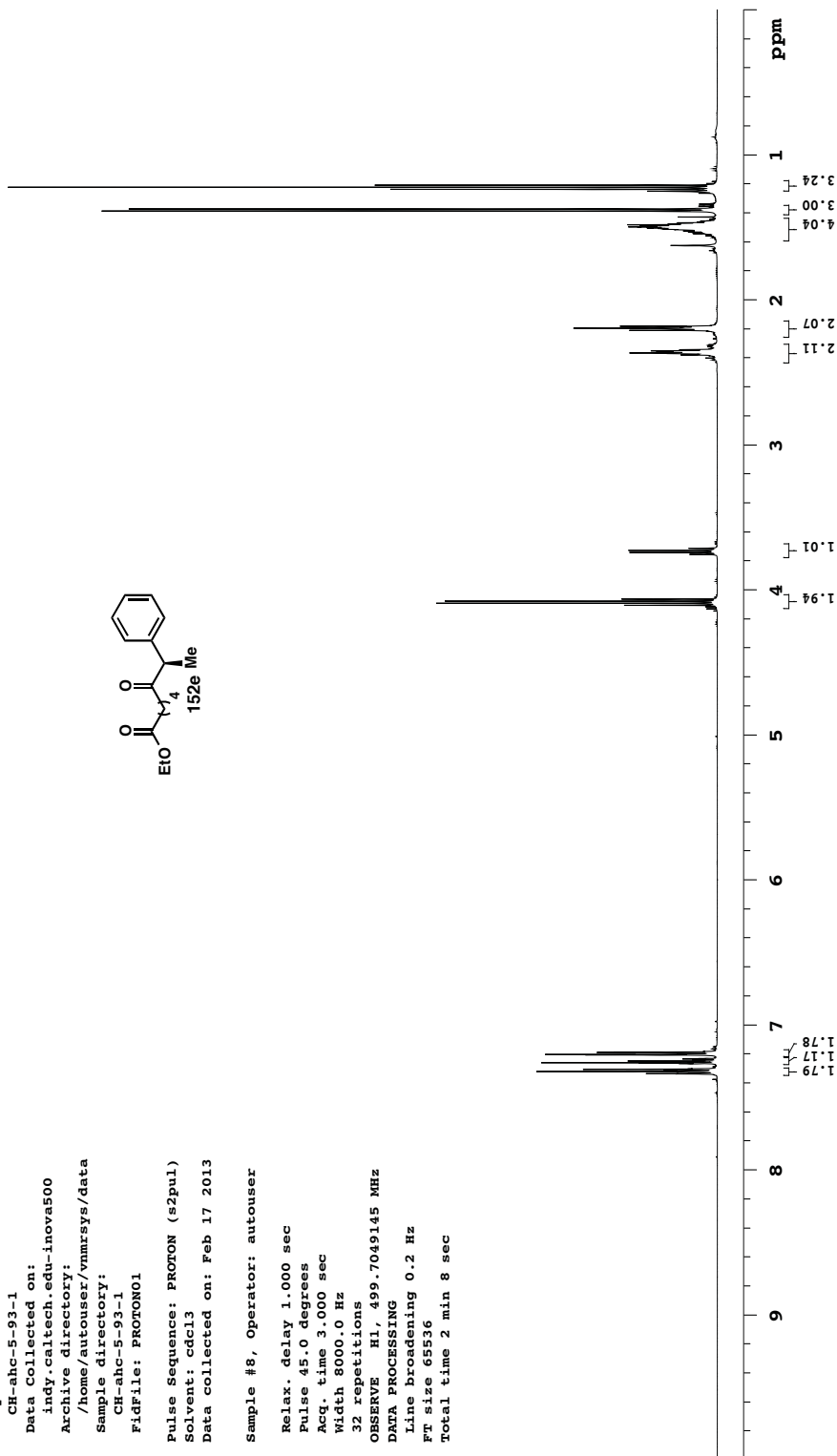
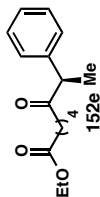


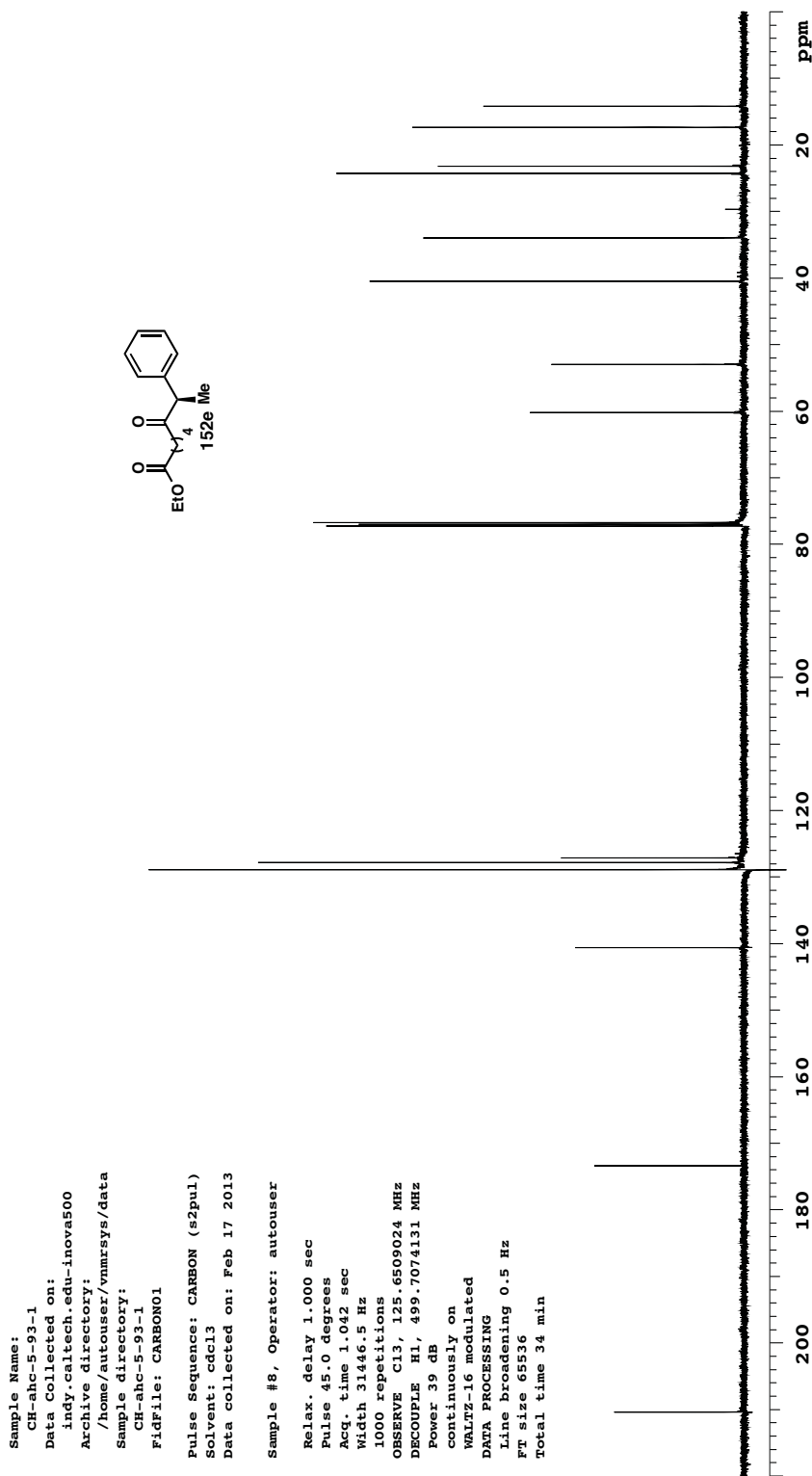


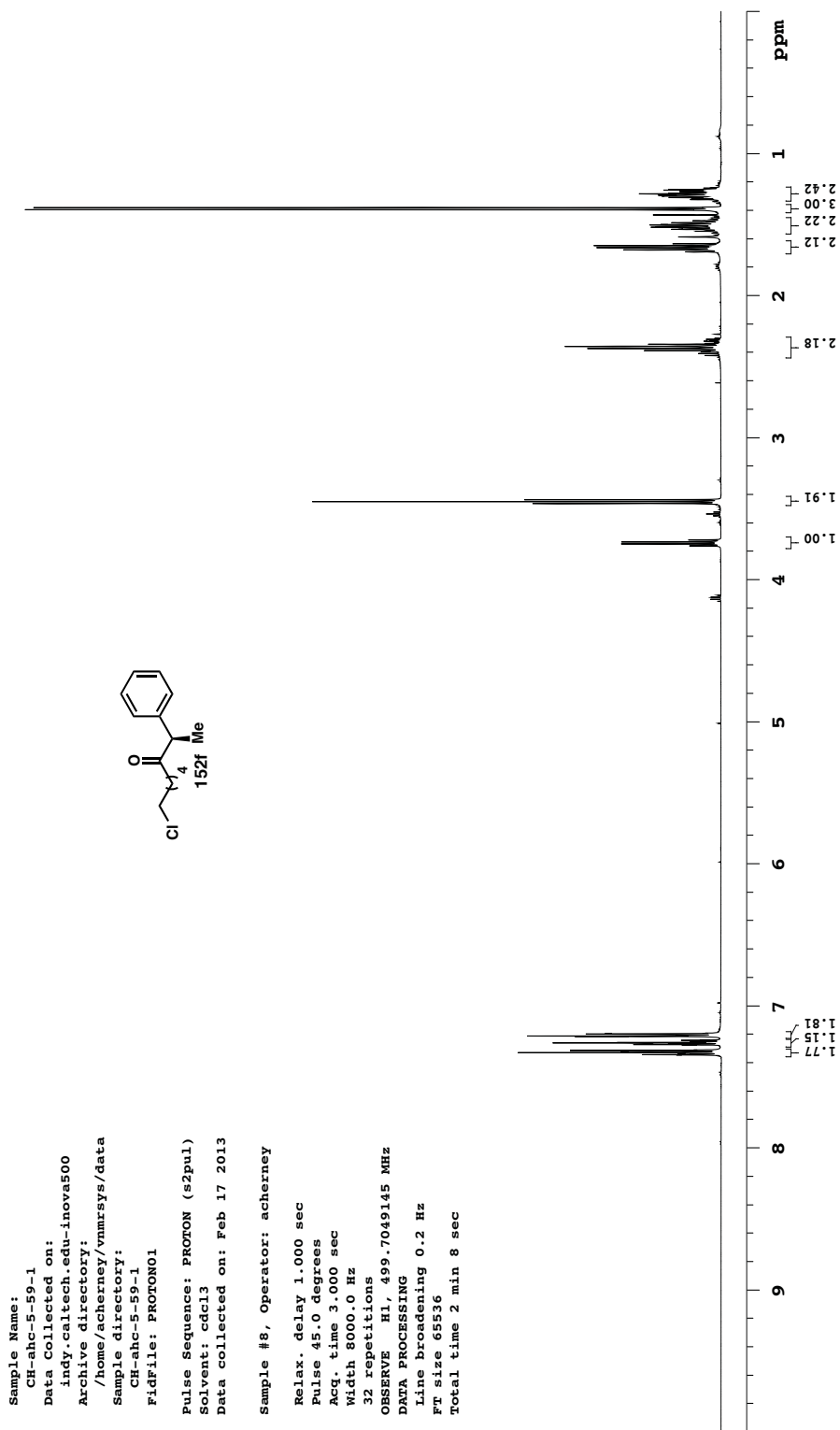


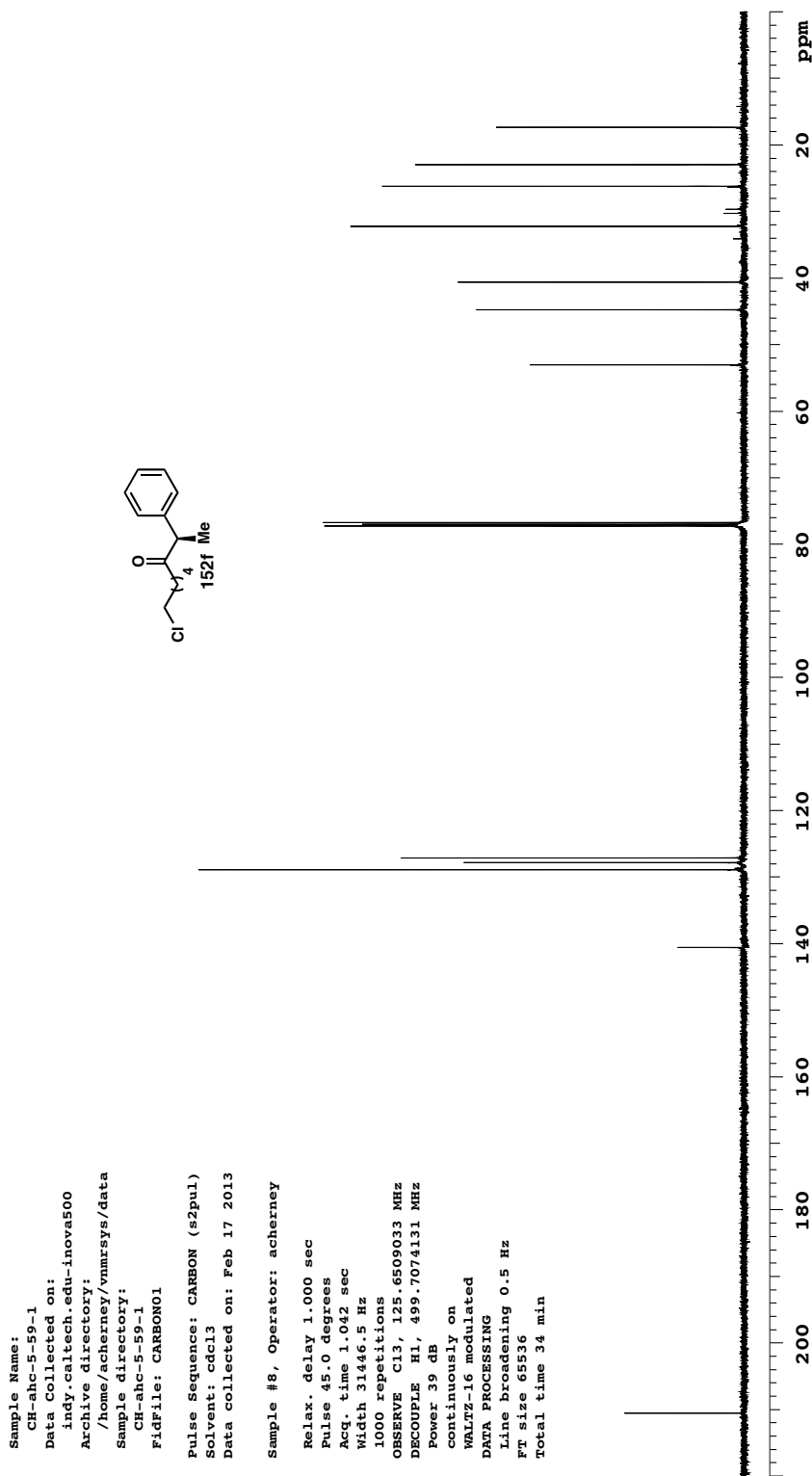


Sample Name: CH-ahc-5-93-1  
 Data Collected on: indy.caltech.edu-inova500  
 Archive directory: /home/autouser/vnmrSYS/data  
 Sample directory: CH-ahc-5-93-1  
 FidFile: PROTON01  
 Pulse Sequence: PROTON (s2pul)  
 Solvent: cdcl3  
 Data collected on: Feb 17 2013  
 Sample #8, Operator: autouser  
 Relax. delay 1.000 sec  
 Pulse 45.0 degrees  
 Acq. time 3.000 sec  
 Width 8000.0 Hz  
 32 repetitions  
 OBSERVE H1, 499.7049145 MHz  
 DATA PROCESSING  
 Line broadening 0.2 Hz  
 FT size 65536  
 Total time 2 min 8 sec

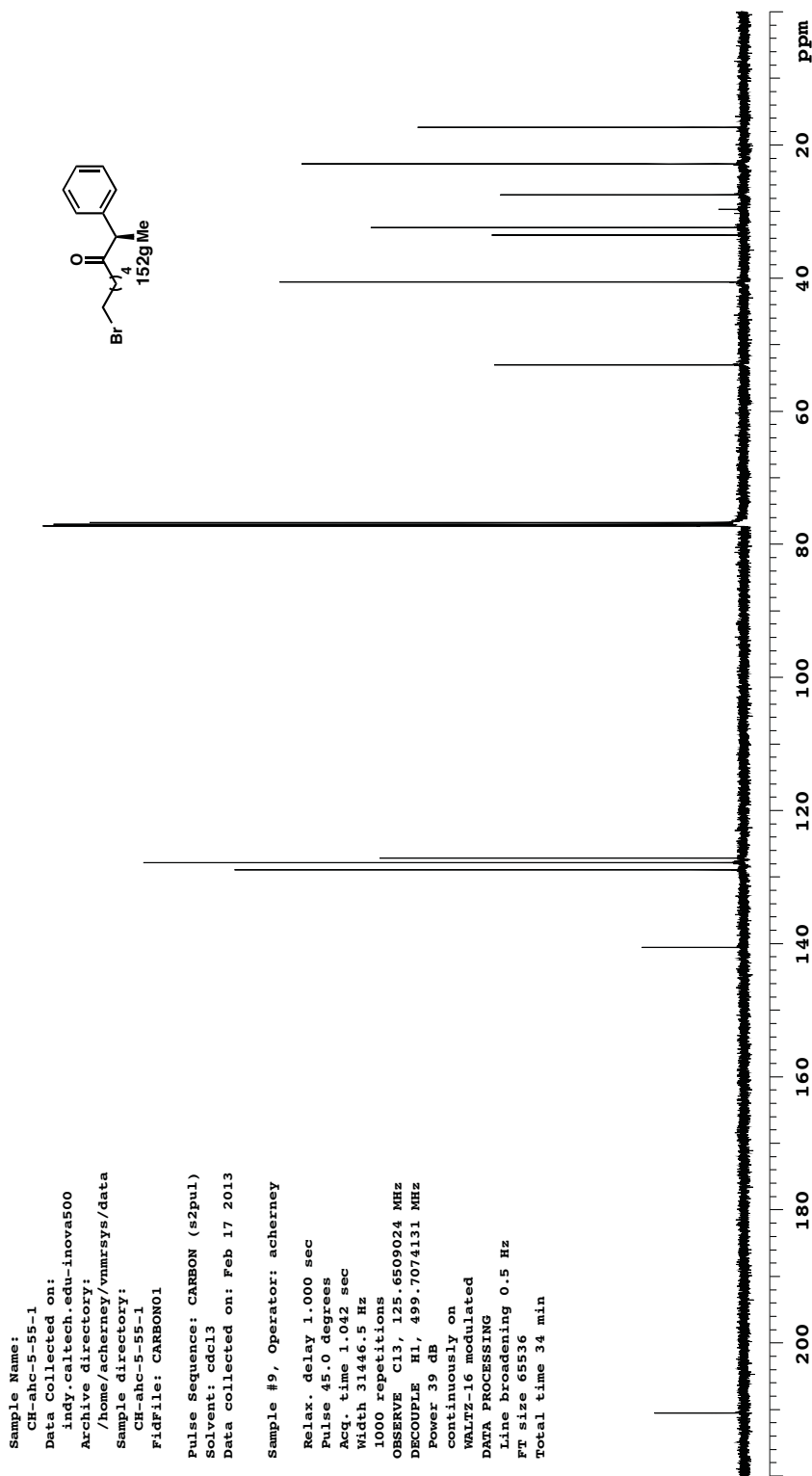


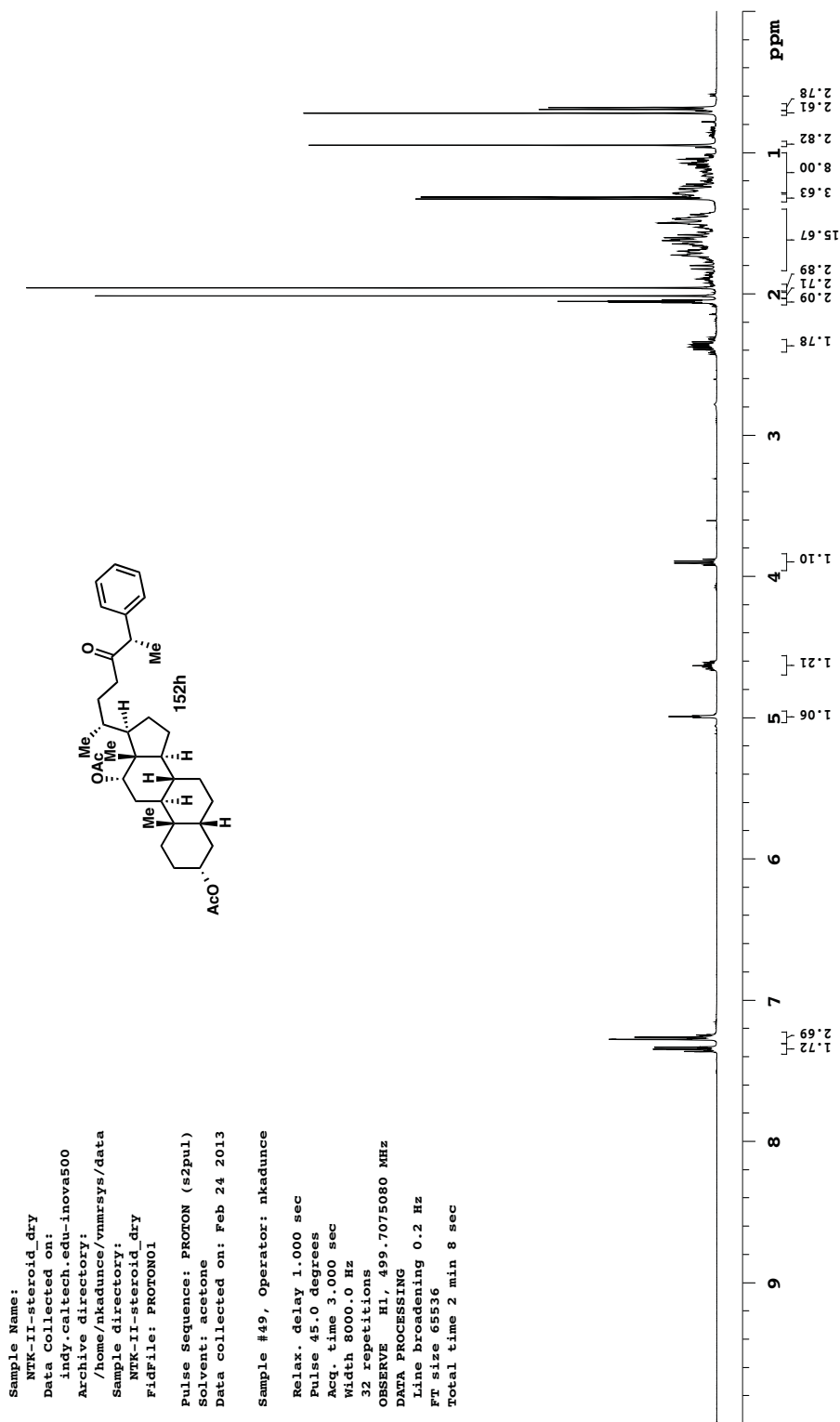














## Chapter 4

### *Nickel-Catalyzed Asymmetric Reductive Cross-Coupling Between Vinyl and Benzyl Electrophiles<sup>†</sup>*

#### 4.1 INTRODUCTION

Ni-catalyzed reductive cross-coupling reactions have recently emerged as direct methods for carbon–carbon bond formation between two organic electrophiles.<sup>1</sup> In these reactions,  $\text{Mn}^0$  or  $\text{Zn}^0$  are typically employed as stoichiometric reductants to turn over a Ni catalyst. Improvements in ligand structure and mechanistic understanding have enabled the cross-coupling between a range of  $\text{C}(\text{sp}^3)$  and  $\text{C}(\text{sp}^2)$  electrophiles bearing a variety of functional groups.<sup>2,3,4</sup> The ability to employ bench stable and readily available organic halides, without the need to pre-generate a reactive organometallic reagent, endows these reductive cross-coupling reactions with a practical advantage over many conventional cross-coupling procedures. In addition, several studies have demonstrated

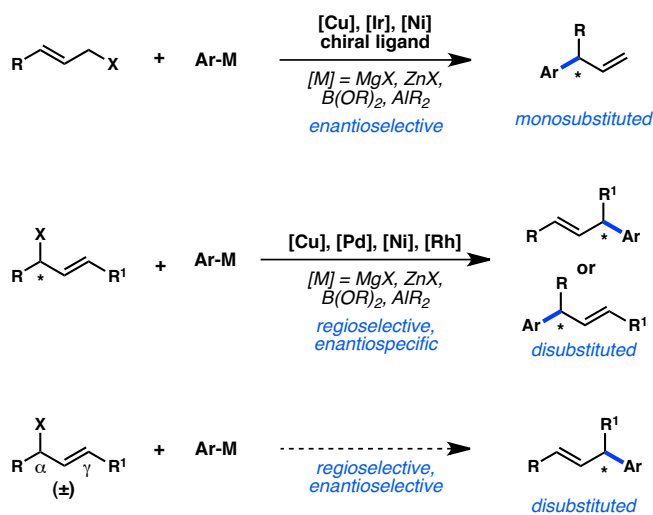
---

<sup>†</sup> Portions of this chapter have been reproduced from published studies (see reference 15) and the supporting information found therein.

that *sec*-alkyl electrophiles are competent reaction partners, providing racemic products bearing stereogenic centers.<sup>2a,b,d,e,h,3a,5</sup> The utility of such transformations would be greatly improved if rendered enantioselective, providing direct access to enantioenriched chiral products from racemic starting materials.

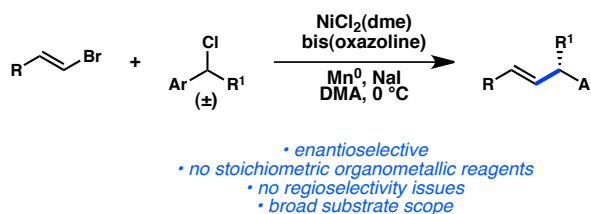
Alkenes bearing stereogenic, aryl-substituted tertiary allylic centers are synthetically useful compounds that can be challenging to prepare using conventional asymmetric allylic substitution reactions (Scheme 4.1).<sup>6,7</sup> Significant progress toward the catalytic enantioselective arylation of allylic electrophiles has been made to selectively form branched over linear *monosubstituted* products.<sup>8</sup> Stereospecific and regioselective arylation of allylic electrophiles to form *disubstituted* products has also been disclosed for a series of organometallic reagents.<sup>9</sup> However, catalysts that simultaneously induce high regio- and enantioselection in the arylation of acyclic, unsymmetrical  $\alpha,\gamma$ -disubstituted allylic electrophiles have not been developed.<sup>10</sup>

**Scheme 4.1.** Enantiocontrolled allylic arylation.



We envisioned that a Ni-catalyzed asymmetric reductive cross-coupling could provide a mild and selective alternative approach to such products.<sup>11</sup> We realized that a complementary disconnection involving a vinyl halide starting material would avoid the regioselectivity issues that often complicate reactions of  $\alpha,\gamma$ -disubstituted allylic electrophiles. Indeed, the reactivity of vinyl halides in Ni-catalyzed reductive cross-coupling reactions is well-precedented, with Semmelhack and coworkers reporting the first Ni-catalyzed homocoupling of such species in 1972.<sup>12</sup> Despite subsequent disclosures of electrochemical Ni-catalyzed couplings,<sup>13</sup> the first reductive *cross*-coupling of a vinyl halide that employed a chemical reductant such as  $\text{Mn}^0$  or  $\text{Zn}^0$  was developed by Weix and coworkers in 2012.<sup>2d</sup> Furthermore, our recent report on asymmetric reductive cross-coupling for the preparation of ketones suggested that secondary benzylic chlorides could be used to promote enantioinduction in the presence of a chiral catalyst.<sup>14</sup> In this chapter, we report a highly enantioselective Ni-catalyzed reductive cross-coupling between vinyl bromides and benzyl chlorides (Figure 4.1).<sup>15,16</sup> A variety of alkenyl products bearing allylic stereogenic centers are prepared in good yields with high enantiomeric excess under mild conditions.

**Figure 4.1.** This work: Asymmetric reductive vinyl cross-coupling.

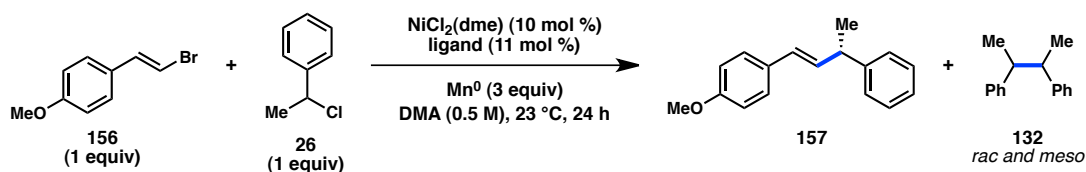


## 4.2 DEVELOPMENT OF AN ASYMMETRIC REDUCTIVE VINYL CROSS-COUPLING

### 4.2.1 Identification of a Chiral Catalyst System

Our investigations commenced with the coupling of an equimolar mixture of vinyl bromide **156** and benzyl chloride **26** using NiCl<sub>2</sub>(dme) (10 mol %), a chiral ligand (11 mol %), Mn<sup>0</sup> as the stoichiometric reductant, and DMA as solvent. A series of bis(oxazoline) ligands delivered a mixture of product **157** and butane-2,3-diylidibenzene (**132**), arising from homocoupling of **26** (Figure 4.2).<sup>17</sup> In all cases, **132** was observed as a 1:1 mixture of the *meso* and *rac* diastereomers. Formation of unreactive chlorostyrene side products, resulting from Ni-catalyzed halide exchange of **156**, was also observed.<sup>18</sup> Among simple isopropylidene-linked Box ligands, **L100** (R = Bn) delivered **157** in 71% ee while the bulky **L66** (R = <sup>t</sup>Bu) provided a nearly racemic product (entries 1–4). Tuning the ligand bite angle by investigating other linkers on the Box scaffold revealed that **L112**, bearing a cyclopropyl bridge, induced formation of **157** in 81% ee (entry 9). We next hypothesized that rigidifying the ligand framework would result in greater enantioinduction. In the event, indanyl-substituted ligands demonstrated that **L104**, also containing a cyclopropyl bridge, furnished the desired product in 89% ee (entry 11).

In addition to Box ligands, several other ligand families were also studied. Bi(oxazoline) ligands bearing less steric bulk delivered promising levels of enantioinduction (entries 12–15). Moderate enantioselectivity could also be achieved with cyanoBox **L106**. On the other hand, the PyOx, PHOX, and PyBox ligands that were tested all resulted in poor levels of asymmetric induction.

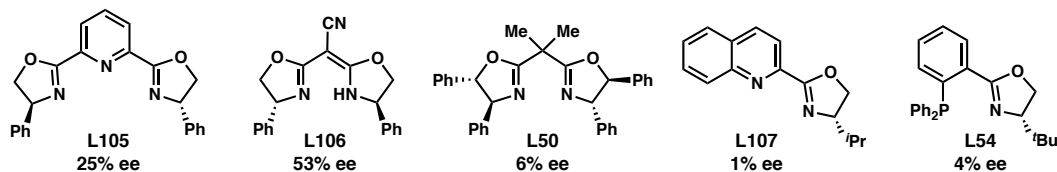
**Figure 4.2.** Evaluation of chiral ligand frameworks.

*Bis(oxazoline) Ligand Scaffold*

Entry	R <sup>1</sup>	R <sup>2</sup>	R <sup>3</sup>	Ligand	ee (%)
1	Me	<sup>t</sup> Pr	H	L99	47
2	Me	<sup>t</sup> Bu	H	L66	2
3	Me	Bn	H	L100	71
4	Me	Ph	H	L36	45
5	Me	Ph	Ph	L109	41
6	Me	<sup>t</sup> Bu	H	L110	32
7	H	Ph	H	L101	9
8	H	<sup>t</sup> Bu	H	L111	1
9	-CH <sub>2</sub> CH <sub>2</sub> -	Bn	H	L112	81
10	Me	indanyl		L51	46
11	-CH <sub>2</sub> CH <sub>2</sub> -	indanyl		L104	89

*Bi(oxazoline) Ligand Scaffold*

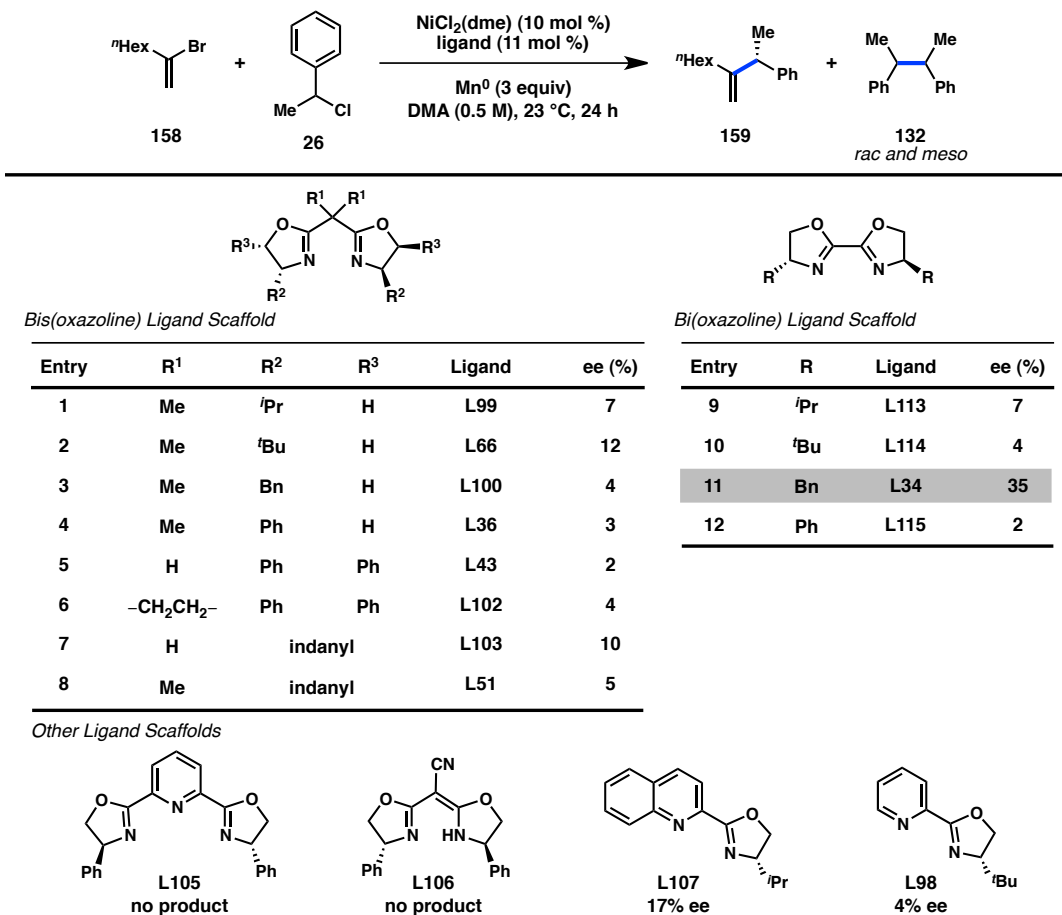
Entry	R	Ligand	ee (%)
12	<sup>t</sup> Pr	L113	33
13	<sup>t</sup> Bu	L114	5
14	Bn	L34	31
15	Ph	L115	1

*Other Ligand Scaffolds*

Having discovered a ligand that furnishes enantioenriched 1,2-disubstituted alkenes, we next pondered whether asymmetric generation of 1,1-disubstituted alkenes could also be achieved. Employing the coupling of vinyl bromide **158** and benzyl chloride **26** as a model system, we screened a variety of chiral ligands (Figure 4.3). In contrast to the reaction with styrenyl bromide **156**, bis(oxazoline) ligands resulted in poor enantioinduction (entries 1–8). On the other hand, bi(oxazoline) **L34** (R = Bn) provided a promising 35% ee of **159** (entry 11). The lower level of asymmetric induction for the

coupling of bromide **158** compared to styrenyl bromide **156** may be due to the increased steric congestion around the nickel center following oxidative addition.

**Figure 4.3.** Preparation of 1,1-disubstituted alkenes.

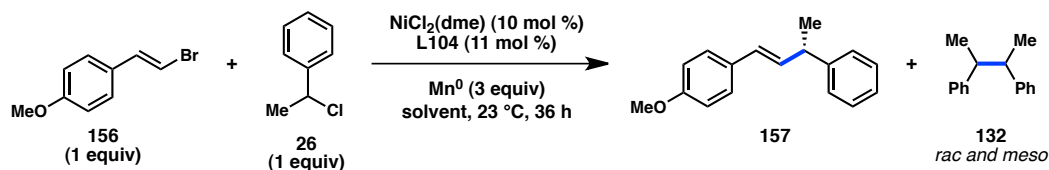


#### 4.2.2 Optimization of Reactivity for an Enantioselective Reaction

With indanyl-substituted ligand **L104** in hand, we next investigated other reaction parameters to increase the yield of our desired transformation. Polar solvents with high dielectric constants provided the greatest yields of product **157** (Table 4.1, entries 1–4). In contrast to our previous acyl coupling, THF delivered reduced enantioinduction

compared to DMA. Overall, the enantioselectivity of the cross-coupling was not very sensitive to the choice of solvent as long as highly polar solvents were chosen. Under the best conditions, product **157** could be obtained in a 3:1 ratio with homocoupled product **132**.

**Table 4.1.** Evaluation of solvents.

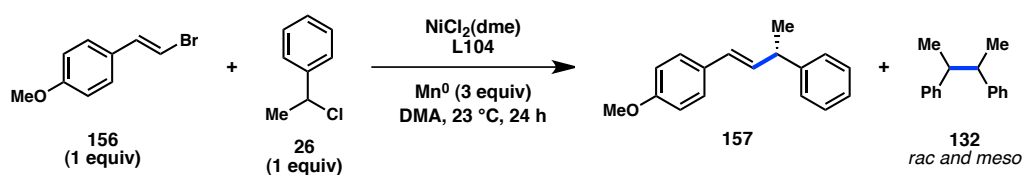


Entry	Solvent	Conversion (%)	Yield (%)	157:132	ee (%)
1	DMA	100	62	3:1	87
2	DMF	100	48	2:1	86
3	DMPU	100	57	2.5:1	89
4	NMP	100	51	2.5:1	91
5	DME	18	trace	--	45
6	dioxane	16	trace	--	3
7	THF	100	38	1.5:1	75
8	MeCN	39	10	1:1	2
9	EtOAc	100	33	1:1	15
10	CH <sub>2</sub> Cl <sub>2</sub>	21	trace	--	3

We next studied the effects of concentration, catalyst loading, and additives. Increasing the reaction concentration to 1.0 M raised the product yield to 69% with a concomitant improvement in the ratio of product to homocoupling (Table 4.2, entries 1–3). We next observed that lowering the catalyst loading below 10% led to a reduction in the selectivity for product formation over homocoupling without significantly altering the enantioinduction (entries 2, 4, and 5). With respect to additives, treatment with 2,6-dimethylbenzoic acid (DMBA), which was employed in our previous acyl coupling, led to a significant drop in yield and favored homodimer formation (entry 6).<sup>14</sup> On the other

hand, exposure to 0.5 equiv NaI improved the yield of product **157** and the selectivity for heterocoupling (entry 7). Several potential factors might be attributed to the beneficial role of NaI, which has previously found use in reductive cross-couplings.<sup>2d</sup> The iodide ion may be able to facilitate electron transfer between Ni and Mn by acting as a bridge between the two metals.<sup>19</sup> Improved reactivity may also be the result of ligand exchange on Ni<sup>20</sup> or the formation of a more reactive nickelate species.<sup>21</sup>

**Table 4.2.** Evaluation of other reaction parameters.



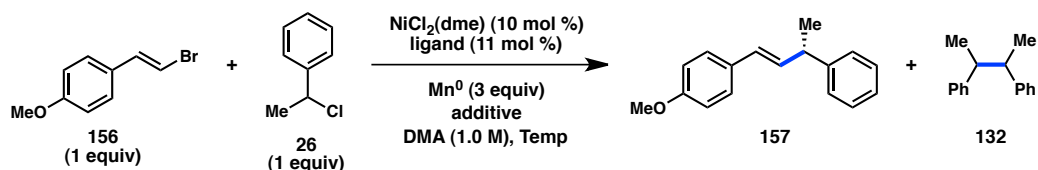
Entry	Concentration (M)	Cat. Loading (%)	Additive	Yield (%)	157:132	ee (%)
1	0.25	10	--	58	3:1	89
2	0.5	10	--	61	3:1	89
3	1.0	10	--	69	4.5:1	87
4	0.5	5	--	50	2:1	91
5	0.5	2.5	--	46	1.5:1	88
6	0.5	5	DMBA	16	1:2.5	76
7	0.5	5	NaI	75	5.5:1	93

Alternatively, excess iodide may lead to in situ formation of organoiodide electrophiles. Generation of benzyl iodide in situ should lead to increased formation of homocoupling and is therefore unlikely. In contrast, crude reaction mixtures that did not proceed with complete conversion often revealed the presence of vinyl bromide **156** with competing amounts of the corresponding vinyl chloride and vinyl iodide. We rationalized that oxidative addition of Ni to bromide **156** is a reversible process; ligand exchange with a chloride followed by irreversible reductive elimination delivers a vinyl chloride side product, reducing the yield of desired product **157**.<sup>22</sup> Chloride ion, derived from benzyl

chloride **26**, increases over the course of the reaction. Addition of excess iodide could produce Ni-iodide complexes instead of Ni-chloride complexes. Importantly, reductive elimination from the vinyl-Ni-iodide complex would be reversible and not lead to a reduction in yield.

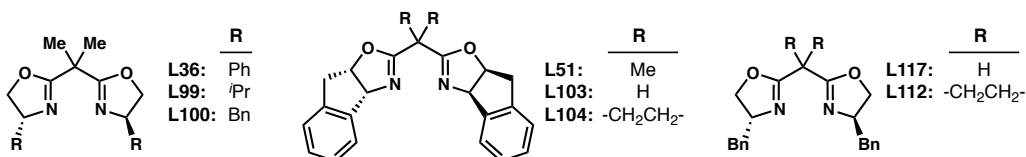
A summary of our optimization efforts for the coupling of vinyl bromide **156** and benzyl chloride **26** is shown in Table 4.3. Several isopropylidene-linked bis(oxazoline) ligands delivered product **157** in moderate yield and enantioselectivity, but favored formation of butane-2,3-diylidibenzene (**132**), arising from homocoupling of **26** (entries 1–3). Formation of unreactive chlorostyrene side products, resulting from Ni-catalyzed halide exchange of **156**, was also observed. Indanyl-substituted ligand **L51** slightly improved the selectivity, permitting formation of **157** in 26% yield and 70% ee (entry 4). Tuning the bite angle of the ligand by changing the central linker revealed that cyclopropyl-linked ligand **L104** produced **157** in 56% yield and 87% ee, favoring heterocoupling over homocoupling (entry 6).

The reaction was further optimized through systematic study of several parameters. Trifluoroacetic acid (TFA) and trimethylsilyl chloride (TMSCl), additives known to activate the  $\text{Mn}^0$  surface, failed to increase reaction efficiency (entries 9 and 10). In contrast, iodide sources, such as NaI or TBAI, improved the yield of **157** and decreased the yield of **132** (entries 11 and 12). Significantly, lowering the reaction temperature to 0 °C produced **157** in 93% yield and 93% ee (entry 13). A series of control experiments confirmed that product was not formed in the absence of  $\text{Mn}^0$ ,  $\text{Ni}^{\text{II}}$  precatalyst, or ligand; significant decomposition of vinyl bromide **156** was also detected in the absence of ligand (entries 15–17).

**Table 4.3.** Optimization of Ni-catalyzed asymmetric reductive coupling.

Entry <sup>a</sup>	Ligand	Additive	Temp (°C)	Yield <b>132</b> (%) <sup>b</sup>	Yield <b>157</b> (%) <sup>b</sup>	ee <b>157</b> (%) <sup>c</sup>
1	L36	--	20	48	50	40
2	L99	--	20	33	21	57
3	L100	--	20	38	25	68
4	L51	--	20	35	26	70
5	L103	--	20	21	33	49
6	L104	--	20	20	56	87
7	L117	--	20	26	20	27
8	L112	--	20	21	56	78
9	L104	TFA	20	30	39	86
10	L104	TMSCl	20	26	33	73
11	L104	Nal <sup>d</sup>	20	17	67	87
12	L104	TBAI <sup>d</sup>	20	13	64	91
13	L104	Nal <sup>d</sup>	0	8	93	93
14 <sup>e</sup>	L104	Nal <sup>d</sup>	0	8	69	89
15 <sup>f</sup>	L104	Nal <sup>d</sup>	0	0	0	--
16 <sup>g</sup>	L104	Nal <sup>d</sup>	0	0	0	--
17	--	Nal <sup>d</sup>	0	0	0	--

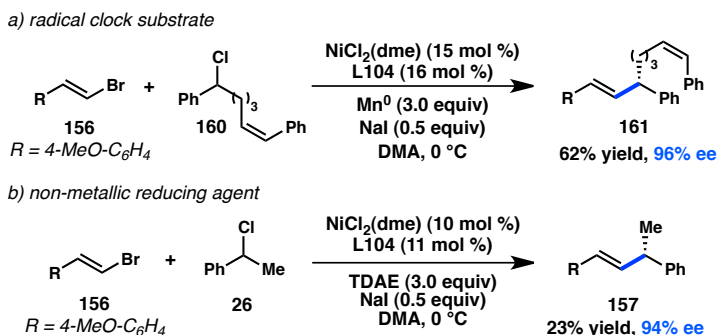
<sup>a</sup> Reactions conducted under  $\text{N}_2$  on 0.2 mmol scale for 6 h. <sup>b</sup> Determined by GC versus an internal standard. <sup>c</sup> Determined by SFC using a chiral stationary phase. <sup>d</sup> 0.5 equiv. <sup>e</sup>  $\text{Zn}^0$  used instead of  $\text{Mn}^0$ . <sup>f</sup> No  $\text{Mn}^0$ . <sup>g</sup> No  $\text{NiCl}_2(\text{dme})$ .



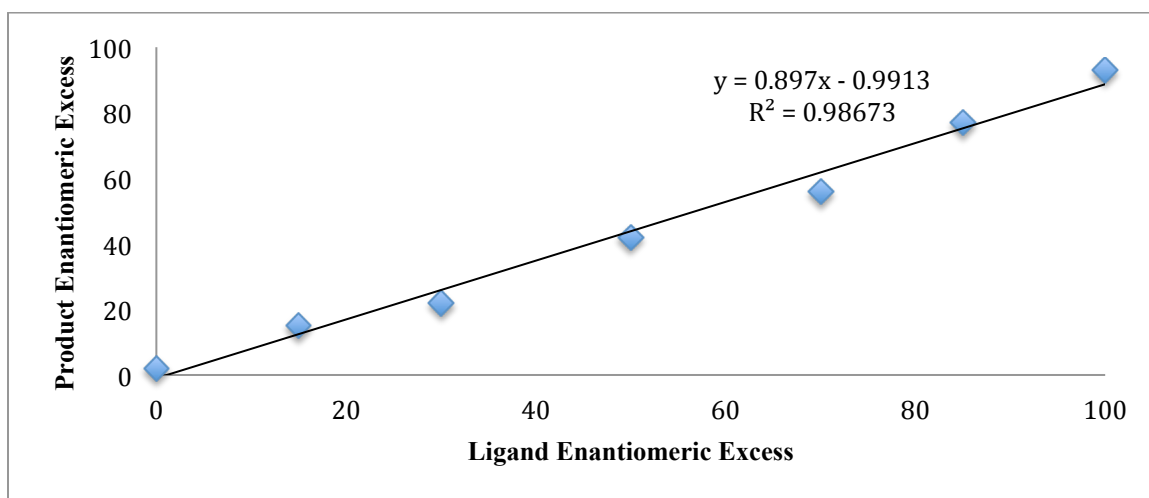
A series of experiments were conducted to provide insight into the reaction mechanism.<sup>23</sup> The reaction proceeds cleanly in the presence of the radical inhibitor 2,6-bis(1,1-dimethylethyl)-4-methylphenol (BHT, as high as 50 mol %).<sup>24</sup> In addition, radical clock substrate **160** was found to couple in good yield, without detection of any cyclized product or isomerization of the olefin geometry (Scheme 4.2, a). Taken together, these

two results appear inconsistent with a radical chain reaction mechanism and suggest that if oxidative addition of **160** occurs by a step-wise mechanism, radical recombination is rapid and precludes cyclization.<sup>25</sup> The reaction proceeds with the same enantioselectivity when tetrakis(*N,N*-dimethylamino)ethylene (TDAE) is employed as the stoichiometric reductant, although the yield is reduced (Scheme 4.2, b).<sup>26</sup> This finding indicates that cross-coupling of an in situ-generated organomanganese reagent is unlikely. Lastly, use of enantioenriched benzyl chloride **26**, in either the presence or absence of NaI under otherwise optimized conditions, still delivers product **157** in 94% ee, illustrating the stereoconvergent nature of the transformation. Additional work is required to fully elucidate the reaction mechanism and the origin of enantioinduction.

**Scheme 4.2.** Mechanistic investigations.



Previous mechanistic studies by Amatore and Jutand have suggested that various reactive intermediates of Ni may aggregate under the reaction conditions.<sup>23a</sup> To assess the role of a reservoir effect in our system, we studied whether our enantioinduction exhibited any non-linear effects. As we increased the ee of scalemic ligand, we observed a linear increase in the ee of cross-coupled product **157** (Figure 4.4). This result suggests that a monomeric Ni complex is responsible for carrying out the cross-coupling reaction and that the active catalyst does not undergo reversible aggregation during the reaction.

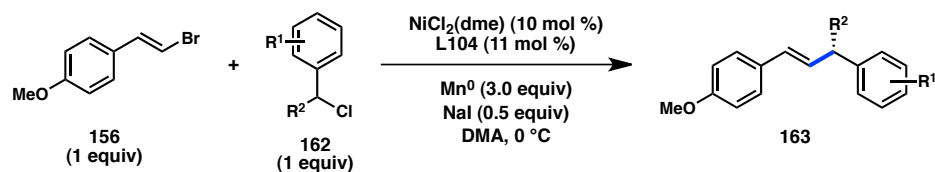
**Figure 4.4.** Examination of non-linear effects.

### 4.2.3 Substrate Scope and Further Studies

With optimized conditions in hand, we investigated the scope of the C(sp<sup>3</sup>) coupling partner. A variety of benzyl chlorides can be coupled in high yield and high enantioselectivity (Table 4.4). Whereas *meta* and *para* substitution is well-tolerated, *ortho* substituents result in lower yield and ee (entries 2–4). Functional groups such as methoxide, fluoride, chloride, bromide, and trifluoromethoxide are tolerated (entries 5–9); however, in some cases increased levels of the butane-2,3-diyldiarene product is observed. We recalled that decreasing the catalyst loading was previously found to erode the selectivity for heterocoupling over homocoupling (see Table 4.2). We reasoned that increasing the catalyst loading might therefore decrease the level of homocoupling. Indeed, for these substrates, improved results are achieved with 15 mol % catalyst loading. For example, the yield of chloride **163g** rises from 54% to 76% when the catalyst loading increases from 10% to 15%. We were pleased to find that  $\beta$ -substituted

benzyl chlorides react with no erosion of ee as compared to the parent substrate **162a** (entries 10–14). Alkenyl substrate **162l**, potentially capable of cyclization under radical conditions, exclusively produced uncyclized product **163l** (entry 12). A substrate bearing a free alcohol can also be coupled in high yield and ee (entry 13).

**Table 4.4.** Substrate scope of benzyl chlorides.



Entry	R <sup>1</sup>	R <sup>2</sup>	Pdt	Yield (%) <sup>a</sup>	ee (%) <sup>b</sup>
1	H	Me	163a	91	93
2	4-Me	Me	163b	82	94
3	3-Me	Me	163c	88	93
4 <sup>c</sup>	2-Me	Me	163d	44	85
5	4-OMe	Me	163e	64	93
6	4-F	Me	163f	81	89
7 <sup>c</sup>	4-Cl	Me	163g	75	88
8	4-Br	Me	163h	59	90
9 <sup>c</sup>	4-OCF <sub>3</sub>	Me	163i	84	88
10	H	Et	163j	80	97
11	H	Bn	163k	82	93
12	H	4-pentenyl	163l	68	94
13	H	2-hydroxyethyl	163m	81	96
14 <sup>c</sup>	H	2-chloroethyl	163n	60	94

<sup>a</sup> Isolated yield, reactions conducted under N<sub>2</sub> on 0.2 mmol scale for 6 h. <sup>b</sup> Determined by SFC using a chiral stationary phase. <sup>c</sup> Run with 15 mol %  $\text{NiCl}_2(\text{dme})$  and 16 mol % **L104**.

A broad scope of styrenyl bromides undergoes the cross-coupling to furnish products in good yields and enantioselectivities (Table 4.5). Regardless of the substitution pattern on the aryl ring of the styrene, a tight window of ee's (93–96%) is achieved. Higher catalyst loadings are sometimes necessary to mitigate formation of **132**. Notably, the dimethylamino (**157g**) and pinacol boronate (**157j**) functional groups are

compatible with the reaction. Both protected and free phenols also deliver the desired product in high yield (entries 6 and 11).

**Table 4.5.** Substrate scope of styrenyl bromides.

Entry	R	Pdt	Yield (%) <sup>a</sup>	ee (%) <sup>b</sup>
1	4-Me-C <sub>6</sub> H <sub>4</sub>	157a	83	96
2	4-F-C <sub>6</sub> H <sub>4</sub>	157b	74	94
3 <sup>c</sup>	4-Cl-C <sub>6</sub> H <sub>4</sub>	157c	66	95
4 <sup>c</sup>	4-CF <sub>3</sub> -C <sub>6</sub> H <sub>4</sub>	157d	49	94
5 <sup>c</sup>	4-OCF <sub>3</sub> -C <sub>6</sub> H <sub>4</sub>	157e	81	94
6 <sup>c</sup>	4-OTBS-C <sub>6</sub> H <sub>4</sub>	157f	82	96
7 <sup>c</sup>	4-NMe <sub>2</sub> -C <sub>6</sub> H <sub>4</sub>	157g	55	95
8 <sup>c</sup>	2,3-diMe-C <sub>6</sub> H <sub>3</sub>	157h	76	96
9 <sup>c</sup>	3,4-diMeO-C <sub>6</sub> H <sub>3</sub>	157i	73	95
10 <sup>c</sup>	4-Bpin-C <sub>6</sub> H <sub>4</sub>	157j	59	94
11	4-OH-C <sub>6</sub> H <sub>4</sub>	157k	86	93

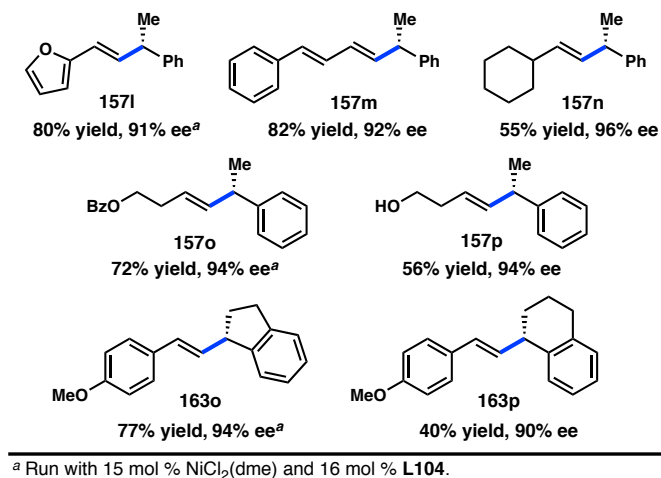
<sup>a</sup> Isolated yield, reactions conducted under N<sub>2</sub> on 0.2 mmol scale for 6 h.

<sup>b</sup> Determined by SFC using a chiral stationary phase. <sup>c</sup> Run with 15 mol % NiCl<sub>2</sub>(dme) and 16 mol % L104.

At this point, it was unclear whether either the reactivity or selectivity profile was dependent on our choice of an activated styrenyl halide. Studies on an asymmetric Kumada–Corriu cross-coupling by Knochel and coworkers demonstrated a significant drop in enantioselectivity as styrenyl halides were replaced with simple alkyl-substituted vinyl halides.<sup>27</sup> In contrast, we were delighted to observe that the reductive cross-coupling can be extended beyond styrenyl systems; for example, furan **157i** and diene **157m** are prepared in good yield and high ee (Figure 4.5). Non-conjugated vinyl bromides are also suitable reaction partners (**157n–p**), allowing for the preparation of products bearing either a free or protected alcohol. Cyclic benzylic halides (**162o** and

**162p**) can be cross-coupled with minimal erosion of enantioselectivity, exemplifying the wide scope of the enantioselective transformation.

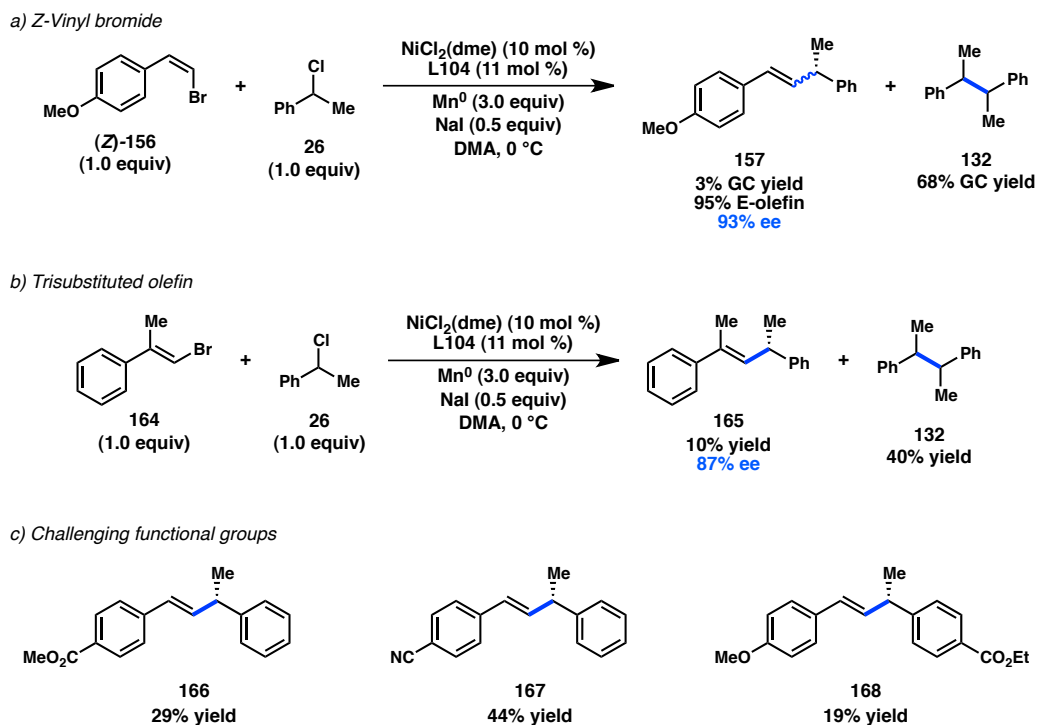
**Figure 4.5.** Beyond styrenyl halides.



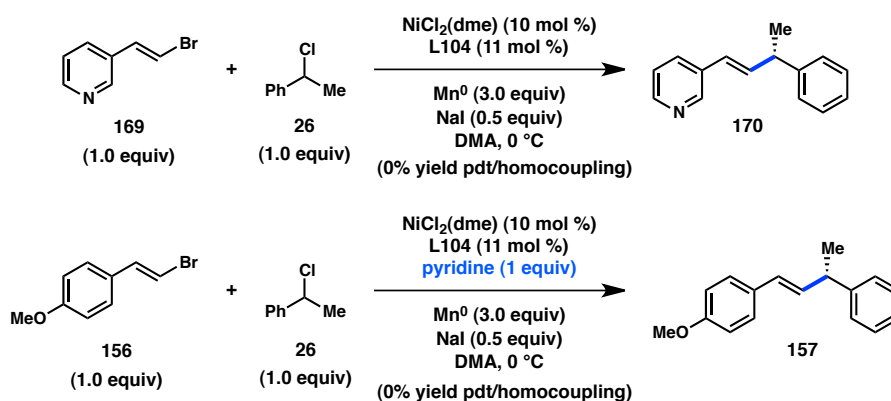
Several key limitations to the established substrate scope still exist. The transformation remains sensitive to increased steric hindrance on either reaction partner, as evidenced by a decreased yield in the coupling of *o*-substituted benzyl chloride **162d**. Similarly, (*Z*)-**156** fails to couple with retention of olefin geometry, instead delivering trace quantities of (*E*)-**157** (Scheme 4.3, a). The poor result may be due to increased steric congestion intrinsic to oxidative addition of a *Z*-olefin compared to an *E*-olefin; sluggish oxidative addition would explain the high yield of homocoupling product **132**. In a similar fashion, trisubstituted olefin **164** delivered high yields of homodimer **132** and only a 10% yield of **165**, albeit with 87% ee (Scheme 4.3, b). This result can also be attributed to an increase in steric congestion on the vinyl bromide coupling partner. Several functional groups still maintain poor compatibility with the optimized reaction conditions, including aryl esters and aryl nitriles (Scheme 4.3, c). In general, substrates

bearing aryl carbonyl groups provide reduced yields of the desired product and increased levels of homocoupling.

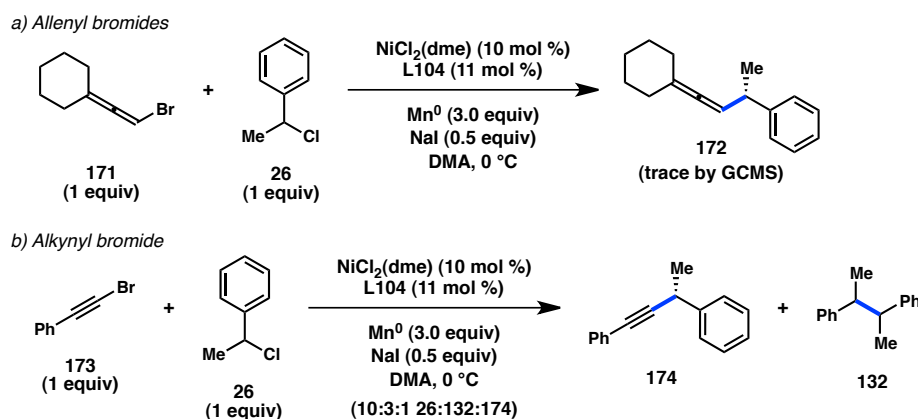
**Scheme 4.3.** Limitations of substrate scope.



Encouraged by positive results in the preparation of furan **1571**, we tested whether a pyridine substituent can be tolerated. Exposure of pyridyl substrate **169** and benzyl chloride **26** to the optimized reaction conditions failed to deliver any cross-coupling or homocoupling products (Scheme 4.4). Reasoning that substrate **169** might inhibit the activity of Ni through coordination, we examined the coupling of styrenyl bromide **156** in the presence of 1 equiv pyridine as an additive. As before, no desired cross-coupling or homocoupling was observed. These studies confirm the inhibitory effect of certain nitrogen heterocycles and highlight the need to develop reaction conditions that are tolerant of such motifs.

**Scheme 4.4.** Tolerance of pyridines.

We hypothesized that unhindered allenyl bromides may react similarly to vinyl bromides. Under our optimized reaction conditions, allene **171** only formed trace amounts of product **172** (Scheme 4.5, a). The main side products were homocoupling of both bromide **171** and chloride **26**. Reexamining racemic coupling conditions with different solvents (DMA, DMPU, NMP, THF) and ligands (dtbpy, terpy, phen) revealed that product **172** was still not detected. Alkynyl bromide **173** was also tested under the optimized conditions, delivering a 10:3:1 ratio of starting material **26** to homodimer **132** to cross-coupled product **174** (Scheme 4.5, b). Further studies on increasing the yield of the C(sp) coupling have not been initiated.

**Scheme 4.5.** Coupling of allenyl and alkynyl bromides.

### 4.3 CONCLUDING REMARKS

In conclusion, a highly enantioselective reductive cross-coupling between vinyl bromides and benzyl chlorides has been developed. The reaction occurs under mild conditions and is tolerant of a variety of functional groups, providing products in good yields and high enantioselectivities. Preliminary mechanistic studies do not support the existence of a long-lived free radical, although further experiments are necessary. This work provides further evidence of the feasibility of developing a broad range of asymmetric reductive cross-coupling reactions, an endeavor that is currently ongoing in our laboratory.

### 4.4 EXPERIMENTAL SECTION

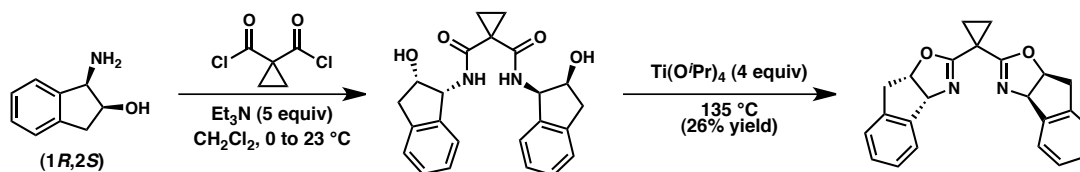
#### 4.4.1 *Materials and Methods*

Unless otherwise stated, reactions were performed under a nitrogen atmosphere using freshly dried solvents. Tetrahydrofuran (THF), methylene chloride ( $\text{CH}_2\text{Cl}_2$ ), and diethyl ether ( $\text{Et}_2\text{O}$ ) were dried by passing through activated alumina columns. Anhydrous dimethylacetamide (DMA) was purchased from Aldrich and stored under inert atmosphere. Manganese powder (– 325 mesh, 99.3%) was purchased from Alfa Aesar.  $\text{NiCl}_2(\text{dme})$  was purchased from Strem and stored in a glovebox under  $\text{N}_2$  when not in use. Unless otherwise stated, chemicals and reagents were used as received. Triethylamine ( $\text{Et}_3\text{N}$ ) was distilled over calcium hydride prior to use. All reactions were monitored by thin-layer chromatography using EMD/Merck silica gel 60 F254 pre-coated plates (0.25 mm) and were visualized by UV, CAM, or  $\text{KMnO}_4$  staining. Flash column

chromatography was performed as described by Still et al.<sup>28</sup> using silica gel (particle size 0.032-0.063) purchased from Silicycle. Optical rotations were measured on a Jasco P-2000 polarimeter using a 100 mm path-length cell at 589 nm. <sup>1</sup>H and <sup>13</sup>C NMR spectra were recorded on a Varian Inova 500 (at 500 MHz and 126 MHz, respectively), and are reported relative to internal CHCl<sub>3</sub> (<sup>1</sup>H, δ = 7.26) and CDCl<sub>3</sub> (<sup>13</sup>C, δ = 77.0). Data for <sup>1</sup>H NMR spectra are reported as follows: chemical shift (δ ppm) (multiplicity, coupling constant (Hz), integration). Multiplicity and qualifier abbreviations are as follows: s = singlet, d = doublet, t = triplet, q = quartet, m = multiplet, br = broad, app = apparent. IR spectra were recorded on a Perkin Elmer Paragon 1000 spectrometer and are reported in frequency of absorption (cm<sup>-1</sup>). HRMS were acquired using an Agilent 6200 Series TOF with an Agilent G1978A Multimode source in electrospray ionization (ESI), atmospheric pressure chemical ionization (APCI), or mixed (MM) ionization mode. Analytical SFC was performed with a Mettler SFC supercritical CO<sub>2</sub> analytical chromatography system with Chiralcel AD-H, OD-H, AS-H, OB-H, and OJ-H columns (4.6 mm x 25 cm) with visualization at 254 nm. Analytical achiral GC-MS was performed with an Agilent 7890A GC and an Agilent 5975C VL MSD with triple axis detector utilizing an Agilent HP-5MS (30.0 m x 0.25 mm) column (0.4 mL/min He carrier gas flow). Analytical chiral HPLC was performed with an Agilent 1100 Series HPLC utilizing Chiralpak AD or Chiralcel OD-H columns (4.6 mm x 25 cm) obtained from Daicel Chemical Industries, Ltd with visualization at 254 nm.

#### 4.4.2 Ligand and Substrate Synthesis

##### Ligand Preparation (L104)



To a flame-dried flask was added (1*R*,2*S*)-(+)-*cis*-1-amino-2-indanol (38 mmol, 2.1 equiv) and CH<sub>2</sub>Cl<sub>2</sub> (70 mL). The reaction was cooled to 0 °C and freshly-distilled Et<sub>3</sub>N (90 mmol, 5 equiv) was added dropwise. Cyclopropane-1,1-dicarbonyl dichloride<sup>29</sup> (18 mmol) was added dropwise and the solution was warmed to room temperature and stirred at 23 °C under N<sub>2</sub> for 6 h. A white precipitate slowly formed over the course of the reaction. The mixture was quenched with 1 M HCl and a white precipitate formed. The mixture was filtered and the white solid was collected and washed several times with an excess of water. The bis-amide product was dried under vacuum and used in the next step without any further purification.

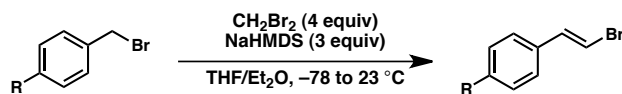
According to procedure by Kurosu and coworkers,<sup>30</sup> to a flame-dried flask was added crude bis-amide (3.6 mmol, 1 equiv) and anhydrous Ti(O<sup>*i*</sup>Pr)<sub>4</sub> (14.4 mmol, 4 equiv). The mixture was equipped with a distillation head and stirred at 135 °C under N<sub>2</sub> for 10 h. The reaction became a brown solution at high temperatures and isopropanol was observed to have been distilled from the solution. The reaction was cooled to 23 °C and 3-(dimethylamino)-1,2-propanediol (4.8 equiv) was added. The reaction was heated with a heat gun until the solution became homogeneous and was then stirred for 30 min. EtOAc (8 mL) and water (8 mL) were added and the reaction was stirred for 1 h. The

organic layer was separated and the aqueous layer was extracted with EtOAc. The combined organic layers were dried ( $\text{Na}_2\text{SO}_4$ ), filtered, and concentrated. The crude residue was purified by flash chromatography (2% methanol/dichloromethane) to isolate a light brown solid. The material was recrystallized from isopropanol to provide a white solid (1.15 g, 26% yield).  $[\alpha]_D^{25} = +274.5^\circ$  ( $c = 1.0$ ,  $\text{CHCl}_3$ );  $^1\text{H NMR}$  (500 MHz,  $\text{CDCl}_3$ )  $\delta$  7.49 – 7.42 (m, 2H), 7.30 – 7.20 (m, 6H), 5.53 (dd,  $J = 7.9, 0.8$  Hz, 2H), 5.34 (ddd,  $J = 7.9, 7.0, 1.9$  Hz, 2H), 3.44 – 3.35 (m, 2H), 3.20 (dd,  $J = 17.9, 1.8$  Hz, 2H), 1.41 – 1.23 (m, 4H);  $^{13}\text{C NMR}$  (126 MHz,  $\text{CDCl}_3$ )  $\delta$  165.8, 141.8, 139.7, 128.3, 127.3, 125.6, 125.1, 83.3, 76.4, 39.6, 18.3, 15.7; FTIR (NaCl, thin film): 3246, 3023, 2917, 1654, 1534, 1479, 1459, 1426, 1364, 1302, 1247, 1159, 1115, 1001, 754, 733  $\text{cm}^{-1}$ ; HRMS (MM) calc'd for  $\text{C}_{23}\text{H}_{20}\text{N}_2\text{O}_2$   $[\text{M}+\text{Na}]^+$  379.1417, found 379.1438.

### Substrate Preparation

Vinyl bromides **156**<sup>31</sup> and **156g**<sup>32</sup> and benzyl chlorides **162m**<sup>33</sup> and **162n**<sup>34</sup> were prepared according to literature precedent.

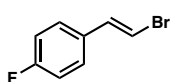
### General Procedure 1: Vinyl Bromide Synthesis from Benzyl Bromides



According to a protocol by Charette and coworkers,<sup>35</sup> to a flame-dried flask under  $\text{N}_2$  was added NaHMDS (9 mmol, 3 equiv, 1 M in THF) and  $\text{Et}_2\text{O}$  (6 mL). The flask was cooled to  $-78$   $^\circ\text{C}$  and wrapped in aluminum foil. To the solution was added freshly-distilled dibromomethane (12 mmol, 4 equiv) dropwise. The solution was stirred at  $-78$   $^\circ\text{C}$  for 20

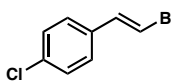
min and then benzyl bromide in 2 mL THF was added dropwise. The solution was stirred at  $-78\text{ }^{\circ}\text{C}$  for an additional 3 h and then slowly warmed to room temperature and stirred in the dark at  $23\text{ }^{\circ}\text{C}$  for 21 h. The mixture was filtered through a pad of celite and silica and concentrated. The crude material was purified by flash chromatography.

**(E)-1-(2-bromovinyl)-4-fluorobenzene (156b)**



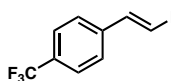
Prepared from 1-(bromomethyl)-4-(fluoromethyl)benzene (3.0 mmol) according to General Procedure 1. The crude residue was purified by silica gel chromatography (hexanes) to yield **156b** (419.2 mg, 70% yield) as a white solid. Spectral data matched those reported in the literature.

**(E)-1-(2-bromovinyl)-4-chlorobenzene (156c)**



Prepared from 1-(bromomethyl)-4-(chloromethyl)benzene (3.0 mmol) according to General Procedure 1. The crude residue was purified by silica gel chromatography (hexanes) to yield **156c** (496.2 mg, 76% yield) as a white solid. Spectral data matched those reported in the literature.

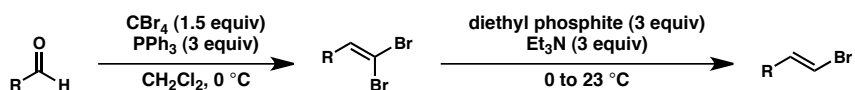
**(E)-1-(2-bromovinyl)-4-(trifluoromethyl)benzene (156d)**



Prepared from 1-(bromomethyl)-4-(trifluoromethyl)benzene (3.0 mmol) according to General Procedure 1. The crude residue was purified by silica gel chromatography (1 to 2% ethyl acetate/hexanes) to yield **156d** (138.4 mg, 18% yield) as a clear oil.  $^1\text{H}$  NMR (500 MHz,  $\text{CDCl}_3$ )  $\delta$  7.60 (d,  $J = 7.7$  Hz, 2H), 7.41 (d,  $J = 8.1$  Hz, 2H), 7.15 (d,  $J = 14.1$  Hz, 1H), 6.92 (d,  $J = 14.0$  Hz, 1H);  $^{13}\text{C}$  NMR (126 MHz,

CDCl<sub>3</sub>) δ 139.2, 135.9, 130.1 (q, *J* = 33 Hz), 126.3, 125.8 (q, *J* = 4 Hz), 124.0 (q, *J* = 276 Hz), 109.4; FTIR (NaCl, thin film): 3074, 1617, 1604, 1574, 1411, 1326, 1166, 1127, 1068, 1017, 935, 848, 785, 739, 724 cm<sup>-1</sup>; HRMS (MM) calc'd for C<sub>9</sub>H<sub>6</sub>BrF<sub>3</sub> [M]<sup>+</sup> 249.9605, found 249.9569.

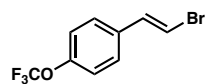
### General Procedure 2: Vinyl Bromide Synthesis from Aldehydes



According to a modified synthetic sequence by Alexakis and coworkers,<sup>36</sup> to a flame-dried flask under N<sub>2</sub> was added aldehyde (10 mmol, 1 equiv), CBr<sub>4</sub> (15 mmol, 1.5 equiv), and CH<sub>2</sub>Cl<sub>2</sub> (80 mL). The flask was cooled to 0 °C. A solution of PPh<sub>3</sub> (30 mmol, 3 equiv), in CH<sub>2</sub>Cl<sub>2</sub> (70 mL) was added to the reaction dropwise via addition funnel over 30 min. The solution was stirred at 0 °C under N<sub>2</sub> for 1 h. The solution was concentrated to remove CH<sub>2</sub>Cl<sub>2</sub> and CHCl<sub>3</sub> was added. The resulting mixture was filtered and washed with CHCl<sub>3</sub> (2 x 20 mL). The filtrate was concentrated to give a thick orange oil. The crude material was purified by flash chromatography to isolate the dibromoalkene.

To a vial containing dibromoalkene was added diethyl phosphite (3 equiv). Additional DMF was added to dissolve solid substrates. The solution was cooled to 0 °C and Et<sub>3</sub>N (3 equiv) was added dropwise. The reaction was warmed to 23 °C and stirred overnight. The mixture was diluted with water. The aqueous layer was extracted with CH<sub>2</sub>Cl<sub>2</sub> and the combined organic layers were washed with brine and dried (Na<sub>2</sub>SO<sub>4</sub>), filtered, and concentrated. The crude material was purified by flash chromatography.

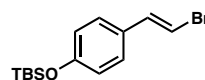
**(E)-1-(2-bromovinyl)-4-(trifluoromethoxy)benzene (156e)**



Prepared from 4-(trifluoromethoxy)benzaldehyde (10.0 mmol) according to General Procedure 2. The crude residue was purified by silica gel chromatography (hexanes) to yield **156e** (2.07 g, 72% yield, 94% E olefin) as a pale yellow oil. <sup>1</sup>H NMR (500 MHz, CDCl<sub>3</sub>) δ 7.38 – 7.24 (m, 2H), 7.24 – 7.16 (m, 2H), 7.10 (d, *J* = 14.0 Hz, 1H), 6.79 (d, *J* = 14.0 Hz, 1H); <sup>13</sup>C NMR (126 MHz, CDCl<sub>3</sub>) δ 148.9 (q, *J* = 2 Hz), 135.7, 134.6, 127.4, 121.2, 120.40 (q, *J* = 257 Hz), 107.5; FTIR (NaCl, thin film): 3073, 2430, 1895, 1607, 1507, 1411, 1261, 1215, 1162, 1104, 1017, 948, 931, 841, 778, 745, 713 cm<sup>-1</sup>; HRMS (MM) calc'd for C<sub>9</sub>H<sub>6</sub>BrF<sub>3</sub>O [M+H<sub>3</sub>O]<sup>+</sup> 284.9733, found 284.9819.

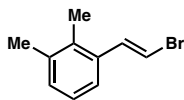
According to Alexakis and coworkers,<sup>36</sup> to a vial containing vinyl bromide **156e** (6 mmol) was added NaOH (0.85 equiv) and IPA (0.5 M). The mixture was stirred at 75 °C for 2 h. The reaction was cooled to room temperature and diluted with pentane and water. The organic layer was washed with water and 1 M HCl. The organic layer was then dried (Na<sub>2</sub>SO<sub>4</sub>), filtered, and concentrated to isolate geometrically pure product (1.44 g, 82% yield).

**(E)-(4-(2-bromovinyl)phenoxy)(tert-butyl)dimethylsilane (156f)**



Prepared from 4-((tert-butyldimethylsilyl)oxy)benzaldehyde (18.0 mmol) according to General Procedure 2. The crude residue was purified by silica gel chromatography (hexanes) to yield **156f** (3.66 g, 66% yield, 88% E olefin) as a pale yellow oil. Spectral data matched those reported in the literature.

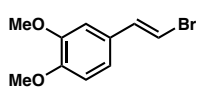
**(E)-1-(2-bromovinyl)-2,3-dimethylbenzene (156h)**



Prepared from 2,3-dimethylbenzaldehyde (10.0 mmol) according to General Procedure 2. The crude residue was purified by silica gel chromatography (hexanes) to yield **156h** (1.73 g, 82% yield, 88% E olefin) as a clear oil.  $^1\text{H}$  NMR (500 MHz,  $\text{CDCl}_3$ )  $\delta$  7.47 – 7.37 (m, 1H), 7.23 – 7.05 (m, 3H), 6.64 – 6.57 (m, 1H), 2.35 (s, 3H), 2.28 (s, 3H);  $^{13}\text{C}$  NMR (126 MHz,  $\text{CDCl}_3$ )  $\delta$  137.1, 136.5, 135.5, 133.8, 130.0, 125.8, 124.3, 107.2, 20.6, 15.6; FTIR (NaCl, thin film): 3068, 2942, 2864, 1725, 1607, 1587, 1456, 1383, 1248, 1203, 1181, 1168, 1092, 938, 784, 757, 707, 668  $\text{cm}^{-1}$ ; HRMS (MM) calc'd for  $\text{C}_{10}\text{H}_{11}\text{Br}$   $[\text{M}]^+$  210.0044, found 209.9930.

According to Alexakis and coworkers,<sup>36</sup> to a vial containing vinyl bromide **156h** (6 mmol) was added NaOH (0.85 equiv) and IPA (0.5 M). The mixture was stirred at 75 °C for 2 h. The reaction was cooled to room temperature and diluted with pentane and water. The organic layer was washed with water and 1 M HCl. The organic layer was then dried ( $\text{Na}_2\text{SO}_4$ ), filtered, and concentrated to isolate geometrically pure product (1.03 g, 81% yield).

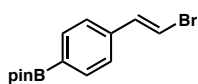
**(E)-4-(2-bromovinyl)-1,2-dimethoxybenzene (156i)**



Prepared from 3,4-dimethoxybenzaldehyde (10.0 mmol) according to General Procedure 2. The crude residue was purified by silica gel chromatography (0 to 5% ethyl acetate/hexanes) to yield **156i** (2.02 g, 83% yield, 93% E olefin) as a white solid. Spectral data matched those reported in the literature.

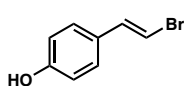
According to Alexakis and coworkers,<sup>36</sup> to a vial containing vinyl bromide **156i** (6 mmol) was added NaOH (0.85 equiv) and IPA (0.5 M). The mixture was stirred at 75 °C for 2 h. The reaction was cooled to room temperature and diluted with Et<sub>2</sub>O and water. The organic layer was washed with water and 1 M HCl. The organic layer was then dried (Na<sub>2</sub>SO<sub>4</sub>), filtered, and concentrated to isolate geometrically pure product (1.35 g, 92% yield).

**(E)-2-(4-(2-bromovinyl)phenyl)-4,4,5,5-tetramethyl-1,3,2-dioxaborolane (156j)**



Prepared from 4-(4,4,5,5-tetramethyl-1,3,2-dioxaborolan-2-yl)benzaldehyde (12.5 mmol) according to General Procedure 2. The crude residue was purified by silica gel chromatography (10 to 20% ethyl acetate/hexanes) to yield **156j** (2.55 g, 68% yield) as a low melting solid. <sup>1</sup>H NMR (500 MHz, CDCl<sub>3</sub>) δ 7.78 (d, *J* = 7.7 Hz, 2H), 7.31 (d, *J* = 8.1 Hz, 2H), 7.12 (d, *J* = 14.5 Hz, 1H), 6.86 (d, *J* = 14.4 Hz, 1H), 1.36 (s, 12H); <sup>13</sup>C NMR (126 MHz, CDCl<sub>3</sub>) δ 138.4, 137.2, 135.2, 125.4, 107.7, 83.9, 24.9; FTIR (NaCl, thin film): 3073, 2978, 2931, 1729, 1607, 1516, 1468, 1401, 1361, 1324, 1269, 1214, 1144, 1090, 1019, 962, 937, 860, 782, 745, 727, 653 cm<sup>-1</sup>; HRMS (MM) calc'd for C<sub>14</sub>H<sub>18</sub>BBrO<sub>2</sub> [M+H]<sup>+</sup> 334.2213, found 334.2030.

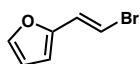
**(E)-4-(2-bromovinyl)phenol (156k)**



To a vial containing vinyl bromide **156f** (6 mmol, obtained from General Procedure 2) was added NaOH (0.85 equiv) and <sup>t</sup>PrOH. The mixture was stirred at 75 °C for 2 h. The reaction was cooled to room temperature and

diluted with Et<sub>2</sub>O and water. The organic layer was washed with water (2x) and 1 M HCl (2x). The organic layer was then dried (MgSO<sub>4</sub>), filtered, and concentrated. The crude residue was purified by flash chromatography (10 to 20% ethyl acetate/hexanes) to yield **156k** (750.0 mg, 63% yield, 92% E olefin) as a white solid. Spectral data for **156k** matched that reported in the literature.

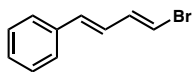
**(E)-2-(2-bromovinyl)furan (156l)**



Prepared from furfural (10.0 mmol) according to General Procedure 2. The crude residue was purified by silica gel chromatography (hexanes) to yield **156l** (745 mg, 49% yield, 71% E olefin) as a yellow oil. Spectral data matched those reported in the literature.

According to Alexakis and coworkers,<sup>36</sup> to a vial containing vinyl bromide **156l** (6 mmol) was added NaOH (0.85 equiv) and IPA (0.5 M). The mixture was stirred at 75 °C for 1 h. The reaction was cooled to room temperature and diluted with pentane and water. The organic layer was washed with water and 1 M HCl. The organic layer was then dried (Na<sub>2</sub>SO<sub>4</sub>), filtered, and concentrated to isolate geometrically pure product (54 mg, 8% yield).

**((1E,3E)-4-bromobuta-1,3-dien-1-yl)benzene (156m)**

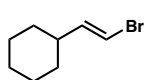


Prepared from cinnamaldehyde (10.0 mmol) according to General Procedure 2. The crude residue was purified by silica gel

chromatography (hexanes) to yield **156m** (910 mg, 44% yield, 73% E olefin) as a white solid. Spectral data matched those reported in the literature.

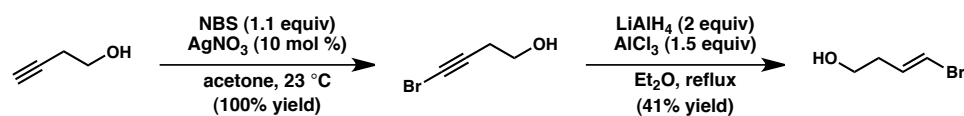
According to Alexakis and coworkers,<sup>36</sup> to a vial containing vinyl bromide **156m** (4.3 mmol) was added NaOH (0.85 equiv) and IPA (0.5 M). The mixture was stirred at 75 °C for 1 h. The reaction was cooled to room temperature and diluted with pentane and water. The organic layer was washed with water and 1 M HCl. The organic layer was then dried (Na<sub>2</sub>SO<sub>4</sub>), filtered, and concentrated to isolate geometrically pure product (584 mg, 66% yield).

**(E)-(2-bromovinyl)cyclohexane (156n)**



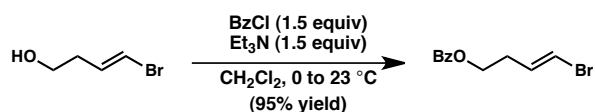
Prepared from cyclohexanecarboxaldehyde (10.0 mmol) according to General Procedure 2, except the debromination was performed at 80 °C for 12 h. The crude residue was purified by silica gel chromatography (hexanes) to yield **156n** (800 mg, 43% yield, 72% E olefin) as a clear oil. Spectral data matched those reported in the literature.

According to Alexakis and coworkers,<sup>36</sup> to a vial containing vinyl bromide **156n** (3.7 mmol) was added NaOH (0.85 equiv) and IPA (0.5 M). The mixture was stirred at 75 °C for 1 h. The reaction was cooled to room temperature and diluted with pentane and water. The organic layer was washed with water and 1 M HCl. The organic layer was then dried (Na<sub>2</sub>SO<sub>4</sub>), filtered, and concentrated to isolate geometrically pure product (480 mg, 61% yield).

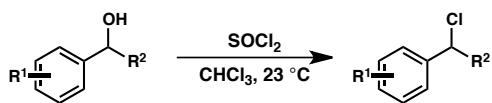
**(E)-4-bromobut-3-en-1-ol (156p)**

According to a procedure by Hofmeister and coworkers,<sup>37</sup> 3-butyne-1-ol (1 equiv, 15 mmol) was dissolved in acetone (50 mL). To the solution was added NBS (16.5 mmol, 1.1 equiv) and AgNO<sub>3</sub> (1.5 mmol, 10 mol %). The reaction was stirred at 23 °C for 2 h. The reaction was concentrated and diluted with Et<sub>2</sub>O and water. The aqueous layer was extracted with Et<sub>2</sub>O and the combined organic layers were dried (MgSO<sub>4</sub>), filtered, and concentrated to give a clear oil (2.22 g, 100% yield).

To a flame-dried flask was added LiAlH<sub>4</sub> (30 mmol, 2 equiv) and Et<sub>2</sub>O (90 mL). The flask was equipped with a reflux condenser and cooled to –5 °C. AlCl<sub>3</sub> (22.5 mmol, 1.5 equiv) was carefully added to the reaction. The reaction was stirred for 10 min at –5 °C under N<sub>2</sub>. Bromoalkyne (15 mmol, 1 equiv) was added dropwise and the reaction was stirred at reflux under N<sub>2</sub> for 2.5 h. The reaction was cooled to 0 °C and Et<sub>2</sub>O (60 mL) was added, followed by 2 M HCl (60 mL) dropwise to quench the reaction. The aqueous layer was extracted with Et<sub>2</sub>O (3 x 40 mL) and the combined organic layers were washed with brine, dried (MgSO<sub>4</sub>), filtered, and concentrated. The crude material was purified by flash chromatography (15 to 30% ethyl acetate/hexanes) to isolate a clear oil (917.6 mg, 41% yield). <sup>1</sup>H NMR (500 MHz, CDCl<sub>3</sub>) δ 6.28 – 6.04 (m, 2H), 3.75 – 3.52 (m, 2H), 2.44 (s, 1H), 2.36 – 2.18 (m, 2H); <sup>13</sup>C NMR (126 MHz, CDCl<sub>3</sub>) δ 134.3, 106.6, 61.1, 36.1; FTIR (NaCl, thin film): 3338, 3065, 2935, 2880, 1622, 1427, 1227, 1168, 1046, 1002, 937, 710 cm<sup>-1</sup>; HRMS (MM) calc'd for C<sub>4</sub>H<sub>7</sub>BrO [M+OH]<sup>+</sup> 166.9702, found 166.9662.

**(E)-4-bromobut-3-en-1-yl benzoate (156o)**

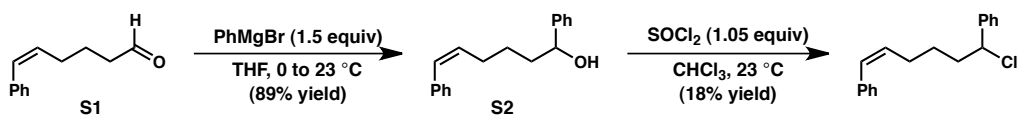
To a flame-dried flask was added alcohol **156p** (1.5 mmol, 1 equiv,) and  $\text{CH}_2\text{Cl}_2$  (5 mL). The solution was cooled to 0 °C and  $\text{Et}_3\text{N}$  (2.25 mmol, 1.5 equiv) and  $\text{BzCl}$  (2.25 mmol, 1.5 equiv) were added. The solution was stirred at 23 °C under  $\text{N}_2$  for 3 h. The reaction was quenched with sat. aqueous  $\text{NH}_4\text{Cl}$  and the aqueous layer was extracted with  $\text{Et}_2\text{O}$ . The combined organic layers were washed with brine, dried ( $\text{MgSO}_4$ ), filtered, and concentrated. The crude oil was purified by flash chromatography (1% ethyl acetate/hexanes) to isolate a clear oil (363.8 mg, 95% yield).  $^1\text{H}$  NMR (500 MHz,  $\text{CDCl}_3$ )  $\delta$  8.09 – 8.01 (m, 2H), 7.61 – 7.53 (m, 1H), 7.45 (td,  $J = 7.7, 1.6$  Hz, 2H), 6.32 – 6.18 (m, 2H), 4.36 (td,  $J = 6.6, 1.8$  Hz, 2H), 2.52 (qd,  $J = 6.6, 2.2$  Hz, 2H);  $^{13}\text{C}$  NMR (126 MHz,  $\text{CDCl}_3$ )  $\delta$  166.3, 133.4, 133.1, 130.0, 129.6, 128.4, 107.1, 63.1, 32.4; FTIR (NaCl, thin film): 3064, 2957, 2898, 1717, 1622, 1602, 1492, 1451, 1382, 1314, 1273, 1176, 1116, 1070, 1026, 937, 710  $\text{cm}^{-1}$ ; HRMS (ESI) calc'd for  $\text{C}_{11}\text{H}_{11}\text{BrO}_2$   $[\text{M}+\text{H}]^+$  255.0015, found 254.9994.

**General Procedure 3: Benzyl Chloride Synthesis**

A flask was charged with the appropriate benzyl alcohol (1.0 equiv) and  $\text{CHCl}_3$  (1.5 M). Thionyl chloride (1.05 equiv) was added dropwise. Evolved gas was quenched via cannula by aqueous  $\text{NaHCO}_3$ . The solution was stirred at 23 °C for 12 h and then

concentrated to afford a yellow oil. The crude residue was purified by Kugelrohr distillation to isolate **162a–l**, **162o**, and **162p** as clear oils. Spectral data for all compounds matched those reported in the literature.

### Preparation of Radical Clock Substrate **160**



Aldehyde **S1** was prepared according to a known procedure from 5-hexyn-1-ol.<sup>38</sup> To a flame-dried flask was added PhMgBr (16 mmol, 1.5 equiv, 3 M in Et<sub>2</sub>O) and THF (33 mL). The solution was cooled to 0 °C and aldehyde **S1** was added dropwise. The solution was slowly warmed to 23 °C and stirred under N<sub>2</sub> overnight. The reaction was quenched with sat. aqueous NH<sub>4</sub>Cl and H<sub>2</sub>O. The aqueous layer was extracted with Et<sub>2</sub>O. The combined organic layers were washed with brine and dried (MgSO<sub>4</sub>), filtered, and concentrated. The crude residue was purified by flash chromatography (10% ethyl acetate/hexanes) to isolate **S2** as a pale yellow oil (2.37 g, 89% yield). <sup>1</sup>H NMR (500 MHz, CDCl<sub>3</sub>) δ 7.49 – 7.11 (m, 10H), 6.46 (d, *J* = 11.4 Hz, 1H), 5.67 (dt, *J* = 11.7, 7.2 Hz, 1H), 4.66 (dd, *J* = 7.5, 5.8 Hz, 1H), 2.52 – 2.28 (m, 2H), 2.12 – 1.93 (m, 1H), 1.93 – 1.68 (m, 2H), 1.68 – 1.36 (m, 2H); <sup>13</sup>C NMR (126 MHz, CDCl<sub>3</sub>) δ 144.7, 137.7, 132.6, 129.2, 128.8, 128.5, 128.2, 127.6, 126.5, 125.9, 74.5, 38.6, 28.4, 26.1; FTIR (NaCl, thin film): 3546, 3350, 3058, 3024, 2935, 2856, 1948, 1880, 1807, 1757, 1599, 1574, 1493, 1453, 1406, 1319, 1269, 1200, 1156, 1069, 1028, 1001, 914, 764, 699; HRMS (MM) calc'd for C<sub>18</sub>H<sub>20</sub>O [M]<sup>+</sup> 252.1514, found 252.1520.

A flask was charged with **S2** (5.2 mmol, 1.0 equiv) and  $\text{CHCl}_3$  (1.5 M). Thionyl chloride (5.5 mmol, 1.05 equiv) was added dropwise. Evolved gas was quenched via cannula by aqueous  $\text{NaHCO}_3$ . The solution was stirred at 23 °C for 12 h and then concentrated to afford a yellow oil. The crude residue was purified by flash chromatography (hexanes) to isolate **160** as a clear oil (250.9 mg, 18% yield).  $^1\text{H}$  NMR (500 MHz,  $\text{CDCl}_3$ )  $\delta$  7.48 – 7.09 (m, 10H), 6.46 (d,  $J$  = 11.8 Hz, 1H), 5.63 (dt,  $J$  = 11.6, 7.2 Hz, 1H), 4.83 (dd,  $J$  = 8.2, 6.4 Hz, 1H), 2.39 (qd,  $J$  = 7.4, 1.9 Hz, 2H), 2.25 – 1.97 (m, 2H), 1.80 – 1.34 (m, 2H);  $^{13}\text{C}$  NMR (126 MHz,  $\text{CDCl}_3$ )  $\delta$  141.7, 137.5, 132.0, 129.5, 128.7, 128.6, 128.24, 128.17, 126.9, 126.6, 63.5, 39.4, 27.8, 27.3; FTIR (NaCl, thin film): 3057, 3024, 2943, 2860, 1599, 1493, 1454, 1235, 1075, 1028, 914, 766, 752, 697  $\text{cm}^{-1}$ ; HRMS (MM) calc'd for  $\text{C}_{18}\text{H}_{19}\text{Cl}$   $[\text{M}+\text{H}_3\text{O}]^+$  289.1354, found 289.1340.

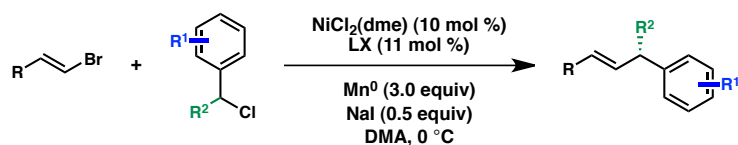
### 4.4.3 Enantioselective Reductive Cross-Coupling

#### General Procedure 4 (Table 4.3): Optimization of Reaction Conditions

On a bench-top, to a 1/2 dram vial was added the appropriate ligand (0.022 mmol, 11 mol %), reductant (0.6 mmol, 3 equiv),  $\text{NiCl}_2(\text{dme})$  (0.02 mmol, 10 mol %), vinyl bromide (0.2 mmol, 1.0 equiv), and NaI (0.1 mmol, 0.5 equiv) if necessary. The vial was transferred into an  $\text{N}_2$ -filled glovebox and charged with the appropriate solvent (0.2 mL, 1.0 M) followed by benzyl chloride (0.2 mmol, 1.0 equiv) and dodecane (internal standard). The vial was sealed and removed from the glovebox. The mixture was stirred vigorously, ensuring that the reductant was uniformly suspended, at 20 °C for 6 h. The dark mixture was diluted with 10% ethyl acetate/hexane and passed through a plug of

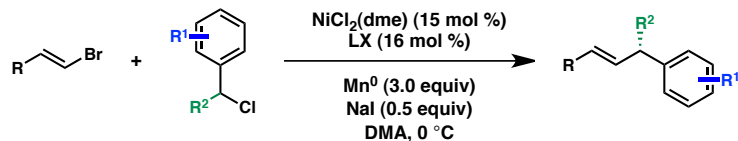
silica, using 10% ethyl acetate/hexane eluent. The solution was concentrated to afford a clear oil. The crude residue was analyzed by GC-MS. Dodecane was used as an internal standard. GC samples were analyzed by flame ionization detection and yields calculated based on a calibrated response factor.

### General Procedure 5: Enantioselective Reductive Coupling of Benzyl Chlorides and Vinyl Bromides



On a bench-top, to a 10 mL round-bottom flask was added **L104** (0.022 mmol, 11 mol),  $\text{Mn}^0$  (0.6 mmol, 3 equiv),  $\text{NiCl}_2(\text{dme})$  (0.02 mmol, 10 mol %), vinyl bromide **156** (if a solid, 0.2 mmol, 1 equiv), and NaI (0.1 mmol, 0.5 equiv). The flask was covered with a rubber septum, purged with  $\text{N}_2$ , and cooled to 0 °C. To the mixture was added DMA (0.2 mL), vinyl bromide **156** (if an oil, 0.2 mmol, 1 equiv), and benzyl chloride **26** (0.2 mmol, 1 equiv). The mixture was stirred vigorously, ensuring that the manganese powder was uniformly suspended. After 6 h, the mixture was allowed to warm to room temperature and was quenched with 1 M HCl (0.5 mL). The mixture was transferred to a separatory funnel using water (5 mL) and  $\text{Et}_2\text{O}$  (10 mL), and the aqueous and organic layers were separated. The aqueous layer was extracted with  $\text{Et}_2\text{O}$  (2 x 10 mL) and the combined organic layers were washed with brine (1 x 5 mL) and dried ( $\text{MgSO}_4$ ), filtered, and concentrated. The crude residue was purified by flash chromatography.

**General Procedure 6: Enantioselective Reductive Coupling of Benzyl Chlorides and Vinyl Bromides – 15% Catalyst Loading**



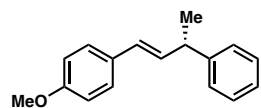
On a bench-top, to a 10 mL round-bottom flask was added **L104** (0.032 mmol, 16 mol %),  $\text{Mn}^0$  (0.6 mmol, 3 equiv),  $\text{NiCl}_2(\text{dme})$  (0.03 mmol, 15 mol %), vinyl bromide **156** (if a solid, 0.2 mmol, 1 equiv), and  $\text{NaI}$  (0.1 mmol, 0.5 equiv). The flask was covered with a rubber septum, purged with  $\text{N}_2$ , and cooled to 0 °C. To the mixture was added DMA (0.2 mL), vinyl bromide **156** (if an oil, 0.2 mmol, 1 equiv), and benzyl chloride **26** (0.2 mmol, 1 equiv). The mixture was stirred vigorously, ensuring that the manganese powder was uniformly suspended. After 6 h, the mixture was allowed to warm to room temperature and was quenched with 1 M  $\text{HCl}$  (0.5 mL). The mixture was transferred to a separatory funnel using water (5 mL) and  $\text{Et}_2\text{O}$  (10 mL), and the aqueous and organic layers were separated. The aqueous layer was extracted with  $\text{Et}_2\text{O}$  (2 x 10 mL) and the combined organic layers were washed with brine (1 x 5 mL) and dried ( $\text{MgSO}_4$ ), filtered, and concentrated. The crude residue was purified by flash chromatography.

**General Procedure 7: Racemic Reductive Cross-Coupling**

On a bench-top, to a 1/2 dram vial was added neocuproine (0.022 mmol, 11 mol %),  $\text{Mn}^0$  (0.6 mmol, 3 equiv),  $\text{NiCl}_2(\text{dme})$  (0.02 mmol, 10 mol %), and vinyl bromide (0.2 mmol, 1.0 equiv). The vial was transferred into an  $\text{N}_2$ -filled glovebox and charged with DMPU (0.2 mL, 1.0 M) followed by benzyl chloride (0.2 mmol, 1.0 equiv). The vial was sealed

and removed from the glovebox. The mixture was stirred vigorously, ensuring that the reductant was uniformly suspended, at 20 °C for 6 h. The mixture was quenched with 1 M HCl (0.5 mL) and transferred to a separatory funnel using water (5 mL) and Et<sub>2</sub>O (10 mL). The aqueous and organic layers were separated. The aqueous layer was extracted with Et<sub>2</sub>O (2 x 10 mL) and the combined organic layers were washed with brine (1 x 5 mL) and dried (MgSO<sub>4</sub>), filtered, and concentrated. The crude residue was purified by flash chromatography.

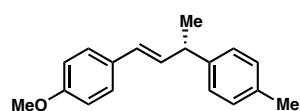
**(*S,E*)-1-methoxy-4-(3-phenylbut-1-en-1-yl)benzene (163a)**



Prepared from (1-chloroethyl)benzene (**162a**, 0.2 mmol) and (*E*)-1-(2-bromovinyl)-4-methoxybenzene (**156**, 0.2 mmol) according to General Procedure 5. The crude residue was purified by silica gel chromatography (5 to 15% toluene/hexanes) to yield **163a** (43.4 mg, 91% yield) in 93% ee as a clear oil. The enantiomeric excess was determined by chiral SFC analysis (OB-H, 2.5 mL/min, 20% IPA in CO<sub>2</sub>, λ = 254 nm): *t<sub>R</sub>* (major) = 7.6 min, *t<sub>R</sub>* (minor) = 9.2 min. [α]<sub>D</sub><sup>25</sup> = -41.9° (c = 1.0, CHCl<sub>3</sub>); <sup>1</sup>H NMR (500 MHz, CDCl<sub>3</sub>) δ 7.39 – 7.20 (m, 7H), 6.90 – 6.83 (m, 2H), 6.40 (d, *J* = 16.2 Hz, 1H), 6.28 (dd, *J* = 15.9, 6.7 Hz, 1H), 3.82 (s, 3H), 3.70 – 3.60 (m, 1H), 1.49 (d, *J* = 7.0 Hz, 3H); <sup>13</sup>C NMR (126 MHz, CDCl<sub>3</sub>) δ 158.9, 145.9, 133.2, 130.5, 128.4, 128.0, 127.3, 127.2, 126.1, 114.0, 55.3, 42.5, 21.3; FTIR (NaCl, thin film): 3026, 2962, 2834, 1607, 1577, 1511, 1492, 1452, 1298, 1251, 1174, 1034, 967, 818, 760 cm<sup>-1</sup>; HRMS (MM) calc'd for C<sub>17</sub>H<sub>18</sub>O [M]<sup>+</sup> 238.1358, found 238.1346.

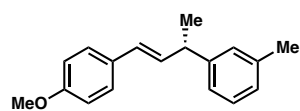
The optical rotation of the product generated in the presence of (*R,R,S,S*)-**L104** was measured as  $[\alpha]_D^{25} = -41.9^\circ$  ( $c = 1.0$ ,  $\text{CHCl}_3$ ). Lit:  $[\alpha]_D^{20} = -16^\circ$  ( $c = 1.28$ ,  $\text{CHCl}_3$ , *S* enantiomer, 94% ee).<sup>39</sup> Based on the literature precedent, we assign our product as the *S* enantiomer.

**(*S,E*)-1-methoxy-4-(3-(*p*-tolyl)but-1-en-1-yl)benzene (163b)**



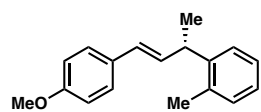
Prepared from 1-(1-chloroethyl)-4-methylbenzene (**162b**, 0.2 mmol) and (*E*)-1-(2-bromovinyl)-4-methoxybenzene (**156**, 0.2 mmol) according to General Procedure 5. The crude residue was purified by silica gel chromatography (5 to 15% toluene/hexanes) to yield **163b** (41.4 mg, 82% yield) in 94% ee as a clear oil. The enantiomeric excess was determined by chiral SFC analysis (OB-H, 2.5 mL/min, 15% IPA in  $\text{CO}_2$ ,  $\lambda = 254$  nm):  $t_R$  (major) = 11.4 min,  $t_R$  (minor) = 13.0 min.  $[\alpha]_D^{25} = -41.1^\circ$  ( $c = 1.1$ ,  $\text{CHCl}_3$ );  $^1\text{H}$  NMR (500 MHz,  $\text{CDCl}_3$ )  $\delta$  7.35 – 7.28 (m, 2H), 7.23 – 7.13 (m, 4H), 6.90 – 6.83 (m, 2H), 6.39 (d,  $J = 16.2$  Hz, 1H), 6.27 (dd,  $J = 15.9, 6.7$  Hz, 1H), 3.82 (s, 3H), 3.66 – 3.58 (m, 1H), 2.37 (s, 3H), 1.47 (d,  $J = 7.0$  Hz, 3H);  $^{13}\text{C}$  NMR (126 MHz,  $\text{CDCl}_3$ )  $\delta$  158.8, 142.9, 135.6, 133.4, 130.5, 129.2, 127.7, 127.23, 127.18, 113.9, 55.3, 42.1, 21.4, 21.0; FTIR (NaCl, thin film): 3019, 2961, 2929, 2834, 1607, 1577, 1511, 1454, 1298, 1273, 1250, 1174, 1036, 967, 814  $\text{cm}^{-1}$ ; HRMS (MM) calc'd for  $\text{C}_{18}\text{H}_{20}\text{O}$   $[\text{M}]^+$  252.1514, found 252.1477.

**(*S,E*)-1-(4-(4-methoxyphenyl)but-3-en-2-yl)-3-methylbenzene (163c)**



Prepared from 1-(1-chloroethyl)-3-methylbenzene (**162c**, 0.2 mmol) and (*E*)-1-(2-bromovinyl)-4-methoxybenzene (**156**, 0.2 mmol) according to General Procedure 5. The crude residue was purified by silica gel chromatography (0 to 2% Et<sub>2</sub>O/hexanes) to yield **163c** (44.6 mg, 88% yield) in 93% ee as a clear oil. The enantiomeric excess was determined by chiral SFC analysis (OB-H, 2.5 mL/min, 15% IPA in CO<sub>2</sub>, λ = 254 nm): *t<sub>R</sub>* (major) = 7.1 min, *t<sub>R</sub>* (minor) = 8.9 min. [α]<sub>D</sub><sup>25</sup> = -40.5° (c = 1.0, CHCl<sub>3</sub>); <sup>1</sup>H NMR (500 MHz, CDCl<sub>3</sub>) δ 7.36 – 7.28 (m, 2H), 7.29 – 7.19 (m, 1H), 7.15 – 7.01 (m, 3H), 6.88 – 6.83 (m, 2H), 6.40 (d, *J* = 16.0 Hz, 1H), 6.28 (dd, *J* = 15.9, 6.8 Hz, 1H), 3.83 (s, 3H), 3.66 – 3.57 (m, 1H), 2.38 (s, 3H), 1.48 (d, *J* = 7.0 Hz, 3H); <sup>13</sup>C NMR (126 MHz, CDCl<sub>3</sub>) δ 158.8, 145.9, 138.0, 133.3, 130.5, 128.3, 128.1, 127.8, 127.2, 126.9, 124.3, 113.9, 55.3, 42.5, 21.5, 21.4; FTIR (NaCl, thin film): 3029, 2962, 2834, 1607, 1577, 1511, 1488, 1463, 1371, 1299, 1251, 1175, 1107, 1036, 967, 848, 817, 785, 767 cm<sup>-1</sup>; HRMS (MM) calc'd for C<sub>18</sub>H<sub>20</sub>O [M]<sup>+</sup> 252.1514, found 252.1443.

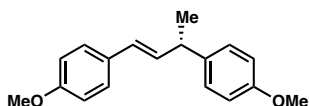
**(*S,E*)-1-(4-(4-methoxyphenyl)but-3-en-2-yl)-2-methylbenzene (163d)**



Prepared from 1-(1-chloroethyl)-2-methylbenzene (**162d**, 0.2 mmol) and (*E*)-1-(2-bromovinyl)-4-methoxybenzene (**156**, 0.2 mmol) according to General Procedure 6. The crude residue was purified by silica gel chromatography (5 to 15% toluene/hexanes) to yield **163d** (22.3 mg, 44% yield) in 85% ee as a clear oil. The enantiomeric excess was determined by chiral SFC analysis (OB-H, 2.5 mL/min, 15% IPA in CO<sub>2</sub>, λ = 254 nm): *t<sub>R</sub>* (major) = 8.7 min, *t<sub>R</sub>* (minor) = 10.4 min.

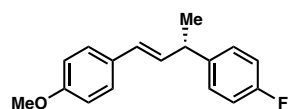
$[\alpha]_D^{25} = -40.3^\circ$  ( $c = 0.9$ ,  $\text{CHCl}_3$ );  $^1\text{H NMR}$  (500 MHz,  $\text{CDCl}_3$ )  $\delta$  7.33 – 7.09 (m, 6H), 6.87 – 6.80 (m, 2H), 6.32 (d,  $J = 15.7$  Hz, 1H), 6.23 (dd,  $J = 16.0, 6.2$  Hz, 1H), 3.89 – 3.82 (m, 1H), 3.81 (s, 3H), 2.39 (s, 3H), 1.45 (d,  $J = 7.0$  Hz, 3H);  $^{13}\text{C NMR}$  (126 MHz,  $\text{CDCl}_3$ )  $\delta$  158.8, 143.8, 135.6, 132.7, 130.42, 130.36, 127.8, 127.2, 126.3, 126.2, 126.0, 113.9, 55.3, 38.0, 20.6, 19.5; FTIR (NaCl, thin film): 3017, 2962, 2929, 2834, 1607, 1576, 1511, 1488, 1462, 1297, 1250, 1174, 1106, 1035, 968, 818, 758, 729  $\text{cm}^{-1}$ ; HRMS (MM) calc'd for  $\text{C}_{18}\text{H}_{20}\text{O}$   $[\text{M}]^+$  252.1514, found 252.1673.

**(*S,E*)-4,4'-(but-1-ene-1,3-diyl)bis(methoxybenzene) (163e)**



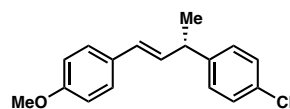
Prepared from 1-(1-chloroethyl)-4-methoxybenzene (**162e**, 0.2 mmol) and (*E*)-1-(2-bromovinyl)-4-methoxybenzene (**156**, 0.2 mmol) according to General Procedure 5. The crude residue was purified by silica gel chromatography (0 to 2%  $\text{Et}_2\text{O}$ /hexanes) to yield **163e** (34.5 mg, 64% yield) in 93% ee as a white solid. The enantiomeric excess was determined by chiral SFC analysis (AD-H, 2.5 mL/min, 20% IPA in  $\text{CO}_2$ ,  $\lambda = 254$  nm):  $t_R$  (major) = 7.3 min,  $t_R$  (minor) = 8.9 min.  $[\alpha]_D^{25} = -32.1^\circ$  ( $c = 0.9$ ,  $\text{CHCl}_3$ );  $^1\text{H NMR}$  (500 MHz,  $\text{CDCl}_3$ )  $\delta$  7.35 – 7.28 (m, 2H), 7.27 – 7.15 (m, 2H), 6.91 – 6.82 (m, 4H), 6.36 (d,  $J = 16.2$  Hz, 1H), 6.25 (dd,  $J = 15.9, 6.7$  Hz, 1H), 3.83 – 3.80 (m, 6H), 3.65 – 3.55 (m, 1H), 1.45 (d,  $J = 7.0$  Hz, 3H);  $^{13}\text{C NMR}$  (126 MHz,  $\text{CDCl}_3$ )  $\delta$  158.8, 158.0, 138.0, 133.6, 130.5, 128.2, 127.7, 127.2, 113.94, 113.88, 55.3 (2C), 41.7, 21.4.; FTIR (NaCl, thin film): 2999, 2960, 2834, 1608, 1582, 1511, 1463, 1441, 1419, 1300, 1248, 1175, 1107, 1036, 968, 830, 818, 767  $\text{cm}^{-1}$ ; HRMS (MM) calc'd for  $\text{C}_{18}\text{H}_{20}\text{O}_2$   $[\text{M}]^+$  268.1463, found 268.1394.

**(*S,E*)-1-fluoro-4-(4-(4-methoxyphenyl)but-3-en-2-yl)benzene (163f)**



Prepared from 1-(1-chloroethyl)-4-fluorobenzene (**162f**, 0.2 mmol) and (*E*)-1-(2-bromovinyl)-4-methoxybenzene (**156**, 0.2 mmol) according to General Procedure 5. The crude residue was purified by silica gel chromatography (0 to 2% Et<sub>2</sub>O/hexanes) to yield **163f** (41.4 mg, 81% yield) in 89% ee as a white solid. The enantiomeric excess was determined by chiral SFC analysis (OB-H, 2.5 mL/min, 15% IPA in CO<sub>2</sub>, λ = 254 nm): *t*<sub>R</sub> (major) = 5.6 min, *t*<sub>R</sub> (minor) = 8.0 min. [α]<sub>D</sub><sup>25</sup> = −35.1° (c = 1.0, CHCl<sub>3</sub>); <sup>1</sup>H NMR (500 MHz, CDCl<sub>3</sub>) δ 7.34 – 7.28 (m, 2H), 7.28 – 7.20 (m, 2H), 7.07 – 6.96 (m, 2H), 6.91 – 6.83 (m, 2H), 6.36 (d, *J* = 16.1 Hz, 1H), 6.23 (dd, *J* = 15.9, 6.7 Hz, 1H), 3.82 (s, 3H), 3.68 – 3.58 (m, 1H), 1.46 (d, *J* = 7.0 Hz, 3H); <sup>13</sup>C NMR (126 MHz, CDCl<sub>3</sub>) δ 161.4 (d, *J* = 244 Hz), 159.0, 141.5, 132.9, 130.3, 128.6 (d, *J* = 8 Hz), 128.1, 127.2, 115.1 (d, *J* = 21 Hz), 114.0, 55.3, 41.8, 21.4; FTIR (NaCl, thin film): 3032, 2963, 2835, 1607, 1577, 1510, 1464, 1419, 1298, 1251, 1223, 1175, 1159, 1107, 1035, 968, 835, 821, 769 cm<sup>−1</sup>; HRMS (MM) calc'd for C<sub>17</sub>H<sub>17</sub>FO [M]<sup>+</sup> 265.1263, found 265.1223.

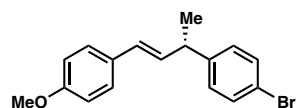
**(*S,E*)-1-chloro-4-(4-(4-methoxyphenyl)but-3-en-2-yl)benzene (163g)**



Prepared from 1-(1-chloroethyl)-4-chlorobenzene (**162g**, 0.2 mmol) and (*E*)-1-(2-bromovinyl)-4-methoxybenzene (**156**, 0.2 mmol) according to General Procedure 6. The crude residue was purified by silica gel chromatography (0 to 2% Et<sub>2</sub>O/hexanes) to yield **163g** (40.9 mg, 75% yield) in 88% ee as a white solid. The enantiomeric excess was determined by chiral SFC analysis (OB-H, 2.5 mL/min, 25% IPA in CO<sub>2</sub>, λ = 254 nm): *t*<sub>R</sub> (major) = 6.6 min, *t*<sub>R</sub> (minor) = 9.4 min.

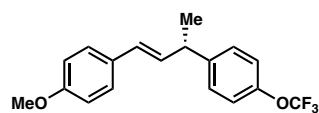
$[\alpha]_D^{25} = -27.9^\circ$  ( $c = 1.0$ ,  $\text{CHCl}_3$ );  $^1\text{H NMR}$  (500 MHz,  $\text{CDCl}_3$ )  $\delta$  7.35 – 7.26 (m, 4H), 7.25 – 7.18 (m, 2H), 6.91 – 6.82 (m, 2H), 6.36 (d,  $J = 16.0$  Hz, 1H), 6.21 (dd,  $J = 15.9, 6.8$  Hz, 1H), 3.82 (s, 3H), 3.66 – 3.56 (m, 1H), 1.45 (d,  $J = 7.0$  Hz, 3H);  $^{13}\text{C NMR}$  (126 MHz,  $\text{CDCl}_3$ )  $\delta$  159.0, 144.4, 132.5, 131.8, 130.2, 128.6, 128.5, 128.4, 127.3, 114.0, 55.3, 41.9, 21.3; FTIR (NaCl, thin film): 3030, 2963, 2834, 1607, 1576, 1511, 1491, 1463, 1408, 1297, 1251, 1174, 1091, 1035, 1012, 967, 828, 817  $\text{cm}^{-1}$ ; HRMS (MM) calc'd for  $\text{C}_{17}\text{H}_{17}\text{ClO}$   $[\text{M}]^+$  272.0968, found 272.0904.

**(*S,E*)-1-bromo-4-(4-(4-methoxyphenyl)but-3-en-2-yl)benzene (163h)**



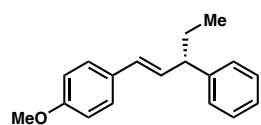
Prepared from 1-(1-chloroethyl)-4-bromobenzene (**162h**, 0.2 mmol) and (*E*)-1-(2-bromovinyl)-4-methoxybenzene (**156**, 0.2 mmol) according to General Procedure 5. The crude residue was purified by silica gel chromatography (5 to 15% toluene/hexanes) to yield **163h** (37.6 mg, 59% yield) in 90% ee as a white solid. The enantiomeric excess was determined by chiral SFC analysis (OB-H, 2.5 mL/min, 35% IPA in  $\text{CO}_2$ ,  $\lambda = 254$  nm):  $t_R$  (major) = 5.4 min,  $t_R$  (minor) = 9.0 min.  $[\alpha]_D^{25} = -30.1^\circ$  ( $c = 0.9$ ,  $\text{CHCl}_3$ );  $^1\text{H NMR}$  (500 MHz,  $\text{CDCl}_3$ )  $\delta$  7.51 – 7.38 (m, 2H), 7.38 – 7.22 (m, 2H), 7.22 – 7.08 (m, 2H), 6.91 – 6.78 (m, 2H), 6.36 (d,  $J = 15.8$  Hz, 1H), 6.20 (dd,  $J = 15.9, 6.8$  Hz, 1H), 3.82 (s, 3H), 3.71 – 3.47 (m, 1H), 1.45 (d,  $J = 6.9$  Hz, 3H);  $^{13}\text{C NMR}$  (126 MHz,  $\text{CDCl}_3$ )  $\delta$  159.0, 144.9, 132.4, 131.5, 130.2, 129.1, 128.4, 127.3, 119.8, 114.0, 55.3, 42.0, 21.2; FTIR (NaCl, thin film): 2962, 2930, 2834, 1607, 1577, 1511, 1487, 1297, 1250, 1174, 1073, 1035, 1008, 967, 816  $\text{cm}^{-1}$ ; HRMS (MM) calc'd for  $\text{C}_{17}\text{H}_{17}\text{BrO}$   $[\text{M}+\text{H}]^+$  317.0536, found 317.0449.

**(*S,E*)-1-methoxy-4-(3-(4-(trifluoromethoxy)phenyl)but-1-en-1-yl)benzene (163i)**



Prepared from 1-(1-chloroethyl)-4-(trifluoromethoxy)benzene (**162i**, 0.2 mmol) and (*E*)-1-(2-bromovinyl)-4-methoxybenzene (**156**, 0.2 mmol) according to General Procedure 6. The crude residue was purified by silica gel chromatography (5 to 15% toluene/hexanes) to yield **163i** (54.2 mg, 84% yield) in 88% ee as a white solid. The enantiomeric excess was determined by chiral SFC analysis (AD-H, 2.5 mL/min, 7% IPA in CO<sub>2</sub>, λ = 254 nm): *t<sub>R</sub>* (major) = 7.7 min, *t<sub>R</sub>* (minor) = 8.8 min. [α]<sub>D</sub><sup>25</sup> = -27.2° (c = 1.1, CHCl<sub>3</sub>); <sup>1</sup>H NMR (500 MHz, CDCl<sub>3</sub>) δ 7.37 – 7.23 (m, 4H), 7.23 – 7.13 (m, 2H), 6.90 – 6.83 (m, 2H), 6.38 (d, *J* = 16.0 Hz, 1H), 6.22 (dd, *J* = 15.9, 6.8 Hz, 1H), 3.82 (s, 3H), 3.70 – 3.61 (m, 1H), 1.47 (d, *J* = 7.1 Hz, 3H); <sup>13</sup>C NMR (126 MHz, CDCl<sub>3</sub>) δ 159.0, 147.6, 144.6, 132.4, 130.2, 128.5, 128.4, 127.3, 120.9, 114.0, 55.3, 41.9, 21.3; FTIR (NaCl, thin film): 3033, 2965, 2836, 1607, 1577, 1511, 1465, 1420, 1374, 1255, 1223, 1174, 1106, 1036, 1015, 968, 849, 819 cm<sup>-1</sup>; HRMS (MM) calc'd for C<sub>18</sub>H<sub>17</sub>F<sub>3</sub>O<sub>2</sub> [M]<sup>+</sup> 322.1181, found 322.1105.

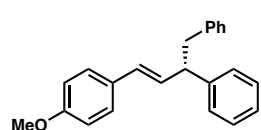
**(*S,E*)-1-methoxy-4-(3-phenylpent-1-en-1-yl)benzene (163j)**



Prepared from (1-chloropropyl)benzene (**162j**, 0.2 mmol) and (*E*)-1-(2-bromovinyl)-4-methoxybenzene (**156**, 0.2 mmol) according to General Procedure 5. The crude residue was purified by silica gel chromatography (5 to 15% toluene/hexanes) to yield **163j** (40.3 mg, 80% yield) in 97% ee as a white solid. The enantiomeric excess was determined by chiral SFC analysis (OB-H, 2.5 mL/min, 15% IPA in CO<sub>2</sub>, λ = 254 nm): *t<sub>R</sub>* (minor) = 7.7 min, *t<sub>R</sub>* (major) = 9.3 min. [α]<sub>D</sub><sup>25</sup> = -47.8° (c = 0.9, CHCl<sub>3</sub>); <sup>1</sup>H NMR (500 MHz, CDCl<sub>3</sub>) δ 7.39 – 7.19 (m, 5H), 6.90 – 6.83 (m, 2H),

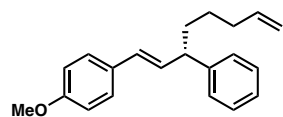
6.38 (d,  $J = 14.8$  Hz, 1H), 6.23 (dd,  $J = 15.8, 7.9$  Hz, 1H), 3.82 (s, 3H), 3.32 (q,  $J = 7.3$  Hz, 1H), 1.86 (pd,  $J = 7.4, 2.4$  Hz, 2H), 0.95 (t,  $J = 7.4$  Hz, 3H);  $^{13}\text{C}$  NMR (126 MHz,  $\text{CDCl}_3$ )  $\delta$  158.9, 144.8, 132.2, 130.6, 128.9, 128.4, 127.7, 127.2, 126.1, 113.9, 55.3, 51.0, 28.9, 12.2; FTIR (NaCl, thin film): 3025, 2958, 2929, 2834, 1607, 1510, 1451, 1300, 1247, 1174, 1107, 1034, 964, 830, 757  $\text{cm}^{-1}$ ; HRMS (MM) calc'd for  $\text{C}_{18}\text{H}_{20}\text{O}$   $[\text{M}]^+$  252.1514, found 252.1466.

**(*S,E*)-(4-(4-methoxyphenyl)but-3-ene-1,2-diyl)dibenzene (163k)**



Prepared from (1-chloroethane-1,2-diyl)dibenzene (**162k**, 0.2 mmol) and (*E*)-1-(2-bromovinyl)-4-methoxybenzene (**156**, 0.2 mmol) according to General Procedure 5. The crude residue was purified by silica gel chromatography (0 to 2%  $\text{Et}_2\text{O}$ /hexanes) to yield **163k** (51.3 mg, 82% yield) in 93% ee as a white solid. The enantiomeric excess was determined by chiral SFC analysis (AS-H, 2.5 mL/min, 10% IPA in  $\text{CO}_2$ ,  $\lambda = 254$  nm):  $t_{\text{R}}$  (minor) = 5.8 min,  $t_{\text{R}}$  (major) = 6.4 min.  $[\alpha]_{\text{D}}^{25} = +18.9^\circ$  ( $c = 1.0$ ,  $\text{CHCl}_3$ );  $^1\text{H}$  NMR (500 MHz,  $\text{CDCl}_3$ )  $\delta$  7.45 – 7.02 (m, 10H), 6.94 – 6.78 (m, 2H), 6.40 – 6.24 (m, 2H), 3.82 (s, 3H), 3.76 (q,  $J = 7.2$  Hz, 1H), 3.22 – 3.09 (m, 2H);  $^{13}\text{C}$  NMR (126 MHz,  $\text{CDCl}_3$ )  $\delta$  158.9, 144.1, 140.1, 131.3, 130.4, 129.4, 129.3, 128.4, 128.1, 127.9, 127.3, 126.3, 125.9, 113.9, 55.3, 50.9, 42.8; FTIR (NaCl, thin film): 3060, 3026, 2932, 2834, 1607, 1577, 1511, 1494, 1452, 1299, 1249, 1174, 1109, 1033, 965, 820, 756  $\text{cm}^{-1}$ ; HRMS (MM) calc'd for  $\text{C}_{23}\text{H}_{22}\text{O}$   $[\text{M}+\text{H}]^+$  315.1743, found 315.1699.

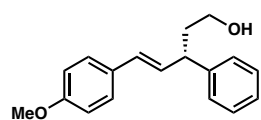
**(*S,E*)-1-methoxy-4-(3-phenylocta-1,7-dien-1-yl)benzene (163l)**



Prepared from (1-chlorohex-5-en-1-yl)benzene (**162l**, 0.2 mmol) and (*E*)-1-(2-bromovinyl)-4-methoxybenzene (**156**, 0.2 mmol)

according to General Procedure 5. The crude residue was purified by silica gel chromatography (5 to 15% toluene/hexanes) to yield **163l** (39.6 mg, 68% yield) in 94% ee as a clear oil. The enantiomeric excess was determined by chiral SFC analysis (AS-H, 2.5 mL/min, 10% IPA in CO<sub>2</sub>, λ = 254 nm): *t*<sub>R</sub> (minor) = 3.1 min, *t*<sub>R</sub> (major) = 3.7 min. [α]<sub>D</sub><sup>25</sup> = -22.7° (c = 1.2, CHCl<sub>3</sub>); <sup>1</sup>H NMR (500 MHz, CDCl<sub>3</sub>) δ 7.39 – 7.19 (m, 7H), 6.89 – 6.81 (m, 2H), 6.36 (d, *J* = 15.8 Hz, 1H), 6.21 (dd, *J* = 15.8, 7.9 Hz, 1H), 5.81 (ddt, *J* = 17.0, 10.2, 6.7 Hz, 1H), 5.06 – 4.93 (m, 2H), 3.81 (s, 3H), 3.41 (q, *J* = 7.6 Hz, 1H), 2.15 – 2.04 (m, 2H), 1.87 – 1.77 (m, 2H), 1.53 – 1.32 (m, 2H); <sup>13</sup>C NMR (126 MHz, CDCl<sub>3</sub>) δ 158.9, 144.8, 138.7, 132.2, 130.4, 128.8, 128.5, 127.6, 127.2, 126.1, 114.5, 113.9, 55.3, 49.1, 35.5, 33.7, 27.0; FTIR (NaCl, thin film): 3060, 3026, 2931, 2856, 2834, 1639, 1607, 1577, 1511, 1493, 1464, 1452, 1441, 1418, 1299, 1250, 1174, 1108, 1036, 965, 910, 828, 759 cm<sup>-1</sup>; HRMS (MM) calc'd for C<sub>21</sub>H<sub>24</sub>O [M+H]<sup>+</sup> 293.1900, found 293.1867.

**(*S,E*)-5-(4-methoxyphenyl)-3-phenylpent-4-en-1-ol (163m)**

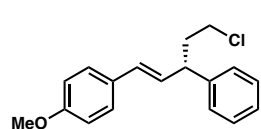


Prepared from 3-chloro-3-phenylpropan-1-ol (**162m**, 0.2 mmol) and (*E*)-1-(2-bromovinyl)-4-methoxybenzene (**156**, 0.2 mmol)

according to General Procedure 5. The crude residue was purified by silica gel chromatography (10 to 20% ethyl acetate/hexanes) to yield **163m** (43.3 mg, 81% yield) in 96% ee as a white solid. The enantiomeric excess was determined by chiral SFC analysis (OB-H, 2.5 mL/min, 30% IPA in CO<sub>2</sub>, λ = 254 nm): *t*<sub>R</sub> (minor) = 5.5 min, *t*<sub>R</sub>

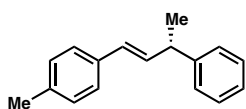
(major) = 6.9 min.  $[\alpha]_D^{25} = -27.5^\circ$  (c = 1.0, CHCl<sub>3</sub>); <sup>1</sup>H NMR (500 MHz, CDCl<sub>3</sub>) δ 7.38 – 7.20 (m, 7H), 6.90 – 6.81 (m, 2H), 6.41 (d, *J* = 15.5 Hz, 1H), 6.22 (dd, *J* = 15.8, 8.0 Hz, 1H), 3.81 (s, 3H), 3.74 – 3.60 (m, 3H), 2.18 – 2.01 (m, 2H); <sup>13</sup>C NMR (126 MHz, CDCl<sub>3</sub>) δ 158.9, 144.1, 131.4, 130.1, 129.1, 128.6, 127.6, 127.3, 126.4, 113.9, 61.0, 55.3, 45.5, 38.5; FTIR (NaCl, thin film): 3350, 3026, 2933, 2835, 1607, 1577, 1511, 1492, 1452, 1300, 1249, 1175, 1033, 967, 809, 760 cm<sup>-1</sup>; HRMS (MM) calc'd for C<sub>18</sub>H<sub>20</sub>O<sub>2</sub> [M+H]<sup>+</sup> 269.1536, found 269.1470.

**(*S,E*)- 1-(5-chloro-3-phenylpent-1-en-1-yl)-4-methoxybenzene (163n)**



Prepared from (1,3-dichloropropyl)benzene (**162n**, 0.2 mmol) and (*E*)-1-(2-bromovinyl)-4-methoxybenzene (**156**, 0.2 mmol) according to General Procedure 6. The crude residue was purified by silica gel chromatography (5 to 20% toluene/hexanes) to yield **163n** (34.3 mg, 60% yield) in 94% ee as a clear oil. The enantiomeric excess was determined by chiral SFC analysis (AS-H, 2.5 mL/min, 3% ACN in CO<sub>2</sub>, λ = 254 nm): *t*<sub>R</sub> (major) = 15.5 min, *t*<sub>R</sub> (minor) = 22.0 min.  $[\alpha]_D^{25} = -10.9^\circ$  (c = 1.0, CHCl<sub>3</sub>); <sup>1</sup>H NMR (500 MHz, CDCl<sub>3</sub>) δ 7.41 – 7.15 (m, 7H), 6.91 – 6.82 (m, 2H), 6.44 (d, *J* = 16.1 Hz, 3H), 6.18 (dd, *J* = 15.8, 8.0 Hz, 1H), 3.81 (s, 3H), 3.76 – 3.68 (m, 1H), 3.61 – 3.45 (m, 2H), 2.34 – 2.19 (m, 2H); <sup>13</sup>C NMR (126 MHz, CDCl<sub>3</sub>) δ 159.0, 143.1, 130.1, 129.9, 129.8, 128.7, 127.6, 127.3, 126.6, 113.9, 55.3, 45.9, 43.1, 38.4; FTIR (NaCl, thin film): 3027, 2956, 2835, 1607, 1576, 1511, 1492, 1452, 1291, 1250, 1175, 1034, 967, 760, 701 cm<sup>-1</sup>; HRMS (MM) calc'd for C<sub>18</sub>H<sub>19</sub>ClO [M]<sup>+</sup> 286.1119, found 286.1119.

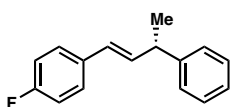
**(*S,E*)-1-methyl-4-(3-phenylbut-1-en-1-yl)benzene (157a)**



Prepared from (1-chloroethyl)benzene (**26**, 0.2 mmol) and (*E*)-1-(2-bromovinyl)-4-methylbenzene (**156a**, 0.2 mmol) according to General Procedure 5. The crude residue was purified by silica gel chromatography (hexanes, 6% AgNO<sub>3</sub>-adsorbed silica gel) to yield **157a** (36.9 mg, 83% yield) in 96% ee as a clear oil. The enantiomeric excess was determined by chiral SFC analysis (OJ-H, 2.5 mL/min, 7% IPA in CO<sub>2</sub>, λ = 254 nm): *t*<sub>R</sub> (minor) = 7.5 min, *t*<sub>R</sub> (major) = 9.3 min. [α]<sub>D</sub><sup>25</sup> = –47.3° (c = 1.1, CHCl<sub>3</sub>); <sup>1</sup>H NMR (500 MHz, CDCl<sub>3</sub>) δ 7.49 – 7.18 (m, 7H), 7.17 – 7.08 (m, 2H), 6.53 – 6.23 (m, 2H), 3.73 – 3.59 (m, 1H), 2.35 (s, 3H), 1.54 – 1.42 (m, 3H); <sup>13</sup>C NMR (126 MHz, CDCl<sub>3</sub>) δ 145.8, 136.8, 134.8, 134.2, 129.2, 128.5, 128.4, 127.3, 126.2, 126.0, 42.6, 21.3, 21.2; FTIR (NaCl, thin film): 3083, 3024, 2964, 2924, 2870, 1602, 1512, 1492, 1451, 1371, 1154, 1017, 967, 803, 759 cm<sup>-1</sup>; HRMS (MM) calc'd for C<sub>17</sub>H<sub>18</sub> [M+H<sub>2</sub>O]<sup>+</sup> 240.1509, found 240.1517.

The optical rotation of the product generated in the presence of (*R,R,S,S*)-**L104** was measured as [α]<sub>D</sub><sup>25</sup> = –47.3° (c = 1.1, CHCl<sub>3</sub>). Lit: [α]<sub>D</sub><sup>20</sup> = +38.4° (c = 0.98, CHCl<sub>3</sub>, *R* enantiomer, 91% ee). Based on the literature precedent, we assign our product as the *S* enantiomer.<sup>40</sup>

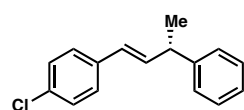
**(*S,E*)-1-fluoro-4-(3-phenylbut-1-en-1-yl)benzene (157b)**



Prepared from (1-chloroethyl)benzene (**26**, 0.2 mmol) and (*E*)-1-(2-bromovinyl)-4-fluorobenzene (**156b**, 0.2 mmol) according to General Procedure 5. The crude residue was purified by silica gel chromatography (hexanes, 6%

AgNO<sub>3</sub>-adsorbed silica gel) to yield **157b** (33.7 mg, 74% yield) in 94% ee as a clear oil. The enantiomeric excess was determined by chiral SFC analysis (OJ-H, 2.5 mL/min, 7% IPA in CO<sub>2</sub>, λ = 254 nm): *t<sub>R</sub>* (minor) = 5.9 min, *t<sub>R</sub>* (major) = 7.1 min. [α]<sub>D</sub><sup>25</sup> = -34.6° (c = 1.1, CHCl<sub>3</sub>); <sup>1</sup>H NMR (500 MHz, CDCl<sub>3</sub>) δ 7.48 – 7.12 (m, 7H), 7.10 – 6.88 (m, 2H), 6.47 – 6.21 (m, 2H), 3.81 – 3.53 (m, 1H), 1.49 (d, *J* = 7.2 Hz, 3H); <sup>13</sup>C NMR (126 MHz, CDCl<sub>3</sub>) δ 162.0 (d, *J* = 246 Hz), 145.5, 135.0, 133.7, 128.5, 127.6 (d, *J* = 8 Hz), 127.35, 127.28, 126.3, 115.3 (d, *J* = 22 Hz), 42.6, 21.2; FTIR (NaCl, thin film): 3025, 2965, 2927, 2871, 1602, 1508, 1492, 1451, 1226, 1157, 1094, 1011, 965, 855, 818, 761 cm<sup>-1</sup>; HRMS (MM) calc'd for C<sub>16</sub>H<sub>15</sub>F [M+Li]<sup>+</sup> 232.1304, found 232.1321.

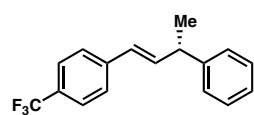
**(*S,E*)-1-chloro-4-(3-phenylbut-1-en-1-yl)benzene (157c)**



Prepared from (1-chloroethyl)benzene (**26**, 0.2 mmol) and (*E*)-1-(2-bromovinyl)-4-chlorobenzene (**156c**, 0.2 mmol) according to General Procedure 6. The crude residue was purified by silica gel chromatography (hexanes, 6% AgNO<sub>3</sub>-adsorbed silica gel) to yield **157c** (32.1 mg, 66% yield) in 95% ee as a clear oil. The enantiomeric excess was determined by chiral SFC analysis (OJ-H, 2.5 mL/min, 10% IPA in CO<sub>2</sub>, λ = 254 nm): *t<sub>R</sub>* (minor) = 6.4 min, *t<sub>R</sub>* (major) = 7.9 min. [α]<sub>D</sub><sup>25</sup> = -42.2° (c = 1.0, CHCl<sub>3</sub>); <sup>1</sup>H NMR (500 MHz, CDCl<sub>3</sub>) δ 7.53 – 7.09 (m, 9H), 6.45 – 6.32 (m, 2H), 3.70 – 3.60 (m, 1H), 1.49 (d, *J* = 7.0 Hz, 3H); <sup>13</sup>C NMR (126 MHz, CDCl<sub>3</sub>) δ 145.3, 136.1, 136.0, 132.6, 128.6, 127.6, 127.4, 127.3, 126.3, 42.6, 21.1; FTIR (NaCl, thin film): 3082, 3060, 3026, 2965, 2927, 2871, 1646, 1602, 1491, 1451, 1404, 1372, 1062, 1012, 966, 858, 810, 761 cm<sup>-1</sup>; HRMS (ESI) calc'd for C<sub>16</sub>H<sub>15</sub>Cl [M+H]<sup>+</sup> 243.0935, found 243.0985.

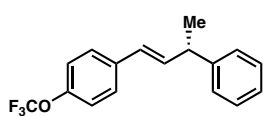
The optical rotation of the product generated in the presence of (*R,R,S,S*)-**L104** was measured as  $[\alpha]_D^{25} = -42.2^\circ$  ( $c = 1.0$ ,  $\text{CHCl}_3$ ). Lit:  $[\alpha]_D^{20} = +33^\circ$  ( $c = 1.0$ ,  $\text{CHCl}_3$ , *R* enantiomer, 91% ee).<sup>41</sup> Based on the literature precedent, we assign our product as the *S* enantiomer.

**(*S,E*)-1-(3-phenylbut-1-en-1-yl)-4-(trifluoromethyl)benzene (157d)**



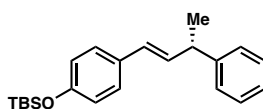
Prepared from (1-chloroethyl)benzene (**26**, 0.2 mmol) and (*E*)-1-(2-bromovinyl)-4-(trifluoromethyl)benzene (**156d**, 0.2 mmol) according to General Procedure 6. The crude residue was purified by silica gel chromatography (hexanes) to yield **157d** (27.0 mg, 49% yield) in 94% ee as a clear oil. The enantiomeric excess was determined by chiral SFC analysis (OJ-H, 2.5 mL/min, 3% IPA in  $\text{CO}_2$ ,  $\lambda = 254$  nm):  $t_R$  (minor) = 5.4 min,  $t_R$  (major) = 6.3 min.  $[\alpha]_D^{25} = -33.1^\circ$  ( $c = 0.9$ ,  $\text{CHCl}_3$ );  $^1\text{H}$  NMR (500 MHz,  $\text{CDCl}_3$ )  $\delta$  7.59 – 7.52 (m, 2H), 7.49 – 7.41 (m, 2H), 7.40 – 7.21 (m, 4H), 6.52 (dd,  $J = 15.9, 6.3$  Hz, 1H), 6.45 (d,  $J = 16.0$  Hz, 1H), 3.73 – 3.63 (m, 1H), 1.50 (d,  $J = 7.0$  Hz, 3H);  $^{13}\text{C}$  NMR (126 MHz,  $\text{CDCl}_3$ )  $\delta$  145.0, 138.0, 128.6, 127.6, 127.33, 127.29, 126.4, 126.3, 125.4 (q,  $J = 4$  Hz), 124.3 (q,  $J = 272$  Hz) 42.6, 21.0; FTIR (NaCl, thin film): 3027, 2967, 1614, 1493, 1452, 1413, 1326, 1164, 1122, 1067, 1016, 967, 864, 820, 760  $\text{cm}^{-1}$ ; HRMS (MM) calc'd for  $\text{C}_{17}\text{H}_{15}\text{F}_3$   $[\text{M}+\text{H}]^+$  227.1199, found 227.1490.

**(*S,E*)-1-(3-phenylbut-1-en-1-yl)-4-(trifluoromethoxy)benzene (157e)**



Prepared from (1-chloroethyl)benzene (**26**, 0.2 mmol) and (*E*)-1-(2-bromovinyl)-4-(trifluoromethoxy)benzene (**156e**, 0.2 mmol) according to General Procedure 6. The crude residue was purified by silica gel chromatography (hexanes, 6% AgNO<sub>3</sub>-adsorbed silica gel) to yield **157e** (47.1 mg, 81% yield) in 94% ee as a clear oil. The enantiomeric excess was determined by chiral SFC analysis (OJ-H, 2.5 mL/min, 10% IPA in CO<sub>2</sub>, λ = 254 nm): *t*<sub>R</sub> (minor) = 2.3 min, *t*<sub>R</sub> (major) = 2.5 min. [α]<sub>D</sub><sup>25</sup> = -27.9° (c = 1.0, CHCl<sub>3</sub>); <sup>1</sup>H NMR (500 MHz, CDCl<sub>3</sub>) δ 7.50 – 7.20 (m, 5H), 7.20 – 7.08 (m, 2H), 6.57 – 6.24 (m, 2H), 3.83 – 3.53 (m, 1H), 1.49 (d, *J* = 7.2 Hz, 3H); <sup>13</sup>C NMR (126 MHz, CDCl<sub>3</sub>) δ 148.1, 145.3, 136.4, 128.6, 128.3, 127.31, 127.28, 127.1, 126.4, 121.1, 42.6, 21.1; FTIR (NaCl, thin film): 3083, 3061, 3027, 2967, 2930, 2873, 1602, 1587, 1507, 1493, 1452, 1260, 1220, 1164, 1017, 965, 864, 762 cm<sup>-1</sup>; HRMS (MM) calc'd for C<sub>17</sub>H<sub>15</sub>F<sub>3</sub>O [M+H]<sup>+</sup> 293.1148, found 293.1237.

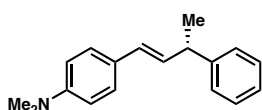
**(*S,E*)-*tert*-butyldimethyl(4-(3-phenylbut-1-en-1-yl)phenoxy)silane (157f)**



Prepared from (1-chloroethyl)benzene (**26**, 0.2 mmol) and (*E*)-(4-(2-bromovinyl)phenoxy)(*tert*-butyl)dimethylsilane (**156f**, 0.2 mmol) according to General Procedure 6. The crude residue was purified by silica gel chromatography (hexanes, 6% AgNO<sub>3</sub>-adsorbed silica gel) to yield **157f** (55.4 mg, 82% yield) in 96% ee as a clear oil. The enantiomeric excess was determined by chiral SFC analysis (OJ-H, 2.5 mL/min, 5% IPA in CO<sub>2</sub>, λ = 254 nm): *t*<sub>R</sub> (major) = 8.6 min, *t*<sub>R</sub> (minor) = 13.2 min. [α]<sub>D</sub><sup>25</sup> = -31.1° (c = 1.1, CHCl<sub>3</sub>); <sup>1</sup>H NMR (500 MHz, CDCl<sub>3</sub>) δ 7.45 – 7.10 (m, 7H), 6.87 – 6.68 (m, 2H), 6.38 (d, *J* = 17.3 Hz, 1H), 6.27 (dd, *J* = 15.9, 6.8 Hz,

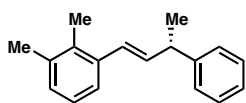
1H), 3.69 – 3.58 (m, 1H), 1.48 (d,  $J = 7.0$  Hz, 3H), 1.00 (s, 9H), 0.21 (s, 6H);  $^{13}\text{C}$  NMR (126 MHz,  $\text{CDCl}_3$ )  $\delta$  154.9, 145.9, 133.2, 130.9, 128.5, 128.0, 127.3, 127.2, 126.1, 120.2, 42.6, 25.7, 21.3, 18.3, –4.4; FTIR (NaCl, thin film): 3060, 3027, 2958, 2929, 2884, 2857, 1604, 1508, 1472, 1462 1451, 1362, 1264, 1168, 1099, 1009, 967, 914, 839, 822, 802, 781  $\text{cm}^{-1}$ ; HRMS (MM) calc'd for  $\text{C}_{22}\text{H}_{30}\text{OSi}$   $[\text{M}+\text{H}]^+$  339.2139, found 339.2118.

**(*S,E*)-*N,N*-dimethyl-4-(3-phenylbut-1-en-1-yl)aniline (**157g**)**



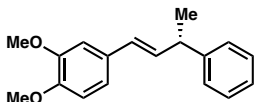
Prepared from (1-chloroethyl)benzene (**26**, 0.2 mmol) and (*E*)-4-(2-bromovinyl)-*N,N*-dimethylaniline (**156g**, 0.2 mmol) according to General Procedure 6. The crude residue was purified by silica gel chromatography (20 to 40% toluene/hexanes) to yield **157g** (27.5 mg, 55% yield) in 95% ee as a white solid. The enantiomeric excess was determined by chiral SFC analysis (OB-H, 2.5 mL/min, 35% IPA in  $\text{CO}_2$ ,  $\lambda = 254$  nm):  $t_{\text{R}}$  (major) = 5.7 min,  $t_{\text{R}}$  (minor) = 9.0 min.  $[\alpha]_{\text{D}}^{25} = -67.3^\circ$  ( $c = 1.1$ ,  $\text{CHCl}_3$ );  $^1\text{H}$  NMR (500 MHz,  $\text{CDCl}_3$ )  $\delta$  7.38 – 7.17 (m, 7H), 6.70 (d,  $J = 8.3$  Hz, 2H), 6.37 (d,  $J = 15.9$  Hz, 1H), 6.21 (dd,  $J = 15.9, 6.8$  Hz, 1H), 3.69 – 3.59 (m, 1H), 2.96 (s, 6H), 1.48 (d,  $J = 7.0$  Hz, 3H);  $^{13}\text{C}$  NMR (126 MHz,  $\text{CDCl}_3$ )  $\delta$  149.8, 146.3, 131.2, 128.4, 128.2, 127.3, 127.0, 126.0, 112.6, 42.5, 40.7, 21.5; FTIR (NaCl, thin film): 3009, 2955, 2870, 2808, 1611, 1525, 1490, 1446, 1359, 1231, 1186, 1168, 1063, 1020, 958, 802, 754  $\text{cm}^{-1}$ ; HRMS (MM) calc'd for  $\text{C}_{18}\text{H}_{21}\text{N}$   $[\text{M}+\text{H}]^+$  252.1747, found 252.1789.

**(*S,E*)-1,2-dimethyl-3-(3-phenylbut-1-en-1-yl)benzene (157h)**



Prepared from (1-chloroethyl)benzene (**26**, 0.2 mmol) and (*E*)-1-(2-bromovinyl)-2,3-dimethylbenzene (**156h**, 0.2 mmol) according to General Procedure 6. The crude residue was purified by silica gel chromatography (hexanes, 6% AgNO<sub>3</sub>-adsorbed silica gel) to yield **157h** (35.9 mg, 76% yield) in 96% ee as a clear oil. The enantiomeric excess was determined by chiral SFC analysis (OB-H, 2.5 mL/min, 4% EtOH in CO<sub>2</sub>, λ = 254 nm): *t*<sub>R</sub> (minor) = 4.4 min, *t*<sub>R</sub> (major) = 5.6 min. [α]<sub>D</sub><sup>25</sup> = −19.4° (c = 1.2, CHCl<sub>3</sub>); <sup>1</sup>H NMR (500 MHz, CDCl<sub>3</sub>) δ 7.46 – 7.16 (m, 7H), 7.08 (d, *J* = 4.7 Hz, 2H), 6.73 (dd, *J* = 15.6, 1.4 Hz, 1H), 6.23 (dd, *J* = 15.7, 6.9 Hz, 1H), 3.75 – 3.66 (m, 1H), 2.33 (s, 3H), 2.28 (s, 3H), 1.52 (d, *J* = 7.0 Hz, 3H); <sup>13</sup>C NMR (126 MHz, CDCl<sub>3</sub>) δ 145.8, 137.2, 137.0, 136.6, 133.8, 128.7, 128.5, 127.4, 127.3, 126.2, 125.5, 124.1, 42.8, 21.5, 20.7, 15.4; FTIR (NaCl, thin film): 3060, 3025, 2963, 2927, 2869, 1600, 1582, 1491, 1451, 1371, 1015, 971, 781, 759 cm<sup>−1</sup>; HRMS (MM) calc'd for C<sub>18</sub>H<sub>20</sub> [M]<sup>+</sup> 236.1565, found 236.1477.

**(*S,E*)-1,2-dimethoxy-4-(3-phenylbut-1-en-1-yl)benzene (157i)**

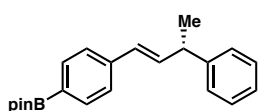


Prepared from (1-chloroethyl)benzene (**26**, 0.2 mmol) and (*E*)-4-(2-bromovinyl)-1,2-dimethoxybenzene (**156i**, 0.2 mmol) according to General Procedure 6. The crude residue was purified by silica gel chromatography (20 to 40% toluene/hexanes) to yield **157i** (39.3 mg, 73% yield) in 95% ee as a clear oil. The enantiomeric excess was determined by chiral SFC analysis (OB-H, 2.5 mL/min, 25% IPA in CO<sub>2</sub>, λ = 254 nm): *t*<sub>R</sub> (minor) = 5.6 min, *t*<sub>R</sub> (major) = 7.8 min. [α]<sub>D</sub><sup>25</sup> = −36.4° (c = 1.1, CHCl<sub>3</sub>); <sup>1</sup>H NMR (500 MHz, CDCl<sub>3</sub>) δ 7.39 – 7.19 (m, 5H), 6.96 – 6.88 (m, 2H),

6.82 (d,  $J = 8.2$  Hz, 1H), 6.38 (d,  $J = 15.9$  Hz, 1H), 6.28 (dd,  $J = 15.8, 6.6$  Hz, 1H), 3.90 (s, 3H), 3.89 (s, 3H), 3.70 – 3.61 (m, 1H), 1.49 (d,  $J = 7.1$  Hz, 3H);  $^{13}\text{C}$  NMR (126 MHz,  $\text{CDCl}_3$ )  $\delta$  149.0, 148.4, 145.8, 133.4, 130.7, 128.5, 128.1, 127.3, 126.2, 119.1, 111.1, 108.5, 55.9, 55.8, 42.5, 21.3; FTIR (NaCl, thin film): 3058, 3024, 2961, 2931, 2833, 1601, 1583, 1513, 1492, 1463 1451, 1417, 1264, 1158, 1139, 1027, 966, 803, 763  $\text{cm}^{-1}$ ; HRMS (MM) calc'd for  $\text{C}_{18}\text{H}_{20}\text{O}_2$   $[\text{M}+\text{H}]^+$  269.1536, found 269.1534.

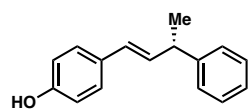
**(*S,E*)-4,4,5,5-tetramethyl-2-(4-(3-phenylbut-1-en-1-yl)phenyl)-1,3,2-dioxaborolane**

**(157j)**



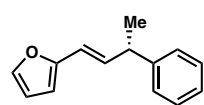
Prepared from (1-chloroethyl)benzene (**26**, 0.2 mmol) and (*E*)-2-(4-(2-bromovinyl)phenyl)-4,4,5,5-tetramethyl-1,3,2-dioxaborolane (**156j**, 0.2 mmol) according to General Procedure 6. The crude residue was purified by silica gel chromatography (20 to 40% hexanes) to yield **157j** (39.4 mg, 59% yield) in 94% ee as a white solid. The enantiomeric excess was determined by chiral SFC analysis (OJ-H, 2.5 mL/min, 15% IPA in  $\text{CO}_2$ ,  $\lambda = 254$  nm):  $t_R$  (major) = 3.9 min,  $t_R$  (minor) = 7.5 min.  $[\alpha]_D^{25} = -33.5^\circ$  ( $c = 0.9$ ,  $\text{CHCl}_3$ );  $^1\text{H}$  NMR (500 MHz,  $\text{CDCl}_3$ )  $\delta$  7.80 – 7.72 (m, 2H), 7.40 – 7.19 (m, 7H), 6.53 – 6.39 (m, 2H), 3.71 – 3.62 (m, 1H), 1.49 (d,  $J = 7.2$  Hz, 3H), 1.36 (s, 12H);  $^{13}\text{C}$  NMR (126 MHz,  $\text{CDCl}_3$ )  $\delta$  145.5, 140.3, 136.4, 135.0, 128.6, 128.5, 127.3, 126.3, 125.5, 83.7, 42.7, 24.9, 21.2; FTIR (NaCl, thin film): 3025, 2975, 2929, 1607, 1602, 1492, 1452, 1397, 1360, 1321, 1270, 1144, 1090, 1017, 962, 860  $\text{cm}^{-1}$ ; HRMS (MM) calc'd for  $\text{C}_{22}\text{H}_{27}\text{BO}_2$   $[\text{M}]^+$  333.2140, found 333.1960.

**(*S,E*)-4-(3-phenylbut-1-en-1-yl)phenol (**157k**)**



Prepared from (1-chloroethyl)benzene (**26**, 0.2 mmol) and (*E*)-4-(2-bromovinyl)phenol (**156k**, 0.2 mmol) according to General Procedure 5. The crude residue was purified by silica gel chromatography (10 to 20% ethyl acetate/hexanes) to yield **157k** (38.6 mg, 86% yield) in 93% ee as a white solid. The enantiomeric excess was determined by chiral SFC analysis (OB-H, 2.5 mL/min, 30% IPA in CO<sub>2</sub>, λ = 254 nm):  $t_R$  (major) = 3.0 min,  $t_R$  (minor) = 3.4 min.  $[\alpha]_D^{25} = -39.1^\circ$  (c = 0.8, CHCl<sub>3</sub>); <sup>1</sup>H NMR (500 MHz, CDCl<sub>3</sub>) δ 7.38 – 7.16 (m, 7H), 6.84 – 6.74 (m, 2H), 6.37 (d, *J* = 16.0 Hz, 1H), 6.26 (dd, *J* = 15.9, 6.7 Hz, 1H), 4.89 (s, 1H), 3.69 – 3.60 (m, 1H), 1.48 (d, *J* = 7.0 Hz, 3H); <sup>13</sup>C NMR (126 MHz, CDCl<sub>3</sub>) δ 154.6, 145.9, 133.2, 130.6, 128.5, 127.8, 127.5, 127.3, 126.2, 115.4, 42.5, 21.3; FTIR (NaCl, thin film): 3368, 3025, 2963, 2927, 2871, 1633, 1608, 1512, 1492, 1451, 1371, 1227, 1170, 1010, 966, 819, 762 cm<sup>-1</sup>; HRMS (MM) calc'd for C<sub>16</sub>H<sub>16</sub>O [M]<sup>+</sup> 224.1201, found 224.1164.

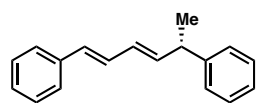
**(*S,E*)-2-(3-phenylbut-1-en-1-yl)furan (**157l**)**



Prepared from (1-chloroethyl)benzene (**26**, 0.2 mmol) and (*E*)-2-(2-bromovinyl)furan (**156l**, 0.2 mmol) according to General Procedure 6. The crude residue was purified by silica gel chromatography (hexanes) to yield **157l** (31.7 mg, 80% yield) in 91% ee as a yellow oil. The enantiomeric excess was determined by chiral SFC analysis (AD-H, 2.5 mL/min, 3% IPA in CO<sub>2</sub>, λ = 254 nm):  $t_R$  (major) = 3.2 min,  $t_R$  (minor) = 3.5 min.  $[\alpha]_D^{25} = -48.3^\circ$  (c = 0.9, CHCl<sub>3</sub>), lit:<sup>39</sup>  $[\alpha]_D^{20} = -48^\circ$  (c = 1.0, CHCl<sub>3</sub>, *S* enantiomer, 95% ee); <sup>1</sup>H NMR (500 MHz, CDCl<sub>3</sub>) δ 7.41 – 7.18 (m, 6H), 6.43 – 6.35 (m, 2H), 6.26 – 6.16 (m, 2H), 3.69 – 3.58 (m, 1H), 1.48 (d, *J* = 7.1 Hz, 3H); <sup>13</sup>C

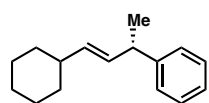
NMR (126 MHz, CDCl<sub>3</sub>)  $\delta$  153.1, 145.3, 141.4, 134.2, 128.5, 127.3, 126.3, 117.4, 111.2, 106.7, 42.3, 21.1; FTIR (NaCl, thin film): 3060, 3026, 2965, 2928, 2871, 1602, 1491, 1452, 1371, 1255, 1151, 1012, 961, 928, 884, 760, 732 cm<sup>-1</sup>; HRMS (MM) calc'd for C<sub>14</sub>H<sub>14</sub>O [M+H]<sup>+</sup> 199.1117, found 199.1067.

**(*S*,1*E*,3*E*)-hexa-1,3-diene-1,5-diyl dibenzene (**157m**)**



Prepared from (1-chloroethyl)benzene (**26**, 0.2 mmol) and ((1*E*,3*E*)-4-bromobuta-1,3-dien-1-yl)benzene (**156m**, 0.2 mmol) according to General Procedure 5. The crude residue was purified by flash chromatography (hexanes, florisil) to yield **157m** (38.5 mg, 82% yield) in 92% ee as a white solid. The enantiomeric excess was determined by chiral SFC analysis (OB-H, 2.5 mL/min, 15% IPA in CO<sub>2</sub>,  $\lambda$  = 254 nm):  $t_R$  (major) = 6.9 min,  $t_R$  (minor) = 9.4 min.  $[\alpha]_D^{25} = -34.1^\circ$  (c = 1.0, CHCl<sub>3</sub>); <sup>1</sup>H NMR (500 MHz, CDCl<sub>3</sub>)  $\delta$  7.43 – 7.16 (m, 9H), 6.80 (dd,  $J = 15.7, 10.4$  Hz, 1H), 6.52 (d,  $J = 15.7$  Hz, 1H), 6.26 (dd,  $J = 15.2, 10.4$  Hz, 1H), 6.03 (dd,  $J = 15.3, 6.8$  Hz, 1H), 3.66 – 3.56 (m, 1H), 1.46 (d,  $J = 7.0$  Hz, 3H); <sup>13</sup>C NMR (126 MHz, CDCl<sub>3</sub>)  $\delta$  145.6, 139.9, 137.5, 131.0, 129.20, 129.18, 128.6, 128.5, 127.3, 127.2, 126.23, 126.19, 42.5, 21.2; FTIR (NaCl, thin film): 3059, 3023, 2964, 2927, 2870, 1638, 1596, 1492, 1448, 1371, 1259, 1154, 1117, 1072, 988, 909, 760, 745 cm<sup>-1</sup>; HRMS (MM) calc'd for C<sub>18</sub>H<sub>18</sub> [M]<sup>+</sup> 234.1409, found 234.1342.

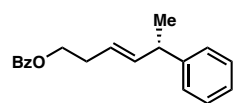
**(*S,E*)-(4-cyclohexylbut-3-en-2-yl)benzene (157n)**



Prepared from (1-chloroethyl)benzene (**26**, 0.2 mmol) and (*E*)-(2-bromovinyl)cyclohexane (**156n**, 0.2 mmol) according to General Procedure 5. The crude residue was purified by flash chromatography (hexanes) to yield **157n** (23.6 mg, 55% yield) in 96% ee as a clear oil. The enantiomeric excess was determined by chiral HPLC analysis (OJ-H, 1 mL/min, 1% IPA in hexanes,  $\lambda = 220$  nm):  $t_R$  (minor) = 5.1 min,  $t_R$  (major) = 5.8 min.  $[\alpha]_D^{25} = -5.5^\circ$  ( $c = 0.8$ ,  $\text{CHCl}_3$ );  $^1\text{H NMR}$  (500 MHz,  $\text{CDCl}_3$ )  $\delta$  7.35 – 7.26 (m, 2H), 7.26 – 7.16 (m, 3H), 5.57 (ddd,  $J = 15.5, 6.7, 1.2$  Hz, 1H), 5.44 (ddd,  $J = 15.4, 6.7, 1.2$  Hz, 1H), 3.47 – 3.37 (m, 1H), 2.01 – 1.89 (m, 1H), 1.78 – 1.61 (m, 4H), 1.35 (d,  $J = 7.0$  Hz, 3H), 1.32 – 1.01 (m, 6H);  $^{13}\text{C NMR}$  (126 MHz,  $\text{CDCl}_3$ )  $\delta$  146.7, 135.2, 132.3, 128.3, 127.2, 125.8, 42.2, 40.6, 33.20, 33.18, 26.2, 26.1, 21.7; FTIR (NaCl, thin film): 3024, 2962, 2922, 2850, 1601, 1492, 1448, 1371, 1009, 965, 759, 698  $\text{cm}^{-1}$ ; HRMS (MM) calc'd for  $\text{C}_{16}\text{H}_{22}$   $[\text{M}]^+$  214.1722, found 214.1689.

The optical rotation of the product generated in the presence of (*R,R,S,S*)-**L104** was measured as  $[\alpha]_D^{25} = -5.5^\circ$  ( $c = 0.8$ ,  $\text{CHCl}_3$ ). Lit:  $[\alpha]_D^{20} = +10.1^\circ$  ( $c = 0.45$ ,  $\text{CHCl}_3$ , *R* enantiomer, 95% ee).<sup>42</sup> Based on the literature precedent, we assign our product as the *S* enantiomer.

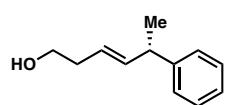
**(*S,E*)-5-phenylhex-3-en-1-yl benzoate (157o)**



Prepared from (1-chloroethyl)benzene (**26**, 0.2 mmol) and (*E*)-4-bromobut-3-en-1-yl benzoate (**156o**, 0.2 mmol) according to General Procedure 6. The crude residue was purified by silica gel chromatography (2%

Et<sub>2</sub>O/hexanes) to yield **157o** (40.5 mg, 72% yield) in 94% ee as a clear oil. The enantiomeric excess was determined by chiral SFC analysis (OJ-H, 2.5 mL/min, 10% IPA in CO<sub>2</sub>, λ = 210 nm): *t<sub>R</sub>* (major) = 5.0 min, *t<sub>R</sub>* (minor) = 5.8 min. [α]<sub>D</sub><sup>25</sup> = 2.8° (c = 1.1, CHCl<sub>3</sub>); <sup>1</sup>H NMR (500 MHz, CDCl<sub>3</sub>) δ 8.09 – 7.99 (m, 2H), 7.63 – 7.54 (m, 1H), 7.51 – 7.40 (m, 2H), 7.31 – 7.14 (m, 5H), 5.78 (ddt, *J* = 15.4, 6.8, 1.4 Hz, 1H), 5.54 (dtd, *J* = 15.2, 6.8, 1.3 Hz, 1H), 4.37 (td, *J* = 6.7, 2.2 Hz, 2H), 3.52 – 3.43 (m, 1H), 2.51 (qt, *J* = 6.7, 1.1 Hz, 2H), 1.36 (d, *J* = 7.0 Hz, 3H); <sup>13</sup>C NMR (126 MHz, CDCl<sub>3</sub>) δ 166.6, 145.9, 138.2, 132.8, 130.4, 129.6, 128.4, 128.3, 127.1, 126.0, 124.1, 64.3, 42.3, 32.1, 21.3; FTIR (NaCl, thin film): 3061, 3027, 2963, 2929, 2898, 2872, 1720, 1602, 1584, 1492, 1451, 1380, 1314, 1274, 1176, 1116, 1070, 1026, 968, 760, 712 cm<sup>-1</sup>; HRMS (MM) calc'd for C<sub>19</sub>H<sub>20</sub>O<sub>2</sub> [M+H]<sup>+</sup> 281.1536, found 281.1522.

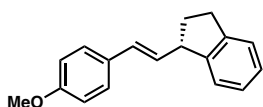
**(*S,E*)-5-phenylhex-3-en-1-ol (157p)**



Prepared from (1-chloroethyl)benzene (**26**, 0.2 mmol) and (*E*)-4-bromobut-3-en-1-ol (**156p**, 0.2 mmol) according to General Procedure 5. The crude residue was purified by silica gel chromatography (10 to 20% ethyl acetate/hexanes) to yield **157p** (19.7 mg, 56% yield) in 94% ee as a clear oil. The enantiomeric excess was determined by chiral SFC analysis (OJ-H, 2.5 mL/min, 2% MeOH in CO<sub>2</sub>, λ = 210 nm): *t<sub>R</sub>* (major) = 9.6 min, *t<sub>R</sub>* (minor) = 10.5 min. [α]<sub>D</sub><sup>25</sup> = +13.1° (c = 0.6, CHCl<sub>3</sub>); <sup>1</sup>H NMR (500 MHz, CDCl<sub>3</sub>) δ 7.35 – 7.27 (m, 2H), 7.25 – 7.15 (m, 3H), 5.77 (ddt, *J* = 15.4, 6.8, 1.4 Hz, 1H), 5.46 (dtd, *J* = 15.4, 7.0, 1.4 Hz, 1H), 3.66 (t, *J* = 6.2 Hz, 2H), 3.52 – 3.43 (m, 1H), 2.37 – 2.27 (m, 2H), 1.37 (d, *J* = 7.0 Hz, 3H); <sup>13</sup>C NMR (126 MHz, CDCl<sub>3</sub>) δ 145.9, 138.7, 128.4, 127.1, 126.1, 124.7, 62.1, 42.4, 35.9,

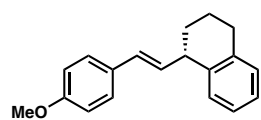
21.4; FTIR (NaCl, thin film): 3337, 3025, 2963, 2928, 1653, 1636, 1491, 1451, 1371, 1258, 1150, 1048, 968, 759  $\text{cm}^{-1}$ ; HRMS (MM) calc'd for  $\text{C}_{12}\text{H}_{16}\text{O}$   $[\text{M}+\text{H}]^+$  177.1274, found 177.1248.

**(*S,E*)-1-(4-methoxystyryl)-2,3-dihydro-1*H*-indene (163o)**



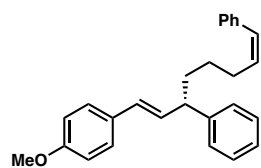
Prepared from 1-chloro-2,3-dihydro-1*H*-indene (**162o**, 0.2 mmol) and (*E*)-1-(2-bromovinyl)-4-methoxybenzene (**156**, 0.2 mmol) according to General Procedure 6. The crude residue was purified by silica gel chromatography (5 to 15% toluene/hexanes) to yield **163o** (38.8 mg, 77% yield) in 94% ee as a white solid. The enantiomeric excess was determined by chiral SFC analysis (OB-H, 2.5 mL/min, 20% IPA in  $\text{CO}_2$ ,  $\lambda = 254$  nm):  $t_R$  (major) = 5.1 min,  $t_R$  (minor) = 8.7 min.  $[\alpha]_D^{25} = -6.5^\circ$  ( $c = 1.1$ ,  $\text{CHCl}_3$ );  $^1\text{H}$  NMR (500 MHz,  $\text{CDCl}_3$ )  $\delta$  7.39 – 7.32 (m, 2H), 7.32 – 7.16 (m, 4H), 6.91 – 6.85 (m, 2H), 6.51 (d,  $J = 15.7$  Hz, 1H), 6.14 (dd,  $J = 15.9, 8.6$  Hz, 1H), 3.97 – 3.88 (m, 1H), 3.83 (s, 3H), 3.06 – 2.89 (m, 2H), 2.49 – 2.38 (m, 1H), 2.01 – 1.89 (m, 1H);  $^{13}\text{C}$  NMR (126 MHz,  $\text{CDCl}_3$ )  $\delta$  158.9, 146.1, 144.0, 130.9, 130.3, 129.7, 127.3, 126.6, 126.2, 124.53, 124.50, 114.0, 55.3, 49.2, 33.7, 31.7; FTIR (NaCl, thin film): 3065, 3018, 2952, 2835, 1606, 1576, 1511, 1476, 1457, 1440, 1292, 1250, 1174, 1036, 965, 844, 811, 754, 740  $\text{cm}^{-1}$ ; HRMS (MM) calc'd for  $\text{C}_{18}\text{H}_{18}\text{O}$   $[\text{M}+\text{H}]^+$  251.1430, found 251.1371.

**(*S,E*)-1-(4-methoxystyryl)-1,2,3,4-tetrahydronaphthalene (163p)**



Prepared from 1-chloro-1,2,3,4-tetrahydronaphthalene (**162p**, 0.2 mmol) and (*E*)-1-(2-bromovinyl)-4-methoxybenzene (**156**, 0.2 mmol) according to General Procedure 5. The crude residue was purified by silica gel chromatography (5 to 15% toluene/hexanes) to yield **163p** (21.2 mg, 40% yield) in 90% ee as a white solid. The enantiomeric excess was determined by chiral SFC analysis (OB-H, 2.5 mL/min, 20% IPA in CO<sub>2</sub>, λ = 254 nm): *t<sub>R</sub>* (major) = 5.4 min, *t<sub>R</sub>* (minor) = 8.3 min. [α]<sub>D</sub><sup>25</sup> = +9.1° (c = 0.9, CHCl<sub>3</sub>); <sup>1</sup>H NMR (500 MHz, CDCl<sub>3</sub>) δ 7.36 – 7.28 (m, 2H), 7.25 – 7.19 (m, 1H), 7.20 – 7.09 (m, 3H), 6.91 – 6.81 (m, 2H), 6.38 (d, *J* = 15.7 Hz, 1H), 6.16 (dd, *J* = 15.7, 8.5 Hz, 1H), 3.82 (s, 3H), 3.66 – 3.58 (m, 1H), 2.91 – 2.77 (m, 2H), 2.10 – 1.91 (m, 2H), 1.86 – 1.72 (m, 2H); <sup>13</sup>C NMR (126 MHz, CDCl<sub>3</sub>) δ 158.8, 138.6, 137.0, 132.9, 130.4, 129.7, 129.6, 129.2, 127.2, 126.0, 125.6, 113.9, 55.3, 42.9, 30.5, 29.7, 21.0; FTIR (NaCl, thin film): 3014, 2930, 2856, 2834, 1607, 1577, 1511, 1489, 1463, 1450, 1297, 1249, 1174, 1035, 965, 843, 814, 755, 735 cm<sup>-1</sup>; HRMS (MM) calc'd for C<sub>19</sub>H<sub>20</sub>O [M+H]<sup>+</sup> 265.1587, found 265.1483.

**((*S,1Z,7E*)-8-(4-methoxyphenyl)octa-1,7-diene-1,6-diyl)dibenzene (161)**

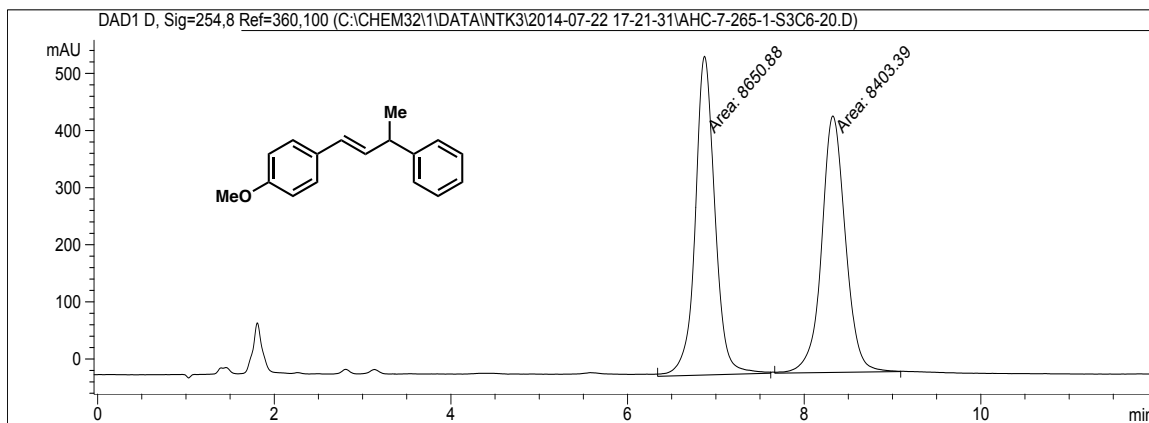


Prepared from **160** (0.2 mmol) and (*E*)-1-(2-bromovinyl)-4-methoxybenzene (**156**, 0.2 mmol) according to General Procedure 6. The crude residue was purified by silica gel chromatography (hexanes) to yield **161** (45.8 mg, 62% yield) in 96% ee as a clear oil. The enantiomeric excess was determined by chiral SFC analysis (OJ-H, 2.5 mL/min, 10% IPA in CO<sub>2</sub>, λ = 254 nm): *t<sub>R</sub>* (minor) = 7.2 min, *t<sub>R</sub>* (major) = 7.9 min. [α]<sub>D</sub><sup>25</sup> = -2.0° (c = 1.1, CHCl<sub>3</sub>); <sup>1</sup>H

NMR (500 MHz, CDCl<sub>3</sub>) δ 7.43 – 7.13 (m, 12H), 6.94 – 6.75 (m, 2H), 6.43 (dt, *J* = 11.7, 1.9 Hz, 1H), 6.34 (d, *J* = 16.4 Hz, 1H), 6.20 (dd, *J* = 15.8, 7.9 Hz, 1H), 5.65 (dt, *J* = 11.7, 7.2 Hz, 1H), 3.81 (s, 3H), 3.50 – 3.30 (m, 1H), 2.39 (qd, *J* = 7.4, 1.8 Hz, 2H), 1.94 – 1.74 (m, 2H), 1.64 – 1.35 (m, 2H); <sup>13</sup>C NMR (126 MHz, CDCl<sub>3</sub>) δ 158.8, 144.7, 137.7, 132.8, 132.1, 130.4, 129.0, 128.8, 128.7, 128.5, 128.1, 127.6, 127.2, 126.5, 126.2, 113.9, 55.3, 49.0, 35.5, 28.5, 27.9; FTIR (NaCl, thin film): 3057, 3024, 2931, 2856, 2834, 1607, 1576, 1511, 1492, 1452, 1300, 1249, 1174, 1035, 965, 914, 829, 804, 760, 699 cm<sup>-1</sup>; HRMS (MM) calc'd for C<sub>27</sub>H<sub>28</sub>O [M+H]<sup>+</sup> 369.2213, found 369.2219.

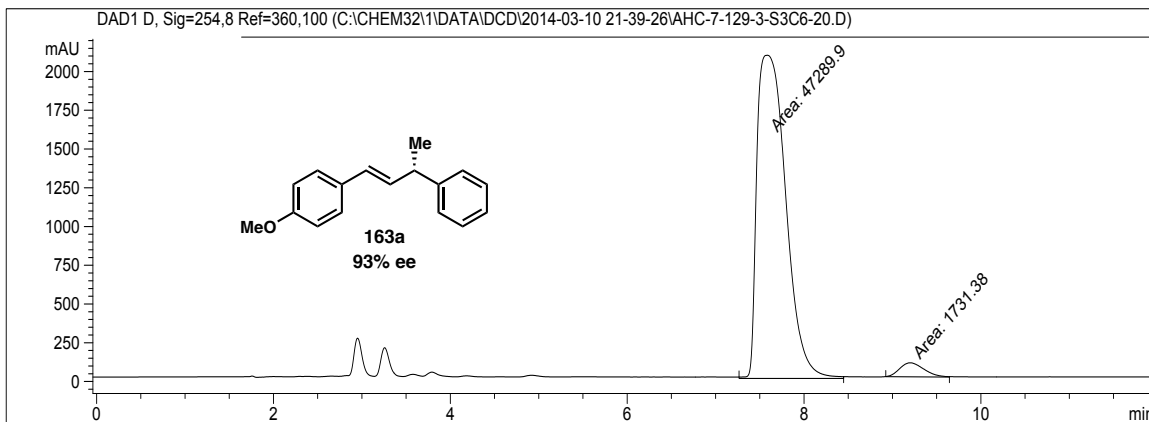
## 4.4.4 SFC Traces of Racemic and Enantioenriched Products

163a (Table 4.4, entry 1): racemic



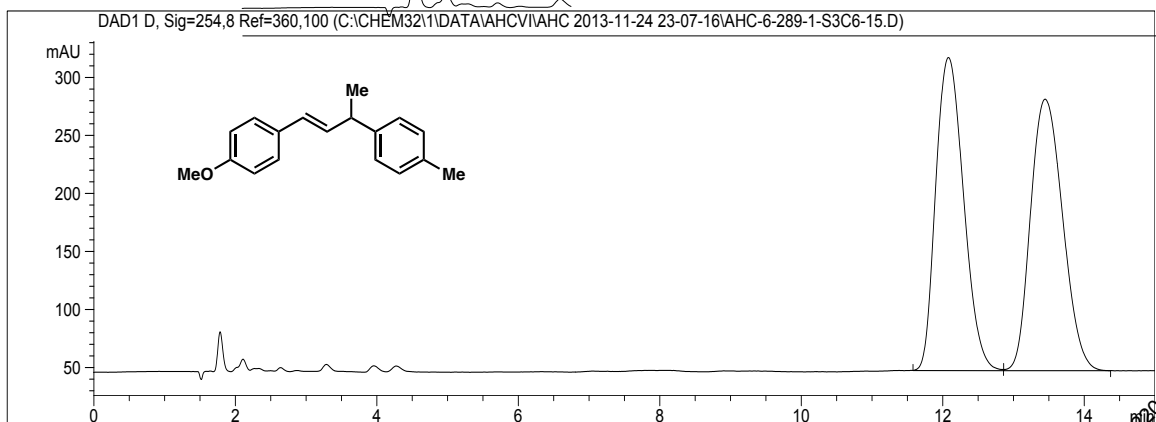
Peak #	RetTime [min]	Type	Width [min]	Area [mAU*s]	Height [mAU]	Area %
1	6.871	MM	0.2583	8650.88281	558.20911	50.7256
2	8.325	MM	0.3119	8403.38672	449.10953	49.2744

163a (Table 4.4, entry 1): enantioenriched, 93% ee



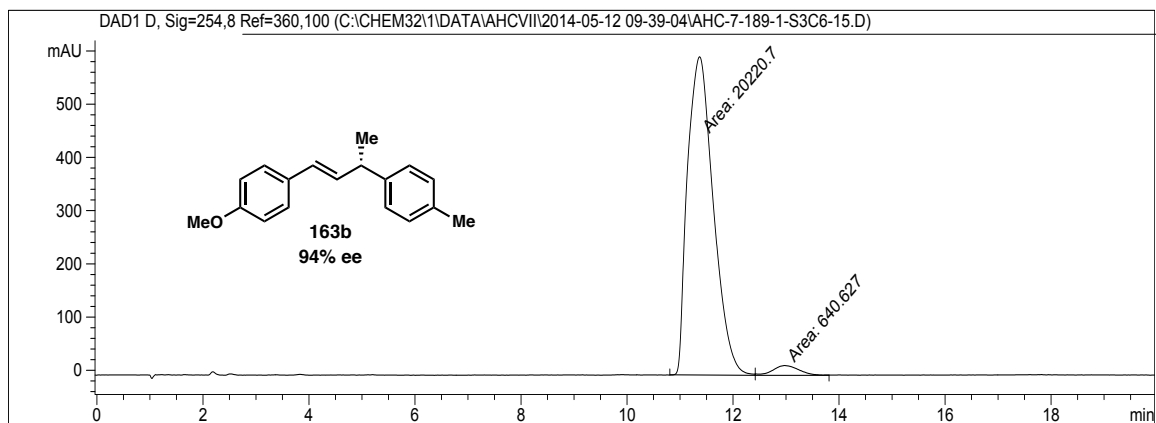
Peak #	RetTime [min]	Type	Width [min]	Area [mAU*s]	Height [mAU]	Area %
1	7.587	MM	0.3780	4.72899e4	2085.26416	96.4681
2	9.201	MM	0.3190	1731.38208	90.45088	3.5319

**163b (Table 4.4, entry 2): racemic**



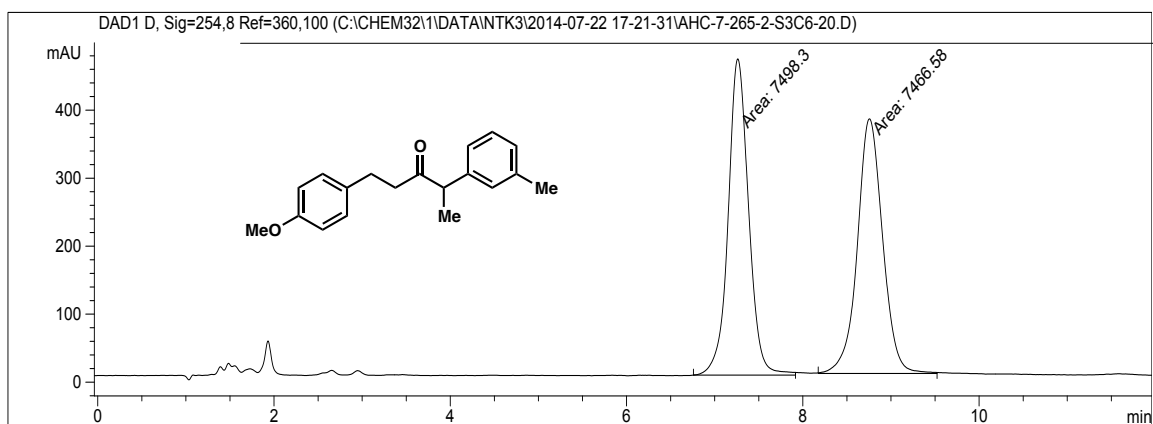
Peak #	RetTime [min]	Type	Width [min]	Area [mAU*s]	Height [mAU]	Area %
1	12.081	BB	0.4356	7393.43018	269.87115	49.9809
2	13.448	BB	0.5069	7399.08838	233.99118	50.0191

**163b (Table 4.4, entry 2): enantioenriched, 94% ee**



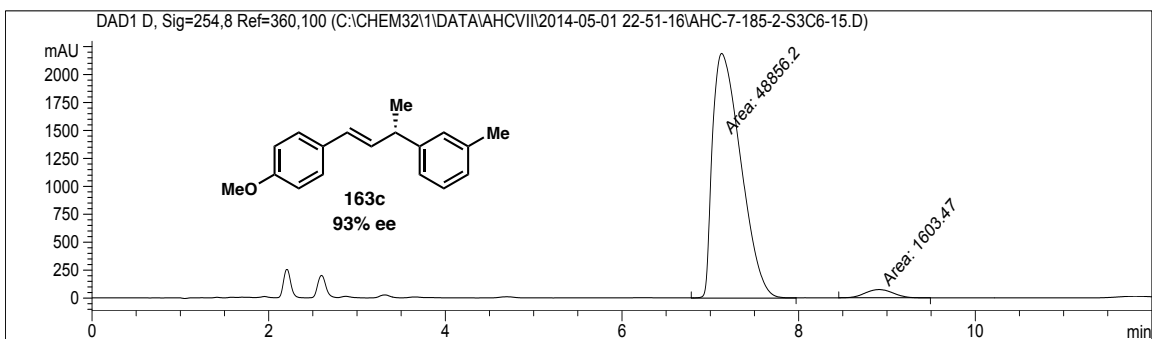
Peak #	RetTime [min]	Type	Width [min]	Area [mAU*s]	Height [mAU]	Area %
1	11.369	MM	0.5638	2.02207e4	597.78845	96.9291
2	12.970	MM	0.5781	640.62689	18.46935	3.0709

**163c (Table 4.4, entry 3): racemic**



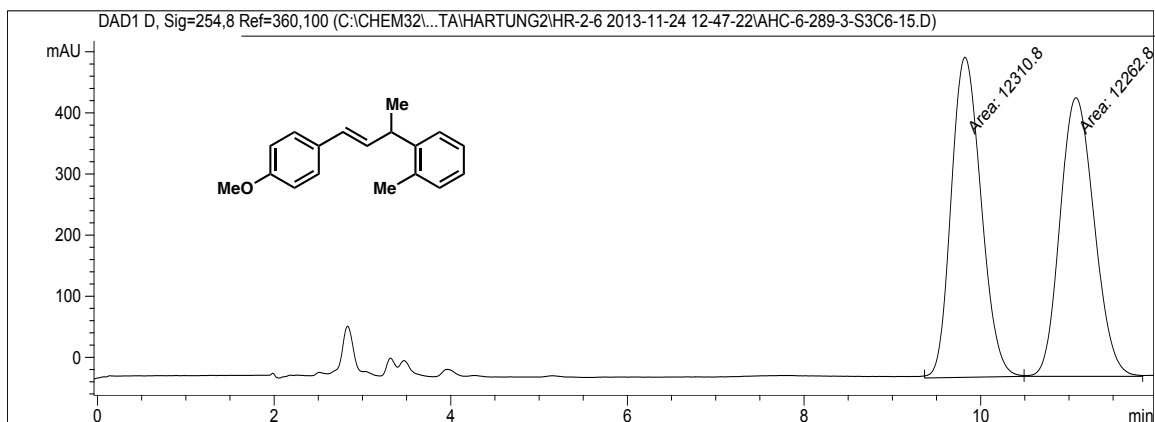
Peak #	RetTime [min]	Type	Width [min]	Area [mAU*s]	Height [mAU]	Area %
1	7.261	MM	0.2686	7498.30225	465.33981	50.1060
2	8.755	MM	0.3322	7466.58496	374.60574	49.8940

**163c (Table 4.4, entry 3): enantioenriched, 93% ee**



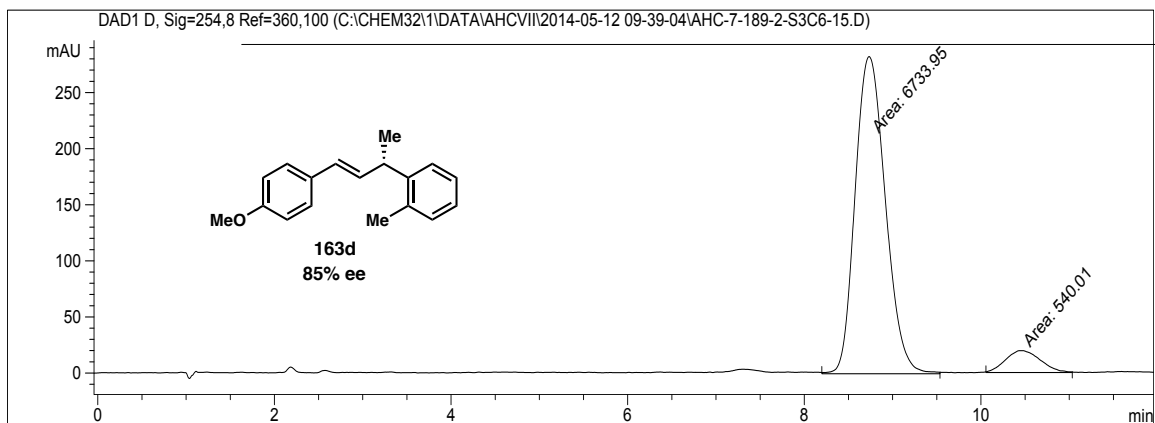
Peak #	RetTime [min]	Type	Width [min]	Area [mAU*s]	Height [mAU]	Area %
1	7.129	MM	0.3720	4.88562e4	2189.11938	96.8223
2	8.913	MM	0.3645	1603.46533	73.32549	3.1777

**163d (Table 4.4, entry 4): racemic**



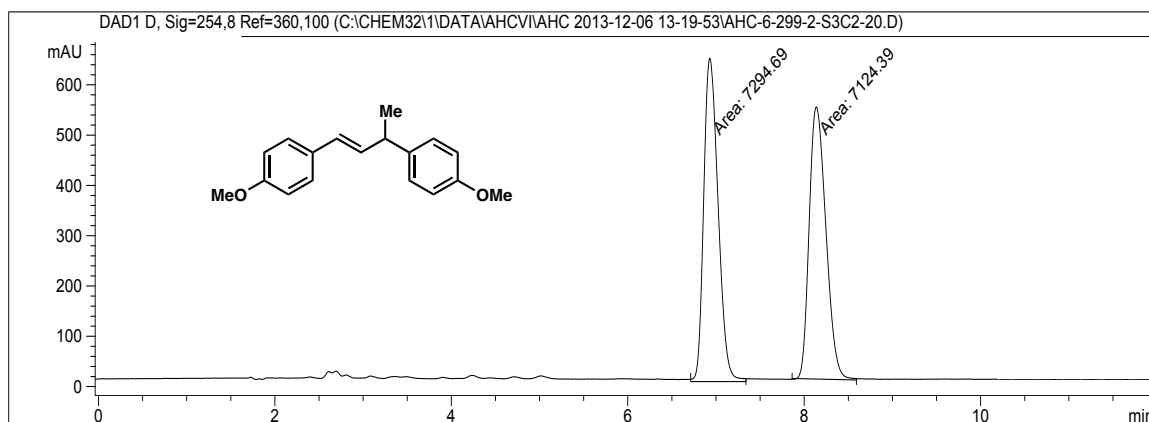
Peak #	RetTime [min]	Type	Width [min]	Area [mAU*s]	Height [mAU]	Area %
1	9.822	MM	0.3917	1.23108e4	523.83447	50.0978
2	11.079	MM	0.4482	1.22628e4	456.04102	49.9022

**163d (Table 4.4, entry 4): enantioenriched, 85% ee**



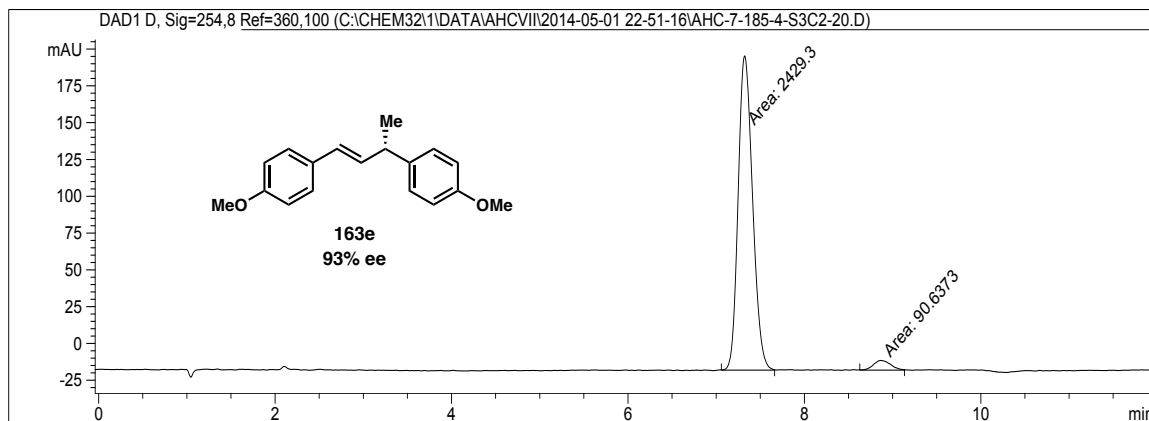
Peak #	RetTime [min]	Type	Width [min]	Area [mAU*s]	Height [mAU]	Area %
1	8.734	MM	0.3969	6733.94727	282.75232	92.5761
2	10.444	MM	0.4602	540.01031	19.55776	7.4239

**163e (Table 4.4, entry 5): racemic**



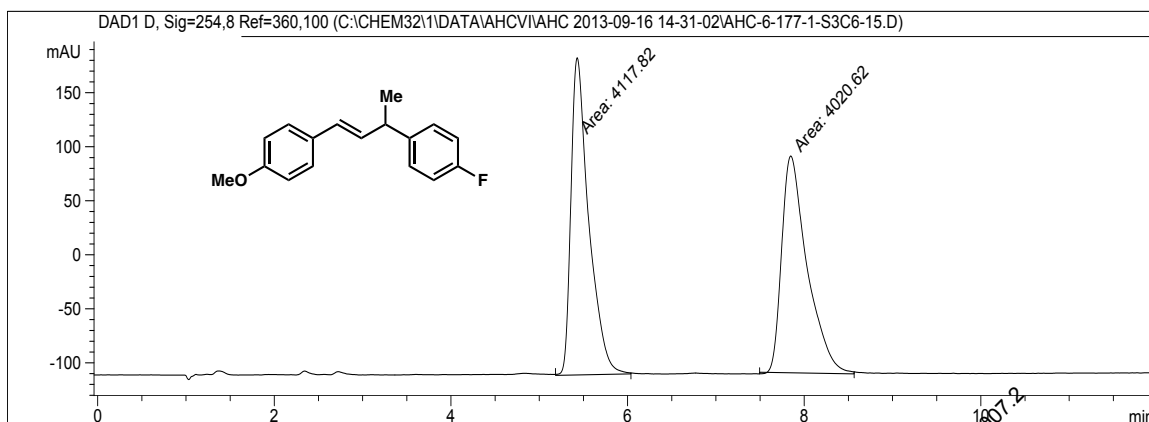
Peak #	RetTime [min]	Type	Width [min]	Area [mAU*s]	Height [mAU]	Area %
1	6.930	MM	0.1890	7294.69238	643.23810	50.5906
2	8.137	MM	0.2193	7124.38721	541.33319	49.4094

**163e (Table 4.4, entry 5): enantioenriched, 93% ee**



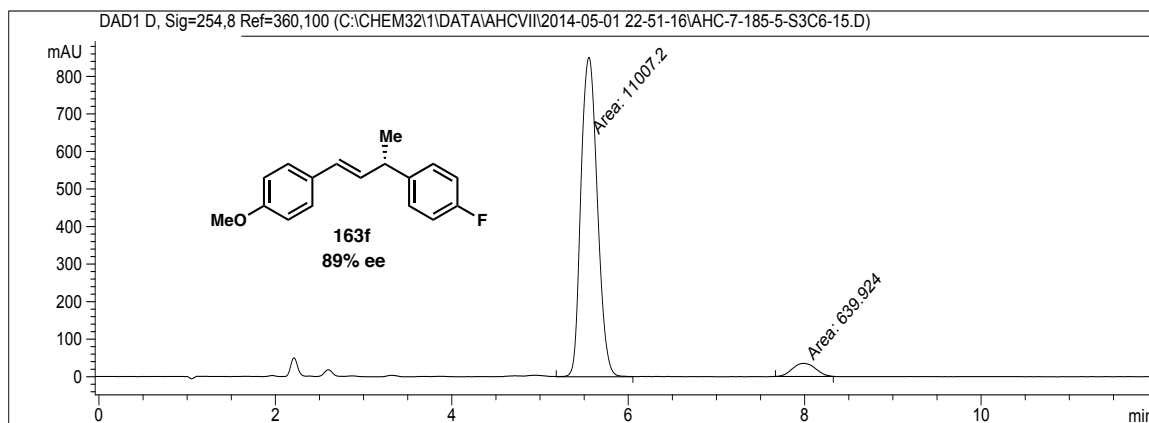
Peak #	RetTime [min]	Type	Width [min]	Area [mAU*s]	Height [mAU]	Area %
1	7.323	MM	0.1893	2429.29541	213.84731	96.4032
2	8.864	MM	0.2287	90.63728	6.60611	3.5968

**163f (Table 4.4, entry 6): racemic**



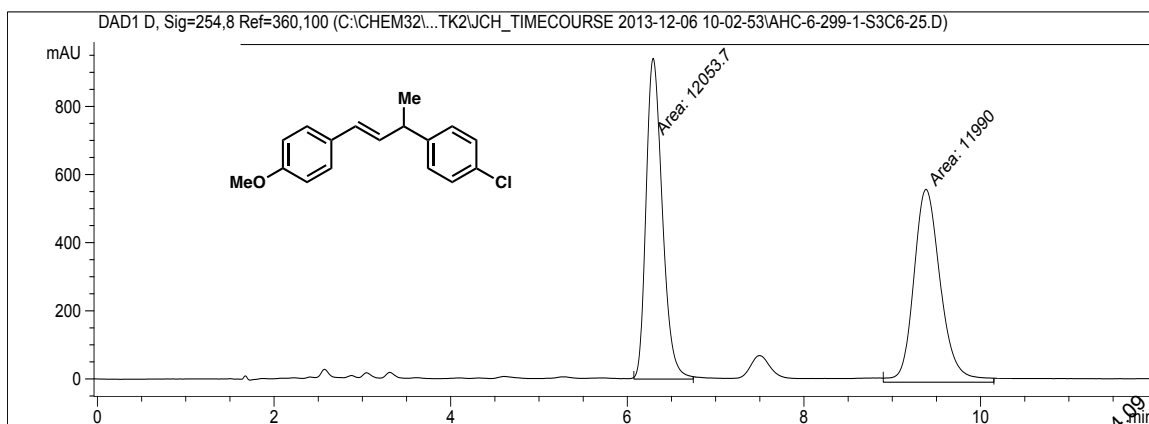
Peak #	RetTime [min]	Type	Width [min]	Area [mAU*s]	Height [mAU]	Area %
1	5.429	MM	0.2337	4117.82129	293.71591	50.5972
2	7.848	MM	0.3339	4020.61816	200.69434	49.4028

**163f (Table 4.4, entry 6): enantioenriched, 89% ee**



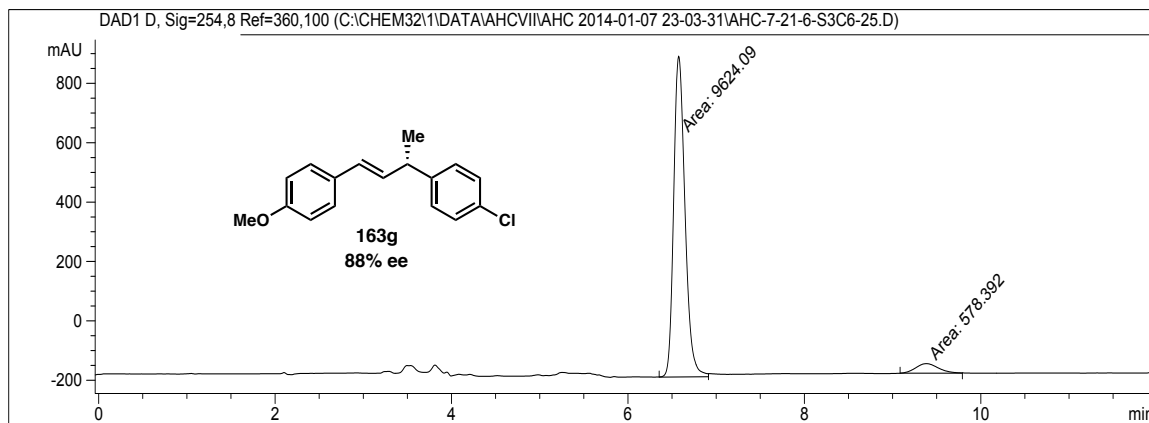
Peak #	RetTime [min]	Type	Width [min]	Area [mAU*s]	Height [mAU]	Area %
1	5.554	MM	0.2155	1.10072e4	851.35431	94.5057
2	7.988	MM	0.3047	639.92358	34.99786	5.4943

**163g (Table 4.4, entry 7): racemic**



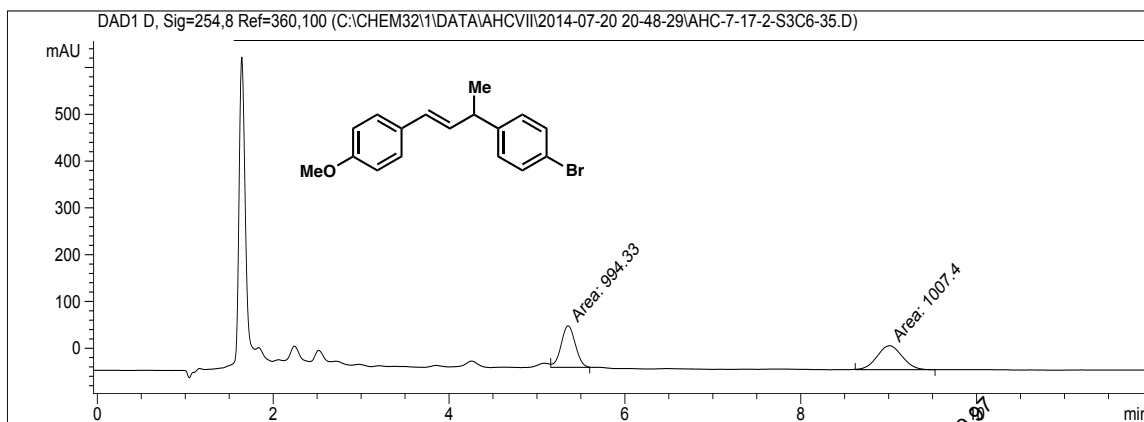
Peak #	RetTime [min]	Type	Width [min]	Area [mAU*s]	Height [mAU]	Area %
1	6.292	MM	0.2133	1.20537e4	941.72620	50.1325
2	9.381	MM	0.3530	1.19900e4	566.09015	49.8675

**163g (Table 4.4, entry 7): enantioenriched, 88% ee**



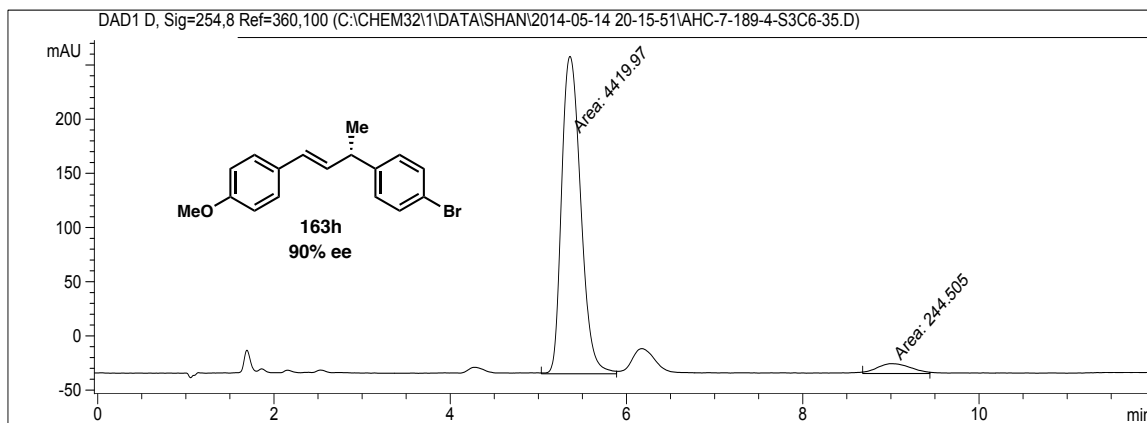
Peak #	RetTime [min]	Type	Width [min]	Area [mAU*s]	Height [mAU]	Area %
1	6.575	MM	0.1483	9624.08691	1081.90076	94.3309
2	9.384	MM	0.2997	578.39185	32.16311	5.6691

**163h (Table 4.4, entry 8): racemic**



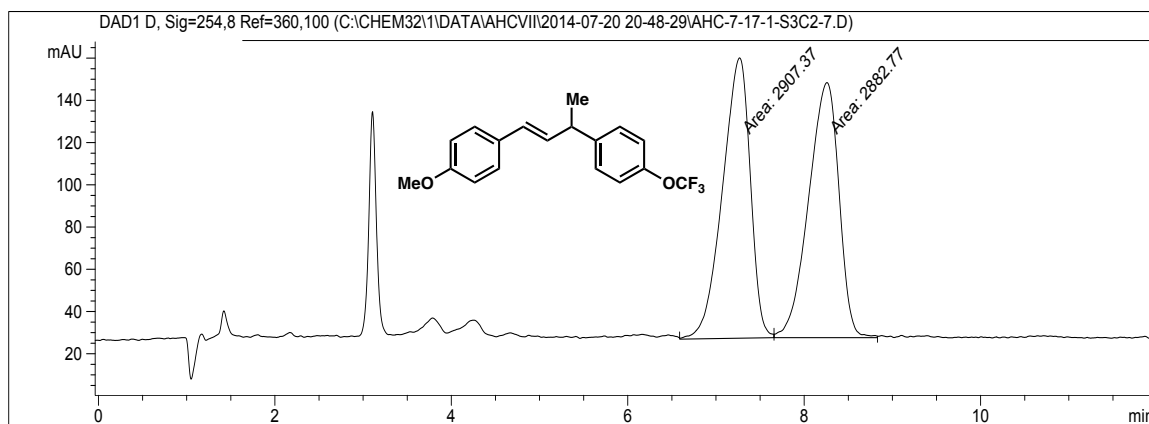
Peak #	RetTime [min]	Type	Width [min]	Area [mAU*s]	Height [mAU]	Area %
1	5.354	MM	0.1867	994.32965	88.77684	49.6736
2	9.010	MM	0.3286	1007.39520	51.08786	50.3264

**163h (Table 4.4, entry 8): enantioenriched, 90% ee**



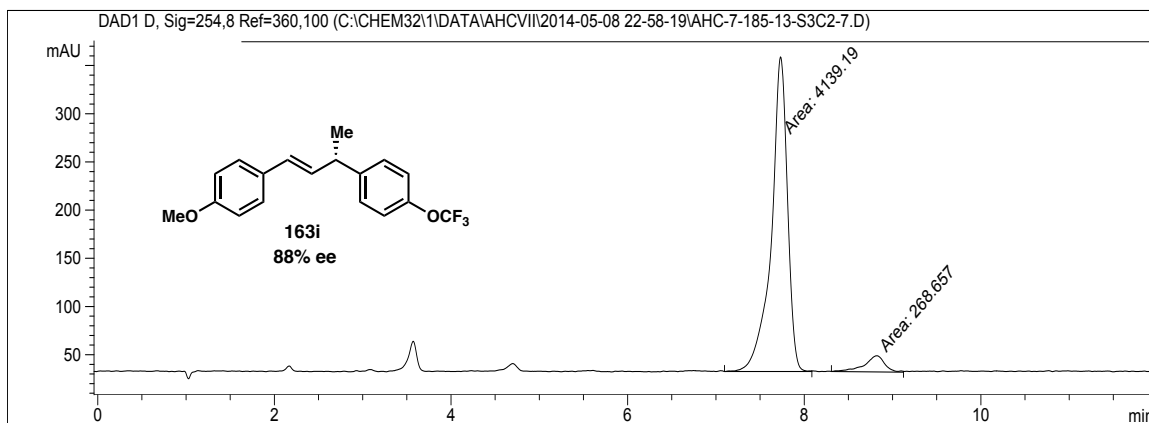
Peak #	RetTime [min]	Type	Width [min]	Area [mAU*s]	Height [mAU]	Area %
1	5.359	MM	0.2515	4419.97461	292.93845	94.7581
2	9.000	MM	0.4463	244.50519	9.13001	5.2419

**163i (Table 4.4, entry 9): racemic**



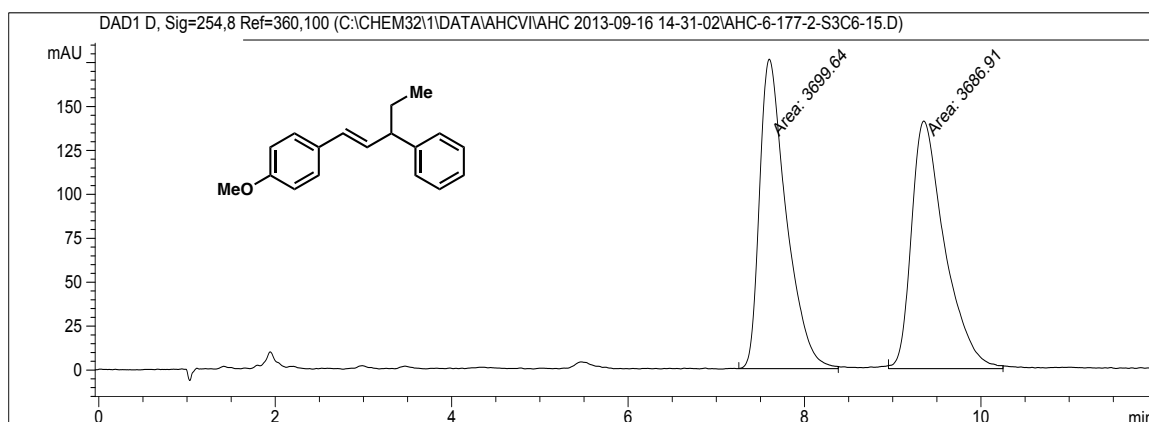
Peak #	RetTime [min]	Type	Width [min]	Area [mAU*s]	Height [mAU]	Area %
1	7.268	MM	0.3649	2907.36719	132.79340	50.2124
2	8.258	MM	0.3976	2882.76611	120.83252	49.7876

**163i (Table 4.4, entry 9): enantioenriched, 88% ee**



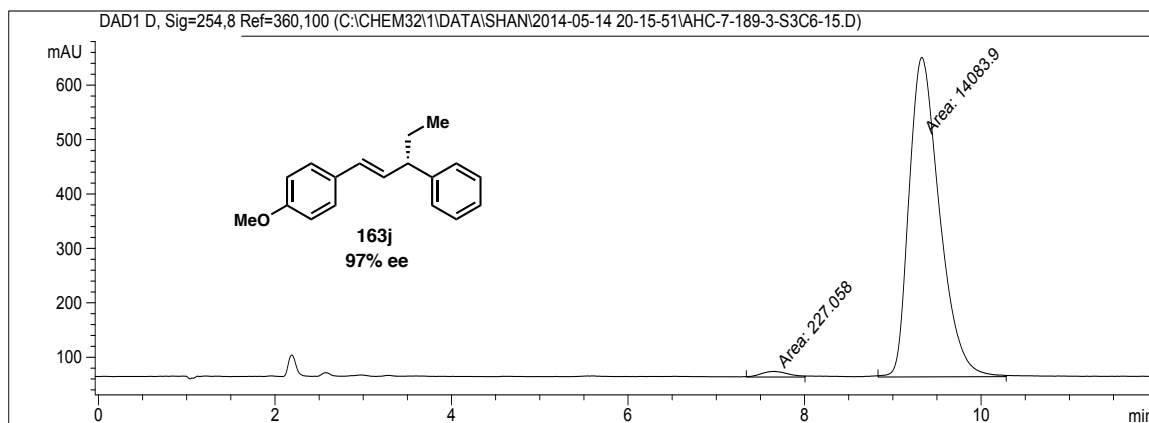
Peak #	RetTime [min]	Type	Width [min]	Area [mAU*s]	Height [mAU]	Area %
1	7.733	MM	0.2112	4139.18750	326.62589	93.9050
2	8.821	MM	0.2665	268.65671	16.80058	6.0950

**163j (Table 4.4, entry 10): racemic**



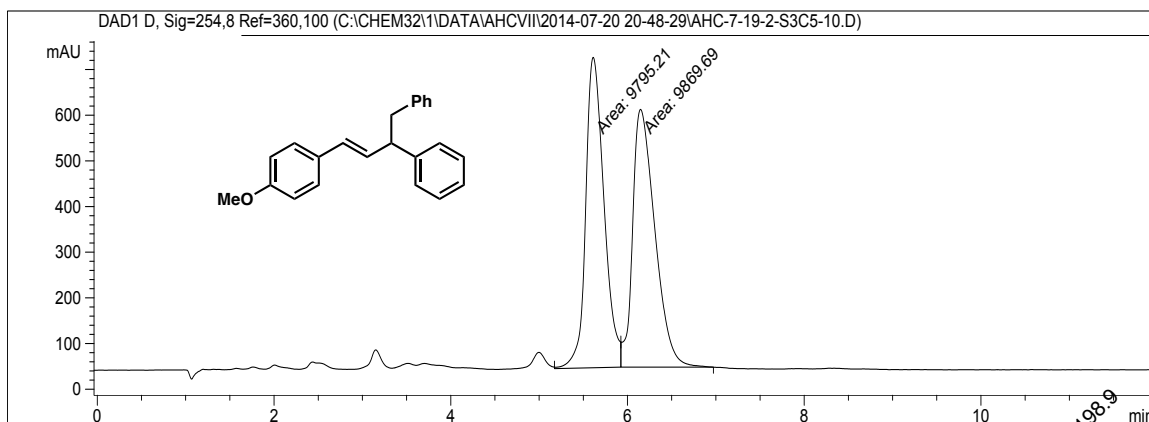
Peak #	RetTime [min]	Type	Width [min]	Area [mAU*s]	Height [mAU]	Area %
1	7.600	MM	0.3500	3699.64233	176.16603	50.0862
2	9.352	MM	0.4361	3686.90503	140.91353	49.9138

**163j (Table 4.4, entry 10): enantioenriched, 97% ee**



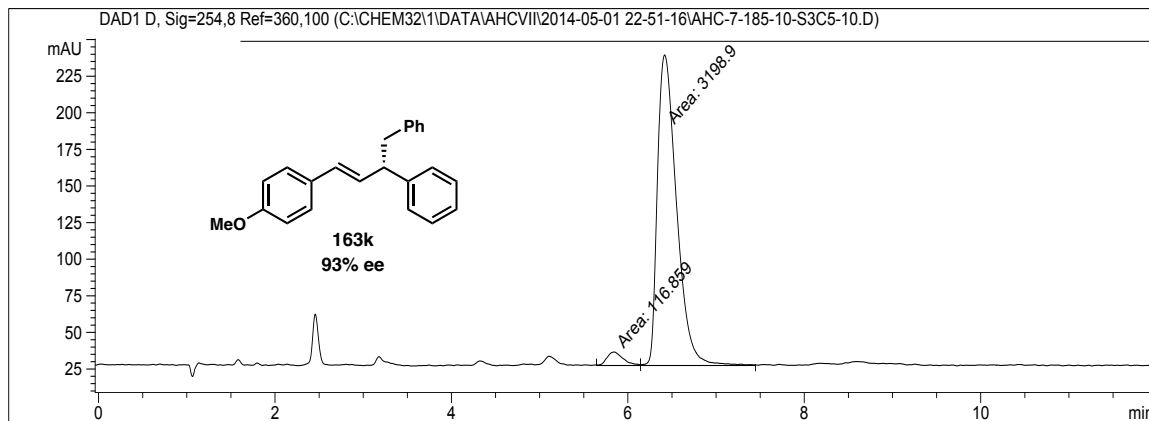
Peak #	RetTime [min]	Type	Width [min]	Area [mAU*s]	Height [mAU]	Area %
1	7.659	MM	0.3658	227.05769	10.34652	1.5866
2	9.329	MM	0.3998	1.40839e4	587.16370	98.4134

**163k (Table 4.4, entry 11): racemic**



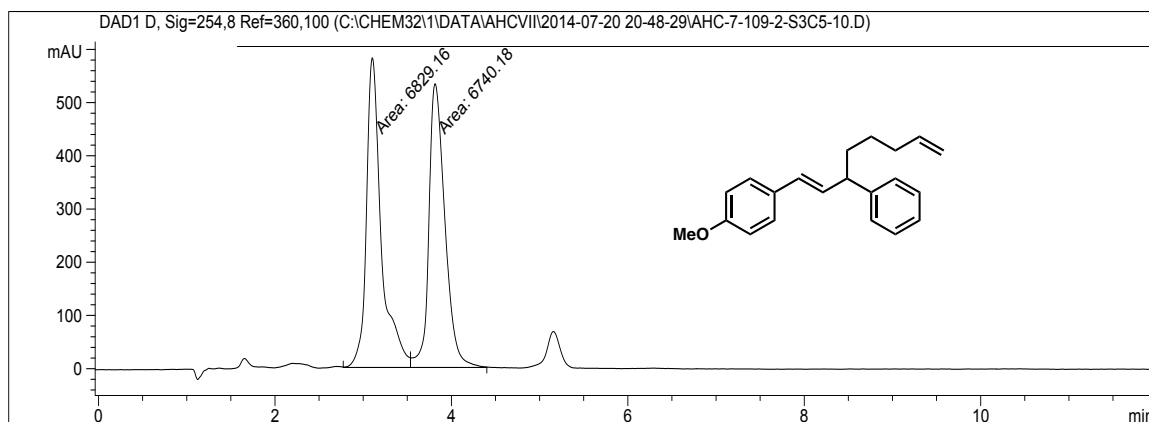
Peak #	RetTime [min]	Type	Width [min]	Area [mAU*s]	Height [mAU]	Area %
1	5.612	MM	0.2400	9795.21289	680.30035	49.8106
2	6.148	MM	0.2913	9869.69043	564.75275	50.1894

**163k (Table 4.4, entry 11): enantioenriched, 93% ee**



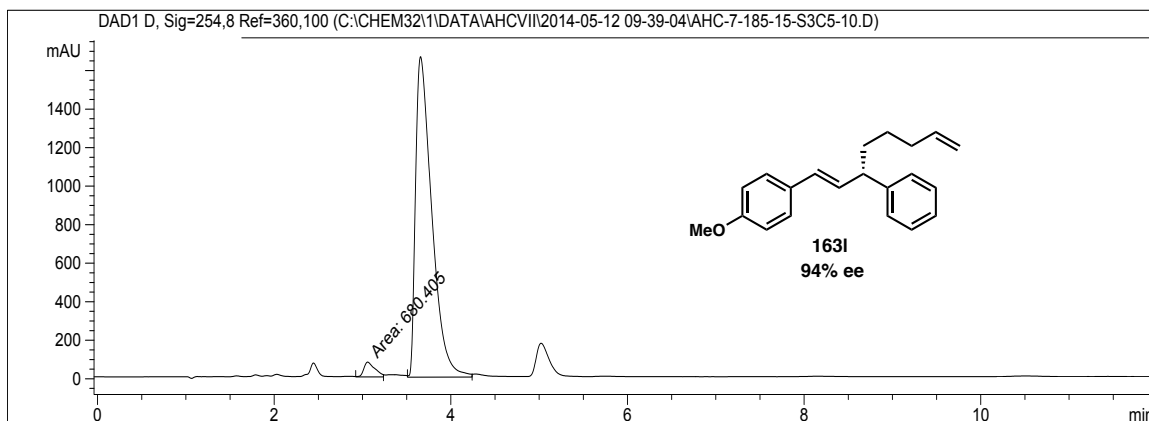
Peak #	RetTime [min]	Type	Width [min]	Area [mAU*s]	Height [mAU]	Area %
1	5.843	MM	0.2131	116.85924	9.14146	3.5244
2	6.416	MM	0.2513	3198.90405	212.16275	96.4756

**163l (Table 4.4, entry 12): racemic**



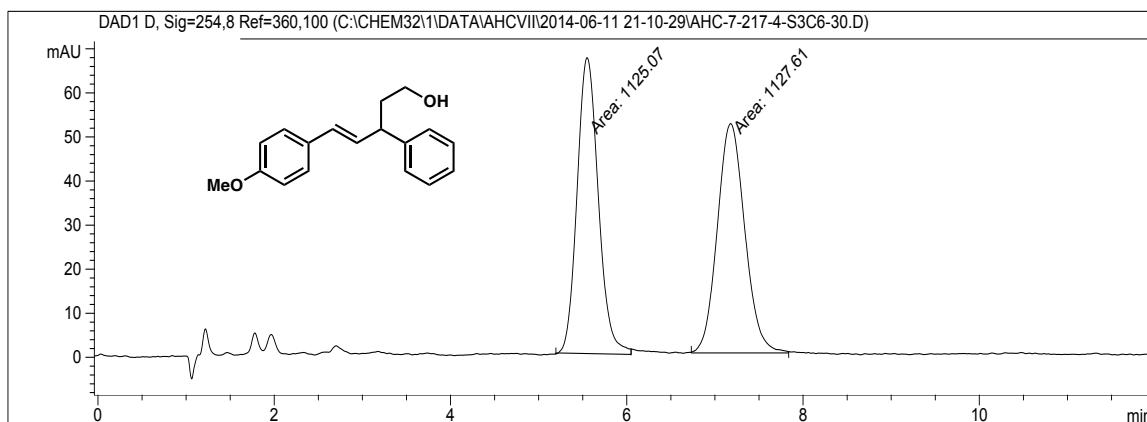
Peak #	RetTime [min]	Type	Width [min]	Area [mAU*s]	Height [mAU]	Area %
1	3.104	MM	0.1953	6829.15918	582.89142	50.3279
2	3.815	MM	0.2105	6740.18213	533.69666	49.6721

**163l (Table 4.4, entry 12): enantioenriched, 94% ee**



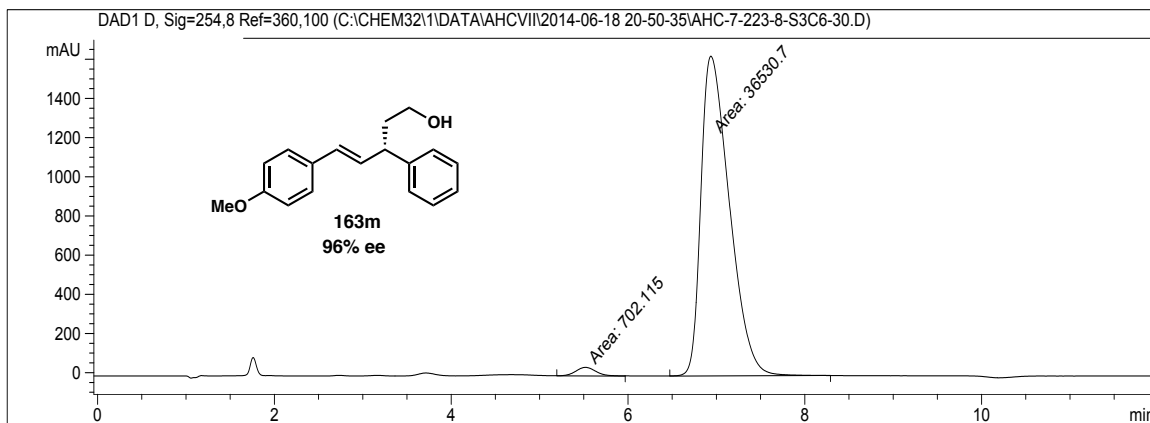
Peak #	RetTime [min]	Type	Width [min]	Area [mAU*s]	Height [mAU]	Area %
1	3.058	MM	0.1470	680.40527	77.13821	3.0921
2	3.659	VV	0.1956	2.13239e4	1663.29028	96.9079

**163m (Table 4.4, entry 13): racemic**



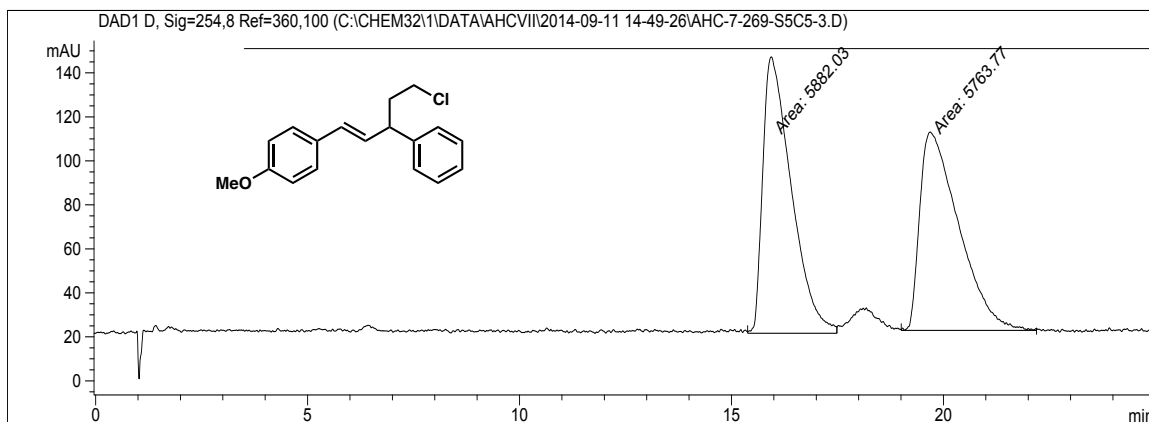
Peak #	RetTime [min]	Type	Width [min]	Area [mAU*s]	Height [mAU]	Area %
1	5.549	MM	0.2793	1125.06787	67.14302	49.9435
2	7.178	MM	0.3612	1127.61450	52.03247	50.0565

**163m (Table 4.4, entry 13): enantioenriched, 96% ee**



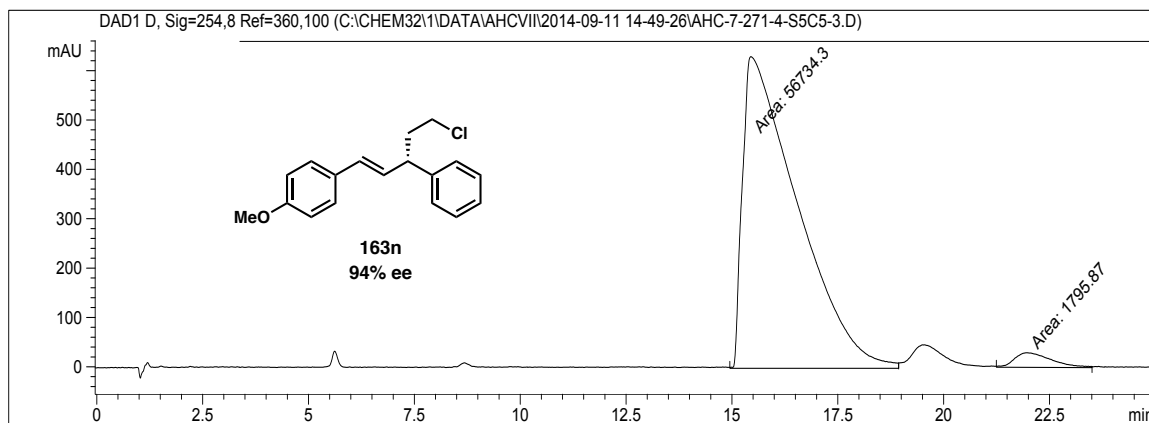
Peak #	RetTime [min]	Type	Width [min]	Area [mAU*s]	Height [mAU]	Area %
1	5.519	MM	0.2665	702.11481	43.90331	1.8857
2	6.938	MM	0.3729	3.65307e4	1632.66406	98.1143

**163n (Table 4.4, entry 14): racemic**



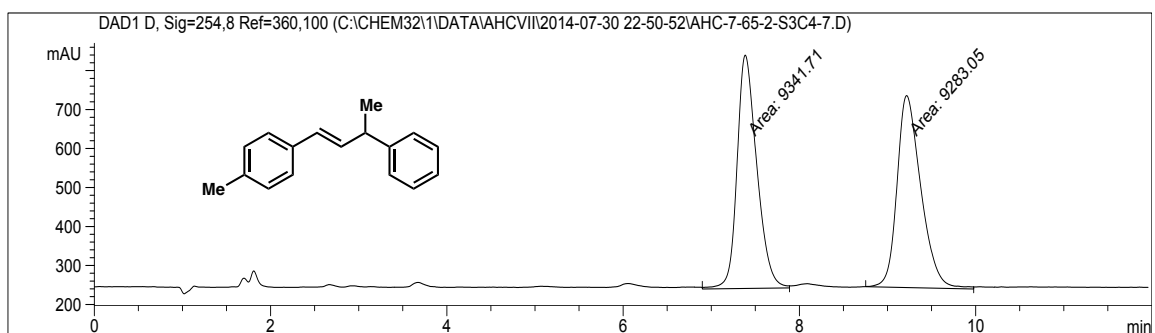
Peak #	RetTime [min]	Type	Width [min]	Area [mAU*s]	Height [mAU]	Area %
1	15.941	MM	0.7802	5882.02979	125.65482	50.5077
2	19.687	MM	1.0651	5763.77490	90.19390	49.4923

**163n (Table 4.4, entry 14): enantioenriched, 94% ee**



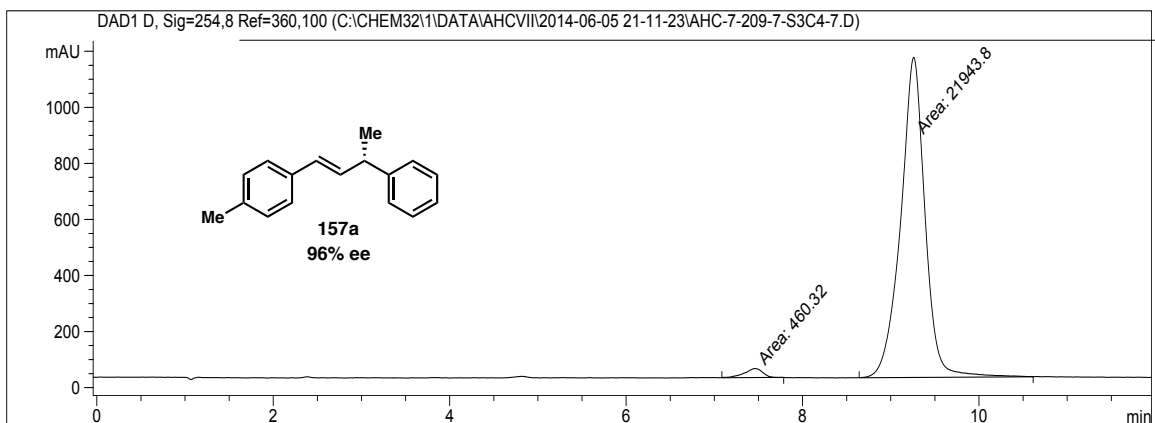
Peak #	RetTime [min]	Type	Width [min]	Area [mAU*s]	Height [mAU]	Area %
1	15.449	MM	1.4976	5.67343e4	631.38782	96.9317
2	21.994	MM	1.0162	1795.87158	29.45459	3.0683

**157a (Table 4.5, entry 1): racemic**



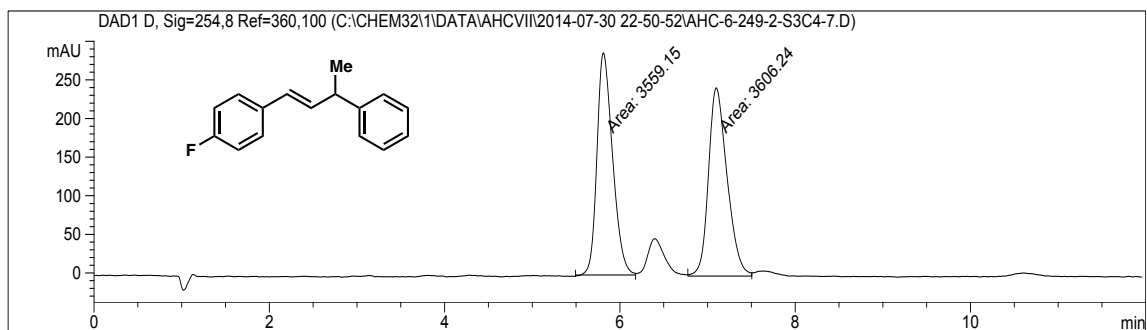
Peak #	RetTime [min]	Type	Width [min]	Area [mAU*s]	Height [mAU]	Area %
1	7.386	MM	0.2600	9341.71094	598.85675	50.1575
2	9.217	MM	0.3140	9283.04590	492.80606	49.8425

**157a (Table 4.5, entry 1): enantioenriched, 96% ee**



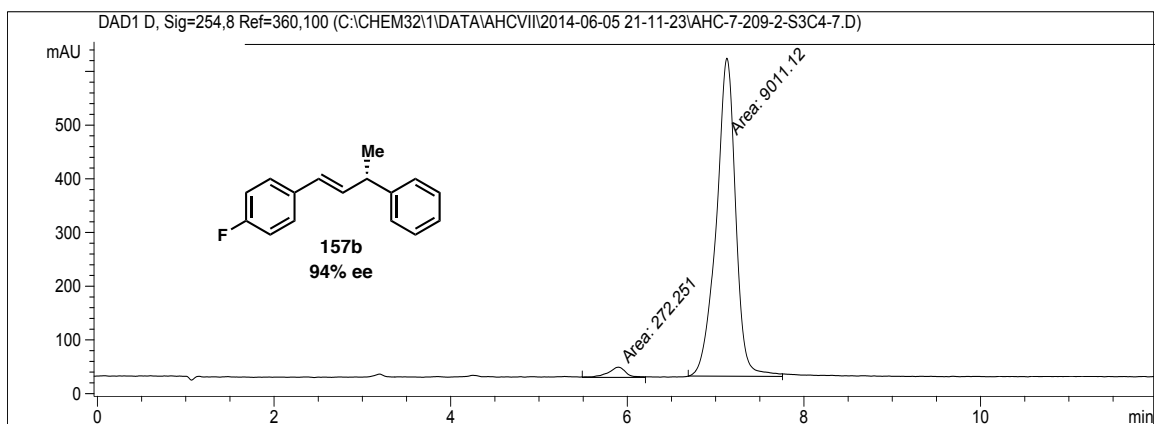
Peak #	RetTime [min]	Type	Width [min]	Area [mAU*s]	Height [mAU]	Area %
1	7.461	MM	0.2411	460.31961	31.82347	2.0546
2	9.260	MM	0.3201	2.19438e4	1142.71289	97.9454

**157b (Table 4.5, entry 2): racemic**



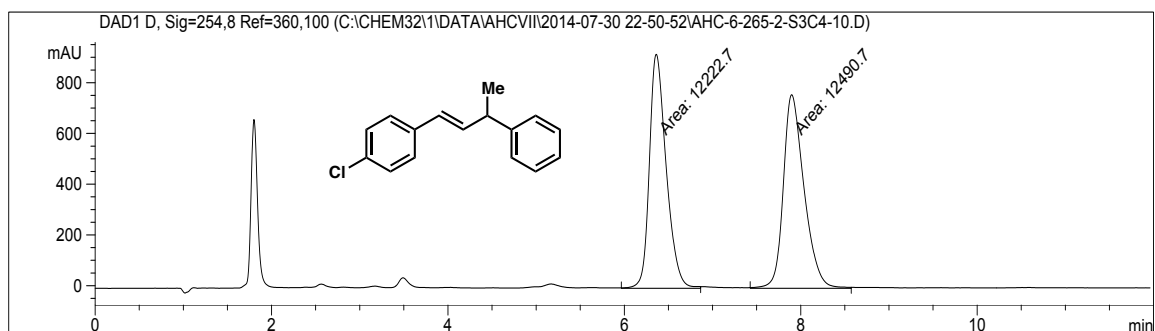
Peak #	RetTime [min]	Type	Width [min]	Area [mAU*s]	Height [mAU]	Area %
1	5.812	MM	0.2061	3559.15161	287.79590	49.6714
2	7.099	MM	0.2464	3606.24365	243.90446	50.3286

**157b (Table 4.5, entry 2): enantioenriched, 94% ee**



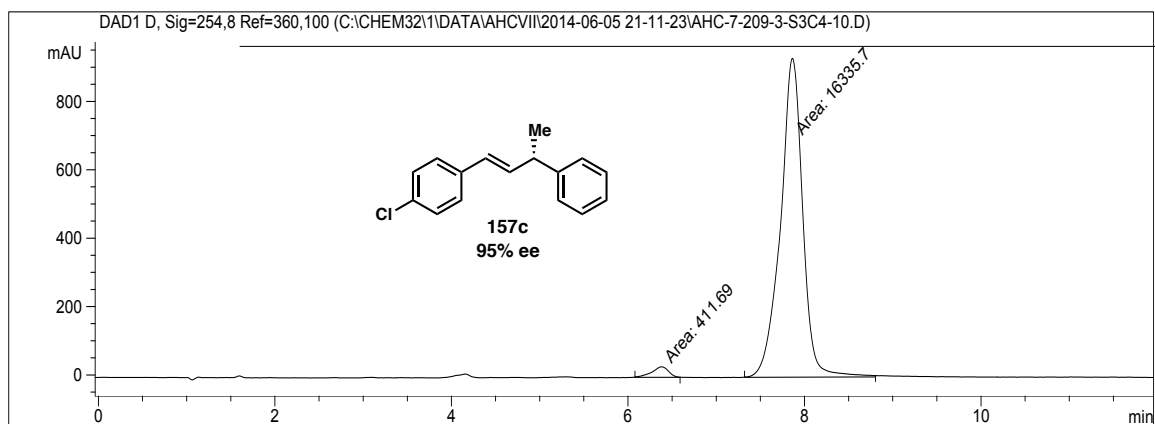
Peak #	RetTime [min]	Type	Width [min]	Area [mAU*s]	Height [mAU]	Area %
1	5.899	MM	0.2386	272.25067	19.01509	2.9327
2	7.128	MM	0.2536	9011.11523	592.32813	97.0673

**157c (Table 4.5, entry 3): racemic**



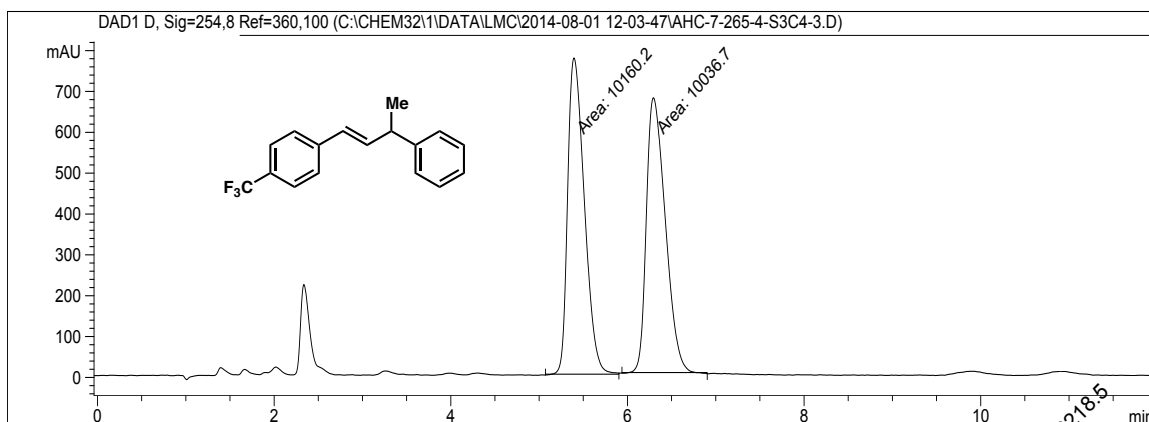
Peak #	RetTime [min]	Type	Width [min]	Area [mAU*s]	Height [mAU]	Area %
1	6.362	MM	0.2207	1.22227e4	922.92114	49.4580
2	7.898	MM	0.2727	1.24907e4	763.51147	50.5420

**157c (Table 4.5, entry 3): enantioenriched, 95% ee**



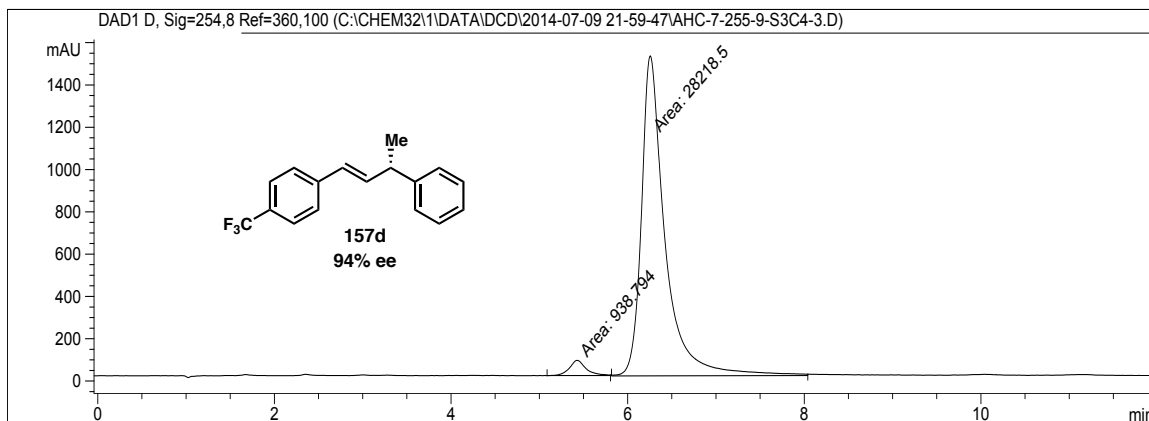
Peak #	RetTime [min]	Type	Width [min]	Area [mAU*s]	Height [mAU]	Area %
1	6.381	MM	0.2204	411.68973	31.13871	2.4582
2	7.864	MM	0.2918	1.63357e4	932.91962	97.5418

**157d (Table 4.5, entry 4): racemic**



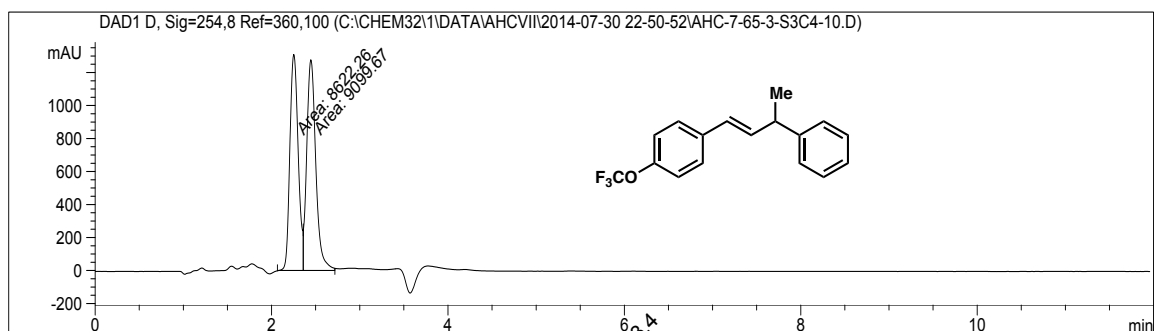
Peak #	RetTime [min]	Type	Width [min]	Area [mAU*s]	Height [mAU]	Area %
1	5.395	MM	0.2185	1.01602e4	774.91656	50.3057
2	6.295	MM	0.2484	1.00367e4	673.30627	49.6943

**157d (Table 4.5, entry 4): enantioenriched, 94% ee**



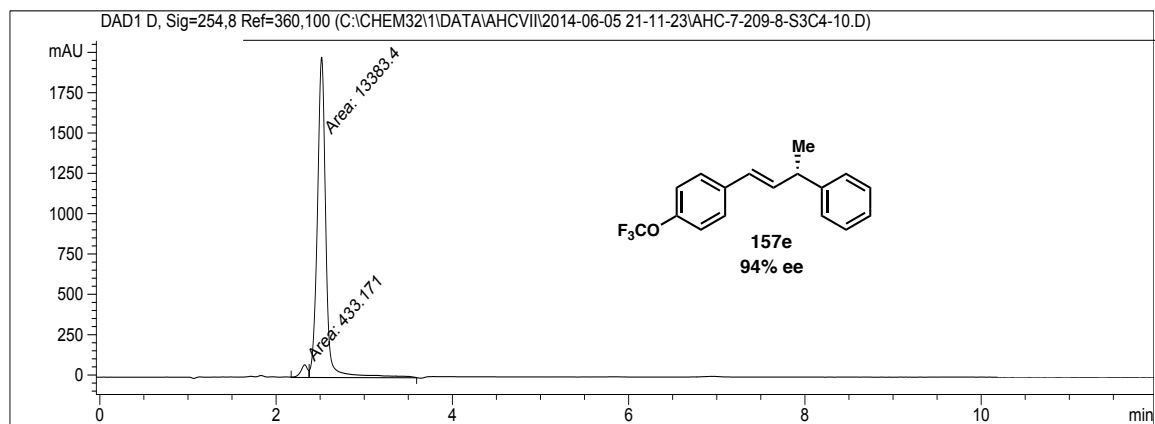
Peak #	RetTime [min]	Type	Width [min]	Area [mAU*s]	Height [mAU]	Area %
1	5.428	MM	0.2175	938.79395	71.92260	3.2198
2	6.256	MM	0.3107	2.82185e4	1513.67834	96.7802

**157e (Table 4.5, entry 5): racemic**



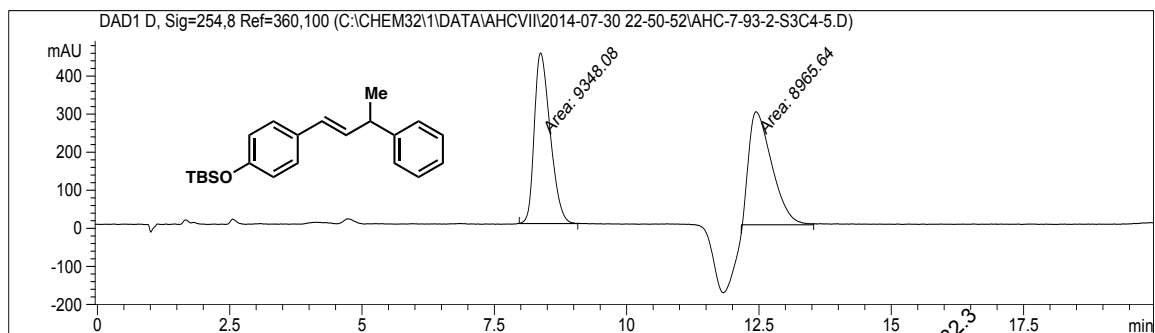
Peak #	RetTime [min]	Type	Width [min]	Area [mAU*s]	Height [mAU]	Area %
1	2.252	MM	0.1095	8622.25586	1312.58875	48.6531
2	2.446	MM	0.1185	9099.66504	1279.80774	51.3469

**157e (Table 4.5, entry 5): enantioenriched, 94% ee**



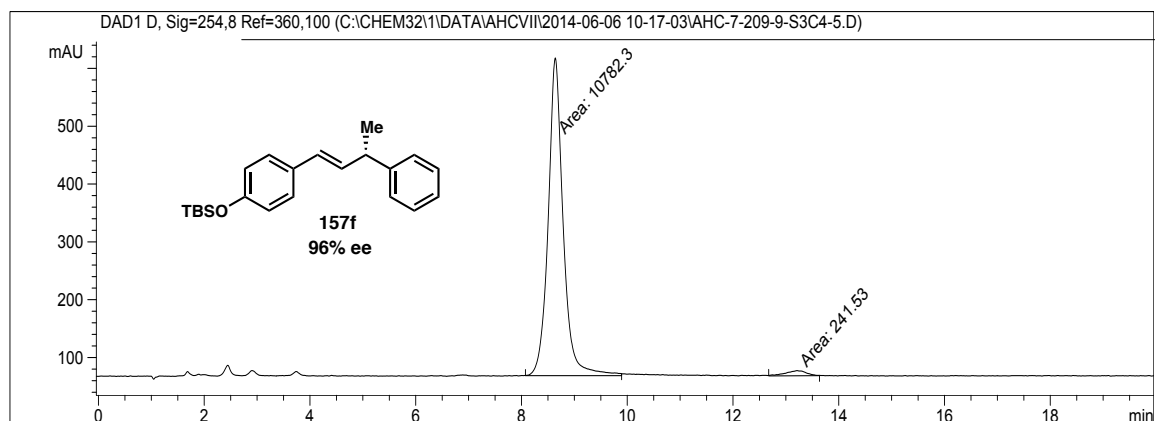
Peak #	RetTime [min]	Type	Width [min]	Area [mAU*s]	Height [mAU]	Area %
1	2.324	MM	0.0917	433.17111	78.69621	3.1352
2	2.517	MM	0.1119	1.33834e4	1993.22083	96.8648

**157f (Table 4.5, entry 6): racemic**



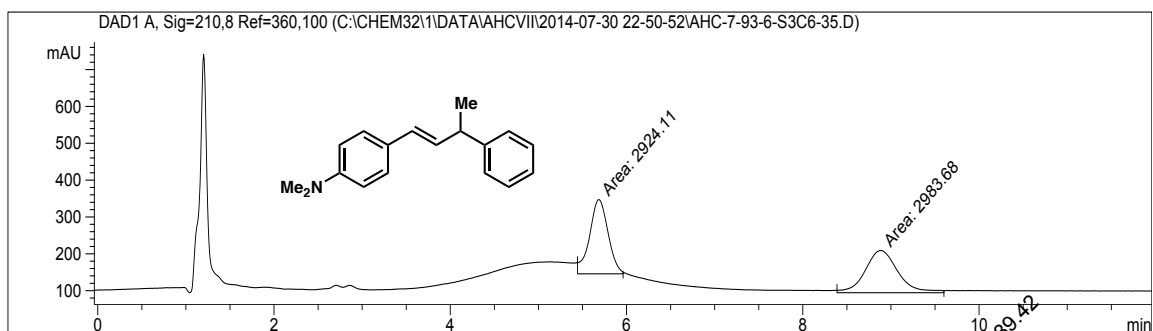
Peak #	RetTime [min]	Type	Width [min]	Area [mAU*s]	Height [mAU]	Area %
1	8.373	MM	0.3477	9348.08398	448.07748	51.0442
2	12.445	MM	0.5034	8965.63672	296.82007	48.9558

**157f (Table 4.5, entry 6): enantioenriched, 96% ee**



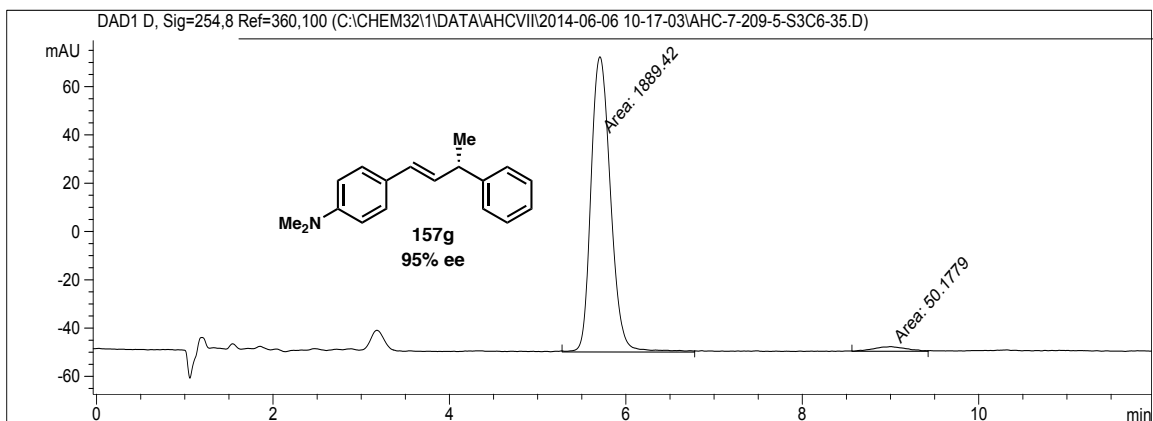
Peak #	RetTime [min]	Type	Width [min]	Area [mAU*s]	Height [mAU]	Area %
1	8.638	MM	0.3270	1.07823e4	549.47449	97.8090
2	13.210	MM	0.4557	241.52989	8.83361	2.1910

**157g (Table 4.5, entry 7): racemic**



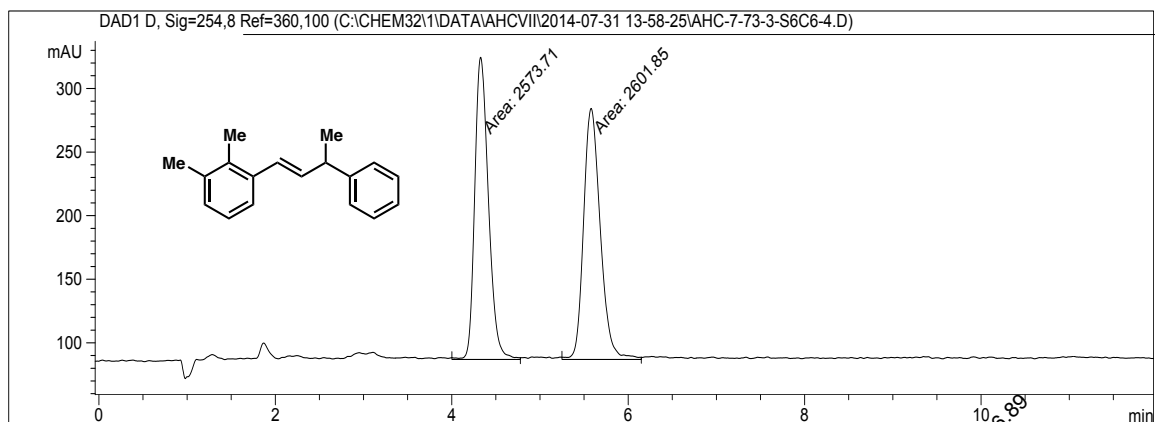
Peak #	RetTime [min]	Type	Width [min]	Area [mAU*s]	Height [mAU]	Area %
1	5.686	MM	0.2419	2924.10986	201.49109	49.4958
2	8.884	MM	0.4337	2983.68335	114.67265	50.5042

**157g (Table 4.5, entry 7): enantioenriched, 95% ee**



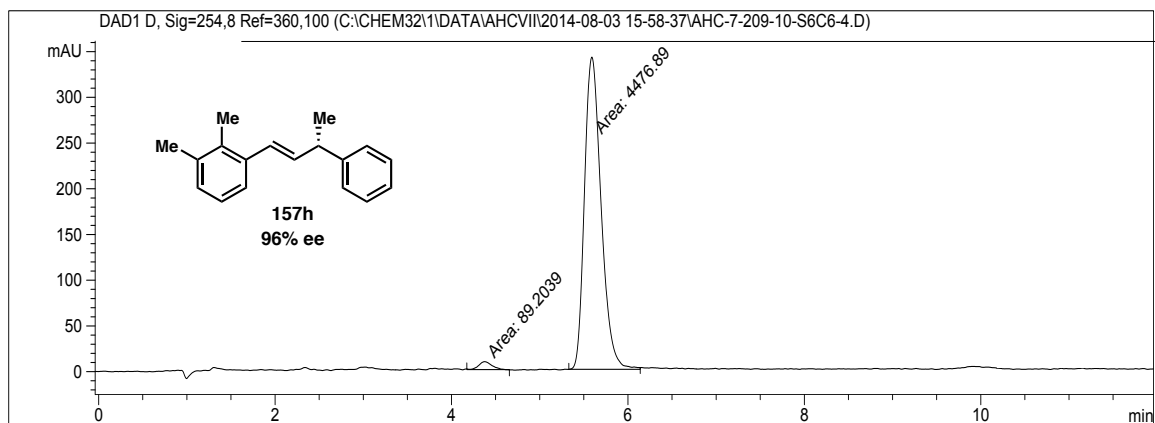
Peak #	RetTime [min]	Type	Width [min]	Area [mAU*s]	Height [mAU]	Area %
1	5.706	MM	0.2574	1889.41882	122.31673	97.4130
2	9.005	MM	0.4300	50.17793	1.94500	2.5870

**157h (Table 4.5, entry 8): racemic**



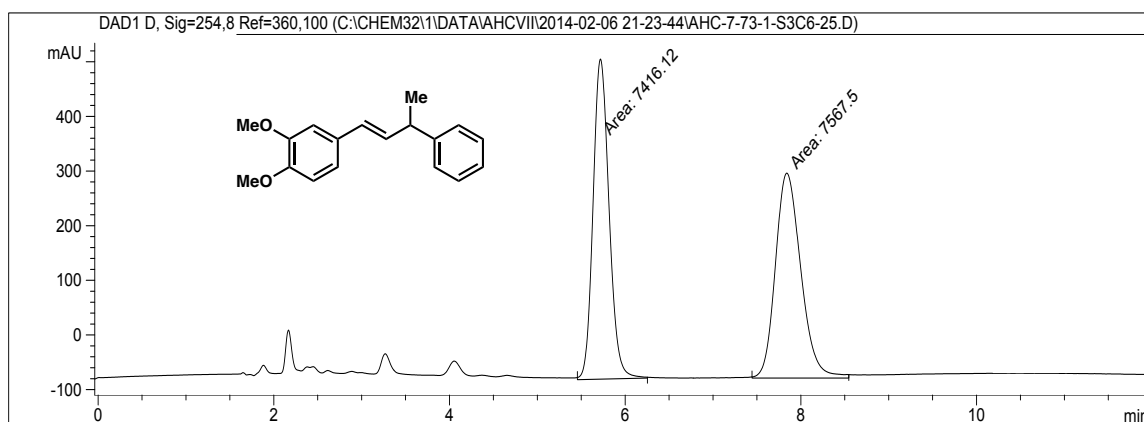
Peak #	RetTime [min]	Type	Width [min]	Area [mAU*s]	Height [mAU]	Area %
1	4.327	MM	0.1803	2573.70605	237.87602	49.7281
2	5.579	MM	0.2195	2601.85254	197.58577	50.2719

**157h (Table 4.5, entry 8): enantioenriched, 96% ee**



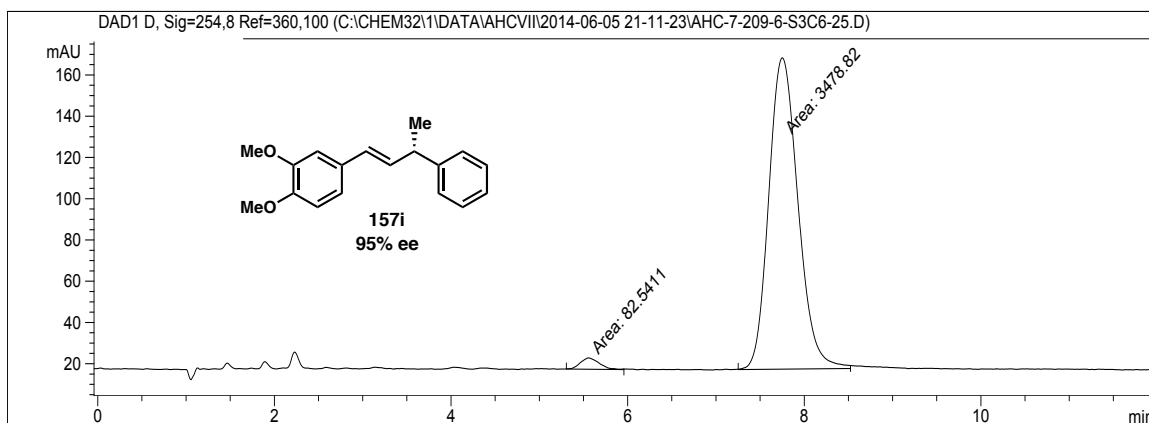
Peak #	RetTime [min]	Type	Width [min]	Area [mAU*s]	Height [mAU]	Area %
1	4.374	MM	0.1704	89.20393	8.72473	1.9536
2	5.590	MM	0.2184	4476.88916	341.59937	98.0464

**157i (Table 4.5, entry 9): racemic**



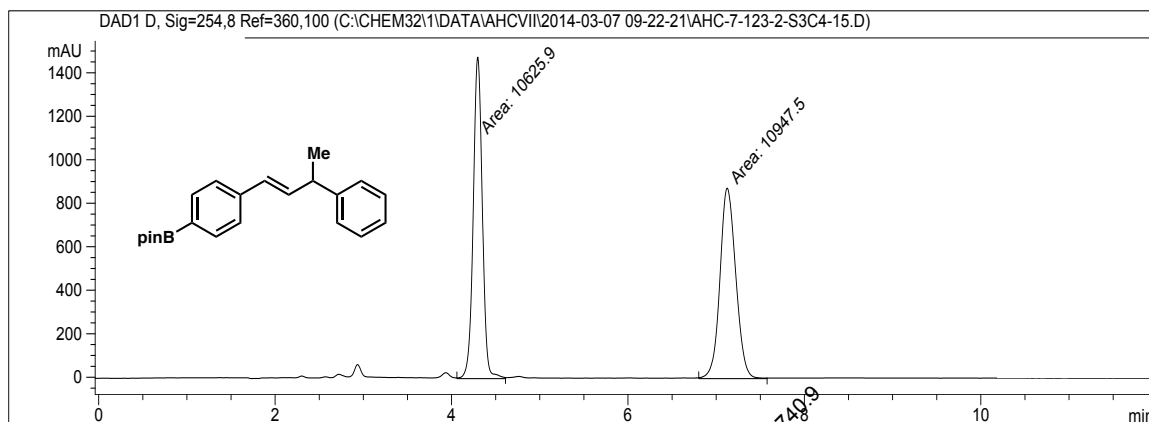
Peak #	RetTime [min]	Type	Width [min]	Area [mAU*s]	Height [mAU]	Area %
1	5.719	MM	0.2109	7416.11523	586.16187	49.4948
2	7.839	MM	0.3362	7567.49658	375.18320	50.5052

**157i (Table 4.5, entry 9): enantioenriched, 95% ee**



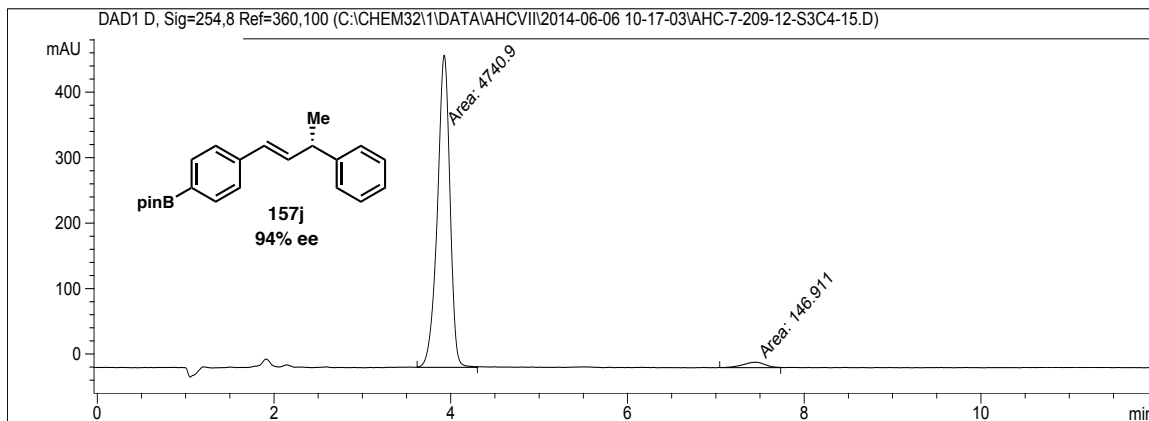
Peak #	RetTime [min]	Type	Width [min]	Area [mAU*s]	Height [mAU]	Area %
1	5.558	MM	0.2489	82.54113	5.52799	2.3177
2	7.751	MM	0.3840	3478.81641	150.97183	97.6823

**157j (Table 4.5, entry 10): racemic**



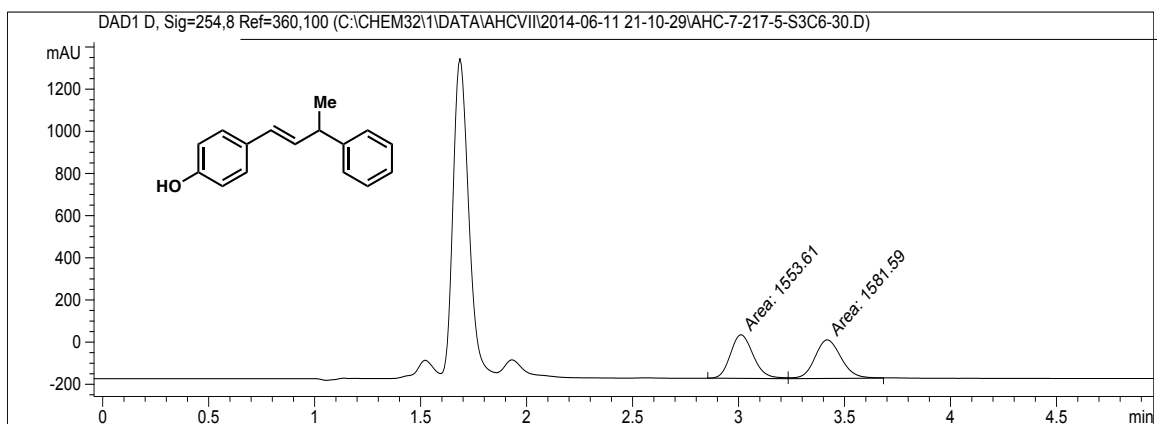
Peak #	RetTime [min]	Type	Width [min]	Area [mAU*s]	Height [mAU]	Area %
1	4.297	MM	0.1195	1.06259e4	1481.47107	49.2547
2	7.125	MM	0.2081	1.09475e4	876.78436	50.7453

**157j (Table 4.5, entry 10): enantioenriched, 94% ee**



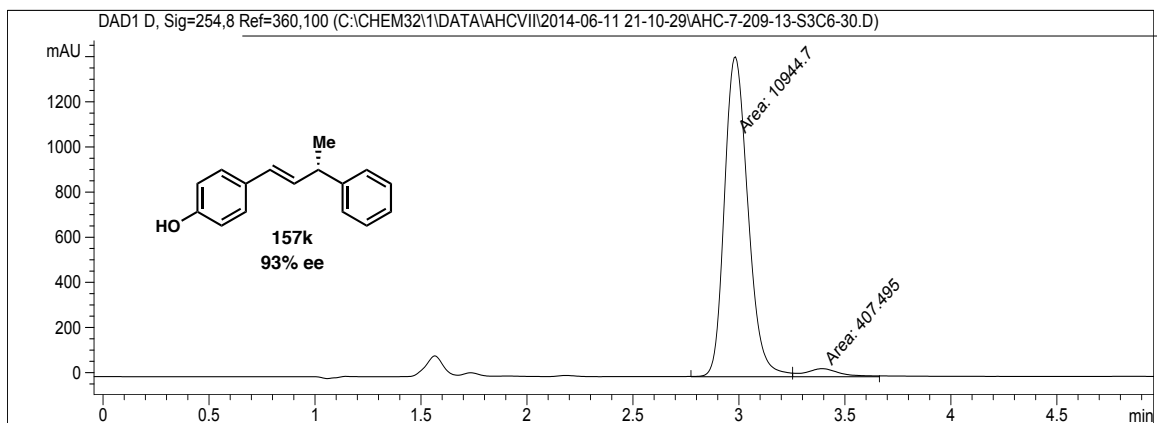
Peak #	RetTime [min]	Type	Width [min]	Area [mAU*s]	Height [mAU]	Area %
1	3.926	MM	0.1654	4740.90332	477.81689	96.9943
2	7.451	MM	0.2946	146.91095	8.30996	3.0057

**157k (Table 4.5, entry 11): racemic**



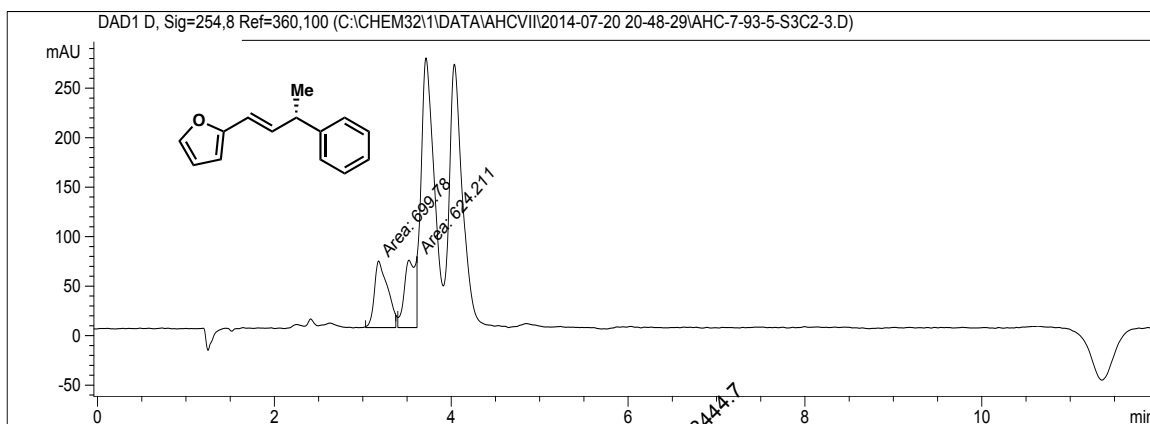
Peak #	RetTime [min]	Type	Width [min]	Area [mAU*s]	Height [mAU]	Area %
1	3.011	MM	0.1249	1553.60925	207.25208	49.5538
2	3.418	MM	0.1438	1581.58533	183.37068	50.4462

**157k (Table 4.5, entry 11): enantioenriched, 93% ee**



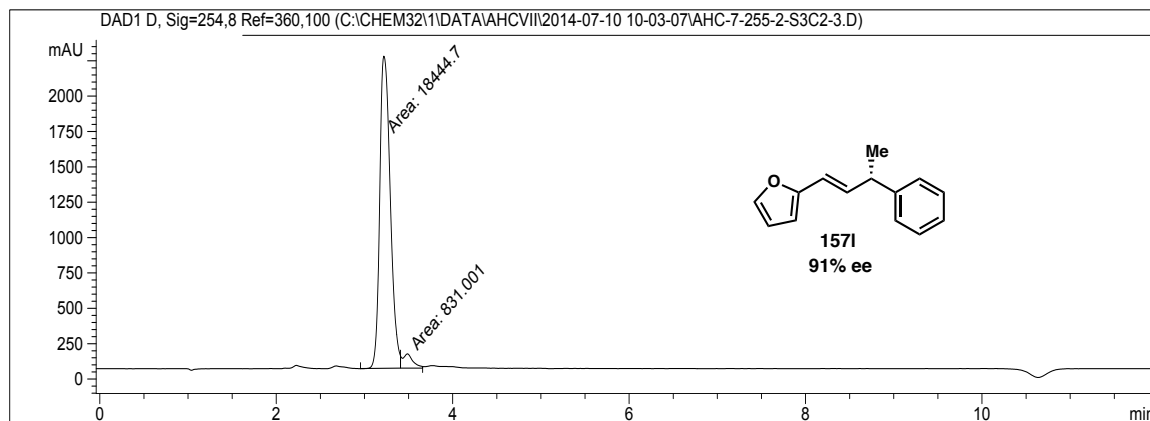
Peak #	RetTime [min]	Type	Width [min]	Area [mAU*s]	Height [mAU]	Area %
1	2.982	MM	0.1285	1.09447e4	1419.67334	96.4104
2	3.392	MM	0.1893	407.49545	35.88238	3.5896

**1571 (Figure 4.5): racemic**



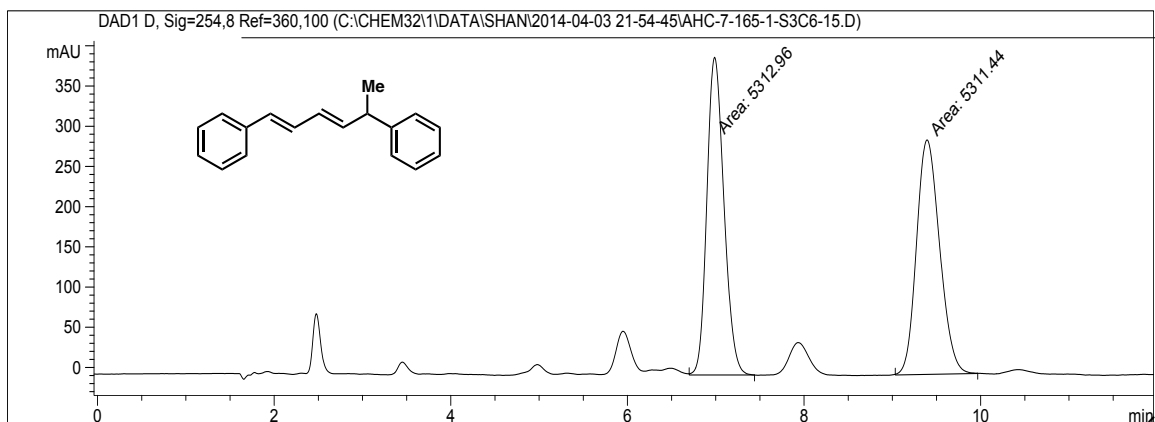
Peak #	RetTime [min]	Type	Width [min]	Area [mAU*s]	Height [mAU]	Area %
1	3.178	MM	0.1734	699.77979	67.27696	52.8538
2	3.611	MM	0.1474	624.21143	70.55936	47.1462

**1571 (Figure 4.5): enantioenriched, 91% ee**



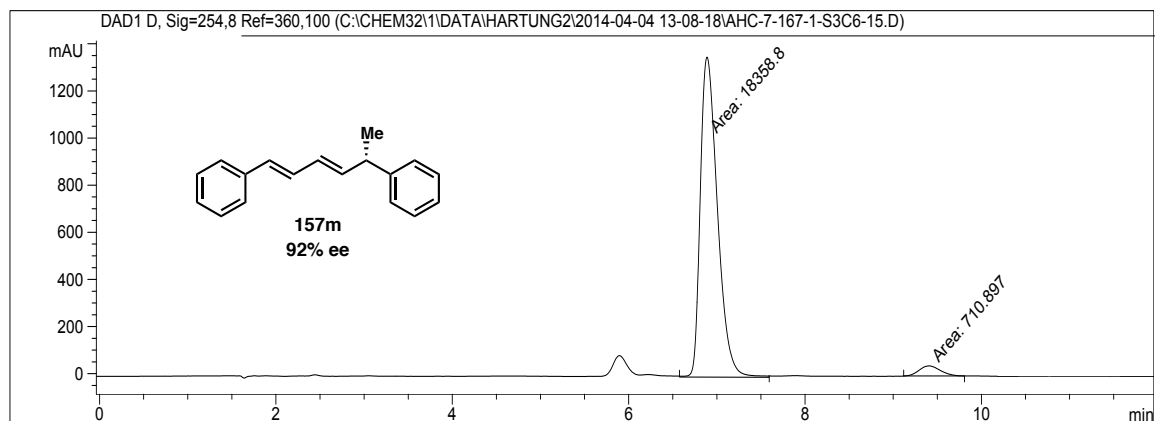
Peak #	RetTime [min]	Type	Width [min]	Area [mAU*s]	Height [mAU]	Area %
1	3.220	MM	0.1391	1.84447e4	2209.27100	95.6889
2	3.487	MM	0.1366	831.00092	101.37794	4.3111

**157m (Figure 4.5): racemic**



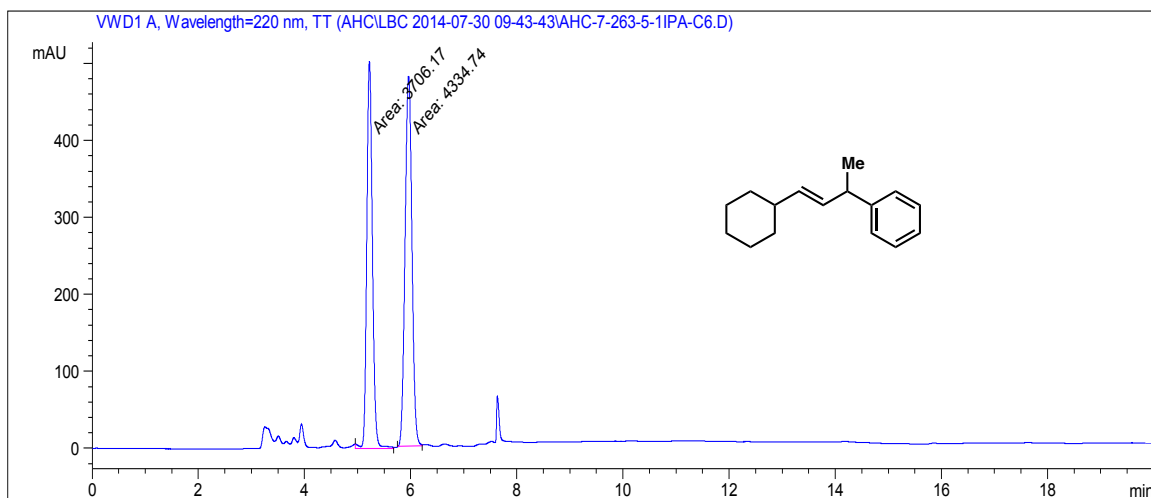
Peak #	RetTime [min]	Type	Width [min]	Area [mAU*s]	Height [mAU]	Area %
1	6.987	MM	0.2241	5312.95996	395.21527	50.0072
2	9.393	MM	0.3035	5311.43506	291.66327	49.9928

**157m (Figure 4.5): enantioenriched, 92% ee**



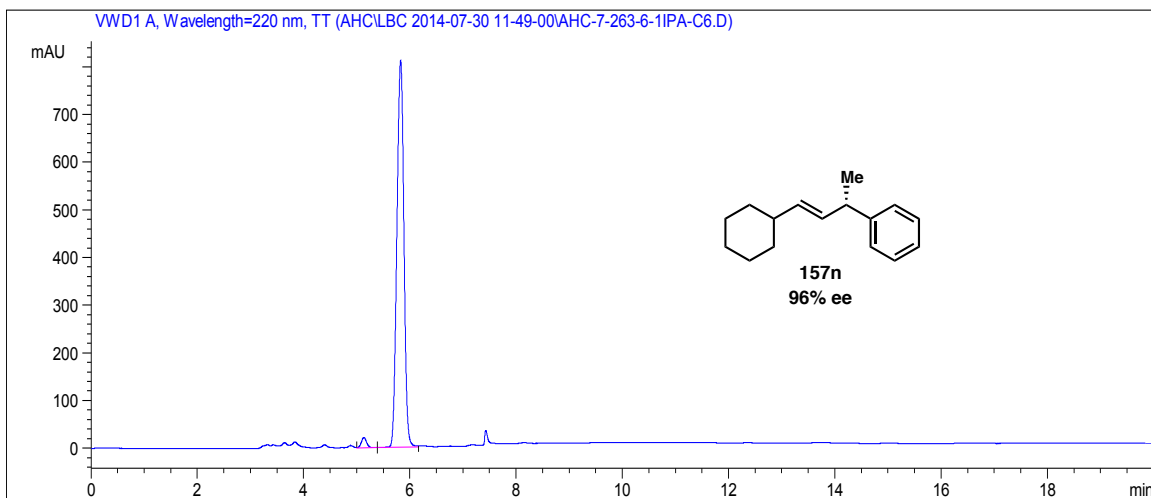
Peak #	RetTime [min]	Type	Width [min]	Area [mAU*s]	Height [mAU]	Area %
1	6.889	MM	0.2251	1.83588e4	1359.02136	96.2721
2	9.404	MM	0.2780	710.89673	42.61983	3.7279

**157n (Figure 4.5): racemic**

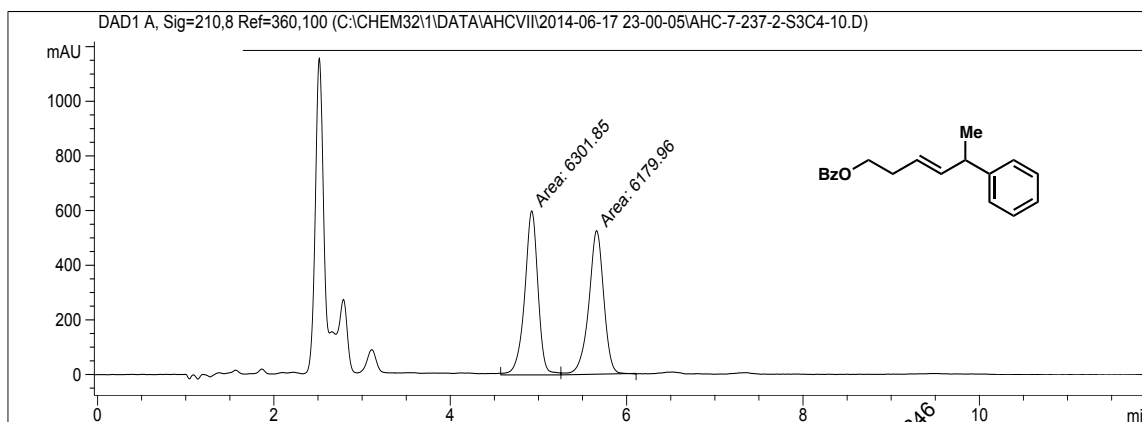


Peak #	RetTime [min]	Type	Width [min]	Area mAU *s	Height [mAU]	Area %
1	5.224	MM	0.1228	3706.16968	503.21298	46.0914
2	5.962	MM	0.1500	4334.74365	481.51410	53.9086

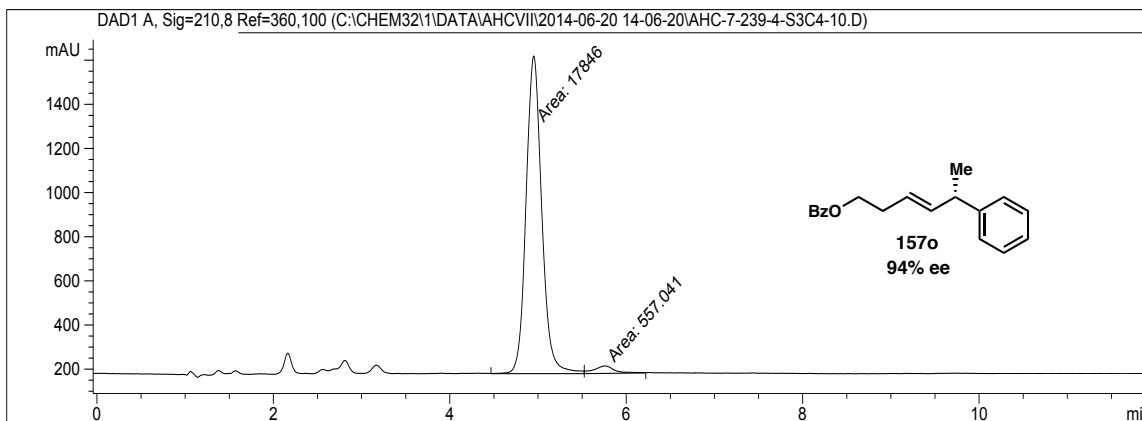
**157n (Figure 4.5): enantioenriched, 96% ee**



Peak #	RetTime [min]	Type	Width [min]	Area mAU *s	Height [mAU]	Area %
1	5.135	VV	0.1050	148.14879	21.73537	1.9461
2	5.828	VV	0.1459	7464.48193	811.72534	98.0539

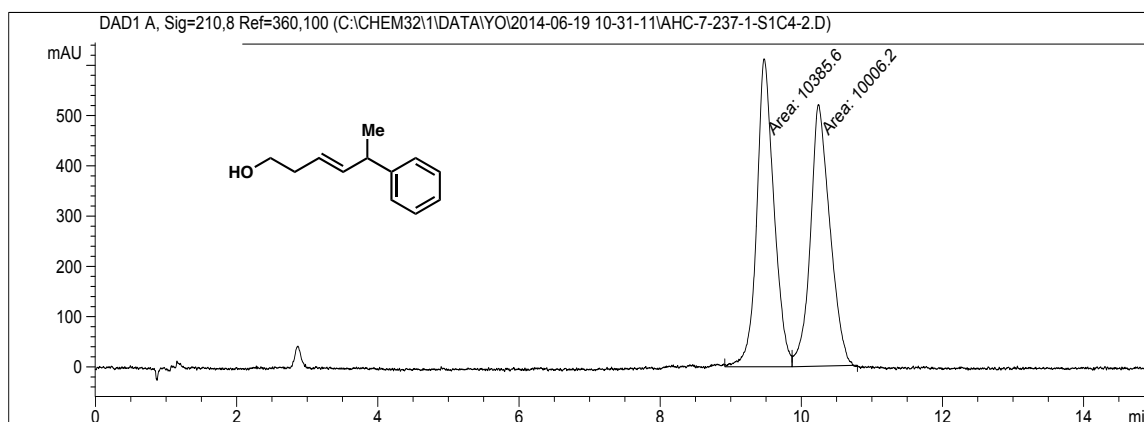
**157o (Figure 4.5): racemic**

Peak #	RetTime [min]	Type	Width [min]	Area [mAU*s]	Height [mAU]	Area %
1	4.924	MM	0.1744	6301.85156	602.20233	50.4883
2	5.660	MM	0.1955	6179.95850	526.80280	49.5117

**157o (Figure 4.5): enantioenriched, 94% ee**

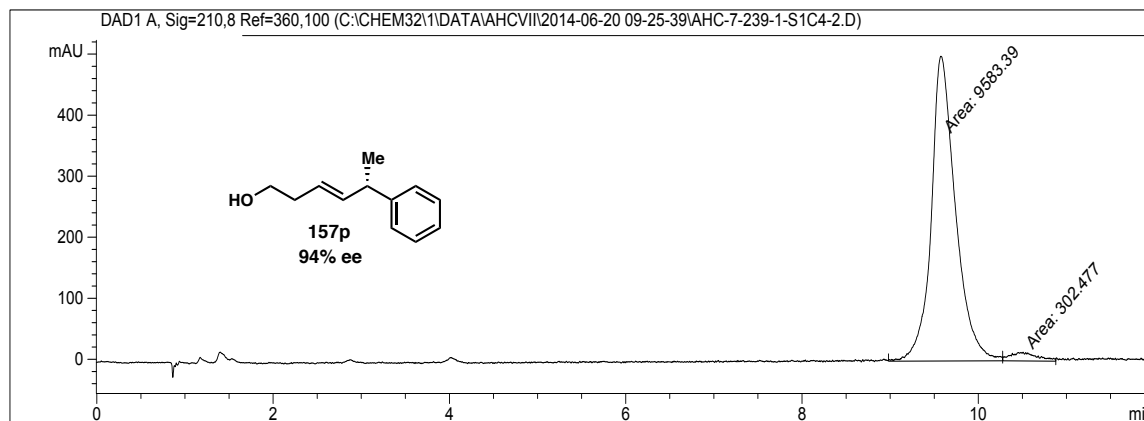
Peak #	RetTime [min]	Type	Width [min]	Area [mAU*s]	Height [mAU]	Area %
1	4.951	MM	0.2063	1.78460e4	1441.90649	96.9731
2	5.755	MM	0.2719	557.04138	34.14230	3.0269

**157p (Figure 4.5): racemic**



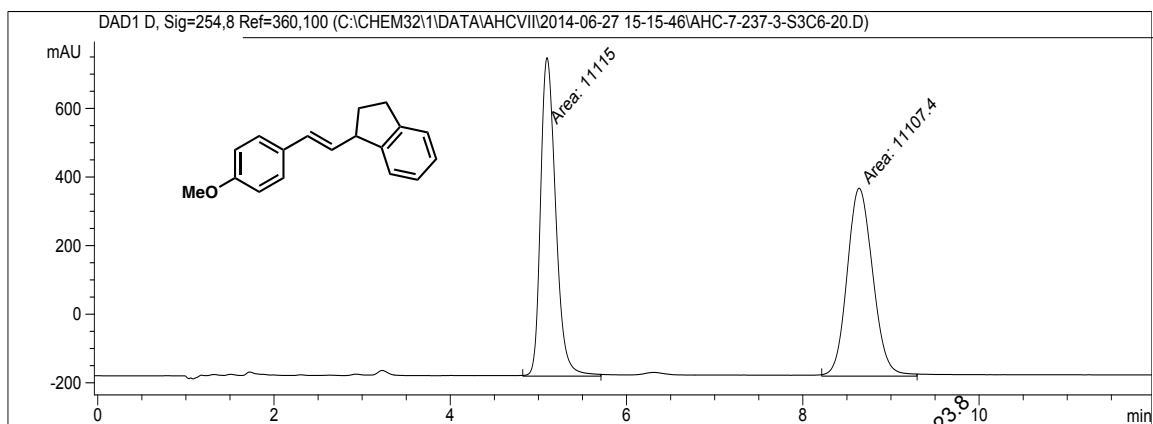
Peak #	RetTime [min]	Type	Width [min]	Area [mAU*s]	Height [mAU]	Area %
1	9.474	MM	0.2823	1.03856e4	613.19647	50.9302
2	10.244	MM	0.3204	1.00062e4	520.49475	49.0698

**157p (Figure 4.5): enantioenriched, 94% ee**



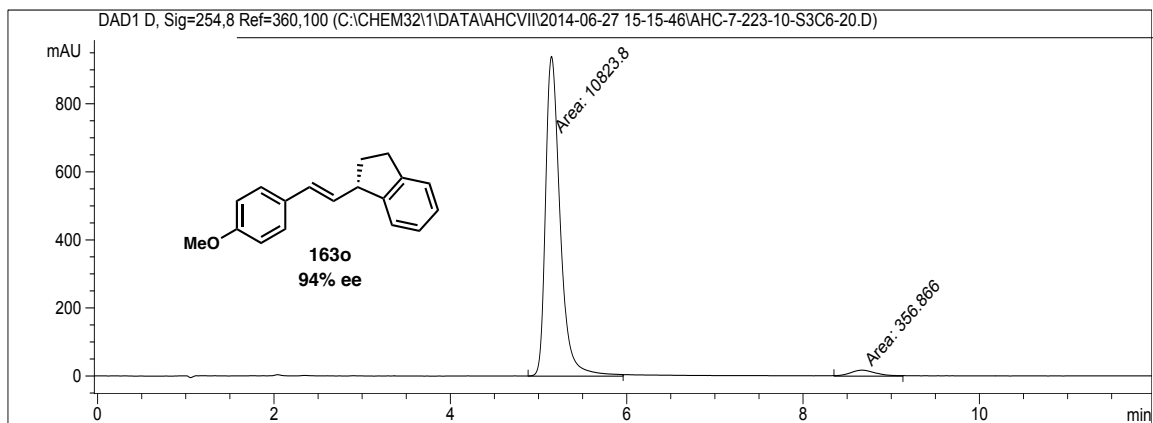
Peak #	RetTime [min]	Type	Width [min]	Area [mAU*s]	Height [mAU]	Area %
1	9.577	MM	0.3197	9583.38965	499.54858	96.9403
2	10.504	MM	0.3286	302.47656	13.89878	3.0597

**163o (Figure 4.5): racemic**



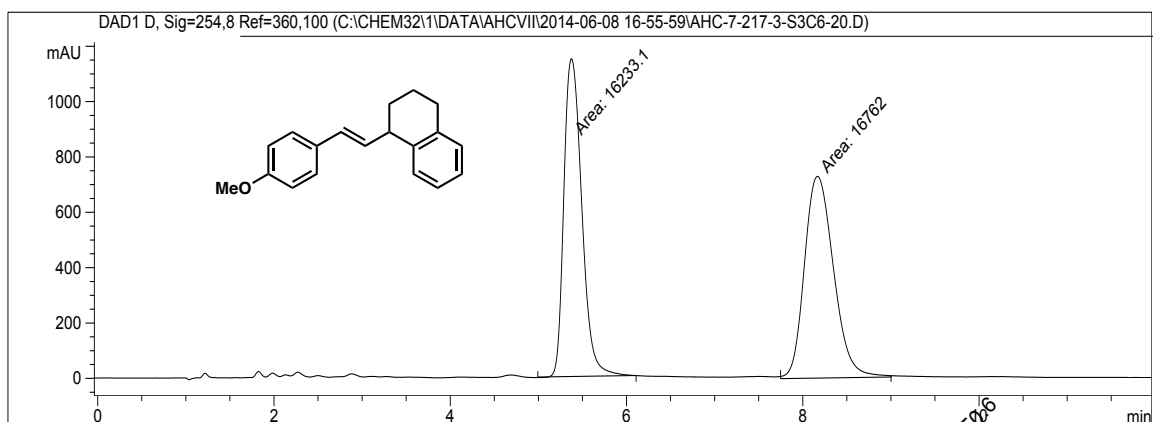
Peak #	RetTime [min]	Type	Width [min]	Area [mAU*s]	Height [mAU]	Area %
1	5.098	MM	0.1994	1.11150e4	929.12982	50.0170
2	8.639	MM	0.3377	1.11074e4	548.26196	49.9830

**163o (Figure 4.5): enantioenriched, 94% ee**



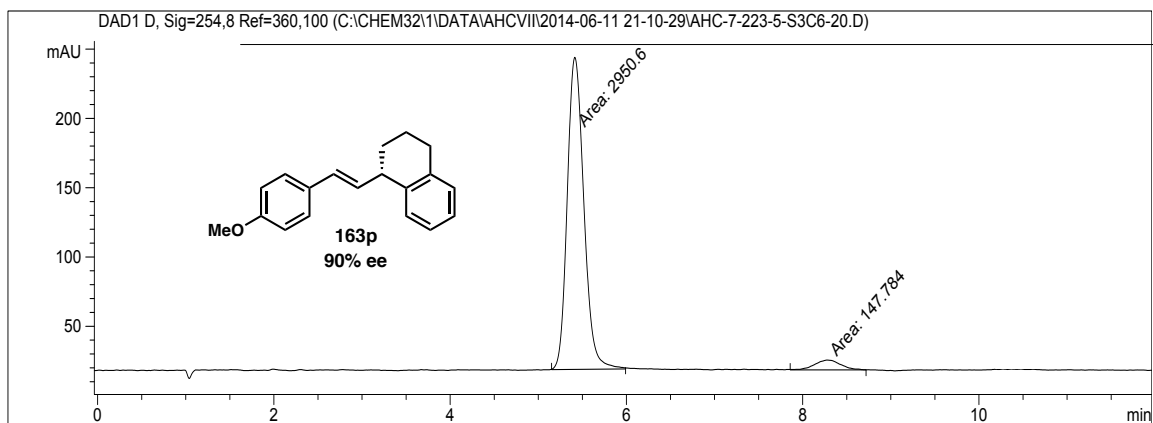
Peak #	RetTime [min]	Type	Width [min]	Area [mAU*s]	Height [mAU]	Area %
1	5.147	MM	0.1918	1.08238e4	940.38129	96.8082
2	8.669	MM	0.3406	356.86603	17.46182	3.1918

**163p (Figure 4.5): racemic**



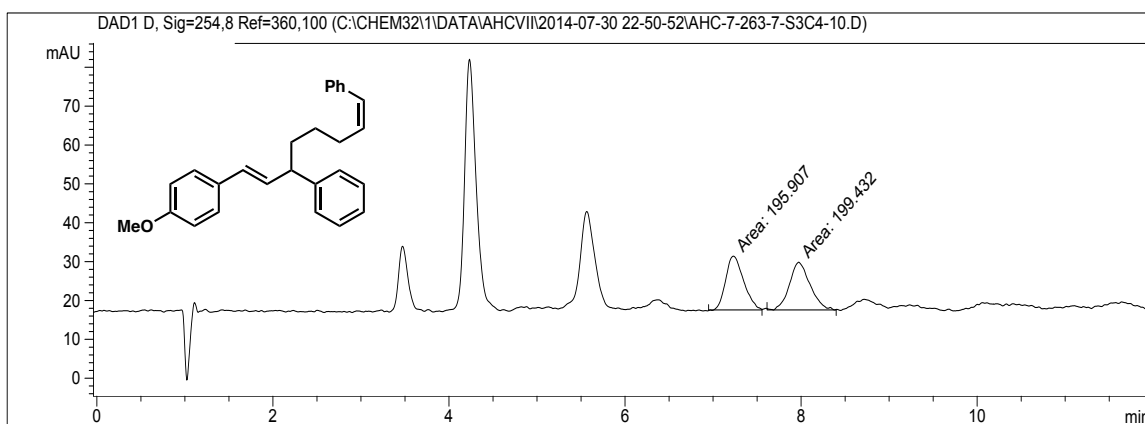
Peak #	RetTime [min]	Type	Width [min]	Area [mAU*s]	Height [mAU]	Area %
1	5.375	MM	0.2355	1.62331e4	1148.88831	49.1985
2	8.167	MM	0.3832	1.67620e4	728.97369	50.8015

**163p (Figure 4.5): enantioenriched, 90% ee**



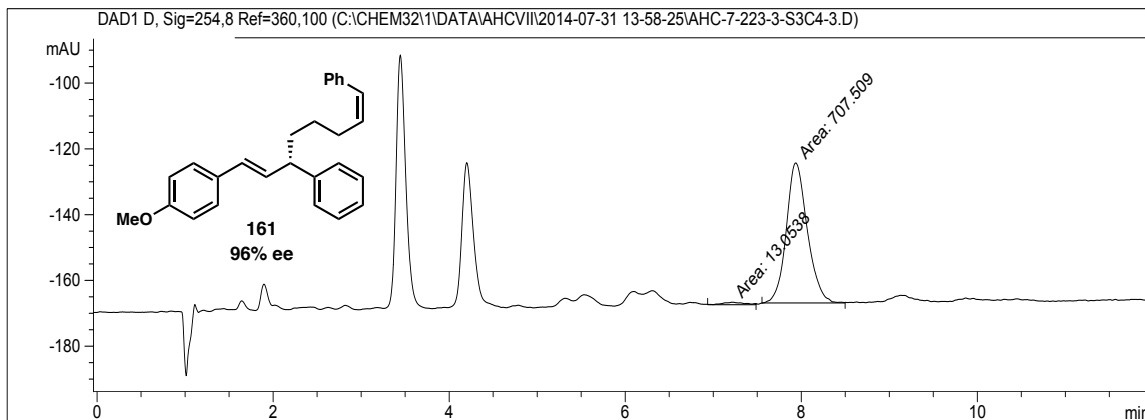
Peak #	RetTime [min]	Type	Width [min]	Area [mAU*s]	Height [mAU]	Area %
1	5.414	MM	0.2183	2950.59619	225.29623	95.2303
2	8.276	MM	0.3454	147.78352	7.13138	4.7697

**161 (Scheme 4.2): racemic**



Peak #	RetTime [min]	Type	Width [min]	Area [mAU*s]	Height [mAU]	Area %
1	7.230	MM	0.2362	195.90703	13.82199	49.5542
2	7.972	MM	0.2706	199.43159	12.28512	50.4458

**161 (Scheme 4.2): enantioenriched, 96% ee**



Peak #	RetTime [min]	Type	Width [min]	Area [mAU*s]	Height [mAU]	Area %
1	7.215	MM	0.2808	13.05381	7.74711e-1	1.8116
2	7.938	MM	0.2768	707.50922	42.60372	98.1884

## 4.5 NOTES AND REFERENCES

- (1) Reviews on reductive cross-couplings: (a) Everson, D. A.; Weix, D. J. *J. Org. Chem.* **2014**, *79*, 4793. (b) Knappke, C. E. I.; Grupe, S.; Gärtner, D.; Corpet, M.; Gosmini, C.; Jacobi von Wangelin, A. *Chem. Eur. J.* **2014**, *20*, 6828. (c) Moragas, T.; Correa, A.; Martin, R. *Chem. Eur. J.* **2014**, *20*, 8242.
- (2) C(sp<sup>3</sup>)-C(sp<sup>2</sup>) couplings: (a) Durandetti, M.; Gosmini, C.; Périchon, J. *Tetrahedron* **2007**, *63*, 1146. (b) Everson, D. A.; Shrestha, R.; Weix, D. J. *J. Am. Chem. Soc.* **2010**, *132*, 920. (c) Shrestha, R.; Weix, D. J. *Org. Lett.* **2011**, *13*, 2766. (d) Everson, D. A.; Jones, B. A.; Weix, D. J. *J. Am. Chem. Soc.* **2012**, *134*, 6146. (e) Wang, S.; Qian, Q.; Gong, H. *Org. Lett.* **2012**, *14*, 3352. (f) Shrestha, R.; Dorn, S. C. M.; Weix, D. J. *J. Am. Chem. Soc.* **2013**, *135*, 751. (g) Wotal, A. C.; Weix, D. J. *Org. Lett.* **2012**, *14*, 1476. (h) Wu, F.; Lu, W.; Qian, Q.; Ren, Q.; Gong, H. *Org. Lett.* **2012**, *14*, 3044.
- (3) C(sp<sup>3</sup>)-C(sp<sup>3</sup>) couplings: (a) Yu, X.; Yang, T.; Wang, S.; Xu, H.; Gong, H. *Org. Lett.* **2011**, *13*, 2138. (b) Xu, H.; Zhao, C.; Qian, Q.; Deng, W.; Gong, H. *Chem. Sci.* **2013**, *4*, 4022.
- (4) Co-catalyzed reductive coupling reactions have also been reported: (a) Amatore, M.; Gosmini, C. *Angew. Chem., Int. Ed.* **2008**, *47*, 2089. (b) Amatore, M.; Gosmini, C. *Chem. Eur. J.* **2010**, *16*, 5848.
- (5) Reviews on alkyl halides in cross-couplings: (a) Netherton, M. R.; Fu, G. C. *Adv. Synth. & Catal.* **2004**, *346*, 1525. (b) Frisch, A. C.; Beller, M. *Angew. Chem., Int. Ed.* **2005**, *44*, 674. (c) Rudolph, A.; Lautens, M. *Angew. Chem., Int. Ed.* **2009**, *48*, 2656.
- (6) (a) Trost, B. M.; Van Vranken, D. L. *Chem. Rev.* **1996**, *96*, 395. (b) Lu, Z.; Ma, S. *Angew. Chem., Int. Ed.* **2008**, *47*, 258.
- (7) Racemic reductive cross-couplings have also been used to couple allyl groups with aryl or alkyl electrophiles: (a) Gomes, P.; Gosmini, C.; Périchon, J. *Org. Lett.* **2003**, *5*, 1043. (b) Anka-Lufford, L. L.; Prinsell, M. R.; Weix, D. J. *J. Org. Chem.* **2012**, *77*, 9989. (c) Dai, Y.; Wu, F.; Zang, Z.; You, H.; Gong, H. *Chem. Eur. J.* **2012**, *18*, 808. (d) Cui, X.; Wang, S.; Zhang, Y.; Deng, W.; Qian, Q.; Gong, H. *Org. Biomol. Chem.* **2013**, *11*, 3094.
- (8) For select examples see: (a) Evans, P. A.; Uraguchi, D. *J. Am. Chem. Soc.* **2003**, *125*, 7158. (b) Ohmiya, H.; Makida, Y.; Li, D.; Tanabe, M.; Sawamura, M. *J. Am. Chem. Soc.* **2010**, *132*, 879. (c) Li, D.; Tanaka, T.; Ohmiya, H.; Sawamura, M. *Org. Lett.* **2010**, *12*, 3344. (d) Thalén, L. K.; Sumic, A.; Bogár, K.; Norinder, J.; Persson, A. K. Å.; Bäckvall, J.-E. *J. Org. Chem.* **2010**, *75*, 6842. (e) Ohmiya, H.; Yokokawa, N.; Sawamura, M. *Org. Lett.* **2010**, *12*, 2438. (f) Lauer, A. M.;

- Mahmud, F.; Wu, J. *J. Am. Chem. Soc.* **2011**, *133*, 9119. (g) Li, C.; Xing, J.; Zhao, J.; Huynh, P.; Zhang, W.; Jiang, P.; Zhang, Y. *J. Org. Lett.* **2012**, *14*, 390.
- (9) (a) Alexakis, A.; Hajjaji, S. El; Polet, D.; Rathgeb, X. *Org. Lett.* **2007**, *9*, 3393. (b) Selim, K. B.; Yamada, K.; Tomioka, K. *Chem. Commun.* **2008**, 5140. (c) Selim, K. B.; Matsumoto, Y.; Yamada, K.; Tomioka, K. *Angew. Chem., Int. Ed* **2009**, *48*, 8733. (d) Polet, D.; Rathgeb, X.; Falciola, C. A.; Langlois, J.-B.; El Hajjaji, S.; Alexakis, A. *Chem. Eur. J.* **2009**, *15*, 1205. (e) Selim, K. B.; Nakanishi, H.; Matsumoto, Y.; Yamamoto, Y.; Yamada, K.; Tomioka, K. *J. Org. Chem.* **2011**, *76*, 1398. (f) Srinivas, H. D.; Zhou, Q.; Watson, M. P. *Org. Lett.* **2014**, *16*, 3596.
- (10) Asymmetric allylic substitution of acyclic, unsymmetrical  $\alpha,\gamma$ -disubstituted allylic electrophiles with alkyl organometallic reagents has been reported: (a) Chung, K.-G.; Miyake, Y.; Uemura, S. *J. Chem. Soc. Perkin Trans. 1* **2000**, 2725. (b) Son, S.; Fu, G. C. *J. Am. Chem. Soc.* **2008**, *130*, 2756.
- (11) For an introduction to Ni-catalyzed reductive cross-couplings, see Chapter 3.
- (12) Semmelhack, M. F.; Helquist, P. M.; Gorzynski, J. D. *J. Am. Chem. Soc.* **1972**, *94*, 9234.
- (13) (a) Takagi, K.; Mimura, H.; Inokawa, S. *Bull. Chem. Soc. Jpn.* **1984**, *57*, 3517. (b) Cannes, C.; Labbé, E.; Durandetti, M.; Devaud, M.; Nédélec, J. Y. *J. Electroanal. Chem.* **1996**, *412*, 85. (c) Cannes, C.; Condon, S.; Durandetti, M.; Périchon, J.; Nédélec, J. *J. Org. Chem.* **2000**, *65*, 4575. (d) Durandetti, M.; Périchon, J. *Synthesis* **2004**, 3079.
- (14) Cherney, A. H.; Kadunce, N. T.; Reisman, S. E. *J. Am. Chem. Soc.* **2013**, *135*, 7442.
- (15) Cherney, A. H.; Reisman, S. E. *J. Am. Chem. Soc.* **2014**, *136*, 14365.
- (16) For a related enantiospecific cross-coupling see: Shacklady-McAtee, D. M.; Roberts, K. M.; Basch, C. H.; Song, Y.-G.; Watson, M. P. *Tetrahedron* **2014**, *70*, 4257.
- (17) For mechanistic studies on homodimer formation see: (a) Yamamoto, T.; Kohara, T.; Yamamoto, A. *Bull. Chem. Soc. Jpn.* **1981**, *54*, 2010. (b) Yamamoto, T.; Kohara, T.; Osakada, K.; Yamamoto, A. *Bull. Chem. Soc. Jpn.* **1983**, *56*, 2147.
- (18) (a) Takagi, K.; Hayama, N.; Inokawa, S. *Chem. Lett.* **1978**, 1435. (b) Tsou, T. T.; Kochi, J. K. *J. Org. Chem.* **1980**, *45*, 1930.

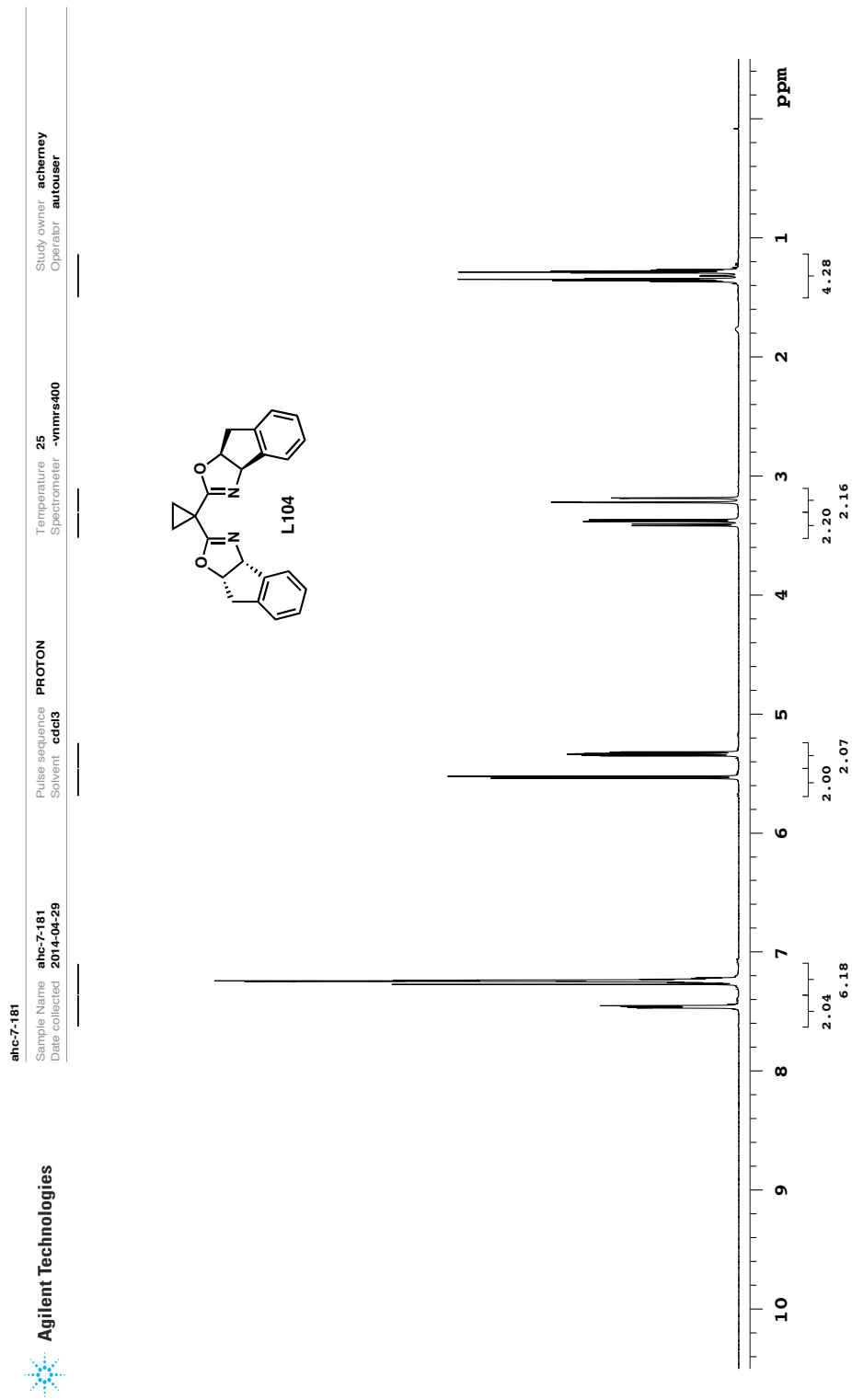
- (19) Colon, I.; Kelsey, D. R. *J. Org. Chem.* **1986**, *51*, 2627.
- (20) Klein, A.; Kaiser, A.; Wielandt, W.; Belaj, F.; Wendel, E.; Bertagnolli, H.; Záliš, S. *Inorg. Chem.* **2008** *47*, 11324.
- (21) Cassar, L.; Foà, A. *J. Organomet. Chem.* **1973**, *51*, 381.
- (22) (a) Takagi, K.; Hayama, N.; Inokawa, S. *Chem. Lett.* **1978**, 1435. (b) Tsou, T. T.; Kochi, J. K. *J. Org. Chem.* **1980**, *45*, 1930.
- (23) Mechanistic studies on reductive homo- and cross-coupling: (a) Amatore, C.; Jutand, A. *Organometallics* **1988**, *7*, 2203. (b) Biswas, S.; Weix, D. J. *J. Am. Chem. Soc.* **2013**, *135*, 16192 and references therein.
- (24) In the presence of 10 and 50 mol % BHT, the desired product is obtained in 86% and 76% yield, respectively.
- (25) Choi, J.; Fu, G. C. *J. Am. Chem. Soc.* **2012**, *134*, 9102.
- (26) Kuroboshi, M.; Tanaka, M.; Kishimoto, S.; Goto, K.; Mochizuki, M.; Tanaka, H. *Tetrahedron Lett.* **2000**, *41*, 81.
- (27) Schwink, L.; Knochel, P. *Chem. Eur. J.* **1998**, *4*, 950.
- (28) Still, W. C.; Kahn, M.; Mitra, A. *J. Org. Chem.* **1978**, *43*, 2923.
- (29) Ginotra, S. K.; Singh, V. K.; *Org. Biomol. Chem.* **2007**, *5*, 3932.
- (30) Kurosu, M.; Porter, J. R.; Foley, M. A. *Tetrahedron Lett.* **2004**, *45*, 145.
- (31) Robiette, R.; Pospíšil, J. *Eur. J. Org. Chem.* **2013**, 836.
- (32) Akiyama, S.; Nakatsuji, S.; Yoshida, K.; Nakashima, K.; Hagiwara, T.; Tsuruta, H.; Yoshida, T. *Bull. Chem. Soc. Jpn.* **1983**, *56*, 361.
- (33) Yoshida, K.; Horikoshi, Y.; Eta, M.; Chikazawa, J.; Ogishima, M.; Fukuda, Y.; Sato, H. *Bioorg. Med. Chem. Lett.* **1998**, *8*, 2967.
- (34) Ayala, C. E.; Villalpando, A.; Nguyen, A. L.; McCandless, G. T.; Kartika, R. *Org. Lett.* **2012**, *14*, 3676.
- (35) Bull, J. A.; Mousseau, J. J.; Charette, A. B. *Org. Lett.* **2008**, *10*, 5485.
- (36) Müller, D.; Alexakis, A. *Chem. Eur. J.* **2013**, *19*, 15226.

- (37) Hofmeister, H.; Annen, K.; Laurent, H.; Wiechert, R. *Angew. Chem., Int. Ed.* **1984**, *23*, 727.
- (38) Petriguet, J.; Boudhar, A.; Blond, G.; Suffert, J. *Angew. Chem., Int. Ed.* **2011**, *50*, 3285.
- (39) Wu, H.-B.; Ma, X.-T.; Tian, S.-K. *Chem. Commun.* **2014**, *50*, 219.
- (40) Ye, J.; Zhao, J.; Xu, J.; Mao, Y.; Zhang, Y. *J. Chem. Commun.* **2013**, *49*, 9761.
- (41) Li, M.-B.; Wang, Y.; Tian, S.-K. *Angew. Chem., Int. Ed.* **2012**, *51*, 2968.
- (42) Zhao, J.; Ye, J.; Zhang, Y. *J. Adv. Synth. Catal.* **2013**, *355*, 491.

## **APPENDIX 3**

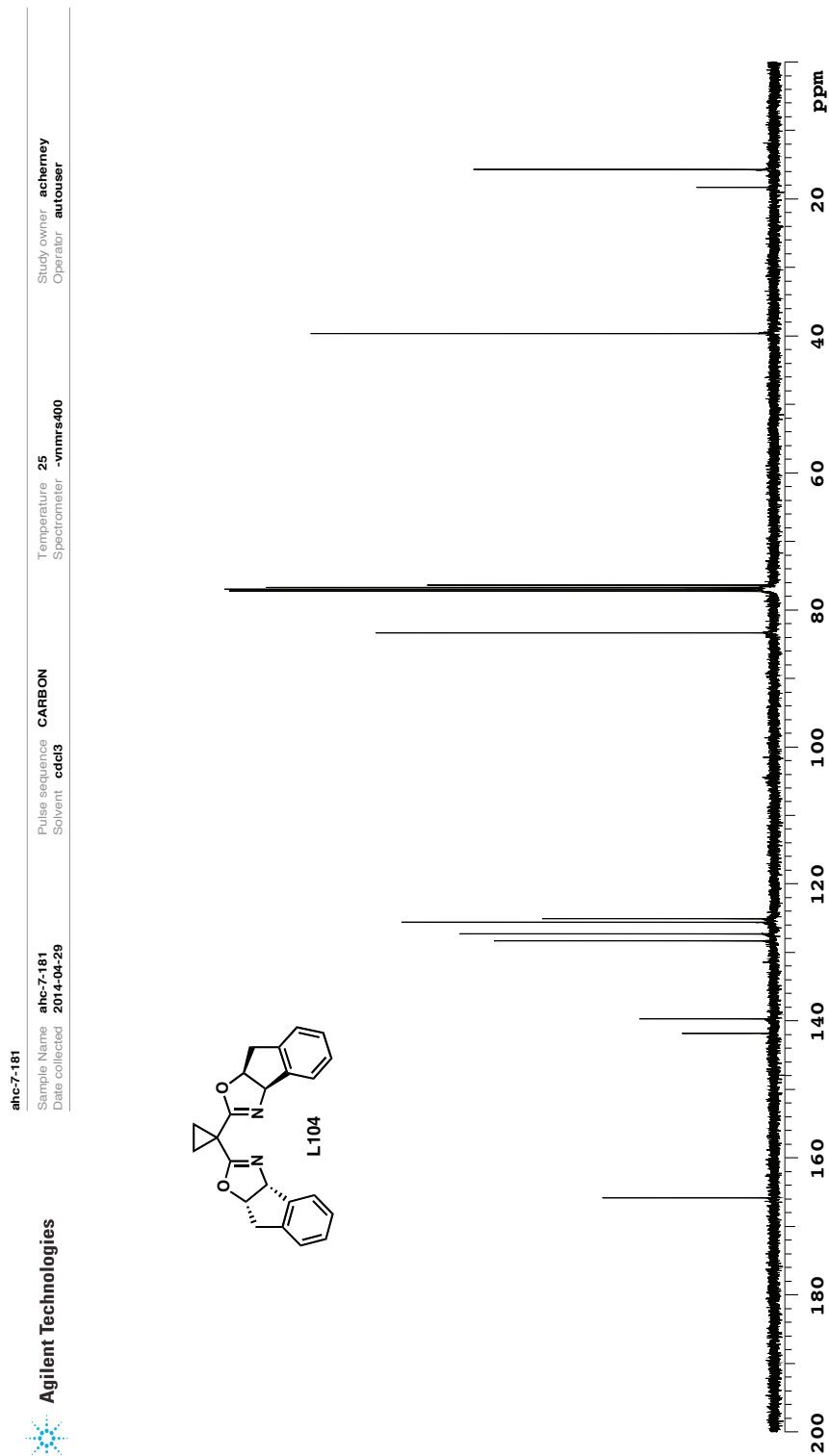
*Spectra Relevant to Chapter 4:*

*Nickel-Catalyzed Asymmetric Reductive Cross-Coupling Between Vinyl  
and Benzyl Electrophiles*



Data file /ndy/acherney/vnmrs/data/ahc-7-181/PROTON01.fid

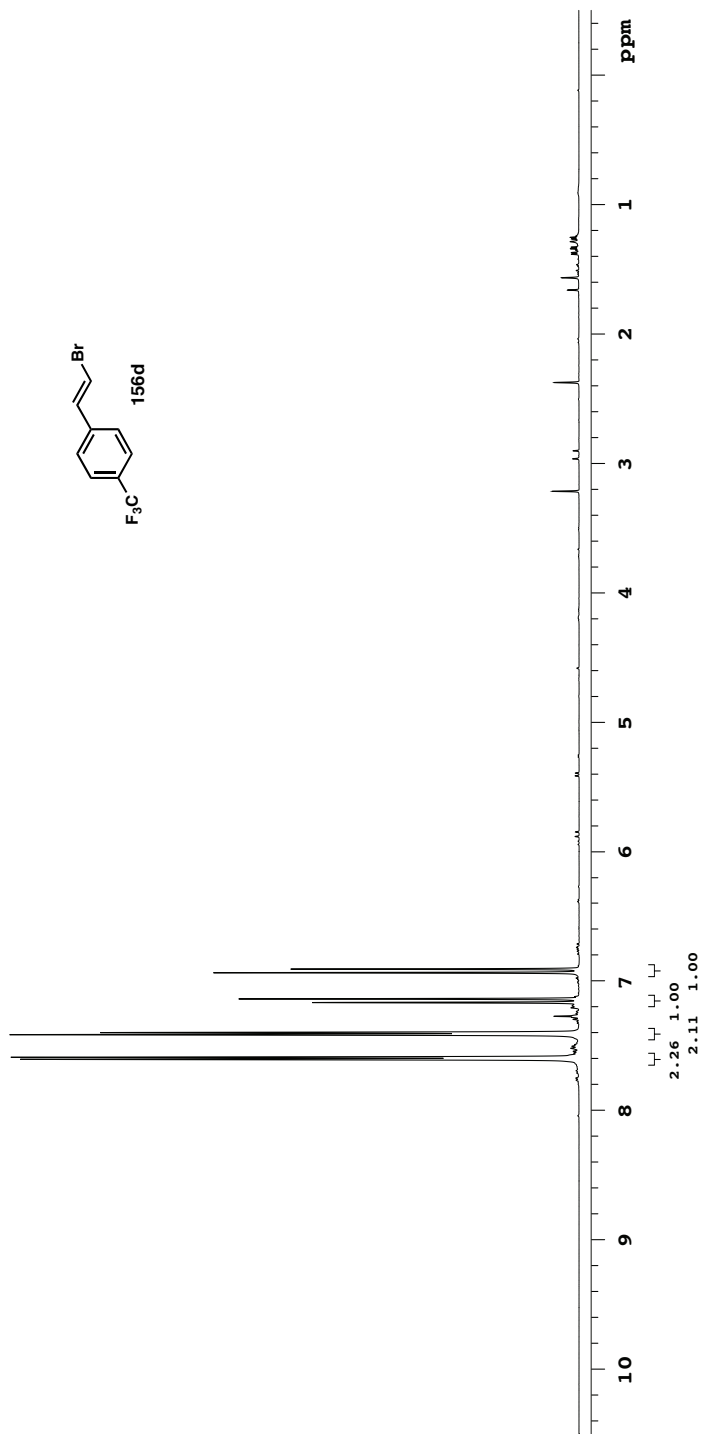
Plot date 2014-08-01



Plot date 2014-08-01

Data file /ndj/acherney/vnmrs/data/ahc-7-181/CARBON01.fid

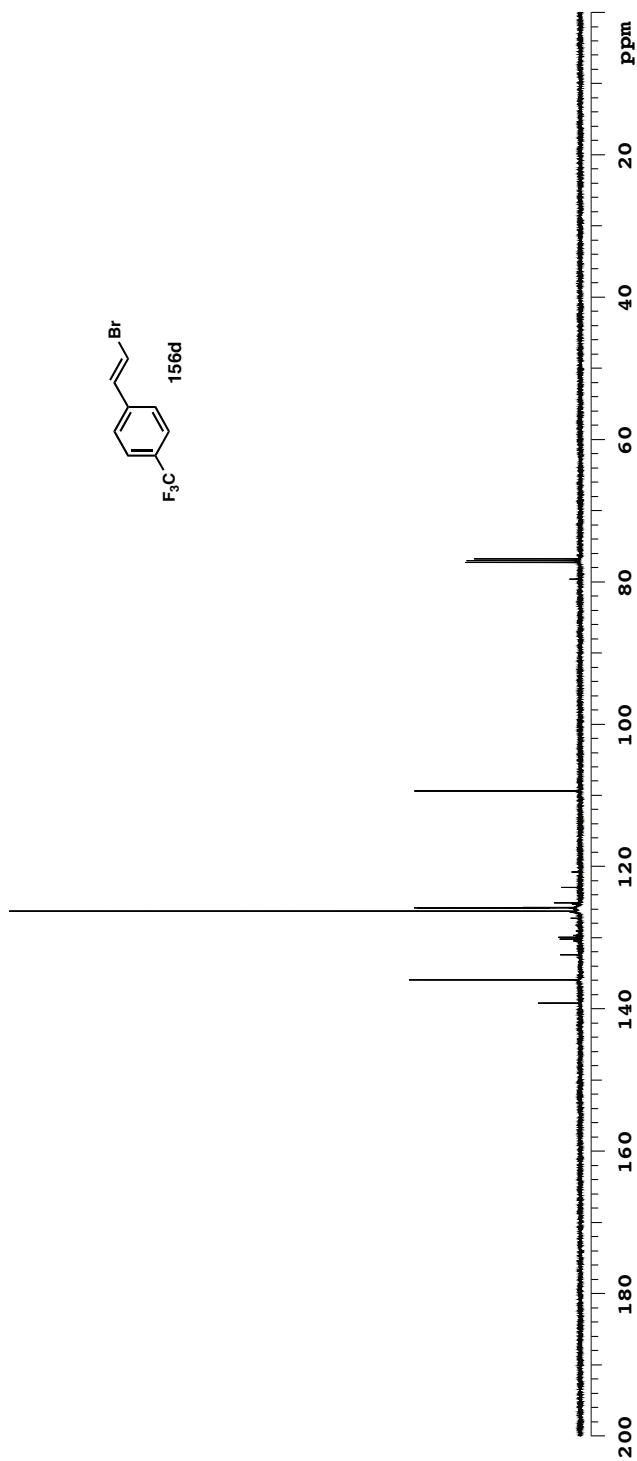
ahc-7-259-2  
 Sample Name **ahc-7-259-2**  
 Date collected **2014-07-16**  
 Pulse sequence **PROTON**  
 Solvent **cdcl3**  
 Temperature Spectrometer **25 -vnmrs-400**  
 Study owner **acherney**  
 Operator **autouser**



Data file /ndj/acherney/vnmrsys\data/ahc-7-259-2/PROTON01.fid

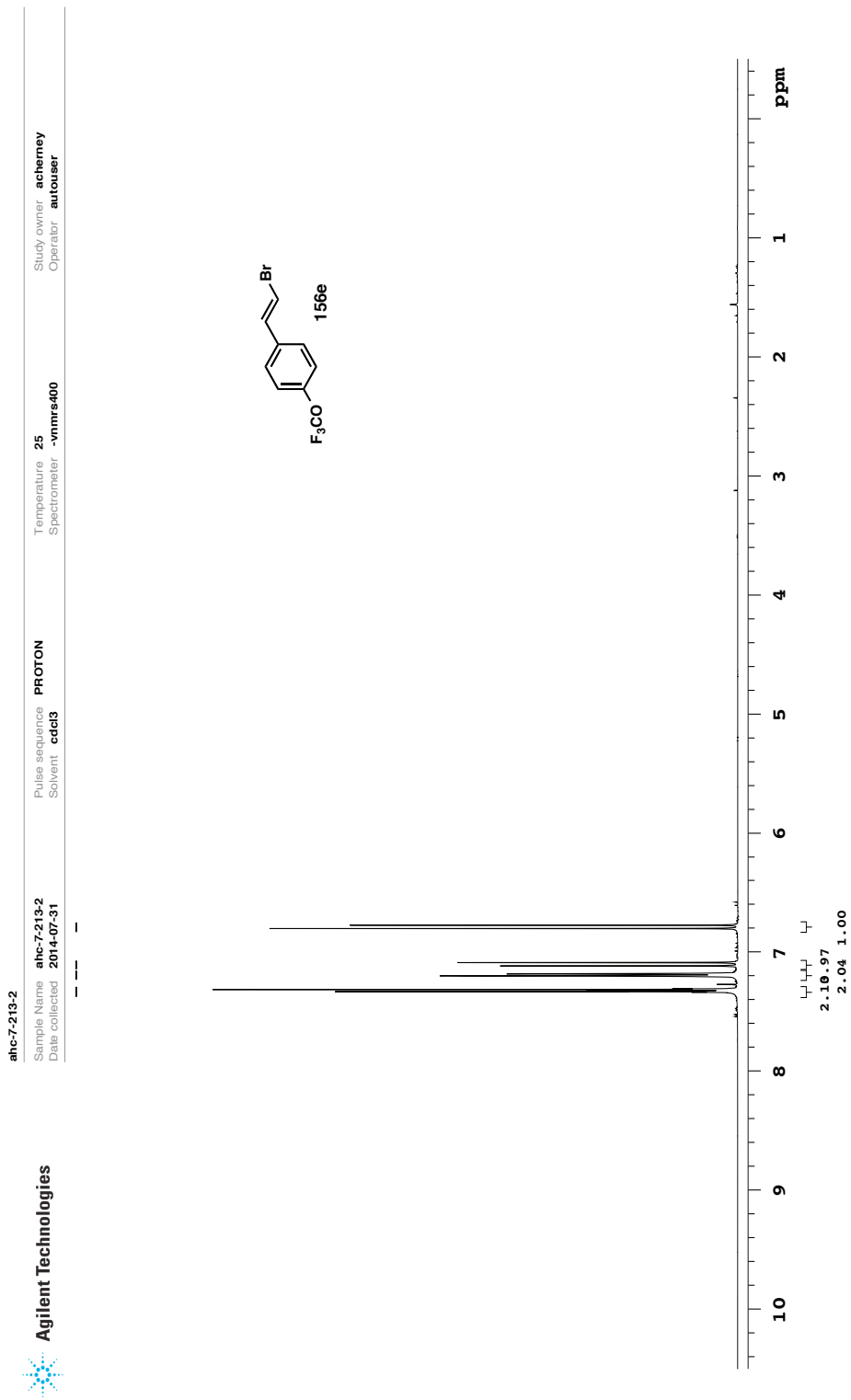
Plot date 2014-07-30

**ahc-7-259-2**  
 Sample Name **ahc-7-259-2**  
 Date collected **2014-07-16**  
 Pulse sequence **CARBON**  
 Solvent **cdcl3**  
 Temperature Spectrometer **25 -vnmrs-400**  
 Study owner **acherney**  
 Operator **autouser**



Data file `/ndj/acherney/vnmrs/data/ahc-7-259-2/CARBON01.fid`

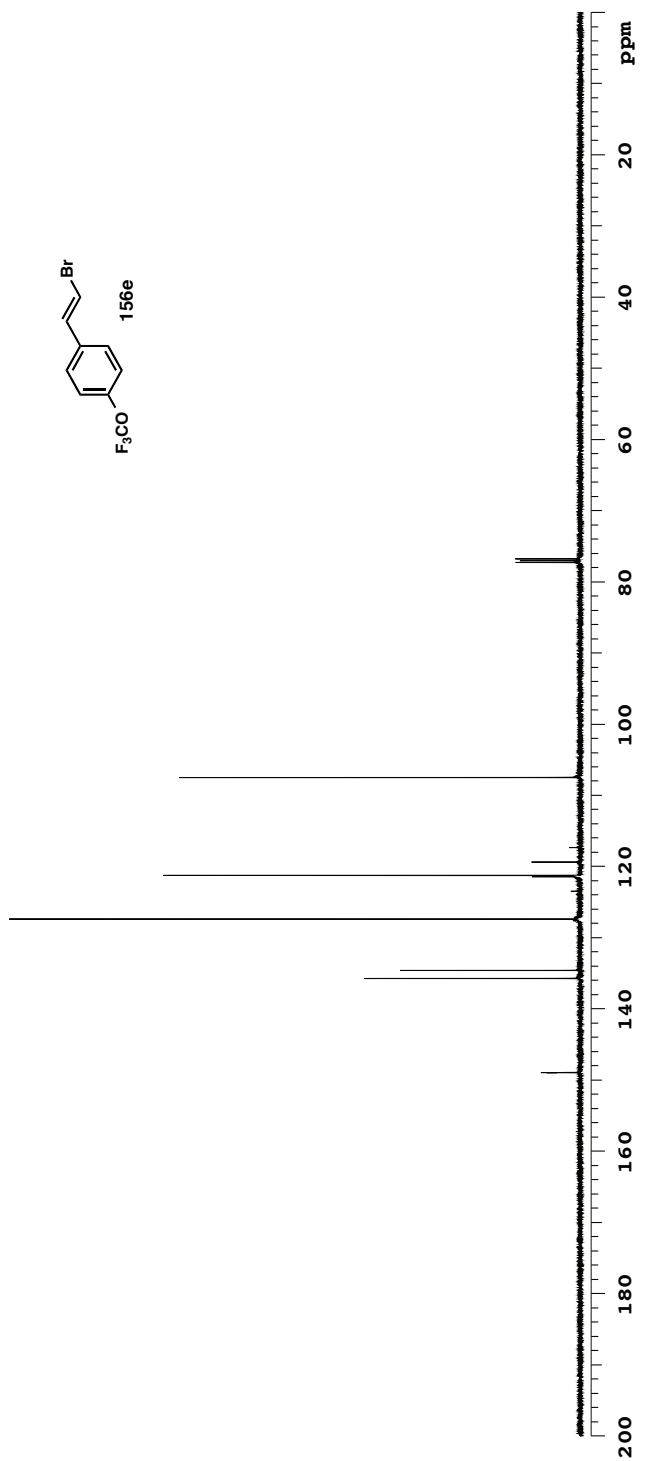
Plot date 2014-07-30



Plot date 2014-08-01

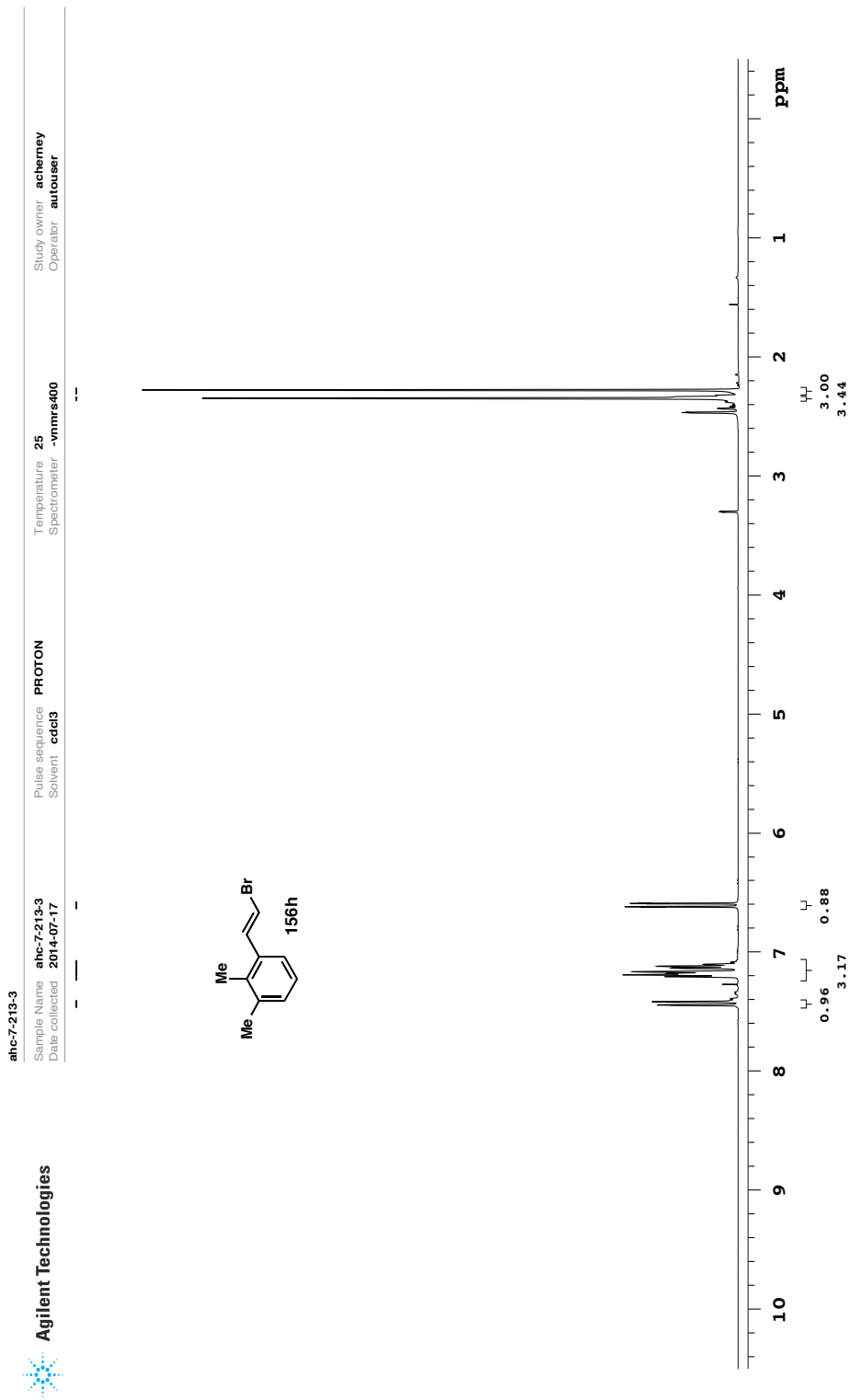
Data file /ndy/acherney/vnmrs/data/ahc-7-213-2/PROTON01.fid

**ahc-7-213-2**  
 Sample Name **ahc-7-213-2**  
 Date collected **2014-07-31**  
 Pulse sequence **CARBON**  
 Solvent **cdcl3**  
 Temperature Spectrometer **25 -vnmrs-400**  
 Study owner **acherney**  
 Operator **autouser**



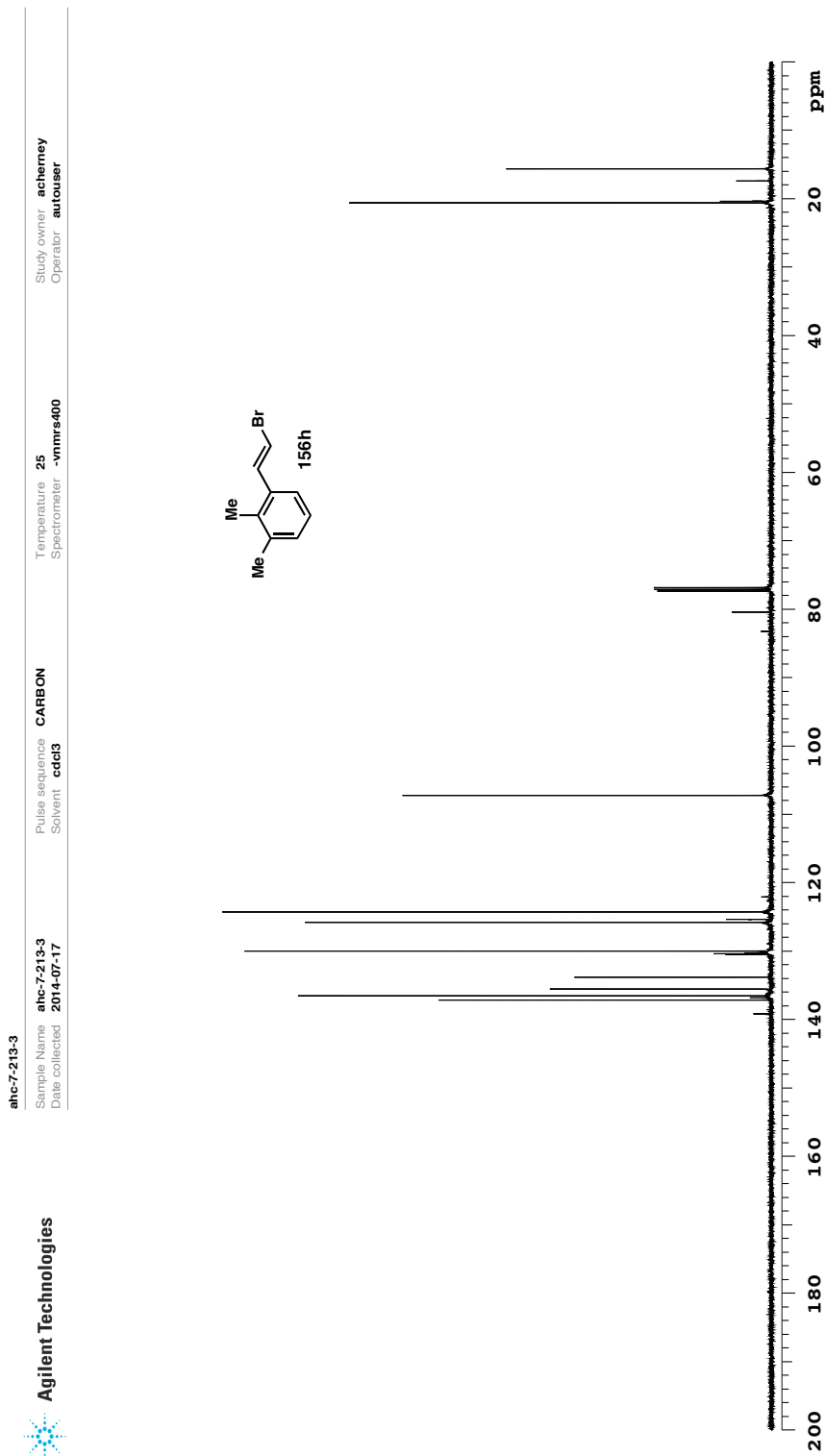
Data file /ndj/acherney/vnmrs/data/ahc-7-213-2/CARBON01.fid

Plot date 2014-08-01



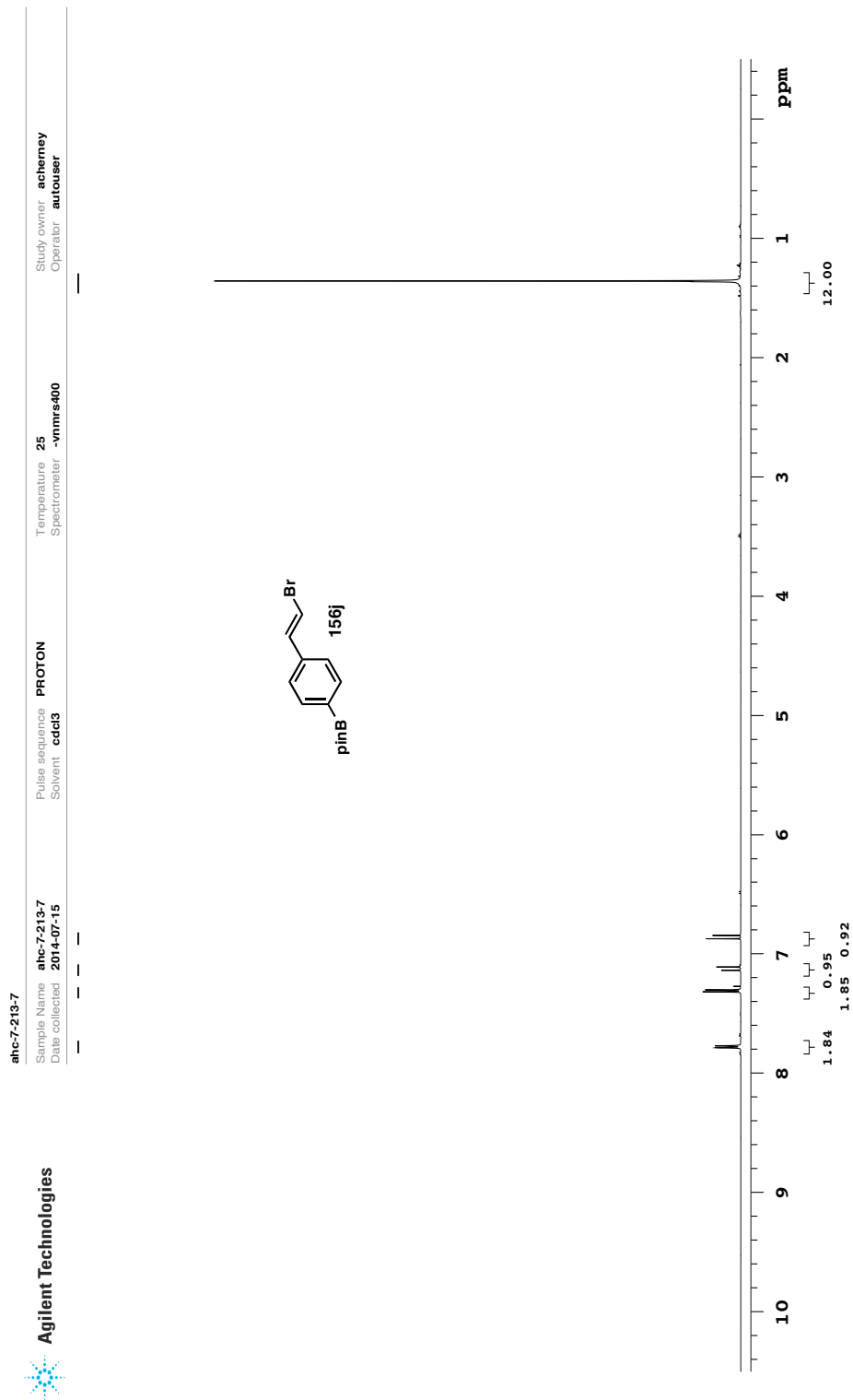
Plot date 2014-07-30

Data file /ndj/acherney/vnmrs/data/ahc-7-213-3/PROTON01.fid



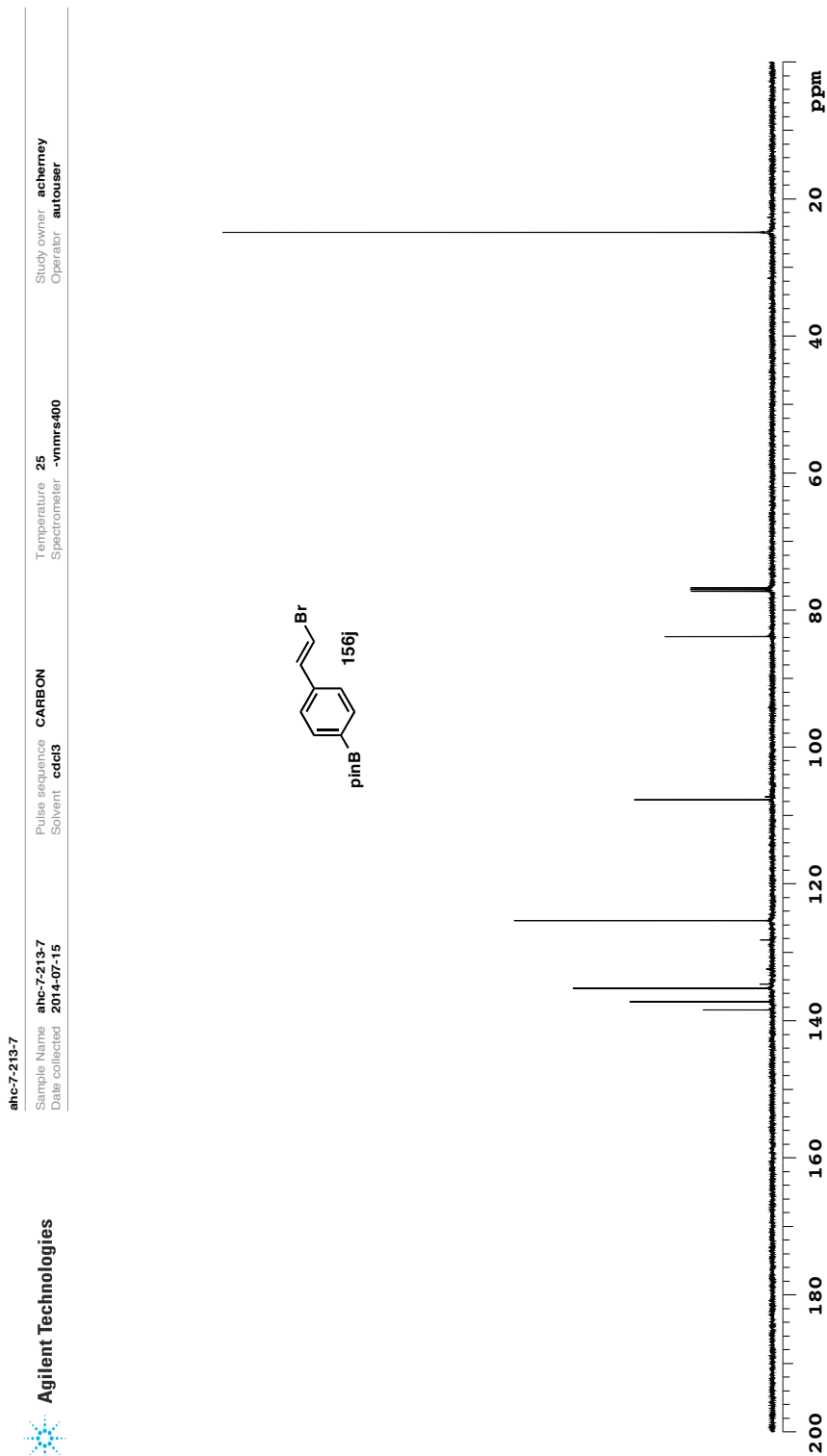
Data file //msj/acherney/vnmrs/data/ahc-7-213-3/CARBON01.fid

Plot date 2014-07-30



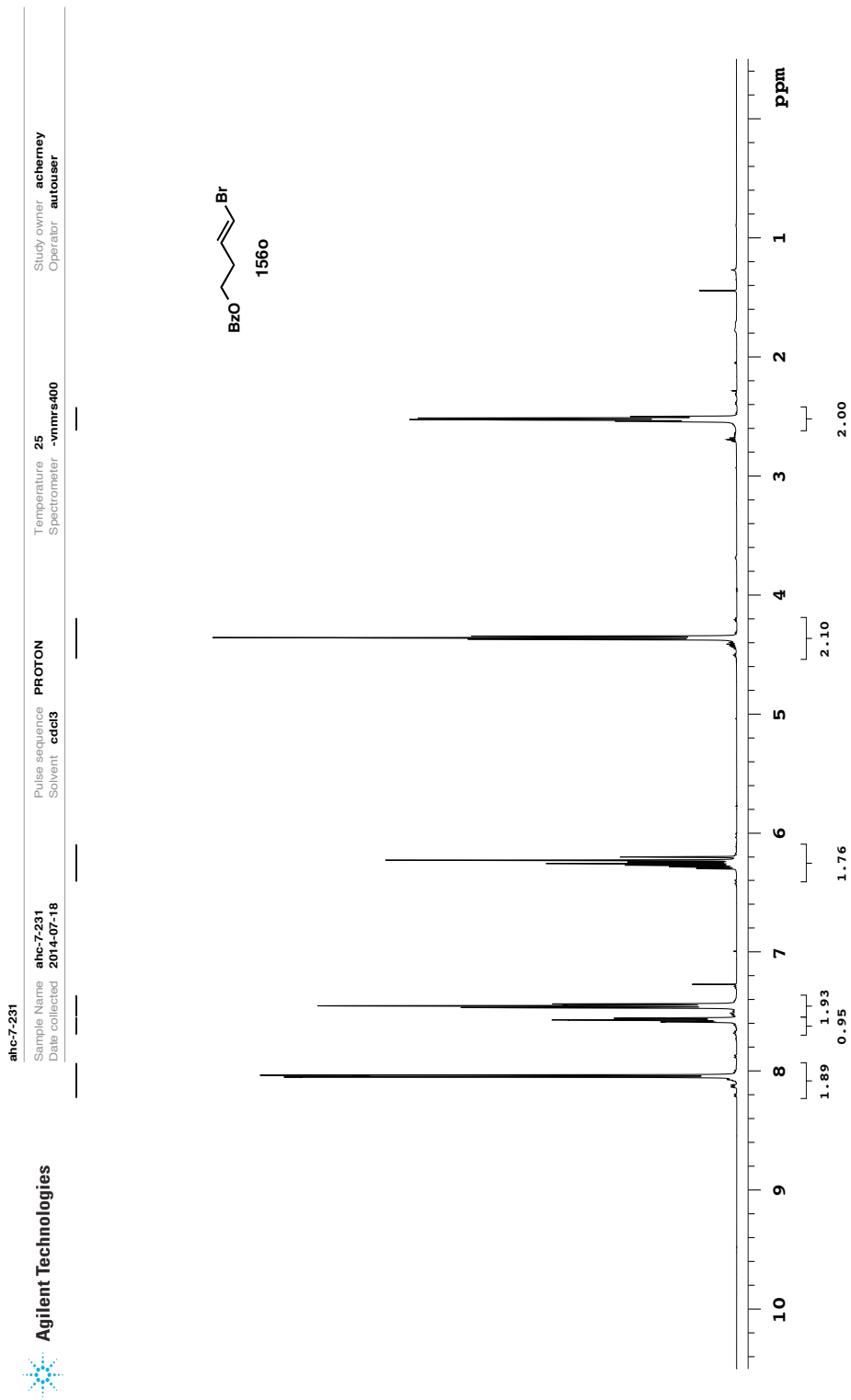
Data file //ndj/acherney/vnmr/ysdata/ahc-7-213-7/PROTON01.fid

Plot date 2014-07-30



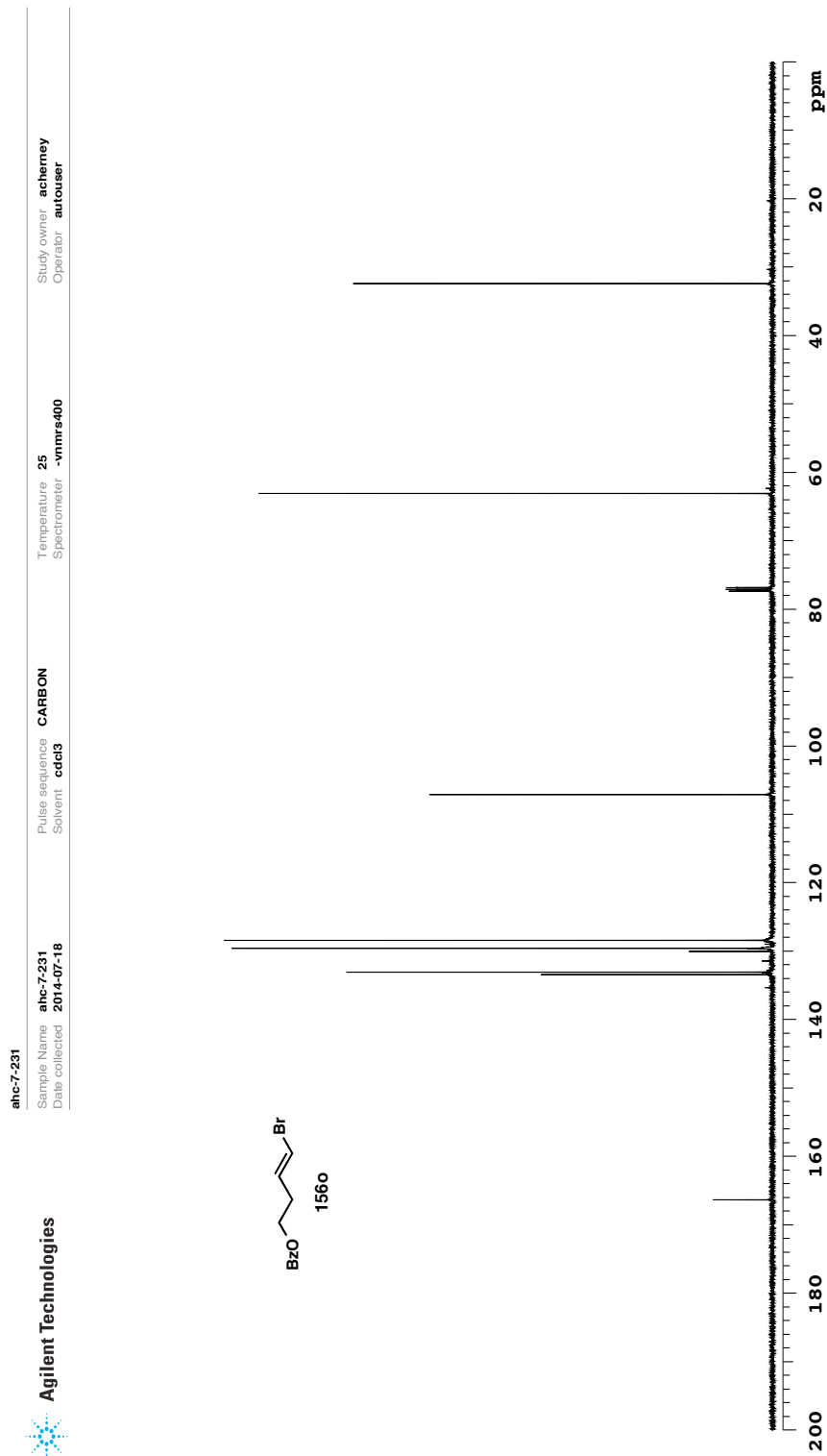
Data file /ndy/acherney/vnmrsys\data/ahc-7-213-7/CARBON01.fid

Plot date 2014-07-30



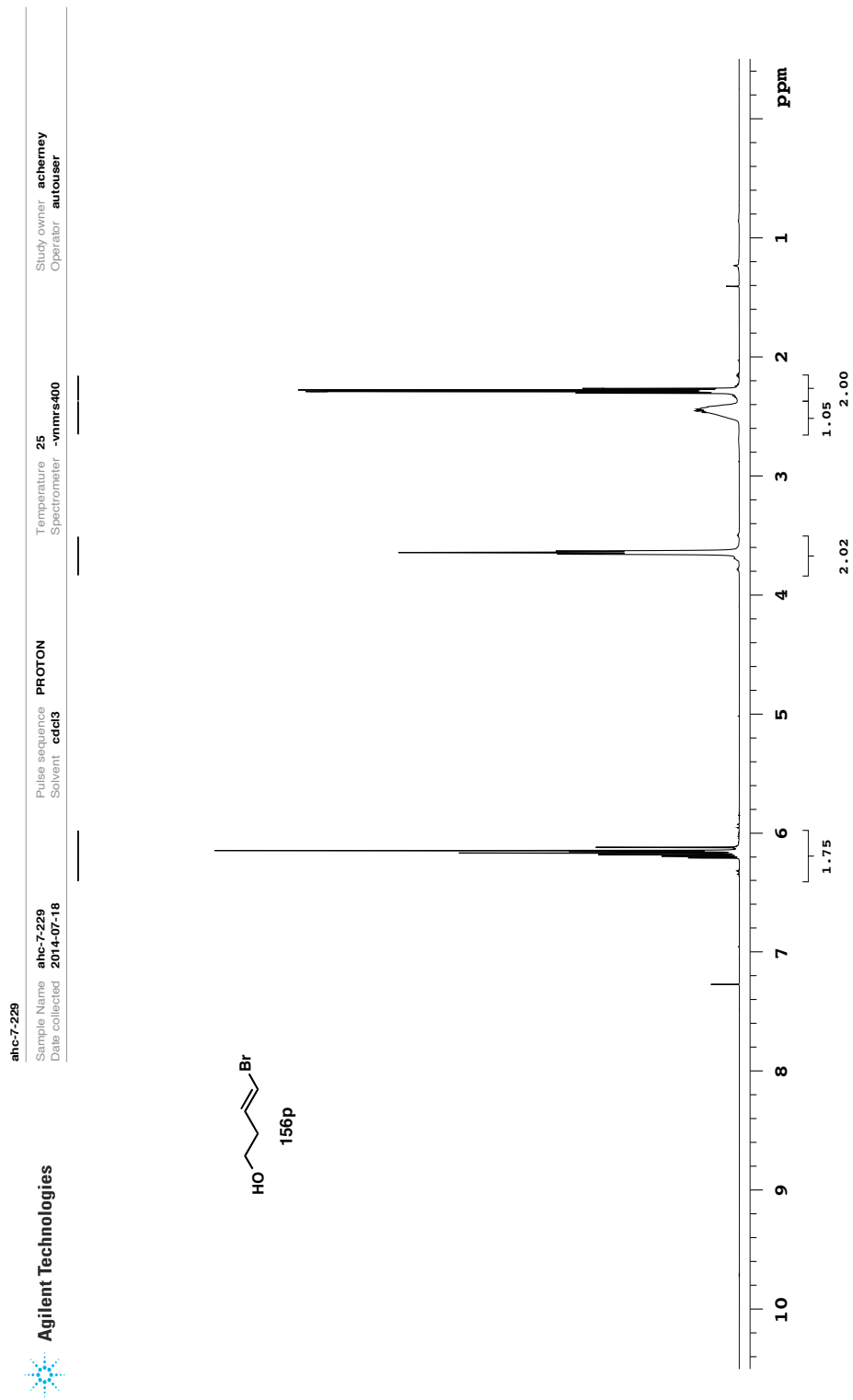
Data file /ndj/acherney/vnmrsysdata/ahc-7-231/PROTON01.fid

Plot date 2014-07-30



Data file /ndj/acherney/vnmr/sys/data/ahc-7-231/CARBON01.fid

Plot date 2014-07-30

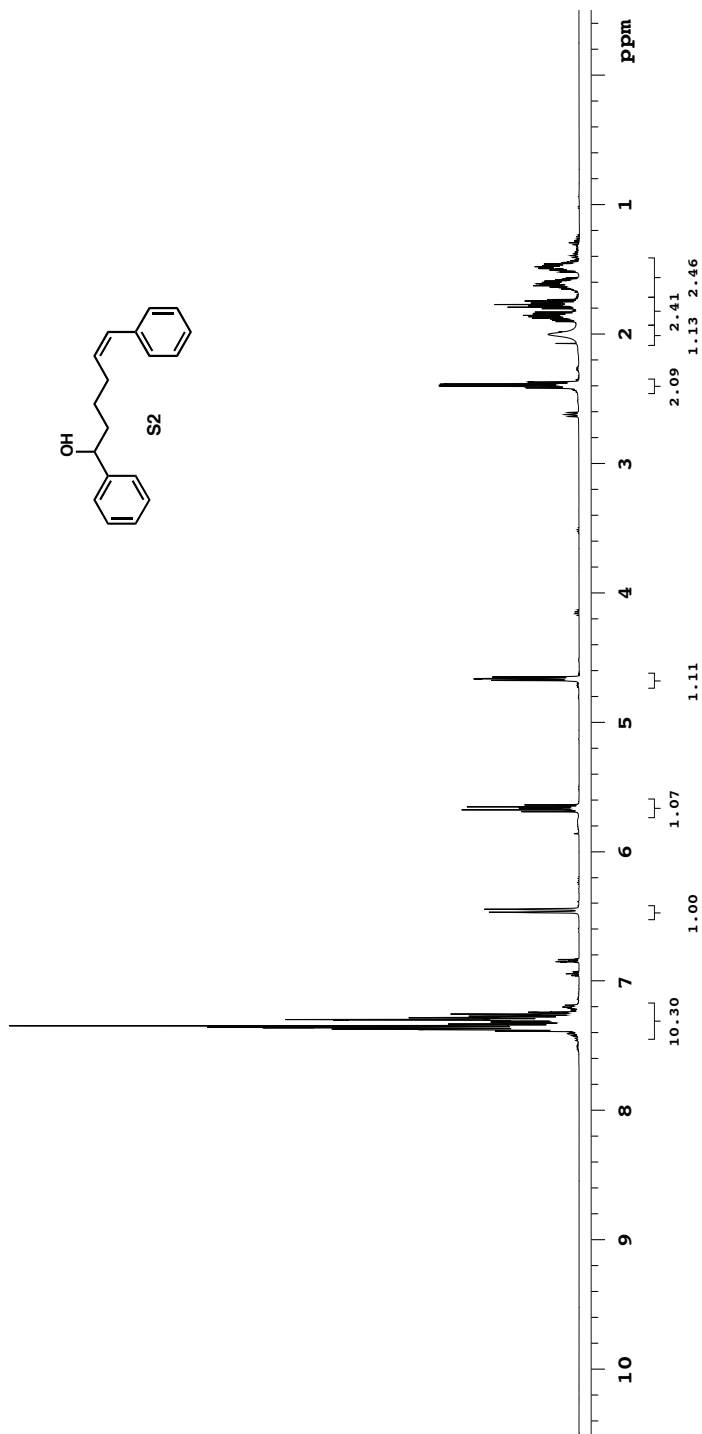


Data file /ndj/acherney/vnmrsys\data/ahc-7-229/PROTON01.fid

Plot date 2014-07-30



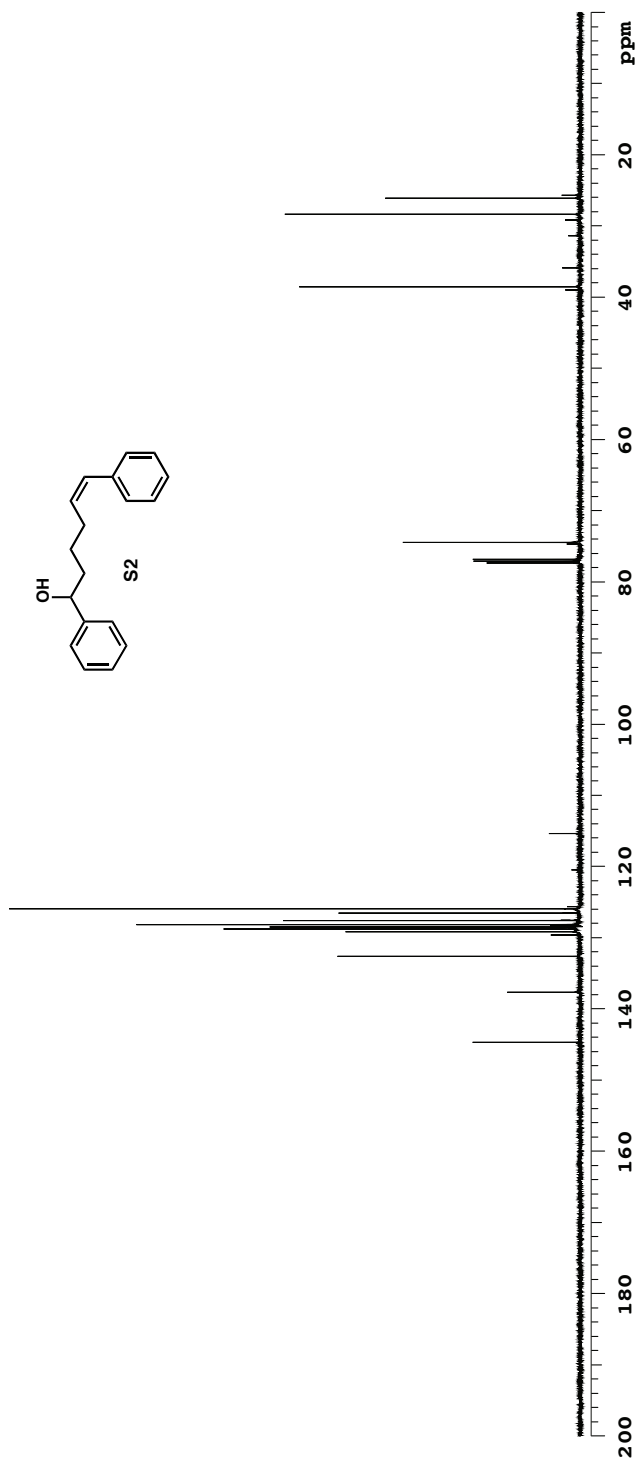
**ahc-7-207**  
 Sample Name **ahc-7-207**  
 Date collected **2014-07-31**  
 Pulse sequence **PROTON**  
 Solvent **cdcl3**  
 Temperature Spectrometer **25 -vnmrs-400**  
 Study owner **acherney**  
 Operator **autouser**



Data file /ndy/acherney/vnmrsysdata/ahc-7-207/PROTON01.fid

Plot date 2014-08-01

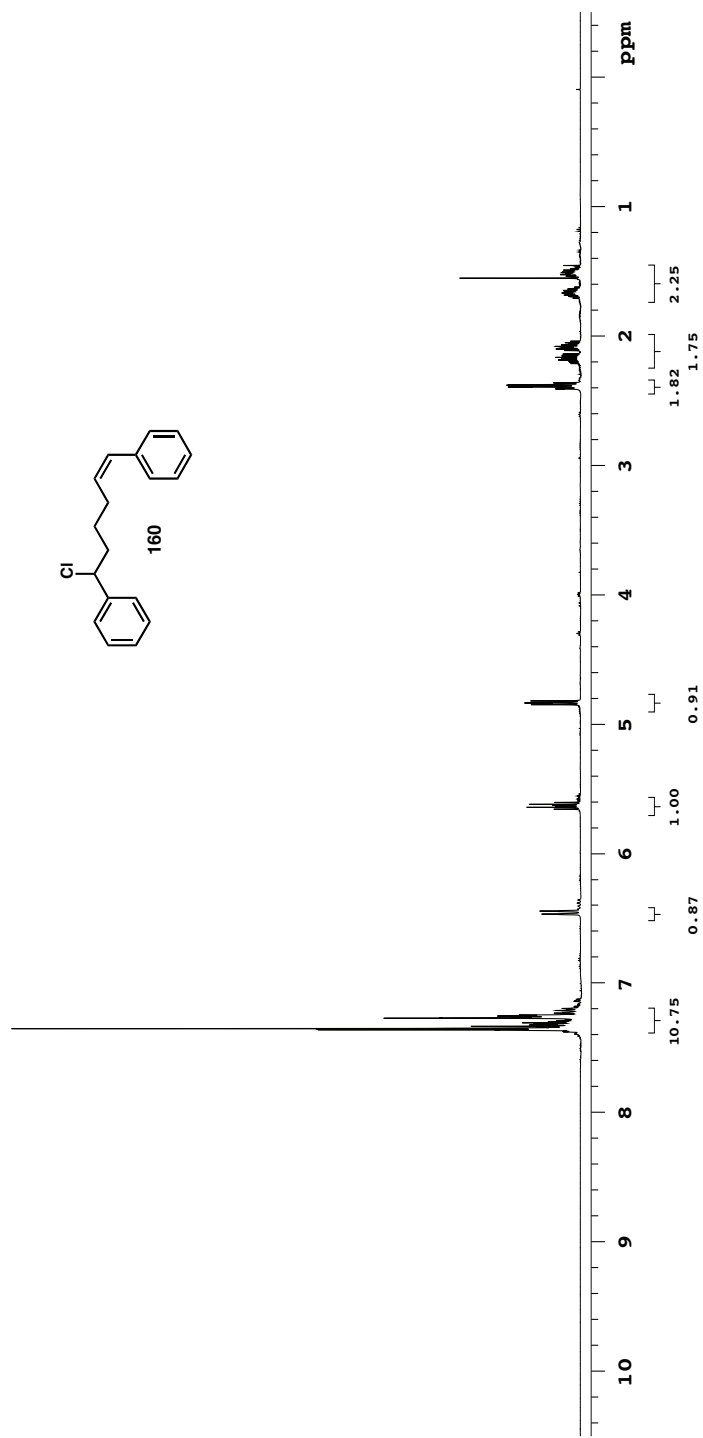
**ahc-7-207**  
 Sample Name **ahc-7-207**  
 Date collected **2014-07-31**  
 Pulse sequence **CARBON**  
 Solvent **cdcl3**  
 Temperature **25**  
 Spectrometer **-vnmrs-400**  
 Study owner **acherney**  
 Operator **autouser**



Data file /ndj/acherney/vnmr/sys/data/ahc-7-207/CARBON01.fid

Plot date 2014-08-01

**ahc-7-211**  
 Sample Name **ahc-7-211**  
 Date collected **2014-07-31**  
 Pulse sequence **PROTON**  
 Solvent **cdcl3**  
 Temperature Spectrometer **25 -vnmrs-400**  
 Study owner **acherney**  
 Operator **autouser**

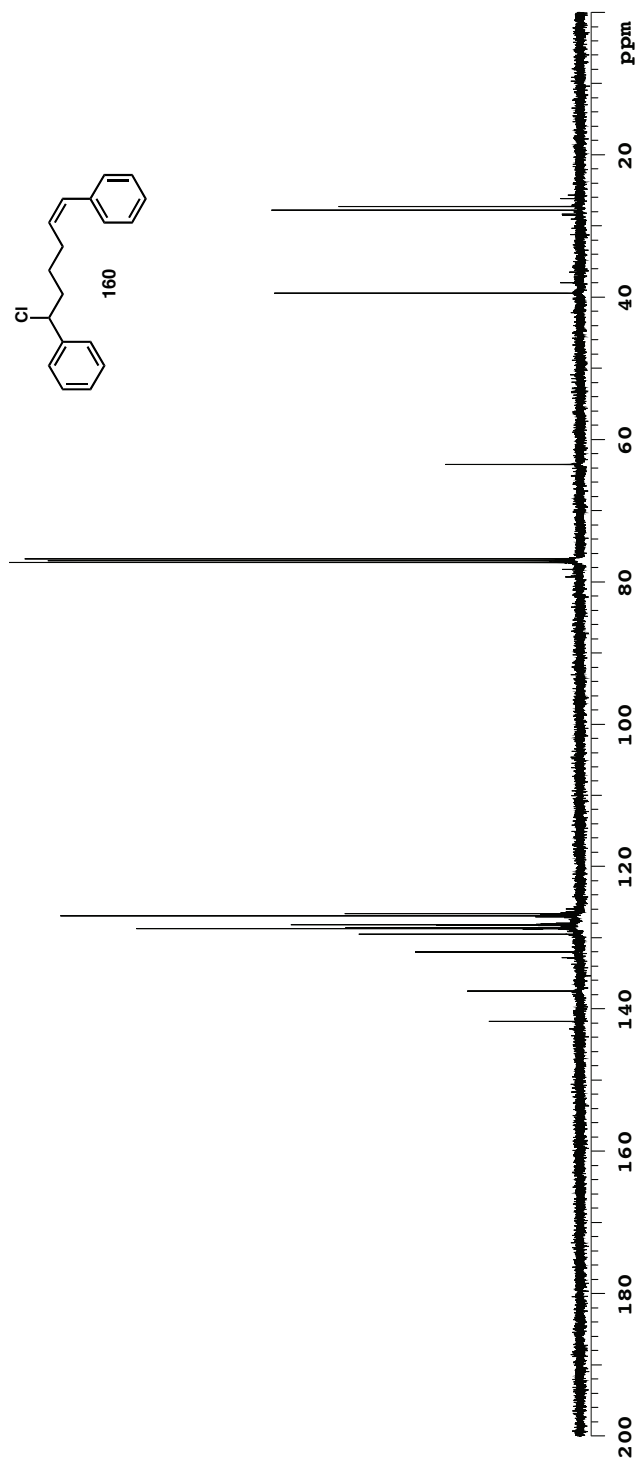
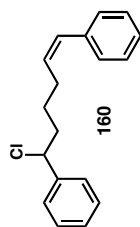


Data file /ndy/acherney/vnmrsysdata/ahc-7-211/PROTON01.fid

Plot date 2014-08-01

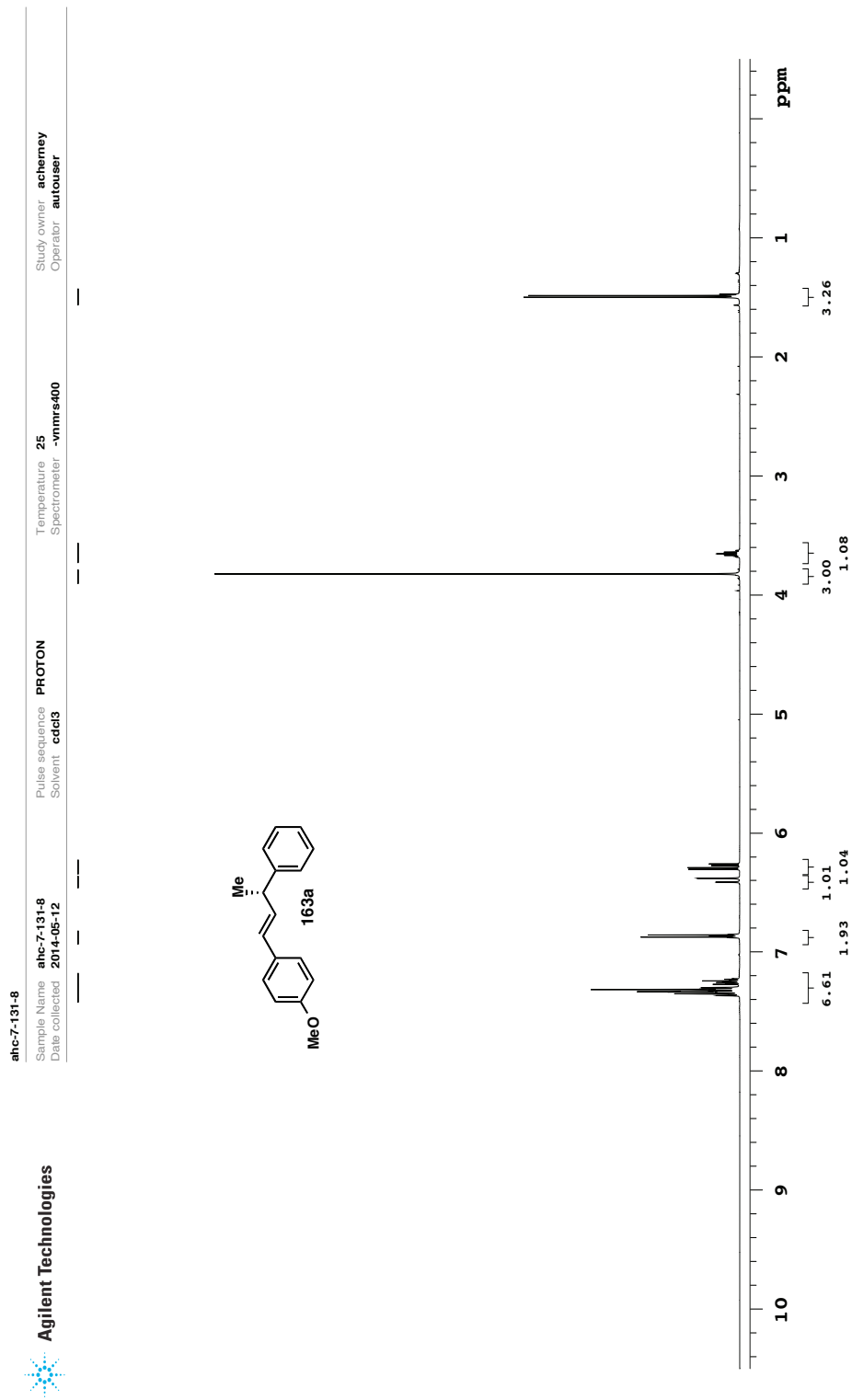


**ahc-7-211**  
 Sample Name **ahc-7-211**  
 Date collected **2014-07-31**  
 Pulse sequence **CARBON**  
 Solvent **cdcl3**  
 Temperature Spectrometer **25 -vnmrs-400**  
 Study owner **acherney**  
 Operator **autouser**



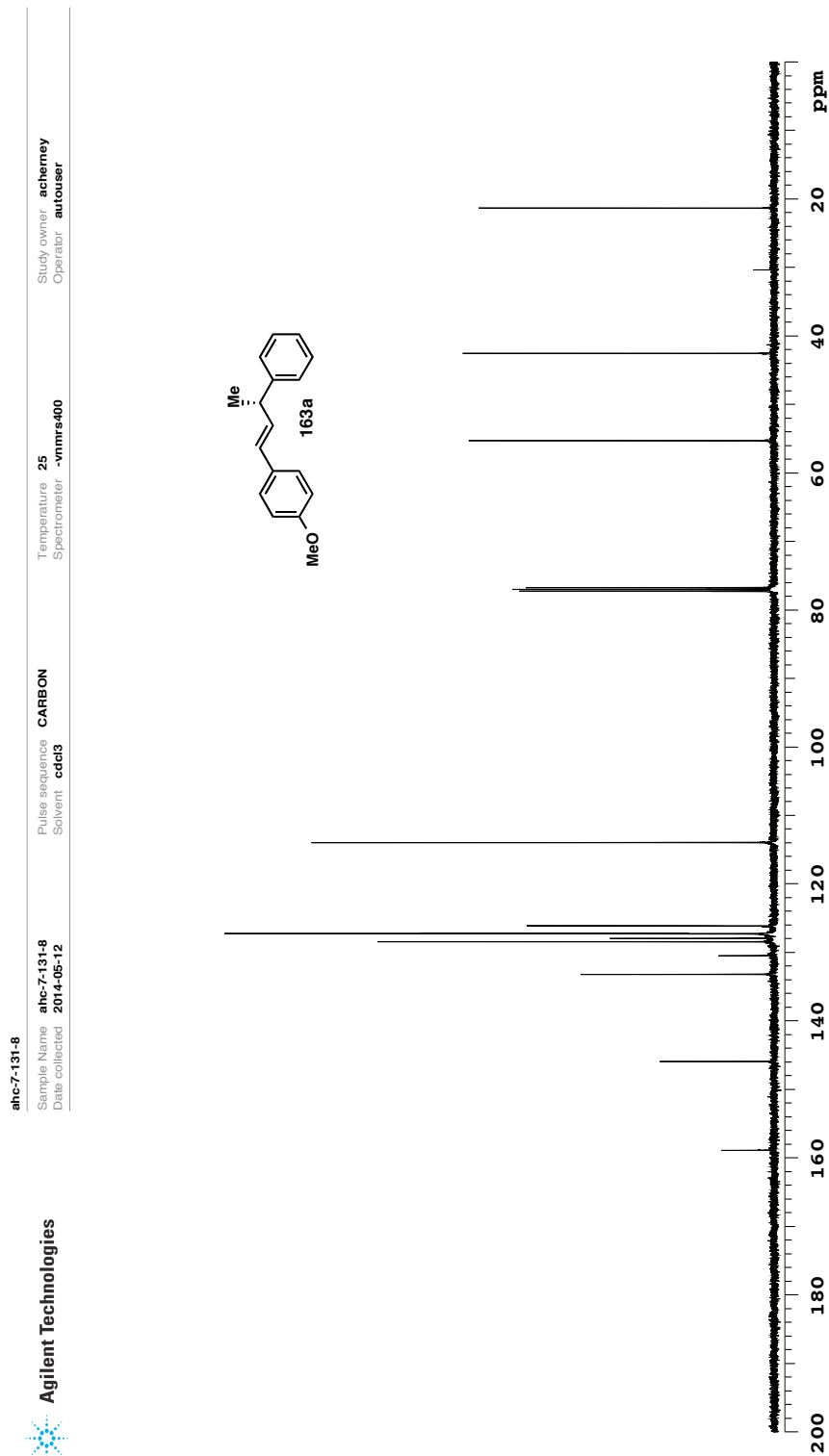
Data file /msd/acherney/vnmrsysdata/ahc-7-211/CARBON01.fid

Plot date 2014-08-01



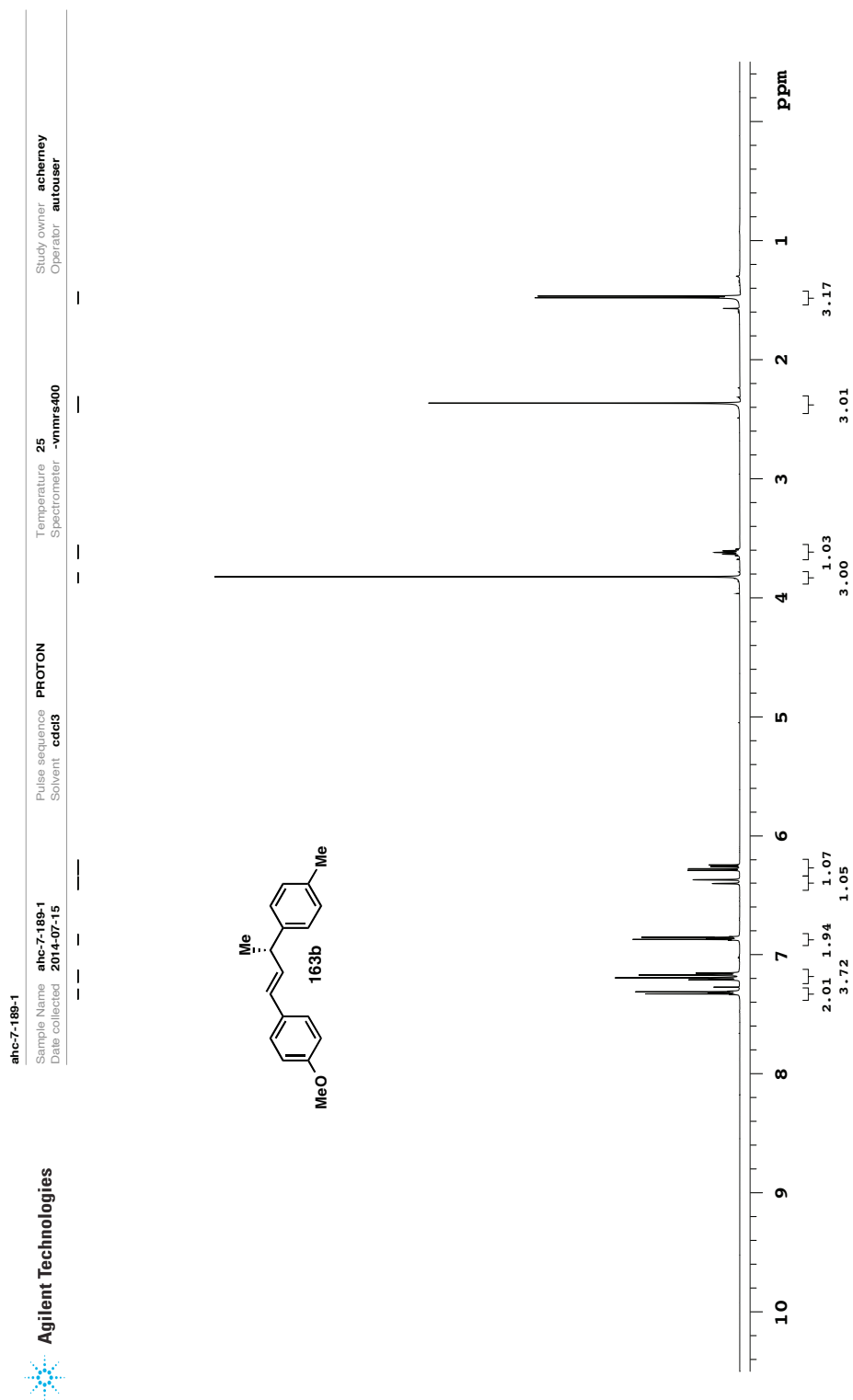
Data file /ndj/acherney/vnmrs/data/ahc-7-131-8/PROTON01.fid

Plot date 2014-07-29



Data file /msd/acherney/vnmrs/data/ahc-7-131-8/CARBON01.fid

Plot date 2014-07-29



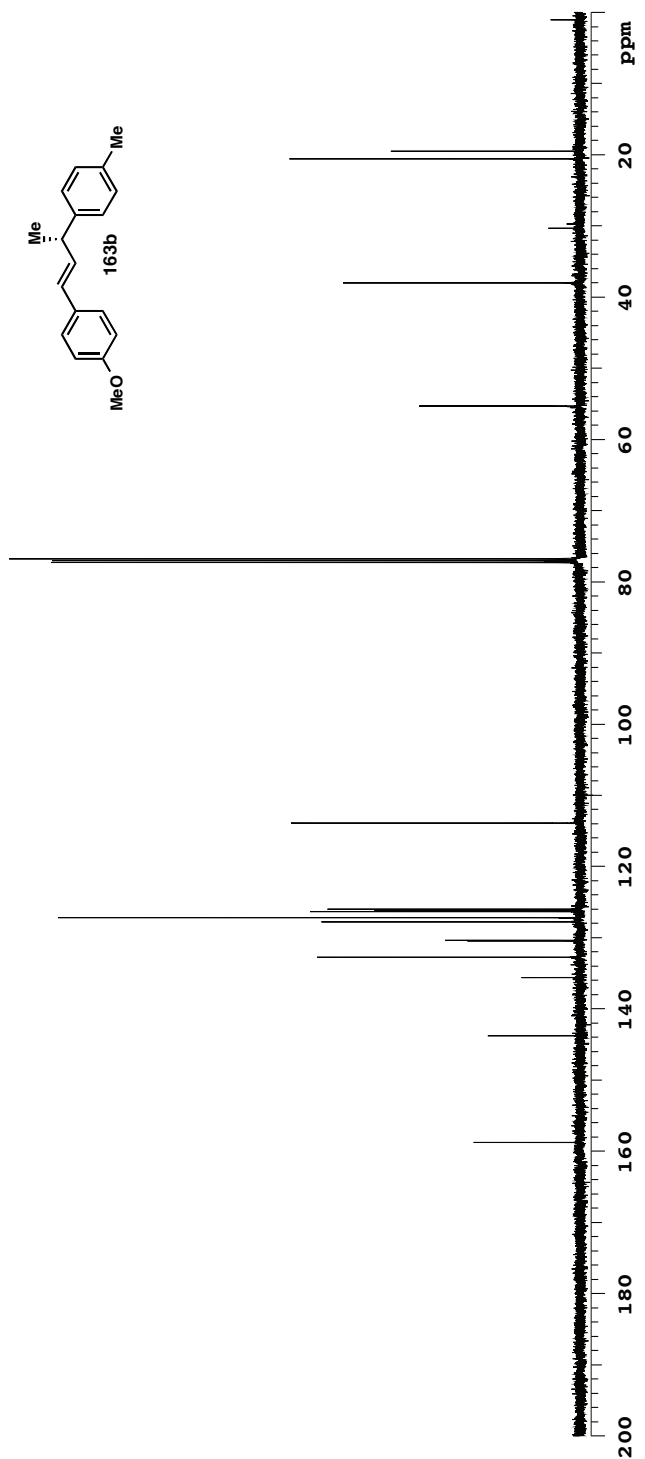
Data file //ndj/acherney/vnmrs/data/ahc-7-189-1/PROTON01.fid

Plot date 2014-07-29



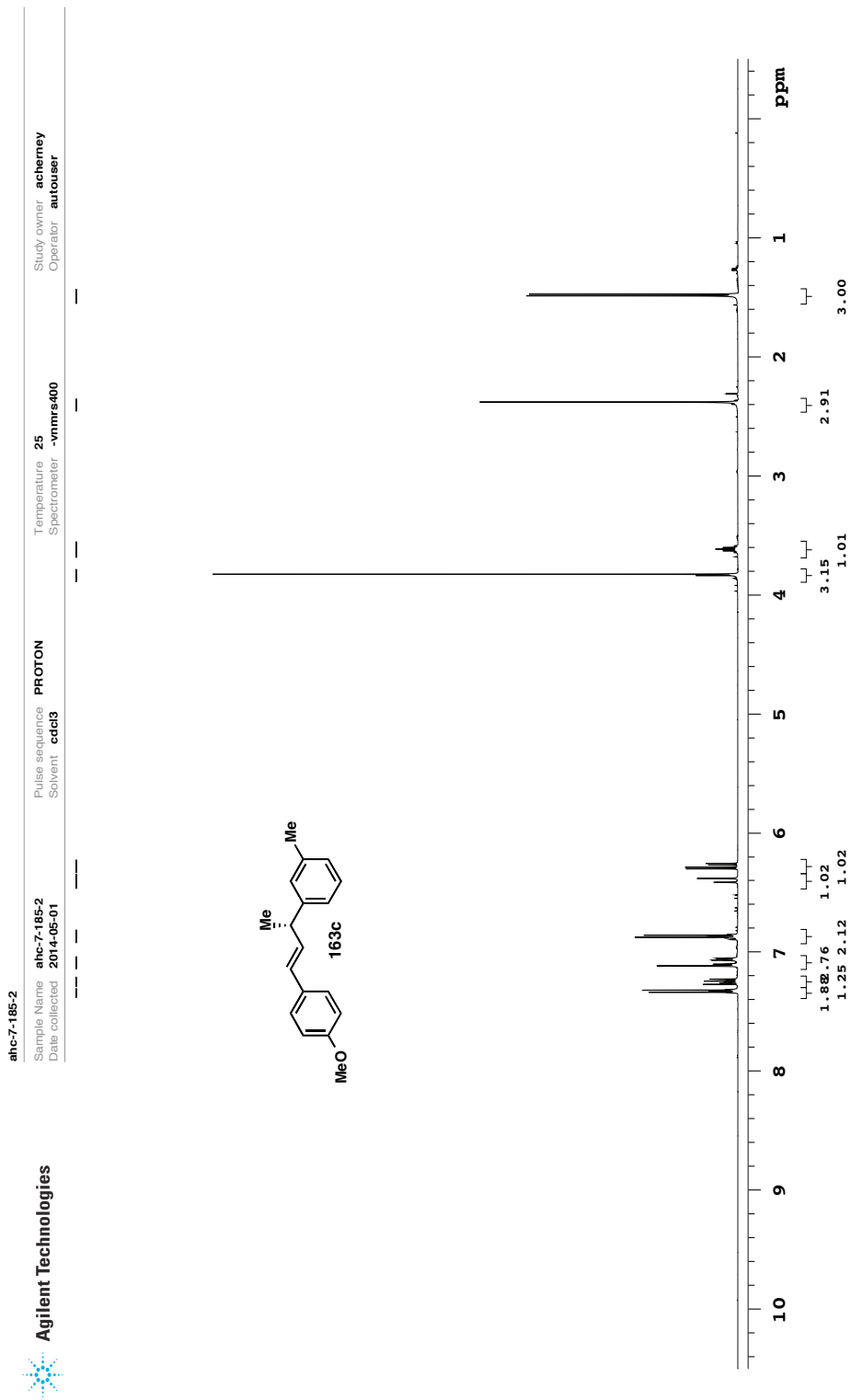
Agilent Technologies

**ahc-7-189-2**  
 Sample Name **ahc-7-189-2**  
 Date collected **2014-07-16**  
 Pulse sequence **CARBON**  
 Solvent **cdcl3**  
 Temperature Spectrometer **25 -vnmrs-400**  
 Study owner **acherney**  
 Operator **autouser**



Data file /msj/acherney/vnmrs/data/ahc-7-189-2/CARBON03.fid

Plot date 2014-07-29

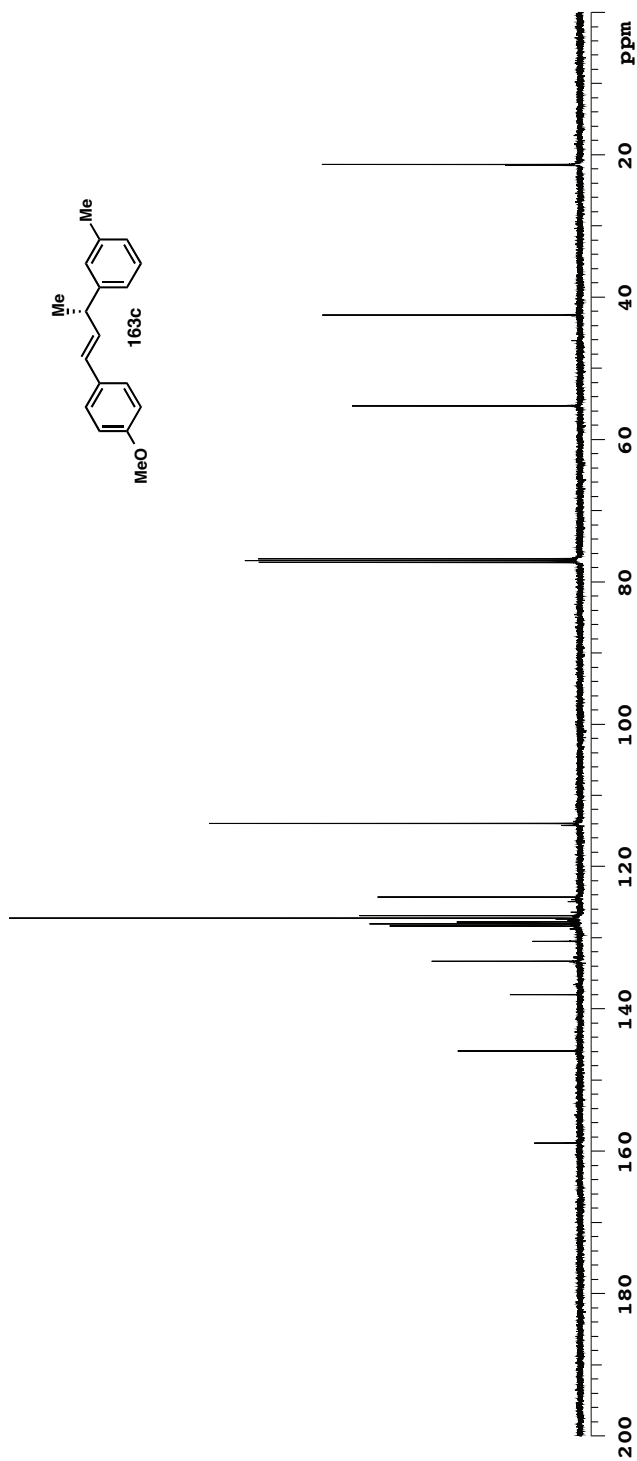


Data file /ndj/acherney/vnmrs/data/ahc-7-185-2/PROTON01.fid

Plot date 2014-07-29

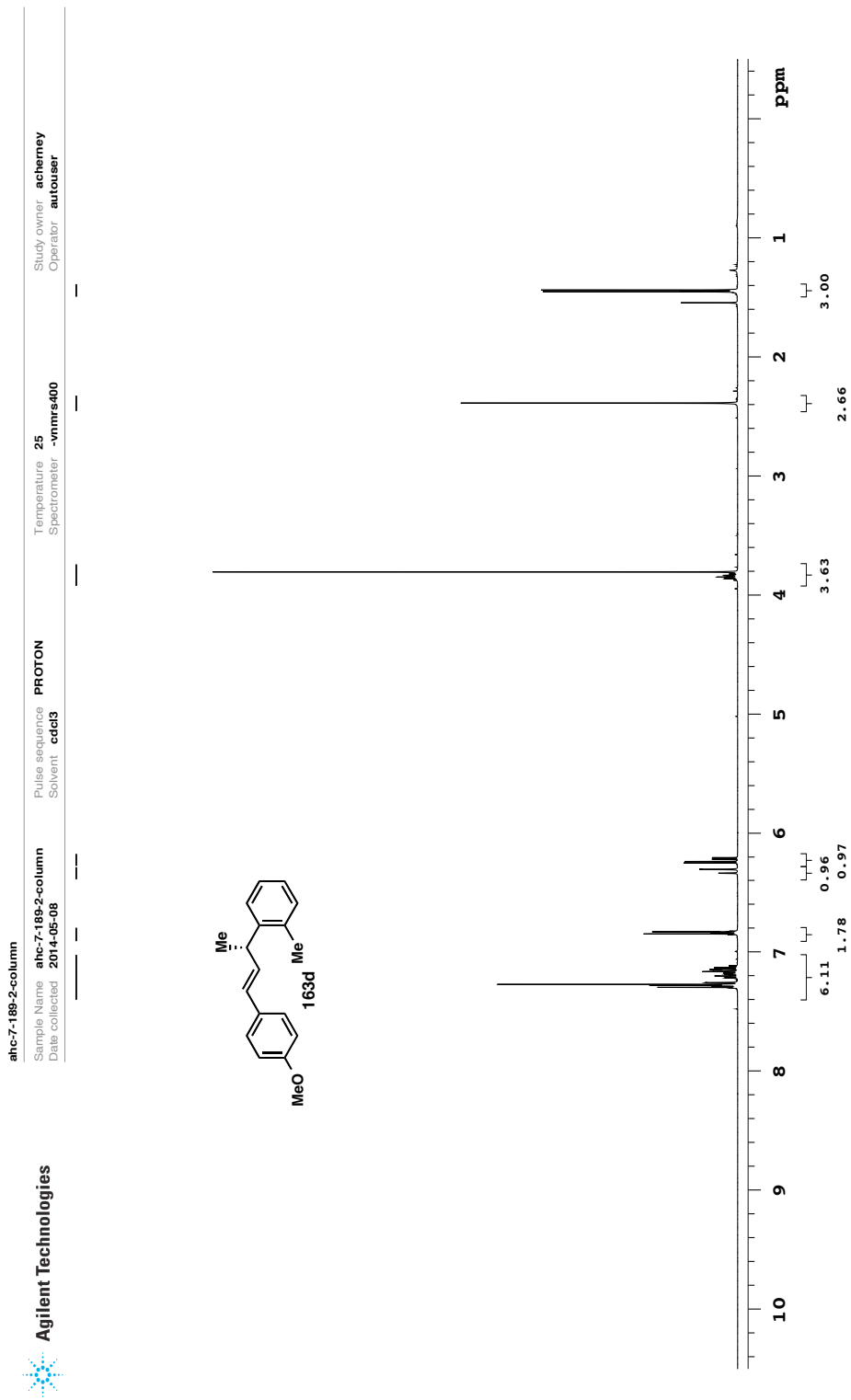


**ahc-7-185-2**  
 Sample Name **ahc-7-185-2**  
 Date collected **2014-05-01**  
 Pulse sequence **CARBON**  
 Solvent **cdcl3**  
 Temperature **25**  
 Spectrometer **-vnmrs-400**  
 Study owner **acherney**  
 Operator **autouser**



Data file /ndj/acherney/vnmrs/data/ahc-7-185-2/CARBON01.fid

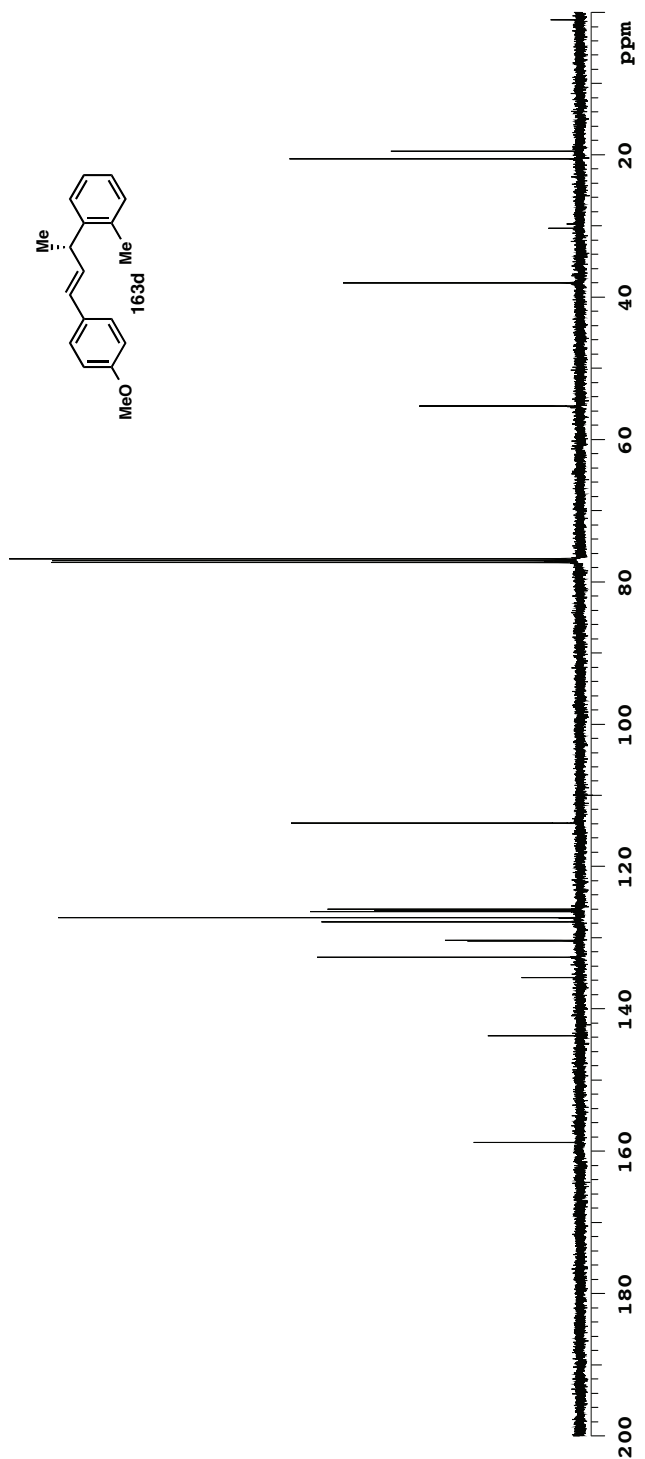
Plot date 2014-07-29



Plot date 2014-07-29

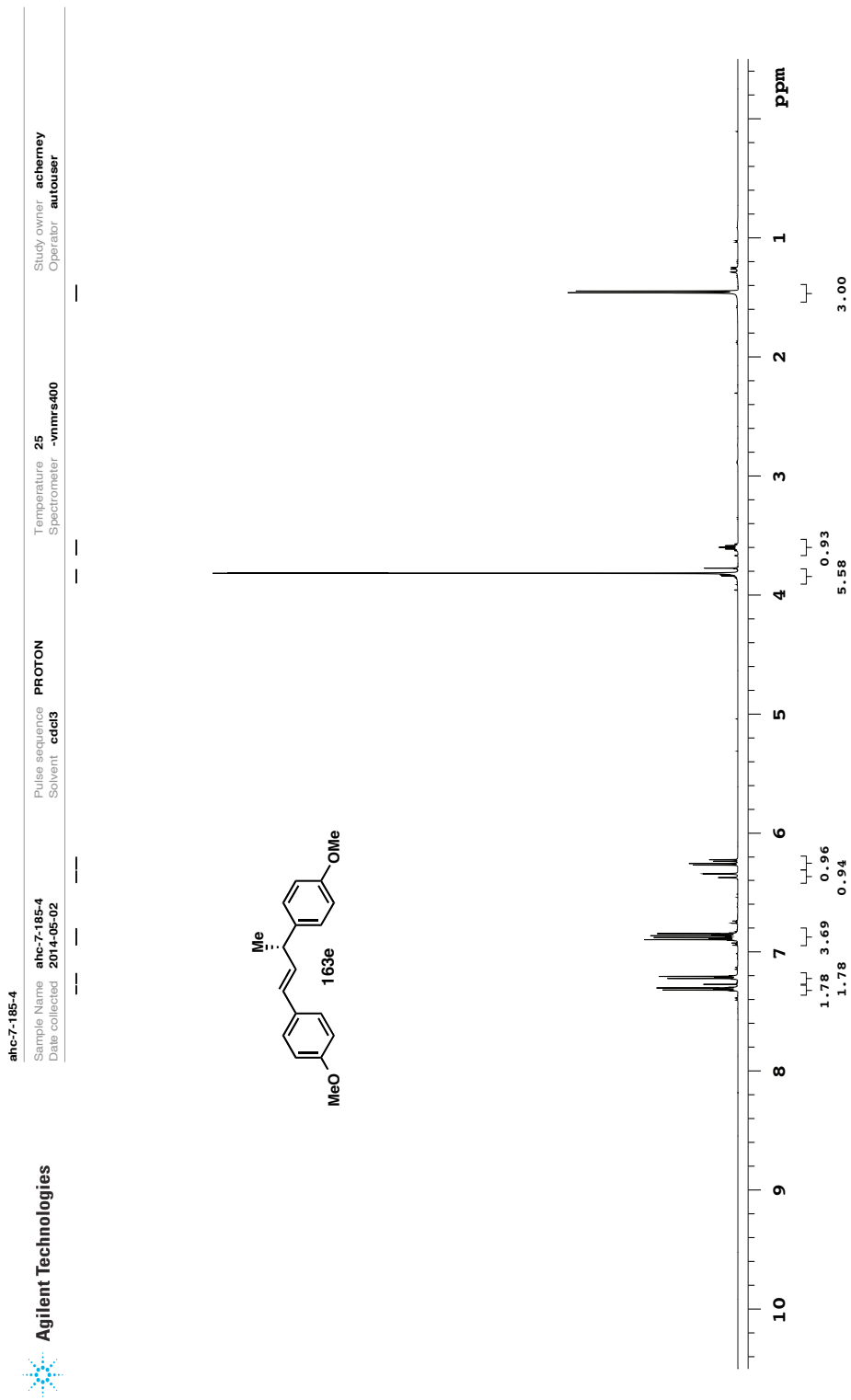
Data file /ndj/acherney/vnmrsys\data/ahc-7-189-2-column/PROTON01.fid

**ahc-7-189-2**  
 Sample Name **ahc-7-189-2**  
 Date collected **2014-07-16**  
 Pulse sequence **CARBON**  
 Solvent **cdcl3**  
 Temperature Spectrometer **25 -vnmrs-400**  
 Study owner **acherney**  
 Operator **autouser**



Plot date 2014-07-29

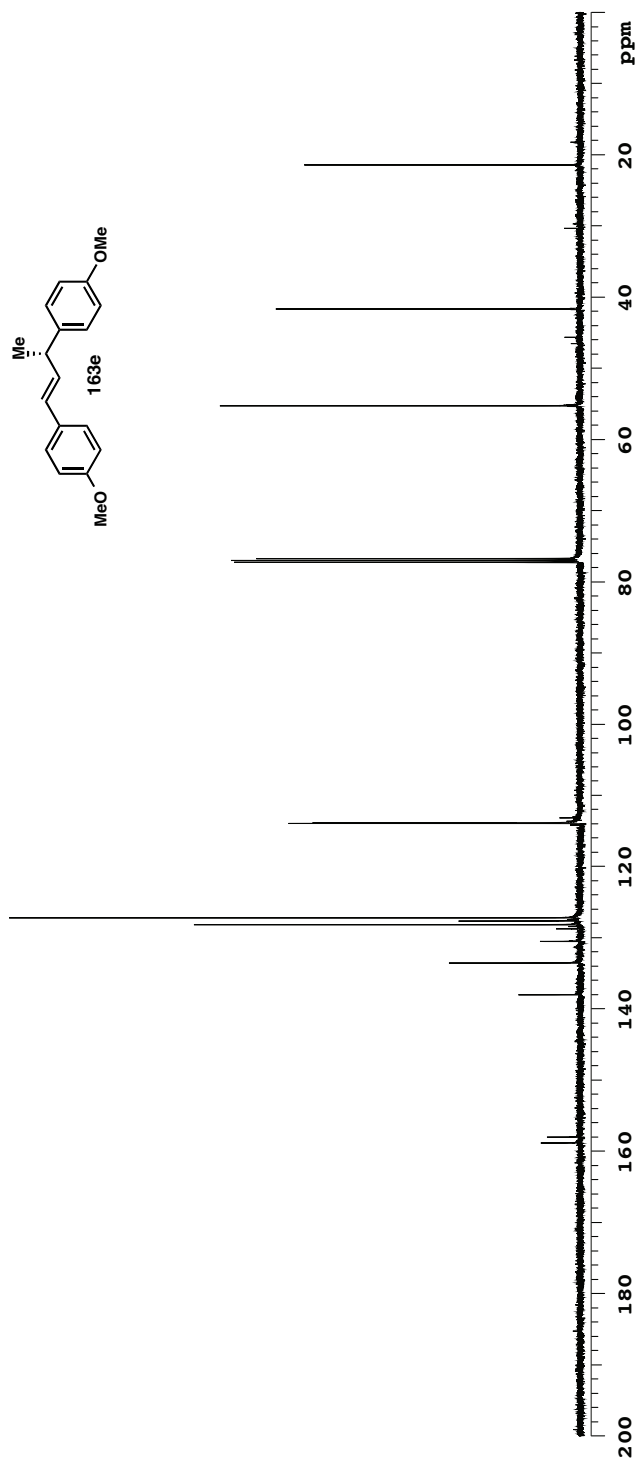
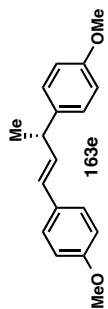
Data file /msj/acherney/vnmrs/data/ahc-7-189-2/CARBON03.fid



Data file //msj/acherney/vnmrs/data/ahc-7-185-4/PROTON01.fid

Plot date 2014-07-29

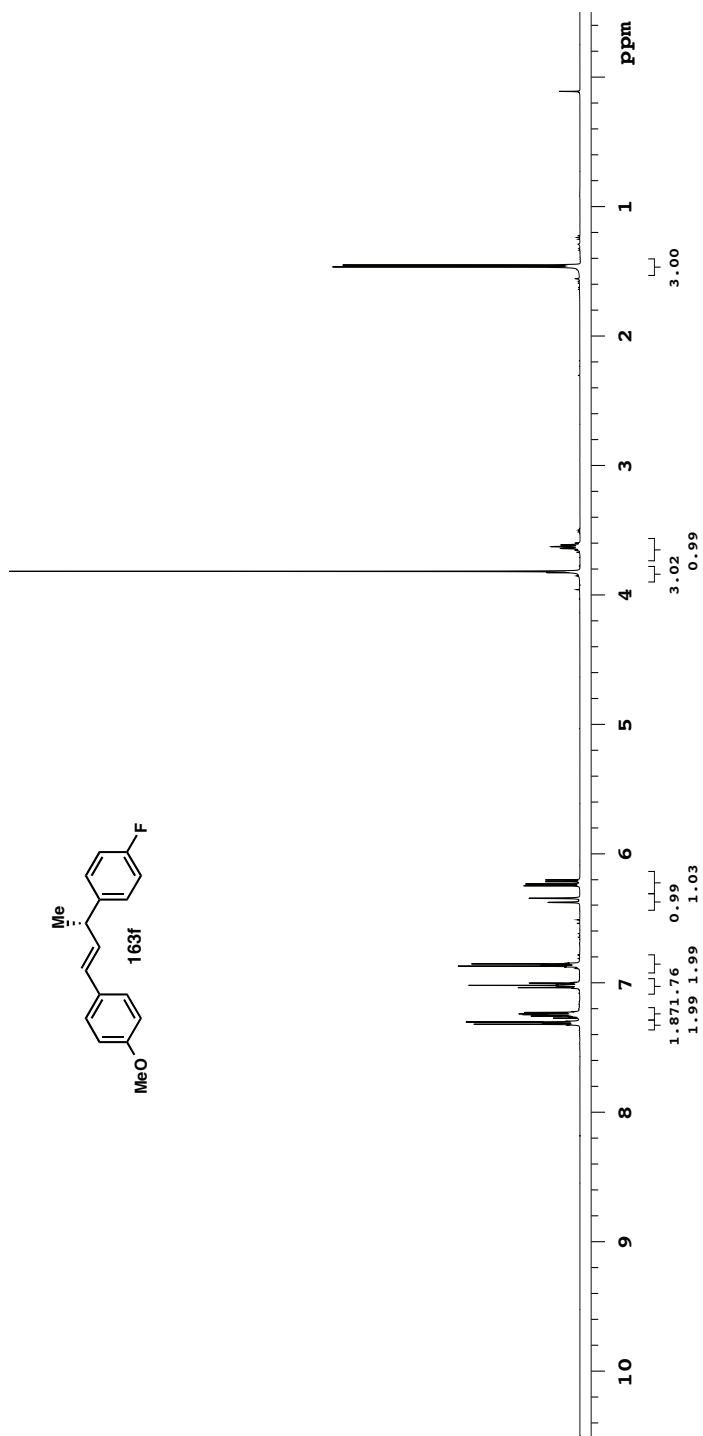
**ahc-7-185-4**  
 Sample Name **ahc-7-185-4**  
 Date collected **2014-05-02**  
 Pulse sequence **CARBON**  
 Solvent **cdcl3**  
 Temperature **25**  
 Spectrometer **-vnmrs-400**  
 Study owner **acherney**  
 Operator **autouser**



Data file /ndy/acherney/vnmrs/data/ahc-7-185-4/CARBON01.fid

Plot date 2014-07-29

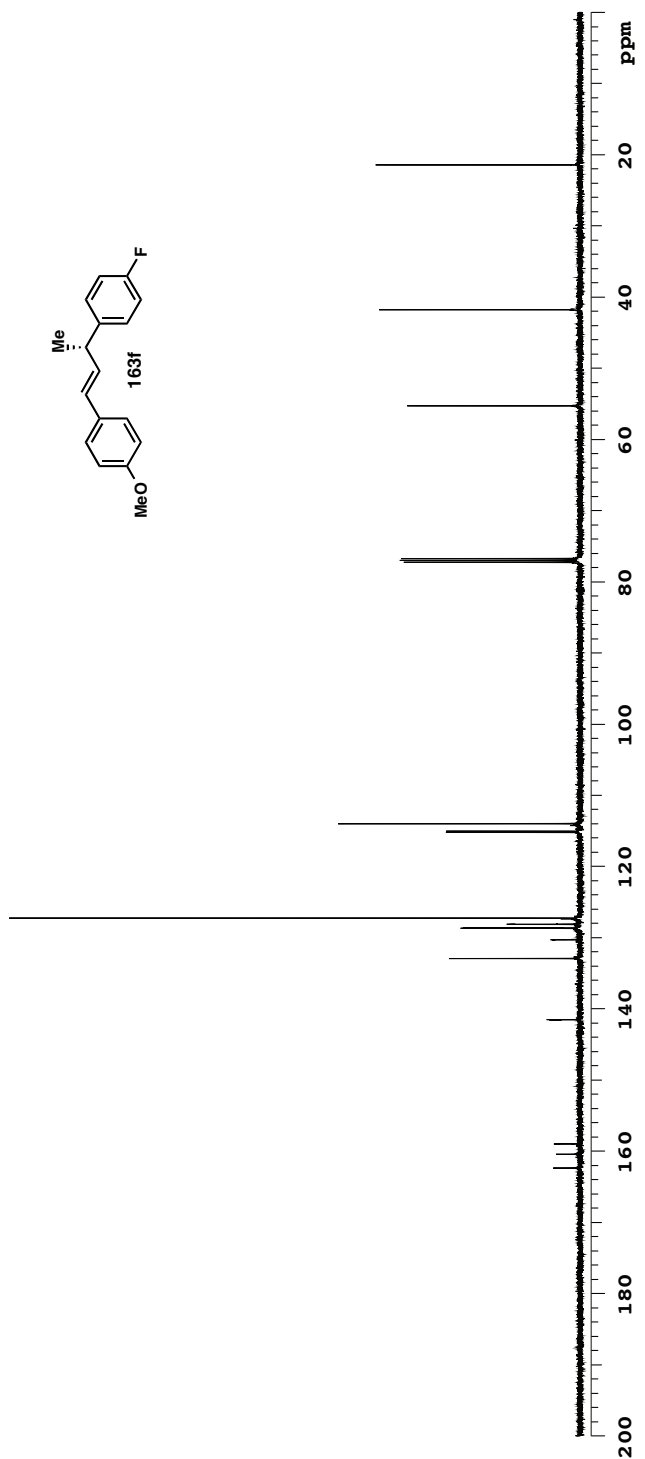
ahc-7-185-5  
 Sample Name **ahc-7-185-5**      Pulse sequence **PROTON**      Temperature **25**      Study owner **acherney**  
 Date collected **2014-05-01**      Solvent **cdcl3**      Spectrometer **-vnmrs-400**      Operator **autouser**



Data file //msj/acherney/vnmrs/data/ahc-7-185-5/PROTON01.fid

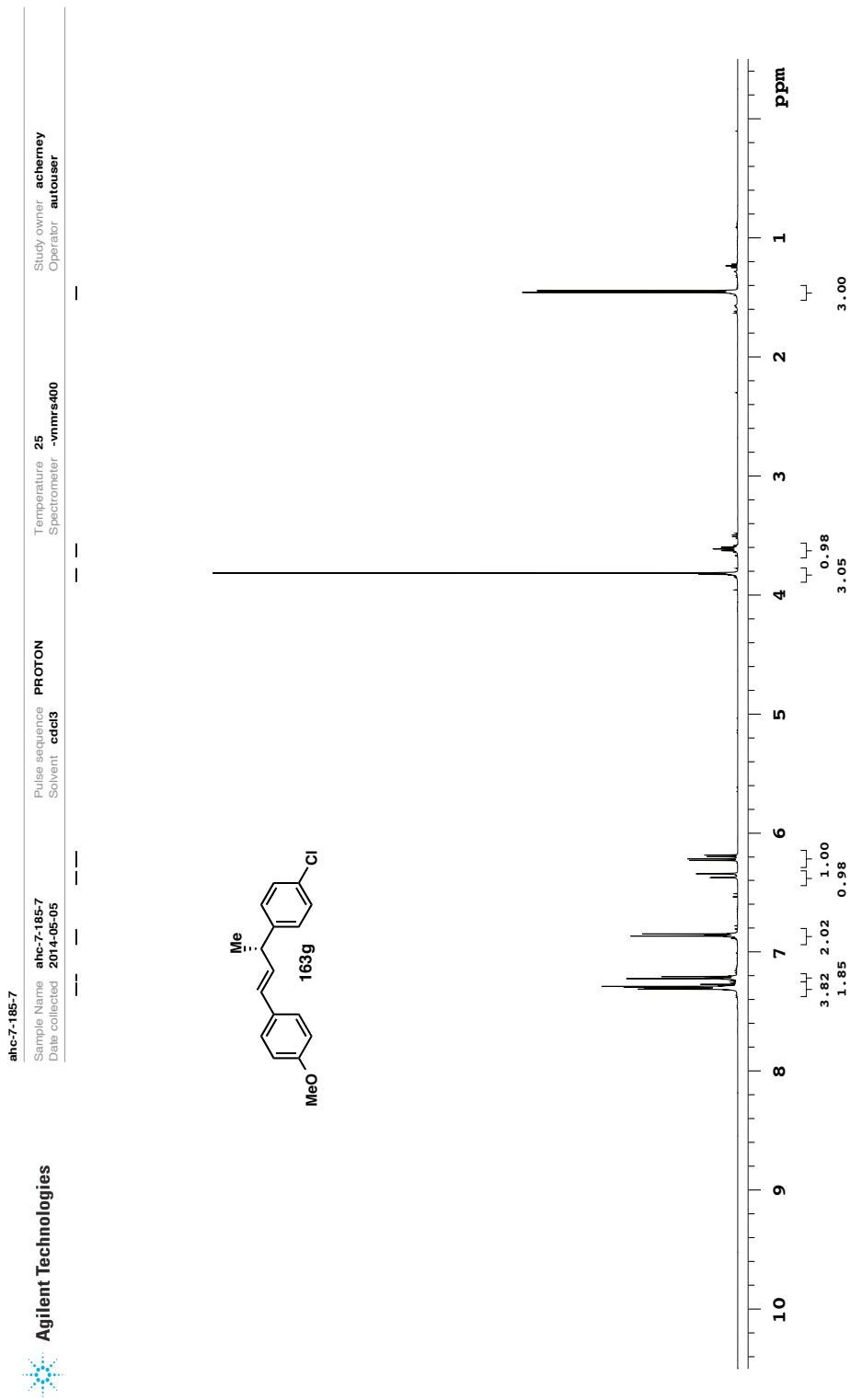
Plot date 2014-07-29

**ahc-7-185-5**  
 Sample Name **ahc-7-185-5**  
 Date collected **2014-05-01**  
 Pulse sequence **CARBON**  
 Solvent **cdcl3**  
 Temperature **25**  
 Spectrometer **-vnmrs-400**  
 Study owner **acherney**  
 Operator **autouser**

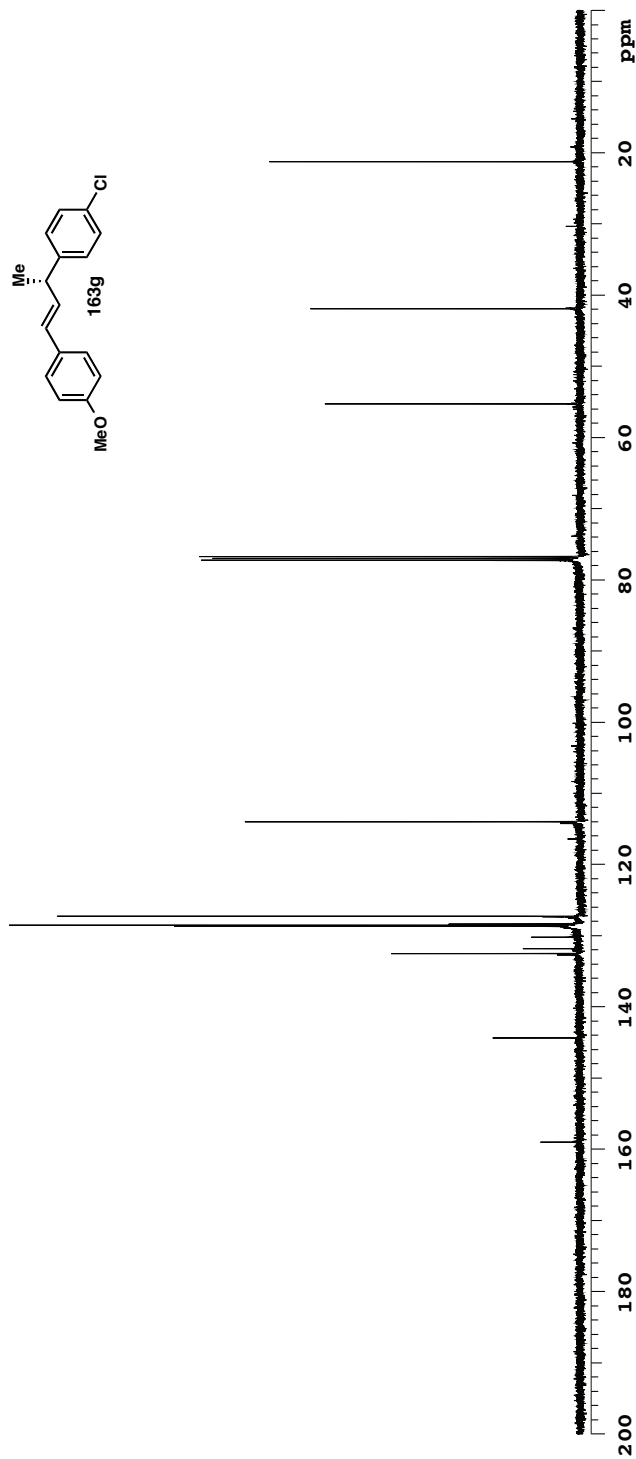
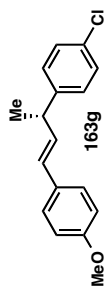


Data file /ndj/acherney/vnmrs/data/ahc-7-185-5/CARBON01.fid

Plot date 2014-07-29

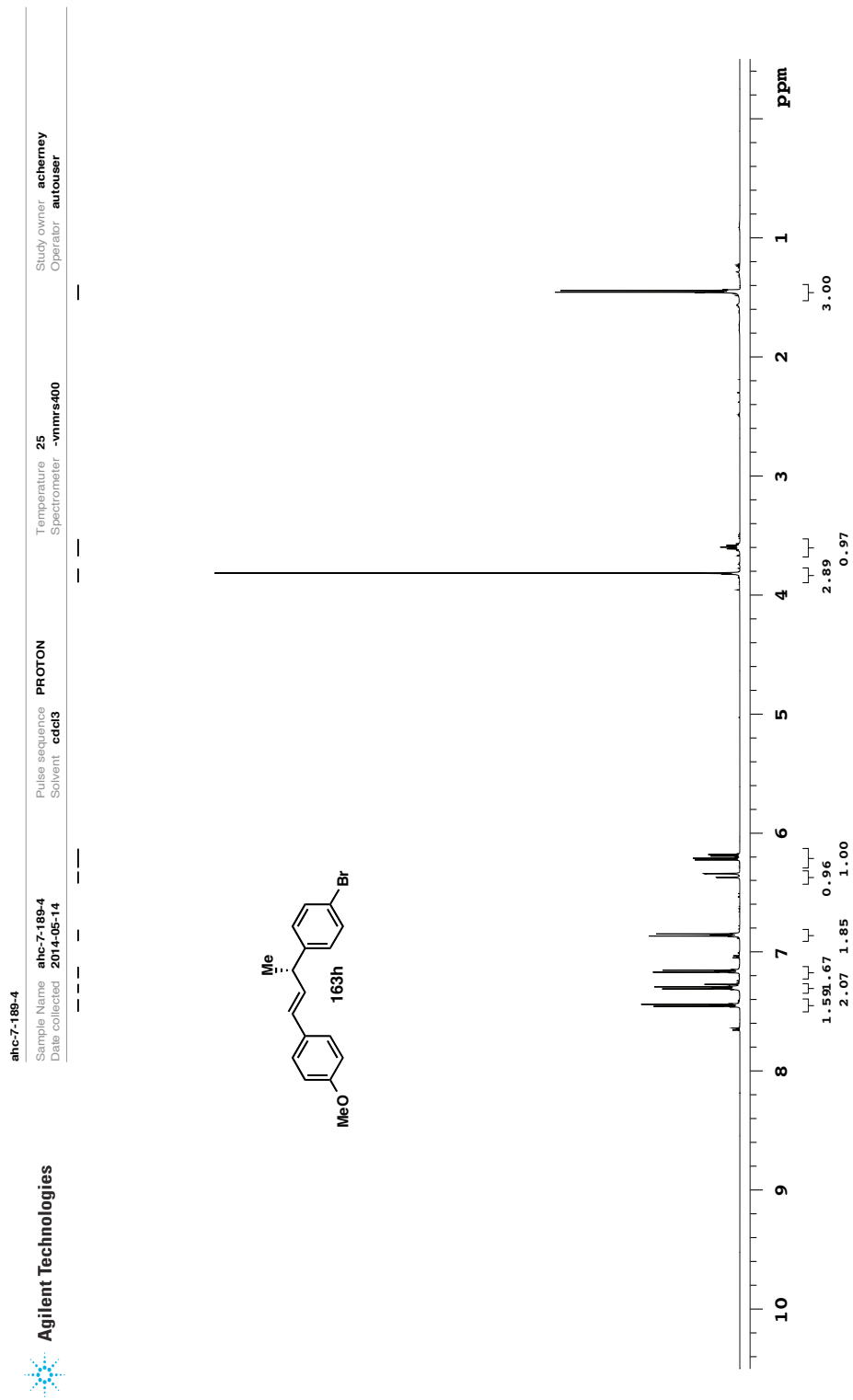


**ahc-7-185-7**  
 Sample Name **ahc-7-185-7**  
 Date collected **2014-05-05**  
 Pulse sequence **CARBON**  
 Solvent **cdcl3**  
 Temperature Spectrometer **25 -vnmrs-400**  
 Study owner **acherney**  
 Operator **autouser**



Data file /ms/acherney/vnmrs/data/ahc-7-185-7/CARBON01.fid

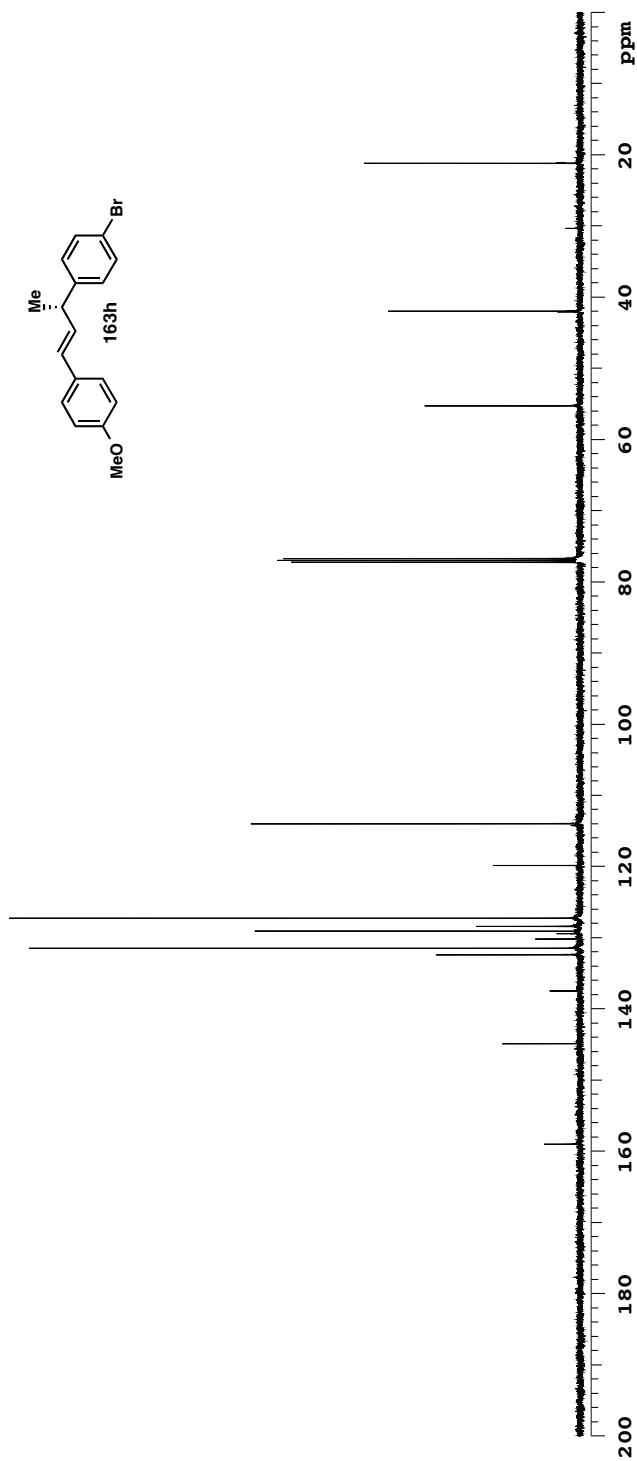
Plot date 2014-07-29



Data file //msj/acherney/vnmrsys\data/ahc-7-189-4/PROTON01.fid

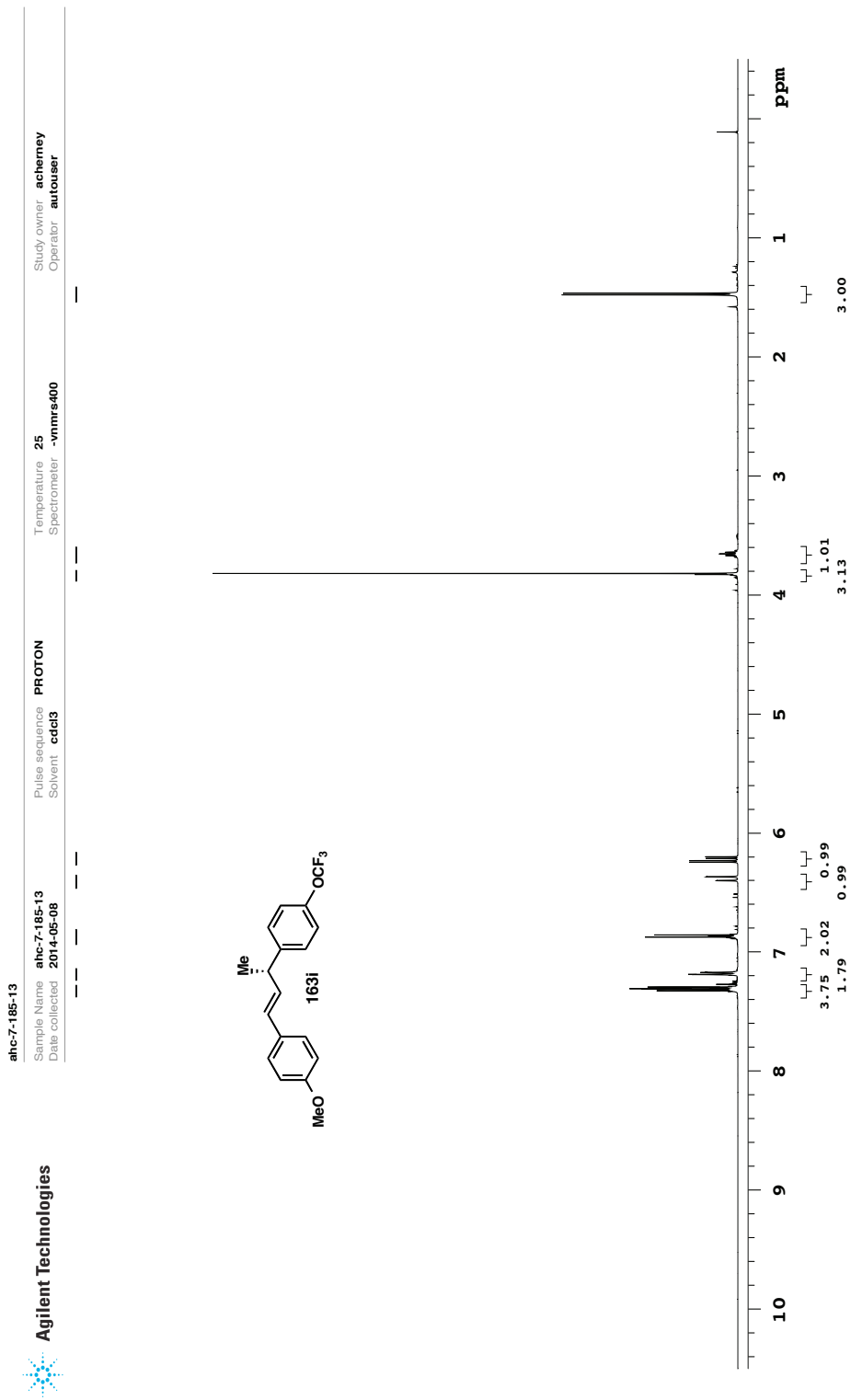
Plot date 2014-07-29

**ahc-7-189-4**  
 Sample Name **ahc-7-189-4**  
 Date collected **2014-05-14**  
 Pulse sequence **CARBON**  
 Solvent **cdcl3**  
 Temperature **25**  
 Spectrometer **-vnmrs-400**  
 Study owner **acherney**  
 Operator **autouser**



Data file /ndy/acherney/vnmrs/data/ahc-7-189-4/CARBON01.fid

Plot date 2014-07-29



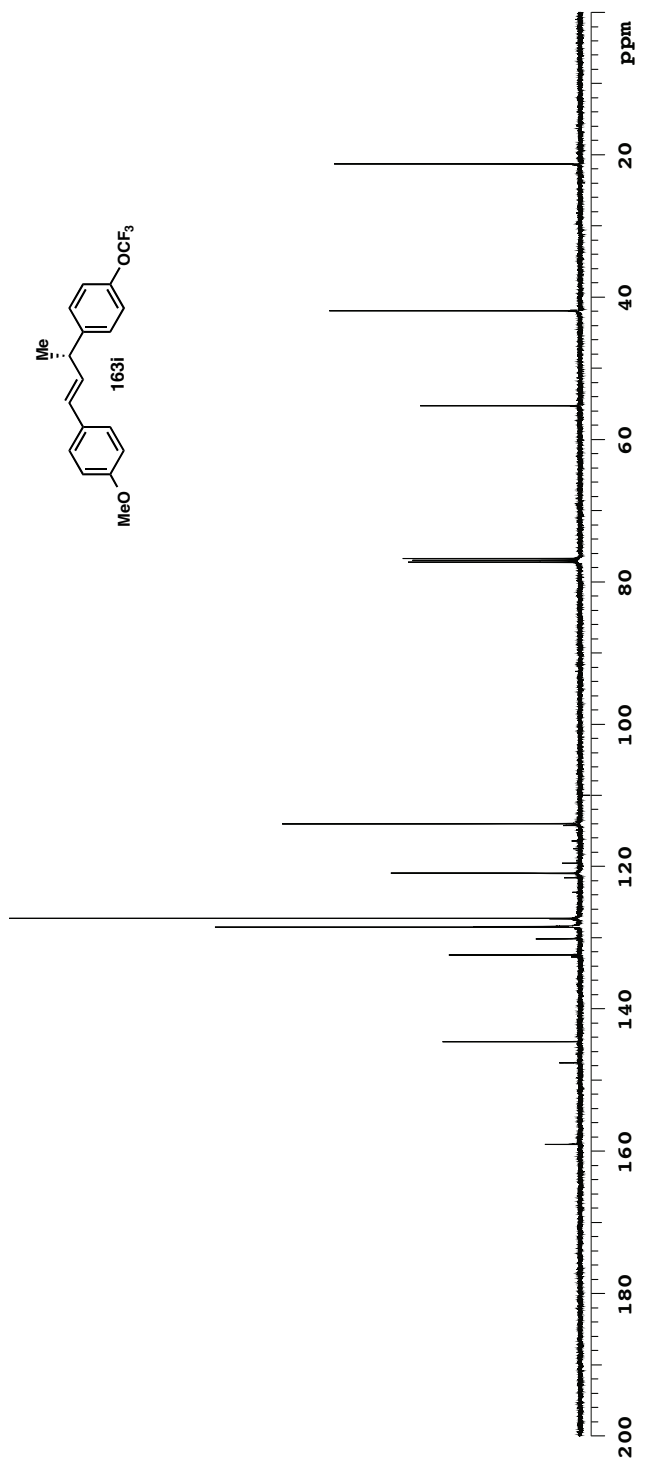
Data file /ndj/acherney/vnmrs/data/ahc-7-185-13/PROTON01.fid

Plot date 2014-07-29



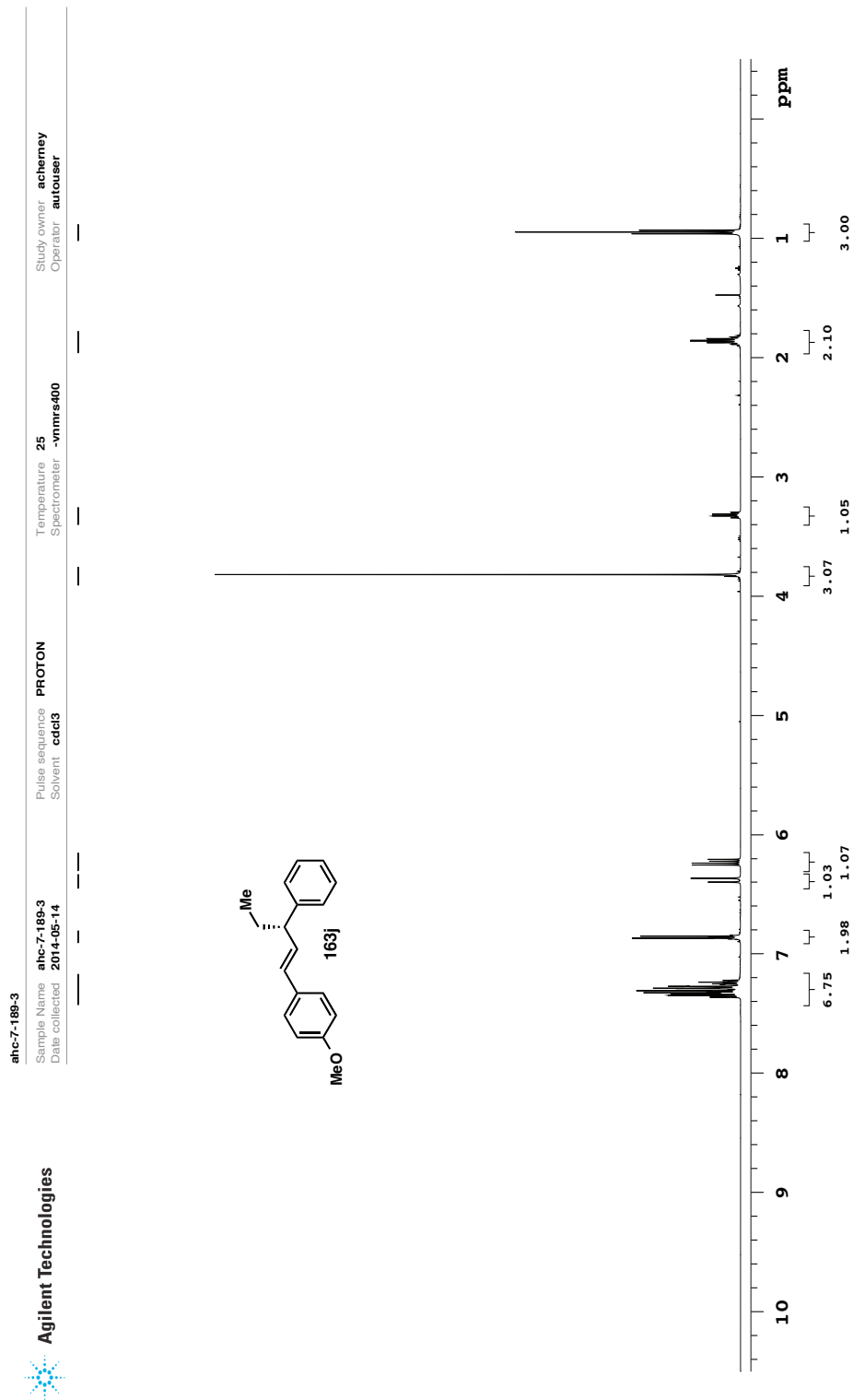
Agilent Technologies

**ahc-7-185-13**  
 Sample Name **ahc-7-185-13**  
 Date collected **2014-05-08**  
 Pulse sequence **CARBON**  
 Solvent **cdcl3**  
 Temperature Spectrometer **25 -vnmrs-400**  
 Study owner **acherney**  
 Operator **autouser**

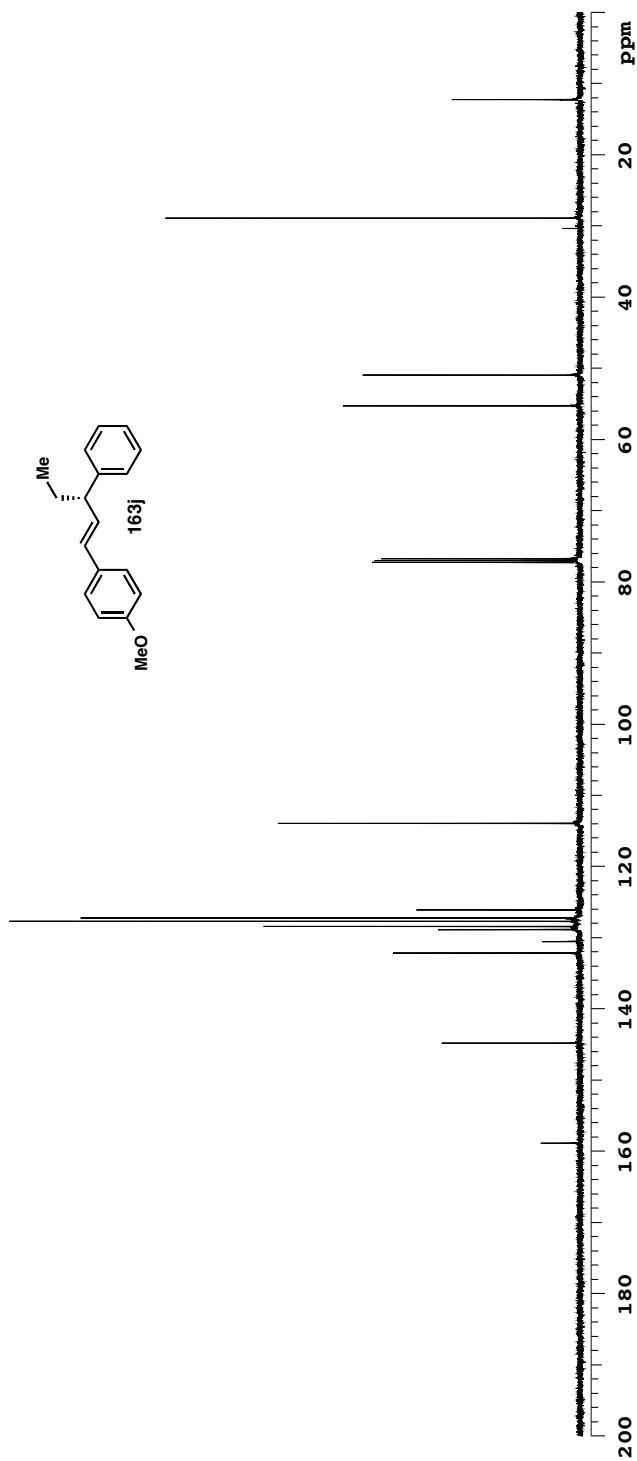


Data file /ndj/acherney/vnmr/ysdata/ahc-7-185-13/CARBON01.fid

Plot date 2014-07-29

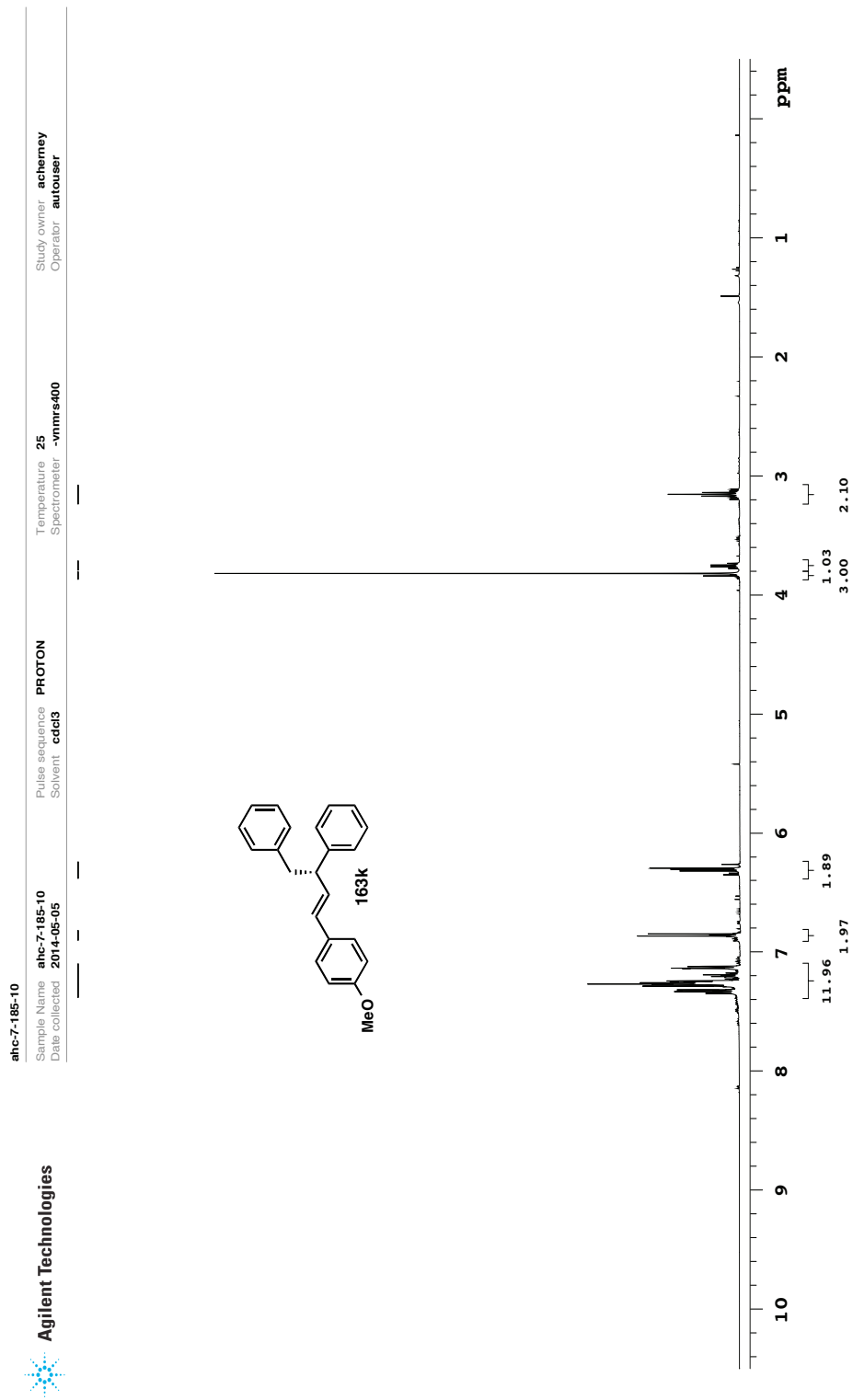


**ahc-7-189-3**  
 Sample Name **ahc-7-189-3**  
 Date collected **2014-05-14**  
 Pulse sequence **CARBON**  
 Solvent **cdcl3**  
 Temperature **25**  
 Spectrometer **-vnmrs-400**  
 Study owner **acherney**  
 Operator **autouser**



Data file /ndj/acherney/vnmrs/data/ahc-7-189-3/CARBON01.fid

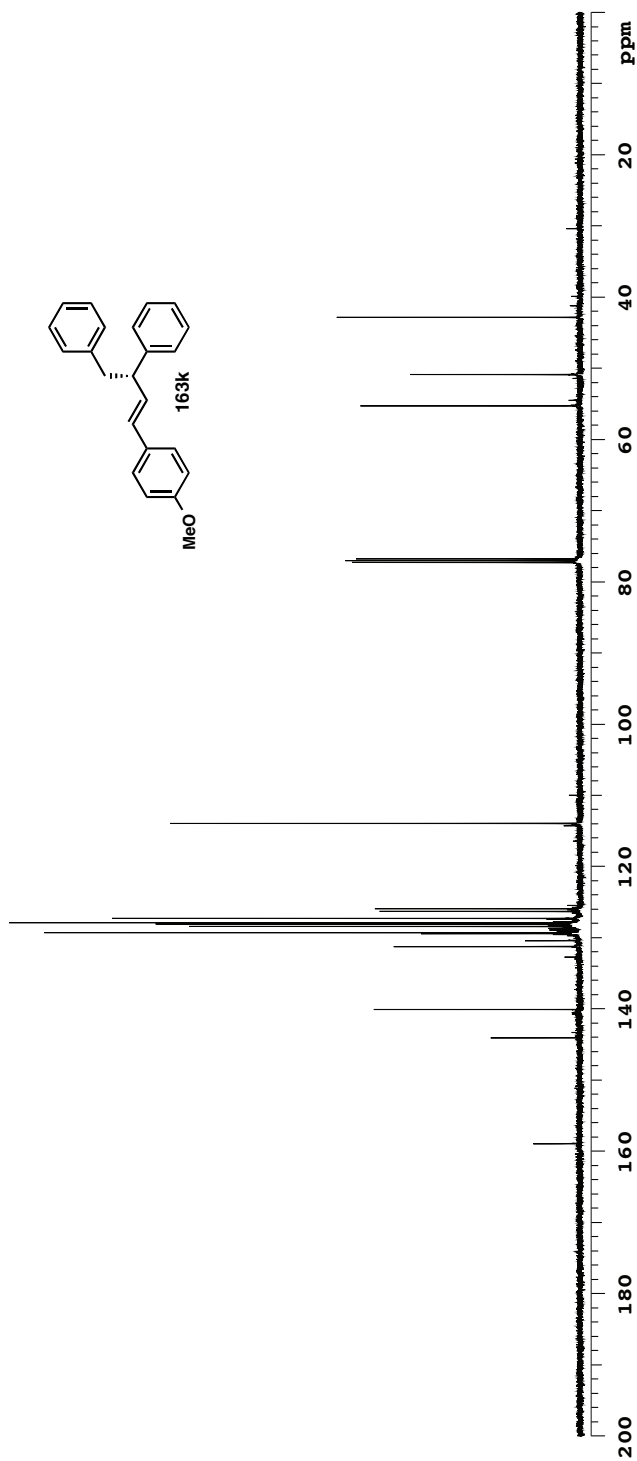
Plot date 2014-07-29



Plot date 2014-07-29

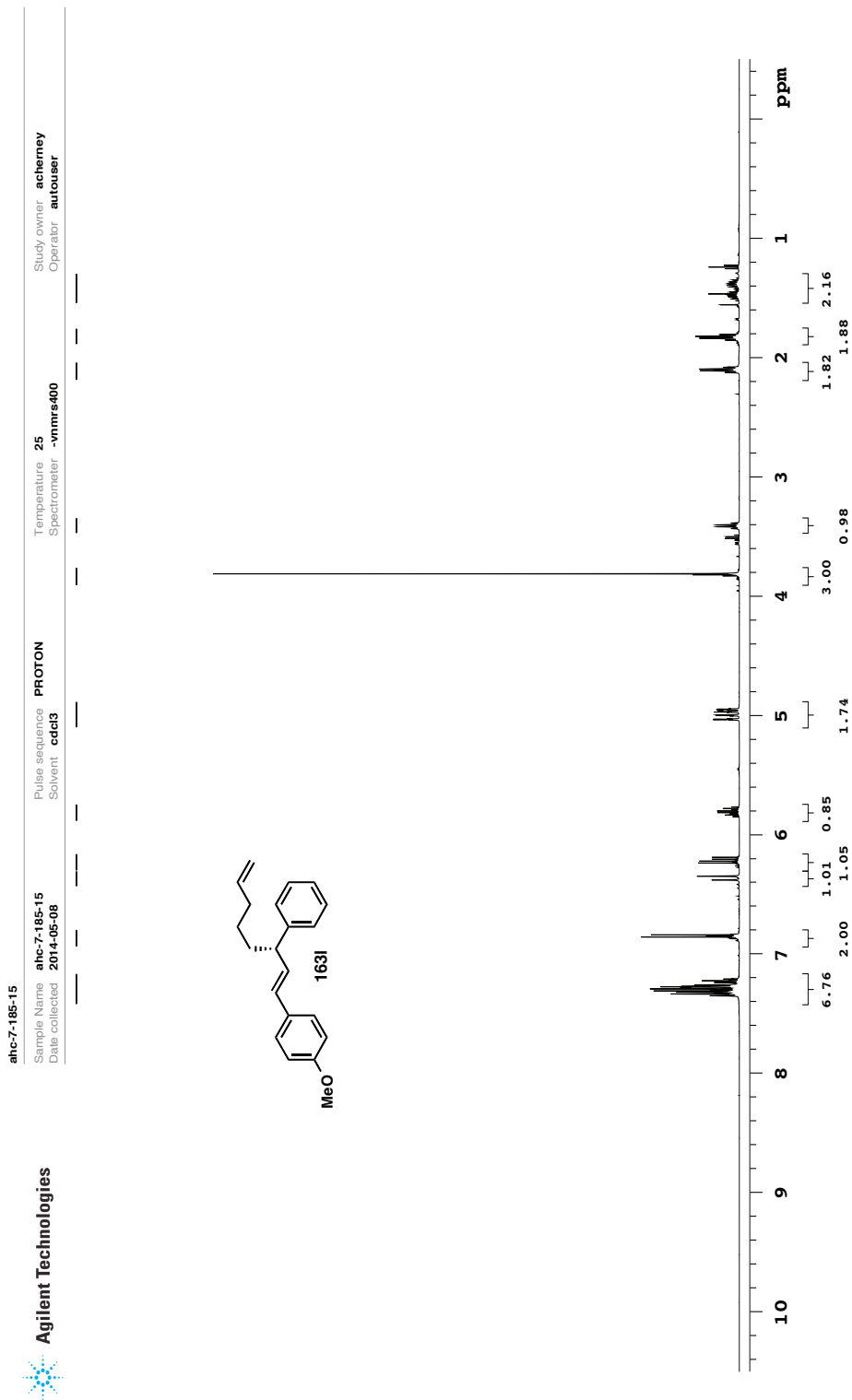
Data file /ndj/acherney/vnmrs/data/ahc-7-185-10/PROTON01.fid

**ahc-7-185-10**  
 Sample Name **ahc-7-185-10**  
 Date collected **2014-05-05**  
 Pulse sequence **CARBON**  
 Solvent **cdcl3**  
 Temperature **25**  
 Spectrometer **-vnmrs-400**  
 Study owner **acherney**  
 Operator **autouser**

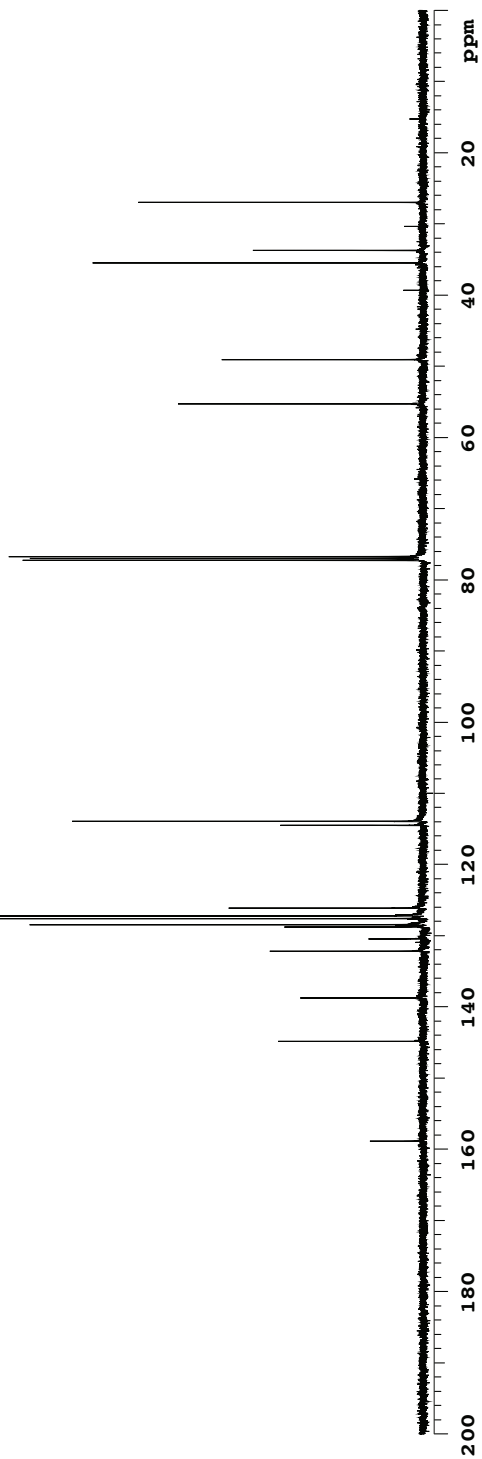
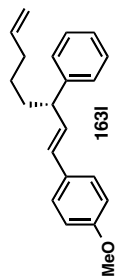


Data file /ndy/acherney/vnmr/ysdata/ahc-7-185-10/CARBON01.fid

Plot date 2014-07-29

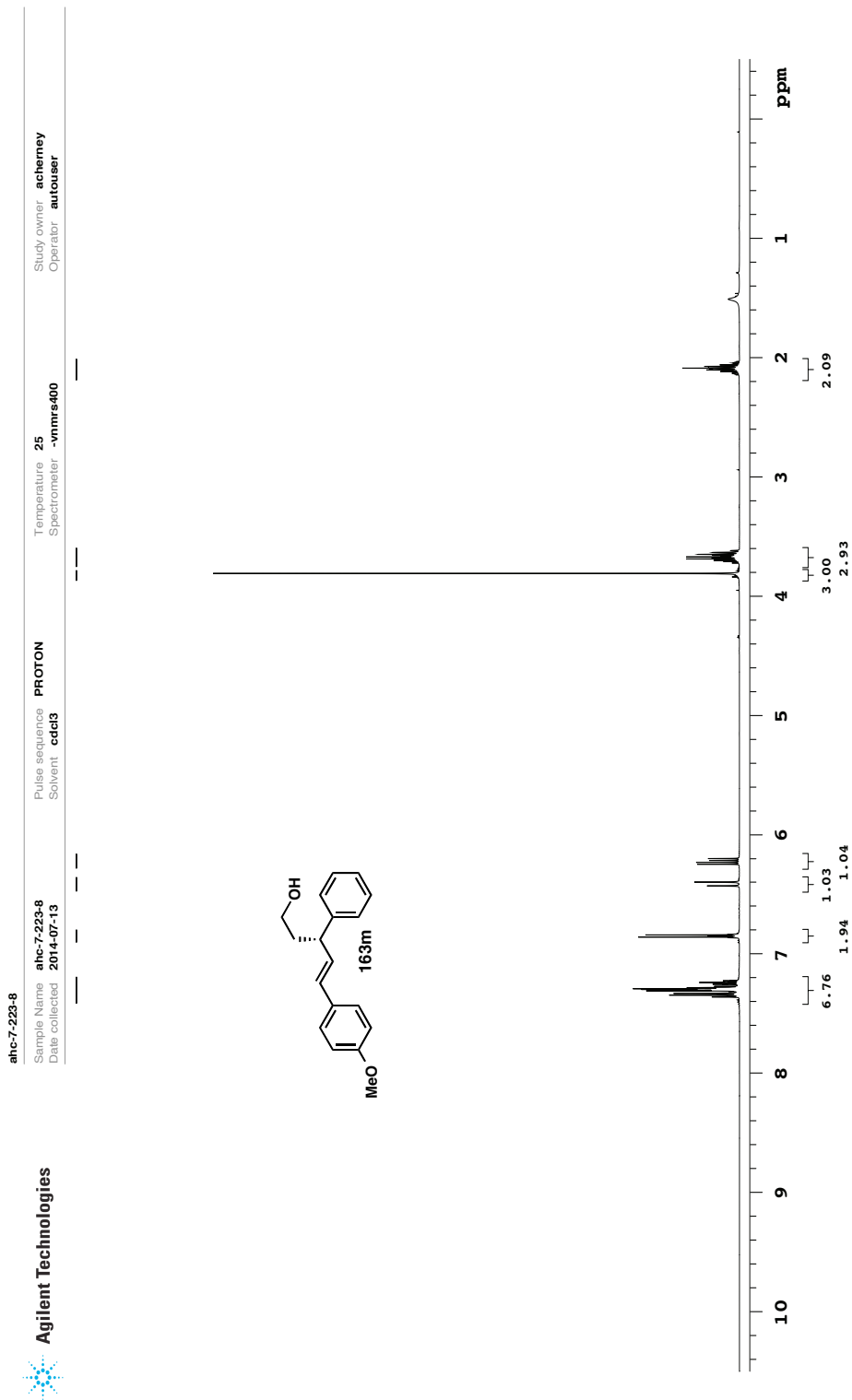


**ahc-7-185-15**  
 Sample Name **ahc-7-185-15**  
 Date collected **2014-05-08**  
 Pulse sequence **CARBON**  
 Solvent **cdcl3**  
 Temperature Spectrometer **25 -vnmrs-400**  
 Study owner **acherney**  
 Operator **autouser**



Data file /ndy/acherney/vnmrs/data/ahc-7-185-15/CARBON01.fid

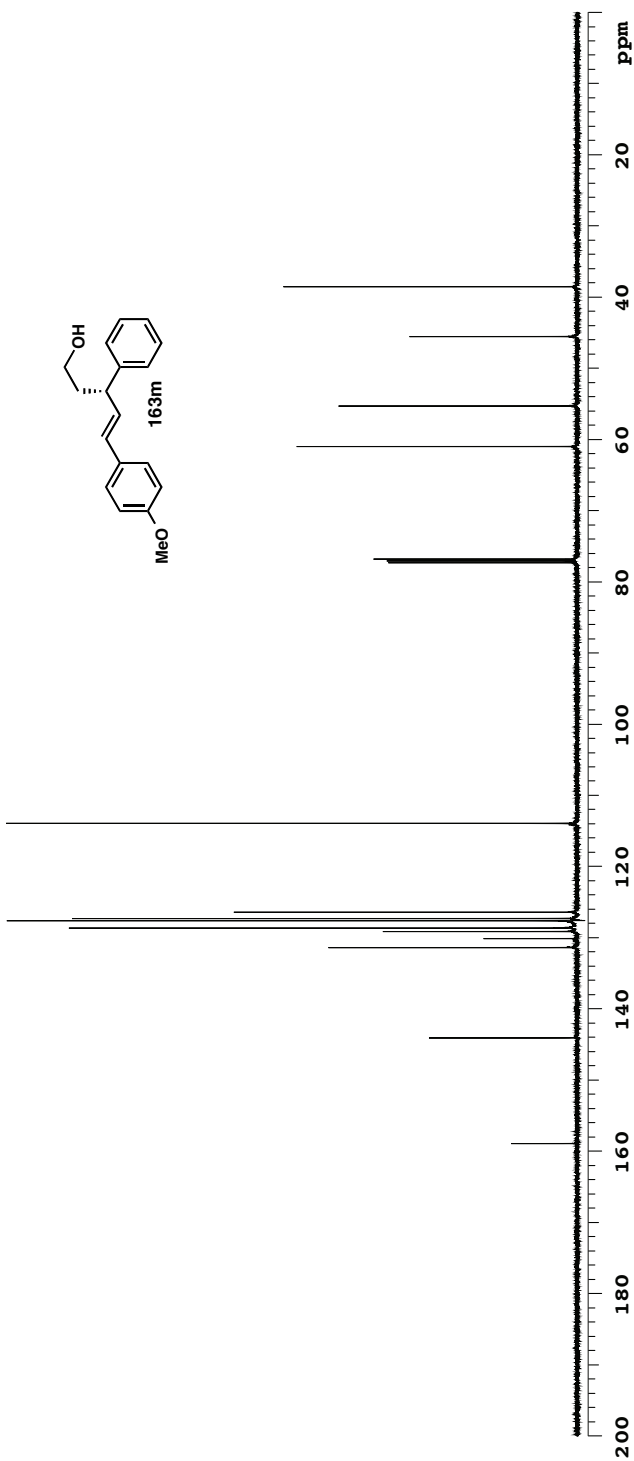
Plot date 2014-07-29



Data file //msj/acherney/vnmrsysdata/ahc-7-223-8/PROTON01.fid

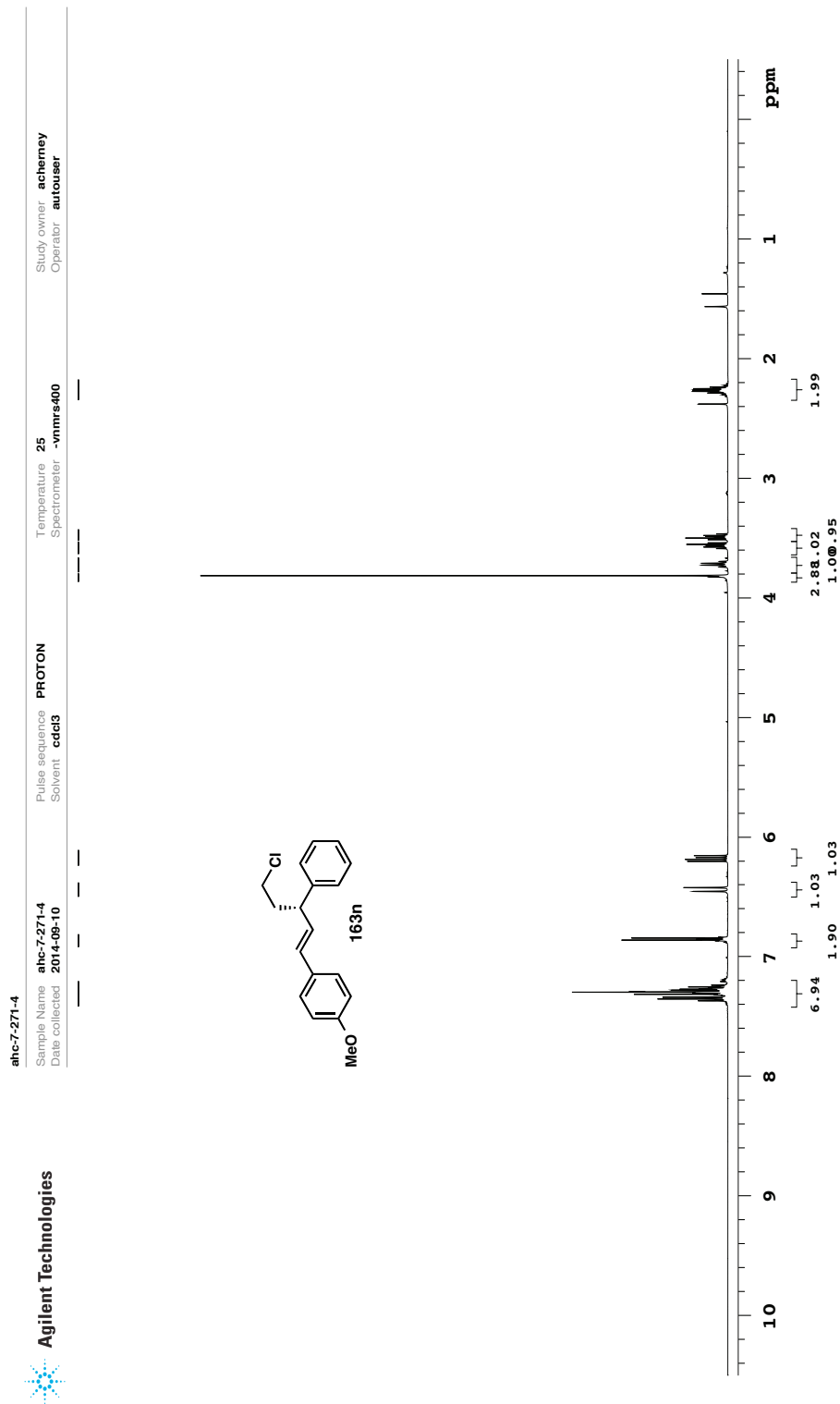
Plot date 2014-07-30

**ahc-7-223-8**  
 Sample Name **ahc-7-223-8**  
 Date collected **2014-07-13**  
 Pulse sequence **CARBON**  
 Solvent **cdcl3**  
 Temperature **25**  
 Spectrometer **-vnmrs-400**  
 Study owner **acherney**  
 Operator **autouser**



Data file /msd/acherney/vnmrsys\data/ahc-7-223-8/CARBON01.fid

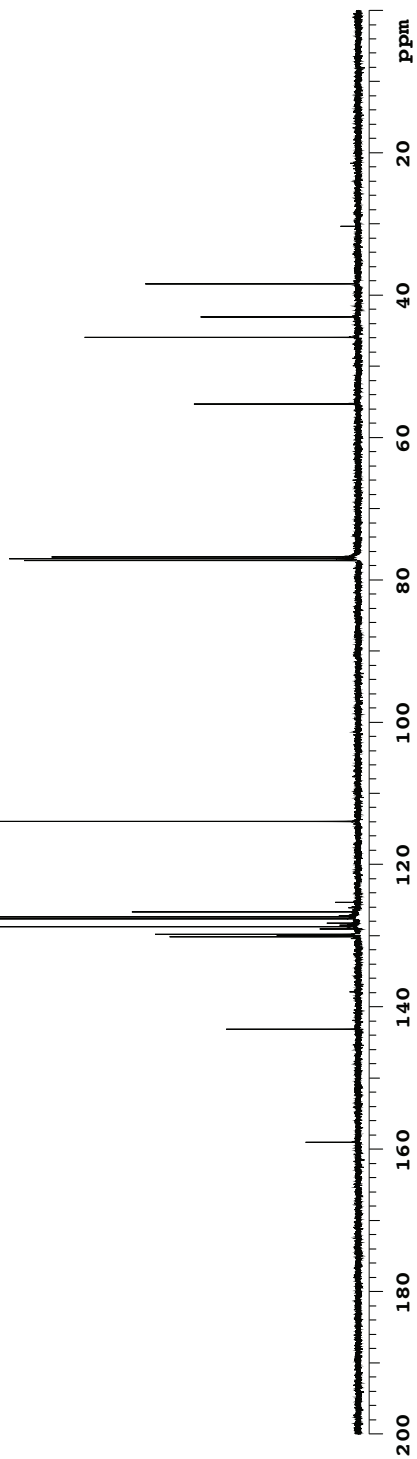
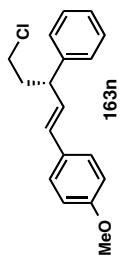
Plot date 2014-07-30



Data file /data/in/acherney/vnmrsys/data/ahc-7-271-4/PROTON01.fid

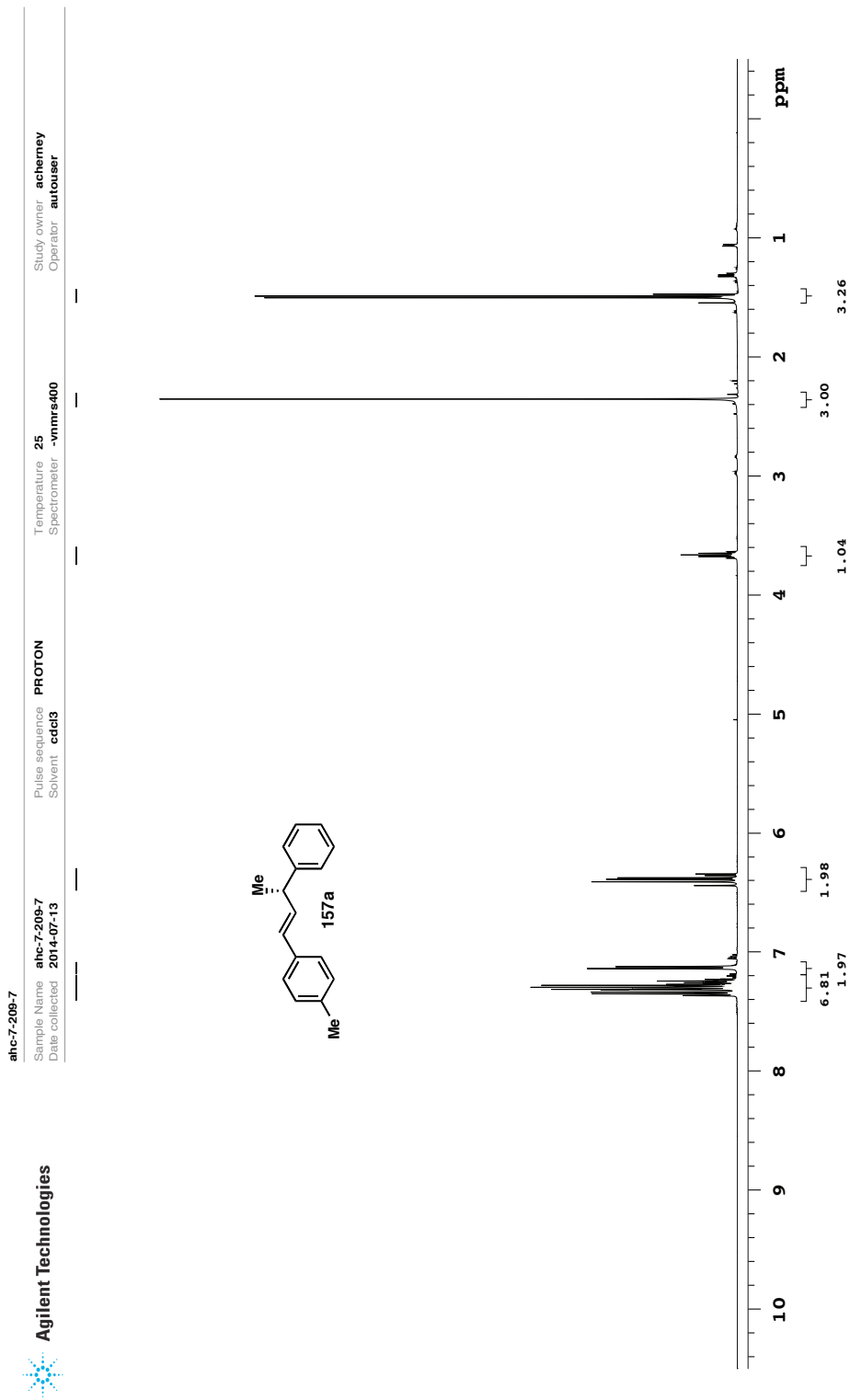
Plot date 2014-09-11

**ahc-7-271-4**  
 Sample Name **ahc-7-271-4**  
 Date collected **2014-09-10**  
 Pulse sequence **CARBON**  
 Solvent **cdcl3**  
 Temperature **25**  
 Spectrometer **-vnmrs-400**  
 Study owner **acherney**  
 Operator **autouser**



Data file /data/inq/acherney/vnmr/sys/data/ahc-7-271-4/CARBON01.fid

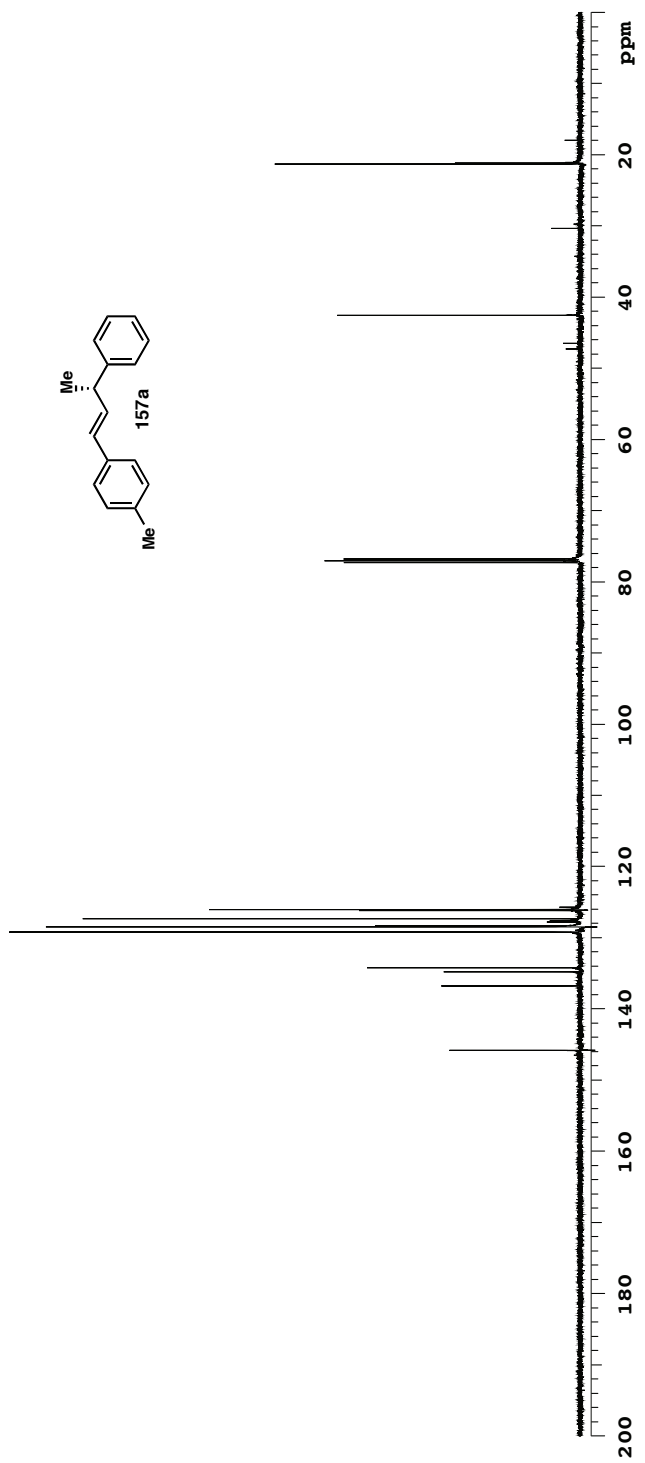
Plot date 2014-09-11



Data file /ndj/acherney/vnmrsysdata/ahc-7-209-7/PROTON01.fid

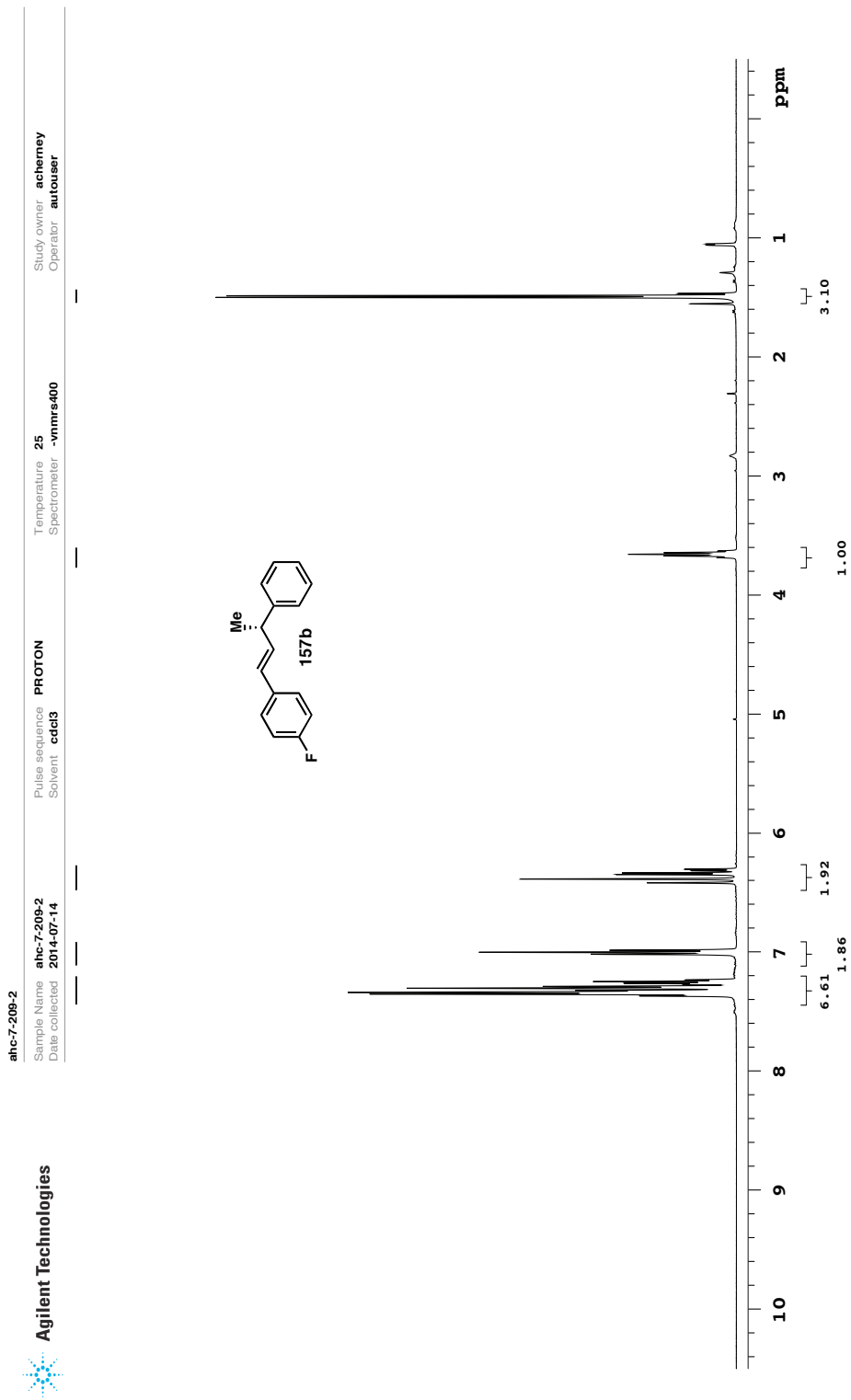
Plot date 2014-07-29

ahc-7-209-7  
 Sample Name ahc-7-209-7  
 Date collected 2014-07-13  
 Pulse sequence CARBON  
 Solvent cdcl3  
 Temperature 25  
 Spectrometer -vnmrs-400  
 Study owner acherney  
 Operator autouser



Data file /ndy/acherney/vnmrsysdata/ahc-7-209-7/CARBON01.fid

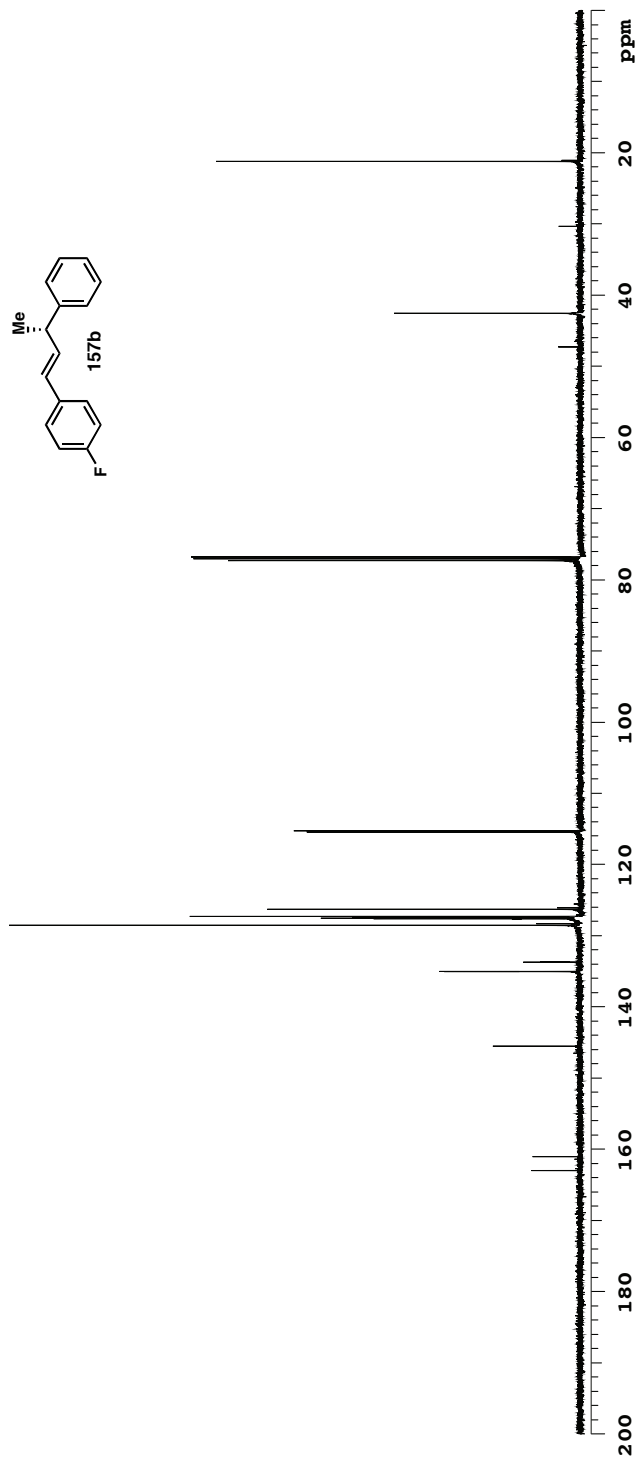
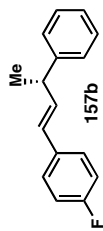
Plot date 2014-07-29

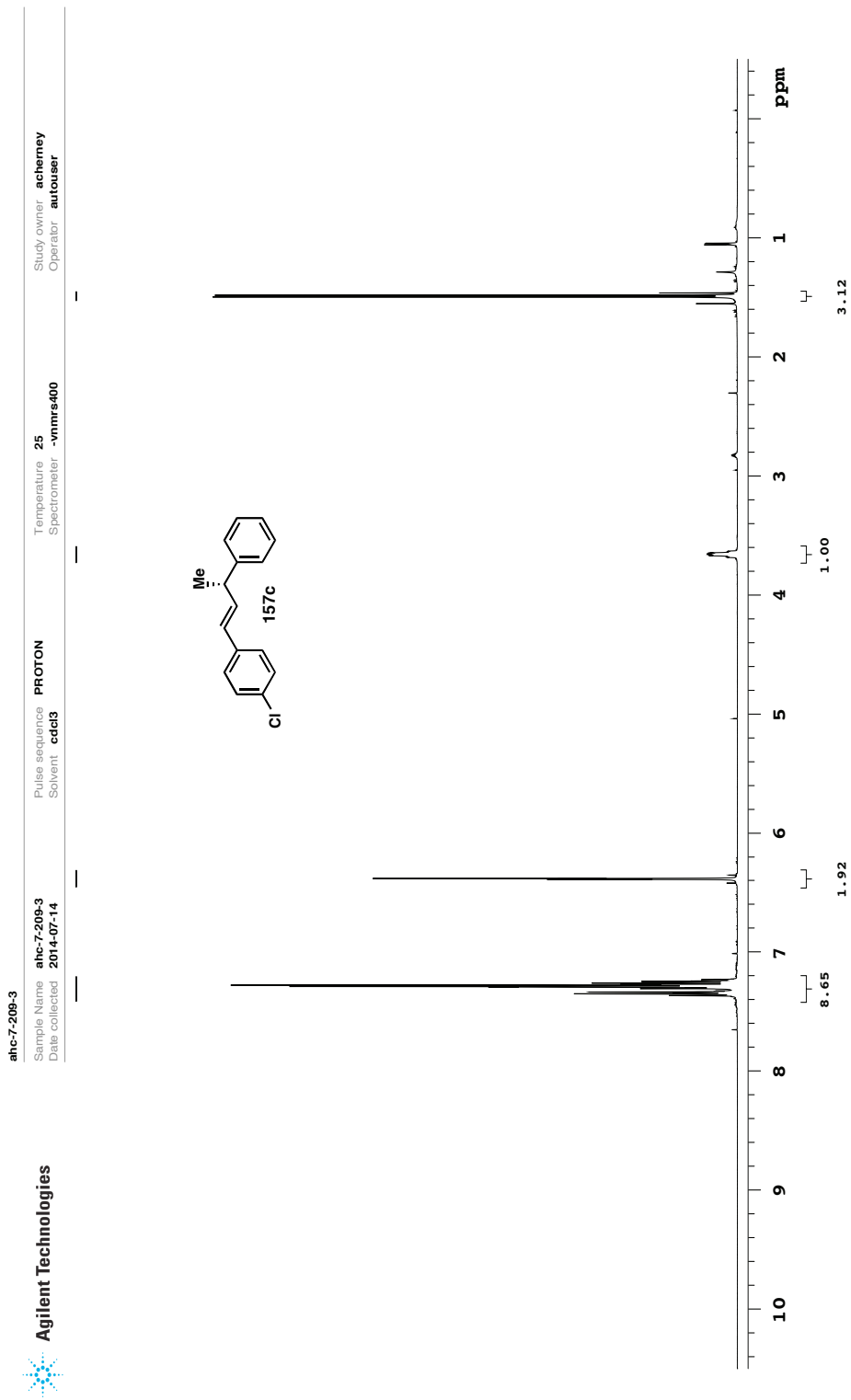


Plot date 2014-07-29

Data file /ndj/acherney/vnmrsysdata/ahc-7-209-2/PROTON01.fid

ahc-7-209-2  
 Sample Name ahc-7-209-2  
 Date collected 2014-07-14  
 Pulse sequence CARBON  
 Solvent cdcl3  
 Temperature 25  
 Spectrometer -vnmrs-400  
 Study owner acherney  
 Operator autouser

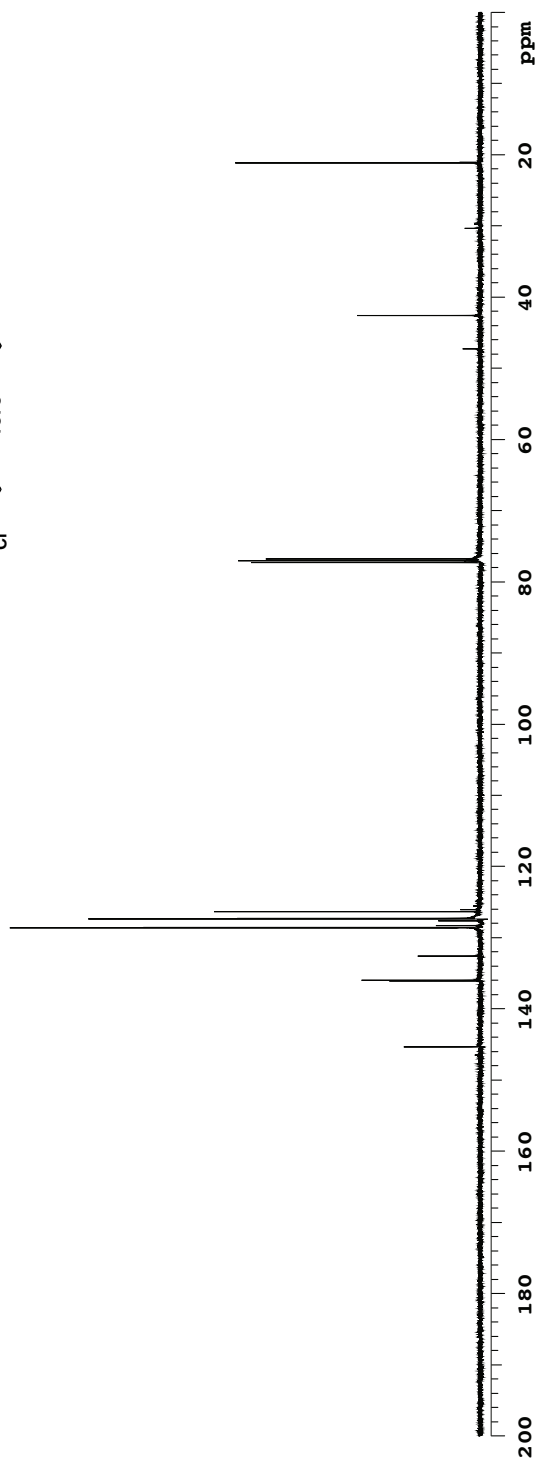
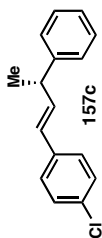




Data file /ndj/acherney/vnmrsysdata/ahc-7-209-3/PROTON01.fid

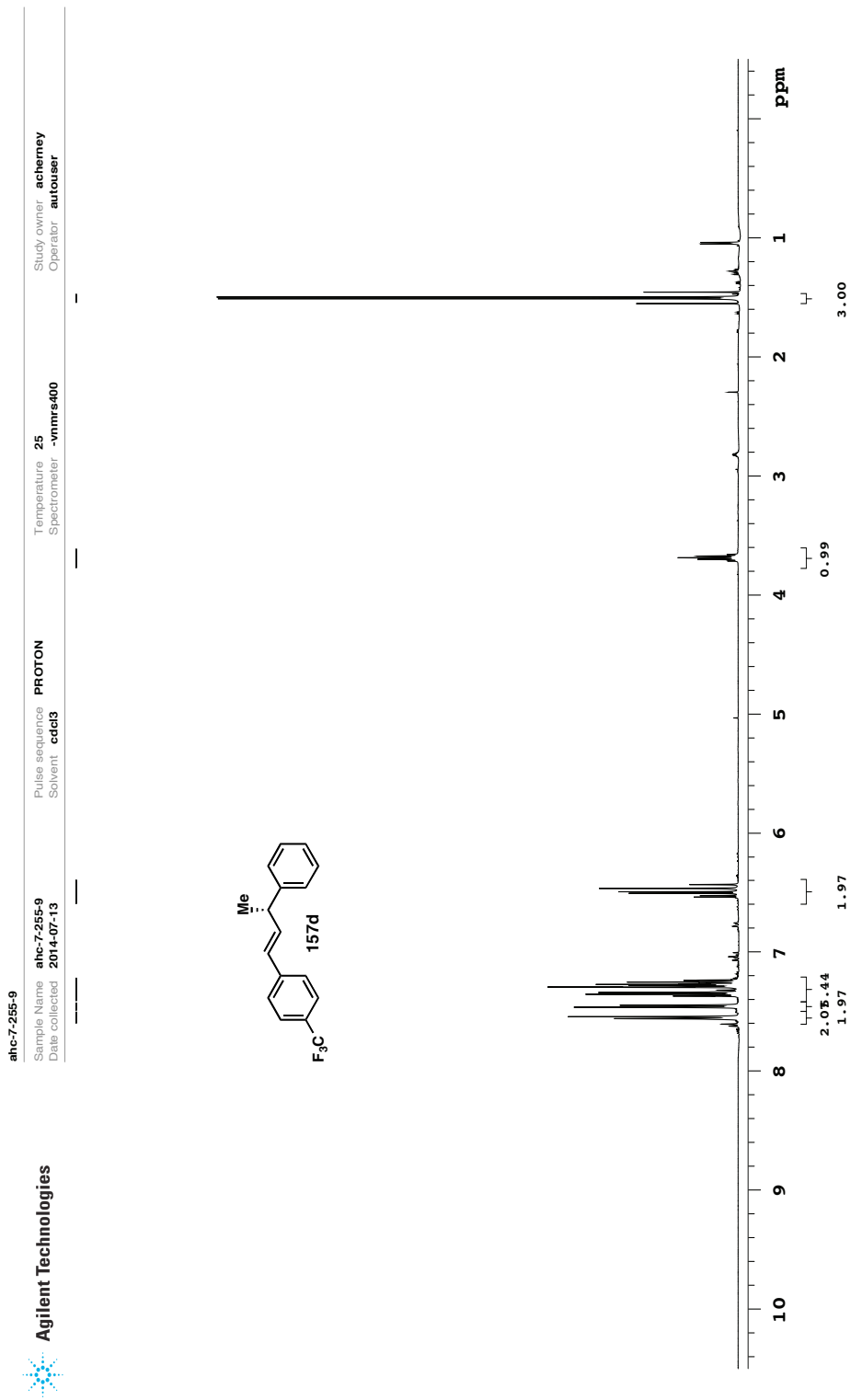
Plot date 2014-07-29

**ahc-7-209-3**  
 Sample Name **ahc-7-209-3**  
 Date collected **2014-07-14**  
 Pulse sequence **CARBON**  
 Solvent **cdcl3**  
 Temperature Spectrometer **25 -vnmrs-400**  
 Study owner **acherney**  
 Operator **autouser**



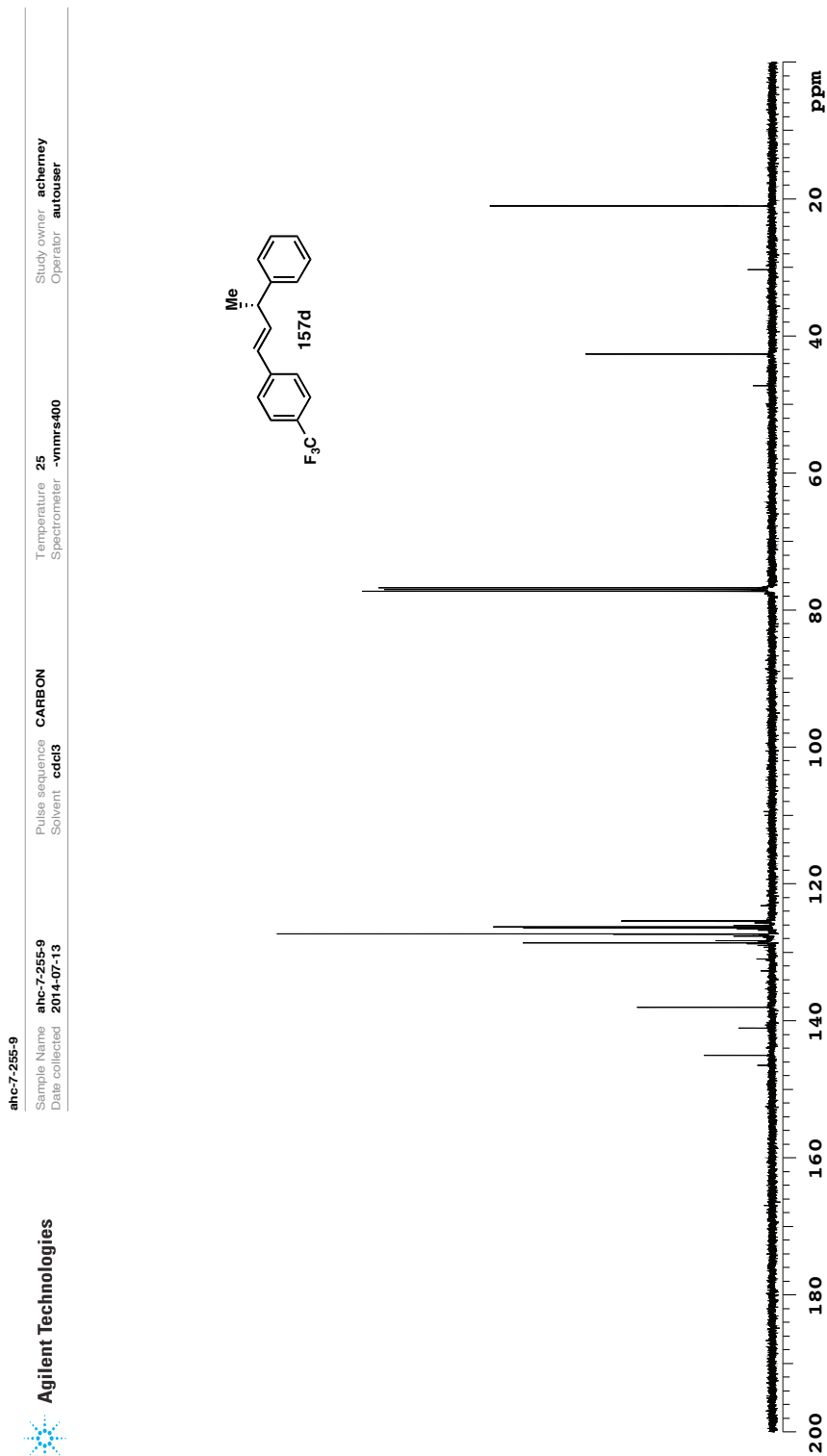
Data file `/ndj/acherney/vnmrsys\data/ahc-7-209-3/CARBON01.fid`

Plot date 2014-07-29



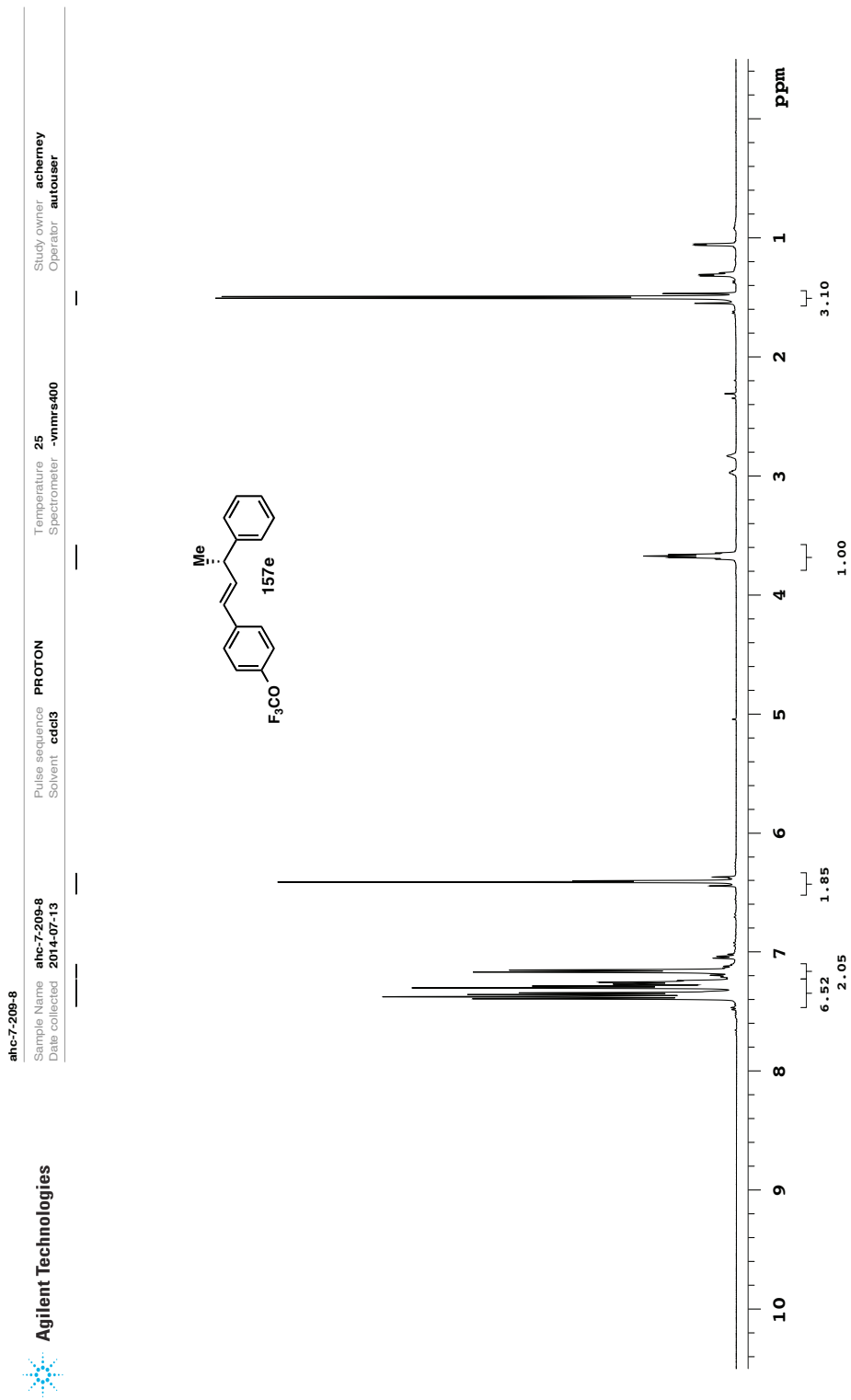
Plot date 2014-07-29

Data file /ndj/acherney/vnmrs/data/ahc-7-255-9/PROTON01.fid



Data file /ndj/acherney/vnmrjrs/data/ahc-7-255-9/CARBON01.fid

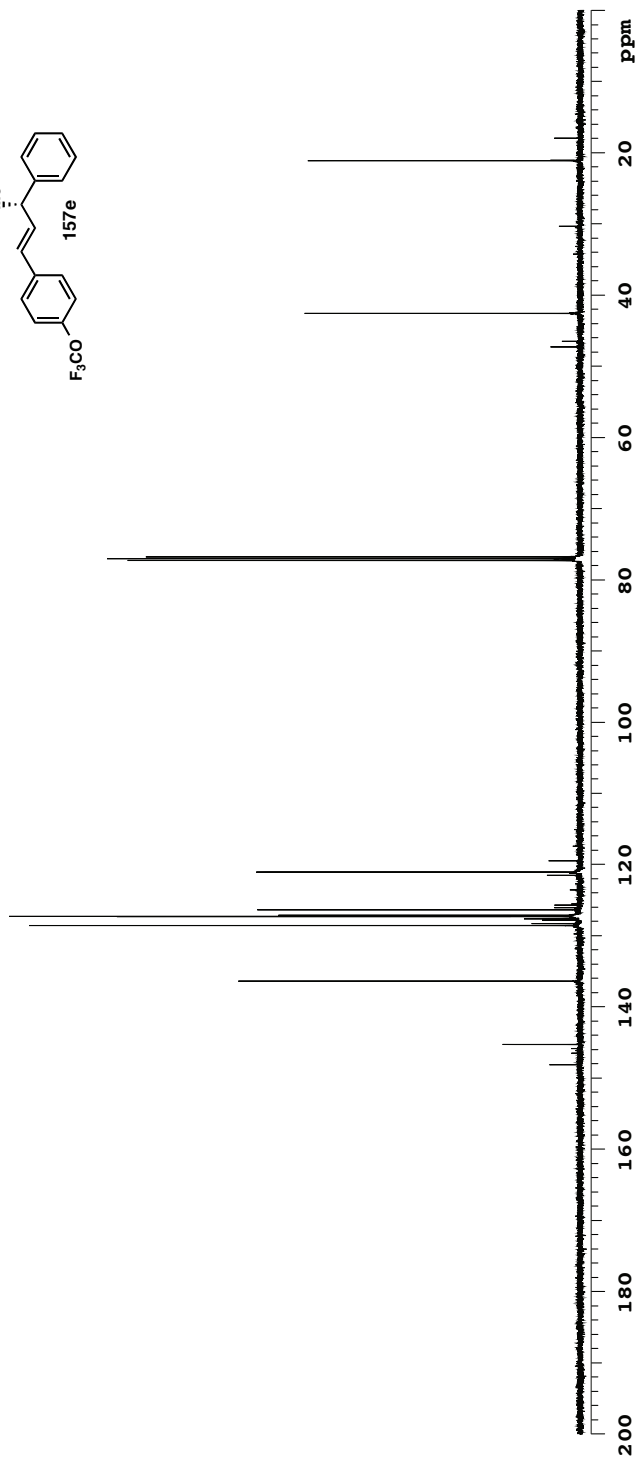
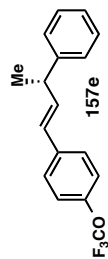
Plot date 2014-07-29



Data file /ndj/acherney/vnmrs/data/ahc-7-209-8/PROTON01.fid

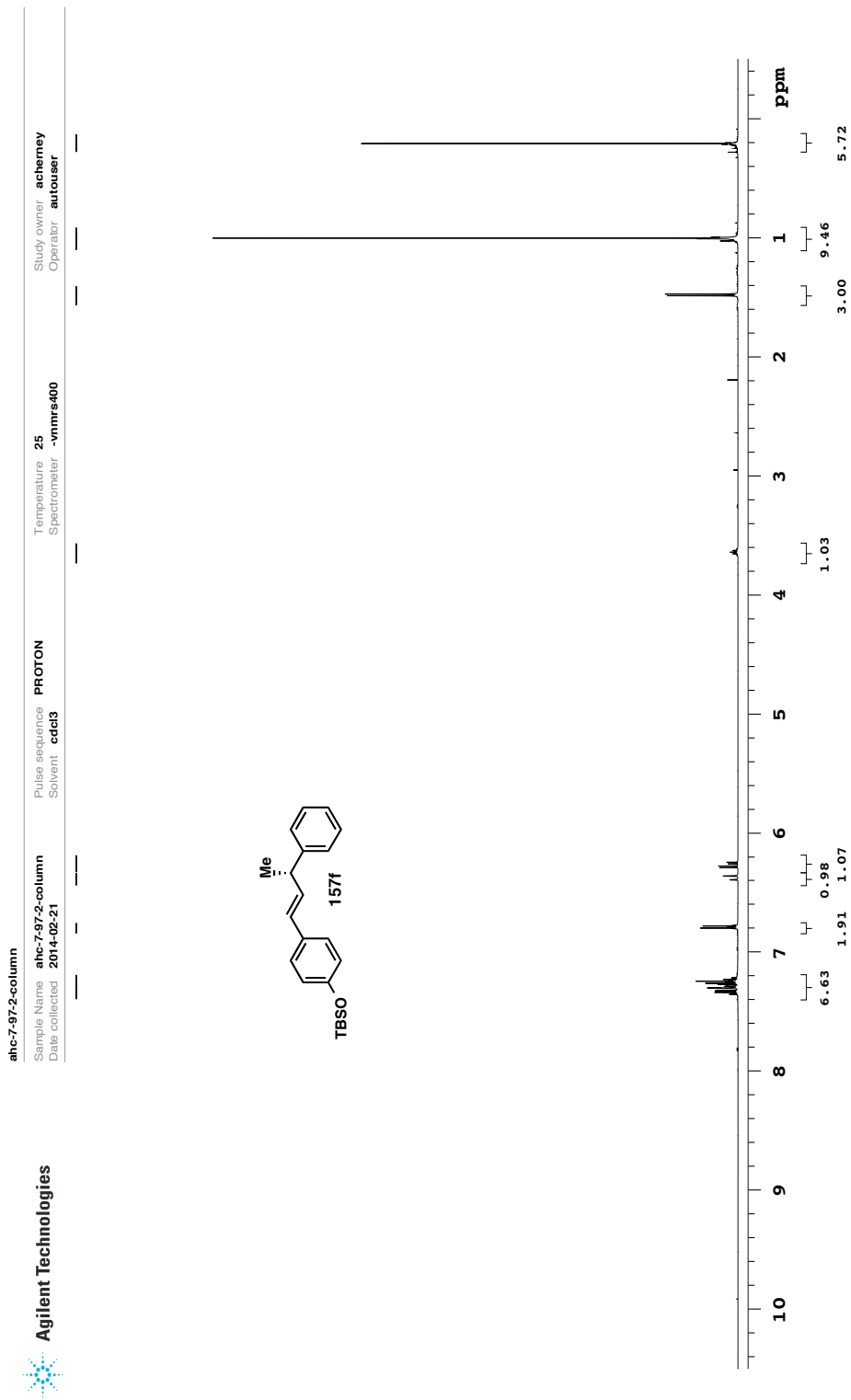
Plot date 2014-07-30

**ahc-7-209-8**  
 Sample Name **ahc-7-209-8**  
 Date collected **2014-07-13**  
 Pulse sequence **CARBON**  
 Solvent **cdcl3**  
 Temperature Spectrometer **25 -vnmrs-400**  
 Study owner **acherney**  
 Operator **autouser**



Data file /msd/acherney/vnmrs/data/ahc-7-209-8/CARBON01.fid

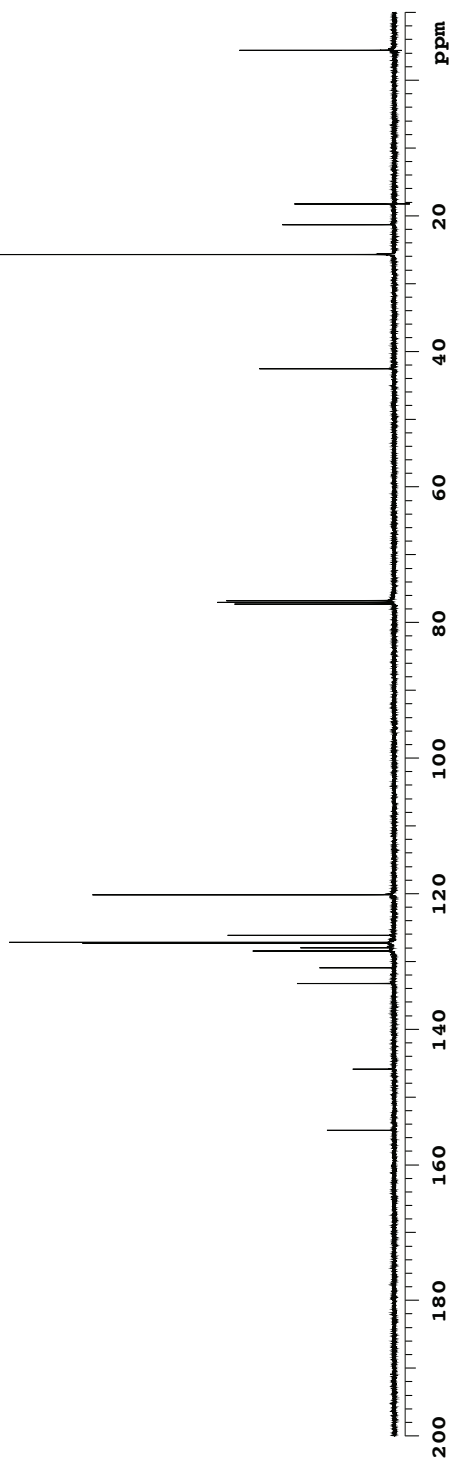
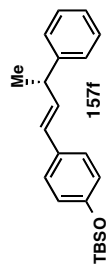
Plot date 2014-07-30

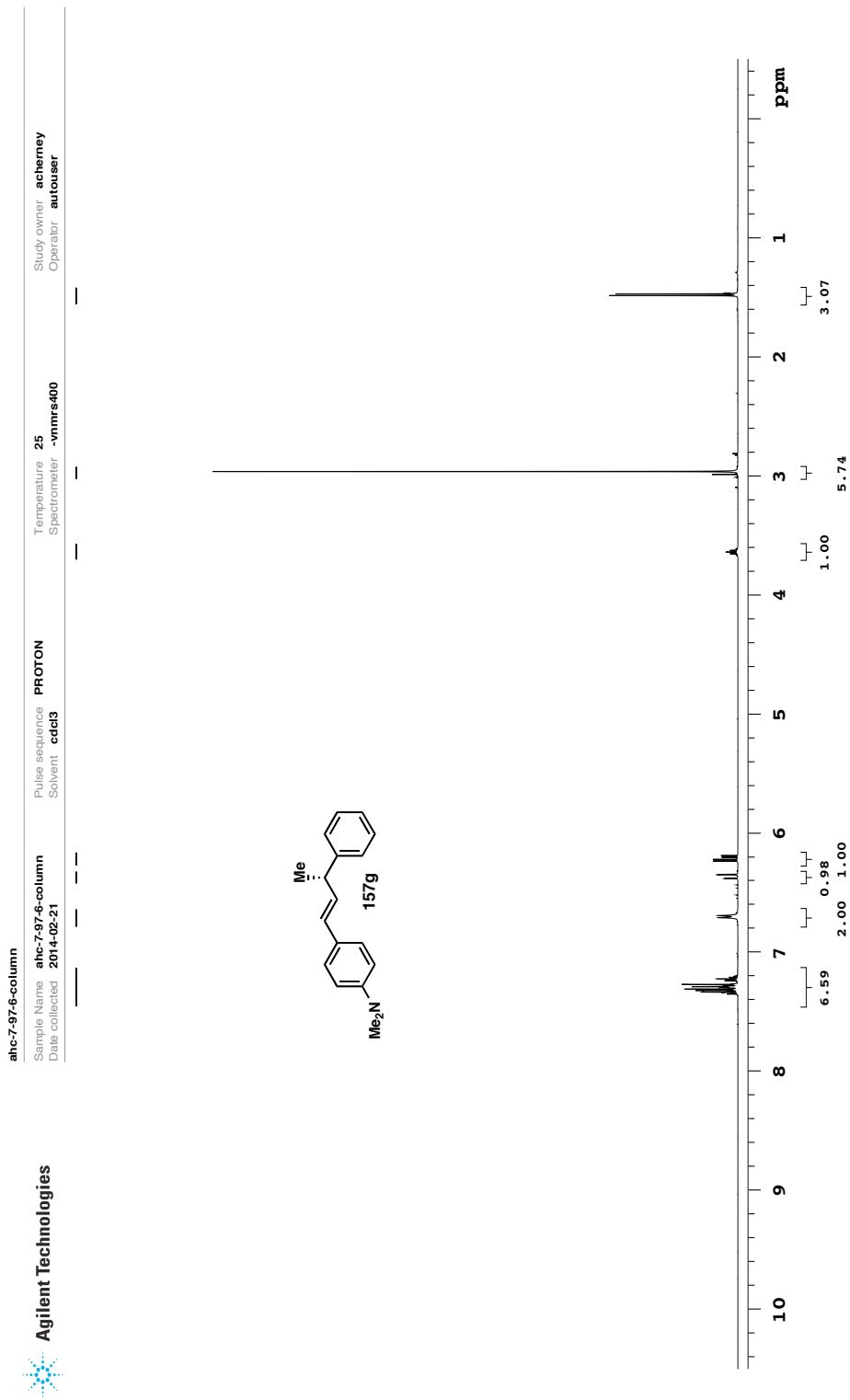


Plot date 2014-07-30

Data file /ndj/acherney/vnmrs/data/ahc-7-97-2-column/PROTON02.fid

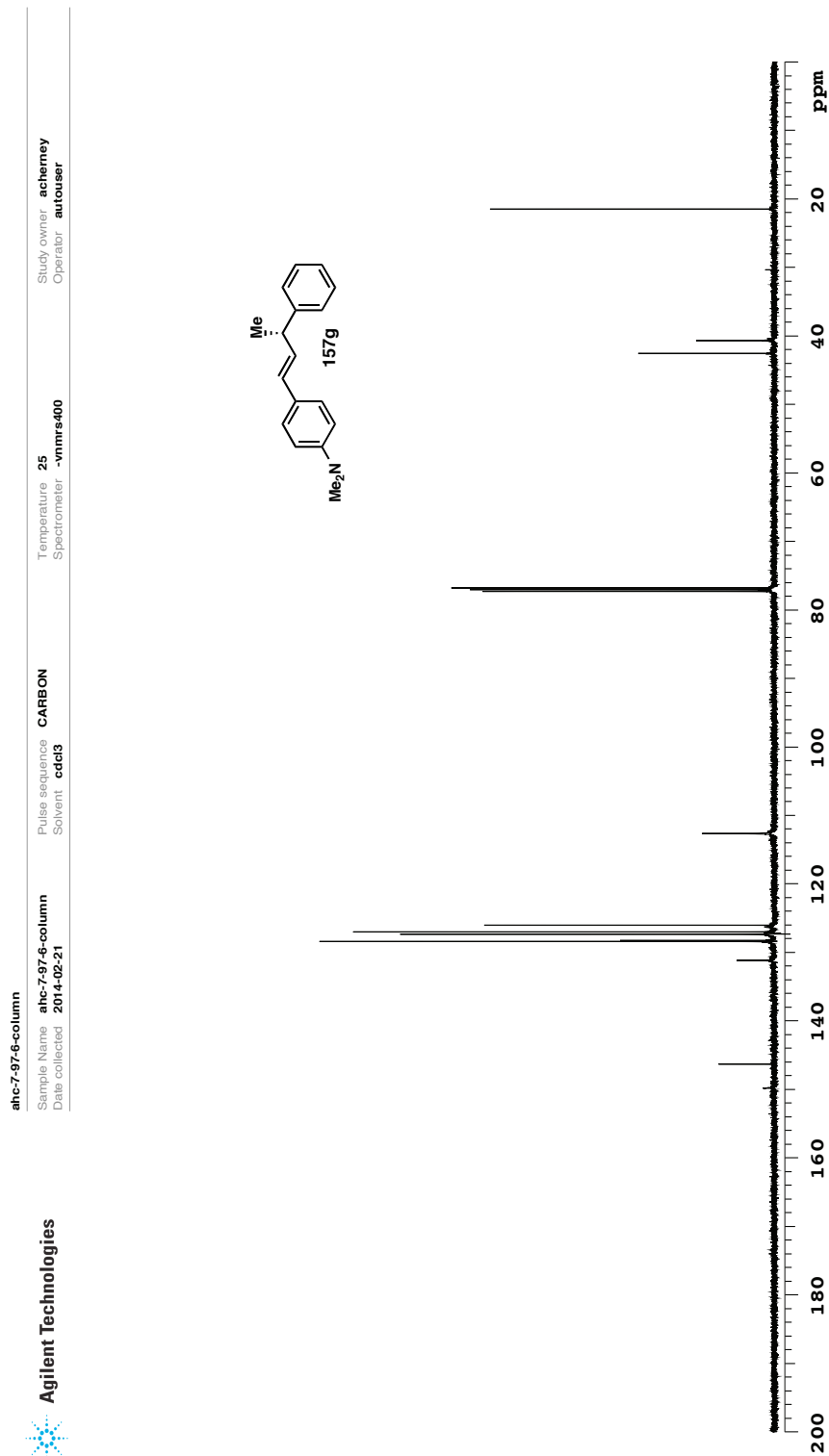
ahc-7-97-2-column  
 Sample Name ahc-7-97-2-column  
 Date collected 2014-02-21  
 Pulse sequence CARBON  
 Solvent cdcl3  
 Temperature 25  
 Spectrometer -vnmrs-400  
 Study owner acherney  
 Operator autouser





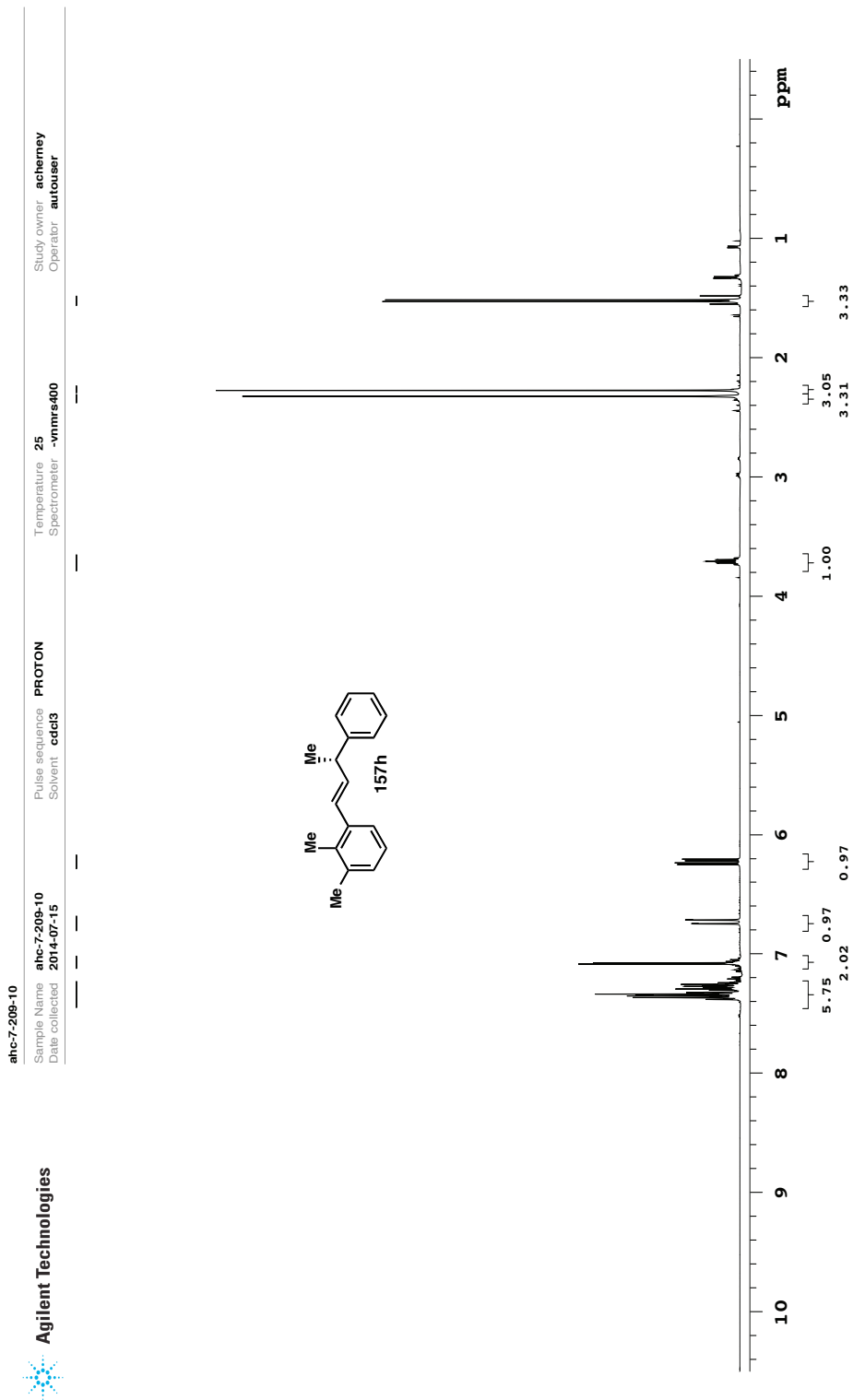
Data file /ndj/acherney/vnmrs/data/ahc-7-97-6-column/PROTON02.fid

Plot date 2014-07-30



Plot date 2014-07-30

Data file /ndj/acherney/vnmrs/data/ahc-7-97-6-column/CARBON01.fid



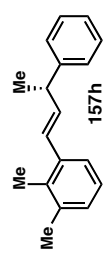
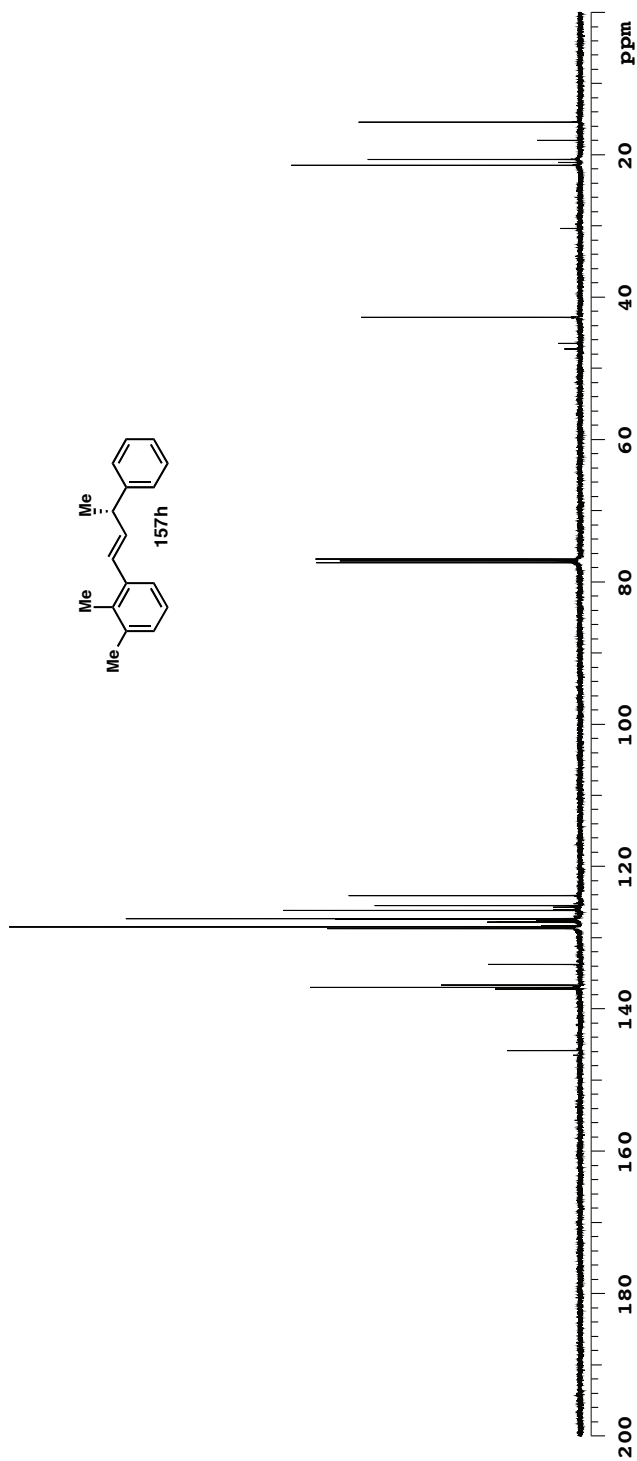
Data file /ndj/acherney/vnmrsysdata/ahc-7-209-10/PROTON01.fid

Plot date 2014-07-30



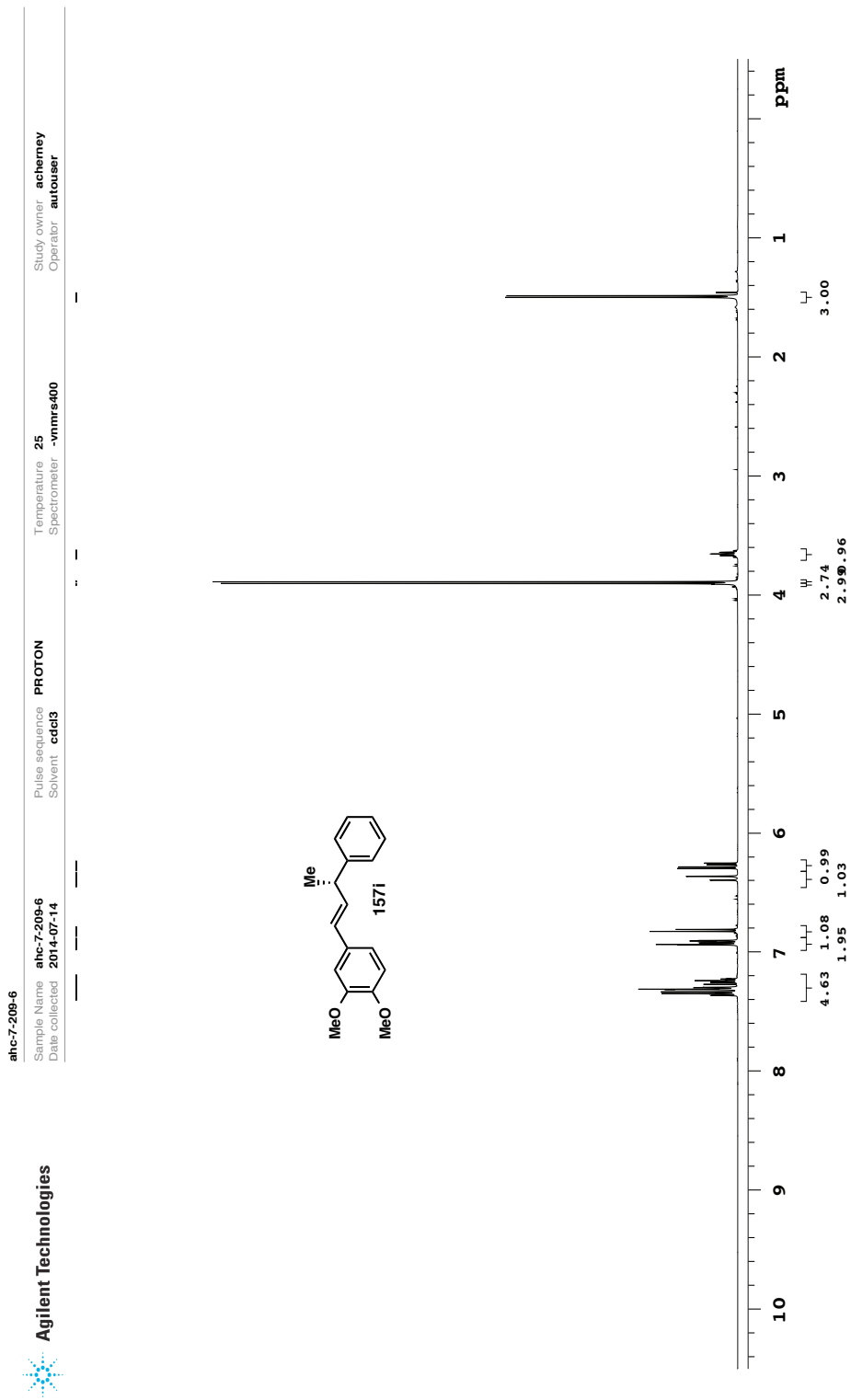
Agilent Technologies

**ahc-7-209-10**  
 Sample Name **ahc-7-209-10**  
 Date collected **2014-07-15**  
 Pulse sequence **CARBON**  
 Solvent **cdcl3**  
 Temperature **25**  
 Spectrometer **-vnmrs-400**  
 Study owner **acherney**  
 Operator **autouser**



Data file /ndy/acherney/vnmrs/data/ahc-7-209-10/CARBON01.fid

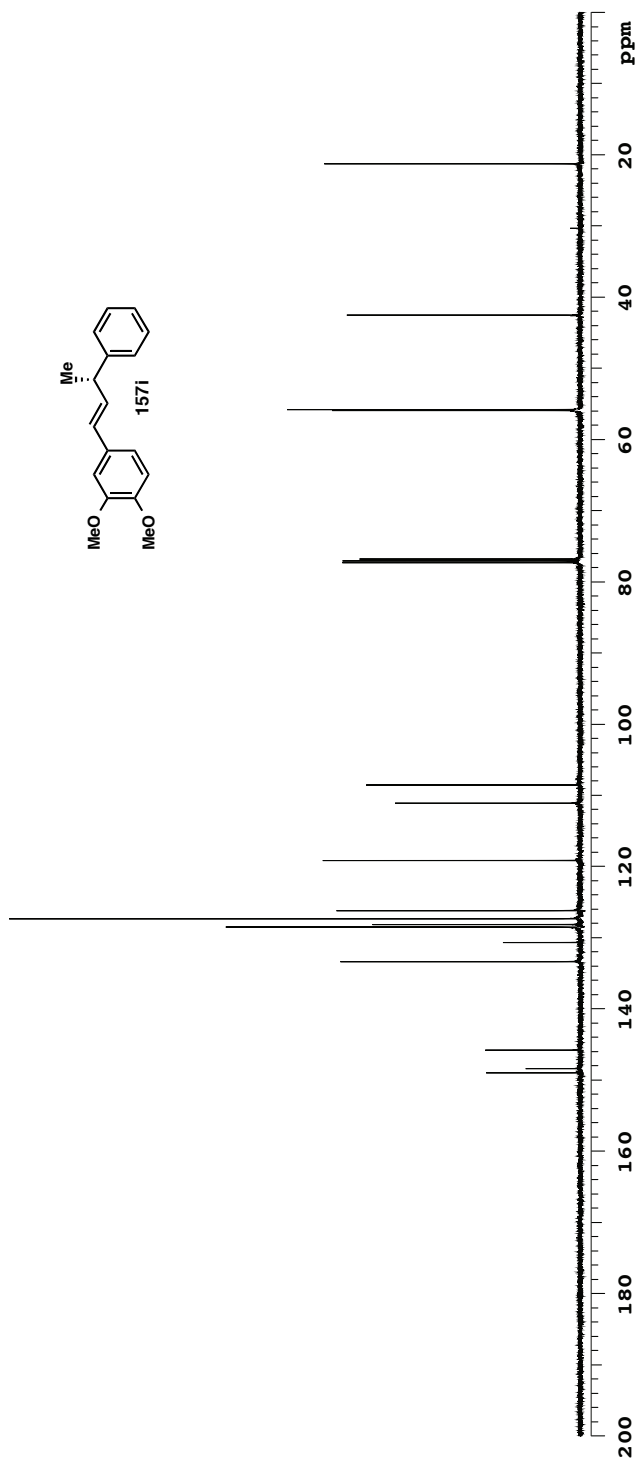
Plot date 2014-07-30



Data file /ndj/acherney/vnmrs/data/ahc-7-209-6/PROTON01.fid

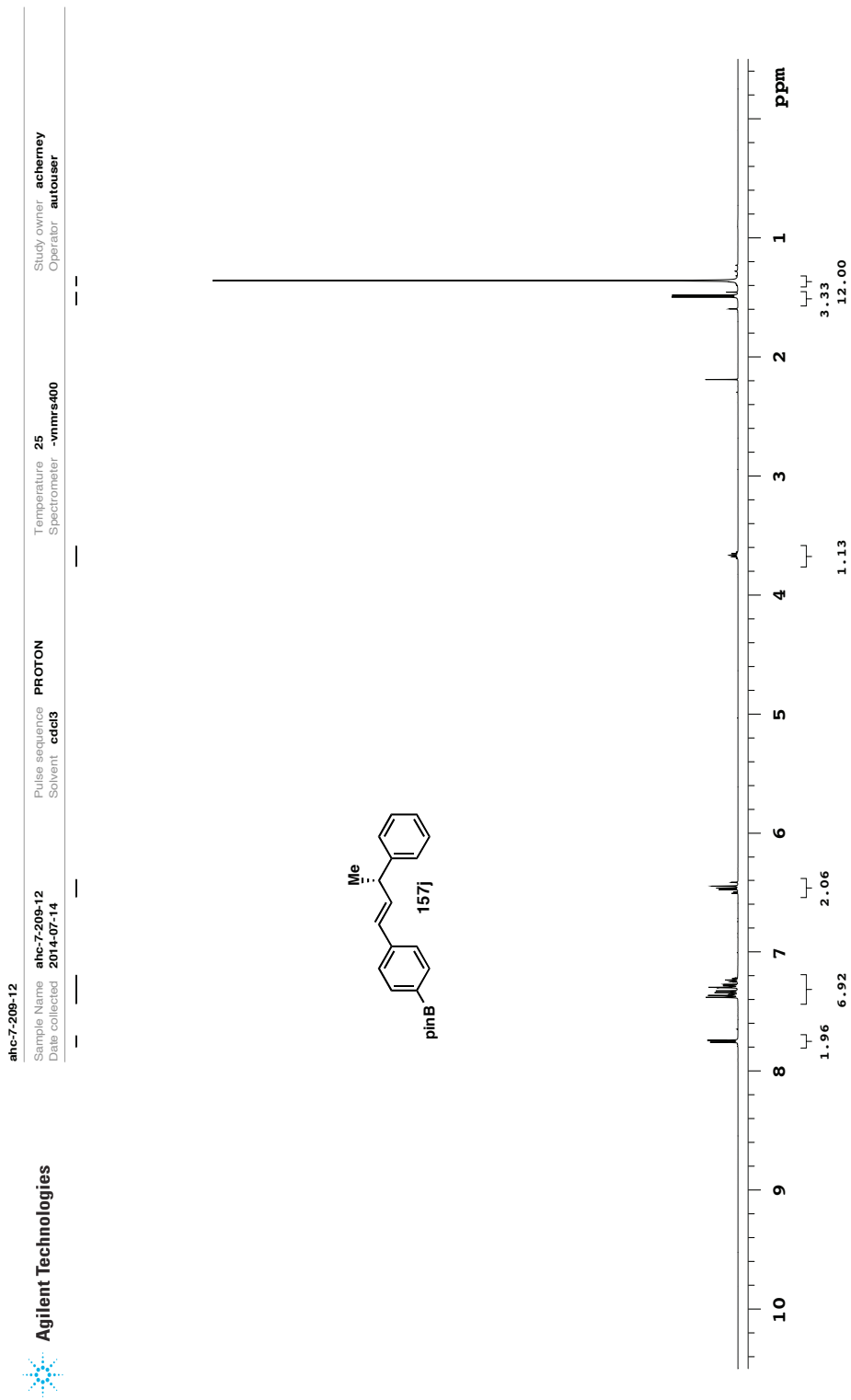
Plot date 2014-07-30

**ahc-7-209-6**  
 Sample Name **ahc-7-209-6**  
 Date collected **2014-07-14**  
 Pulse sequence **CARBON**  
 Solvent **cdcl3**  
 Temperature **25**  
 Spectrometer **-vnmrs-400**  
 Study owner **acherney**  
 Operator **autouser**



Data file /msd/acherney/vnmrs/data/ahc-7-209-6/CARBON01.fid

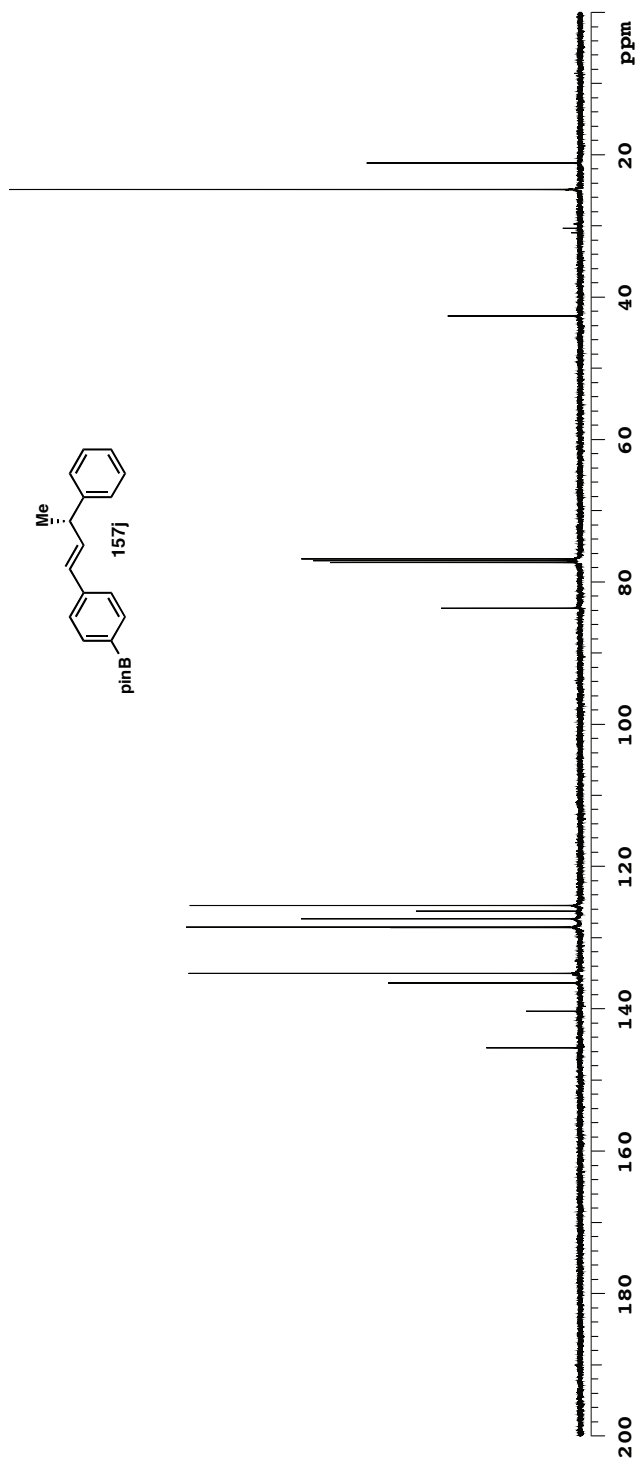
Plot date 2014-07-30



Plot date 2014-07-30

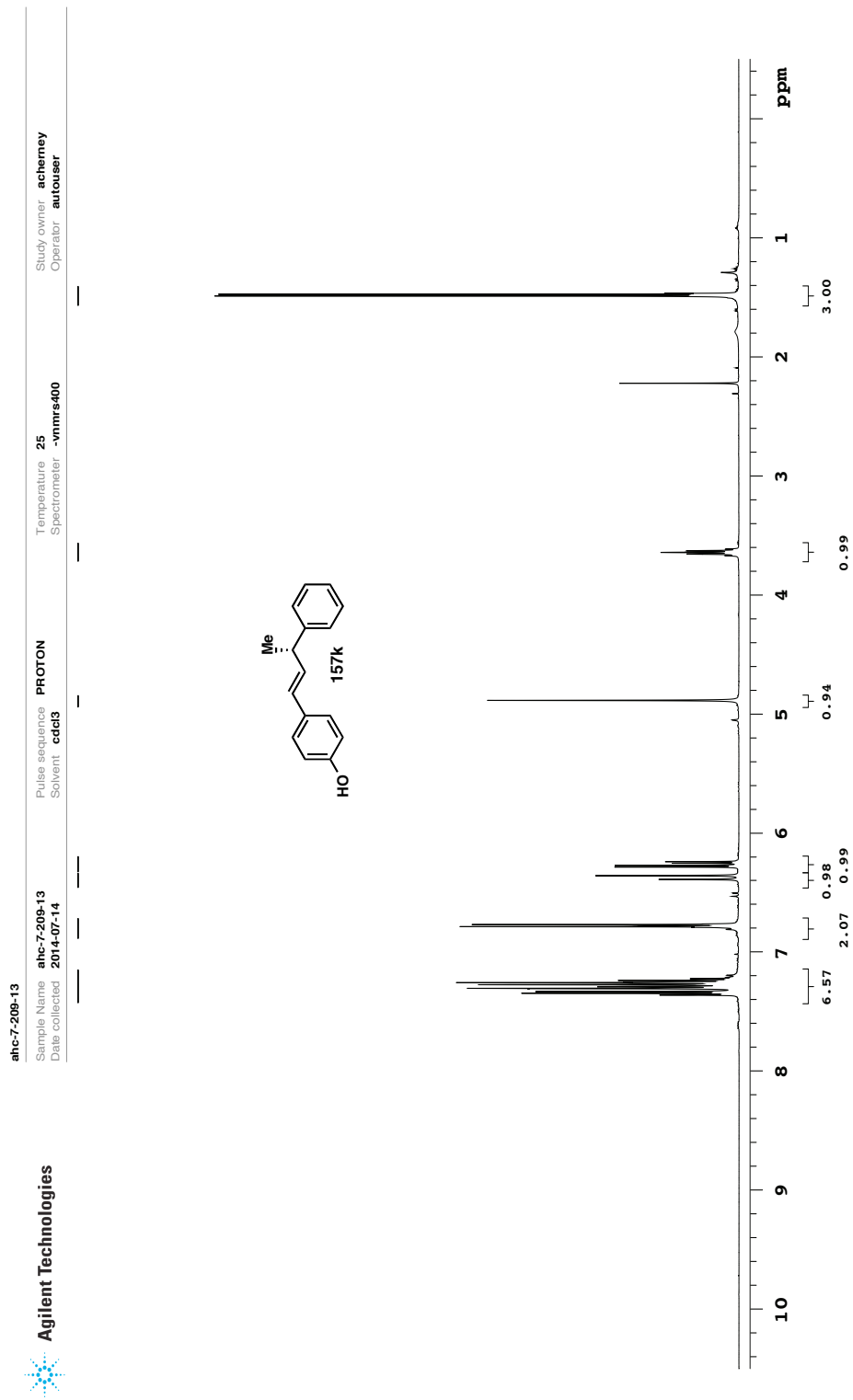
Data file /ndj/acherney/vnmrsysdata/ahc-7-209-12/PROTON01.fid

**ahc-7-209-12**  
 Sample Name **ahc-7-209-12**  
 Date collected **2014-07-14**  
 Pulse sequence **CARBON**  
 Solvent **cdcl3**  
 Temperature **25**  
 Spectrometer **-vnmrs-400**  
 Study owner **acherney**  
 Operator **autouser**



Data file /msd/acherney/vnmrs/data/ahc-7-209-12/CARBON01.fid

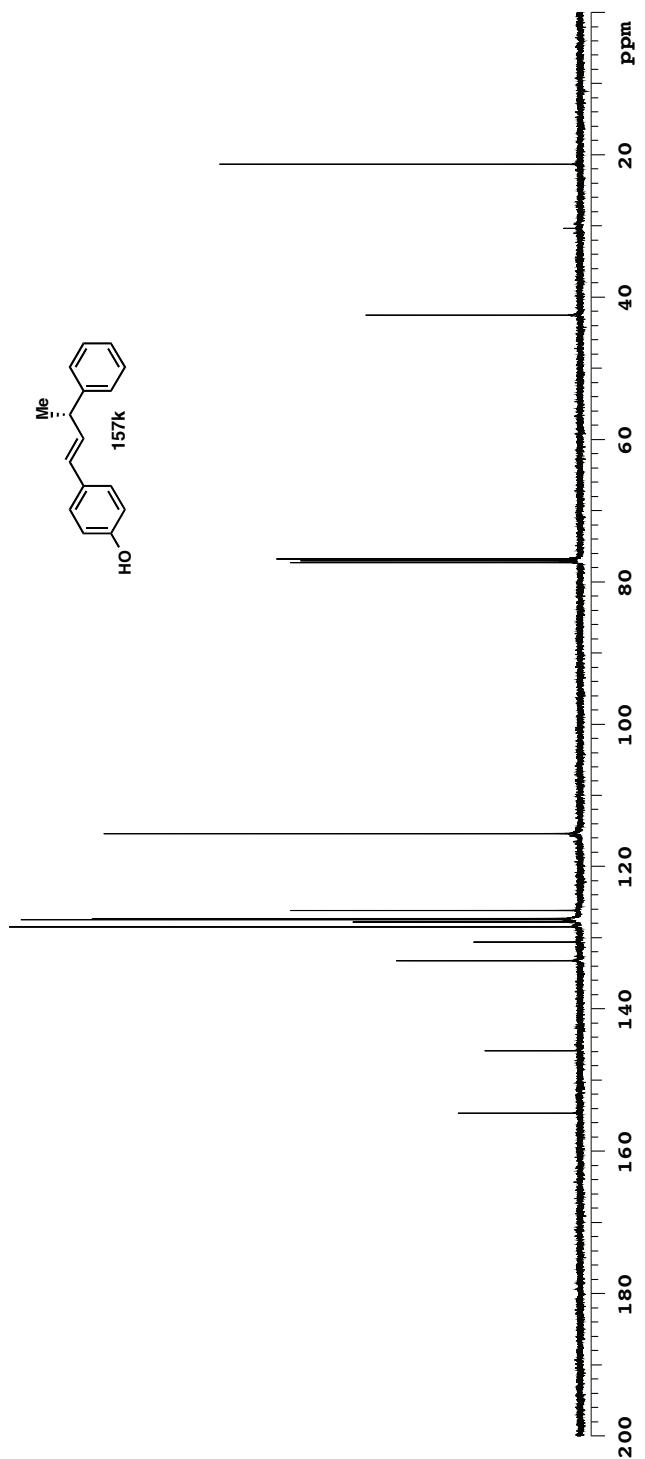
Plot date 2014-07-30



Plot date 2014-07-30

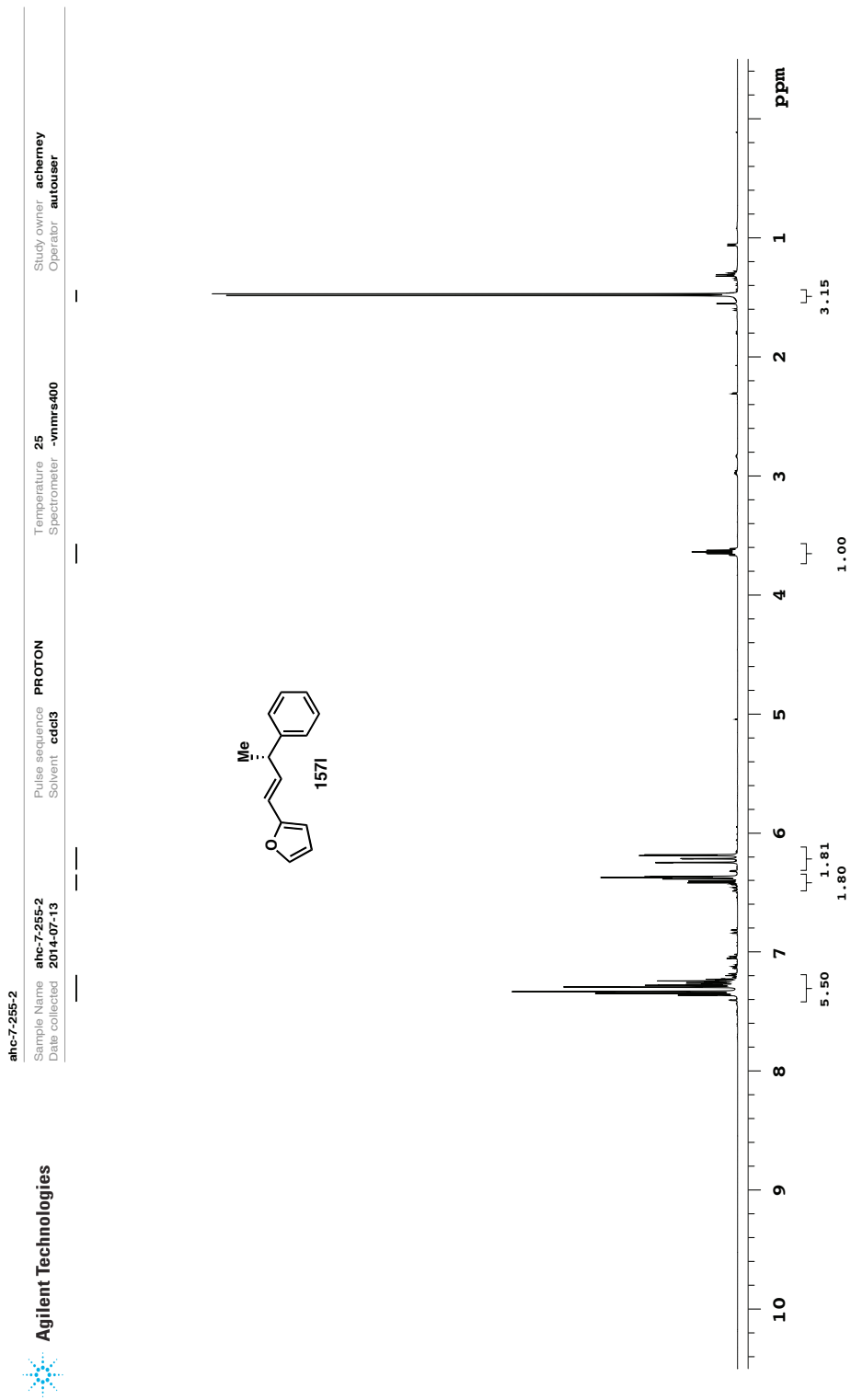
Data file /msj/acherney/vnmrsysdata/ahc-7-209-13/PROTON01.fid

**ahc-7-209-13**  
 Sample Name **ahc-7-209-13**  
 Date collected **2014-07-14**  
 Pulse sequence **CARBON**  
 Solvent **cdcl3**  
 Temperature **25**  
 Spectrometer **-vnmrs-400**  
 Study owner **acherney**  
 Operator **autouser**



Data file /ndy/acherney/vnmrsys\data/ahc-7-209-13/CARBON01.fid

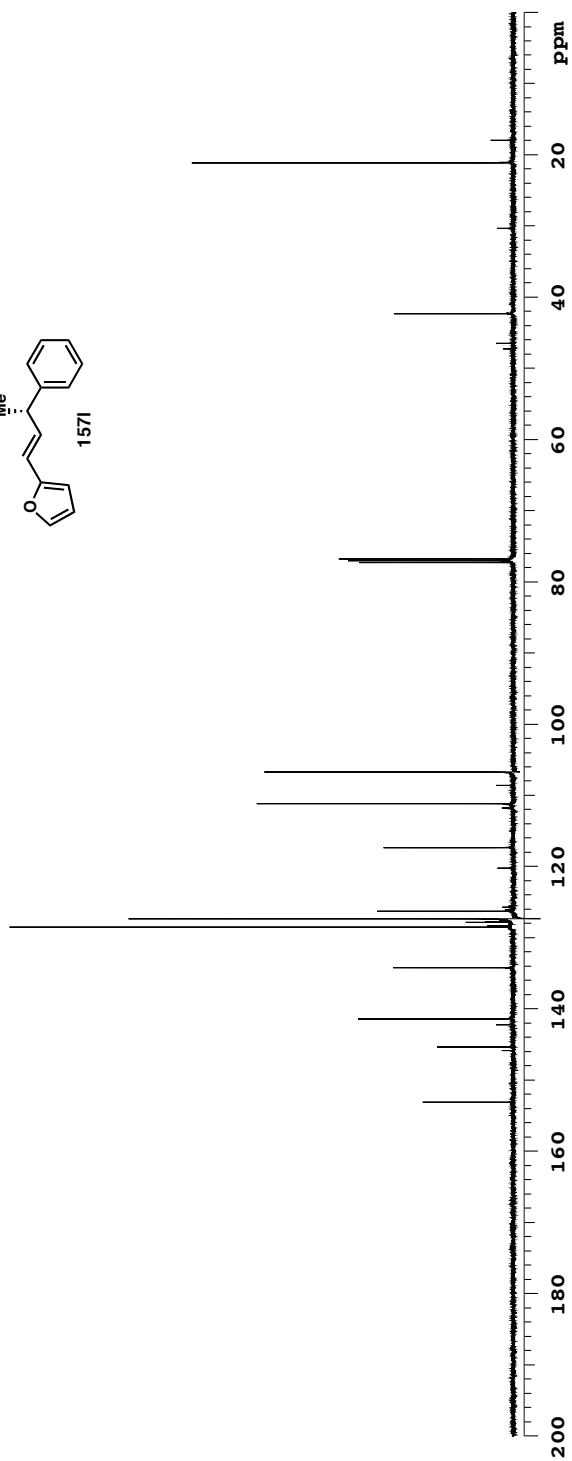
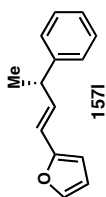
Plot date 2014-07-30



Plot date 2014-07-30

Data file /ndj/acherney/vnmrs/data/ahc-7-255-2/PROTON01.fid

**ahc-7-255-2**  
 Sample Name **ahc-7-255-2**  
 Date collected **2014-07-13**  
 Pulse sequence **CARBON**  
 Solvent **cdcl3**  
 Temperature **25**  
 Spectrometer **-vnmrs-400**  
 Study owner **acherney**  
 Operator **autouser**

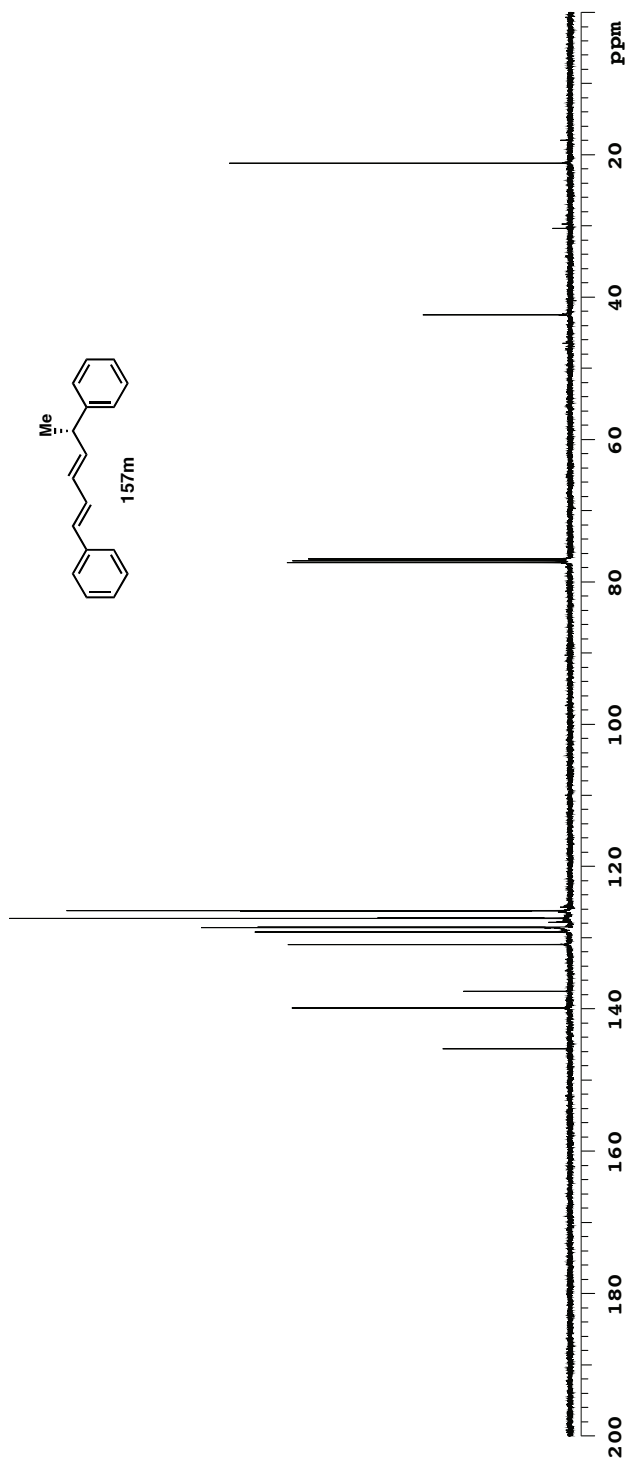


Data file /msd/acherney/vnmrs/data/ahc-7-255-2/CARBON01.fid

Plot date 2014-07-30



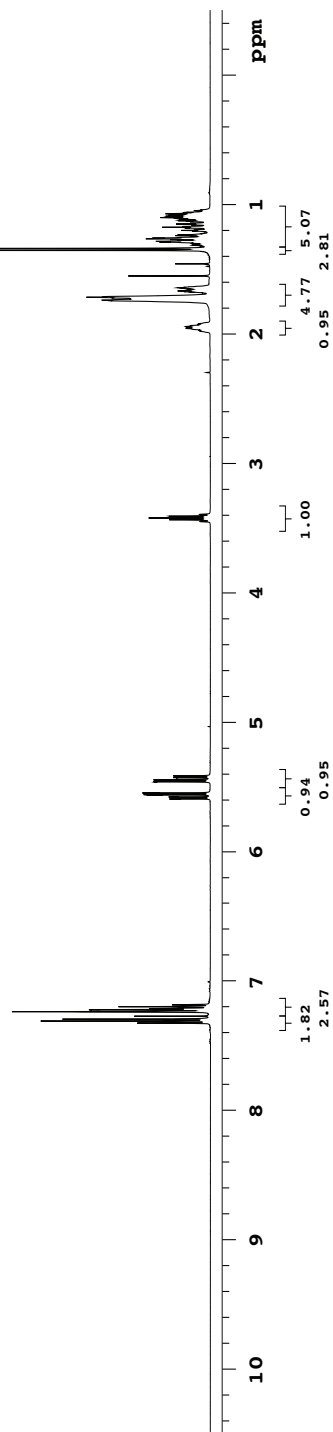
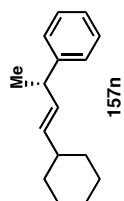
**ahc-7-255-5**  
 Sample Name **ahc-7-255-5**  
 Date collected **2014-07-13**  
 Pulse sequence **CARBON**  
 Solvent **cdcl3**  
 Temperature **25**  
 Spectrometer **-vnmrs-400**  
 Study owner **acherney**  
 Operator **autouser**

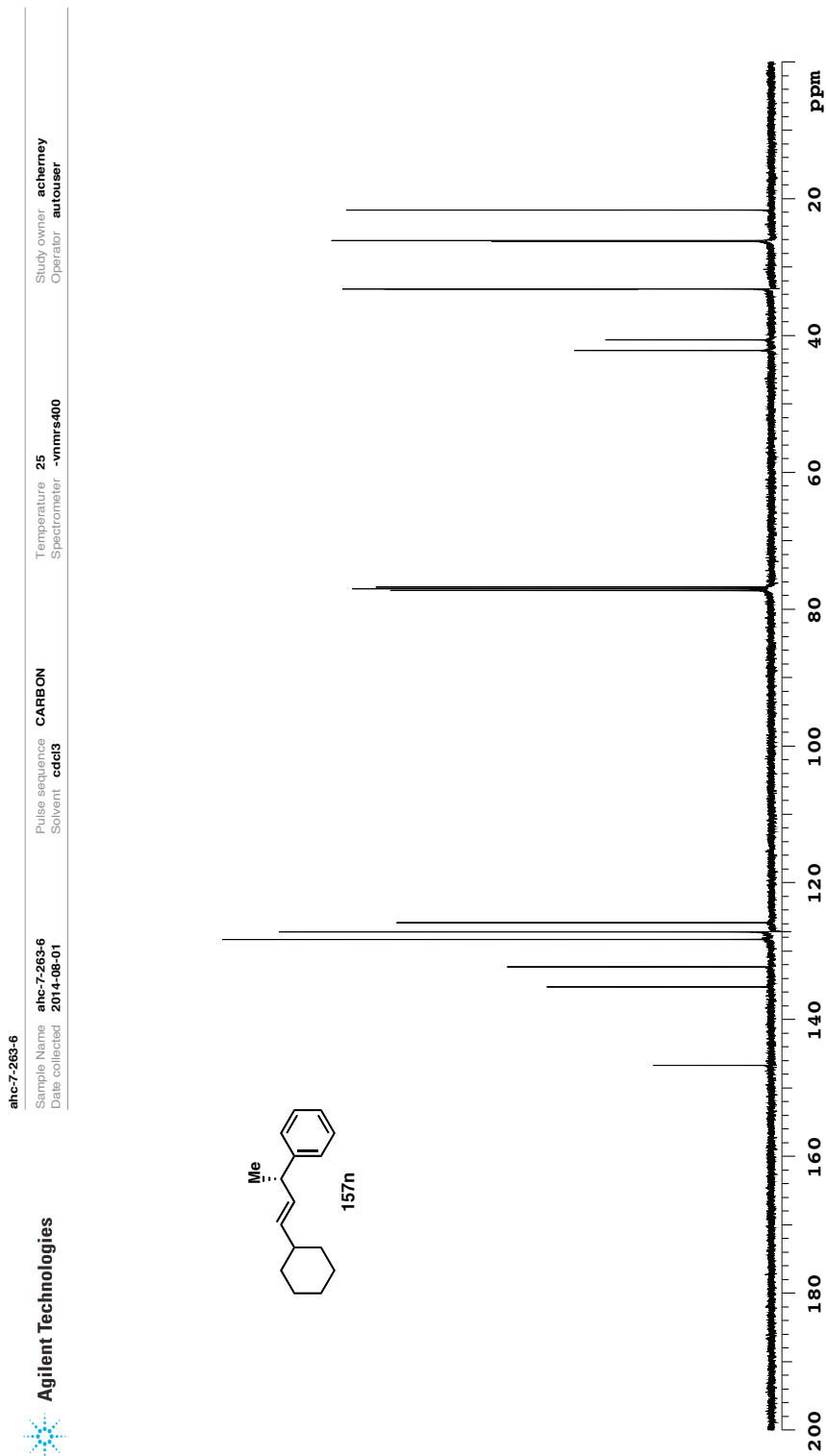


Data file /ndj/acherney/vnmrs/data/ahc-7-255-5/CARBON01.fid

Plot date 2014-07-30

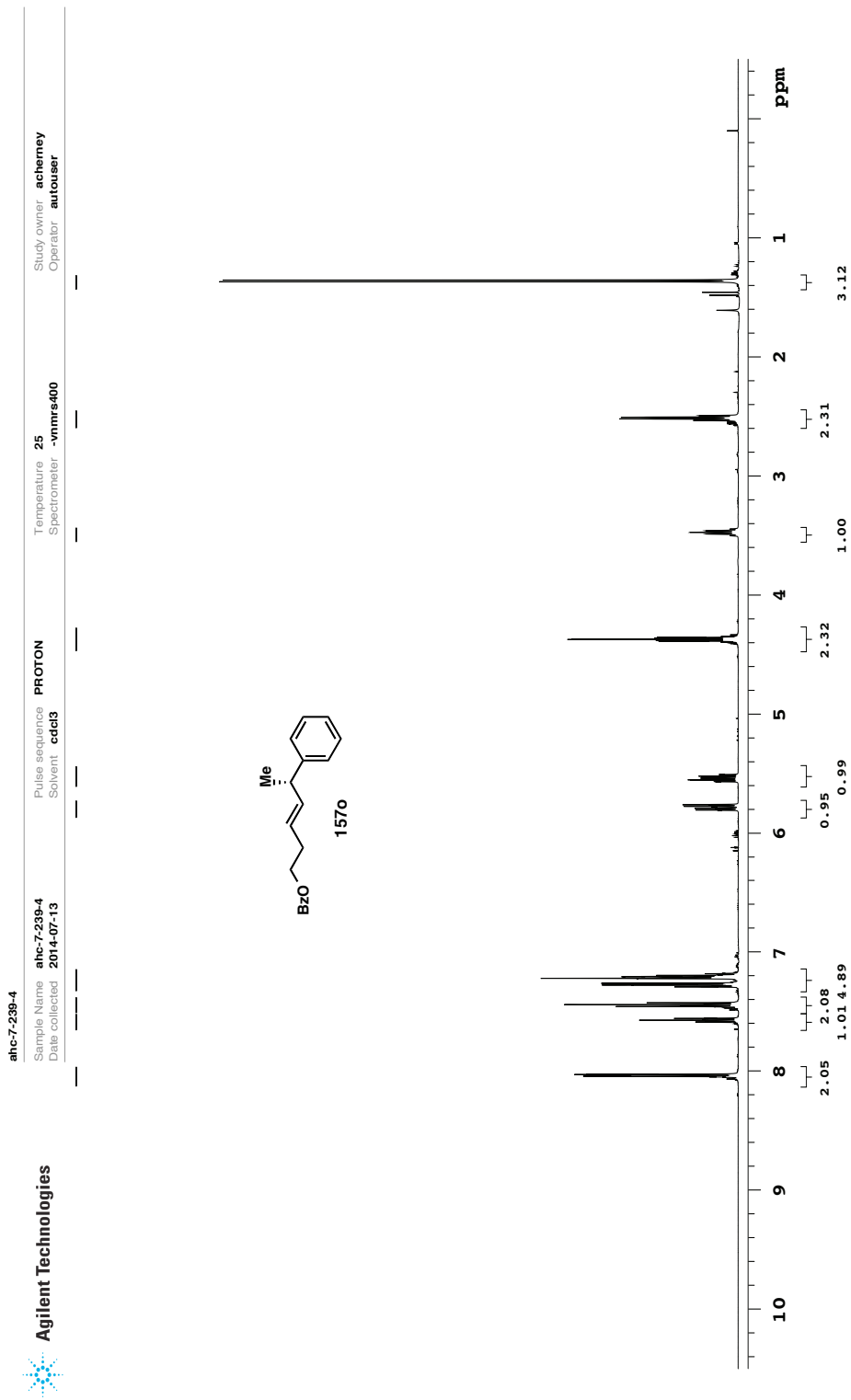
ahc-7-263-6  
 Sample Name **ahc-7-263-6** Pulse sequence **PROTON** Study owner **acherney**  
 Date collected **2014-08-01** Solvent **cdcl3** Spectrometer **25 -vnmrs-400** Operator **autouser**





Plot date 2014-08-01

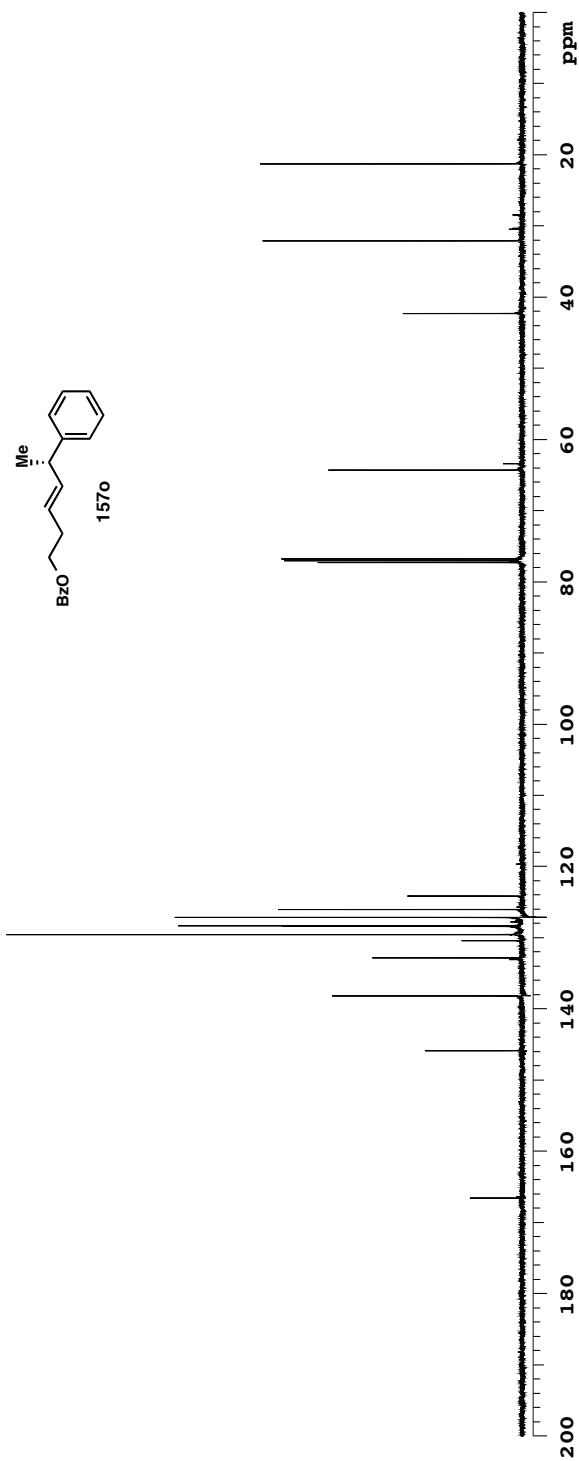
Data file /msd/acherney/vnmrsys\data/ahc-7-263-6/CARBON01.fid



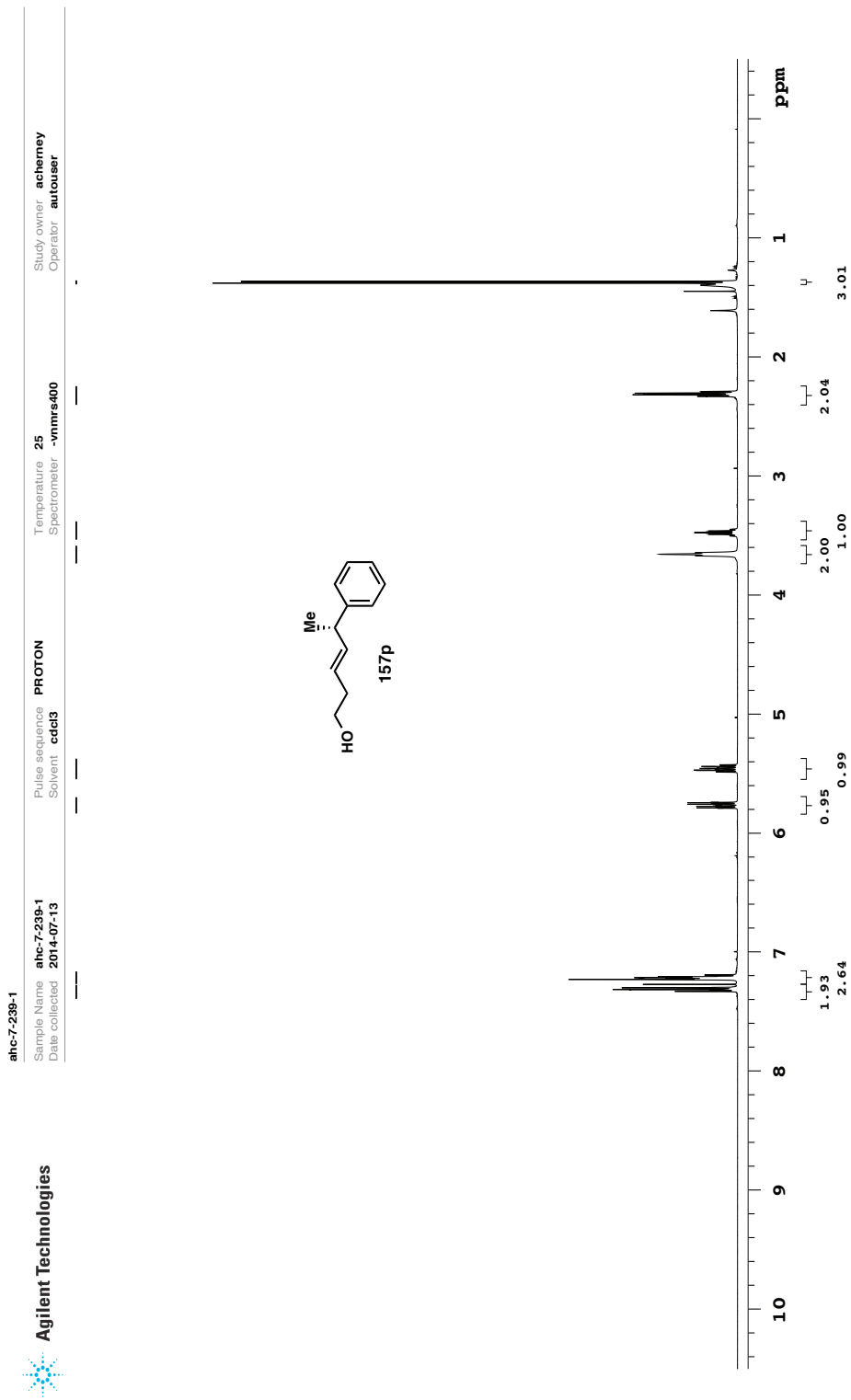
Plot date 2014-07-30

Data file /ndj/acherney/vnmrs/data/ahc-7-239-4/PROTON01.fid

ahc-7-239-4  
 Sample Name **ahc-7-239-4**  
 Date collected **2014-07-13**  
 Pulse sequence **CARBON**  
 Solvent **cdcl3**  
 Temperature **25**  
 Spectrometer **-vnmrs-400**  
 Study owner **acherney**  
 Operator **autouser**



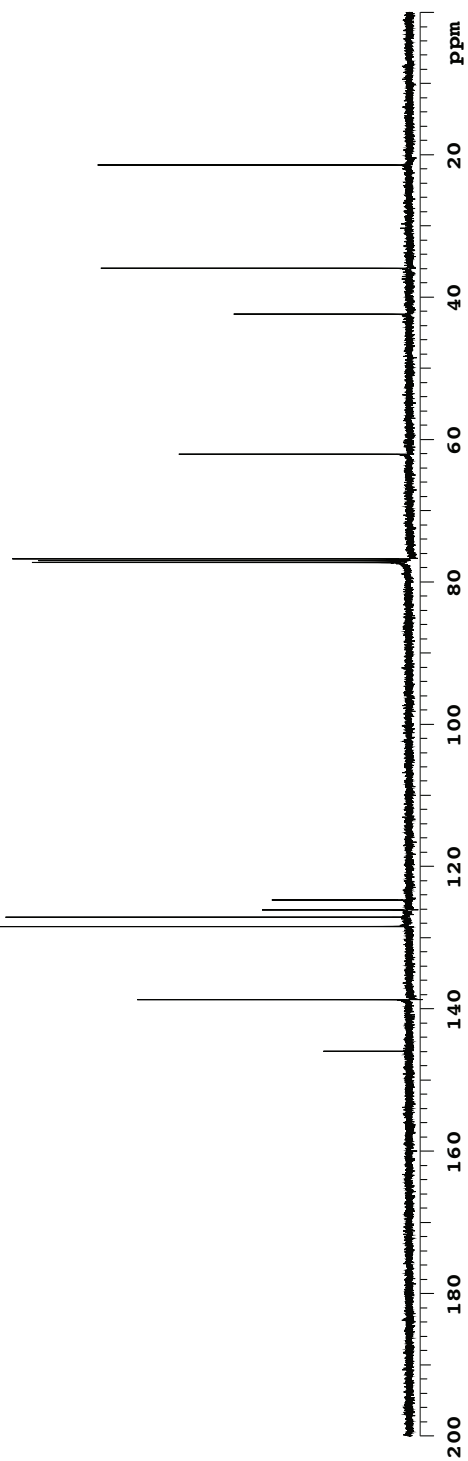
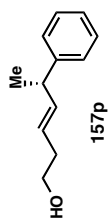
Data file `/ndj/acherney/vnmrs/data/ahc-7-239-4/CARBON01.fid`  
 Plot date 2014-07-30



Plot date 2014-07-30

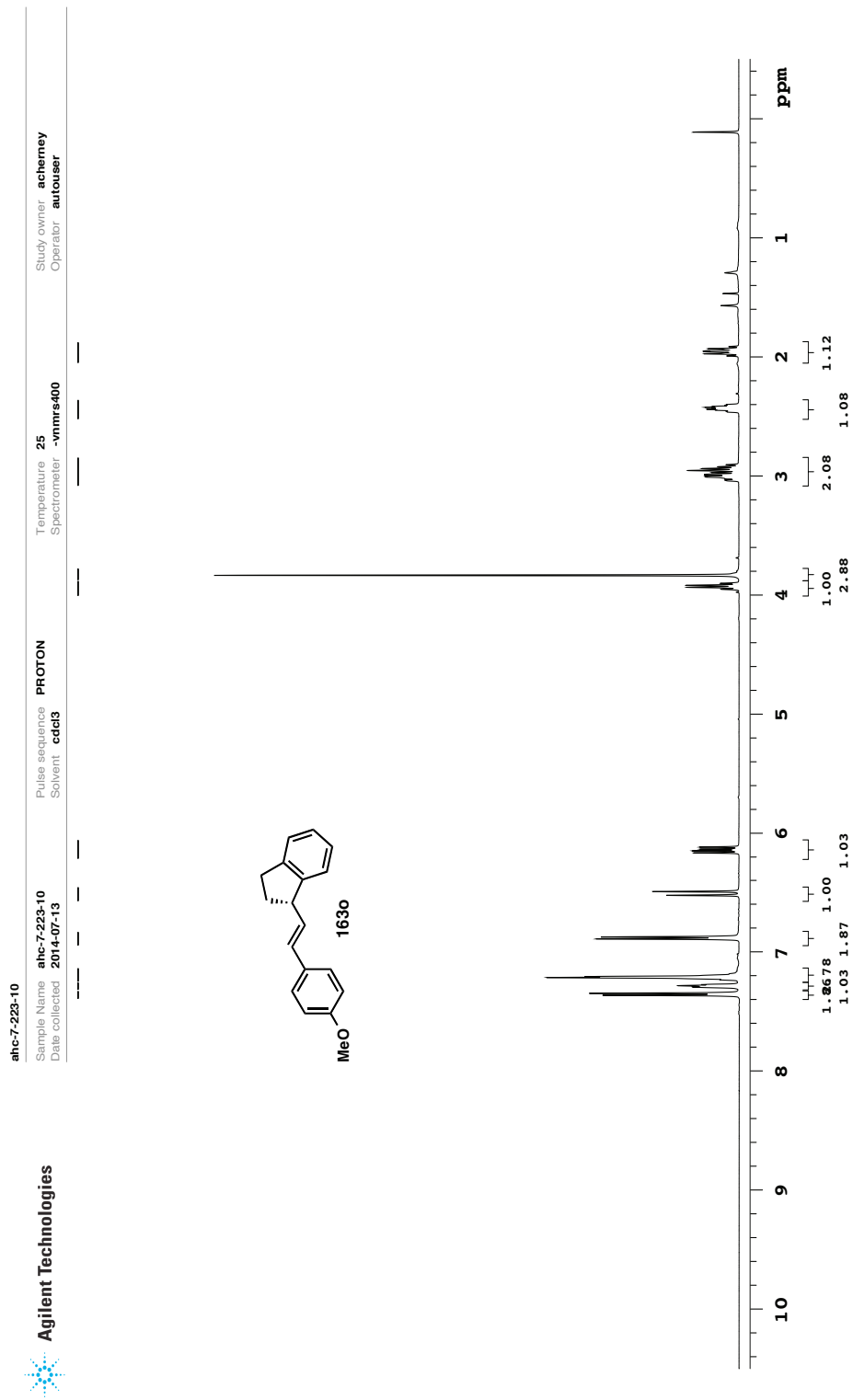
Data file /ndj/acherney/vnmrs/data/ahc-7-239-1/PROTON01.fid

ahc-7-239-1  
 Sample Name ahc-7-239-1  
 Date collected 2014-07-13  
 Pulse sequence CARBON  
 Solvent cdcl3  
 Temperature Spectrometer 25 -vnmrs-400  
 Study owner acherney  
 Operator autouser



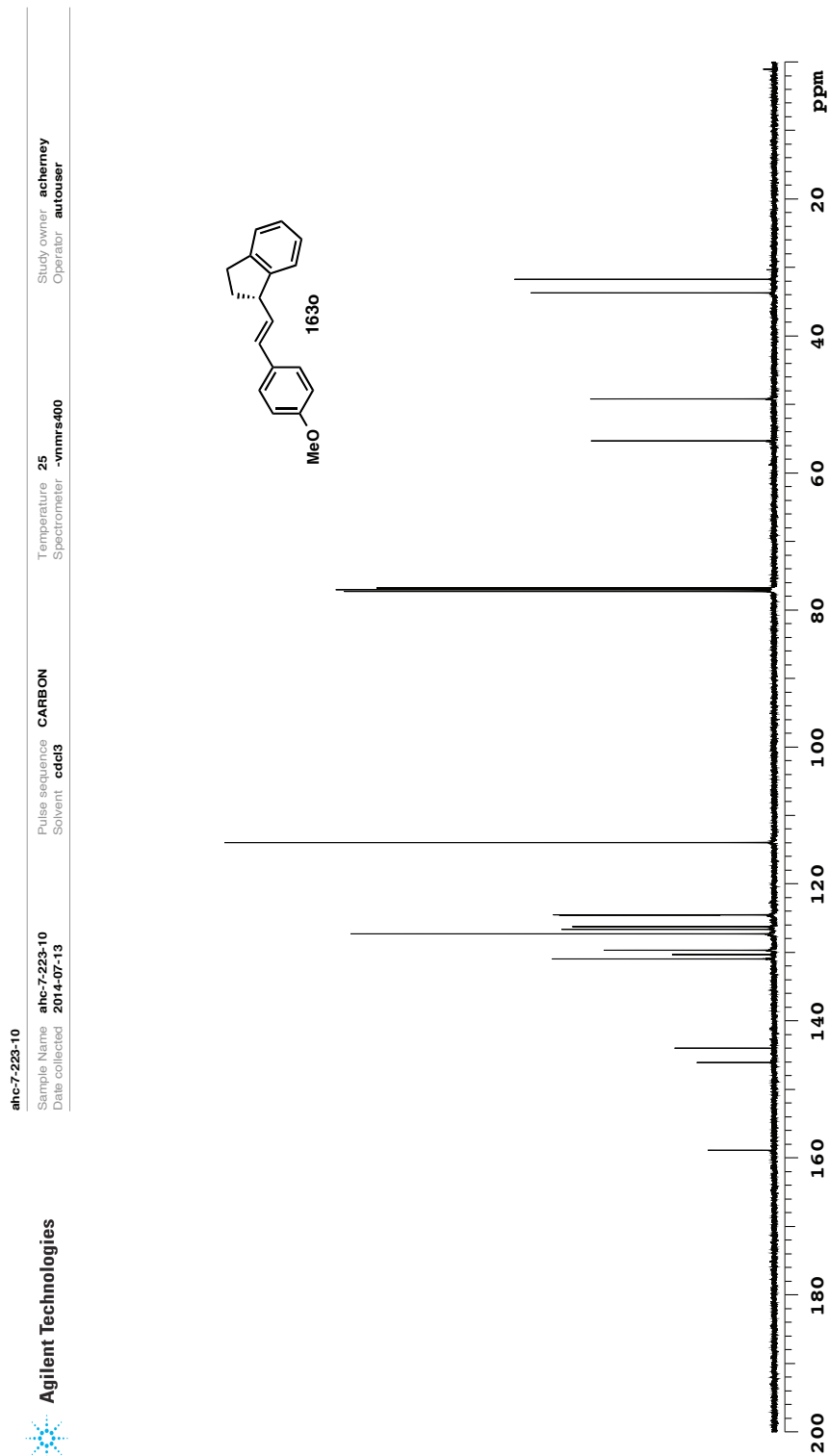
Data file /ndj/acherney/vnmrsys\data/ahc-7-239-1/CARBON01.fid

Plot date 2014-07-30



Data file /ndj/acherney/vnmrsys\data/ahc-7-223-10/PROTON01.fid

Plot date 2014-07-30

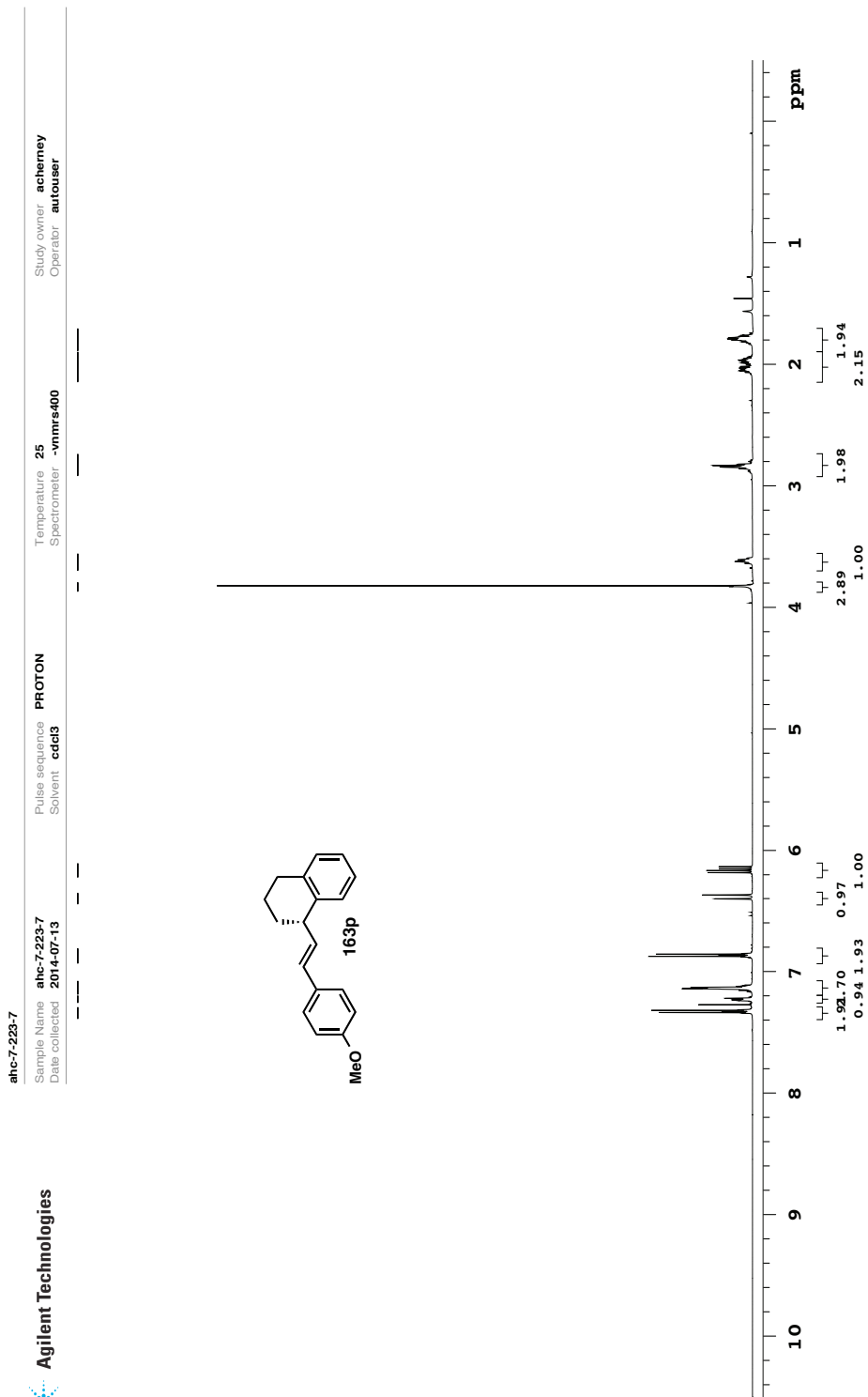


Data file /ndy/acherney/vnmrsys\data/ahc-7-223-10/CARBON01.fid

Plot date 2014-07-30



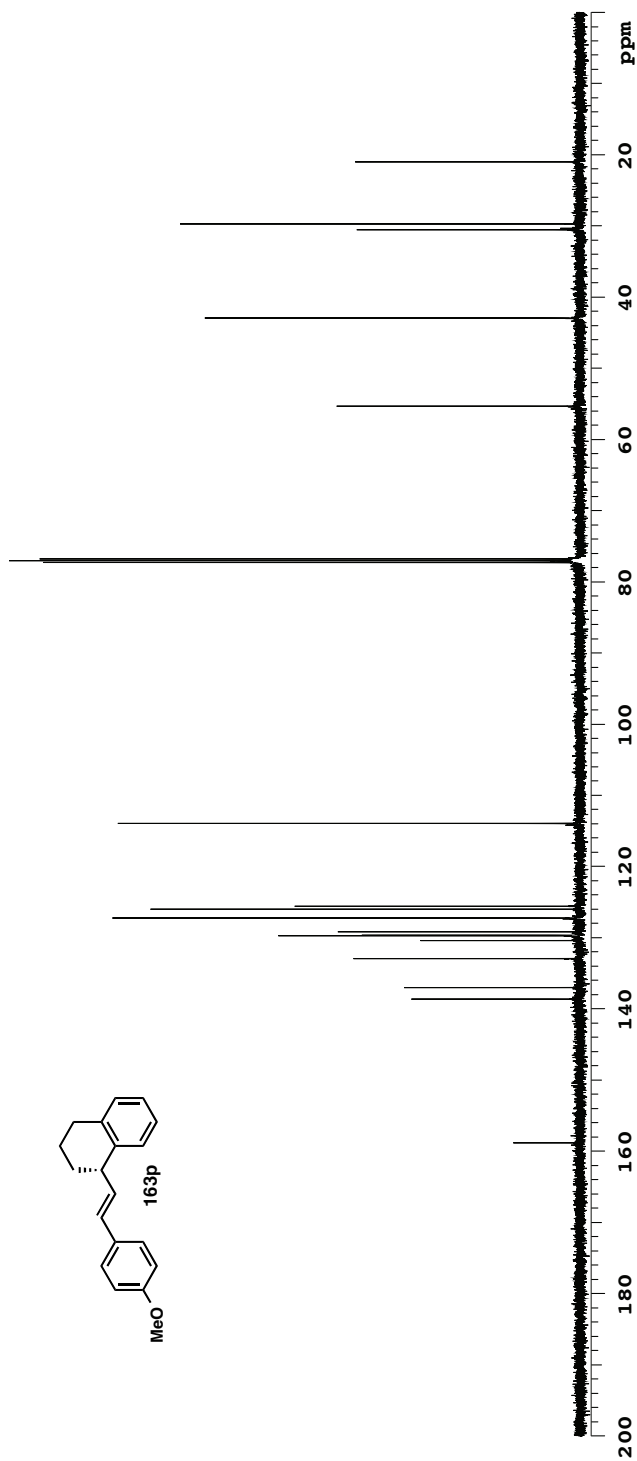
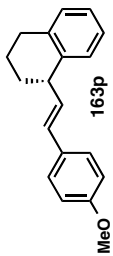
Agilent Technologies



Plot date 2014-07-30

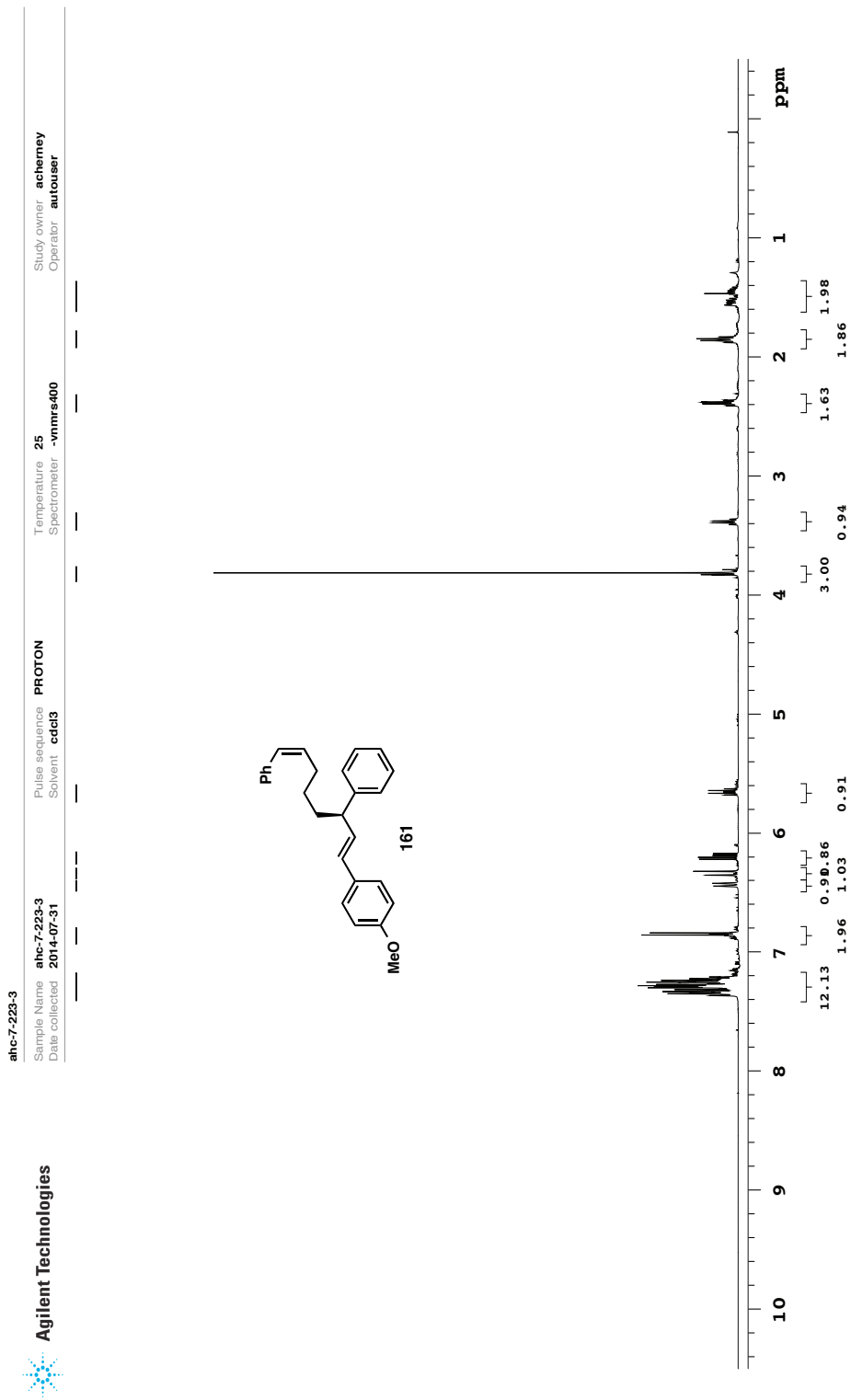
Data file /ndj/acherney/vnmrs/data/ahc-7-223-7/PROTON01.fid

ahc-7-223-7  
 Sample Name ahc-7-223-7  
 Date collected 2014-07-13  
 Pulse sequence CARBON  
 Solvent cdcl3  
 Temperature 25  
 Spectrometer -vnmrs-400  
 Study owner acherney  
 Operator autouser



Data file /msj/acherney/vnmrs/data/ahc-7-223-7/CARBON01.fid

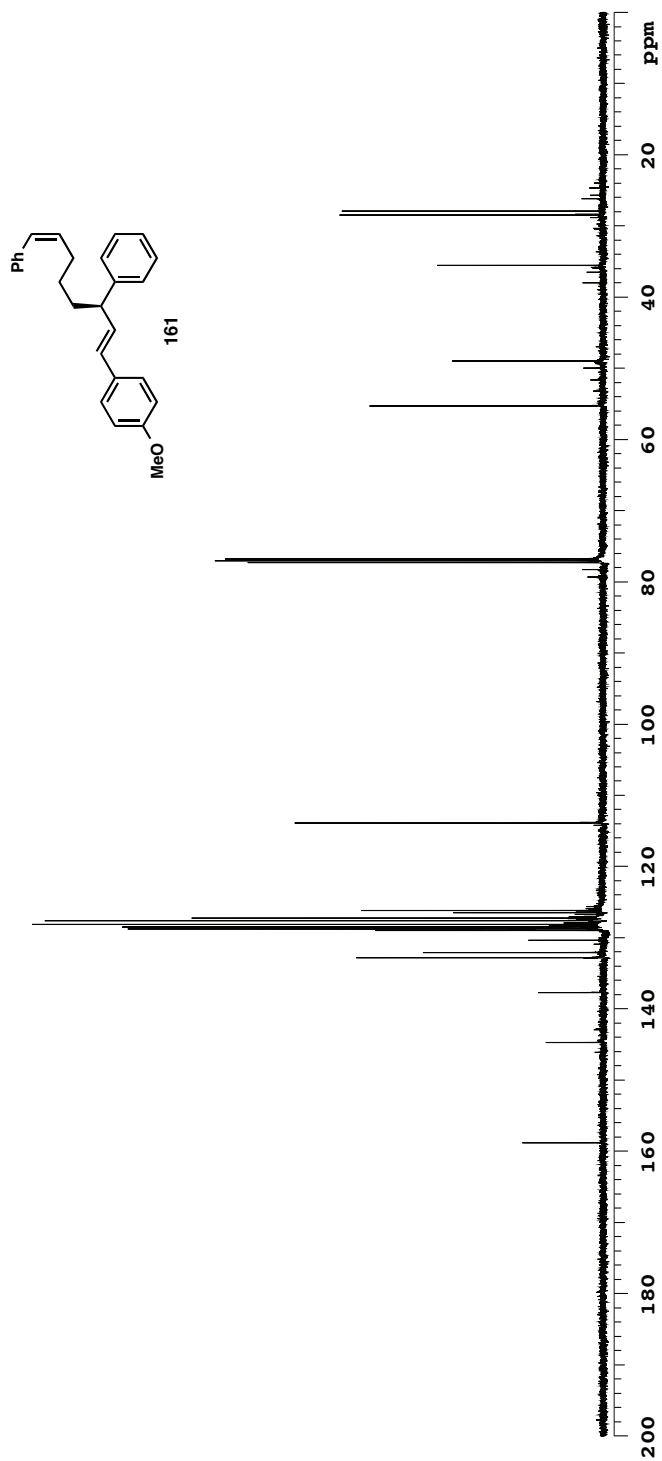
Plot date 2014-07-30



Data file /ndj/acherney/vnmrsysdata/ahc-7-223-3/PROTON01.fid

Plot date 2014-08-01

ahc-7-223-3  
 Sample Name ahc-7-223-3  
 Date collected 2014-07-31  
 Pulse sequence CARBON  
 Solvent cdcl3  
 Temperature 25  
 Spectrometer -vnmrs-400  
 Study owner acherney  
 Operator autouser



Data file /msj/acherney/vnmrs/data/ahc-7-223-3/CARBON01.fid

Plot date 2014-08-01

## Chapter 5

### *Toward New Coupling Partners for Asymmetric Ni-Catalyzed Reductive Cross-Coupling*

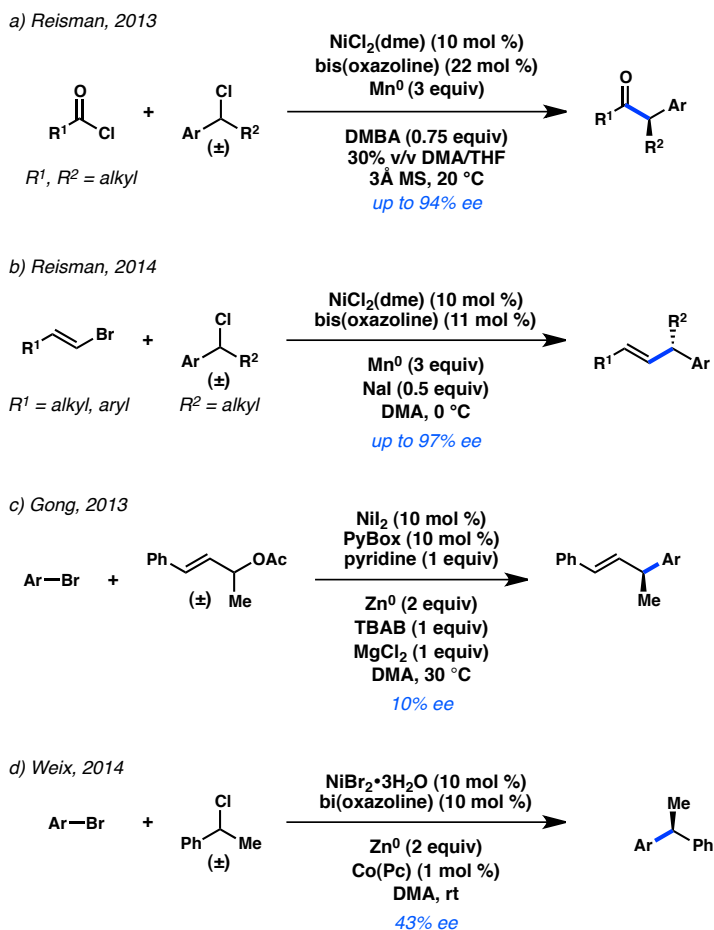
#### 5.1 INTRODUCTION

The last several years have witnessed a renaissance in Ni-catalyzed reductive cross-coupling methodologies because of its wide functional group tolerance, operational simplicity, use of readily available air- and moisture-stable starting materials, and utilization of earth-abundant first-row transition metals (see Chapter 3).<sup>1</sup> Ni catalysts have also shown a proficiency in the coupling of C(sp<sup>3</sup>)-hybridized reaction partners, allowing for a natural expansion of Ni-catalyzed reductive cross-couplings toward the regime of alkyl coupling.<sup>2</sup> The ability to generate C(sp<sup>3</sup>)-C(sp<sup>x</sup>) bonds raises additional considerations with respect to control of the newly-formed stereogenic center.

Prior to our own studies, no enantioconvergent Ni-catalyzed reductive cross-couplings of organohalide electrophiles had been reported in the literature. In 2013, we

disclosed the highly enantioselective coupling of benzyl chlorides and acid chlorides to furnish  $\alpha,\alpha$ -disubstituted ketone products (Scheme 5.1, a).<sup>3</sup> The next year, we extended our protocol to the coupling of benzyl chlorides and vinyl bromides, achieving up to 97% ee (Scheme 5.1, b).<sup>4</sup> Concurrent investigations by other laboratories have also resulted in promising levels of enantioinduction. Gong and coworkers demonstrated that allylic acetates could be arylated in 10% ee by a Ni/PyBox system (Scheme 5.1, c).<sup>5</sup> Weix and coworkers have recently shown that a benzyl chloride and an aryl bromide can be coupled to yield a diarylalkane in 43% ee (Scheme 5.1, d).<sup>6,7</sup>

**Scheme 5.1.** Enantioconvergent Ni-catalyzed reductive cross-coupling.

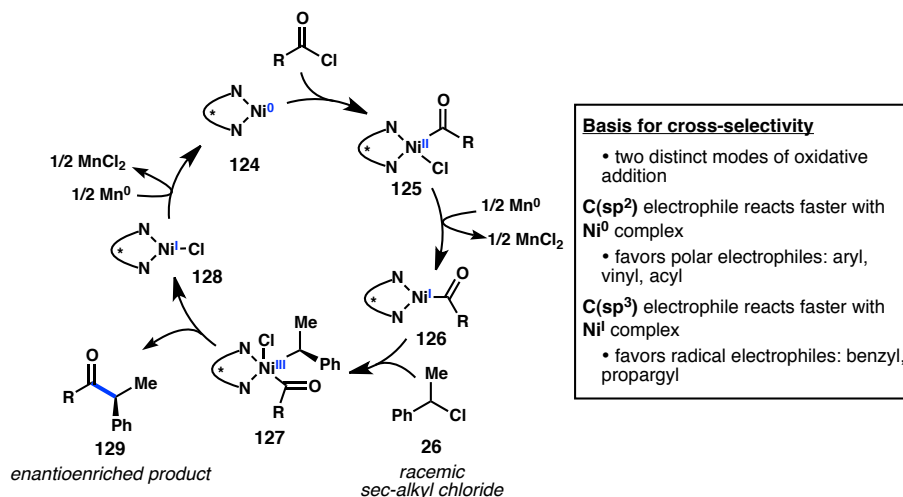


While these results illustrate the general potential of asymmetric Ni-catalyzed reductive cross-coupling, a number of challenges still remain for the development of novel transformations. For example, all highly enantioselective reductive couplings in the literature have required the use of a benzyl halide starting material. Furthermore, while certain racemic reductive couplings are tolerant of heteroaromatic groups, such a substrate scope has not yet been achieved under asymmetric conditions employing bis(oxazoline) ligands. Lastly, while achiral ligand tuning is often performed to minimize homocoupling in reductive methodologies, it is still difficult to engineer a ligand that simultaneously delivers high enantioinduction as well as high cross-selectivity.

Greater mechanistic understanding of these transformations will increase our ability to rationally optimize reaction conditions and will also provide a basis for initial identification of reaction partners. While further mechanistic investigations are necessary, we currently look to a sequential reduction mechanism as a model for thinking about our desired reactivity (Figure 5.1, also see Chapter 3). Importantly, this model can help explain the origin of cross-selectivity in our systems. We hypothesize that this selectivity arises from two distinct modes of oxidative addition within the sequential reduction mechanism: 1) oxidative addition by a  $\text{Ni}^0$  complex, which often proceeds via a polar two-electron mechanism that allows polar-type electrophiles, including aryl, vinyl, and acyl halides to react readily and 2) oxidative addition by a  $\text{Ni}^I$  complex that is more likely to occur through single-electron elementary steps. These steps include halide abstraction to form a  $\text{Ni}^{II}$  complex and a carbon-centered radical, followed by rapid recombination to give  $\text{Ni}^{III}$  complex **127**. Electrophiles that can stabilize the formation of a transient radical, such as benzyl or propargyl halides, would react faster under these conditions

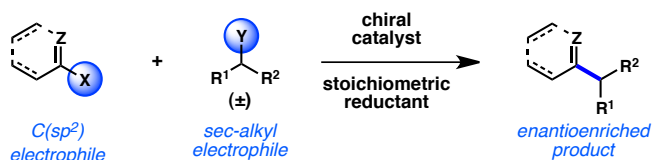
than polar-type electrophiles. Homocoupling can arise if  $\text{Ni}^0$  reacts with benzyl chloride **26** in an  $\text{S}_{\text{N}}2$ -type oxidative addition, followed by a second radical-type oxidative addition of  $\text{Ni}^{\text{I}}$  to **26** and subsequent reductive elimination.

**Figure 5.1.** Model for cross-selectivity.



With these concepts in mind, we became interested in the idea that these couplings could serve as a general platform for the synthesis of enantioenriched small molecule building blocks. We envisioned that with a judicious choice of both a polar electrophile and a radical electrophile, a wide variety of enantioselective Ni-catalyzed reductive cross-couplings could be developed, provided that an appropriate chiral catalyst is identified (Figure 5.2). Critically, in order to facilitate enantioinduction, we reasoned that the alkyl coupling partner must either contain a directing group or bear sterically- or electronically-differentiated  $\text{R}^1$  and  $\text{R}^2$  groups.

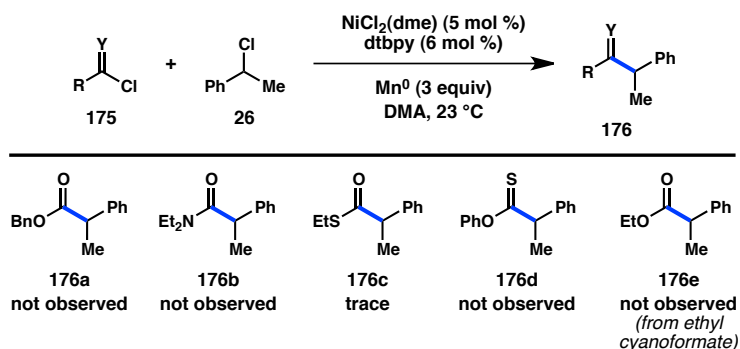
**Figure 5.2.** Outline of a general platform for asymmetric reductive cross-coupling.



## 5.2 DEVELOPMENT OF NEW NI-CATALYZED REDUCTIVE CROSS-COUPPLINGS (RACEMIC OR ACHIRAL)

Acid chlorides are widely available starting materials that readily react with Ni catalysts under reductive conditions. In 2012, Weix and Gong independently disclosed the reductive cross-coupling of alkyl halides with alkyl or aryl acid chlorides, respectively.<sup>8</sup> Building on these results, we reported an asymmetric coupling of alkyl acid chlorides and benzyl chlorides.<sup>3</sup> In an attempt to increase the substrate scope toward other carbonyl derivatives, we investigated substrates of general formula **175** in the presence of NiCl<sub>2</sub>(dme)/dtbpy (Figure 5.3). Under these conditions, we failed to observe product formation when using a chloroformate or a carbamoyl chloride. Thioester **176c** is generated in a trace amount, but competitive levels of homocoupling are also observed. Lastly, we found that cyanoformates do not provide **176e** as the desired product.

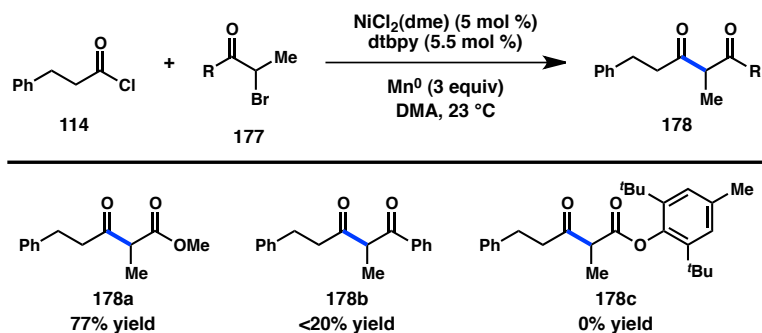
**Figure 5.3.** Coupling of other carbonyl chlorides with benzyl chlorides.



With respect to acid chlorides, we have tried to identify additional radical-type electrophiles that will facilitate cross-coupling over homocoupling. Durandetti and coworkers have demonstrated that  $\alpha$ -chloroesters react with aryl halides under reductive Ni catalysis.<sup>9</sup> We investigated the racemic coupling of acid chloride **114** with several  $\alpha$ -

bromocarbonyl compounds (Figure 5.4).  $\alpha$ -Bromoester **177a** delivered  $\beta$ -ketoester **178a** in 77% yield; a screen of chiral ligands provided no enantioinduction, likely because the low pKa of **178a** would allow racemization under very mild conditions. Under identical coupling conditions, a lower yield was realized for  $\alpha$ -bromoketone **177b** and no product was observed for aryl ester **177c**. The high selectivity for the coupling of  $\alpha$ -bromoester **177a** should be studied further to better understand the reactivity that may permit the development of an enantioselective transformation.

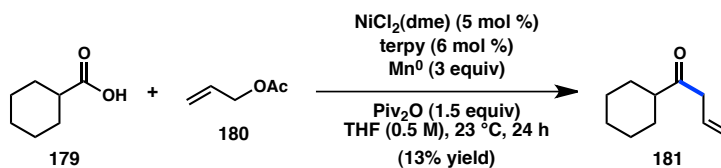
**Figure 5.4.** Coupling of  $\alpha$ -halocarbonyl compounds with acid chlorides.



We next studied the reductive cross-coupling of acyl equivalents and allyl electrophiles. Over the last several years, allyl acetates<sup>5,10</sup> and carbonates<sup>11</sup> have each been shown to react with aryl and alkyl halides in the presence of a Ni catalyst. Allyl electrophiles are distinct from benzyl ones in that regioselectivity issues arise and that they can readily react with  $\text{Ni}^0$  to form a  $\pi$ -allyl Ni complex. We questioned whether an in situ-generated mixed anhydride, prepared from a free carboxylic acid, would be amenable to reductive cross-coupling with allyl acetate (**180**).<sup>8d,12</sup> We commenced by screening several ligand (dtbpy, terpy, phen) and solvent (DMA, DMF, DMPU, THF) combinations with  $\text{NiCl}_2(\text{dme})$ ,  $\text{Mn}^0$ , and  $\text{Piv}_2\text{O}$  (Scheme 5.2). Only when running the

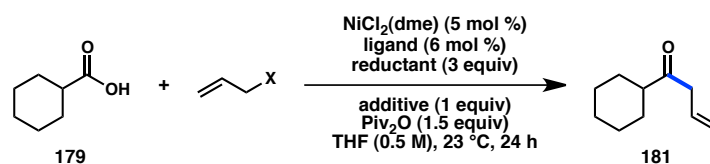
reaction with terpy in THF were we able to form ketone **181**, resulting in a 13% yield; the isomerized  $\alpha,\beta$ -unsaturated ketone was not detected in the crude reaction mixture.

**Scheme 5.2.** Initial result for an acyl-allyl reductive cross-coupling.



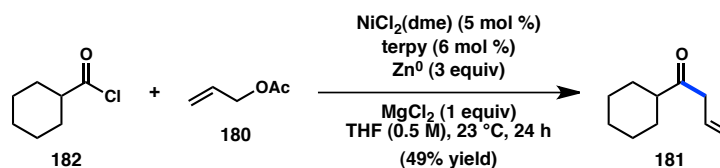
Using these conditions as a starting point, we screened a variety of parameters to increase the yield of the coupling reaction. When either  $\text{Mn}^0$  or  $\text{Zn}^0$  is used as the reductant, allyl carbonate and allyl bromide fail to form ketone **181** (Table 5.1). In the presence of  $\text{Mn}^0$ , electron-rich ligand  $t\text{Bu-terpy}$  performs better than unsubstituted terpy (entries 1 and 4). While  $\text{MgCl}_2$  inhibits product formation for  $\text{Mn}^0$ -mediated reactions, it was found to be critical to promote  $\text{Zn}^0$ -mediated reactivity (entries 6–9). Under these conditions, terpy delivered ketone **181** in 23% yield, but more electron-rich  $t\text{Bu-terpy}$  produced **181** in only 7% yield (entries 9 and 12). Additional studies examining Ni source, solvent, catalyst loading, and ligand loading were unsuccessful at increasing the product yield;  $\text{Boc}_2\text{O}$  was also inefficient as a replacement for  $\text{Piv}_2\text{O}$ . Interestingly, running the reaction at 60 °C provided the corresponding  $\alpha,\beta$ -unsaturated ketone instead of desired  $\beta,\gamma$ -unsaturated ketone **181**.

For the reductive coupling of the free carboxylic acid to be successful, mixed anhydride formation must be fast relative to oxidative addition of the electrophiles. The coupling of pregenerated acyl electrophiles were studied in order to understand whether the low yields were due to inefficient anhydride formation or problematic steps in the catalytic cycle itself. 2-Pyridyl thioesters reacted poorly under the previously optimized

**Table 5.1.** Exploration of an acyl-allyl reductive cross-coupling.

Entry	Reductant	Ligand	X	Additive	Yield (%)
1	Mn <sup>0</sup>	terpy	OAc	--	13
2	Mn <sup>0</sup>	terpy	OCO <sub>2</sub> Me	--	0
3	Mn <sup>0</sup>	terpy	Br	--	0
4	Mn <sup>0</sup>	<sup>t</sup> Bu-terpy	OAc	--	22
5	Mn <sup>0</sup>	<sup>t</sup> Bu-terpy	OCO <sub>2</sub> Me	--	0
6	Mn <sup>0</sup>	<sup>t</sup> Bu-terpy	Br	--	0
7	Mn <sup>0</sup>	terpy	OAc	MgCl <sub>2</sub>	0
8	Zn <sup>0</sup>	terpy	OAc	--	0
9	Zn <sup>0</sup>	terpy	OAc	MgCl <sub>2</sub>	23
10	Zn <sup>0</sup>	terpy	OCO <sub>2</sub> Me	MgCl <sub>2</sub>	3
11	Zn <sup>0</sup>	terpy	Br	MgCl <sub>2</sub>	0
12	Zn <sup>0</sup>	<sup>t</sup> Bu-terpy	OAc	MgCl <sub>2</sub>	7
13	Zn <sup>0</sup>	<sup>t</sup> Bu-terpy	OCO <sub>2</sub> Me	MgCl <sub>2</sub>	0
14	Zn <sup>0</sup>	<sup>t</sup> Bu-terpy	Br	MgCl <sub>2</sub>	0

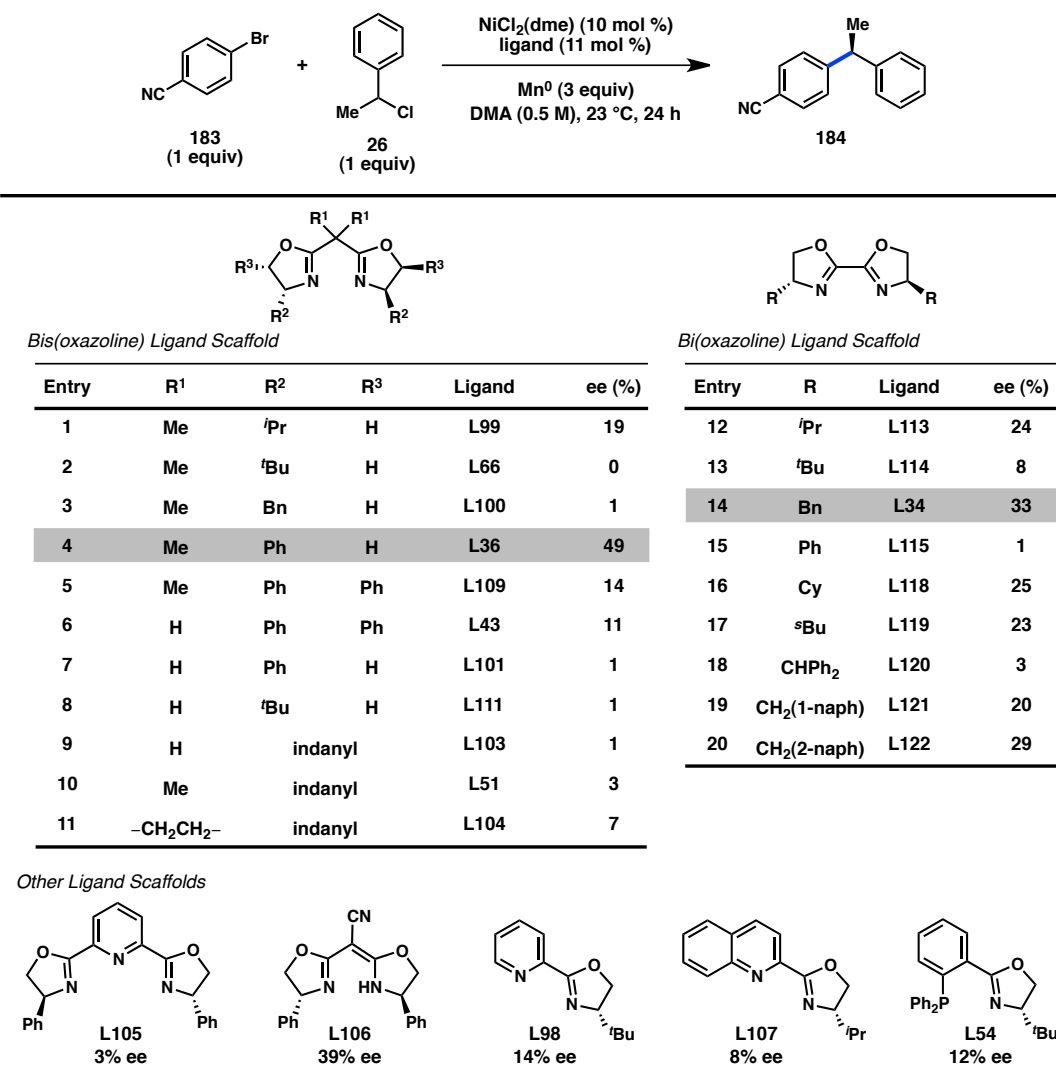
reaction conditions. When switching to acid chloride **182**, improvement in the yield of ketone **181** was not achieved with Mn<sup>0</sup> as the reductant. In contrast, Zn<sup>0</sup> allowed **181** to be formed in 49% yield from acid chloride **182** (Scheme 5.3). Further enhancement in the yield might be possible with an acid chloride lacking branching at the α position, as seen in our asymmetric reductive acyl coupling (see Chapter 3). Future efforts should also focus on more functionalized allylic acetates to assess regio- and enantioselectivity.

**Scheme 5.3.** Acyl-allyl reductive cross-coupling with an acid chloride.

### 5.3 DEVELOPMENT OF NEW NI-CATALYZED REDUCTIVE CROSS-COUPPLINGS (ASYMMETRIC)

In our studies on asymmetric reductive cross-couplings, we have identified (1-chloroethyl)benzene (**26**) as capable of inducing high enantioselectivity in couplings with C(sp<sup>2</sup>)-hybridized electrophiles, such as acid chlorides and vinyl bromides. We hypothesized that the coupling of chloride **26** and aryl halides should also be amenable to enantioinduction. The union of these two fragments would generate enantioenriched diarylalkanes, prevalent motifs in medicinal chemistry.<sup>13</sup> Elegant studies by Fu and coworkers have shown that bi(oxazoline) ligands promote asymmetric Ni-catalyzed Negishi cross-couplings for the preparation of diarylalkanes.<sup>14</sup> Investigations by Weix and Molander under reductive conditions have also identified bi(oxazoline) ligands, but their asymmetric induction for diarylalkanes remains modest.<sup>6,7</sup>

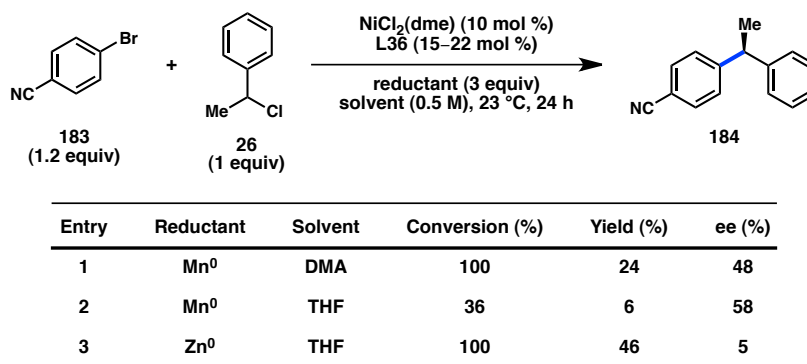
In our preliminary studies on diarylalkanes, we realized that both coupling partners readily undergo homocoupling in addition to heterocoupling. Nonetheless, we performed a ligand screen for the coupling of 4-bromobenzonitrile (**183**) and benzyl chloride **26** (Figure 5.5). In general, bis(oxazoline) ligands delivered very low levels of enantioinduction (entries 1–11); encouragingly, phenyl-substituted **L36** provided diarylalkane **184** in 49% ee (entry 4). We next tested several bi(oxazoline) ligands and observed the highest ee of 33% with benzyl-substituted **L34** (entries 12–17). We tried to enhance our enantioinduction by incorporating diphenyl or naphthyl moieties into our ligand, but greater ee was not observed (entries 18–20). Other ligand families gave poor enantioselective results.

**Figure 5.5.** Ligand screen for aryl-benzyl reductive cross-coupling.

We first chose to optimize reaction conditions with bis(oxazoline) **L36**. Unfortunately, reactions with **L36** were plagued with low yields and competitive homocoupling. The reaction also proved to be sensitive to ligand loading, with at least a 1.5:1 ligand/Ni ratio necessary for reproducible enantioinduction. Changing the solvent from DMA to THF reduced the yield and conversion but increased the ee of **184** to 58% (Table 5.2, entries 1 and 2). Using Zn<sup>0</sup> in place of Mn<sup>0</sup> provided complete conversion of benzyl chloride **26** and delivered diarylalkane **184** in 46% yield, albeit with near-

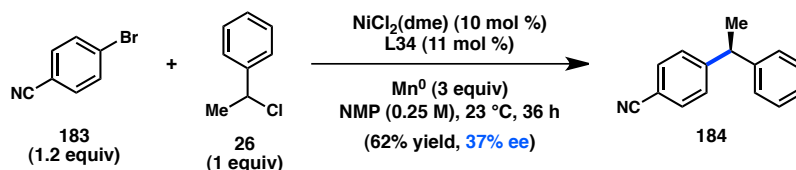
complete erosion of enantioinduction (entry 3). The loss of ee may result from in situ-generation of an organozinc reagent in the presence of  $\text{Zn}^0$  as a reductant, altering the mechanism from a reductive coupling to a conventional Negishi cross-coupling.

**Table 5.2.** Bis(oxazoline) ligand in aryl-benzyl reductive cross-coupling.



We also studied diarylalkane generation mediated by benzyl-substituted bi(oxazoline) **L34**. Lowering the reaction concentration and employing a slight excess of aryl bromide **183** in NMP allowed product **184** to be formed in 62% yield (Scheme 5.4). Additional modifications to the reaction conditions did not increase the enantioselectivity of the transformation above 37% ee.

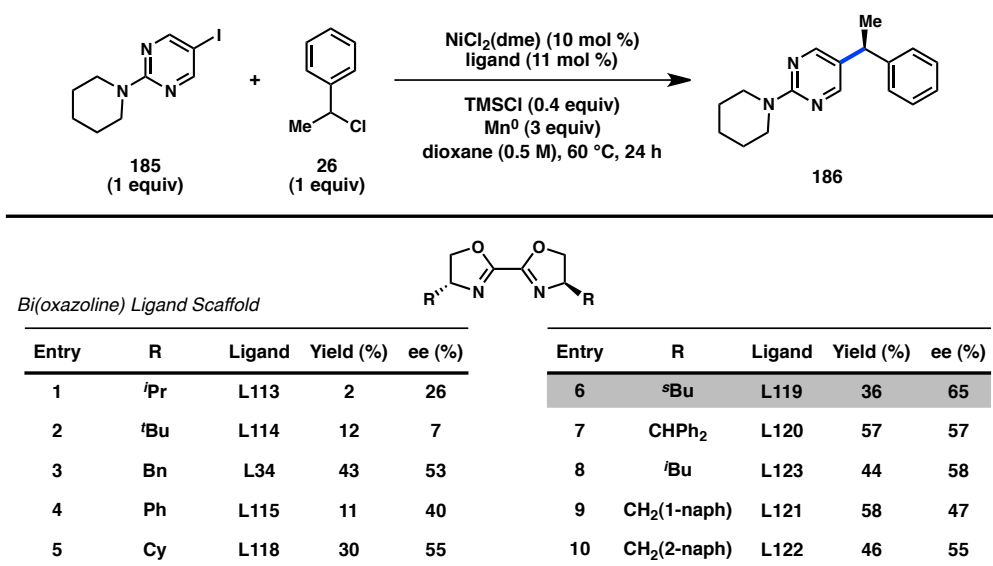
**Scheme 5.4.** Bi(oxazoline) ligand in aryl-benzyl reductive cross-coupling.



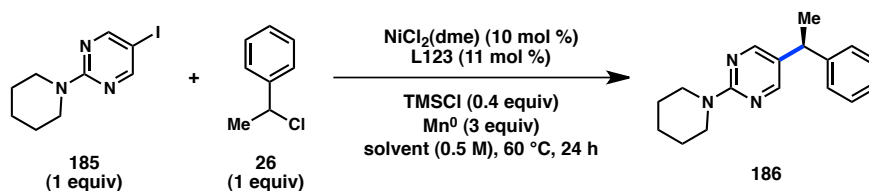
Approaching the transformation from a different direction, we decided to examine the cross-coupling between benzyl chloride **26** and heteroaryl halides. Pyrimidine **185** exhibited promising reactivity only when heated to 60 °C with additional activation by catalytic  $\text{TMSCl}$ . A screen of chiral scaffolds revealed that PHOX ligands gave moderate

yields but no enantioinduction and that Box ligands provided low reactivity. An analysis of bi(oxazolines) was more fruitful: **L34** (R = Bn) delivered diarylalkane **186** in 43% yield and 53% ee (Table 5.3, entry 3). The highest enantioselectivity was attained with **L119** (R = <sup>s</sup>Bu), furnishing **186** in 65% ee (entry 6). Additional optimization studies were performed with **L123** (R = <sup>t</sup>Bu), another promising ligand (entry 8).

**Table 5.3.** Bi(oxazoline) ligands in heteroaryl-benzyl reductive cross-coupling.



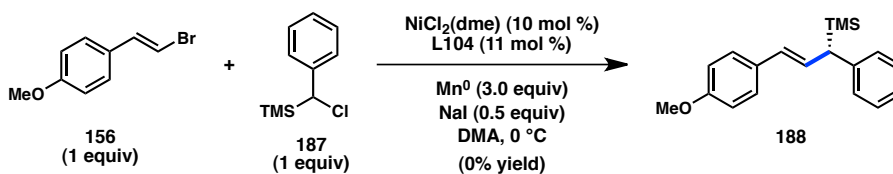
Analysis of crude reaction mixtures revealed formation of benzyl homocoupling, aryl homocoupling, and hydrodehalogenation of aryl iodide **185**. A solvent screen was conducted to increase product yields and ee's (Table 5.4). THF led to a large reduction in enantioinduction, while the highest ee was still observed with dioxane (entries 1 and 2). In the absence of TMSCl, no desired product was formed (entry 7). Interestingly, only a trace of **186** was observed when Mn<sup>0</sup> was replaced with Zn<sup>0</sup> (entry 8). Future work on this coupling should focus on the scope of heteroaryl halide and investigate different cyclic benzyl chlorides that may enhance the enantioselectivity of the transformation.

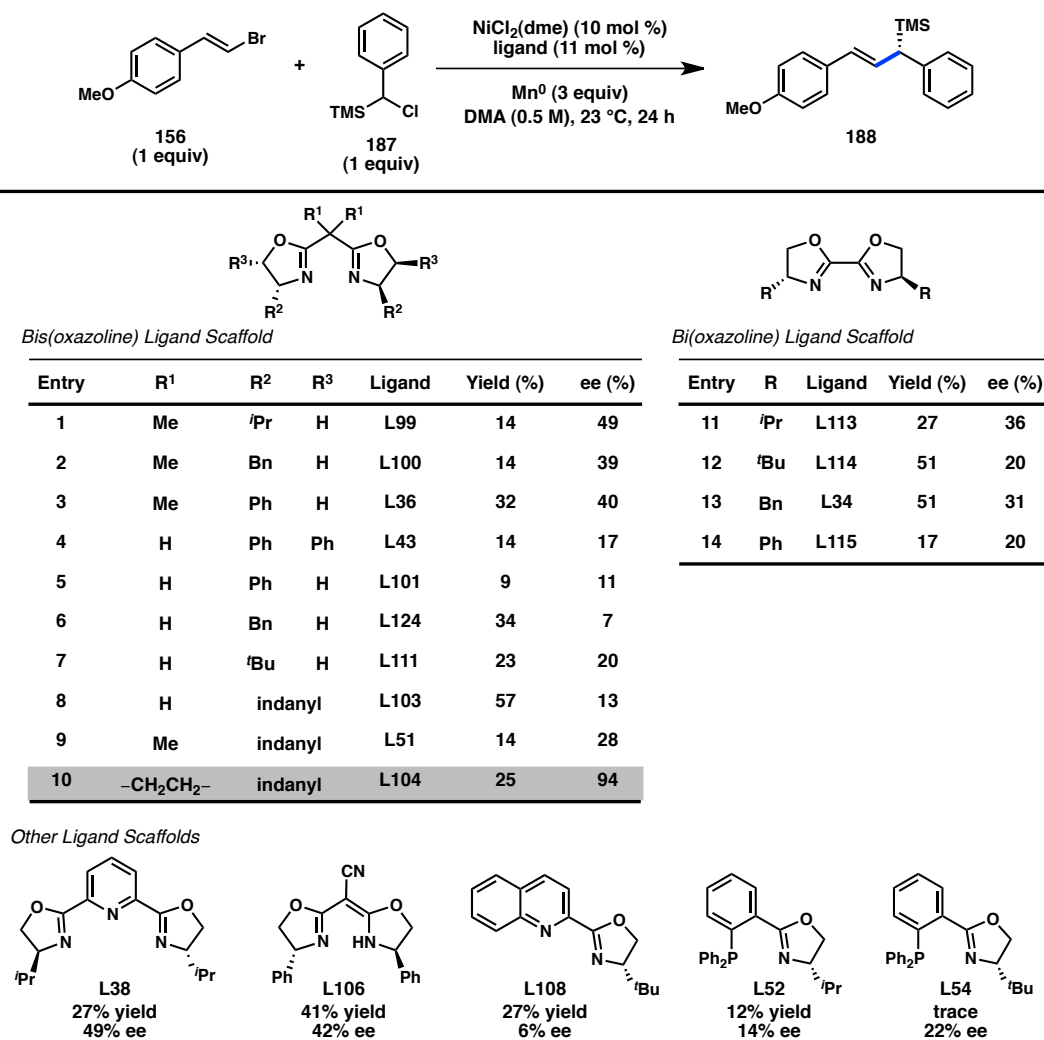
**Table 5.4.** Exploration of heteroaryl-benzyl reductive cross-coupling.

Entry	Solvent	Yield (%)	ee (%)
1	dioxane	34	59
2	THF	55	8
3	DMA	67	44
4	DMPU	38	42
5	NMP	47	39
6	DMF	44	33
7 <sup>a</sup>	dioxane	0	--
8 <sup>b</sup>	dioxane	3	--

<sup>a</sup> No  $\text{TMSCl}$ . <sup>b</sup>  $\text{Zn}^0$  used instead of  $\text{Mn}^0$ .

We next turned our attention to the coupling of vinyl bromide **156** and (chloro(phenyl)methyl)trimethylsilane (**187**) to form allylsilane **188** (Scheme 5.5).<sup>15</sup> Under our previously optimized conditions for vinyl couplings, no desired product was formed.<sup>4</sup> Undeterred, a ligand screen revealed that bis(oxazoline) ligands containing an isopropylidene linker were inefficient at imparting asymmetric induction (Figure 5.6, see Chapter 4 for comparison to chloride **26**). To our delight, cyclopropyl-linked ligand **L104** still furnished allylsilane **188** in 25% yield and 94% ee (entry 10). Bi(oxazoline) ligands delivered lower enantioinduction but sometimes provided higher yields of **188** (entries 11–14). Other ligand families did not perform better than bis(oxazoline) **L104**.

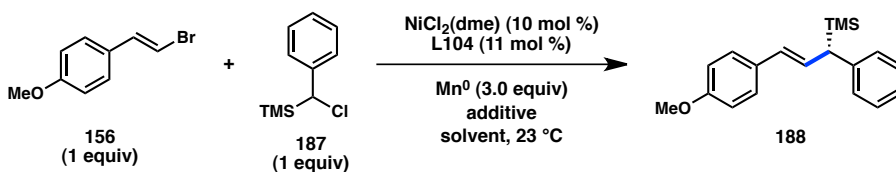
**Scheme 5.5.** Initial attempt toward an allylsilane product.

**Figure 5.6.** Ligand evaluation for the preparation of allylsilanes.

Additional optimization of the reaction conditions demonstrated similar results for solvents DMA, NMP, and DMF, although both DMPU and THF failed to deliver product **188** (Table 5.5, entries 1–5). We were surprised to find that addition of 1 mol % cobalt(II) phthalocyanine (Co(Pc)) improved the yield of allylsilane **188** to 40% without affecting the ee (entry 6). Increasing the loading of Co(Pc) had little impact on the reaction yield, although changing the solvent to NMP delivered **188** in 49% yield and 96% ee (entry 9). While the role of Co(Pc) remains unclear, the compound is capable of

displacing halides in a two-electron fashion followed by homolytic cleavage of the resulting Co–C bond to generate a carbon-centered radical.<sup>16</sup> This strategy has been employed by Weix and coworkers for the coupling of benzylic electrophiles, wherein activation with cobalt and a mesylate leaving group prevents the high level of homocoupling observed with a chloride leaving group.<sup>6</sup> Follow-up studies are needed to elucidate the role of Co(Pc) and evaluate the generality of the allylsilane synthesis.

**Table 5.5.** Optimization of reaction parameters for the preparation of allylsilanes.



Entry	Solvent	Additive	Yield (%)	ee (%)
1	DMA	--	28	94
2	DMPU	--	0	--
3	NMP	--	32	94
4	DMF	--	18	90
5	THF	--	0	--
6	DMA	Co(Pc) (1 mol %)	40	95
7	DMA	Co(Pc) (3 mol %)	42	96
8	DMA	Co(Pc) (5 mol %)	42	95
9	NMP	Co(Pc) (2 mol %)	49	96

Co(Pc) = cobalt(II) phthalocyanine

## 5.4 CONCLUDING REMARKS

In conclusion, we have disclosed a model for cross-selectivity in the Ni-catalyzed reductive coupling of two distinct organohalide electrophiles. Improved yields can be achieved when a polar-type electrophile is combined with an electrophile that can stabilize formation of a transient radical. With respect to enantioinduction, electrophiles

that have a directing group or bear steric and electronic differences between both faces perform best. Several examples of promising cross-reactivity and enantioinduction have been presented, including couplings of  $\alpha$ -halo carbonyls, benzyl chlorides, and  $\alpha$ -silyl benzyl chlorides with C(sp<sup>2</sup>)-hybridized coupling partners. Investigations to expand the substrate scope of enantioselective Ni-catalyzed reductive cross-couplings are currently underway in our laboratory.

## 5.5 EXPERIMENTAL SECTION

### 5.5.1 Materials and Methods

Unless otherwise stated, reactions were performed under a nitrogen atmosphere using freshly dried solvents. Tetrahydrofuran (THF), methylene chloride (CH<sub>2</sub>Cl<sub>2</sub>), and diethyl ether (Et<sub>2</sub>O) were dried by passing through activated alumina columns. Anhydrous dimethylacetamide (DMA) was purchased from Aldrich and stored under inert atmosphere. Manganese powder (– 325 mesh, 99.3%) was purchased from Alfa Aesar. NiCl<sub>2</sub>(dme) was purchased from Strem and stored in a glovebox under N<sub>2</sub> when not in use. Unless otherwise stated, chemicals and reagents were used as received. Triethylamine (Et<sub>3</sub>N) was distilled over calcium hydride prior to use. All reactions were monitored by thin-layer chromatography using EMD/Merck silica gel 60 F254 pre-coated plates (0.25 mm) and were visualized by UV, CAM, or KMnO<sub>4</sub> staining. Flash column chromatography was performed as described by Still et al.<sup>17</sup> using silica gel (particle size 0.032-0.063) purchased from Silicycle. Optical rotations were measured on a Jasco P-2000 polarimeter using a 100 mm path-length cell at 589 nm. <sup>1</sup>H and <sup>13</sup>C NMR spectra

were recorded on a Varian Inova 500 (at 500 MHz and 126 MHz, respectively), and are reported relative to internal  $\text{CHCl}_3$  ( $^1\text{H}$ ,  $\delta = 7.26$ ) and  $\text{CDCl}_3$  ( $^{13}\text{C}$ ,  $\delta = 77.0$ ). Data for  $^1\text{H}$  NMR spectra are reported as follows: chemical shift ( $\delta$  ppm) (multiplicity, coupling constant (Hz), integration). Multiplicity and qualifier abbreviations are as follows: s = singlet, d = doublet, t = triplet, q = quartet, m = multiplet, br = broad, app = apparent. IR spectra were recorded on a Perkin Elmer Paragon 1000 spectrometer and are reported in frequency of absorption ( $\text{cm}^{-1}$ ). HRMS were acquired using an Agilent 6200 Series TOF with an Agilent G1978A Multimode source in electrospray ionization (ESI), atmospheric pressure chemical ionization (APCI), or mixed (MM) ionization mode. Analytical SFC was performed with a Mettler SFC supercritical  $\text{CO}_2$  analytical chromatography system with Chiralcel AD-H, OD-H, AS-H, OB-H, and OJ-H columns (4.6 mm x 25 cm) with visualization at 210, 254, and 280 nm. Analytical achiral GC-MS was performed with an Agilent 7890A GC and an Agilent 5975C VL MSD with triple axis detector utilizing an Agilent HP-5MS (30.0 m x 0.25 mm) column (0.4 mL/min He carrier gas flow).

### 5.5.2 Ni-Catalyzed Reductive Cross-Coupling

#### Acyl-Allyl Coupling (Table 5.1):

On a bench-top, to a 1/2 dram vial was added the appropriate ligand (0.006 mmol, 6 mol %), reductant (0.3 mmol, 3 equiv),  $\text{NiCl}_2(\text{dme})$  (0.005 mmol, 5 mol %), and  $\text{MgCl}_2$  (0.1 mmol, 1 equiv) if necessary. The vial was transferred into an  $\text{N}_2$ -filled glovebox and charged with the appropriate solvent (0.2 mL, 0.5 M) followed by cyclohexanecarboxylic acid (0.1 mmol, 1.0 equiv) and benzyl ether (internal standard). Allyl electrophile (0.2

mmol, 2 equiv) and pivalic anhydride (0.15 mmol, 1.5 equiv) were each added in one portion. The vial was sealed and removed from the glovebox. The mixture was stirred vigorously, ensuring that the reductant was uniformly suspended, at 23 °C for 24 h. The dark mixture was diluted with 10% ethyl acetate/hexane and passed through a plug of silica, using 10% ethyl acetate/hexane eluent. The solution was concentrated, and the crude reaction mixture was analyzed by <sup>1</sup>H NMR.

#### **Aryl-Benzyl Coupling (Figure 5.5):**

On a bench-top, to a 1/2 dram vial was added the appropriate ligand (0.011 mmol, 11 mol %), Mn<sup>0</sup> (0.3 mmol, 3 equiv), NiCl<sub>2</sub>(dme) (0.01 mmol, 10 mol %), and 4-bromobenzonitrile (0.1 mmol, 1 equiv). The vial was transferred into an N<sub>2</sub>-filled glovebox and charged with DMA (0.2 mL, 0.5 M) followed by (1-chloroethyl)benzene (0.1 mmol, 1.0 equiv) and benzyl ether (internal standard). The vial was sealed and removed from the glovebox. The mixture was stirred vigorously, ensuring that the reductant was uniformly suspended, at 23 °C for 24 h. The dark mixture was diluted with 20% ethyl acetate/hexane and passed through a plug of silica, using 20% ethyl acetate/hexane eluent. The solution was concentrated and the crude reaction mixture was analyzed by <sup>1</sup>H NMR and chiral SFC.

#### **Heteroaryl-Benzyl Coupling (Table 5.3):**

On a bench-top, to a 1/2 dram vial was added the appropriate ligand (0.0055 mmol, 11 mol %), Mn<sup>0</sup> (0.15 mmol, 3 equiv), NiCl<sub>2</sub>(dme) (0.005 mmol, 10 mol %), and heteroaryl iodide (0.05 mmol, 1 equiv). The vial was transferred into an N<sub>2</sub>-filled glovebox and

charged with DMA (0.1 mL, 0.5 M) followed by (1-chloroethyl)benzene (0.05 mmol, 1.0 equiv) and benzyl ether (internal standard). The vial was sealed and removed from the glovebox. The mixture was stirred vigorously, ensuring that the reductant was uniformly suspended, at 60 °C for 18 h. The dark mixture was diluted with 20% ethyl acetate/hexane and passed through a plug of silica, using 20% ethyl acetate/hexane eluent. The solution was concentrated and the crude reaction mixture was analyzed by <sup>1</sup>H NMR and chiral SFC.

**Vinyl-Benzyl Coupling (Figure 5.6):**

On a bench-top, to a 1/2 dram vial was added the appropriate ligand (0.0055 mmol, 11 mol %), Mn<sup>0</sup> (0.15 mmol, 3 equiv), NiCl<sub>2</sub>(dme) (0.005 mmol, 10 mol %), and vinyl bromide (0.05 mmol, 1 equiv). The vial was transferred into an N<sub>2</sub>-filled glovebox and charged with DMA (0.1 mL, 0.5 M) followed by (chloro(phenyl)methyl)trimethylsilane (0.05 mmol, 1.0 equiv) and benzyl ether (internal standard). The vial was sealed and removed from the glovebox. The mixture was stirred vigorously, ensuring that the reductant was uniformly suspended, at 23 °C for 18 h. The dark mixture was diluted with 20% ethyl acetate/hexane and passed through a plug of silica, using 20% ethyl acetate/hexane eluent. The solution was concentrated and the crude reaction mixture was analyzed by <sup>1</sup>H NMR and chiral SFC.

## 5.6 NOTES AND REFERENCES

- (1) Reviews on reductive cross-couplings: (a) Everson, D. A.; Weix, D. J. *J. Org. Chem.* **2014**, *79*, 4793. (b) Knappke, C. E. I.; Grupe, S.; Gärtner, D.; Corpet, M.; Gosmini, C.; Jacobi von Wangelin, A. *Chem. Eur. J.* **2014**, *20*, 6828. (c) Moragas, T.; Correa, A.; Martin, R. *Chem. Eur. J.* **2014**, *20*, 8242.
- (2) (a) Netherton, M. R.; Fu, G. C. *Adv. Synth. & Catal.* **2004**, *346*, 1525. (b) Frisch, A. C.; Beller, M. *Angew. Chem., Int. Ed.* **2005**, *44*, 674. (c) Rudolph, A.; Lautens, M. *Angew. Chem., Int. Ed.* **2009**, *48*, 2656. (d) Jana, R.; Pathak, T. P.; Sigman, M. S. *Chem. Rev.* **2011**, *111*, 1417.
- (3) Cherney, A. H.; Kadunce, N. T.; Reisman, S. E. *J. Am. Chem. Soc.* **2013**, *135*, 7442.
- (4) Cherney, A. H.; Reisman, S. E. *J. Am. Chem. Soc.* **2014**, *136*, 14365.
- (5) Cui, X.; Wang, S.; Zhang, Y.; Deng, W.; Qian, Q.; Gong, H. *Org. Biomol. Chem.* **2013**, *11*, 3094.
- (6) Ackerman, L. K. G.; Anka-Lufford, L. L.; Naodovic, M.; Weix, D. J. *Chem. Sci.* **2015**, *6*, 1115.
- (7) For a related stereoconvergent transformation: Tellis, J. C.; Primer, D. N.; Molander, G. A. *Science* **2014**, *345*, 433.
- (8) (a) Wotal, A. C.; Weix, D. J. *Org. Lett.* **2012**, *14*, 1476. (b) Wotal, A. C.; Ribson, R. D.; Weix, D. J. *Organometallics* **2014**, *33*, 5874. (c) Wu, F.; Lu, W.; Qian, Q.; Ren, Q.; Gong, H. *Org. Lett.* **2012**, *14*, 3044. (d) Yin, H.; Zhao, C.; You, H.; Lin, K.; Gong, H. *Chem. Commun.* **2012**, *48*, 7034. (e) Zhao, C.; Jia, X.; Wang, X.; Gong, H. *J. Am. Chem. Soc.* **2014**, *136*, 17645.
- (9) Durandetti, M.; Gosmini, C.; Périchon, J. *Tetrahedron* **2007**, *63*, 1146.
- (10) (a) Wang, S.; Qian, Q.; Gong, H. *Org. Lett.* **2012**, *14*, 3352. (b) Anka-Lufford, L. L.; Prinsell, M. R.; Weix, D. J. *J. Org. Chem.* **2012**, *77*, 9989. For a Co-catalyzed method: (c) Gomes, P.; Gosmini, C.; Périchon, J. *Org. Lett.* **2003**, *5*, 1043.
- (11) Dai, Y.; Wu, F.; Zang, Z.; You, H.; Gong, H. *Chem. Eur. J.* **2012**, *18*, 808.
- (12) Gooßen, L. J.; Ghosh, K. *Angew. Chem., Int. Ed.* **2001**, *40*, 3458.
- (13) Yonova, I. M.; Johnson, a. G.; Osborne, C. A.; Moore, C. E.; Morrissette, N. S.; Jarvo, E. R. *Angew. Chem., Int. Ed.* **2014**, *53*, 2422 and references cited therein.

- (14) Do, H. Q.; Chandrashekar, E. R. R.; Fu, G. C. *J. Am. Chem. Soc.* **2013**, *135*, 16288.
- (15) For a related Kumada–Corriu coupling: (a) Hayashi, T.; Konishi, M.; Ito, H.; Kumada, M. *J. Am. Chem. Soc.* **1982**, *104*, 4962. (b) Hayashi, T.; Konishi, M.; Okamoto, Y.; Kabeta, K.; Kumada, M. *J. Org. Chem.* **1986**, *51*, 3772.
- (16) K. Takai, K. Nitta, O. Fujimura, K. Utimoto, *J. Org. Chem.* **1989**, *54*, 4732.
- (17) Still, W. C.; Kahn, M.; Mitra, A. *J. Org. Chem.* **1978**, *43*, 2923.

## ABOUT THE AUTHOR

Alan Hayden Cherney was born on April 28, 1988 to Marc and Leora Cherney in Chicago, Illinois. He was raised in nearby Skokie and Morton Grove, graduating from Niles North High School in 2006. That same year, Alan moved downstate to pursue his undergraduate education at the University of Illinois at Urbana-Champaign. While an interest in the chemical sciences compelled him to pursue a degree in chemical engineering, a passion for the complexities of organic synthesis was fostered during his second year of education. Joining the laboratory of Prof. Martin Burke gave Alan his first taste of organic chemistry research, resulting in a study on the scope of Suzuki–Miyaura cross-couplings of allenes. After receiving his B.S. degree in chemical engineering in 2010, Alan decided to join the dark side and pursue a future as a chemist.

This future took Alan from the golden cornfields of Illinois to the golden skies of California, where he enrolled at the California Institute of Technology in Pasadena. He commenced his doctoral studies under the supervision of Prof. Sarah Reisman and focused his research on the development of asymmetric nickel-catalyzed reductive cross-coupling reactions. His time in Pasadena came to a happy end when he was awarded his Ph.D. in chemistry in 2015. In the fall of 2015, Alan will remain in California, making the short move to Thousand Oaks to begin his industrial career within a process chemistry group at Amgen.